

Catalytic Chemical Bond Activation for New Molecular Transformations

著者	HO HON EONG
学位授与機関	Tohoku University
学位授与番号	11301甲第17146号
URL	http://hdl.handle.net/10097/00096933

DOCTORAL DISSERTATION

Catalytic Chemical Bond Activation for New Molecular Transformations

(触媒的結合活性化による新規分子変換反応の開発)

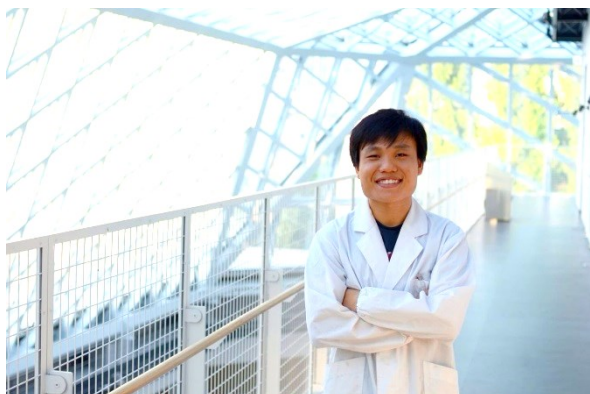
Ho Hon Eong

2016

Department of Chemistry
Graduate School of Science
Tohoku University

Dissertation Examiner
Assoc. Professor Tienan Jin
Tohoku University

Bibliography



Ho Hon Eong was born in Johor Bahru, Malaysia in 1987. He graduated from Universiti Malaysia Sabah in BSc. Industrial Chemistry (First Class Hons.) in 2010. He is awarded the MEXT Scholarship of Japan and entered his Master studies in organic chemistry in Dept. of Chemistry, Tohoku University, from 2011-2013. He graduated with the Master Thesis titled: Highly

Efficient Heterogeneous Aerobic Cross-dehydrogenative Coupling *via* C–H Functionalization of Tertiary Amines using A Nanoporous Gold Skeleton Catalyst, under the supervision of Prof. Yamamoto Yoshinori. He further developed research interest in synthetic methodology and began doctoral studies in 2013, under the academic advice of Associate Prof. Jin Tienan of WPI-AIMR (Advanced Institute for Materials Research), Tohoku University, Japan. Currently, his research focused on the transition-metals catalyzed methodology development for new molecular transformations (particularly enjoy the challenge of C-H bond activations) for functional organic materials.

Contents

Contents	i
List of Publication	ii
Abbreviation	iii
Numbering	iv
 Introduction	 1
 Chapter 1. Highly Efficient Heterogeneous Aerobic Cross-dehydrogenative Coupling via C–H Functionalization of Tertiary Amines using A Nanoporous Gold Skeleton Catalyst	 7
 Chapter 2. <i>N</i> -Methyl Transfer Induced Copper-Mediated Oxidative Diamination of Alkynes.	 58
 Chapter 3. Pd(II)-catalyzed Intramolecular Annulations of <i>ortho</i> -Alkynylaniline for Polyheterocyclics via C–N and <i>peri</i> C–H Bond Activation	 132
 Chapter 4. Carboxylic Acid-Catalyzed Highly Efficient and Selective Hydroboration of Alkynes with Pinacolborane	 170
 Acknowledgement	

List of Publications

1. *N*-Methyl Transfer Induced Copper-Mediated Oxidative Diamination of Alkynes. Ho, H. E.; Oniwa, K.; Yamamoto, Y.; Jin, T. *Org. Lett.* **2016**, *18*, 2487.
2. Highly Efficient Heterogeneous Aerobic Cross-dehydrogenative Coupling *via* C–H Functionalization of Tertiary Amines using A Nanoporous Gold Skeleton Catalyst. Ho, H. E.; Ishikawa, Y.; Asao, N.; Yamamoto, Y.; Jin, T. *Chem. Commun.* **2015**, *51*, 12764.
3. Carboxylic Acid-Catalyzed Highly Efficient and Selective Hydroboration of Alkynes with Pinacolborane. Ho H. E.; Asao, N.; Yamamoto, Y.; Jin, T. *Org. Lett.* **2014**, *16*, 4670.
4. Unsupported Nanoporous Gold Catalyst for Highly Selective Hydrogenation of Quinolines. Yan, M.; Jin, T.; Chen, Q.; Ho, H. E.; Fujita, T.; Chen, L-Y.; Bao, M.; Chen, M-W.; Asao, N.; Yamamoto, Y. *Org. Lett.* **2012**, *15*, 1484.

STATEMENT OF COPYRIGHT CLEARANCE

I hereby declare that request for copyright has been granted by the respective publishers to reprint the journal and related contents in print and electronic format.

In Sendai, 05.08.2016

Signature:

Abbreviation

M	Metal
A	Carboxylic acid
Cat.	Catalyst
L	Ligand
CDC	Cross-dehydrogenative coupling
THIQ	1,2,3,4-Tetrahydroisoquinoline
AuNPore	Nanoporous gold
AgNPore	Nanoporous silver
CuNPore	Nanoporous copper
PtNPore	Nanoporous platinum
PdNPore	Nanoporous palladium
Fe ₃ O ₄ NPs	Ferric oxide nanoparticles
TBHP	<i>tert</i> -butyl hydroperoxide
h	Hour
rt.	Room temperature
equiv.	Equivalent
EDX	Energy dispersive X-Ray
SEM	Scanning electron microscopy
XPS	X-Ray photoelectron spectroscopy
HRTEM	High-resolution transmission electron microscopy
mCPBA	<i>m</i> -chloroperoxybenzoic acid
DTBP	Di- <i>tert</i> -butyl peroxide
TEMPO	(2,2,6,6-Tetramethylpiperidin-1-yl)oxyl
BHT	2,6-Di- <i>tert</i> -butyl-4-methyl phenol
Et ₃ N	Triethylamine
DHII	5,10-Dihydroindolo[3,2- <i>b</i>] indole
PAH	Polycyclic aromatic hydrocarbon
PHA	Polyheteroaromatic
AAI	7-Alkyl-7H-acetonaptho[1,2- <i>b</i>] indole
DBU	1,8-Diazabicycloundec-7-ene
DABCO	1, 4-Diazabicyclo[2.2.2]octane
HBPIn	Pinacolborane
B ₂ Pin ₂	Bis(pinacolato)diboron
PPh ₃	Triphenylphosphine

Numbering

Compounds, tables, schemes, equations, and figures are numbered independently in each chapter.

Introduction

1. General Introduction

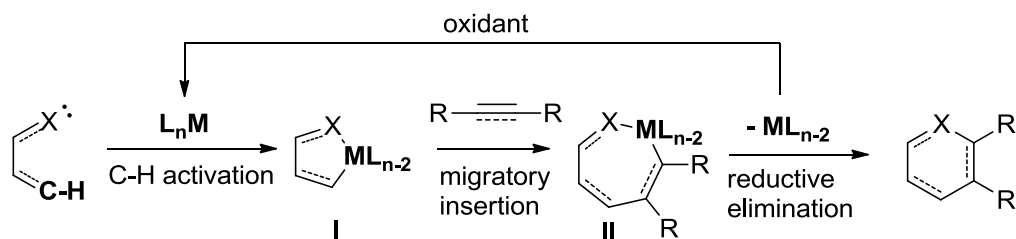
“Let's create reactions and concepts which will become the milestone contributions in organic chemistry”

As Prof. Yamamoto Yoshinori's once called, building a chemistry that can inspire the next and many generations to come is indeed the highest philosophy in synthetic chemistry. Over the last 50 years, a substantial list of great discoveries in synthetic methodology for new molecular transformations has continue to drive the community forward and play an important role in modernization of human society. Synthetic chemistry has since progressed rapidly from the classical alteration of functional groups towards direct functionalization of the hitherto inactive chemical bonds.¹ Wide range of chemical classes can be now considered as starting materials for the building of more complex molecules or functional targets compounds such as polymer, bioactive compounds, natural products, and metal organic compounds.

1.1. C-H Bond Activations

The development of transition metals catalysis for direct activation of C-H bonds has reshape the landscape of both organometallic and synthetic chemistry. Despite the relatively high activation energy of C-H bond cleavage ($\approx 110 \text{ kcal mol}^{-1}$, for C(aryl)-H bonds), we have witnessed the rapid development of transition metals catalysis in C-H activation. Progressive development of C-H activation has moved from the early serendipitous discovery of catalytic combination for metal insertion into the inactive C-H bond towards the recent examples of practical and general functionalization of C-H bonds as a synthetic tool.² As a result, a new horizon of synthetic approach is being adopted by synthetic community to maximize the functionalization the ubiquitous-present C-H bond for an atom-/step-economy synthesis, and bring an overall simplicity in synthetic design.

Taking an example of common scenario of metal-catalyzed annulation reaction *via* C-H activation as depicted in Scheme 1, the electrophilic metal-species undergo oxidative addition and generate active heterometallacycle **I** intermediate followed by coordination with unsaturated coupling partner to form the intermediate **II**, and finally reductive elimination step under oxidative condition to regenerate the active metal-species. In most cases, stoichiometric oxidants are required to accept the redundant electron and regenerate the active catalyst.

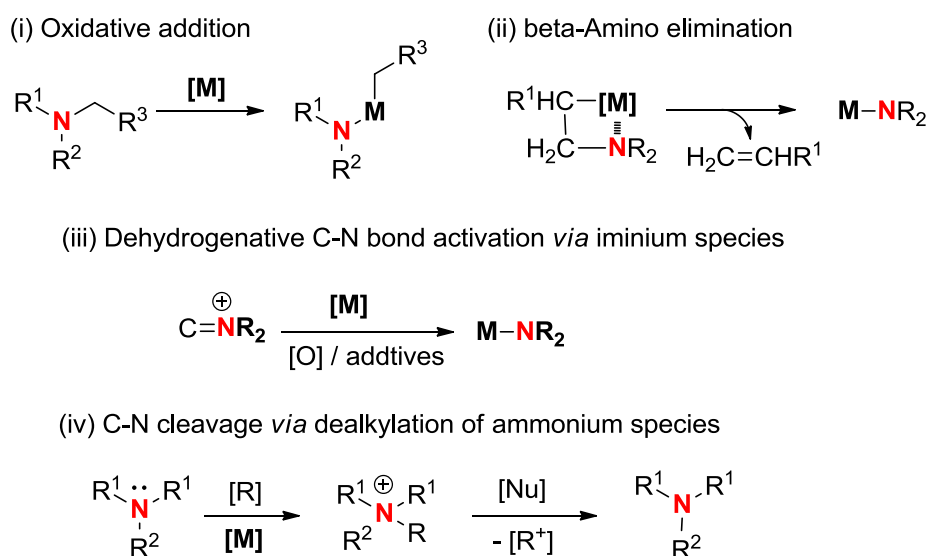


Scheme 1. Metal-catalyzed annulation reactions involving C-H activation.

In the rapid development for C-H functionalization, Pd-complexes is undisputable the dominant catalyst for general C-H activation.³ This phenomena might be due to the high electrophilicity of Pd-complexes that can readily undergo electropalladation with C-H bond to generate reactive intermediate.

1.2 C-N Bond Activations

Nitrogen-containing molecules is widely found in natural products, drug targets, and material science. The report of C-N bond related transformations is on the rise and represent one of most important issue in organic chemistry, organometallics, and biochemistry. The high bond dissociation energy of C-N bond containing molecules has make C-N bond a prevalent and too stable for modifications in synthetic chemistry.⁴ Nonetheless, transition-metal catalyzed C-N bond activation reactions have received much attentions in recent years and emerged as a powerful synthetic tool to construct N-containing compounds in a mild and efficient manners.⁵

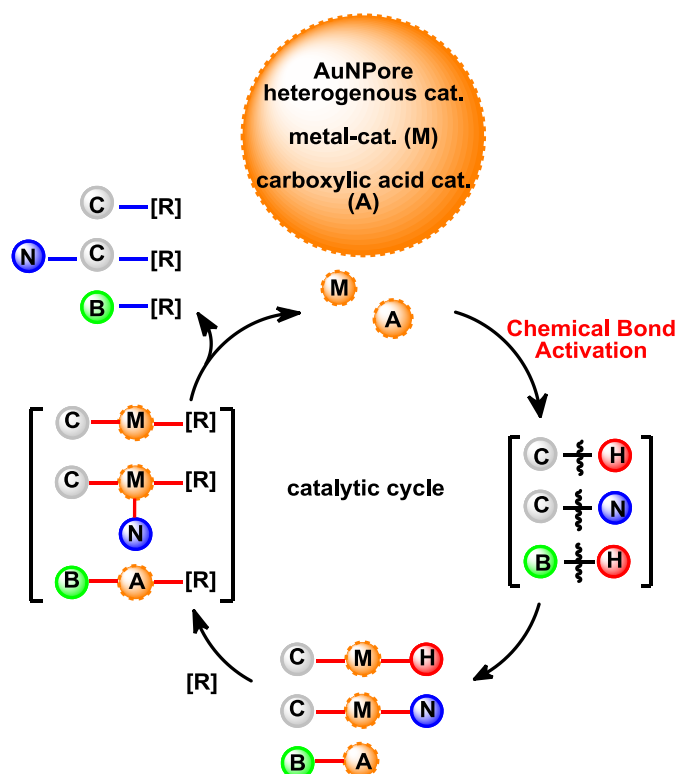


Scheme 2. C-N activation/cleavage strategies.

Generally, transition metal-catalyzed C-N activation/cleavage strategy is analogous to that of C-X (halogen) bonds metalations which can generate the more reactive C-M or M-N species. The general transition metal-catalyzed C-N metalation as depicted in Scheme 2, can be categorized into: (i) Oxidative addition with low-valent transition metals, (ii) β -amino elimination, (iii) dehydrogenative C-N bond activation *via* formation of iminium species, and (iv) metal -induced generation of ammonium species and followed by dealkylation *via* C-N cleavage.

2 Brief Introduction of The Dissertation

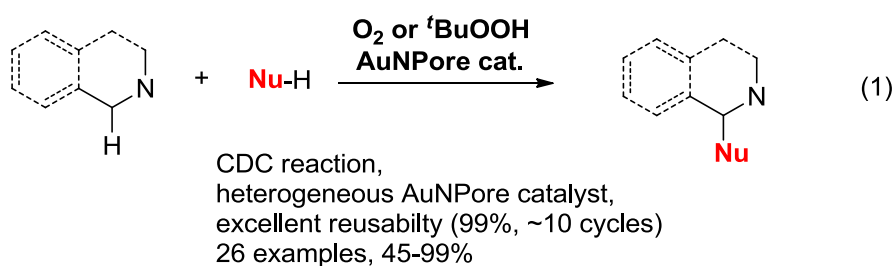
In the landscape of synthetic methodology, our research group has been relentless in addressing and undertaking the most fundamental challenges. Under a systematic approach, we are interested to functionalize the inactive chemical bonds (especially a catalysis feat.) for new methodology development. That being said, serendipitous discovery is never left unnoticed and has often led to the greatest joy of new discovery in chemistry that follows soon after. To date, we have contributed several creative strategies to activate chemical bonds for new molecular transformations, using both homogenous and heterogeneous catalysis,⁶ for various functional organic molecules.⁷



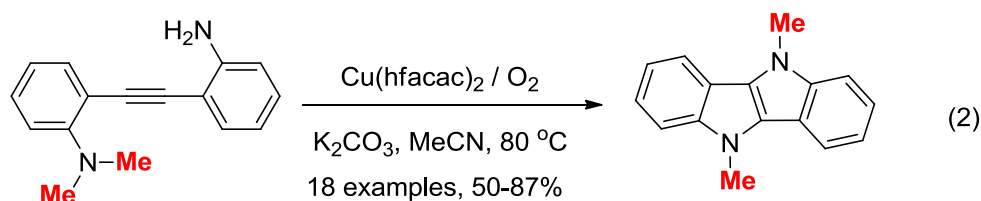
Scheme 3. Catalytic cycle of chemical bonds using heterogeneous AuNPore, transition-metal catalyst (M), and carboxylic acid catalyst (A).

In agreement with the development of globally sustainable society and a response to Prof. Yamamoto Yoshinori's calling, I decided to challenge my PhD studies with the following research theme: Catalytic Chemical Bond Activation for New Molecular Transformations. This dissertation represents our research interest to undertake the most fundamental issues in synthetic chemistry, i.e. to discover, activate, and functionalize different reactivities of different chemical bonds, namely C-H, C-N, and H-B bonds for new molecular transformations. The strategies include homogeneous catalysis using transition metals (M) and carboxylic acid (A), as well as using the zero-valent nanoporous gold heterogeneous catalyst (AuNPore) to activate different chemical bonds. (Scheme 3)

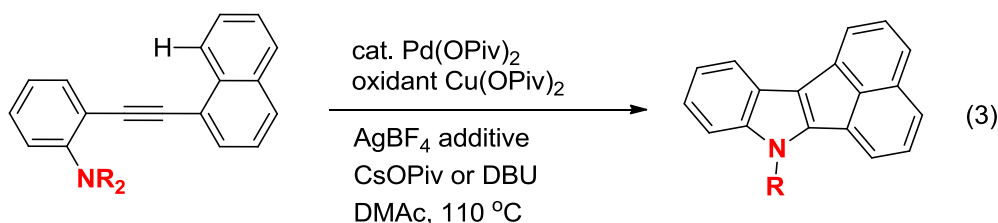
In Chapter 1, I summarize the zero-valent nanoporous gold (AuNPore) as a robust and green heterogeneous catalyst for α -C-H functionalization of various tertiary amines. AuNPore combines with molecular oxygen at 80 °C or *tert*-butyl hydrogen peroxide at room temperature and catalyzes the heterogeneous cross-dehydrogenative coupling (CDC) reaction efficiently to afford the corresponding C-C and C-heteroatom coupling products in good to excellent yields with excellent reusability as shown in eq. 1. This work was completed in 2013 and represents the first application of AuNPore catalysts for complex transformation involving C-H functionalization, apart from the other successful applications of AuNPore heterogeneous system for oxidation and reduction reactions reported by our research group.⁸ The well-defined structure of AuNPore densely covered by low-coordinated Au-atom is established catalytic active sites.⁹



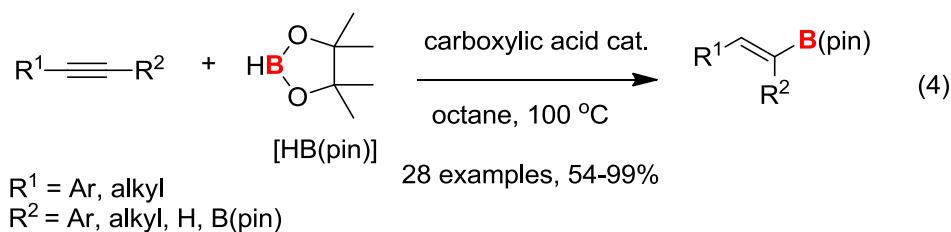
In Chapter 2, a novel intramolecular oxidative diamination of bis(2-aminophenyl)acetylene is developed for the synthesis of the structurally intriguing π -conjugated polyheterocyclic scaffold, 5,10-dihydroindolo[3,2-*b*]indole (DHII), under $\text{Cu}(\text{hfacac})_2/\text{O}_2$ oxidation systems (eq. 2). The structure design of bis(2-aminophenyl)acetylene bearing both *N,N*-dimethylamine and primary amine groups is crucial for constructing the corresponding DHII scaffold. Notably, an intermolecular *N*-methyl transfer from the nitrogen atom of *N,N*-dimethylamine to the primary amine takes place, which is a critical step for the successful implementation of the present annulation process.¹⁰



In Chapter 3, a Pd(II)-catalyzed intramolecular annulation of *o*-alkynylaniline via C-N and *peri* C-H bond activations has been developed for the construction of highly π -conjugated polyheteroaromatic (PHAs) as low-band gap organoelectronic material (eq. 3). Pd(II)-catalyzed tandem intramolecular annulation of *N,N*-dialkyl-2-(naphthalen-1-ylethynyl)aniline to construct 7-alkyl-7*H*-acenaphtho[1,2-*b*]indole (AAIs) scaffold via tandem C-N and *peri* C-H activation is discussed. The role of suitable additives and bases are essential for the efficient intramolecular cascade annulation process.



In Chapter 4, I report for the first time that carboxylic acids as active catalyst for the direct hydroboration of various terminal and internal alkynes with pinacolborane without using any metal catalysts (eq. 4). This unprecedented carboxylic acid-catalyzed H-B bond activation for hydroboration of various alkynes exhibits a broad functional groups compatibility, giving the corresponding alkenyl diboronates and monoboronates in good to high yields with exclusive regio- and stereoselectivities.¹¹



3. References and notes

1. For selected review on transition-metal catalyzed chemical bonds activations: (a) Gensch, T.; Hopkinson, M. N.; Glorius, F.; J. Wencel-Delord, J. *Chem. Soc. Rev.* **2016**, *45*, 2900. (b) Bariwal, J.; der Eycken, E. V. *Chem. Soc. Rev.* **2013**, *42*, 9283.
2. For recent review of C-H bond activations: (a) Liu, C.; Zhang, H.; Shi, W.; Lei, A.; *Chem. Rev.* **2011**, *111*, 1780. (b) Yeung, C. S.; Dong, V. M. *Chem. Rev.* **2011**, *111*, 1215. (c) Yamaguchi, J.; Yamaguchi, A. D.; Itami, K. *Angew. Chem. Int. Ed.* **2012**, *51*, 8960. (d) Lyons, T. W.; Sanford, M. S. *Chem. Rev.* **2010**, *110*, 1147. (e) Chen, X.; Engle, K. M.; Wang, D.-H.; Yu, J.-Q. *Angew. Chem. Int. Ed.* **2009**, *48*, 5094. (f) F. Gulías, M.; Mascareñas, J. L. *Angew. Chem. Int. Ed.* **2016**, *55*, 27. (g) Glorius, F.; Wencel-Delord, J. *Nat. Chem.* **2013**, *5*, 369–375.
3. Dyker, G. *Handbook of C–H Transformations: Applications in Organic Synthesis*; Wiley-VCH: Weinheim, **2005**.
4. Blanksby, S. J.; Ellison, G. B. *Acc. Chem. Res.* **2003**, *36*, 255.
5. For recent review of C-N bond activations: (a) Quanjun Wang, Q.; Su, Y.; Li, L.; Huang, H. *Chem. Soc. Rev.* **2016**, *45*, 1257. (b) Ouyang, K.; Hao, W.; Zhang, W.-X.; Xi, Z. *Chem. Rev.* **2015**, *115*, 12045.
6. For heterogeneous catalytic system using nanoporous-metal: (a) Yan, M.; Jin, T.; Ishikawa, Y.; Minato, T.; Fujita, T.; Chen, L.-Y.; Bao, M.; Asao, N.; Chen, M.; Yamamoto, Y. *J. Am. Chem. Soc.* **2012**, *134*, 17536. (b) Yan, M.; Jin, T.; Chen, Q.; Ho, E. H.; Fujita, T.; Chen, L.-Y.; Bao, M.; Chen, M.; Asao, N.; Yamamoto, Y. *Org. Lett.* **2013**, *15*, 1484. (c) Asao, N.; Hatakeyama, N.; Menggenbateer; Minato, T.; Ito, E.; Hara, M.; Kim, Y.; Yamamoto, Y.; Chen, M.; Zhang, W.; Inoue, A. *Chem. Commun.* **2012**, *48*, 4540. (d) Asao, N.; Ishikawa, Y.; Hatakeyama, N.; Menggenbateer; Yamamoto, Y.; Chen, M.; Zhang, W.; Inoue, A. *Angew. Chem. Int. Ed.* **2010**, *49*, 10093. (e) Wagh, Y. S.; Asao, N. *J. Org. Chem.* **2015**, *80*, 847.
7. (a) Zhao, J.; Oniwa, K.; Asao, N.; Yamamoto, Y.; Jin, T. *J. Am. Chem. Soc.* **2013**, *135*, 10222. (b) Zhao, J.; Asao, N.; Yamamoto, Y.; Jin, T. *J. Am. Chem. Soc.* **2014**, *136*, 9540. (c) Jin, T.; Zhao, J.; Asao, N.; Yamamoto, Y. *Chem. Eur. J.* **2014**, *20*, 3554. (d) Zhao, J.; Xu, Z.; Oniwa, K.; Asao, N.; Yamamoto, Y.; Jin, T. *Angew. Chem. Int. Ed.* **2016**, *55*, 259. (e) Jiang, H.; Ferrara, G.; Zhang, X.; Oniwa, K.; Islam, A.; Han, L.; Sun, Y.-J.; Bao, M.; Asao, N.; Yamamoto, Y.; Jin, T.; *Chem –Eur. J.* **2015**, *21*, 4065.
8. Ho, H. E.; Ishikawa, Y.; Asao, N.; Yamamoto, Y.; Jin, T. *Chem. Commun.* **2015**, *51*, 12764.
9. Fujita, T.; Guan, P.; McKenna, K.; Lang, X.; Hirata, A.; Zhang, L.; Tokunaga, T.; Arai, S.; Yamamoto, Y.; Tanaka, N.; Ishikawa, Y.; Asao, N.; Yamamoto, Y.; Erlebacher, J.; Chen, M. *W. Nat. Mater.* **2012**, *11*, 775.
10. Ho, H. E.; Oniwa, K.; Yamamoto, Y.; Jin, T. *Org. Lett.* **2016**, *18*, 2487
11. Ho, H. E.; Asao, N.; Yamamoto, Y.; Jin, T. *Org. Lett.* **2014**, *16*, 4670

Chapter 1

Highly Efficient Heterogeneous Aerobic Cross-dehydrogenative Coupling *via* C-H Functionalization of Tertiary Amines by nanoporous Gold Skeleton Catalyst

1. Introduction

Since the seminal works on the cross-dehydrogenative coupling (CDC) demonstrated by Murahashi and Li through the activation of the α -C(sp³)-H bond of tertiary amines,¹ tremendous progress has been made mostly employing high-valent transition-metal catalysts combined with oxidants.^{2,3} However, the use of recoverable and reusable heterogeneous catalysts sustaining a high catalytic activity for C-H functionalizations, would be more desirable from the viewpoint of green and sustainable chemistry.⁴ In spite of the remarkable progress made in the homogeneous transition-metal catalysis, the heterogeneous catalysis of such C-H bond functionalization remains a challenging issue.⁵ So far, very few reports describing heterogeneous catalytic CDC reactions of tertiary amines have been reported,⁶ such as using Fe₃O₄ nanoparticles, SBA-15 supported Fe(II) terpyridine complex, RuO₂ nanoparticles on graphene, and light-mediated TiO₂ nanoparticles, while in most cases, their use limited to the active 1,2,3,4-tetrahydroisoquinoline (THIQ) derivatives and required high temperatures. In addition, they did not show a satisfactory high catalytic activity with respect to the catalyst's reusability.

Recently, we and other groups disclosed that the self-supporting nanoporous gold (AuNPore) etched from bulk Au-Ag alloys is as a promising heterogeneous catalyst for green and sustainable chemical transformations.⁷⁻⁹ In particular, AuNPore showed a remarkable activity and selectivity for the oxidation of carbon monoxide and alcohols through the oxygen chemisorption,^{7,8} most likely due to the bicontinuous 3D nanostructure and the hyperboloid-shape of gold ligaments with concave and convex columnar curvatures, which provide many highly active sites to catalysis.¹⁰ Moreover, a small amount of residual Ag (1-3%) remaining in AuNPore is also an important element for activity of oxidation reactions via dissociation of molecular oxygen. Taking into consideration the remarkable oxidation catalytic properties of AuNPore together with its high surface area, high resistances for versatile chemicals and thermal coarsening, non-toxic nature, simple recovery operation, and high reusability, we reasoned that AuNPore should be a promising heterogeneous catalyst for oxidative C-H functionalization to construct new C-C bonds, which has never been reported to date. In our continual efforts to explore new catalytic activity and selectivity of nanoporous metals toward synthetic transformations,^{8,9,11} we report for the first time that the zero-valent AuNPore serves as a very active, highly reusable, and green heterogeneous

catalyst for α -C-H functionalization of tertiary amines with nucleophiles under aerobic conditions, either by using molecular oxygen at 80 °C or TBHP at room temperature. Various kinds of tertiary amines and nucleophiles were employed to the present heterogeneous CDC reactions, giving the corresponding coupling products in good to excellent yields. AuNPore can be readily recovered and reused up to 10 cycles without losing any catalytic activity.

The unsupported AuNPore catalyst was prepared by etching the homogeneous Au₃₀Ag₇₀ alloy with a 200 μ m thickness in 70 wt% of nitric acid at room temperature for 18 h.^{9a} The energy dispersive X-ray (EDX) measurement showed that the resulting AuNPore material composed of Au in 97% and the residual Ag in 3%. The scanning electron microscopy (SEM) images indicated that this nanoporous structure has an average ligament size of approximately 30 nm (Figure 1a). Our previous works on the characterization AuNPore revealed that AuNPore is zero-valent gold by means of X-ray photoelectron spectroscopy (XPS) and a high density of atomic steps and kinks at the curved surfaces of ligaments observed from high resolution transmission electron microscopy (HRTEM), should be the origin of catalytic activity.^{9a}

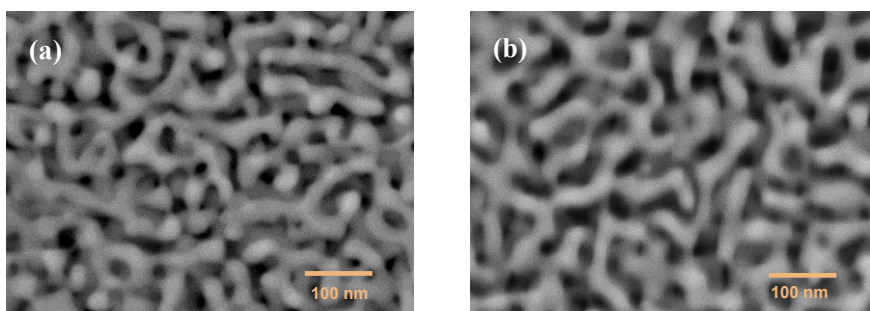


Figure 1. SEM images of nanoporous gold (AuNPore) catalyst. (a) fresh AuNPore, (b) after tenth cycle.

2. Results and Discussion

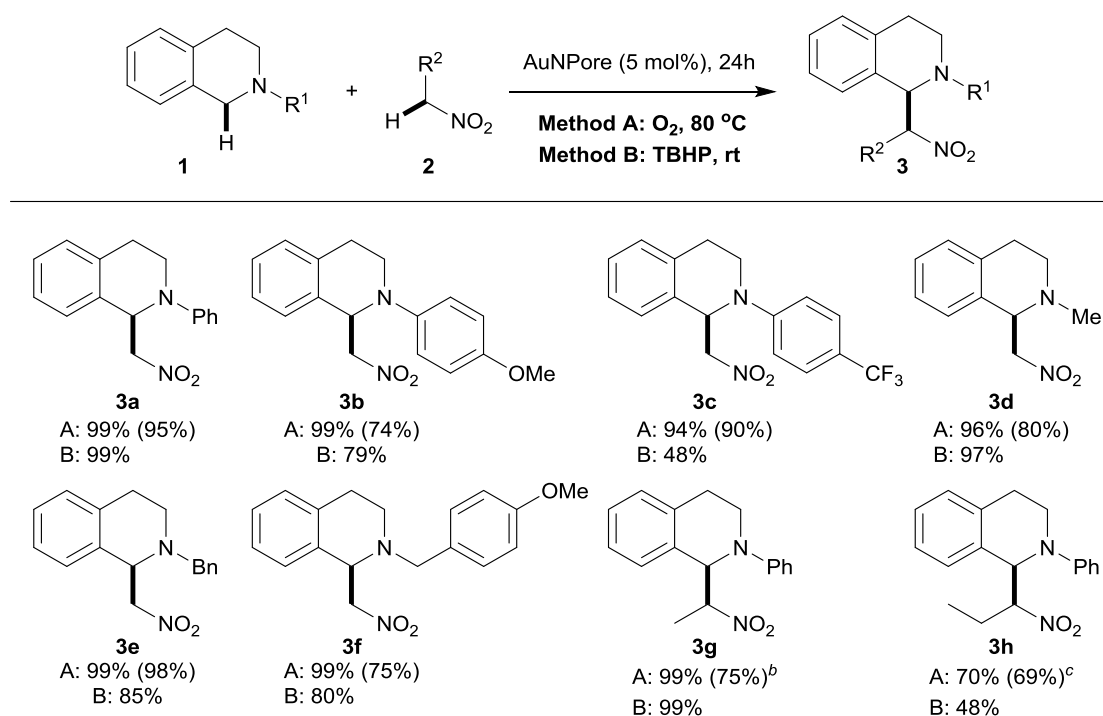
Initially, various nanostructured metal catalysts were investigated for the Nitro-Mannich type reaction of THIQ **1a** with nitromethane (**2a**) in the presence of molecular oxygen (1 atm) at 80 °C for 24 h. (Table 1). To our delight, AuNPore exhibited a very high catalytic activity for the present aerobic oxidative CDC reaction, giving the corresponding coupling product **3a** in almost quantitative yield (entry 1). Other nanoporous metals such as AgNPore prepared from Ag-Al alloy,^{9b} CuNPore prepared from Cu-Mn alloy,^{11a,b} PdNPore prepared from Pd-Al alloy,^{11d,e} and PtNPore prepared from Pt-Cu alloy,^{9e} showed an inferior catalytic activity compared with AuNPore, affording **3a** in 50% to 85% yields (entries 2-5). The use of gold nanoparticles (AuNPs) as catalyst produced **3a** in 80% yield and Fe₃O₄ nanoparticles (Fe₃O₄NPs) and the later has been reported by Li et al,^{6a} showed a low activity under the present conditions (entries 6 and 7). The reaction under an air atmosphere decreased the yield of **2a** dramatically (entry 8) and no reaction took place under an inert argon atmosphere, indicating the critical role of molecular oxygen with respect to the high chemical yield. Thus, we examined various oxidants for the present CDC reaction using AuNPore as a catalyst. Interestingly, when *tert*-butyl hydroperoxide (TBHP) in decane solution was used, the reaction could proceed at room temperature with a quantitative yield of **3a** (entry 9). Other oxidants, such as *m*-chloroperoxybenzoic acid (mCPBA) and di-*tert*-butyl peroxide (DTBP) exhibited poor activities and H₂O₂ resulted in a very low yield of **3a** due to its rapid decomposition by AuNPore. (entries 10-12). Thus, two optimal conditions, method A (O₂ at 80 °C, entry 1) and method B (TBHP in decane at rt, entry 9) were used for further studying the substrate scope.

Table 1. Screening of various nano-metal catalysts and oxidants for the CDC of THIQ (**1a**) and nitromethane (**2a**)^a

Reaction scheme: **1a** + **2a** $\xrightarrow[\text{oxidant, rt or 80 } ^\circ\text{C, 24 h}]{\text{nano-metal catalyst (5 mol\%)}}$ **3a**

Entry	MNPore (5 mol%)	Oxidant	T (°C)	Yield (%) ^b
1	AuNPore	O ₂	80	99
2	AgNPore	O ₂	80	51
3	CuNPore	O ₂	80	85
4	PdNPore	O ₂	80	55
5	PtNPore	O ₂	80	50
6	AuNPs on TiO ₂ ^c	O ₂	80	80
7	Fe ₃ O ₄ NPs ^d	O ₂	80	50
8	AuNPore	air	80	54
9	AuNPore	TBHP ^e	rt	99
10	AuNPore	mCPBA	rt	62
11	AuNPore	DTBP	rt	80
12	AuNPore	H ₂ O ₂	rt	38

^a Reaction conditions: **1a** (0.6 mmol), nitromethane **2a** (0.5 M for entries 1-8, 0.6 M for entries 9-12), nano-metal catalysts (5 mol%), oxidant (1 atm for O₂, 1 equiv for others), rt or 80 °C for 24 h. ^b ¹H NMR yield determined by using CH₂Br₂ as an internal standard. ^c The average size of AuNPs supported on TiO₂ is 5 nm. ^d The size is in the range of 50-100 nm. ^e A decane solution (5.5 M) was used. TBHP = *tert*-butyl hydroperoxide. mCPBA = *m*-chloroperoxybenzoic acid. DTBP = di-*tert*-butyl peroxide.

Table 2. AuNPore-catalyzed CDC reaction of various THIQs and nitroalkanes^a

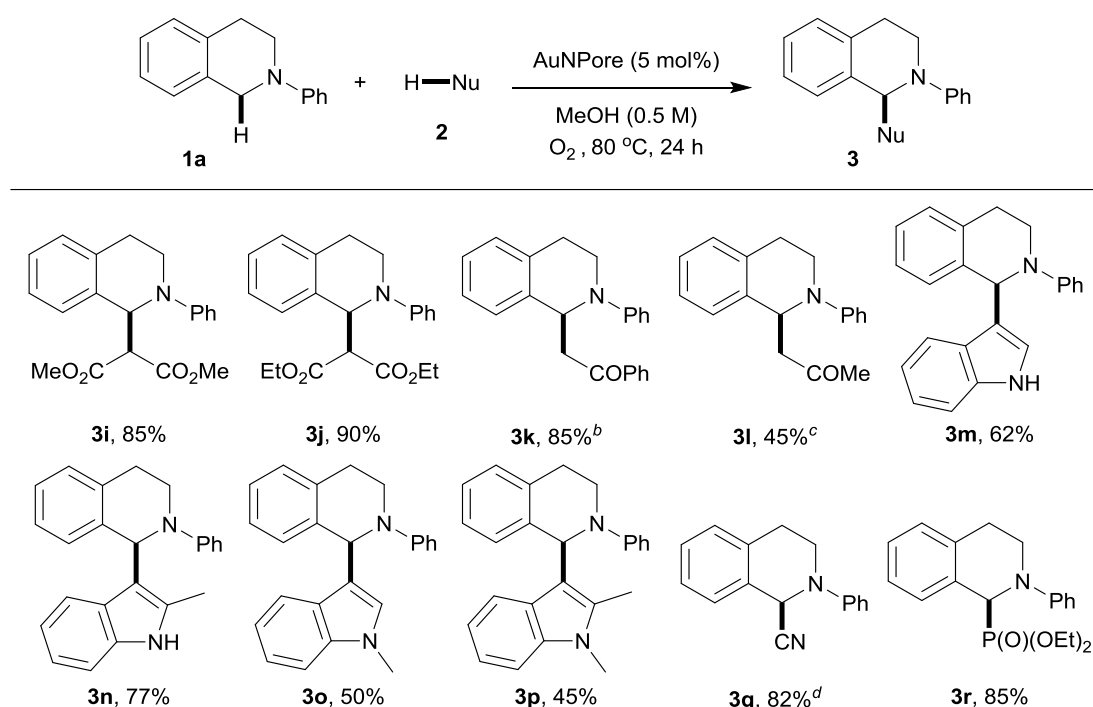
^a Method A: **1** (0.6 mmol), nitroalkane (0.5 M), AuNPore (5 mol%), O₂ (1 atm), 80 °C, 24 h. Method B: **1** (0.6 mmol), nitroalkane (1.0 M), TBHP in decane (5.5 M, 1 equiv), AuNPore (5 mol%), rt, 24 h. ¹H NMR yield determined by using CH₂Br₂ as an internal standard. Isolated yields are shown in parentheses. ^b Diastereomeric ratio is 1:1.7. ^c Diastereomeric ratio is 1:1.3.

The substrate scope of THIQs was examined using nitroalkanes as nucleophiles under the optimized conditions (Table 2). Similar to the *N*-phenyl-protected THIQ **1a**, the *N*-aryl-protected THIQs **1b** and **1c** having an electron-donating group of methoxy and an electron-withdrawing group of trifluoromethyl on the phenyl ring, afforded the corresponding nitromethyl-substituted products **3b** and **3c** in high yields under the method A. However, the reactions of **1b** and **1c** with method B showed lower reactivities, especially with the electron-deficient *N*-protected **1c**. THIQs having other *N*-protecting groups, such as methyl (**1d**) and benzyl groups (**1e** and **1f**) were also good substrates, giving the nitromethyl substituted products **3d-f** in high yields under both methods A and B. Other nitroalkanes such as nitroethane and nitropropane also can be used as nucleophiles under both conditions A and B to give the corresponding products **3g** and **3h** in good to high yields, while nitropropane was found to be less active.

Without limiting to the Nitro-Mannich type reaction, other nucleophiles were also found to be compatible with the AuNPore-catalyzed CDC reaction systems. It was noted that during the optimization of solvents for the reaction of **1a** with nitromethane, we found that the reaction in

MeOH showed a comparable reactivity with nitromethane (Table S1). Thus, the nucleophile scope was investigated in MeOH using O₂ as an oxidant due to its higher reactivity for the THIQ substrates unless otherwise noted (Table 3). The dialkyl malonates were proved to be active nucleophiles, affording the desired CDC products **3i** and **3j** in high yields. Although acetophenone exhibited an efficient reactivity to give the corresponding product **3k** in 85% yield, acetone showed a lower reactivity, which was conducted with TBHP to give **3l** in 45% yield. Indole derivatives were also tolerated under the present conditions to afford the dehydrogenative C(sp²)-C(sp³) coupling products **3m-p** in good yields with an exclusive regioselectivity. Trimethylsilyl cyanide was also an active nucleophile, furnishing the corresponding cyanation product **3q** in high yield. In addition to the C-C bond formation, the present conditions can be applied to the C-P bond formation. For example, the reaction of **1a** with diethyl phosphonate under the standard conditions produced the corresponding phosphonate **3r** in 85% yield.

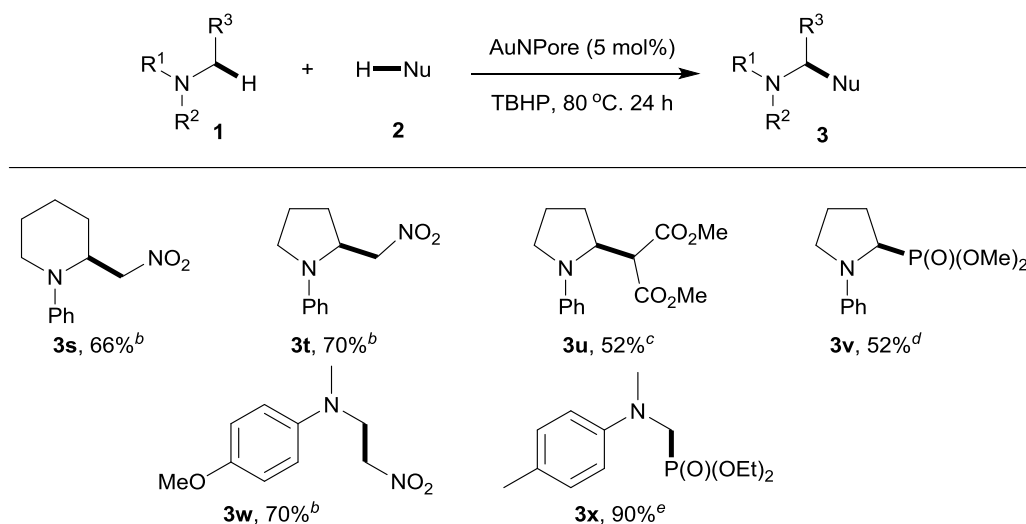
Table 3. AuNPore-Catalyzed CDC reactions of THIQ **1a** with various nucleophiles^a



^a Reaction conditions: **1a** (0.3 mmol), nucleophiles (3 equiv), MeOH (0.5 M), AuNPore (5 mol%), 80 °C, O₂ (1 atm), 24 h. Isolated yields are shown. ^b Acetophenone (5 equiv) was used. ^c TBHP (1 equiv) was used instead of O₂ and acetone (0.5 M) was used instead of MeOH. ^d TMS-CN (3 equiv) was used as a nucleophile at 50 °C for 48 h.

The current catalysis was further extended to the simple cyclic and acyclic tertiary amines using TBHP as an oxidant at 80 °C (Table 4). The reactions of cyclic amines, such as 1-phenylpiperidine and 1-phenylpyrrolidine with nitromethane, produced the corresponding α -nitromethyl amines **3s** and **3t** in 66% and 70% yields, respectively. 1-Phenylpyrrolidine was also reacted with other nucleophiles, such dimethyl malonate and dimethyl phosphonate, respectively, to give the corresponding substituted amines **3u** and **3v** in good yields using acetonitrile as solvent. Acyclic tertiary amines, such as 4-methoxy-*N,N*-dimethylaniline and *N,N*,4-trimethylaniline were also examined to be suitable substrates, which reacted with excess amounts of nitromethane and diethyl phosphonate efficiently to give the corresponding cross-coupling products **3w** and **3x** in 70% and 90% yields, respectively. It was noted that the aliphatic amine such as 1-ethylpiperidine was examined to be ineffective.

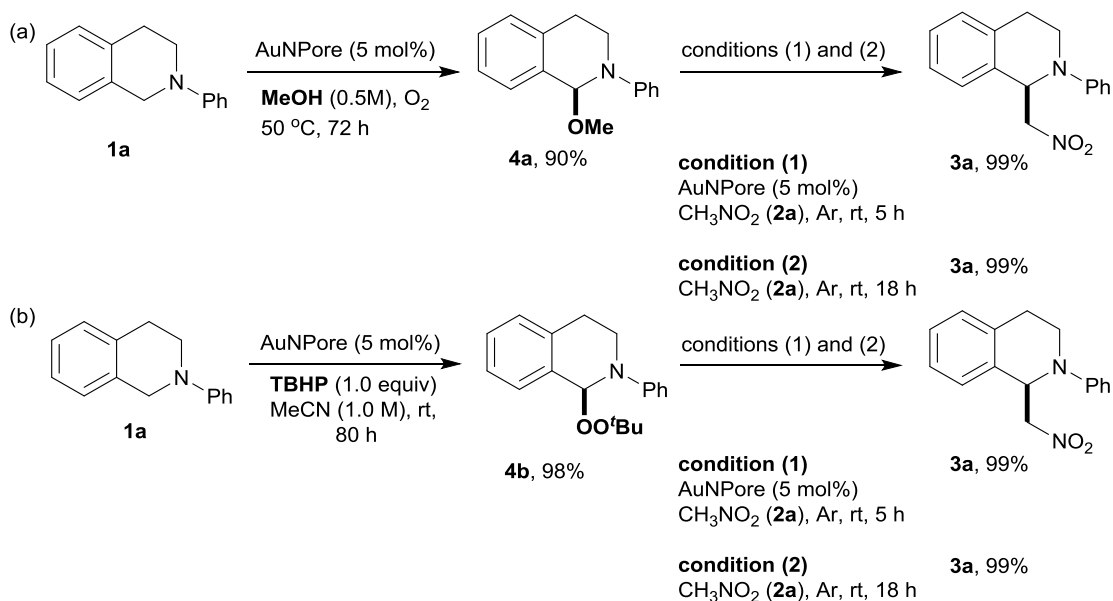
Table 4. AuNPore-Catalyzed CDC reactions of various tertiary amines with nucleophiles^a



^a Reaction conditions: amines (**1**, 0.3 mmol), TBHP in decane (5.5 M, 1 equiv), AuNPore (5 mol%), 80 °C, 24 h. Isolated yields are shown. ^b Nitromethane (0.5 M) was used as solvent. ^c Dimethyl malonate (3 equiv) was used in MeCN (0.5 M). ^d TBHP (2 equiv.) and dimethyl phosphonate (5 equiv) were used in MeCN (0.5 M) for 36 h. ^e Diethyl phosphonate (5 equiv) was used in MeCN (0.5 M).

AuNPore showed an excellently sustained and reproducible catalytic activity for the reaction of **1a** with nitromethane under O₂, which was used for ten cycles without losing any catalytic activity; the yield of **3a** was still 99% after the tenth cycle (Figure S1). AuNPore can be recovered readily by simple filtration without cumbersome work-up procedures. The SEM images of AuNPore after the tenth cycle showed that the ligand and pore sizes, and nanoporosity of

AuNPore did not show obvious changes compared to the fresh AuNPore, indicating the durability and robustness of AuNPore under the present aerobic conditions (Figures 1). Moreover, the inductively coupled plasma (ICP-MS) analysis of the reactions in entries 1 and 9 (Table 1) and leaching experiments (Scheme S1) indicate that no Au atoms were leached to the reaction solution, confirming that the present catalysis proceeds in a heterogeneous manner.



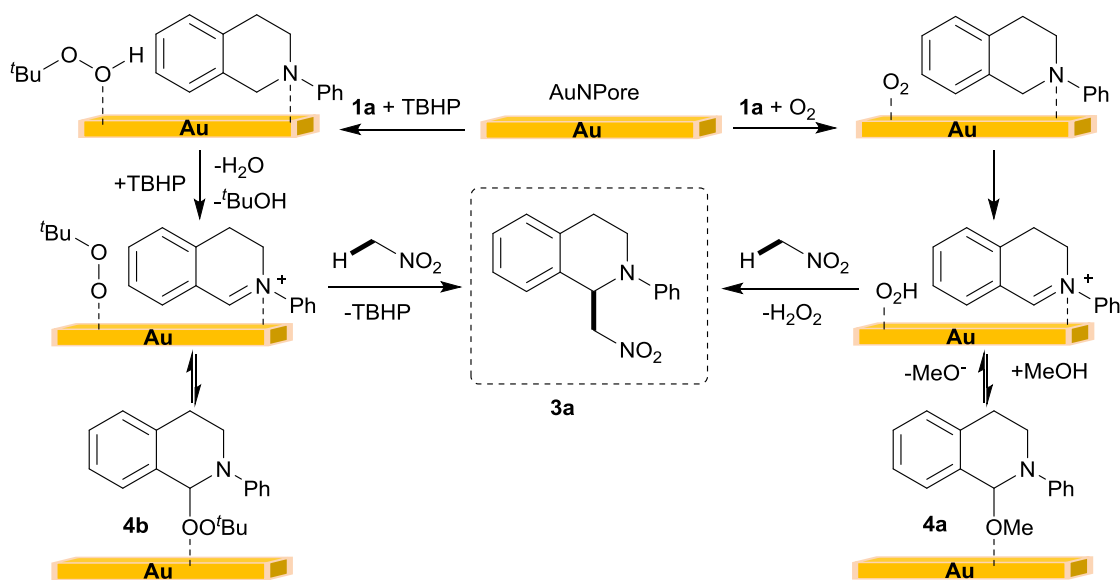
Scheme 1 Control experiments (a) using O₂ as an oxidant in MeOH; (b) using TBHP as an oxidant in MeCN.

To gain further insight into the reaction details, several control experiments were carried out. In the absence of nucleophiles, the reaction of **1a** with the AuNPore catalyst in MeOH under O₂ at 50 °C for 72 h produced the methoxy-substituted product **4a** in a 90% ¹H NMR yield (Scheme 1a). Subsequently, the reaction of **4a** with nitromethane in the presence of AuNPore under an argon atmosphere was completed in 5 h, affording the cross-coupling product **3a** in 99% yield. As a comparison, the similar reaction in the absence of AuNPore catalyst required 18 h to afford **3a** in same yield. Similarly, the *tert*-butylperoxyl-substituted product **4b** was isolated in 98% yield for the reaction of **1a** with TBHP, which was further reacted with nitromethane in the presence of AuNPore to give **3a** in high yield after 5 h, while the reaction without using AuNPore was completed after 18 h (Scheme 1b). These results indicate that the intermediates **4a** and **4b** are formed in the present CDC reactions and AuNPore also promotes the second nucleophilic substitution process. In addition, the reactions of **1a** and **2a** under both methods A and B in the presence of the additional radical inhibitors (1 equiv), such as 2,2,6,6-tetramethylpiperidine 1-oxyl (TEMPO) and 2,6-di-*tert*-butyl-4-methylphenol (BHT), did not affect the reaction rate and

yields, implying that the involvement of radical species was unlikely in the present heterogeneous catalysis.¹²

It is noteworthy to highlight that a vigorous gas evolution was observed when TBHP got in contact with AuNPore, which was assumed to be molecular oxygen released by dissociation of TBHP on AuNPore and the AuNPore surface remained unchanged. In contrast, this gas evolution was suppressed when the amine substrate was present, while the CDC reaction proceeds efficiently, implying the interaction of the adsorbed TBHP and amine substrate on AuNPore.

On the basis of the aforementioned experimental observations, a conceivable mechanism was proposed as shown in Scheme 2. In the O₂-based method, the adsorption of both O₂ and THIQ **1a** onto the active sites of AuNPore initiate the cleavage of the α -C-H bond of **1a**, leading to the formation of an iminium intermediate, which should be stabilized by AuNPore or through the interconversion with the methoxy-substituted **4a** in MeOH. In presence of strong nucleophile (MeNO₂), the forward reaction of the iminium intermediate or **4a** proceeds smoothly to give the desired product **3a**. Likewise, in the TBHP-based method, the *t*-BuO species dissociated from TBHP on AuNPore promotes the cleavage of the α -C-H bond of **1a** to form the iminium intermediate, which may be stabilized by the formation of *tert*-butylperoxyl-substituted **4b**. Similarly, the iminium intermediate and **4b** adsorbed on AuNPore further react with nitromethane to afford the corresponding product **3a**.



Scheme 2 Proposed reaction mechanism.

3. Conclusion

In conclusion, I reported for the first time that the zero-valent AuNPore showed a highly efficient and reusable heterogeneous catalytic activity for the C-H functionalization of tertiary amines. In the presence of molecular oxygen or TBHP, the α -C(sp³)-H bond of tertiary amines can be cleaved by the AuNPore catalyst under mild conditions. A wide range of tertiary amines and nucleophiles are compatible with the present heterogeneous cross-coupling conditions to form new C-C, C-P, and C-O bonds. AuNPore was reused for ten cycles without any activity loss and leaching of gold atoms. The present remarkable heterogeneous catalytic activity of AuNPore for C-H functionalization has the potential to be widely applicable in developing new types of synthetic transformations

4. References and notes

- 1 (a) Murahashi, S.-I. *Angew. Chem. Int. Ed. Engl.* **1995**, *34*, 2443; (b) Li, C.-J. *Acc. Chem. Res.* **2009**, *42*, 335.
- 2 For selected reviews on CDC reactions, see: (a) Murahashi, S.-I.; Zhang, D. *Chem. Soc. Rev.* **2008**, *37*, 1490; (b) Scheuermann, C. J. *Chem. Asian. J.* **2010**, *5*, 436. (c) Wendlandt, A. E.; Suess, A. M.; Stahl, S. S. *Angew. Chem. Int. Ed.* **2011**, *50*, 11062. (d) Liu, C.; Zhang, H.; Shi, W.; Lei, A. *Chem. Rev.* **2011**, *111*, 1780. (e) Yeung, C. S.; Dong, V. M. *Chem. Rev.* **2011**, *111*, 1215. (f) Girard, S. A.; Knauber, T.; Li, C.-J. *Angew. Chem. Int. Ed.* **2014**, *53*, 74.
- 3 (a) Schweitzer-Chaput, B.; Klussmann, M. *Eur. J. Org. Chem.* **2013**, 666; (b) Ueda, H.; Yoshida, K.; Tokuyama, H. *Org. Lett.* **2014**, *16*, 4194. (c) Nobuta, T.; Tada, N.; Fujiya, A.; Kariya, A.; Miura, T.; Itoh, A. *Org. Lett.* **2013**, *15*, 574.
- 4 Anastas, P. T.; Eghbali, N. *Chem. Soc. Rev.* **2010**, *39*, 301.
- 5 Zaera, F. *Catal. Lett.* **2012**, *142*, 501.
- 6 (a) Zeng, T.; Song, G.; Moores, A.; Li, C.-J. *Synlett.* **2010**, *13*, 2002; (b) Liu, P.; Zhou, C.-Y.; Xiang, S.; Che, C.-M. *Chem. Commun.* **2010**, 46, 2739. (c) Meng, Q.-Y.; Liu, Q.; Zhong, J.-J.; Zhang, H.-H.; Li, Z.-J.; Chen, B.; Tung, C.-H.; Wu, L.-Z. *Org. Lett.* **2012**, *14*, 5992. (d) Rueping, M.; Zoller, J.; Fabry, D. C.; Poschorny, K.; Koenigs, R. M.; Weirich, T. E.; Mayer, J. *Chem. Eur. J.* **2012**, *18*, 3478.
- 7 (a) Zielasek, V.; Jürgens, B.; Schulz, C.; Biener, J.; Biener, M. M.; Hamza, A. V. Bäumer, M. *Angew. Chem., Int. Ed.* **2006**, *45*, 8241. (b) Xu, C.; Su, J.; Xu, X.; Liu, P.; Zhao, H.; Tian, F.; Ding, Y. *J. Am. Chem. Soc.* **2007**, *129*, 42. (c) Wittstock, A.; Zielasek, V.; Biener, J.; Friend, C. M.; Bäumer, M. *Science*. **2010**, *327*, 319. (d) Kosuda, K. M. Wittstock, A.; Friend, C. M.; Bäumer, M. *Angew. Chem., Int. Ed.* **2012**, *51*, 1698.

- 8 Our previous reports on AuNPore-catalyzed oxidation reactions, see: (a) Asao, N.; Hatakeyama, N.; Menggenbateer.; Minato, T.; Ito, E.; Hara, M.; Kim, Y.; Yamamoto, Y.; Chen, M.; Zhang, W.; Inoue, A. *Chem. Commun.* **2012**, 48, 4540. (b) Tanaka, S.; Minato, T.; Ito, E.; Hara, M.; Kim, Y.; Yamamoto, Y.; Asao, N. *Chem. Eur. J.* **2013**, 19, 11832 (c) Asao, N.; Ishikawa, Y.; Hatakeyama, N.; Menggenbateer.; Yamamoto, Y.; Chen, M.; Zhang, W.; Inoue, A. *Angew. Chem. Int. Ed.* **2010**, 49, 10093.
- 9 (a) Yan, M.; Jin, T.; Ishikawa, Y.; Minato, T.; Fujita, T.; Chen, L.-Y.; Bao, M.; Asao, N.; Chen, M.-W.; Yamamoto, Y. *J. Am. Chem. Soc.* **2012**, 134, 17536. (b) Yan, M.; Jin, T.; Chen, Q.; Ho, H. E.; Fujita, T.; Chen, L.-Y.; Bao, M.; Chen, M.-W.; Asao, N.; Yamamoto, Y. *Org. Lett.* **2013**, 15, 1484. (c) Ishikawa, Y.; Yamamoto, Y.; Asao, N. *Catal. Sci. Technol.* **2013**, 3, 2902. (d) Asao, N.; Jin, T.; Tanaka, S.; Yamamoto, Y. *Pure Appl. Chem.* **2012**, 84, 1771. (e) Chen, Q.; Zhao, J.; Ishikawa, Y.; Asao, N.; Yamamoto, Y.; Jin, T. *Org. Lett.* **2013**, 15, 5766. (f) Takale, B. S.; Tao, S. M.; Yu, X. Q.; Feng, X. J.; Jin, T.; Bao, M.; Yamamoto, Y. *Org. Lett.* **2014**, 16, 2558. (g) Takale, B. S.; Wang, S.; Zhang, X.; Feng, X.; Yu, X.; Jin, T.; Bao, M.; Yamamoto, Y. *Chem. Commun.* **2014**, 50, 14401. (h) Takale, B.; Bao, M.; Yamamoto, Y. *Org. Biomol. Chem.* **2014**, 12, 2005. (i) Yamamoto, Y. *Tetrahedron.* **2014**, 70, 2305.
- 10 Fujita, T.; Guan, P.; McKenna, K.; Lang, X.; Hirata, A.; Zhang, L.; Tokunaga, T.; Arai, S.; Yamamoto, Y.; Tanaka, N.; Ishikawa, Y.; Asao, N.; Yamamoto, Y.; Erlebacher, J.; Chen, M. W. *Nat. Mater.* **2012**, 11, 775.
- 11 (a) Jin, T.; Yan, M.; Menggenbateer.; Minato, T.; Bao, M. Yamamoto, Y. *Adv. Synth. Catal.* **2011**, 353, 3095. (b) Jin, T.; Yan, M.; Yamamoto, Y. *ChemCatChem.* **2012**, 4, 1217. (c) Chen, Q.; Tanaka, S.; Fujita, T.; Chen, L.; Minato, T.; Ishikawa, Y.; Chen, M.-W.; Asao, N.; Yamamoto, Y.; Jin, T. *Chem. Commun.* **2014**, 50, 3344 (d) Tanaka, S.; Kaneko, T.; Asao, N.; Yamamoto, Y.; Chen, M.-W.; Zhang, W.; Inoue, A. *Chem. Commun.* **2011**, 47, 5985. (e) Kaneko, T.; Tanaka, S.; Asao, N.; Yamamoto, Y.; Chen, M.-W.; Zhang, W.; Inoue, A. *Adv. Synth. Catal.* **2011**, 353, 2927.
- 12 Xie, J.; Li, H.; Zhou, J.; Cheng, Y.; Zhu, C. *Angew. Chem. Int. Ed.* **2012**, 51, 1252.

5. Experimental Section

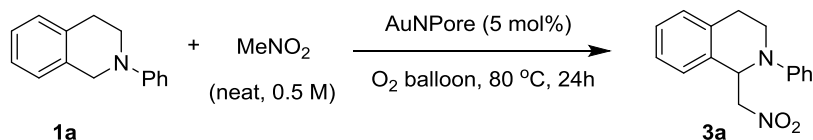
General Information: GC-MS analysis was performed on an Agilent 6890N GC interfaced to an Agilent 5973 mass-selective detector (30 m × 0.25 mm capillary column, HP-5MS). Scanning electron microscope (SEM) observation was carried out using a JEOL JSM-6500F instrument operated at an accelerating voltage of 30 kV. TEM characterization was performed using a JEM-2100F TEM (JEOL, 200 kV) equipped with double spherical aberration (Cs) correctors for both the probe-forming and image-forming lenses. ¹H NMR and ¹³C NMR spectra were recorded on JEOL JNM AL 400 (400, 700 MHz) spectrometers. ¹¹B NMR spectra were recorded on JEOL JNM AL 700 (225 MHz) spectrometers. ¹H NMR spectra are reported as follows: chemical shift in ppm (δ) relative to the chemical shift of CDCl₃ at 7.26 ppm, integration, multiplicities (s = singlet, d = doublet, t = triplet, q = quartet, m = multiplet and br = broadened), and coupling constants (Hz). ¹³C NMR spectra were recorded on JEOL JNM AL 400 (100.5 MHz) spectrometers with complete proton decoupling, and chemical shift reported in ppm (δ) relative to the central line of triplet for CDCl₃ at 77 ppm. High-resolution mass spectra were obtained on a BRUKER APEXIII spectrometer and JEOL JMS-700 MStation operator. Column chromatography was carried out employing Merck silica (spherical, neutral, Merck Chemical Co.) and the florisil (particle size 150 -250 μm, Kanto Chemical Co.). Analytical thin-layer chromatography (TLC) was performed on 0.2 mm precoated plate Kieselgel 60 F254 (Merck).

Materials. The commercially available chemicals were used as received. Au (99.99%) and Ag (99.99%) are purchased from Tanaka Kikinzoku Hanbai K. K. and Mitsuwa's Pure Chemical, respectively. *N*-Protected 1,2,3,4-tetrahydroisoquinolines were prepared following the reported methods.^[1] Structures of the products were identified by ¹H, ¹³C NMR, HRMS, and compared with reported compounds.^[2-4]

References

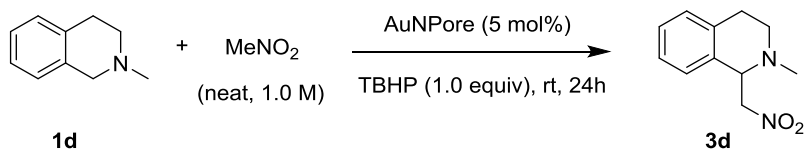
1. (a) B. Buckley, C. Steven, M. Elsegood, C. Gillings, P. Page and W. Pardoe, *Synlett*, **2010**, 6, 939. (b) M. Ebden, N. Simpskin and D. Fox, *Tetrahedron*, **1998**, 54, 12923.
2. (a) Z. Li, D. Bohle and C.-J. Li, *Proc. Natl. Acad. Sci. USA.*, **2006**, 103, 8928. (b) Z. Li and C.-J. Li, *J. Am. Chem. Soc.* **2005**, 127, 3672. (c) J. Xie, H. Li, J. Zhou, Y. Cheng and C. Zhu, *Angew. Chem., Int. Ed.* **2012**, 51, 1252. (d) K. Alagiri and K. Prabhu, *Tetrahedron Lett.* **2012**, 12, 1456. (e) J. Dhineskumar, M. Lamani, K. Alagiri and K. Prabhu, *Org. Lett.* **2013**, 15, 1092. (f) K. Jones, P. Karier and M. Klusmann, *ChemCatChem*. **2012**, 4, 51. (g) Z. Li and C. J. Li, *Eur. J. Org. Chem.* **2005**, 3173.
3. M. Ratnikov, X. Xu and M. Doyle, *J. Am. Chem. Soc.* **2013**, 135, 9475.
4. W. Han, P. Mayer, and A. Ofial, *Adv. Synth. Catal.* **2010**, 352, 166.

Representative procedure for AuNPore-catalyzed cross-dehydrogenative coupling of **1a with nitromethane: Method A**



To a 5 mL reaction vial were added starting material **1a** (0.3 mmol, 62.7 mg) and nitromethane **2a** (0.5 M, 0.6 mL) and stirred for 5 min at room temperature before adding AuNPore catalyst (5 mol%, 2.97 mg). The vial cap was sealed under oxygen flow and oxygen balloon was attached. Reaction mixture was stirred at 80 °C for 24 hours. AuNPore catalyst was recovered by filtration, and the solvent was removed under vacuum. AuNPore catalyst was recovered and washed with acetone, and dried under vacuum. The residue was purified with short silica gel chromatography (Merck Chemical Co, hexane:ethyl acetate = 10:1, R_f = 0.3) to afford **3a** (77 mg, 95%) as a yellow oil.

Representative procedure for AuNPore-catalyzed cross-dehydrogenative coupling of **1d with nitromethane: Method B**



To a 5 mL reaction vial were added starting material **1d** (0.6 mmol, 88.3 μL) and nitromethane **2a** (1.0 M, 0.6 mL) and TBHP (5.5 M in decane solution; 0.6 mmol, 109 μL) and stirred for 5 min at room temperature before adding AuNPore catalyst (5 mol%, 5.9 mg). The reaction mixture was stirred at room temperature for 24 hours. The reaction was monitored by using TLC chromatography. The AuNPore catalyst was recovered by filtration, and the solvent was removed under vacuum. The recovered AuNPore catalyst was washed with acetone and dried under vacuum before being used for another cycle. The residue was purified with silica gel chromatography (Merck Chemical Co, hexane:ethyl acetate: Et_3N = 5:1:0.01, R_f = 0.4) to afford **3d** (99 mg, 80%) as a yellow oil.

Fabrication of AuNPore Catalyst

Au (99.99%) and Ag (99.99%) were melted with electric arc-melting furnace under Ar atmosphere to form Au/Ag alloy (30:70, in at.%), which was rolled down to thickness of 0.04 mm. The resulting foil was annealed at 850 °C for 20 h. The foil was cut into small pieces (5 \times 2

mm square). Treatment of the resulting chips (67.1 mg) with 70 wt% nitric acid (7.5 mL) for 18 h at room temperature in a shaking apparatus resulted in the formation of the nanoporous structure by selective leaching of silver. The material was washed with a saturated aqueous solution of NaHCO₃, pure water, and acetone, successively. Drying of the material under reduced pressure gave the nanoporous gold (30.2 mg), and its composition was found to be Au₉₈Ag₂ from EDX analysis.

Table S1. Screening of solvents under an oxygen atmosphere (method A).^[a]

c1ccc2c(c1)CN(C2) + MeNO2 >> c1ccc2c(c1)C(N(C2)C(=O)N) + MeNO2

1a + MeNO₂ $\xrightarrow[\text{Solvent, O}_2, 80\text{ }^\circ\text{C, 24 h}]{\text{AuNPore (5 mol\%)}}$ **3a**

Entry	Solvent	Yield (%) ^[b]
1	MeNO ₂	99
2	MeOH	99
3	MeCN	93
4	Toluene	41
5	Octane	46
6	H ₂ O	50
7	MeNO ₂	73 ^[c]

[a] Reaction conditions: **1a** (0.3 mmol), nitromethane (0.5 M, neat or 5 equiv. when used with other solvents), AuNPore (5 mol%), oxygen sealed vial. [b] ¹H NMR yield determined using CH₂Br₂ as an internal standard. [c] Reaction temperature is 60 °C.

Reusability of nanoporous gold

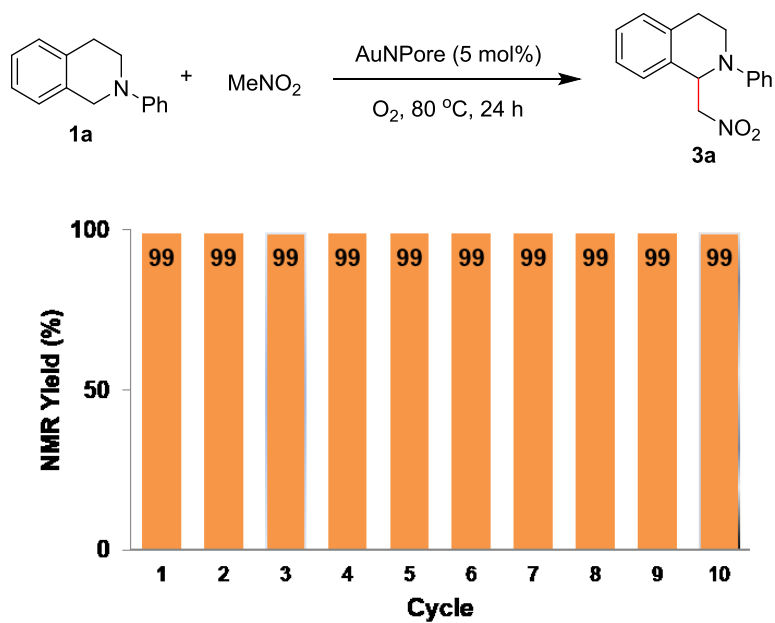
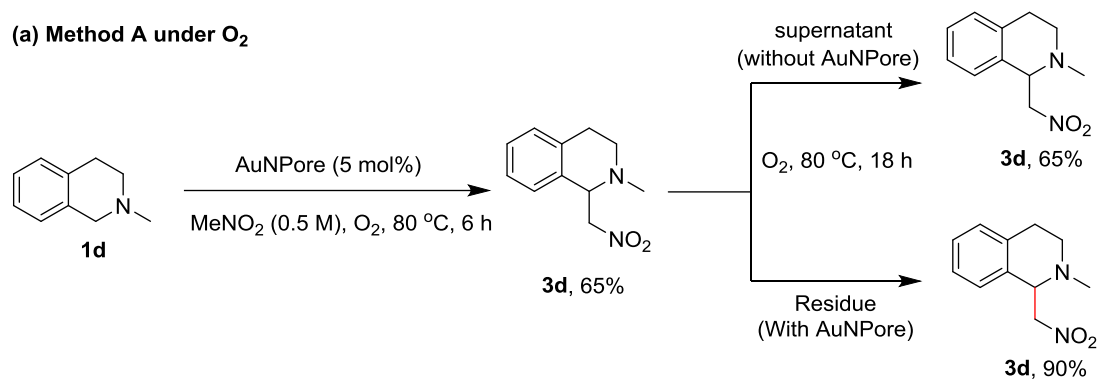


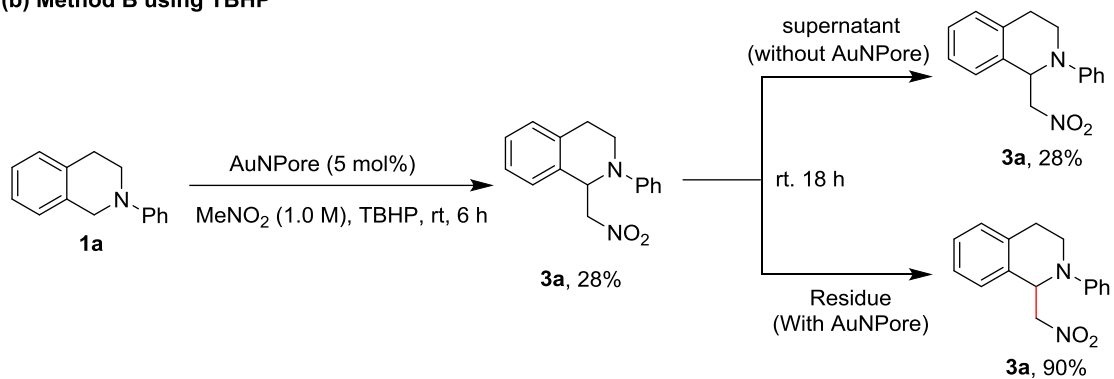
Figure S1. AuNPore was used for ten cycles and the yield was still 99% after tenth cycle. The ^1H NMR yields are shown using CH_2Br_2 as an internal standard.

Leaching experiments

(a) Method A under O₂



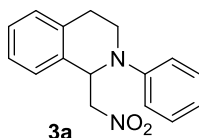
(b) Method B using TBHP



Scheme S1. Leaching experiment under methods A and B. 1,2,4-trimethylbenzene was used as an internal standard for ¹H NMR yield determination.

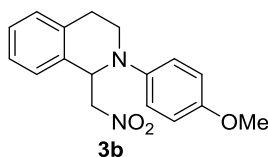
Analytical data of products^[2-4]

1-(Nitromethyl)-2-phenyl-1,2,3,4-tetrahydroisoquinoline (3a)



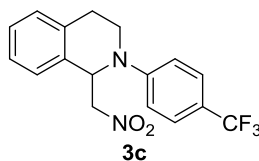
Yellow oil; ¹H NMR (400 MHz, CDCl₃) δ 7.30-7.18 (m, 5H); 7.13 (d, *J* = 8.0 Hz, 1H), 6.96 (d, *J* = 8.0 Hz, 2H), 6.85 (dd, *J* = 7.6, 7.6 Hz, 1H), 5.55 (dd, *J* = 8.0, 7.8 Hz, 1H), 4.87 (dd, *J* = 12.0, 8.0 Hz, 1H), 4.56 (dd, *J* = 12.0, 7.8 Hz, 1H), 3.70-3.59 (m, 2H), 3.13-3.05 (m, 1H), 2.80 (dt, *J* = 16.4, 4.8 Hz, 1H); ¹³C NMR (100 MHz, CDCl₃) δ 148.2, 135.1, 132.7, 129.3, 129.0, 127.9, 126.8, 126.5, 119.2, 114.9, 78.6, 58.1, 42.0, 26.4.

2-(4-Methoxyphenyl)-1-(nitromethyl)-1,2,3,4-tetrahydroisoquinoline (3b)



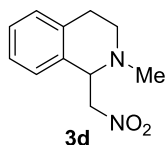
Yellow oil; ¹H NMR (400 MHz, CDCl₃) δ 7.28-7.16 (m, 5H), 6.94 (d, *J* = 9.2 Hz, 2H), 6.84 (d, *J* = 9.2 Hz, 2H), 5.42 (dd, *J* = 8.4, 5.6 Hz, 1H), 4.85 (dd, *J* = 12.0, 8.4 Hz, 1H), 4.58 (dd, *J* = 12.0, 5.6 Hz, 1H), 3.78 (s, 3H), 3.61-3.55 (m, 2H), 3.08-3.00 (m, 1H), 2.72 (dt, *J* = 16.4, 4.0 Hz, 1H); ¹³C NMR (100 MHz, CDCl₃) δ 153.7, 142.9, 135.3, 132.7, 129.3, 127.7, 126.7, 126.4, 118.7, 114.5, 78.8, 58.8, 55.5, 43.0, 25.7.

1-(Nitromethyl)-2-(4-(trifluoromethyl)phenyl)-1,2,3,4-tetrahydroisoquinoline (3c)



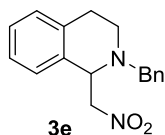
Yellow oil; ¹H NMR (400 MHz, CDCl₃) δ 7.54 (d, *J* = 8.4 Hz, 2H), 7.33-7.24 (m, 3H), 7.17 (d, *J* = 7.6 Hz, 1H), 7.04 (d, *J* = 8.4 Hz, 2H), 5.63 (dd, *J* = 7.2, 7.2 Hz, 1H), 4.90 (dd, *J* = 12.0, 7.2 Hz, 1H), 4.62 (dd, *J* = 12.0, 7.2 Hz, 1H), 3.75-3.68 (m, 2H), 3.17-3.11 (m, 1H), 2.90 (dt, *J* = 16.4, 5.6 Hz, 1H); ¹³C NMR (100 MHz, CDCl₃) δ 150.3, 134.7, 132.2, 129.0, 128.3, 126.9, 126.8, 126.7 (q, *J*³ = 3.3 Hz), 124.5 (q, *J*¹ = 269.0 Hz), 120.3 (q, *J*² = 33.0 Hz), 113.2, 78.3, 57.7, 41.7, 26.5. HRMS (ESI positive) calcd for C₁₇H₁₅F₃N₂O₂ [M + H]⁺: 337.1158, found: 337.1157.

2-Methyl-1-(nitromethyl)-1,2,3,4-tetrahydroisoquinoline (3d)



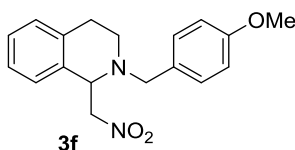
Yellow oil; ^1H NMR (400 MHz, CDCl_3) δ 7.23-7.18 (m, 2H), 7.16-7.09 (m, 2H), 4.69 (dd, J = 12.0, 9.6 Hz, 1H), 4.50 (dd, J = 12.0, 4.4 Hz, 1H), 4.43 (dd, J = 9.6, 4.4 Hz, 1H), 3.24 (dd, J = 9.6, 4.4 Hz, 1H), 3.22-3.15 (m, 1H), 3.03-2.95 (m, 1H), 2.91-2.85 (m, 1H), 2.60 (dt, J = 16.8, 4.0 Hz, 1H), 2.51 (s, 3H); ^{13}C NMR (100 MHz, CDCl_3) δ 135.0, 132.1, 129.3, 127.3, 127.2, 126.3, 79.3, 61.3, 45.5, 42.1, 23.7. HRMS (ESI positive) calcd for $\text{C}_{11}\text{H}_{14}\text{N}_2\text{O}_2$ $[\text{M} + \text{H}]^+$: 207.1128, found: 207.1127.

2-Benzyl-1-(nitromethyl)-1,2,3,4-tetrahydroisoquinoline (3e)



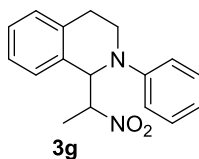
Yellow oil; ^1H NMR (400 MHz, CDCl_3) δ 7.29-7.14 (m, 8H), 7.07 (d, J = 6.8 Hz, 1H), 4.71 (dd, J = 11.6, 10.0 Hz, 1H), 4.53 (dd, J = 10.0, 4.4 Hz, 1H), 4.45 (dd, J = 11.6, 4.4 Hz, 1H), 3.82 (d, J = 13.2 Hz, 1H), 3.73 (d, J = 13.2 Hz, 1H), 3.06-2.89 (m, 2H), 2.50 (dd, J = 16.4, 4.0 Hz, 1H); ^{13}C NMR (100 MHz, CDCl_3) δ 138.1, 135.2, 132.0, 129.6, 128.6, 128.2, 127.6, 127.4, 127.2, 126.4, 79.4, 59.6, 57.5, 41.7, 22.8. HRMS (ESI positive) calcd for $\text{C}_{17}\text{H}_{18}\text{N}_2\text{O}_2$ $[\text{M} + \text{H}]^+$: 283.1441, found: 283.1440.

2-(4-Methoxybenzyl)-1-(nitromethyl)-1,2,3,4-tetrahydroisoquinoline (3f)



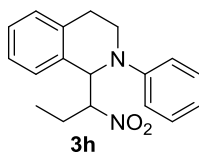
Yellow oil; ^1H NMR (400 MHz, CDCl_3) δ 7.30-7.12 (m, 6H), 6.90 (d, J = 8.8 Hz, 2H), 4.77 (dd, J = 11.6, 10.0 Hz, 1H), 4.58 (dd, J = 10.0, 4.4 Hz, 1H), 4.51 (dd, J = 11.6, 4.4 Hz, 1H), 3.85 (s, 3H), 3.82 (d, J = 12.8 Hz, 1H), 3.73 (d, J = 12.8 Hz, 1H), 3.28-3.20 (m, 1H), 3.11-2.95 (m, 2H), 2.76 (dd, J = 16.8, 3.2 Hz, 1H); ^{13}C NMR (100 MHz, CDCl_3) δ 158.7, 135.2, 132.0, 130.1, 129.8, 129.5, 127.6, 127.4, 126.4, 113.6, 79.4, 59.3, 56.8, 55.2, 41.6, 22.8. HRMS (ESI positive) calcd for $\text{C}_{18}\text{H}_{20}\text{N}_2\text{O}_3$ $[\text{M} + \text{H}]^+$: 313.1546, found 313.1545.

1-(1-Nitroethyl)-2-phenyl-1,2,3,4-tetrahydroisoquinoline (3g)



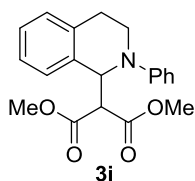
Yellow oil. Isolated diastereomeric ratio = 1.7:1; Major isomer: ^1H NMR (400 MHz, CDCl_3) δ 7.30-7.20 (m, mixture of isomers), 7.18-7.10 (m, mixture of isomers), 7.02-6.98 (m, mixture of isomers), 6.85-6.80 (m, mixture of isomers), 5.25 (m, 1H, mixture of isomers), 5.05 (dq, $J = 8.4$, 6.8 Hz, 1H, major isomer), 4.89 (dq, $J = 8.8$, 6.8 Hz, 1H, minor isomer), 3.88-3.81 (m, 1H, major isomer), 3.64-3.54 (m, 3H, mixture of isomers), 3.10-3.02 (m, 1H, mixture of isomers), 2.95-2.85 (m, mixture of isomers), 1.71 (d, $J = 6.8$, 3H, minor isomer), 1.55 (d, $J = 6.8$, 3H, major isomer); ^{13}C NMR (100 MHz, CDCl_3 , mixture of isomers) δ 148.7 (149.0), 135.5 (134.6), 131.9 (133.7), 129.2 (129.3), 129.0 (128.6), 128.2 (128.1), 127.1 (128.1), 126.0 (126.5), 119.2 (118.7), 115.3 (114.4), 85.3 (88.9), 62.7 (61.1), 42.6 (43.5), 26.4 (26.7), 16.4 (17.4); HRMS (ESI positive) calcd for $\text{C}_{17}\text{H}_{18}\text{N}_2\text{O}_2$ $[\text{M} + \text{H}]^+$: 283.1441, found: 283.14401.

1-(1-Nitropropyl)-2-phenyl-1,2,3,4-tetrahydroisoquinoline (3h)



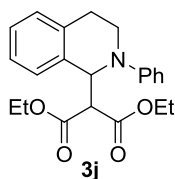
Yellow oil. Isolated diastereomeric ratio = 1.3:1; Major isomer: ^1H NMR (400 MHz, CDCl_3) δ 7.35-7.19 (m, mixture of isomers), 7.06-6.99 (m, mixture of isomers), 6.89-6.83 (m, mixture of isomers), 5.30 (d, $J = 9.2$ Hz, 1H, minor isomer), 5.19 (d, $J = 9.6$ Hz, 1H, major isomer), 4.96-4.90 (m, 1H, major isomer), 4.77-4.71 (m, 1H, minor isomer), 3.94-3.88 (m, 1H, major isomer), 3.76-3.55 (m, 3H, mixture of isomers), 3.16-3.09 (m, mixture of isomers), 3.00-2.91 (m, 1H, mixture of isomers), 2.27-2.16 (m, 3H, mixture of isomers), 1.92-1.86 (m, 1H, major isomer), 1.02-0.98 (m, 3H, mixture of isomers); ^{13}C NMR (100 MHz, CDCl_3 , mixture of isomers) δ 148.9 (149.0), 135.4 (134.6), 133.8 (132.5), 129.3 (129.1), 129.2, 128.5 (128.6), 128.0 (128.1), 127.1, 125.8 (126.5), 119.2 (118.5), 115.8 (114.1), 96.1 (93.0), 62.1 (60.7), 43.5 (42.4), 25.7 (26.8), 25.0 (24.6), 10.7; HRMS (ESI positive) calcd for $\text{C}_{18}\text{H}_{20}\text{N}_2\text{O}_2$ $[\text{M} + \text{H}]^+$: 297.1597, found: 297.1598.

Dimethyl 2-(2-phenyl-1,2,3,4-tetrahydroisoquinolin-1-yl)malonate (3i)



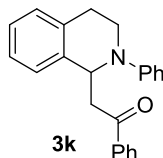
Yellow oil; ^1H NMR (400 MHz, CDCl_3) δ 7.23-7.09 (m, 6H), 6.98 (d, J = 8.0 Hz, 2H), 6.76 (dd, J = 7.2, 7.2 Hz, 1H), 5.71 (d, J = 9.2 Hz, 1H), 3.95 (d, J = 9.2 Hz, 1H), 3.73-3.60 (m, 2H), 3.66 (s, 3H), 3.55 (s, 3H), 3.11-3.03 (m, 1H), 2.88 (dt, J = 16.4, 5.2 Hz, 1H); ^{13}C NMR (100 MHz, CDCl_3) δ 168.1, 167.2, 148.6, 135.5, 134.6, 128.9, 128.8, 127.5, 126.9, 125.9, 118.5, 115.0, 59.1, 58.1, 52.5, 52.4, 42.2, 26.1; HRMS (ESI positive) calcd for $\text{C}_{20}\text{H}_{21}\text{NO}_4$ $[\text{M} + \text{H}]^+$: 340.1543, found: 340.1542.

Diethyl 2-(2-phenyl-1,2,3,4-tetrahydroisoquinolin-1-yl)malonate (3j)



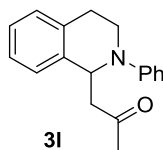
Yellow oil; ^1H NMR (400 MHz, CDCl_3) δ 7.31-7.13 (m, 7H), 7.03 (d, J = 8.8 Hz, 2H), 6.80 (dd, J = 8.0, 8.0 Hz, 1H), 5.78 (d, J = 9.6 Hz, 1H), 4.24-3.99 (m, 4H), 3.95 (d, J = 9.6 Hz, 1H), 3.79-3.65 (m, 2H), 3.16-3.08 (m, 1H), 2.93 (dt, J = 16.4, 5.2 Hz, 1H), 1.22 (t, J = 7.2 Hz, 3H), 1.14 (t, J = 7.2 Hz, 3H); ^{13}C NMR (100 MHz, CDCl_3) δ 167.7, 166.9, 148.6, 135.8, 134.6, 128.9, 128.7, 127.3, 127.0, 125.8, 118.3, 114.9, 61.5(4), 61.5(3), 59.5, 57.8, 42.2, 26.1, 14.0, 13.9(7), 13.9(1); HRMS (ESI positive) calcd for $\text{C}_{22}\text{H}_{25}\text{NO}_4$ $[\text{M} + \text{H}]^+$: 368.1856, found: 368.1856.

1-Phenyl-2-(2-phenyl-1,2,3,4-tetrahydroisoquinolin-1-yl)ethanone (3k)



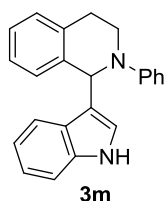
Yellow solid; ^1H NMR (400 MHz, CDCl_3) δ 7.88 (d, J = 8.0 Hz, 1H), 7.57-7.54 (m, 1H), 7.46-7.42 (m, 2H), 7.29-7.15 (m, 6H), 7.01 (d, J = 8.0, 2H), 6.79 (dd, J = 7.6, 7.6 Hz, 1H), 5.70 (dd, J = 7.2, 7.2 Hz, 1H), 3.72-3.59 (m, 3H), 3.42 (dd, J = 16.8, 7.6 Hz, 1H), 3.19-3.12 (m, 1H), 2.97 (dt, J = 16.0, 5.2 Hz, 1H); ^{13}C NMR (100 MHz, CDCl_3) δ 198.4, 148.6, 138.4, 137.1, 134.4, 132.9, 129.2, 128.4, 128.0, 127.0, 126.7, 126.1, 117.8, 114.2, 55.0, 45.3, 42.1, 27.6; HRMS (ESI positive) calcd for $\text{C}_{23}\text{H}_{21}\text{NO}$ $[\text{M} + \text{H}]^+$: 328.1696, found: 328.1695.

1-(2-Phenyl-1,2,3,4-tetrahydroisoquinolin-1-yl)propan-2-one (3l)



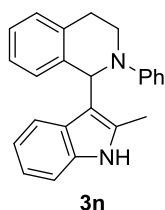
White solid; ^1H NMR (400 MHz, CDCl_3) δ 7.26-7.22 (m, 3H), 7.17-7.13 (m, 4H), 6.93 (d, J = 8.8, 2H), 6.78 (dd, J = 6.8, 6.8 Hz, 1H), 5.40 (dd, J = 6.4, 6.4 Hz, 1H), 3.68-3.62 (m, 1H), 3.57-3.50 (m, 1H), 3.09-3.03 (m, 2H), 2.83 (dt, J = 16.4, 3.6 Hz, 2H), 2.07 (s, 3H); ^{13}C NMR (100 MHz, CDCl_3) δ 207.0, 148.7, 138.1, 134.3, 129.2, 128.5, 126.8, 126.7, 126.2, 118.1, 114.7, 54.8, 50.2, 42.0, 31.1, 27.2; HRMS (ESI positive) calcd for $\text{C}_{18}\text{H}_{19}\text{NO}$ $[\text{M} + \text{H}]^+$: 266.1539, found: 266.1539.

1-(1*H*-Indol-3-yl)-2-phenyl-1,2,3,4-tetrahydroisoquinoline (3m)



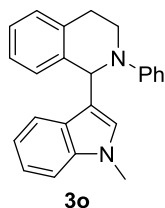
Yellow solid; ^1H NMR (400 MHz, CDCl_3) δ 7.92 (bs, 1H), 7.55 (d, J = 8.0 Hz, 1H), 7.33-7.14 (m, 8H), 7.05-7.02 (m, 3H), 6.78 (dd, J = 7.6, 7.6 Hz, 1H), 6.63 (s, 1H), 6.18 (s, 1H), 3.64 (dd, J = 7.6, 4.8 Hz, 2H), 3.12-3.04 (m, 1H), 2.82 (dt, J = 16.0, 4.8 Hz, 1H); ^{13}C NMR (100 MHz, CDCl_3) δ 149.6, 137.3, 136.5, 135.4, 129.1, 128.7, 127.9, 126.5, 126.3, 125.4, 124.0, 122.0, 119.5, 119.2, 118.0, 115.7, 110.9, 56.6, 42.3, 26.6; HRMS (ESI positive) calcd for $\text{C}_{23}\text{H}_{20}\text{N}_2$ $[\text{M} + \text{Na}]^+$: 347.1518, found: 347.1518.

1-(2-Methyl-1*H*-indol-3-yl)-2-phenyl-1,2,3,4-tetrahydroisoquinoline (3n):



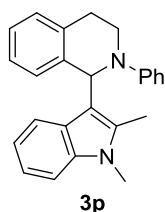
White solid; ^1H NMR (400 MHz, CDCl_3) δ 7.65 (bs, 1H), 7.22-7.02 (m, 11H), 6.92 (dd, J = 8.0, 8.0 Hz, 1H), 6.87 (dd, J = 7.6, 7.6 Hz, 1H), 5.99 (s, 1H), 3.74-3.61 (m, 2H), 3.15-2.99 (m, 2H), 2.01 (s, 3H); ^{13}C NMR (100 MHz, CDCl_3) δ 150.7, 137.8, 135.1, 134.7, 133.2, 128.7, 128.5, 128.1, 126.1, 125.9, 120.6, 120.0, 119.5, 119.3, 119.0, 113.2, 109.9, 57.0, 45.7, 27.9, 12.2; HRMS (ESI positive) calcd for $\text{C}_{24}\text{H}_{22}\text{N}_2$ $[\text{M} + \text{H}]^+$: 339.1069, found: 339.1069.

1-(1-Methyl-1*H*-indol-3-yl)-2-phenyl-1,2,3,4-tetrahydroisoquinoline (3o)



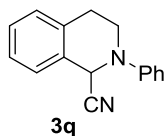
Yellow solid; ^1H NMR (400 MHz, CDCl_3) δ 7.56 (d, $J = 8.0$ Hz, 1H), 7.32-7.17 (m, 9H), 7.04-7.02 (m, 3H), 6.78 (dd, $J = 7.2, 7.2$ Hz, 1H), 6.51 (s, 1H), 6.19 (s, 1H), 3.66 (s, 3H), 3.75-3.60 (m, 2H), 3.12-3.04 (m, 1H), 2.83 (dt, $J = 16.4, 4.4$ Hz, 1H); ^{13}C NMR (100 MHz, CDCl_3) δ 149.6, 137.5, 137.2, 135.4, 129.1, 128.7, 128.6, 127.9, 126.7, 126.5, 125.6, 121.5, 120.0, 119.0, 117.8, 117.5, 115.5, 109.0, 56.5, 42.1, 32.7, 26.6; HRMS (ESI positive) calcd for $\text{C}_{24}\text{H}_{24}\text{N}_2$ $[\text{M} + \text{H}]^+$: 339.1855, found: 339.1854.

1-(1,2-Dimethyl-1H-indol-3-yl)-2-phenyl-1,2,3,4-tetrahydroisoquinoline (3p)



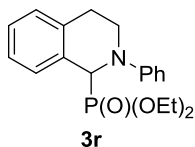
White solid; ^1H NMR (400 MHz, CDCl_3) δ 7.21-7.16 (m, 5H), 7.09-7.01 (m, 5H), 6.94-6.81 (m, 3H), 6.00 (s, 1H), 3.73-3.55 (m, 2H), 3.59 (s, 3H), 3.13-2.96 (m, 2H), 2.12 (s, 3H); ^{13}C NMR (100 MHz, CDCl_3) δ 150.8, 138.0, 136.2, 135.2, 128.6, 128.5, 128.2, 127.6, 126.1, 120.1, 120.0, 119.4, 118.99, 118.97, 112.6, 108.3, 57.1, 45.9, 29.4, 27.8, 10.6; HRMS (ESI positive) calcd for $\text{C}_{25}\text{H}_{24}\text{N}_2$ $[\text{M} + \text{H}]^+$: 353.2012, found: 353.2011.

2-Phenyl-1,2,3,4-tetrahydroisoquinoline-1-carbonitrile (3q)



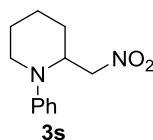
White solid; ^1H NMR (400 MHz, CDCl_3) δ 7.35-7.19 (m, 6H), 7.07-6.96 (d, $J = 7.6$ Hz, 2H), 6.98 (d, $J = 7.6$ Hz, 1H), 5.48 (s, 1H), 3.77-3.71 (m, 1H), 3.48-3.42 (m, 1H), 3.17-3.08 (m, 1H), 2.93 (dt, $J = 16.4, 3.6$ Hz, 1H); ^{13}C NMR (100 MHz, CDCl_3) δ 148.2, 134.4, 129.4, 129.2, 128.6, 126.9, 126.7, 121.7, 117.6, 117.4, 53.1, 44.1, 28.5; HRMS (ESI positive) calcd for $\text{C}_{16}\text{H}_{14}\text{N}_2$ $[\text{M} + \text{H}]^+$: 235.1229, found: 235.1229.

Diethyl 2-phenyl-1,2,3,4-tetrahydroisoquinolin-1-ylphosphonate (3r)



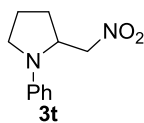
Pale yellow oil; ^1H NMR (400 MHz, CDCl_3) δ 7.38 (d, $J = 6.8$, 1H), 7.28-7.14 (m, 5H), 6.99 (d, $J = 8.0$ Hz, 2H), 6.80 (dd, $J = 6.8$, 6.8 Hz, 1H), 5.20 (d, $J = 20.0$ Hz, 1H), 4.15-3.86 (m, 5H), 3.64 (dt, $J = 12.4$, 6.0 Hz, 1H), 3.12-2.97 (m, 2H), 1.26 (t, $J = 7.2$ Hz, 3H), 1.15 (t, $J = 7.2$ Hz, 3H); ^{13}C NMR (100 MHz, CDCl_3) δ 149.2 (d, $J = 5.8$ Hz), 136.2 (d, $J = 5.7$ Hz), 130.5, 129.0, 128.6 (d, $J = 2.4$ Hz), 128.0 (d, $J = 4.9$ Hz), 127.3 (d, $J = 3.3$ Hz), 125.7 (d, $J = 3.3$ Hz), 118.3, 114.6, 63.3 (d, $J = 7.4$ Hz), 62.2 (d, $J = 7.4$ Hz), 58.7 (d, $J = 158.4$ Hz), 43.4, 26.7, 16.5 (d, $J = 5.0$ Hz), 16.4 (d, $J = 5.7$ Hz); HRMS (ESI positive) calcd for $\text{C}_{19}\text{H}_{24}\text{NO}_3\text{P}$ $[\text{M} + \text{H}]^+$: 346.1566, found: 346.1566.

2-(Nitromethyl)-1-phenylpiperidine (3s)



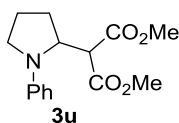
Pale yellow oil; ^1H NMR (400 MHz, CDCl_3) δ 7.28 – 7.22 (m, 2H), 6.95 (d, $J = 8.0$ Hz, 2H), 6.86 (dd, $J = 8.0$, 8.0 Hz, 1H), 4.55-4.51 (m, 2H), 4.45-4.38 (m, 1H), 3.39 (dt, $J = 12.8$, 3.2 Hz, 1H), 2.90-2.84 (m, 1H), 1.93-1.87 (m, 1H), 1.80-1.57 (m, 5H); ^{13}C NMR (100 MHz, CDCl_3) δ 149.1, 129.4, 120.3, 116.8, 73.2, 54.9, 44.5, 26.4, 25.0, 19.1; HRMS (ESI positive) calcd for $\text{C}_{12}\text{H}_{16}\text{N}_2\text{O}_2$ $[\text{M} + \text{H}]^+$: 221.1284, found: 221.1283.

2-(Nitromethyl)-1-phenylpyrrolidine (3t)



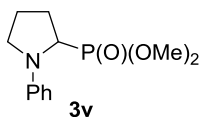
Pale yellow oil; ^1H NMR (400 MHz, CDCl_3) δ 7.28-7.22 (m, 2H), 6.75 (dd, $J = 7.6$, 7.6 Hz, 1H), 6.66 (d, $J = 7.6$ Hz, 2H), 4.60 (dd, $J = 11.2$, 2.8 Hz, 1H), 4.42-4.37 (m, 1H), 4.18-4.13 (m, 1H), 3.48-3.44 (m, 1H), 3.21-3.15 (m, 1H), 2.13-2.04 (m, 4H); ^{13}C NMR (100 MHz, CDCl_3) δ 145.6, 129.5, 117.2, 111.9, 75.7, 57.4, 48.1, 29.3, 22.8; HRMS (ESI positive) calcd for $\text{C}_{11}\text{H}_{14}\text{N}_2\text{O}_2$ $[\text{M} + \text{H}]^+$: 207.1128, found: 207.1127.

Dimethyl 2-(1-phenylpyrrolidin-2-yl)malonate (3u)



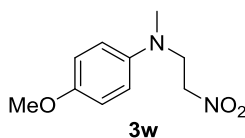
Yellow oil; ^1H NMR (400 MHz, CDCl_3) δ 7.29-7.24 (m, 2H), 6.73 (dd, $J = 7.2, 7.2$ Hz, 1H), 6.67 (d, $J = 8.0$ Hz, 2H), 4.65-4.61 (m, 1H), 3.85 (d, $J = 6.0$ Hz, 1H), 3.74 (s, 3H), 3.61 (s, 3H), 3.55-3.50 (m, 1H), 3.25 (m, 1H), 2.19-2.14 (m, 2H), 2.108-2.00 (m, 2H); ^{13}C NMR (100 MHz, CDCl_3) δ 168.4(9), 168.4(4), 146.4, 129.1, 116.4, 112.3, 57.7, 53.1, 52.4, 52.3, 48.6, 29.5, 23.0; HRMS (ESI positive) calcd for $\text{C}_{15}\text{H}_{19}\text{NO}_4$ $[\text{M} + \text{H}]^+$: 278.1386, found: 278.1386.

Dimethyl 1-phenylpyrrolidin-2-ylphosphonate (**3v**)



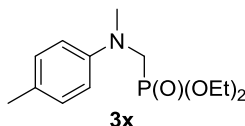
Yellow oil; ^1H NMR (400 MHz, CDCl_3) δ 7.28-7.24 (m, 2H), 6.81 (d, $J = 8.0$ Hz, 2H), 6.77 (dd, $J = 7.2, 7.2$ Hz, 1H), 4.09 (d, $J = 9.6$ Hz, 1H), 3.77 (dd, $J = 9.6, 0.8$ Hz, 3H), 3.64 (dd, $J = 9.6, 0.8$ Hz, 3H), 3.63-3.59 (m, 1H), 3.23-3.16 (m, 1H), 2.44-2.33 (m, 2H), 2.18-2.02 (m, 2H); ^{13}C NMR (100 MHz, CDCl_3) δ 147.5, 128.8, 117.1, 112.9, 56.2 (d, $J = 167.5$ Hz), 53.2 (d, $J = 6.6$ Hz), 52.5 (d, $J = 7.4$ Hz), 49.6 (d, $J = 2.5$ Hz), 27.8, 24.3; HRMS (ESI positive) calcd for $\text{C}_{12}\text{H}_{18}\text{NO}_3\text{P}$ $[\text{M} + \text{H}]^+$: 256.1097, found: 256.1096.

4-Methoxy-*N*-methyl-*N*-(2-nitroethyl)aniline (**3w**)



Yellow oil; ^1H NMR (400 MHz, CDCl_3) δ 6.85 (d, $J = 8.8$ Hz, 2H), 6.75 (d, $J = 8.8$ Hz, 2H), 4.54 (t, $J = 6.4$ Hz, 2H), 3.89 (t, $J = 6.4$ Hz, 2H), 3.77 (s, 3H), 2.90 (s, 3H); ^{13}C NMR (100 MHz, CDCl_3) δ 152.7, 142.6, 115.4, 114.8, 72.7, 55.7, 51.9, 39.5; HRMS (ESI positive) calcd for $\text{C}_{10}\text{H}_{14}\text{N}_2\text{O}_3$ $[\text{M} + \text{H}]^+$: 211.1077, found: 211.1076.

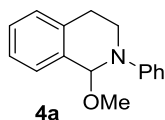
Diethyl ((methyl(*p*-tolyl)amino)methyl)phosphonate (**3x**)



White solid: ^1H NMR (400 MHz, CDCl_3) δ 7.04 (d, $J = 8.4$ Hz, 2H), 6.74 (d, $J = 8.4$ Hz, 2H), 4.14-4.04 (m, 4H), 3.66 (d, $J = 7.6$ Hz, 2H), 3.00 (s, 3H), 2.25 (s, 3H), 1.27 (t, $J = 7.2$ Hz, 6H); ^{13}C NMR (100 MHz, CDCl_3) δ 147.4, 129.4, 126.7, 113.2, 62.1 (d, $J = 6.6$ Hz), 50.4 (d, $J = 161.7$ Hz).

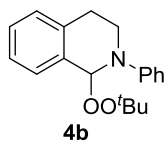
Hz), 39.4, 20.2, 16.5 (d, $J = 5.8$ Hz); HRMS (ESI positive) calcd for $C_{13}H_{22}NO_3P$ $[M + H]^+$: 272.1410, found: 272.1408.

1-Methoxy-2-phenyl-1,2,3,4-tetrahydroisoquinoline (4a): crude NMR using CH_2Br_2 as an internal standard

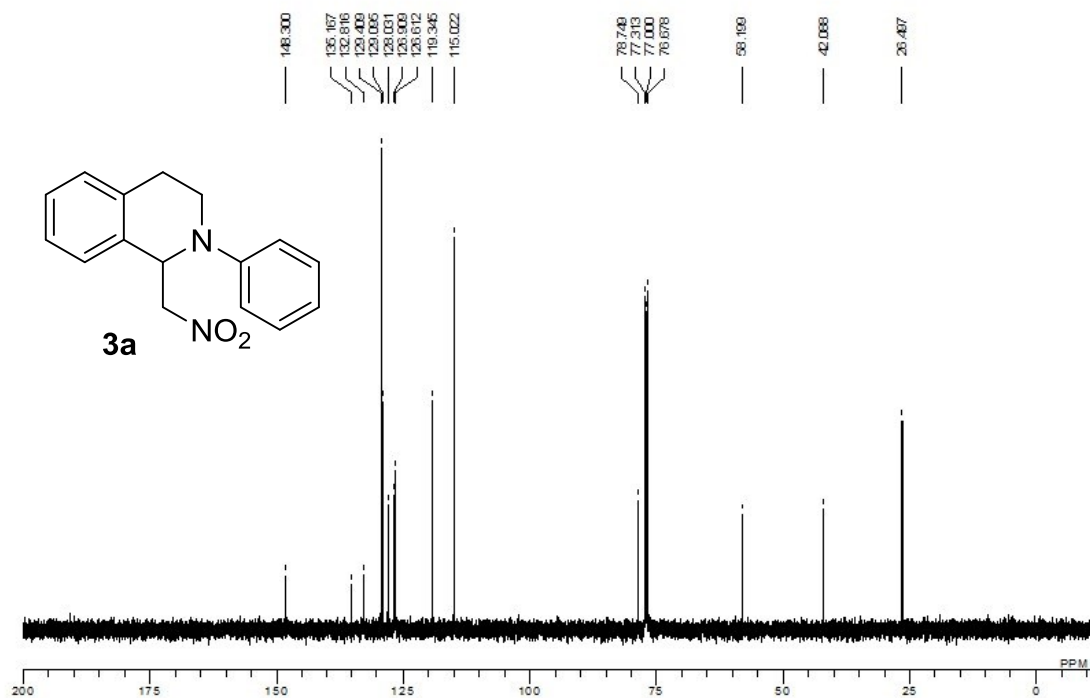
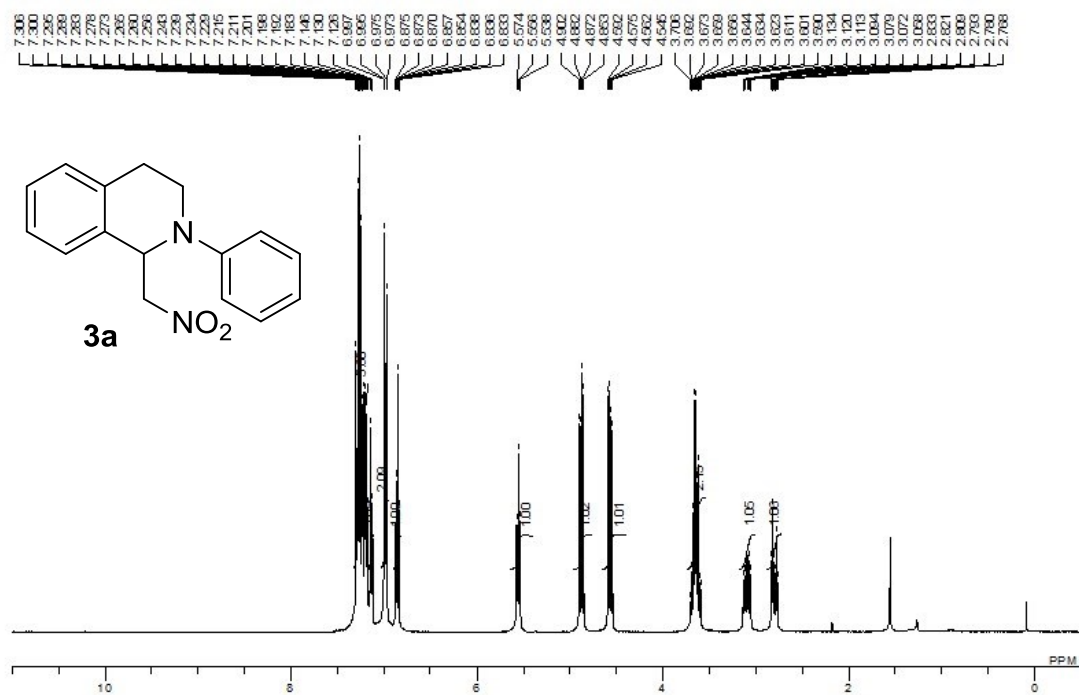


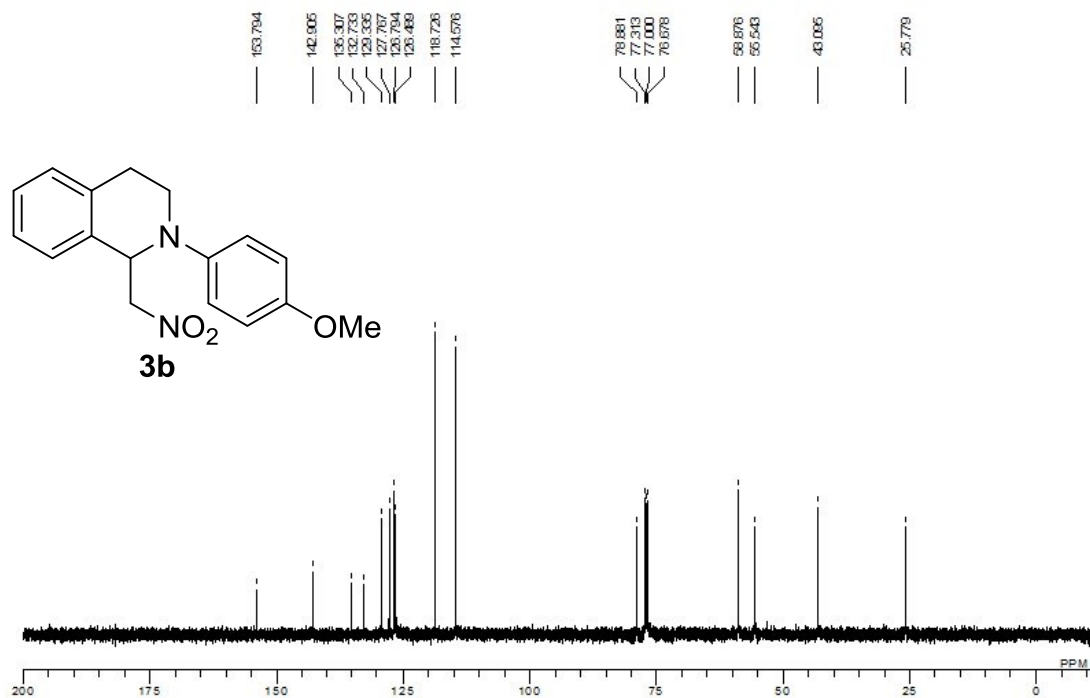
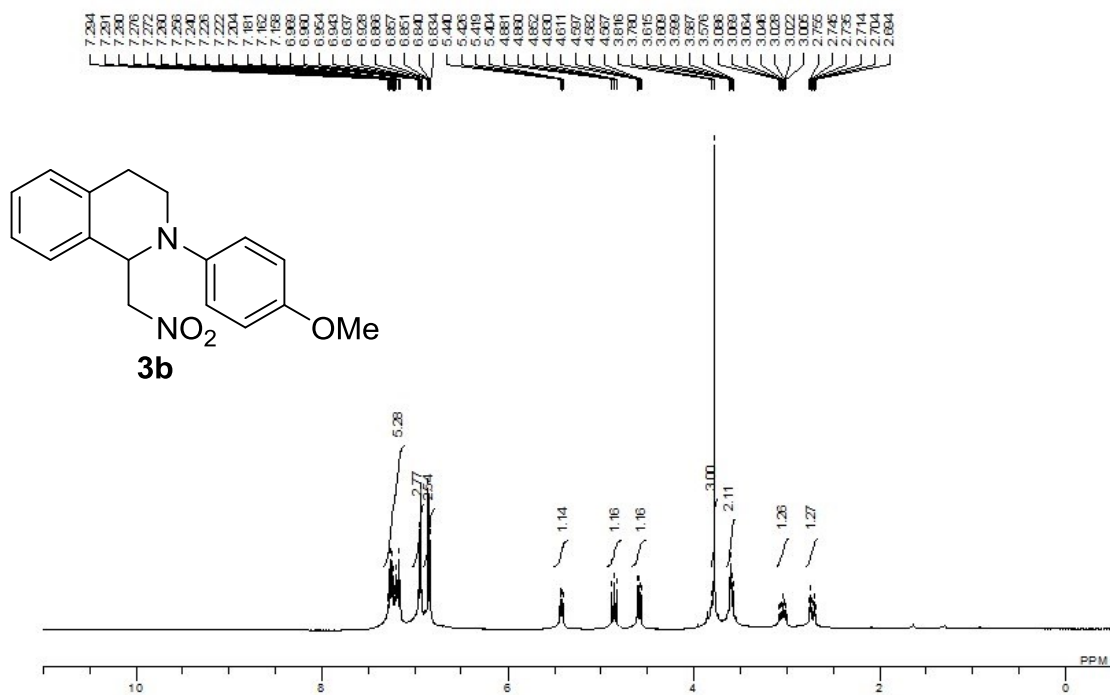
Crude product was pure enough for characterization; product decomposes when subject to silica column chromatography. Colourless oil; 1H NMR (400 MHz, $CDCl_3$) δ 7.30-7.18 (m, 6H), 7.00 (d, $J = 8.4$ Hz, 2H), 6.84 (dd, $J = 7.2, 7.2$ Hz, 1H), 5.63 (s, 1H), 3.73-3.67 (m, 1H), 3.57-3.51 (m, 1H), 3.28 (s, 3H), 3.10-3.03 (m, 1H), 2.97-2.90 (m, 1H); ^{13}C NMR (100 MHz, $CDCl_3$): δ 148.8, 135.9, 135.35, 129.0, 128.2, 128.1, 127.9, 127.8, 125.9, 114.6, 88.2, 53.4, 43.8, 27.82; HRMS (ESI positive) calcd for $C_{16}H_{17}NO$ $[M + Na]^+$: 262.1201; found: 262.1202.

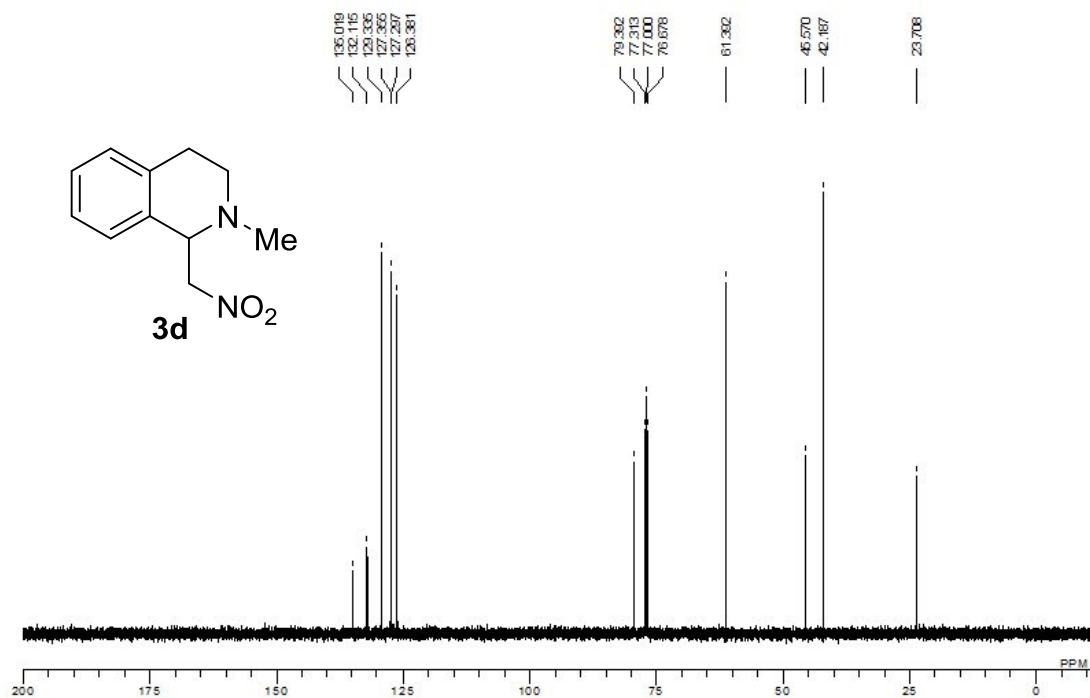
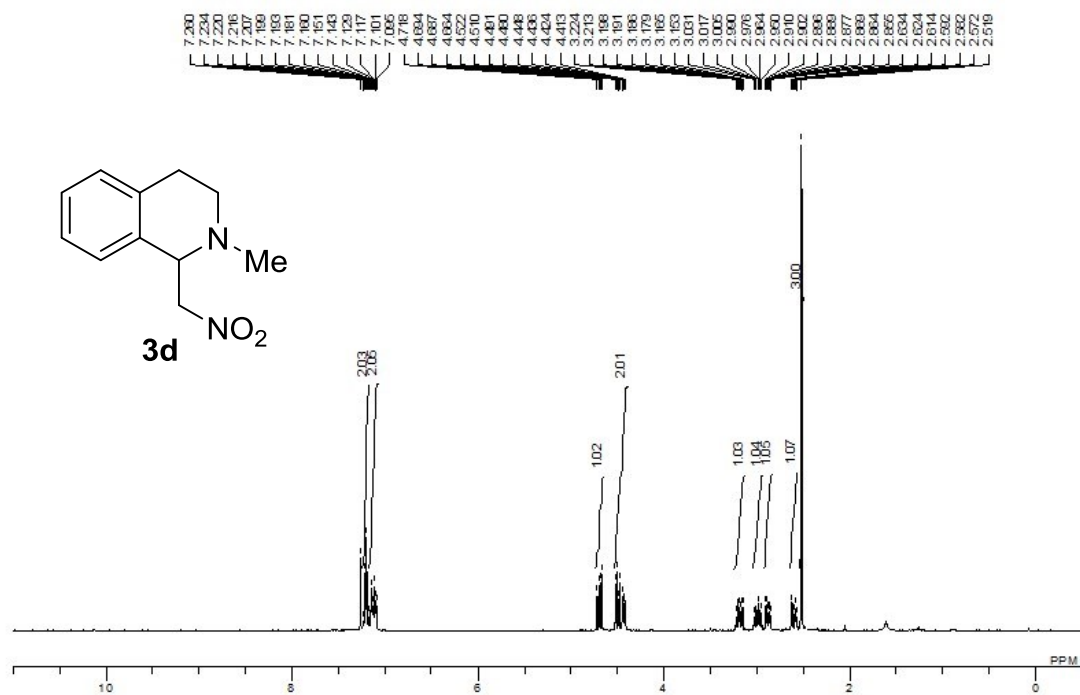
1-(*Tert*-butylperoxy)-2-phenyl-1,2,3,4-tetrahydroisoquinoline (4b)

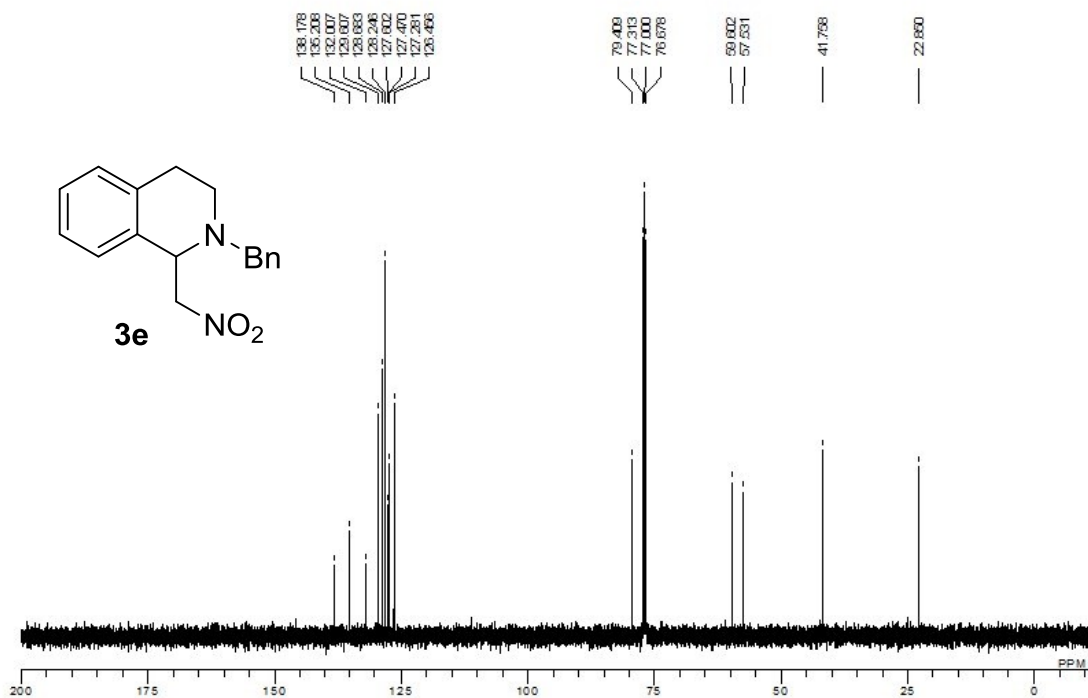
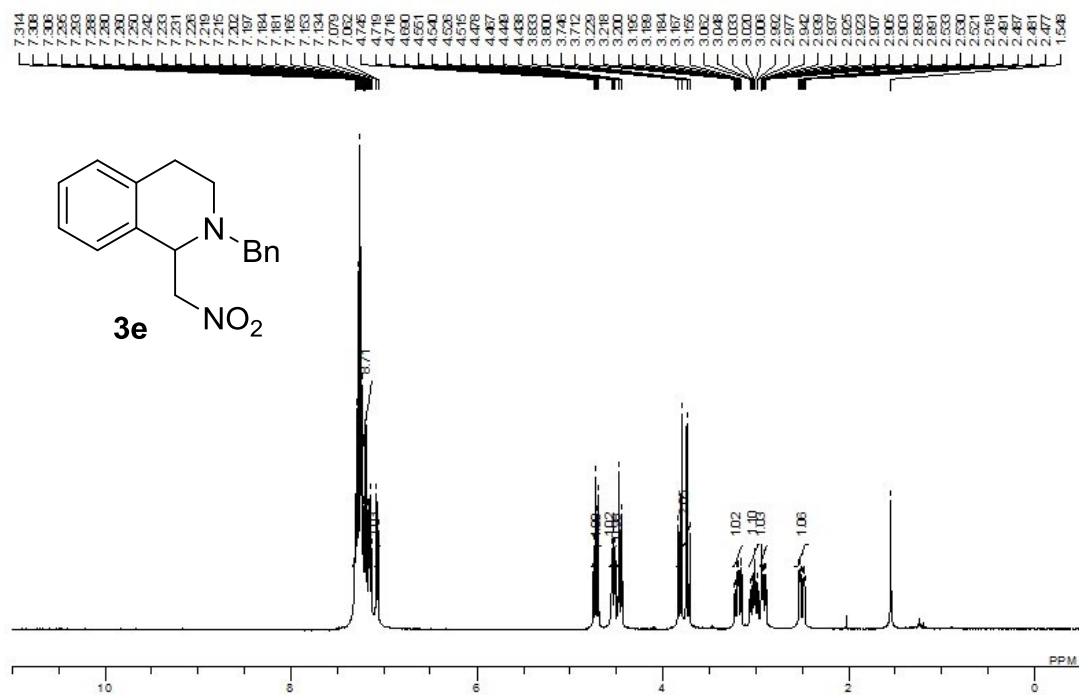


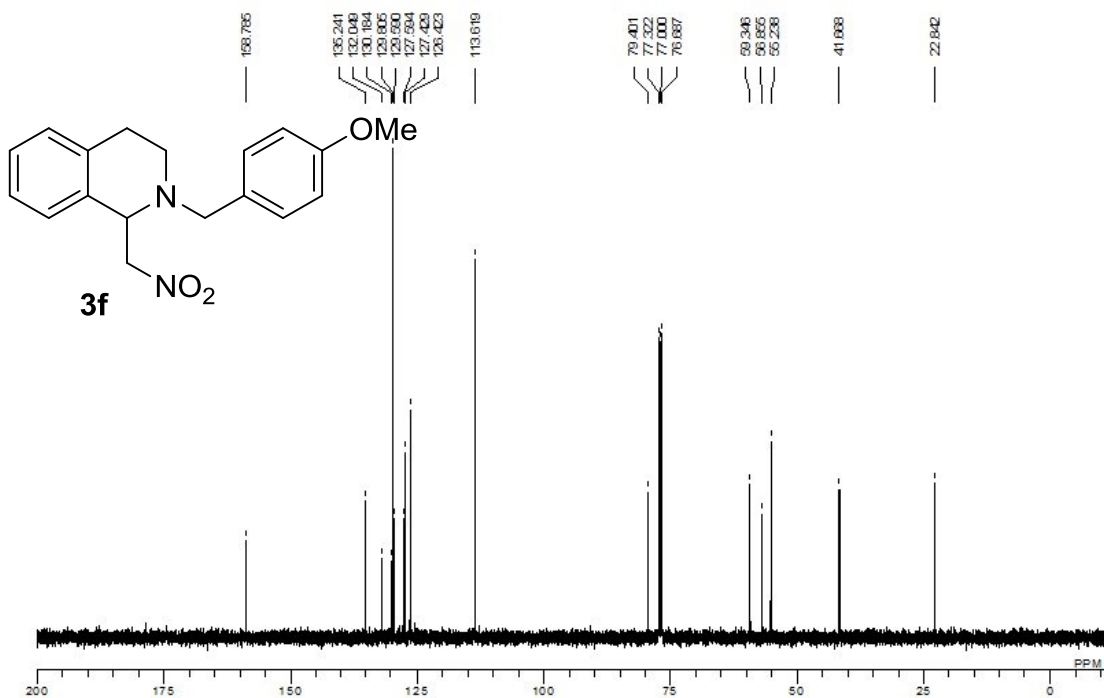
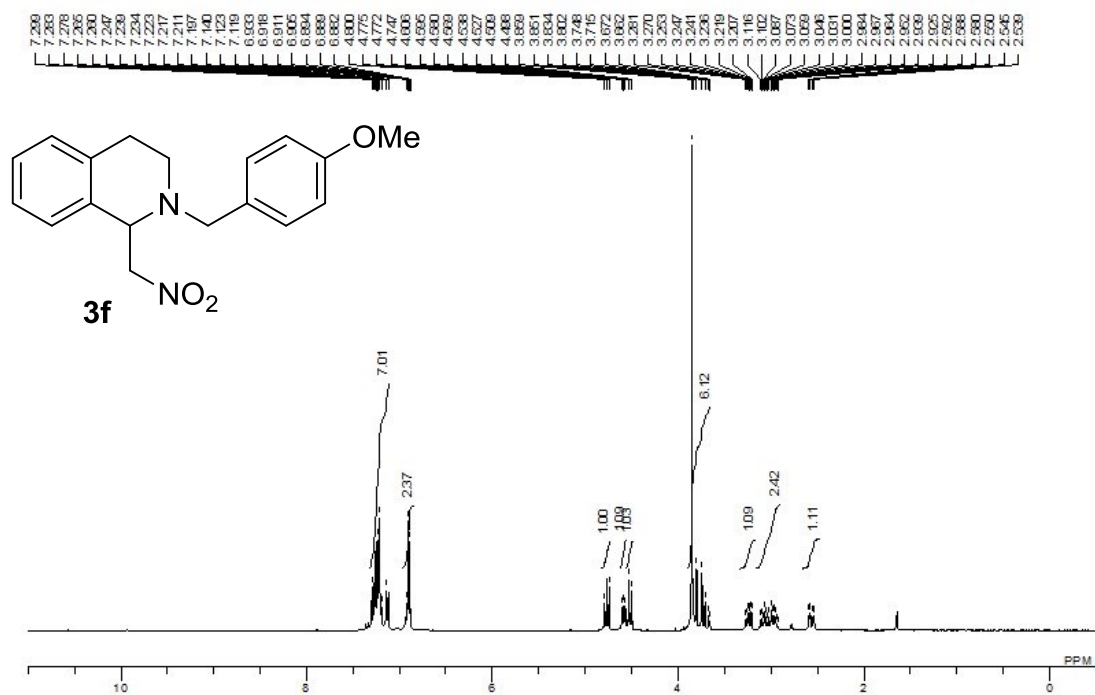
Colourless oil; 1H NMR (400 MHz, $DMSO-d_6$) δ 7.38 (d, $J = 7.2$ Hz, 1H), 7.32-7.21 (m, 5H), 7.09 (d, $J = 8.4$ Hz, 2H), 6.77 (dd, $J = 7.2, 7.2$ Hz, 1H), 6.24 (s, 1H), 3.62-3.56 (m, 1H), 3.52-3.46 (m, 1H), 3.03-2.90 (m, 2H), 3.02-2.97 (m, 1H), 1.04 (s, 9H); ^{13}C NMR (100 MHz, $DMSO-d_6$) δ 148.1, 136.1, 132.4, 128.7, 128.6, 128.4, 127.4, 125.7, 118.2, 114.2, 89.6, 79.2, 41.8, 27.4, 26.2. HRMS (ESI positive) calcd for $C_{19}H_{23}NO_2$ $[M + H]^+$: 298.1801, found: 298.1801.

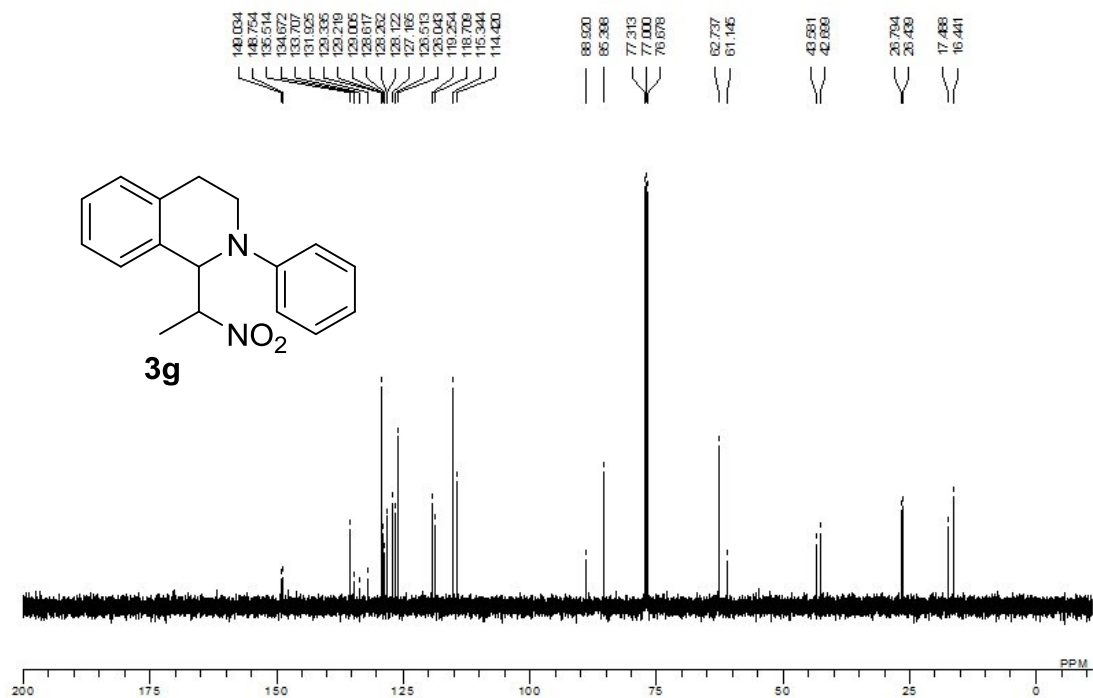
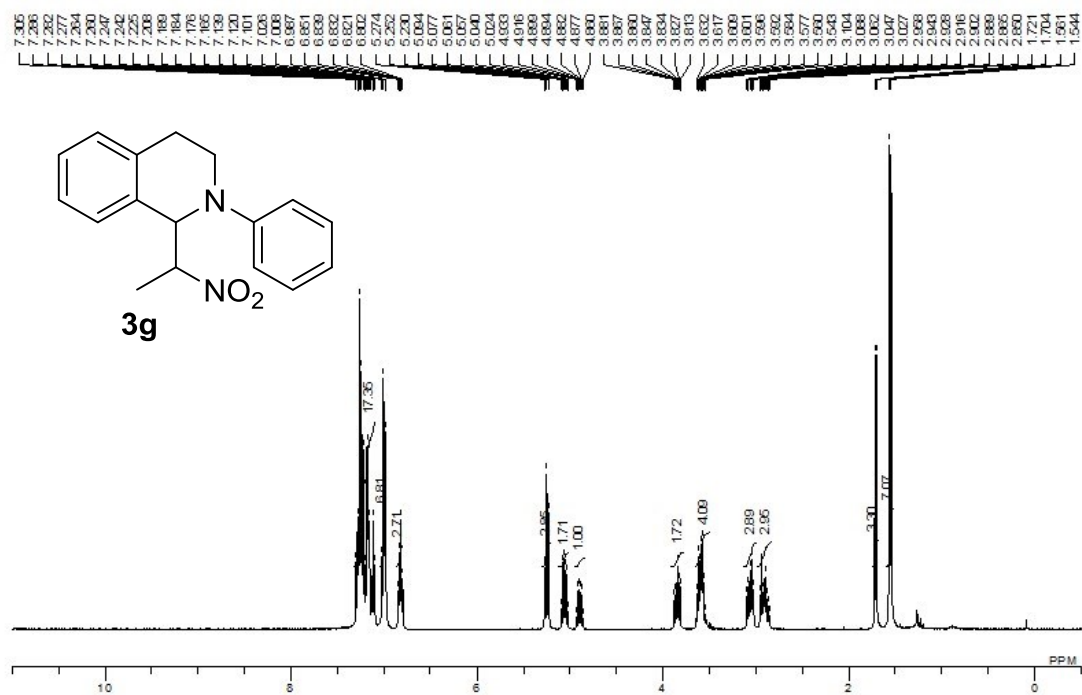


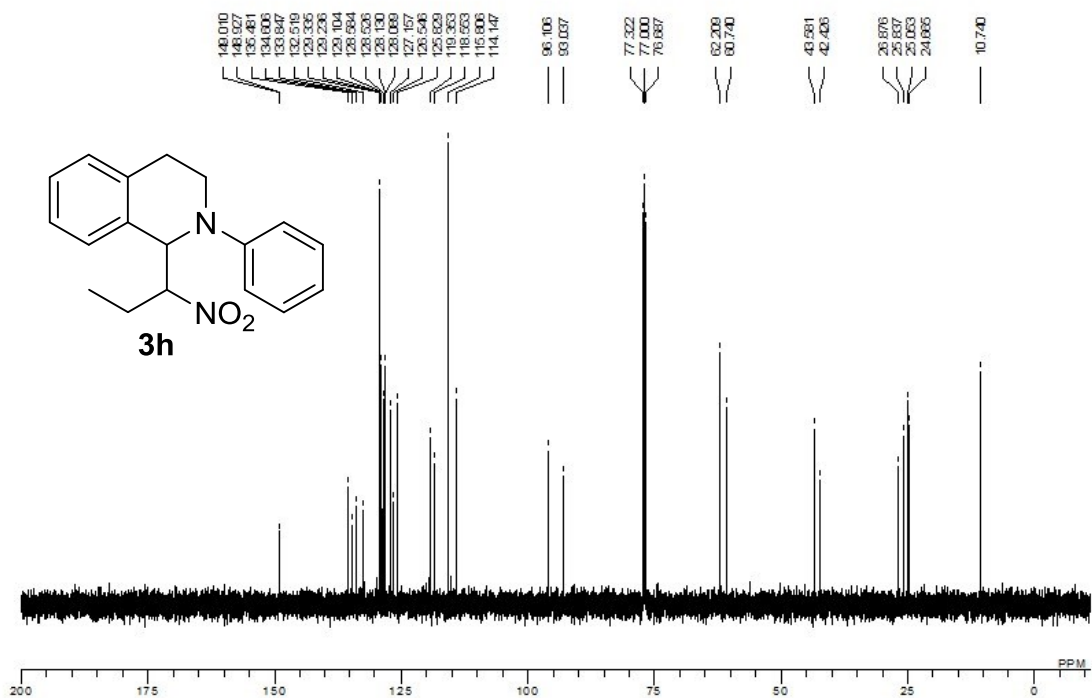
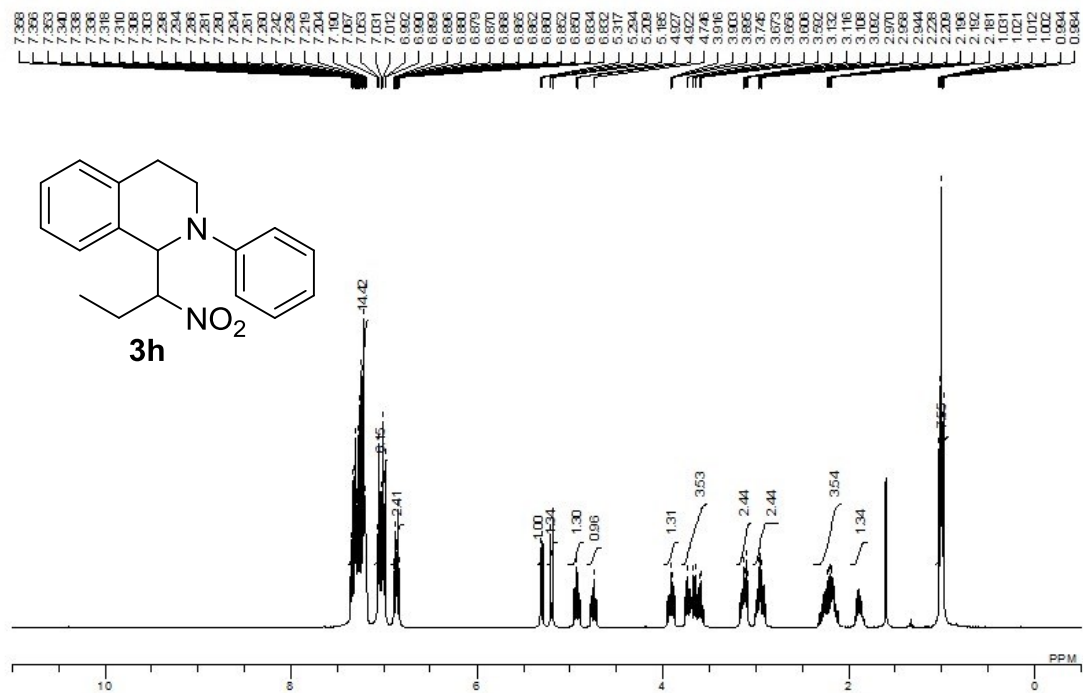


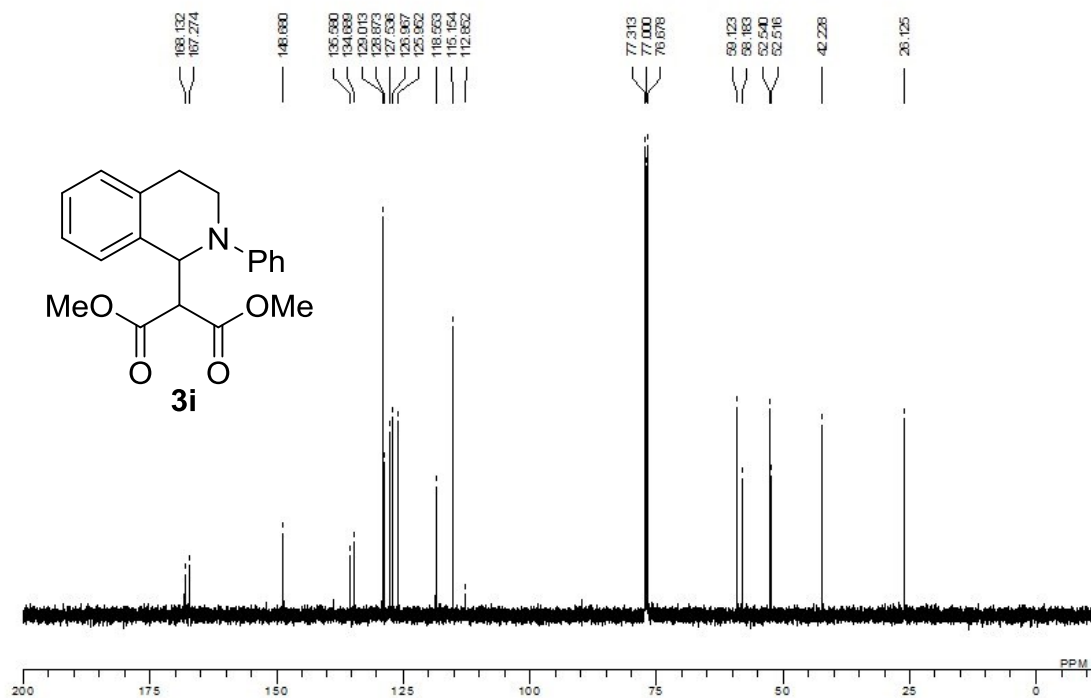
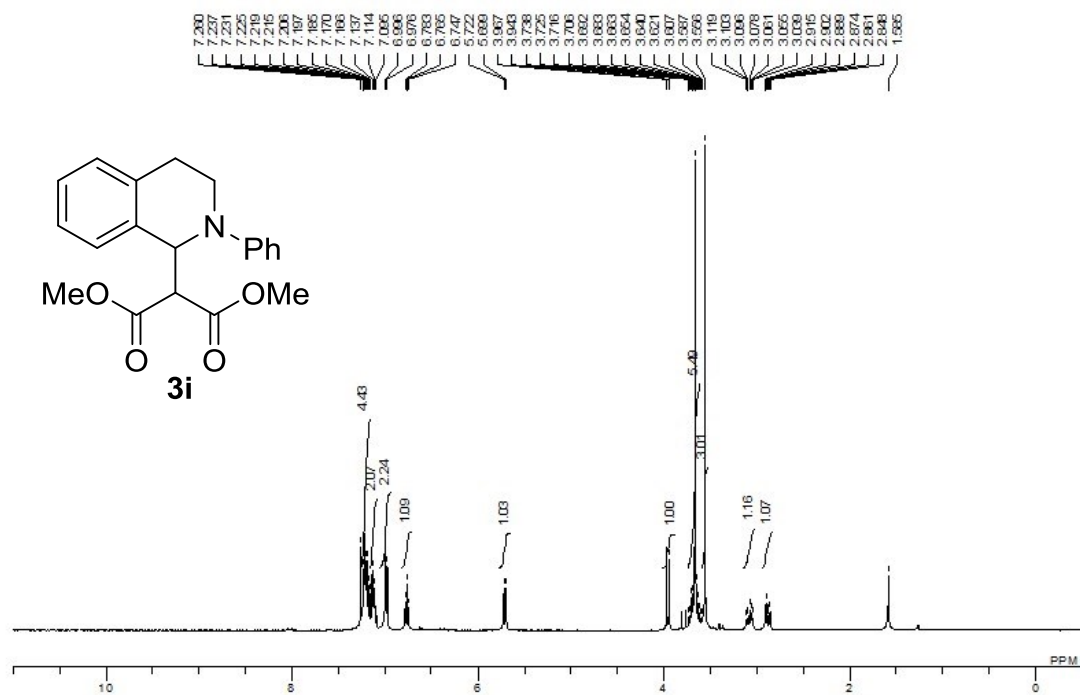


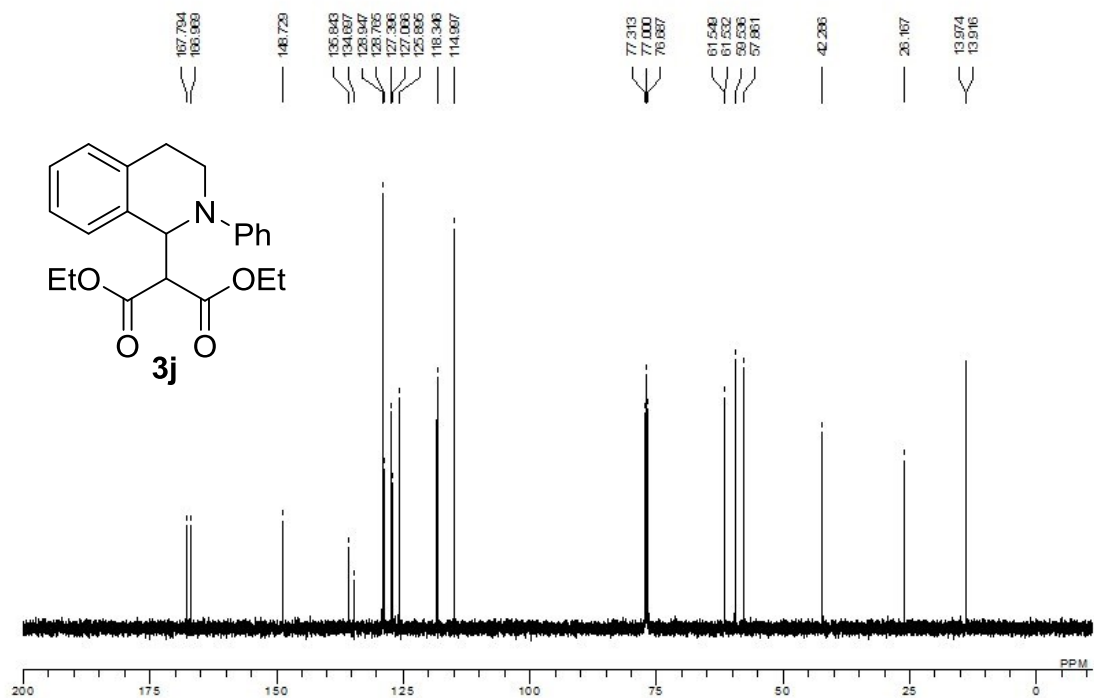
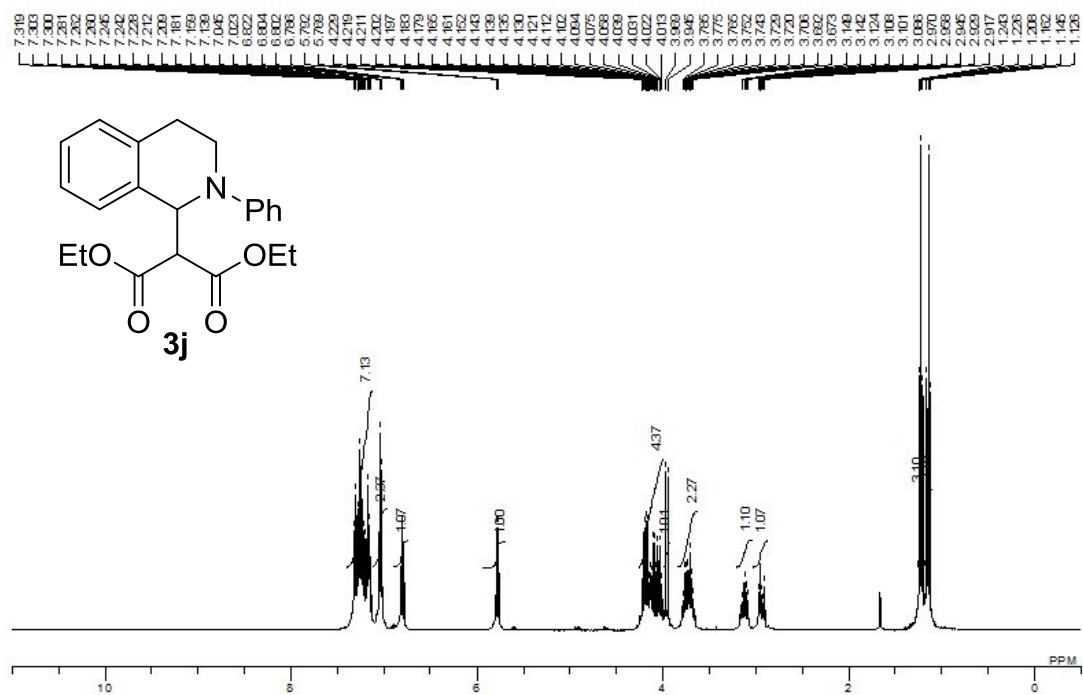


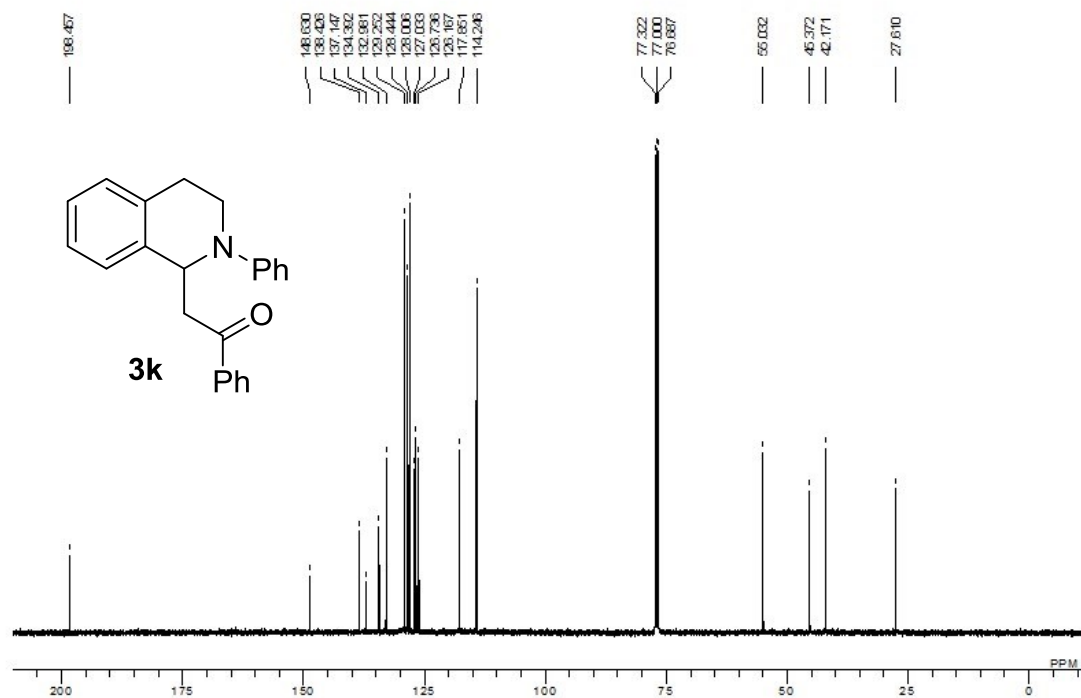
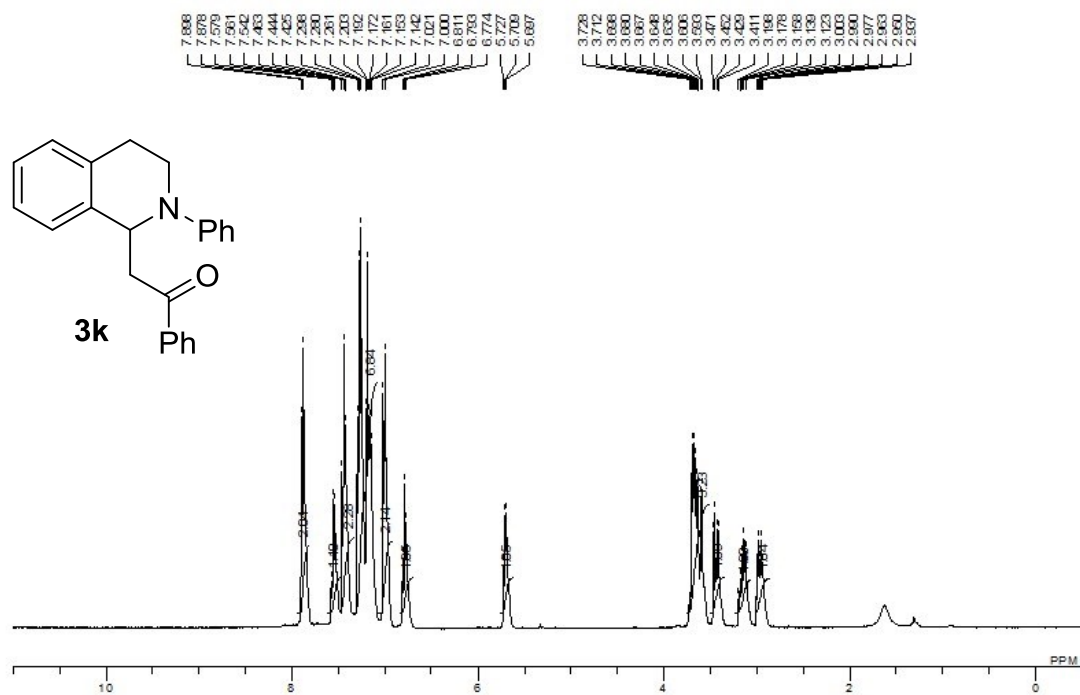


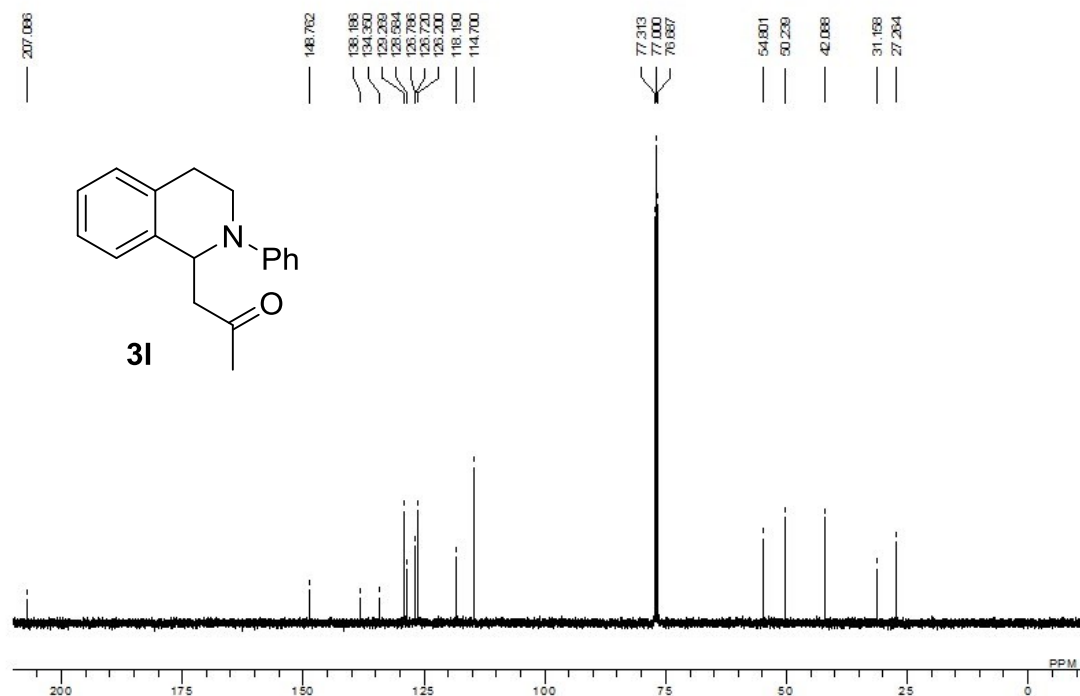
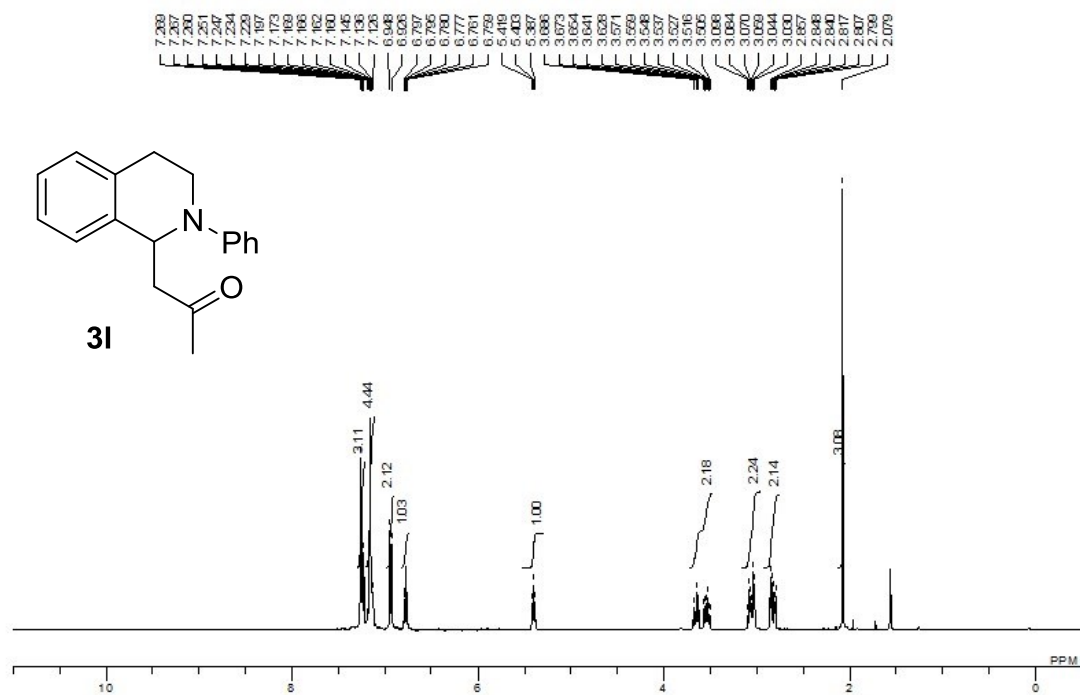


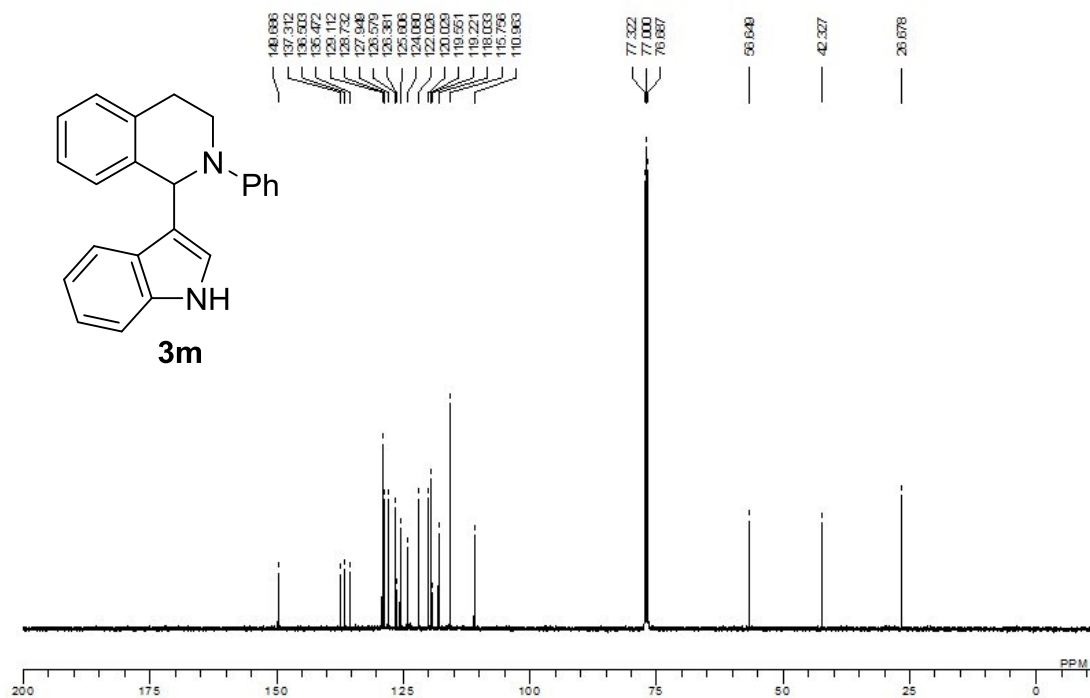
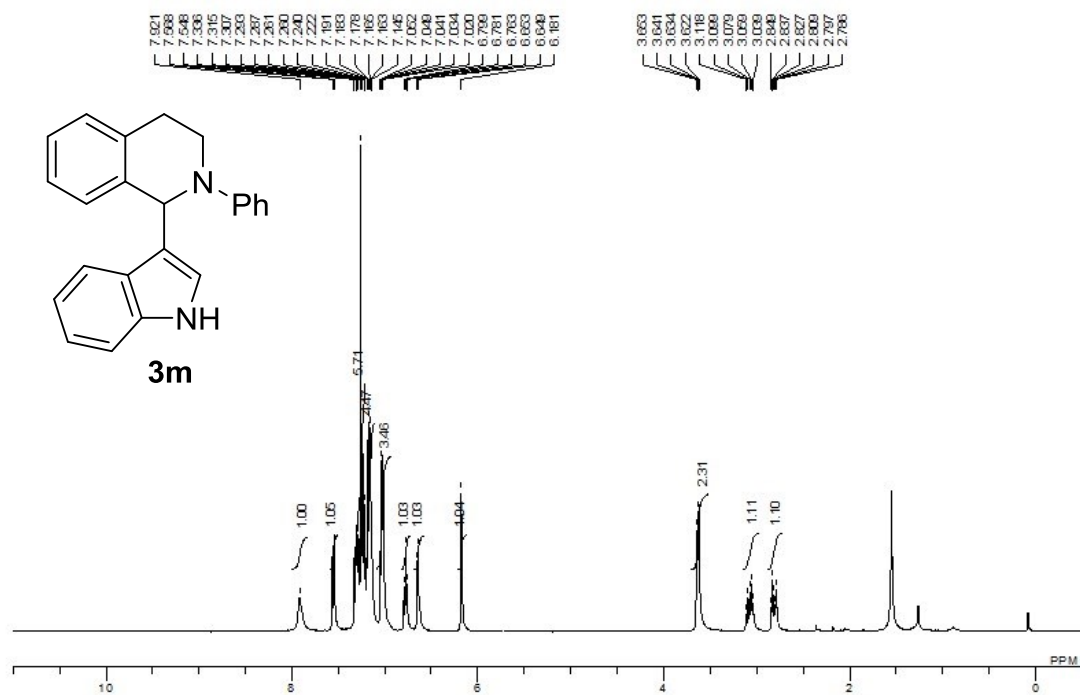


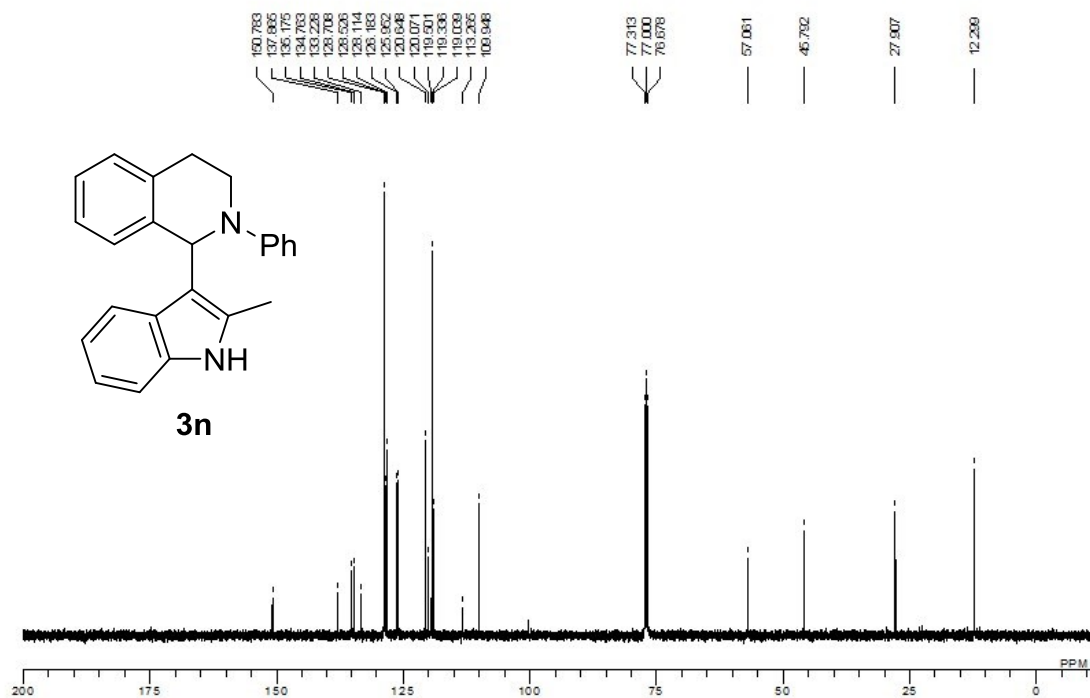
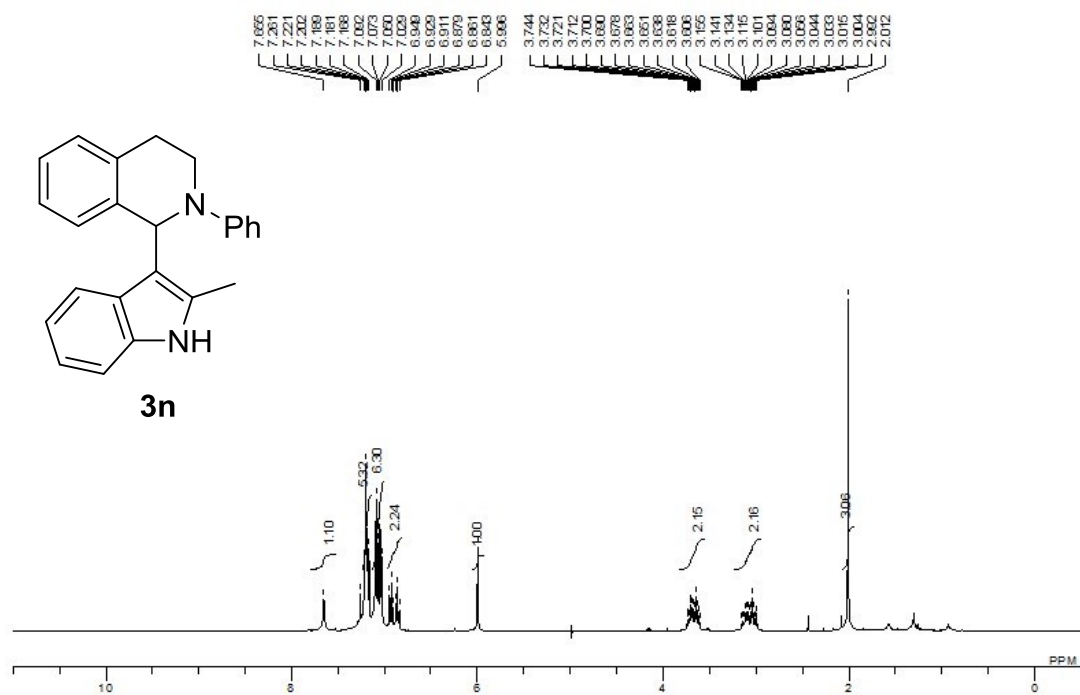


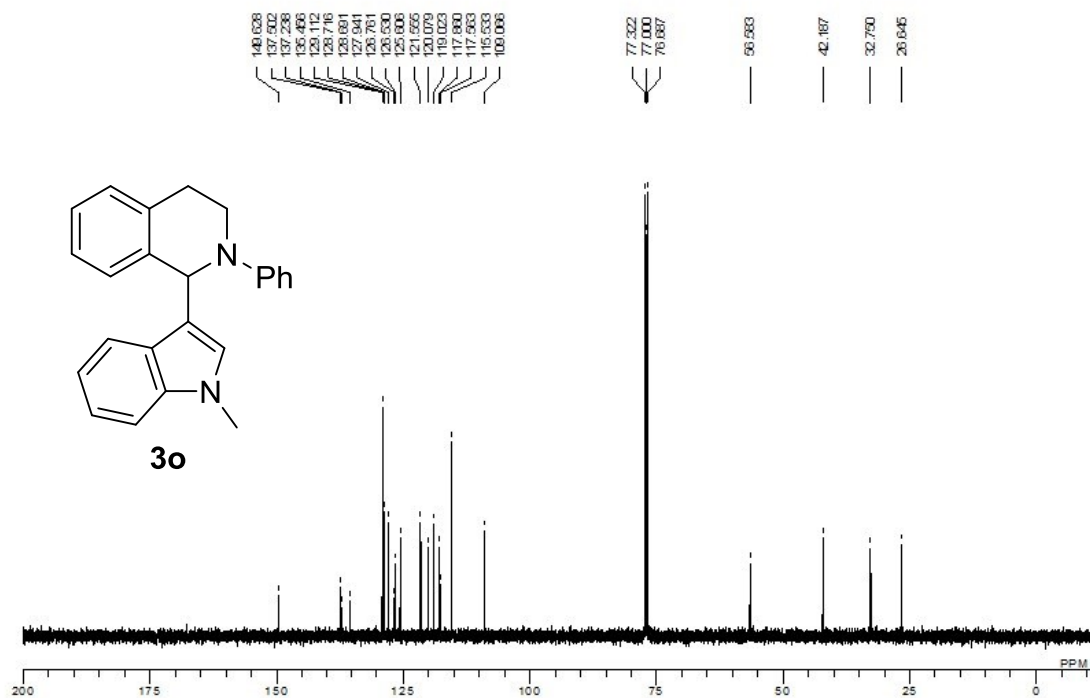
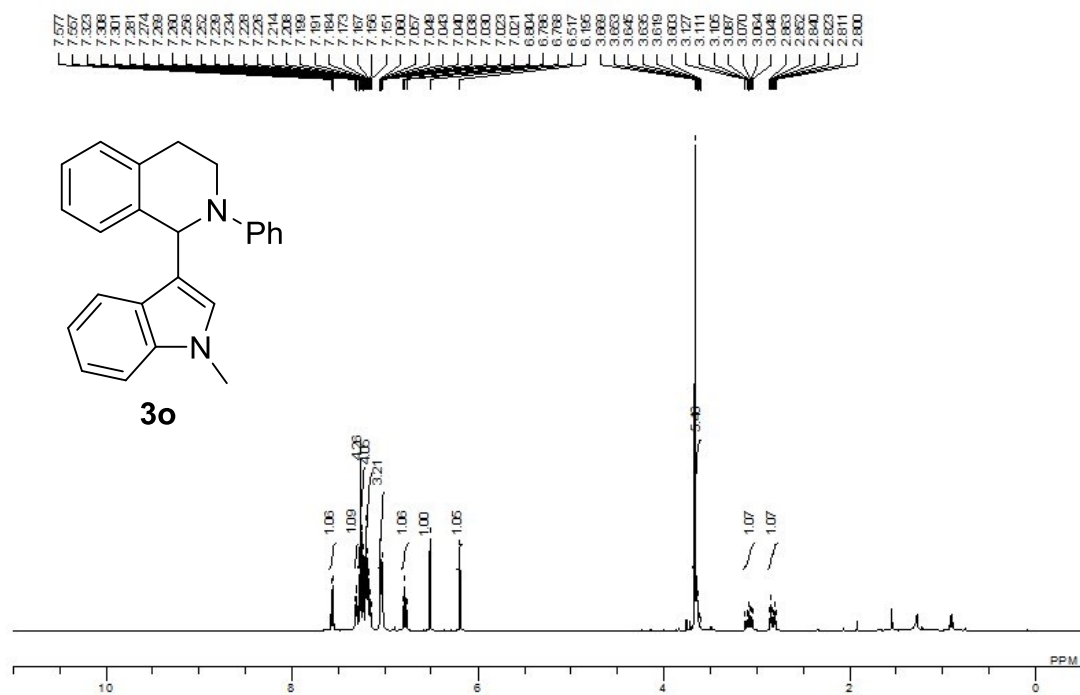


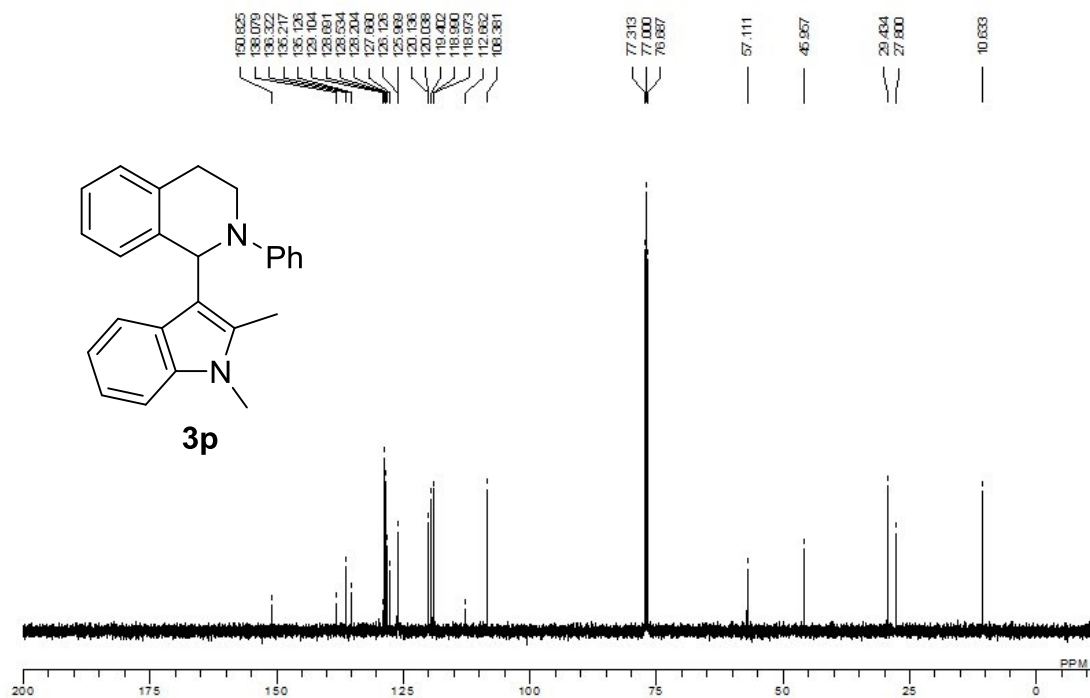
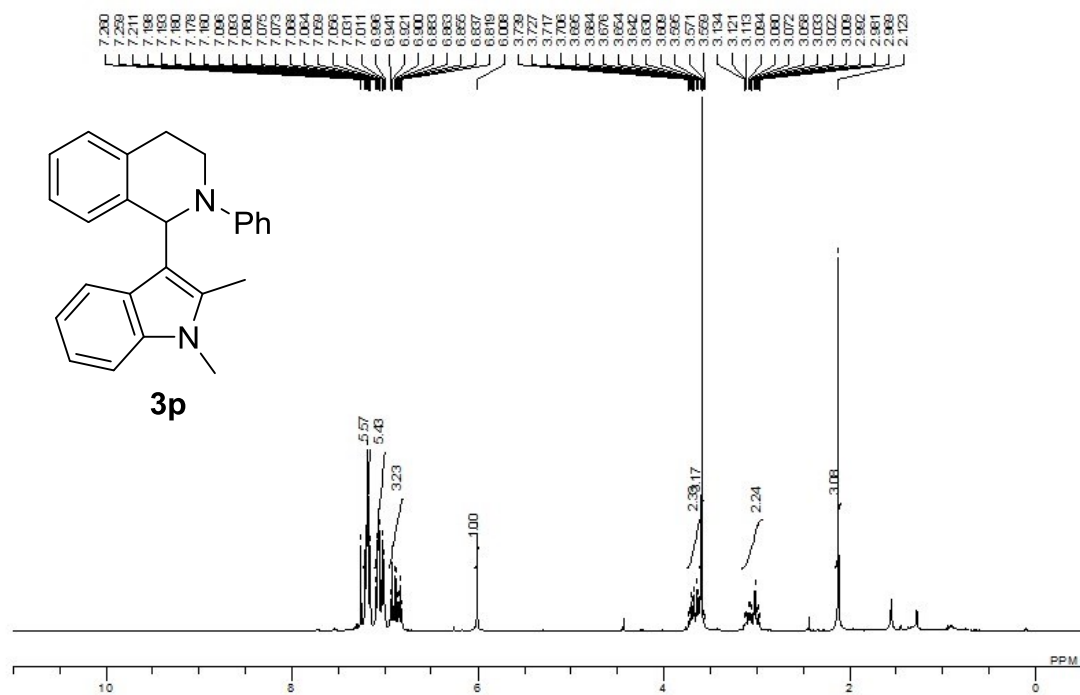


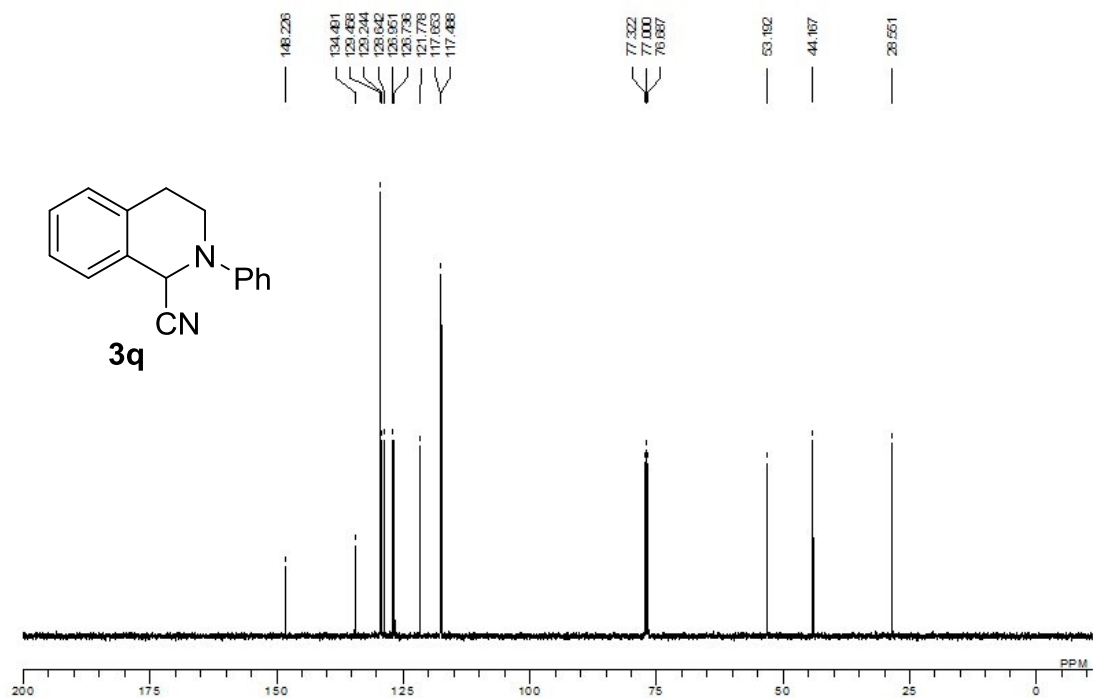
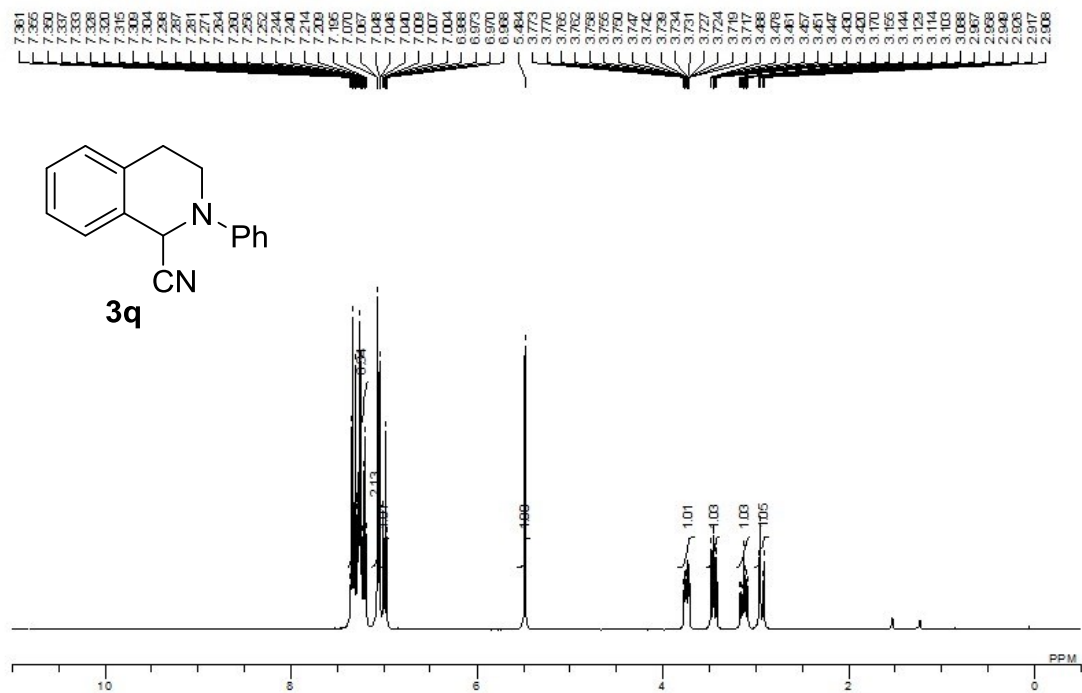


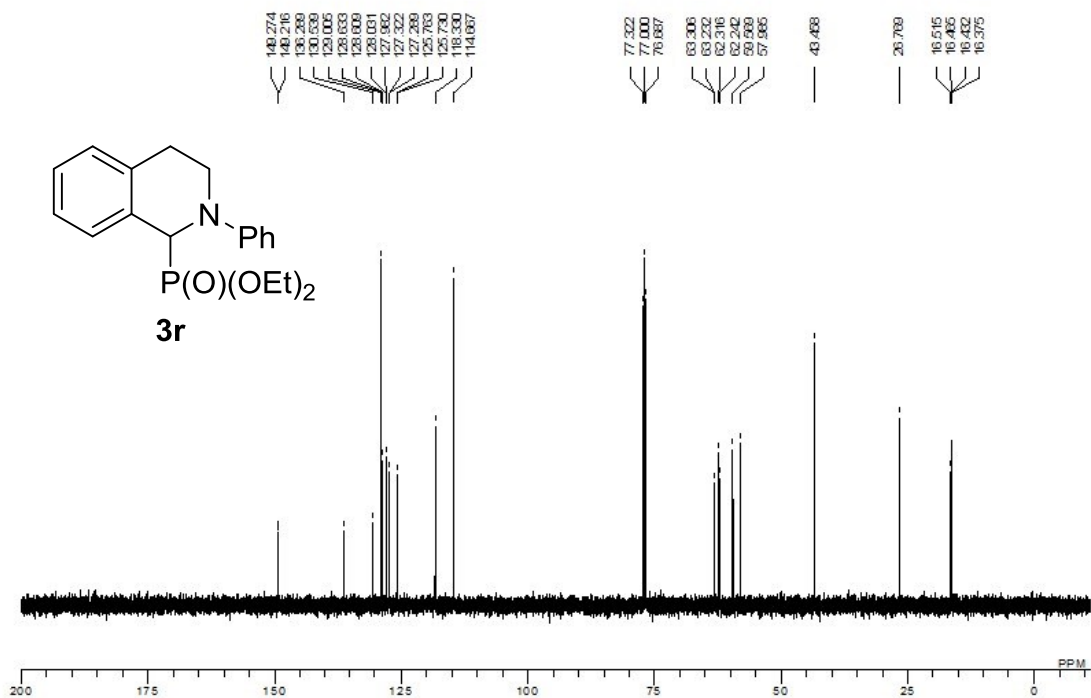
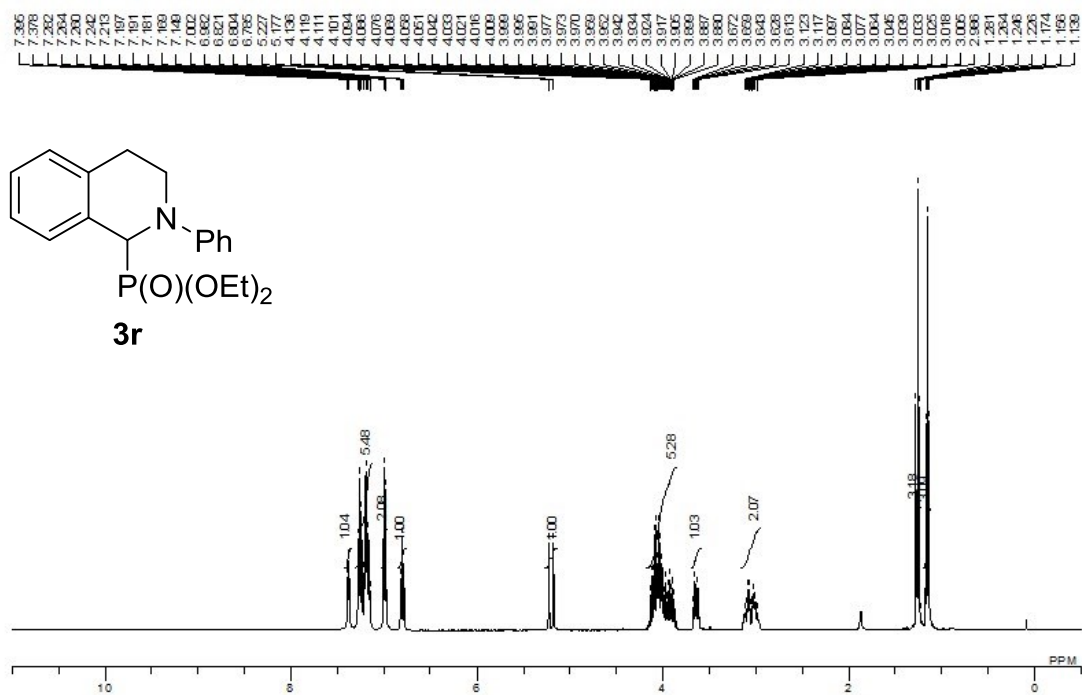


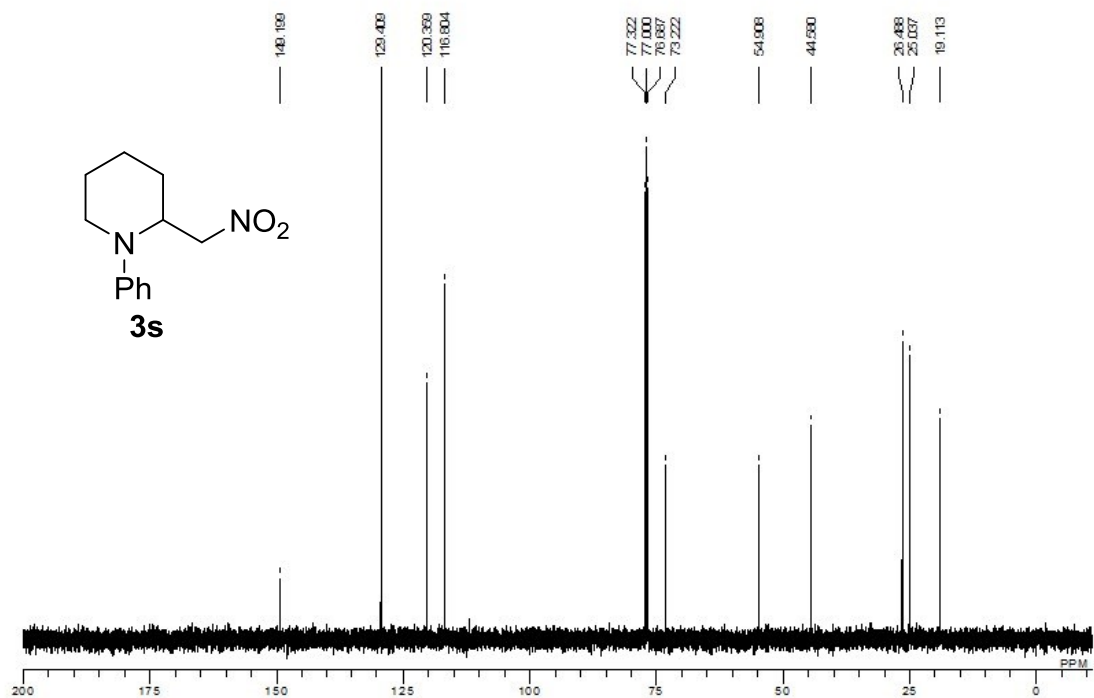
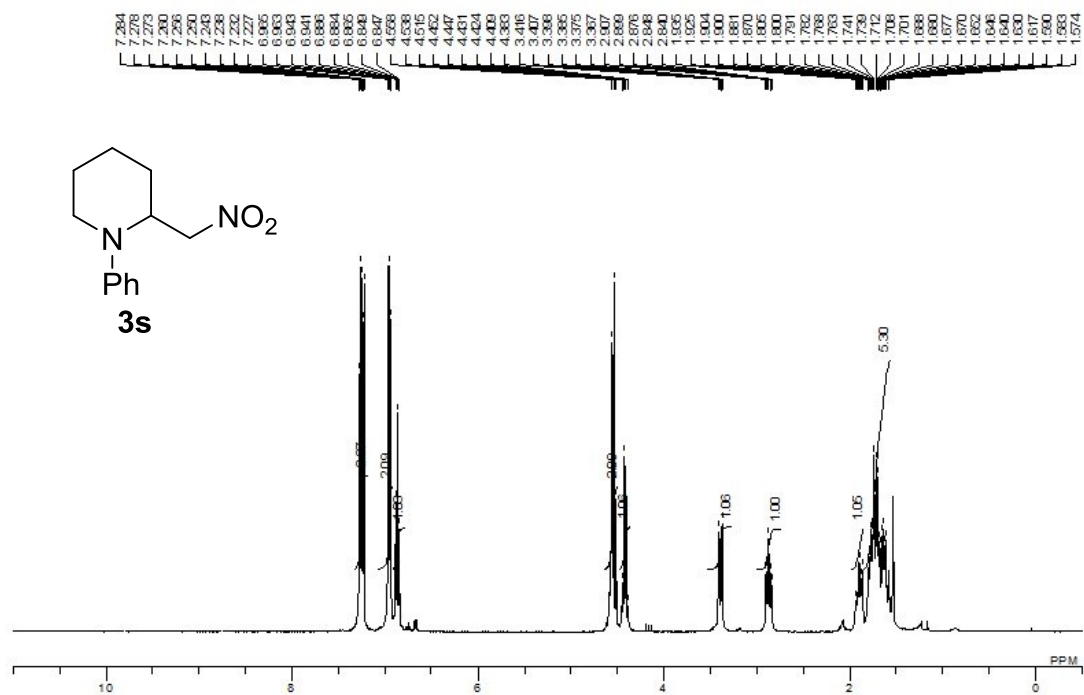


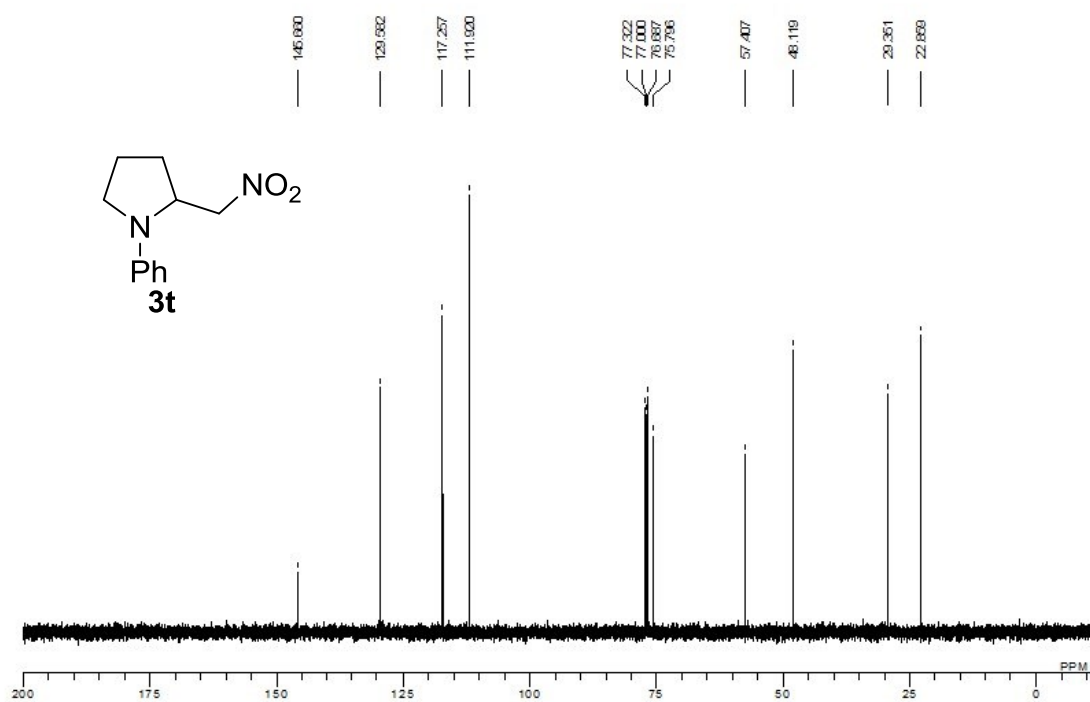
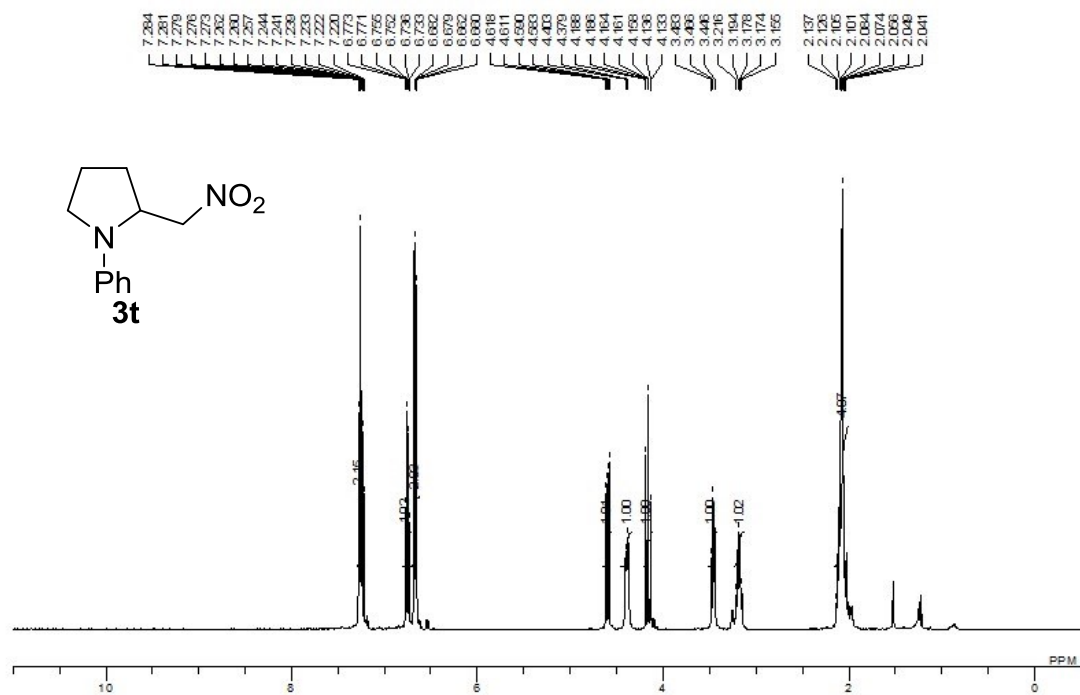


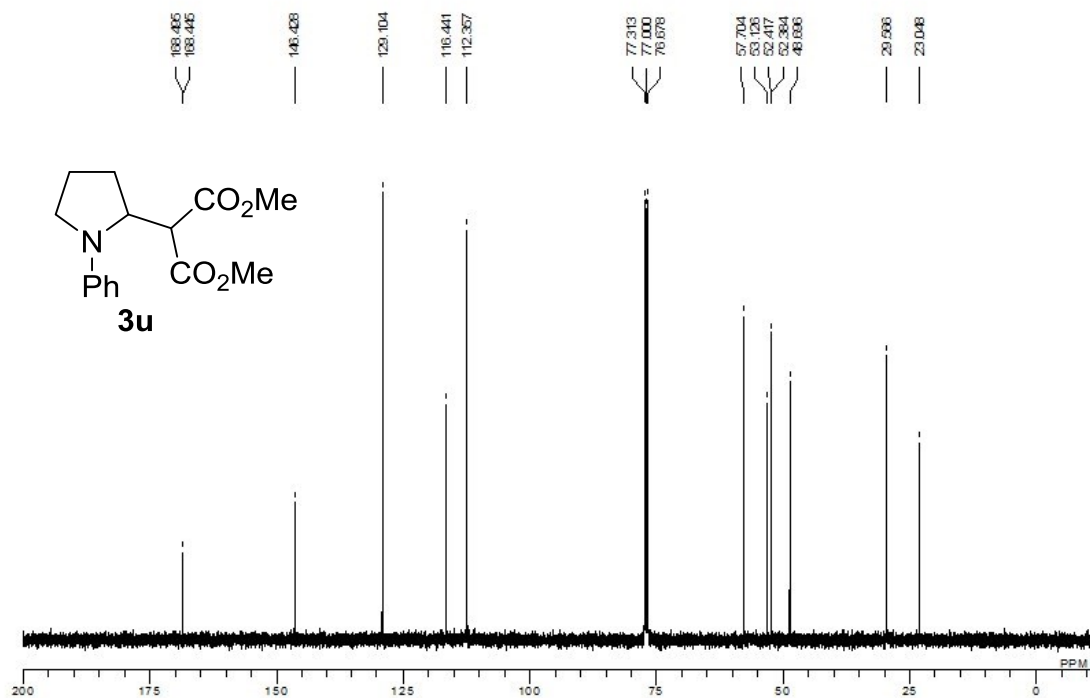
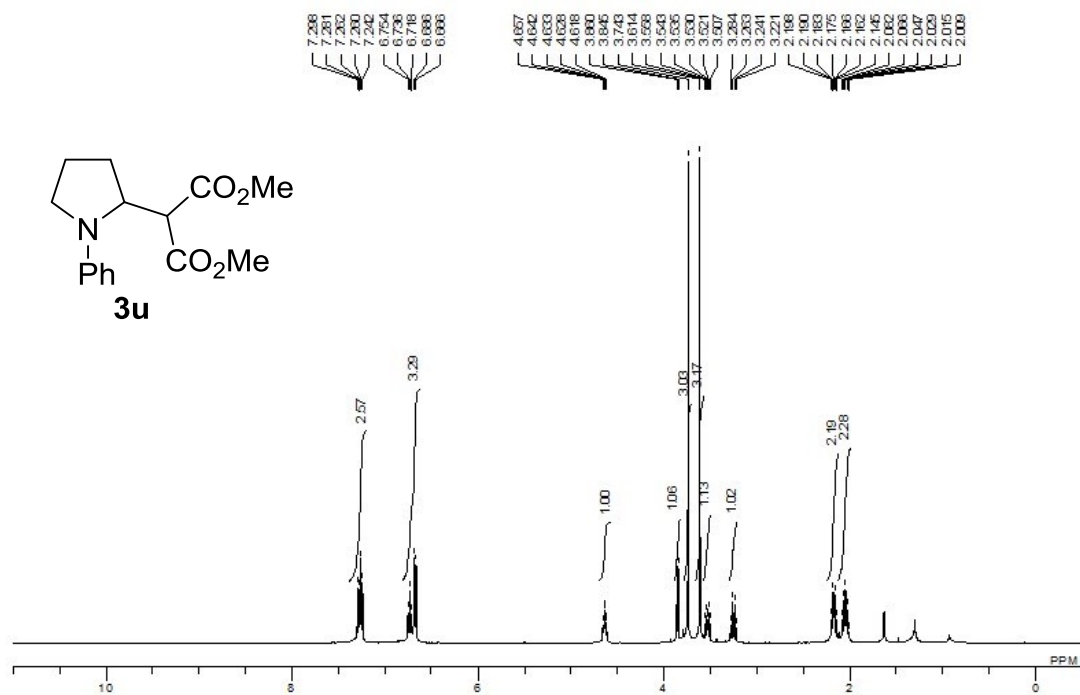


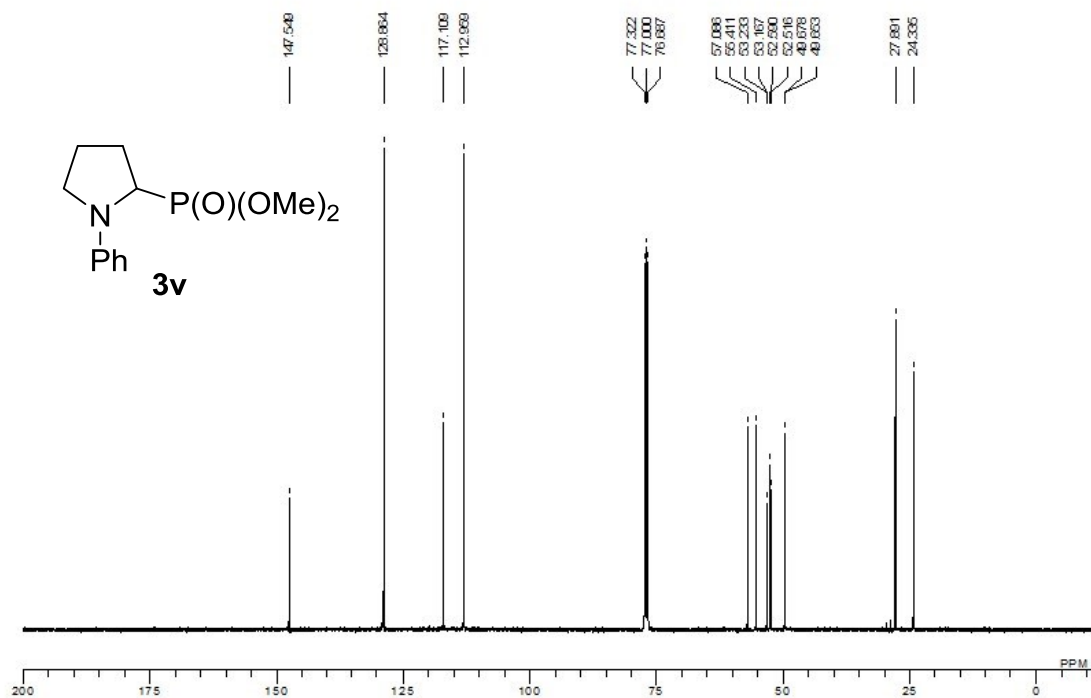
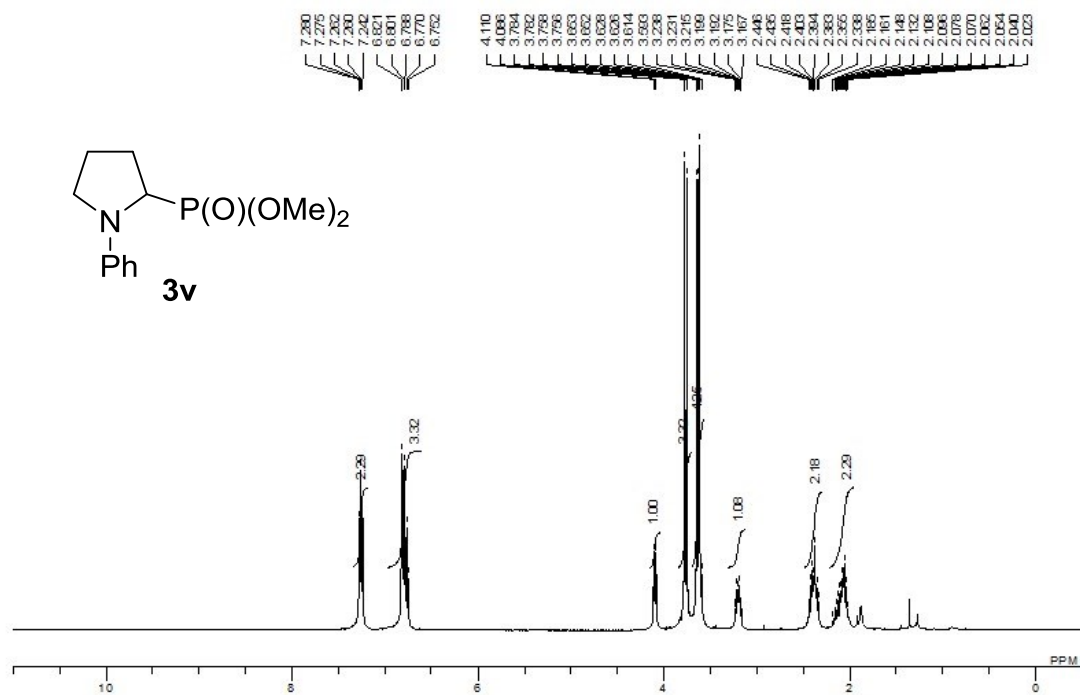


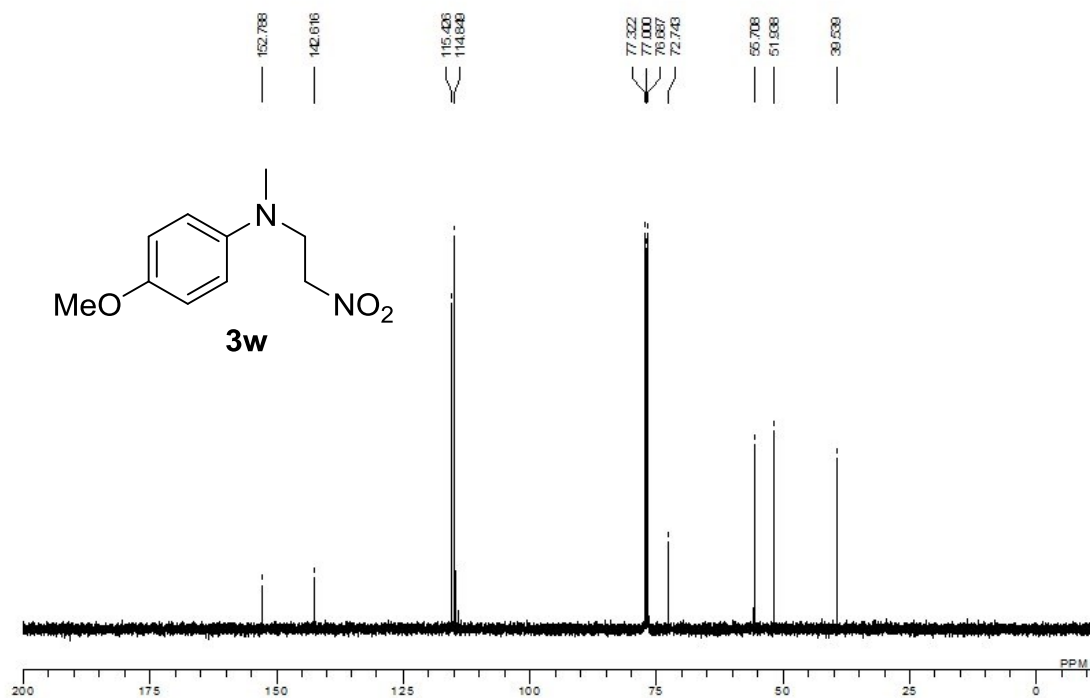
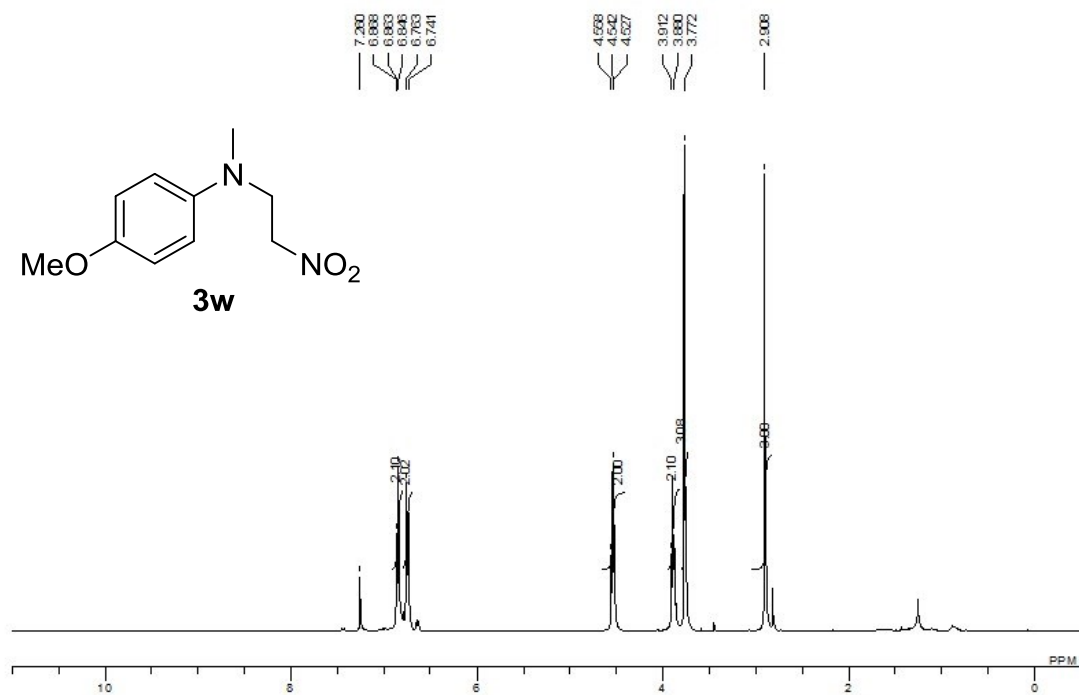


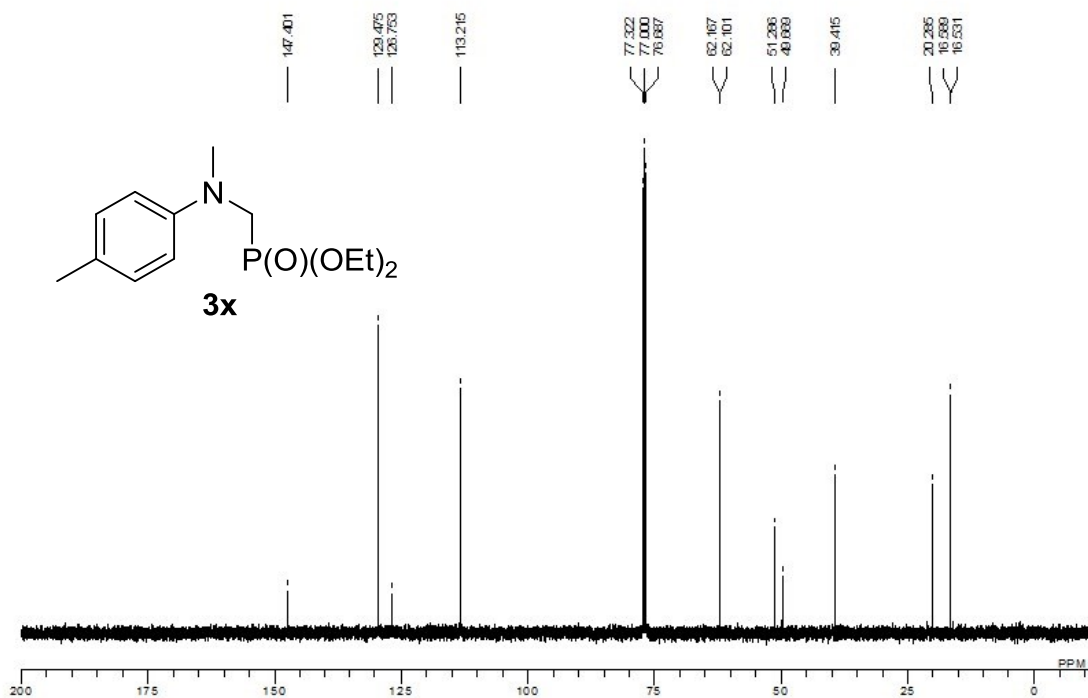
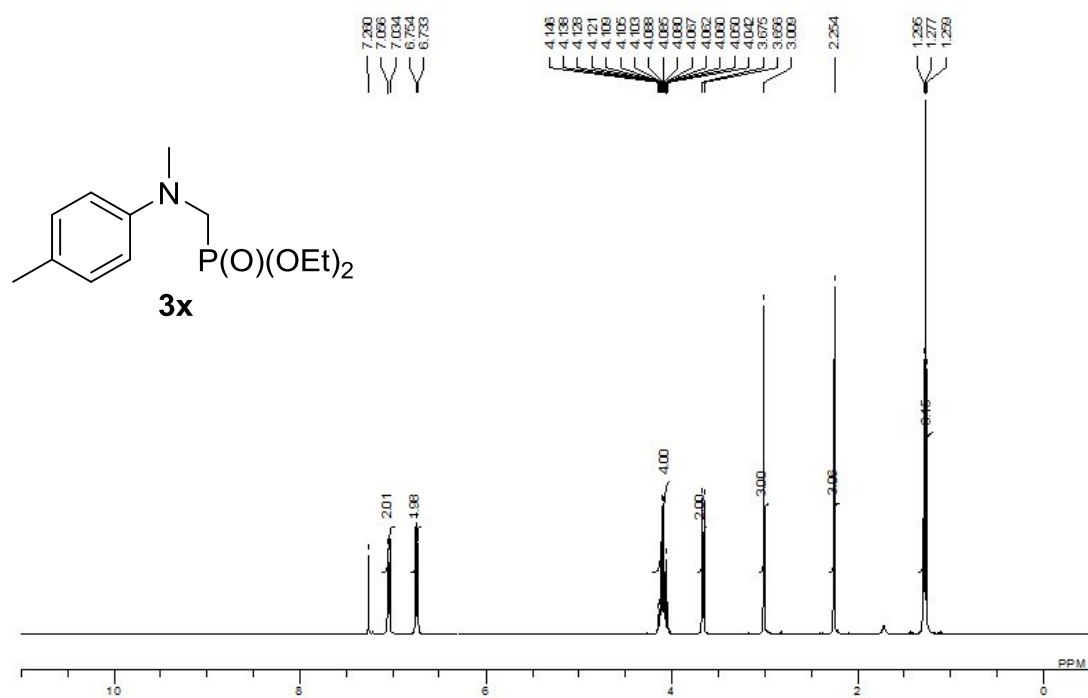


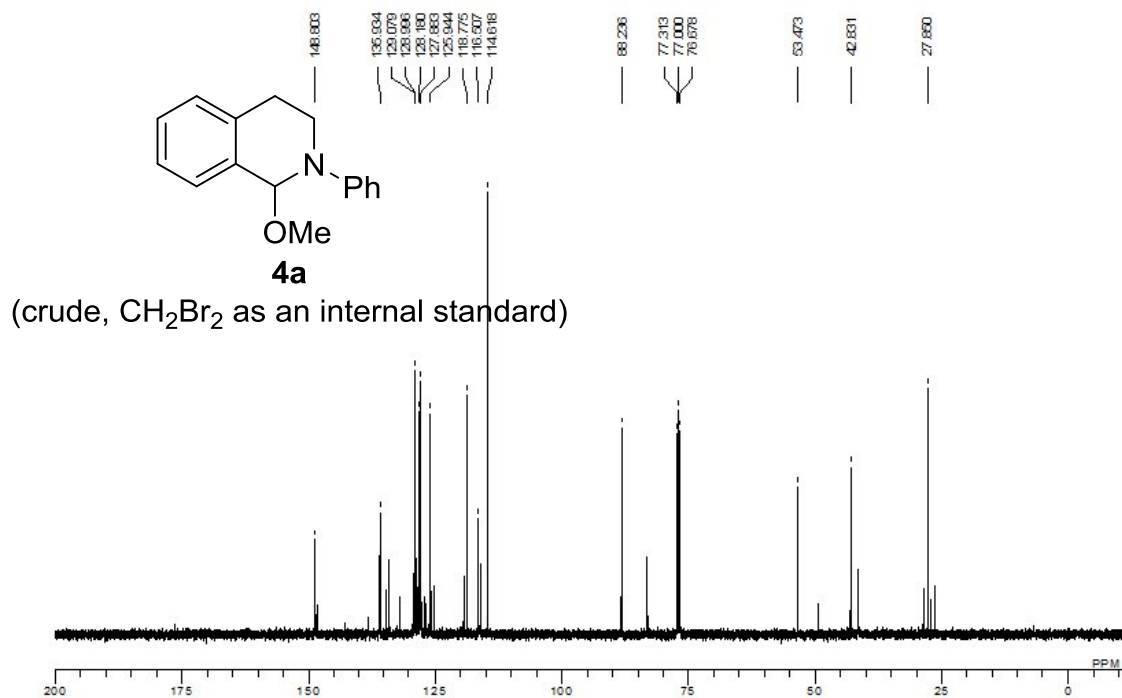
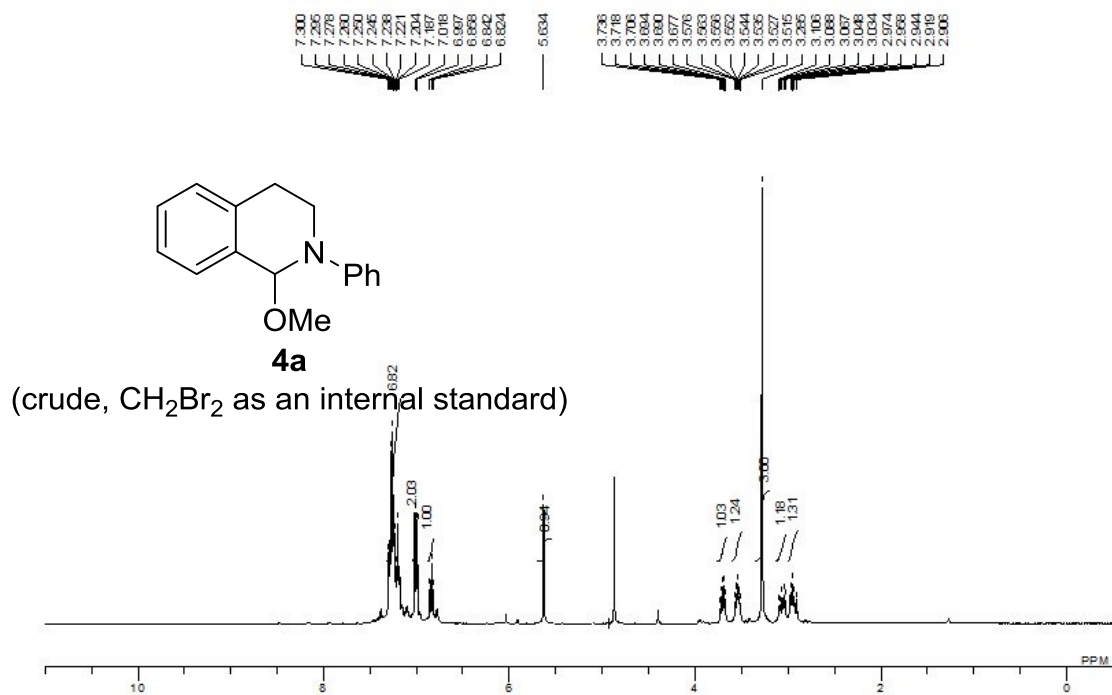


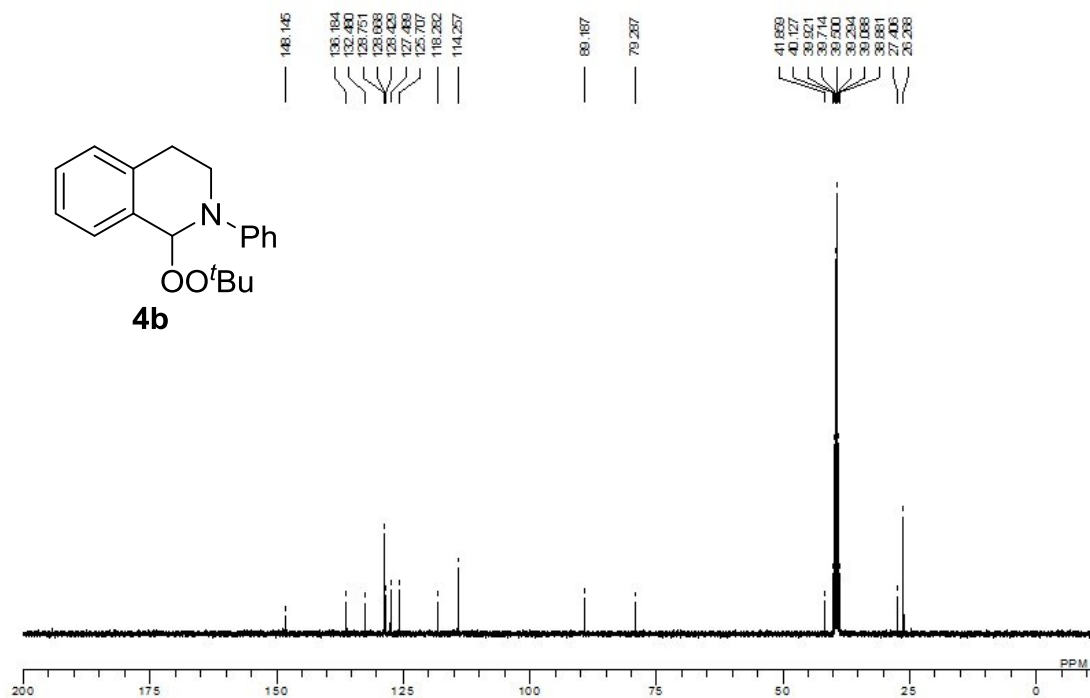
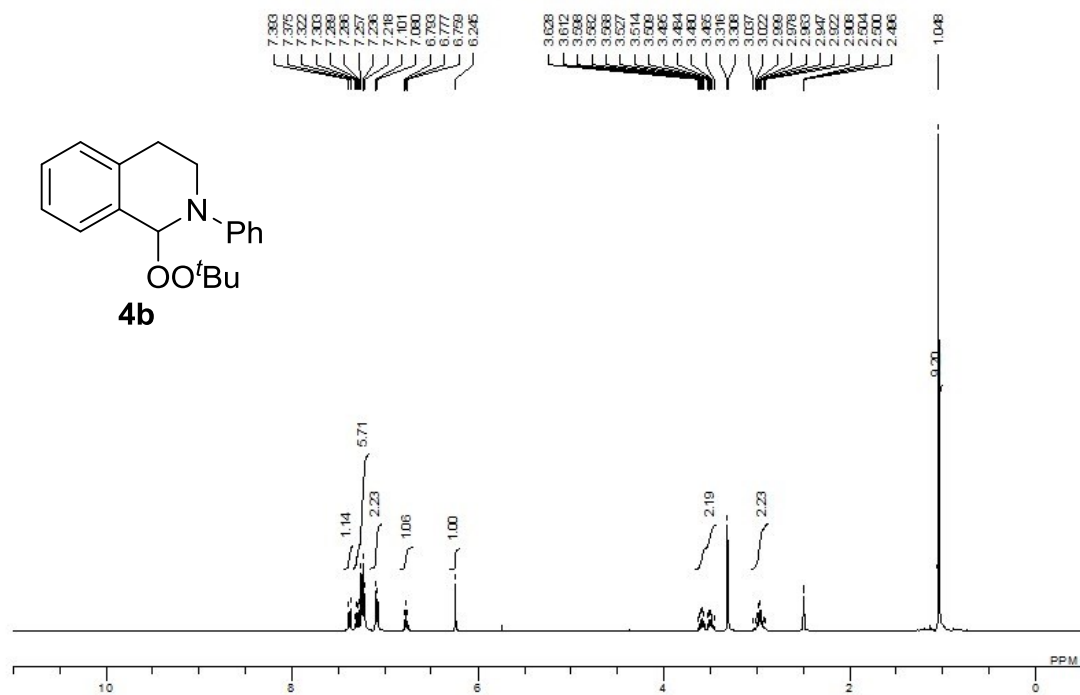












Chapter 2

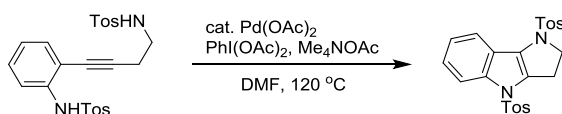
N-Methyl Transfer Induced Copper-Mediated Oxidative Diamination of Alkynes

1. Introduction

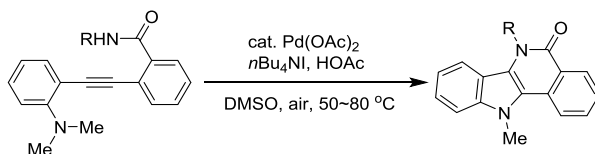
The diamination of C-C multiple bonds provides one of the most effective and straightforward approaches for construction of vicinal diamine components which are important functional frameworks in numerous biologically active compounds and chemically significant molecules.^{1,2} However, compared with those well-established direct diamination reactions of alkenes,¹ the diamination of alkynes has been far less developed.³ The successful diamination of alkynes is anticipated to provide efficient synthetic methodologies for facile construction of various functionally important nitrogen-containing polyheterocycles from readily available chemical building blocks, which still remains challenging. Nonetheless, a few examples toward direct diamination of alkynes has been reported.³ For example, a sole example of intramolecular alkyne diamination was first reported by Muñiz in his pioneering study of alkene diamination,^{3a} in which *N*-tosylated 2-(4-aminobut-1-yn-1-yl)aniline was found to proceed in the oxidative diamination in the presence of a Pd-catalyst and hypervalent iodine oxidant to form a 1,2,3,4-tetrahydropyrrolo[3,2-*b*]indole structure (Scheme 1a). As of late, Zhu and co-workers have demonstrated that 2-(*N,N*-dimethylamino)-phenylethynyl benzamides underwent the demethylation-accompanied intramolecular alkyne diamination under the Pd-catalyzed aerobic conditions to give the tetracyclic indoloisoquinolinone scaffold (Scheme 1b).^{3c,d}

Scheme 1. Intramolecular Diamination of Alkynes for Heterocycle Synthesis

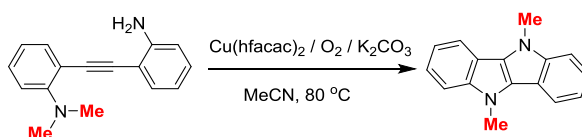
(a) Diamination of alkyne with tosylamides: a sole example by Muñiz



(b) Diamination of alkyne with *N,N*-dimethylamine and benzamide: Zhu *et al*



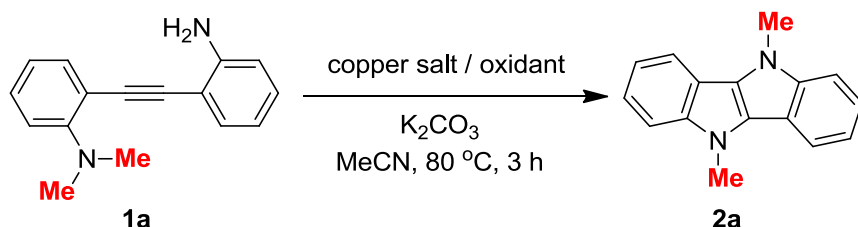
(c) Diamination of alkyne with *N,N*-dimethylamine and primary amine: **this study**



In light of the logical progression on the direct alkyne diamination toward heterocycle synthesis,³ I envisaged that if bis(2-aminophenyl)acetylene having an appropriate *N*-protecting group is used as a substrate under aerobic conditions, the π -conjugated tetracyclic 5,10-dihydroindolo[3,2-*b*]indole (DHII) scaffold would be formed through a direct intramolecular diamination of an alkyne (Scheme 1c), while the related transformations have rarely been reported.^{3a,3c} Owing to the electron-rich and facile oxidizing natures of the DHII scaffold, the DHII-containing materials have been widely applied in organic electronics⁴ including prototypical polaronic ferromagnetic materials,^{4a,b} organic photovoltaics,^{4c-e} and organic light-emitting diodes.^{4f} DHIIs are also expected to exhibit potential biological activities due to the existence of the indole moiety.^{4g} In general, the DHII scaffold could be synthesized by the reduction of 2,2'-dinitrobenzil with a Zn or Sn reductant under acidic conditions, or from the eight-membered dibenzo[*b,f*]-[1,5]diazocine-6,12(*5H*,11*H*)-dione through a multistep process under harsh conditions.^{4,5} Taking into consideration the aforementioned scenarios and our recent research project on developing new synthetic methodologies of π -conjugated polycycles,⁶ herein a novel synthetic method of DHII scaffold is reported through a Cu-mediated intramolecular oxidative diamination of 2-((2-aminophenyl)ethynyl)-*N,N*-dimethylaniline under aerobic conditions using molecular oxygen as an oxidant (Scheme 1c). Notably, an *N*-methyl transfer takes place from the *N,N*-dimethylamine to the primary amine during the annulation, which is an essential step for implementation of the present alkyne diamination.

2. Results and Discussion

Table 1. Optimization of Reaction Conditions for Diamination of **1a**^a



entry	Cu salt (equiv)	Oxidant (2 equiv)	2a (%) ^b	1a (%) ^b
1	CuCl (0.2)	O ₂ (1 atm)	11	5
2	CuCl ₂ (0.2)	O ₂ (1 atm)	10	3
3	Cu(OAc) ₂ (0.2)	O ₂ (1 atm)	4	0
4	Cu(OTf) ₂ (0.2)	O ₂ (1 atm)	17	19
5	Cu(acac) ₂ (0.2)	O ₂ (1 atm)	0	99
6	Cu(hfacac) ₂ (0.2)	O ₂ (1 atm)	31	57
7 ^c	Cu(hfacac) ₂ (0.2)	O ₂ (1 atm)	30	0
8	Cu(hfacac) ₂ (1.0)	O ₂ (1 atm)	85 (80)	0
9	Cu(hfacac) ₂ (1.0)	air (1 atm)	3	37
10	Cu(hfacac) ₂ (1.0)	TBHP	12	0
11	Cu(hfacac) ₂ (1.0)	DTBP	50	0
12	Cu(hfacac) ₂ (1.0)	PhI(OAc) ₂	13	0
13	Cu(hfacac) ₂ (1.0)	<i>o</i> -chloranil	0	0
14 ^c	Cu(hfacac) ₂ (1.0)	O ₂ (1 atm)	0	0

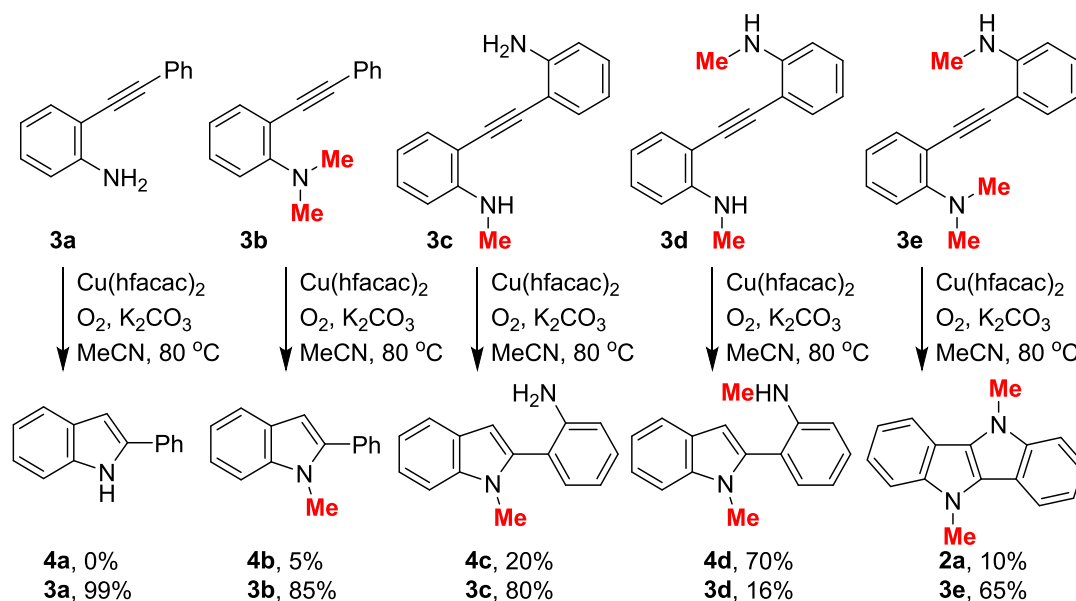
^a Reaction conditions: **1a** (0.2 mmol), copper salt (0.2-1.0 equiv), oxidant (1 atm or 2 equiv), K₂CO₃ (entries 1-7: 0.6 equiv, 12 h; entries 8-14: 3 equiv, 3 h) in MeCN (0.2 M) at 80 °C unless otherwise noted. ^b The ¹H NMR yield determined using CH₂Br₂ as an internal standard. Isolated yield is shown in parentheses. ^c In the absence of K₂CO₃.

In preliminary experiments, the reaction of 2-((2-aminophenyl)ethynyl)-*N,N*-dimethylaniline (**1a**) with Muñiz's conditions (Scheme 1a)^{3a} resulted in a complete decomposition of the starting substrate **1a** without formation of any products, while with Zhu's conditions (Scheme 1b)^{3c} only produced the indole product **4c** (Scheme 2) in 70% yield. After optimization of a variety of oxidative diamination conditions using various metal complexes by employing **1a** as a starting substrate, copper salts were found to be the most effective for implementation of the present

transformation and the results are summarized in Table 1. Various catalytic amounts of copper salts were examined in the presence of molecular oxygen and K₂CO₃ base in CH₃CN solvent at 80 °C for the reaction of **1a**. The use of catalytic amounts of CuCl, CuCl₂, Cu(OAc)₂, Cu(OTf)₂, Cu(acac)₂ (acac: acetylacetonate), and Cu(hfacac)₂ (hfacac: hexafluoroacetylacetonate) proved to be inferior to the formation of the expected product **2a** (entries 1-6), in which Cu(hfacac)₂ afforded **2a** with the highest yield of 31% with recovery of **1a**. It was mentioned that in the absence of K₂CO₃, the catalytic Cu(hfacac)₂ did afford **2a** in 30% yield, but the remaining **1a** was completely decomposed (entry 7). However, further efforts to render catalytic transformations using Cu(hfacac)₂ as a catalyst gave unsatisfactory results (SI, Table S1). The structure of **2a** was determined unambiguously by single crystal X-ray crystallography (SI, Figure S1). Interestingly, in the crystal structure of **2a**, the two methyl groups are substituted at two nitrogen atoms of the DHII core, respectively, indicating the involvement of an *N*-methyl transfer process in the present transformation. To our delight, a significantly improved yield (80%) of **2a** was obtained using a stoichiometric amount of Cu(hfacac)₂ (1 equiv) in conjunction with K₂CO₃ (3 equiv) under oxygen (entry 8). It was noted that Cu(hfacac)₂ was highly superior to the other copper salts in this stoichiometric reaction (SI, Table S2). The reaction under an air atmosphere led to a very poor yield of **2a** with a serious decomposition of **1a** (entry 9), indicating the critical role of molecular oxygen. The use of other oxidants instead of O₂, such as *tert*-butyl hydroperoxide (TBHP), di-*tert*-butylperoxide (DTBP), PhI(OAc)₂, and *o*-chloranil, resulted in a serious decomposition of **1a** (entries 10-13). K₂CO₃ proved to be the most effective base (SI, Table S2) and without bases the reaction led to complete decomposition (entry 14).

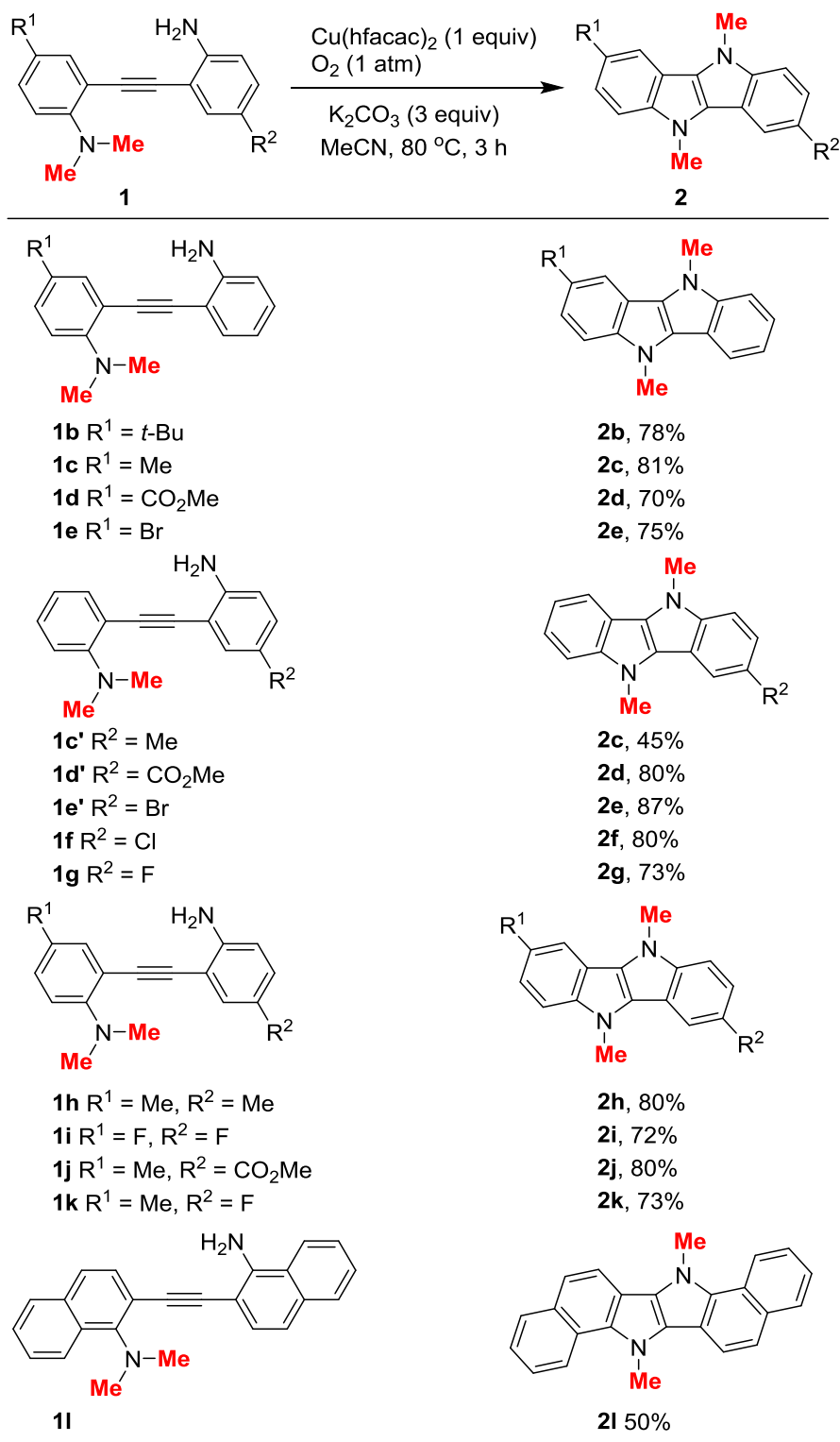
Under the optimal conditions obtained from entry 8 in Table 1, several structurally similar *o*-alkynylanilines **3a-d** were examined as shown in Scheme 2. No reaction occurred with 2-(phenylethynyl)aniline (**3a**), but *N,N*-dimethyl-2-(phenylethynyl)aniline (**3b**) afforded the desired indole product **4b** in 5% yield. The reactions of 2-((2-aminophenyl)ethynyl)-*N*-methylaniline (**3c**) and 2,2'-(ethyne-1,2-diyl)bis(*N*-methylaniline) (**3d**) afforded the *N*-methyl-protected indole products **4c** and **4d** in 20% and 70% yields, respectively, without forming the corresponding DHII products. Although the diaryl alkyne **3e** bearing both *N,N*-dimethylamine and secondary *N*-methylamine groups at the *ortho*-position of two phenyl rings, respectively, underwent the mechanistically related reaction to produce the corresponding product **2a** via a demethylation, the yield was as low as 10%. The significant reactivity difference between the reactions of **1a** and **3a-f** revealed the indispensable role of the molecular structure of **1a** for the efficient construction of the DHII scaffold.

Scheme 2. Optimization of *o*-Alkynylaniline Substrates



The electronic effect of substituents on the starting aniline moieties has been studied under the standard conditions as shown in Scheme 3. It was noted that all the reactions were completed within 3 h without formation of other byproducts including the corresponding indoles. 2-((2-Aminophenyl)ethynyl)-*N,N*-dimethylanilines with electron-rich substituents, such as *t*-Bu (**1b**) and Me (**1c**) at the *para*-position (R^1) of *N,N*-dimethylamine afforded slightly higher yields of the corresponding DHIs **2b** and **2c** as compared to the substrates with electron-poor substituents, such as CO₂Me (**1d**) and Br (**1e**) at R^1 . The introduction of an electron-rich substituent of methyl (**1c'**) at the *para*-position (R^2) of the primary amine lowered the yield of **2c** (45%). In contrast, the substrates with electron-poor substituents, such as CO₂Me (**1d'**), Br (**1e'**), Cl (**1f**), and F (**1g**) at R^2 afforded high yields of the corresponding DHIs. Comparatively, the presence of both electron-rich (**1h**) and -poor (**1i**) substituents at R^1 and R^2 , respectively, did not affect the efficiency in achieving high yields of **2h** and **2i**. As expected, the substrates **1j** and **1k** having both electron-rich and -poor substituents at R^1 and R^2 , respectively, showed high compatibility and efficiency to furnish the corresponding DHIs **2j** and **2k** in high yields. Interestingly, **1l** composed of bis(naphthalen-1-amine) also underwent the present diamination smoothly to give the highly π -extended DHII derivative **2l** in 50% yield. It is noted that presumably the relatively low mass balance of the present reactions is in correlation with the low stability of the proposed radical species **B** and **C** as shown in Scheme 6.

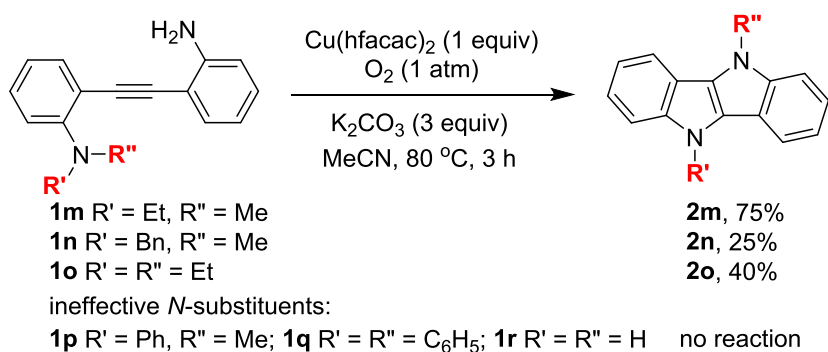
Scheme 3. Electronic Effect of Substituents^a



^a Reaction conditions: **1** (0.2 mmol), $\text{Cu}(\text{hfacac})_2 \cdot x\text{H}_2\text{O}$ (1 equiv), O_2 balloon (1 atm), K_2CO_3 (3 equiv), CH_3CN (0.2 M), at 80 °C for 3 h. The isolated yields are shown.

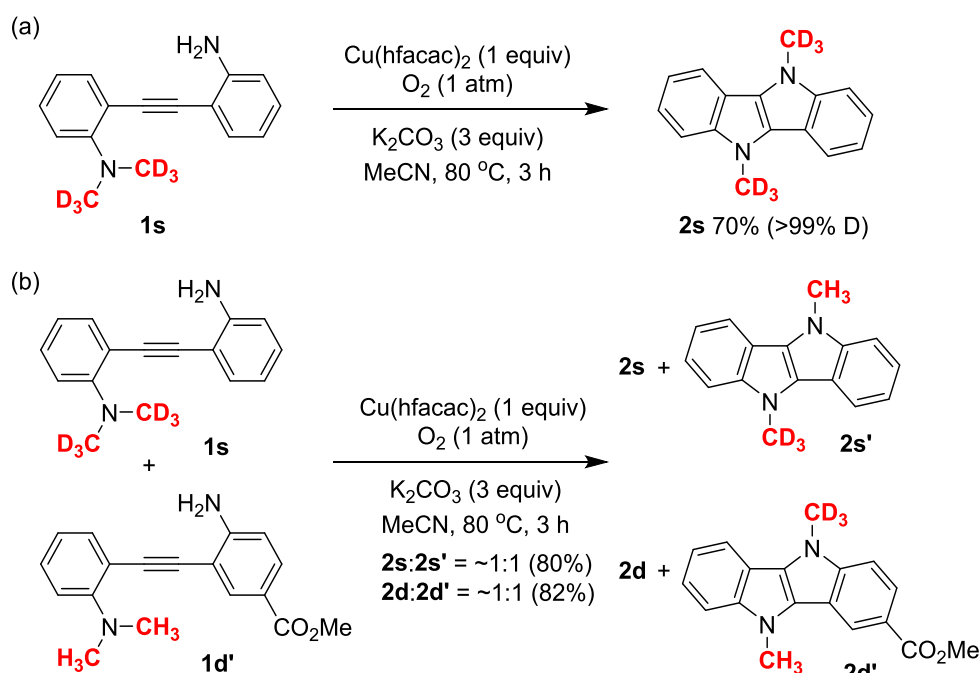
We also examined other bis(2-aminophenyl)acetylenes (**1m-r**) by replacement of *N,N*-dimethylamine with other *N,N*-difunctional amines without changing the primary amine group under the standard conditions (Scheme 4). Substrate **1m** having an *N*-ethyl-*N*-methyl group showed a comparable reactivity for constructing the corresponding DHII **2m**. The reactions with **1n** and **1o** bearing *N*-benzyl-*N*-methylamine and *N,N*-diethylamine, respectively, did afford the corresponding products **2n** and **2o**, but the yields were relatively low. In contrast, other *N*-substituents such as *N*-methyl-*N*-phenylamine (**1p**), *N,N*-diphenylamine (**1q**), and -NH₂ (**1r**) did not yield any products, demonstrating the importance of the *N,N*-dialkylamine group for constructing the DHII scaffold.

Scheme 4. Investigation of Other *N*-Substituents



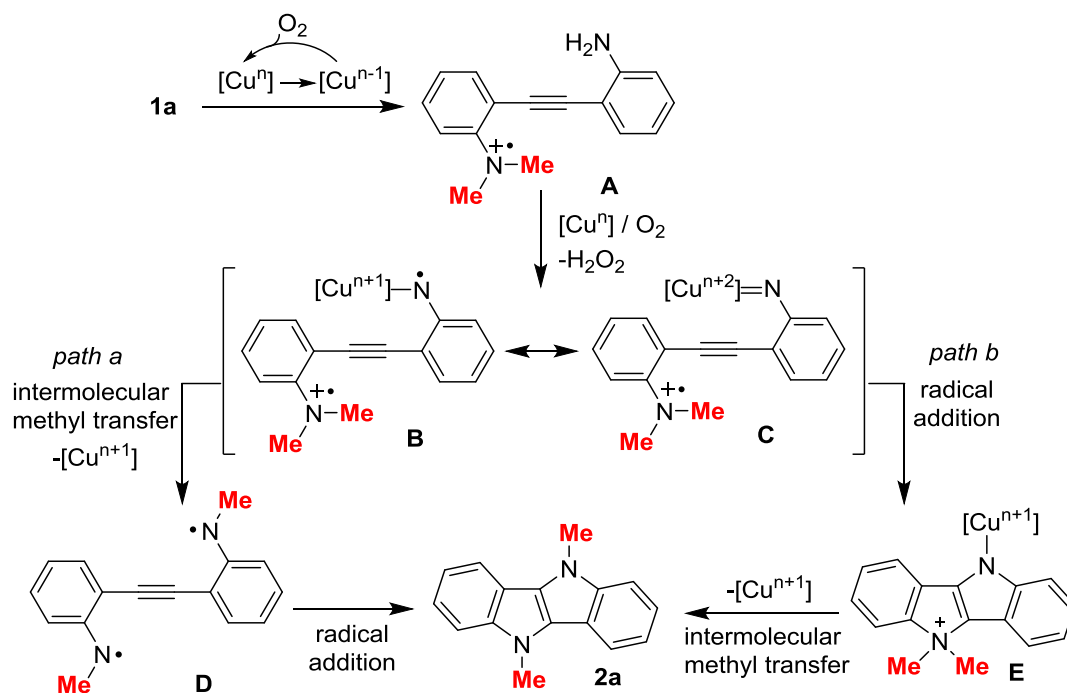
The deuterium labeling experiments were performed to gain some mechanistic insights. Under the standard conditions, the substrate **1s** having an *N,N*-bis(methyl-*d*₃)amine group yielded the corresponding product **2s** with two methyl-*d*₃ substituents at the two nitrogen atoms of the DHII core, respectively, without observation of a D-H exchange (Scheme 5a). This result clearly demonstrated that the methyl-*d*₃ group on the DHII core is originated from the *N,N*-bis(methyl-*d*₃)amine group. Moreover, a crossover reaction between the deuterated **1s** and the protonated **1d'** (1:1 ratio) was performed (Scheme 5b). Other than the corresponding products **2s** and **2d**, the crossover products **2s'** and **2d'** having both CH₃ and CD₃ at the DHII core were obtained with nearly a 1:1 ratio for **2s** vs **2s'** and **2d** vs **2d'** (also see SI, Scheme S1). The formation of the crossover products in an ~1:1 ratio implied that the *N*-methyl transfer should mainly proceed through an intermolecular pathway. In addition, the presence of 1 equiv of the radical scavengers, such as 3,5-di-*tert*-butyl-4-hydroxytoluene (BHT) or (2,2,6,6-tetramethylpiperidin-1-yl)oxyl (TEMPO), completely or partially inhibited the reaction of **1a** under the standard conditions (SI, Scheme S2), indicating the involvement of the radical species in the mechanism.

Scheme 5. Deuterium Labeling Experiments



While the exact mechanism remains to be confirmed, a tentative reaction pathway is outlined in Scheme 6 in terms of the experimental information, such as the crucial roles of the Cu salt and oxygen, electronic effect of substituents, unique structural design of the starting substrate, deuterium labeling experiments, and radical inhibiting reactions. Initially, a one-electron oxidation of the electron-rich *N,N*-dimethylamine by a copper salt takes place to form a radical cation **A**.⁷ The combination of copper with oxygen oxidizes the primary amine to afford an aniline-copper radical **B** along with the exclusion of H_2O_2 . The radical species **B** should be stabilized by its resonance form of the Cu-nitrenoid complex **C**.⁸ The role of K_2CO_3 is thought to decompose H_2O_2 generated in situ, which may be unfavorable for the stabilization of the less stable radical species **B** and/or **C**. Subsequently, an intermolecular *N*-methyl transfer⁹ takes place from the *N,N*-dimethylamine radical cation to the N-Cu radical in **B** or **C** to give the *N*-methylamine radical species **D** which undergoes an intramolecular radical addition to alkyne to form the corresponding product **2a** (path a). Alternately, an intramolecular radical addition to the alkyne moiety in **B** or **C** occurs prior to the *N*-methyl transfer to form a Cu-DHII indolium **E** which subsequently undergoes an intermolecular *N*-methyl transfer to afford **2a** (path b).

Scheme 6. Plausible Reaction Mechanism



3. Conclusion

In summary, a novel copper-mediated intramolecular oxidative diamination of alkyne has been developed through an *N*-methyl transfer process. The present diamination of the designed bis(2-aminophenyl)acetylenes bearing both *N,N*-dimethylamine and primary amine moieties enables structurally intriguing π -conjugated polyheterocyclic DHIs to be constructed in good to high yields with broad functional group compatibility. The combination of $Cu(hfacac)_2$ with molecular oxygen in the presence of K_2CO_3 is unique for achieving a high conversion efficiency. Notably, the *N*-methyl transfer is a critical process for the successful implementation of the present double annulation. Further mechanistic studies and application of the present methodology for synthesis of highly π -expanded heteropolyaromatic functional materials are in progress.

4. References and notes:

1. For related reviews, see: (a) Minatti, A.; Muñiz, K. *Chem. Soc. Rev.* **2007**, *36*, 1142. (b) Jensen, K. H.; Sigman, M. S. *Org. Biomol. Chem.* **2008**, *6*, 4083. (c) Cardona, F.; Goti, A. *Nat. Chem.* **2009**, *1*, 269. (d) Muñiz, K.; Martínez, J. *J. Org. Chem.* **2013**, *78*, 2168. (e) Zhu, Y.; Cornwall, R. G.; Du, H.; Zhao, B.; Shi, Y. *Acc. Chem. Res.* **2014**, *47*, 3665.
2. (a) Lucet, D.; Le Gall, T.; Mioskowski, C. *Angew. Chem., Int. Ed.* **1998**, *37*, 2580. (b) Saibabu Kotti, S. R. S.; Timmons, C.; Li, G. *Chem. Biol. Drug Des.* **2006**, *67*, 101.
3. For intramolecular diamination of alkynes, see: (a) Muñiz, K. *J. Am. Chem. Soc.* **2007**, *129*, 14542. (b) Okano, A.; Tsukamoto, K.; Kosaka, S.; Maeda, H.; Oishi, S.; Tanaka, T.; Fujii, N.; Ohno, H. *Chem. Eur. J.* **2010**, *16*, 8410. (c) Yao, B.; Wang, Q.; Zhu, J. *Angew. Chem., Int. Ed.* **2012**, *51*, 5170. (d) Ha, T. M.; Yao, B.; Wang, Q.; Zhu, J. *Org. Lett.* **2015**, *17*, 1750. For intermolecular deamination of alkynes, see: (e) Fukudome, Y.; Naito, H.; Hata, T.; Urabe, H. *J. Am. Chem. Soc.* **2008**, *130*, 1820. (f) Wang, W.; Shen, Y.; Meng, X.; Zhao, M.; Chen, Y.; Chen, B. *Org. Lett.* **2011**, *13*, 4514. (g) Zeng, J.; Tan, Y. J.; Leow, M. L.; Liu, X.-W. *Org. Lett.* **2012**, *14*, 4386. (h) Li, J.; Neuville, L. *Org. Lett.* **2013**, *15*, 1752.
4. (a) Kaszynski, P.; Dougherty, D. A. *J. Org. Chem.* **1993**, *58*, 5209. (b) Murray, M. M.; Kaszynski, P.; Kaisaki, D. A.; Chang, W.; Dougherty, D. A. *J. Am. Chem. Soc.* **1994**, *116*, 8152. (c) Owczarczyk, Z. R.; Braunecker, W. A.; Garcia, A.; Larsen, R.; Nardes, A. M.; Kopidakis, N.; Ginley, D. S. Olson, D. C. *Macromolecules* **2013**, *46*, 1350. (d) Lai, Y.-Y.; Yeh, J.-M.; Tsai, C.-E.; Cheng, Y.-J. *Eur. J. Org. Chem.* **2013**, 5076. (e) Sim, J.; Do, K.; Song, K.; Sharma, A.; Biswas, A.; Sharma, G. D.; Ko, J. *Org. Electron.* **2016**, *30*, 122. (f) Jin, Y.; Kim, K.; Song, S.; Kim, J.; Kim, J.; Park, S. H.; Lee, K.; Suh, H. *Bull. Korean Chem. Soc.* **2006**, *27*, 1043. (g) Bergman, J.; Janosik, T.; Wahlstrom, N. *Adv. Heterocycl. Chem.* **2001**, *80*, 1. (h) Qiu, L.; Yu, C.; Zhao, N.; Chen, W.; Guo, Y.; Wan, X.; Yang, R.; Liu, Y. *Chem. Commun.* **2012**, *48*, 12225.
5. (a) Janiga, A.; Gryko, D. T. *Chem.-Asian J.* **2014**, *9*, 3036. (b) Hung, T. Q.; Hancker, S.; Villinger, A.; Lochbrunner, S.; Dang, T. T.; Friedrich, A.; Breitsprecher, W.; Langer, P. *Org. Biomol. Chem.* **2015**, *13*, 583.
6. (a) Zhao, J.; Oniwa, K.; Asao, N.; Yamamoto, Y.; Jin, T. *J. Am. Chem. Soc.* **2013**, *135*, 10222. (b) Zhao, J.; Asao, N.; Yamamoto, Y.; Jin, T. *J. Am. Chem. Soc.* **2014**, *136*, 9540. (c) Jiang, H.; Ferrara, G.; Zhang, X.; Oniwa, K.; Islam, A.; Han, L.; Sun, Y.-J.; Bao, M.; Asao, N.; Yamamoto, Y.; Jin, T. *Chem.-Eur. J.* **2015**, *21*, 4065. (d) Zhao, J.; Xu, Z.; Oniwa, K.; Asao, N.; Yamamoto, Y.; Jin, T. *Angew. Chem., Int. Ed.* **2016**, *55*, 259. (e) Jin, T.; Zhao, J.; Asao, N.; Yamamoto, Y. *Chem.-Eur. J.* **2014**, *20*, 3554.
7. For selected reviews on aerobic copper-mediated reactions, see: (a) Wendlandt, A. E.; Suess,

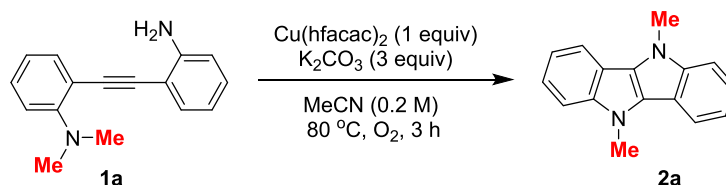
- A. M.; Stahl, S. S. *Angew. Chem., Int. Ed.* **2011**, *50*, 11062. (b) Allen, S. E.; Walvoord, R. R.; Padilla-Salinas, R.; Kozłowski, M. C. *Chem. Rev.* **2013**, *113*, 6234. (c) Girard, S. A.; Knauber, T.; Li, C.-J. *Angew. Chem., Int. Ed.* **2014**, *53*, 74. (d) Guo, X.-X.; Gu, D.-W.; Wu, Z.; Zhang, W. *Chem. Rev.* **2015**, *115*, 1622.
8. For reviews on metal-nitrenoid-mediated reactions, see: (a) Davies, H. M. L.; Manning, J. R. *Nature* **2008**, *451*, 417. (b) Fantauzzi, S.; Caselli, A.; Gallo, E. *Dalton Trans.* **2009**, 5434. (c) Gephart, R. T.; Warren, T. H. *Organometallics* **2012**, *31*, 7728. (d) Dequierez, G.; Pons, V.; Dauban, P. *Angew. Chem., Int. Ed.* **2012**, *51*, 7384. (e) Shin, K.; Kim, H.; Chang, S. *Acc. Chem. Res.* **2015**, *48*, 1040.
 9. Nakamura, I.; Gima, S.; Kudo, Y.; Terada, M. *Angew. Chem., Int. Ed.* **2015**, *54*, 7154.

5. Experimental Section

General Information. ^1H NMR, ^{13}C NMR and ^{19}F NMR spectra were recorded on JEOL JNM AL 400 (400 MHz), JEOL JNM AL 700 (700 MHz), and JNM ECA 700 (700MHz) spectrometers. ^1H NMR spectra are reported as follows: chemical shift in ppm (δ) relative to the chemical shift of CDCl_3 at 7.26 ppm, CD_2Cl_2 at 5.32 ppm, acetone- d_6 at 2.04 ppm, THF- d_8 at 3.58 ppm integration, multiplicities (s = singlet, d = doublet, t = triplet, q = quartet, m = multiplet, and br = broadened), and coupling constants (Hz). ^{13}C NMR spectra were recorded on JEOL JNM AL 400 (100.5 MHz) and JEOL JNM AL 400 (176.0 MHz) spectrometers with complete proton decoupling, and chemical shift reported in ppm (δ) relative to the central line for CDCl_3 at 77 ppm, CD_2Cl_2 at 53.8 ppm, Acetone- d_6 at 29.8 ppm, and THF- d_8 at 66.5 ppm. ^{19}F NMR were recorded on JNM ECA-700 (658.8 MHz, ppm) spectrophotometer with chemical shift reported in ppm (δ) relative to CFCl_3 as an external standard ($\delta = 0$ ppm). High-resolution mass spectra were obtained on a BRUKER APEXIII spectrometer and JEOL JMS-700 MStation operator. Column chromatography was carried out employing silica gel 60 N (spherical, neutral, 40–63 μm , Merck Chemicals) and basic silica gel NH-DM1020 (Fuji Silysia Chemical Ltd). Analytical thin-layer chromatography (TLC) was performed on 0.2 mm precoated plate Kieselgel 60 F254 (Merck).

Materials. The commercially available chemicals were used as received. Structures of the products were identified by ^1H NMR, ^{13}C NMR, HRMS, and compared with **2a** which was confirmed unambiguously by X-ray crystallography: CCDC 1469095 contains the supplementary crystallography data of **2a**. This data can be download free of charge via www.ccdc.cam.ac.uk/conts/retrieving.html.

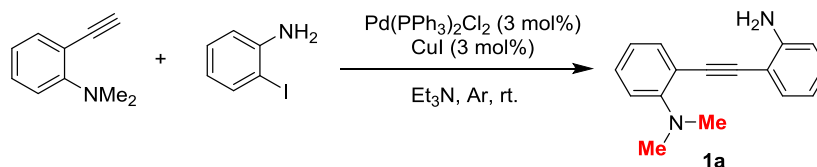
Representative procedure for Cu-mediated synthesis of 5,10-dimethyl-5,10-dihydroindolo[3,2-*b*]indole **2a**



To a solution of starting material **1a** (47.2 mg, 0.2 mmol) in MeCN (1.0 mL) were added $\text{Cu}(\text{hfacac})_2 \cdot x\text{H}_2\text{O}$ (95.5 mg, 0.2 mmol) and K_2CO_3 (82.8 mg, 0.6 mmol). The reaction mixture was stirred for 3 h at 80 °C under O_2 balloon. The resulting mixture was filtered through a short basic silica pad (Fuji Silysia) using Et_2O or hexane/ EtOAc as eluent. After concentration, the residue was purified by quick column chromatography using basic silica gel (hexane: EtOAc =

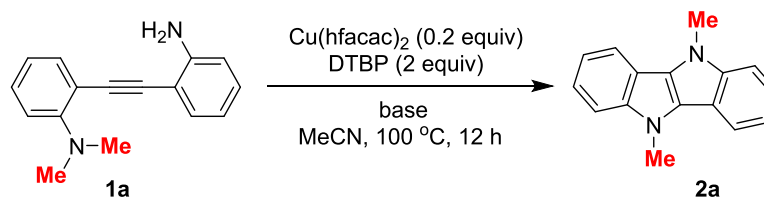
10:1) to give **2a** (37.5 mg, 0.16 mmol) in 80% yield as white solid.

Representative procedure for synthesis of 2-((2-aminophenyl)ethynyl)-*N,N*-dimethylaniline **1a**



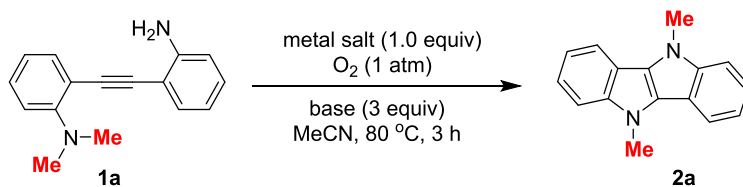
To a mixture of 2-ethynyl-*N,N*-dimethylaniline (1.59 g, 11 mmol), 2-iodoaniline (2.19 g, 10 mmol), PdCl₂(PPh₃)₃ (210 mg, 0.3 mmol), and CuI (5.7 mg, 0.3 mmol) was added triethylamine (0.3 M, 33 mL) in a 50 mL of Schlenk tube under Ar atmosphere. The reaction mixture was stirred for 12 h at room temperature. The resulting mixture was washed with Et₂O and filtered through a Celite pad. The filtrate was concentrated under reduced pressure to afford crude product, which was purified by silica gel chromatography (hexane:EtOAc = 7:1) to give **1a** (2.24 g, 9.5 mmol) in 95% yield as pale yellow oil.

Table S1. Optimization of bases for catalytic reaction conditions^a



entry	Base (0.6 equiv)	2a (%) ^b	1a (%) ^b
1 ^c	K ₂ CO ₃	31	57
2	K ₂ CO ₃	50	48
3	K ₃ PO ₄	35	61
4	CS ₂ CO ₃	30	66
5	Na ₂ CO ₃	37	0
6	Ag ₂ CO ₃	25	0
7	Na(hfacac) ₂	18	0
8	KBF ₄	27	10

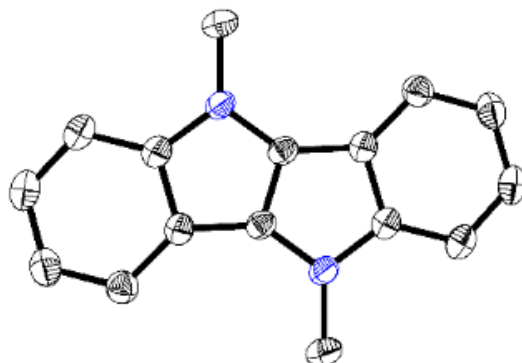
^a Reaction conditions: **1a** (0.2 mmol), Cu(hfacac)₂·xH₂O (0.2 equiv), base (0.6 equiv), DTBP (2 equiv) in MeCN (0.2 M) at 100 °C for 12 h. ^b ¹H NMR yield determined using CH₂Br₂ as an internal standard. ^c O₂ was used instead of DTBP at 80 °C.

Table S2. Optimization of stoichiometric reaction conditions^a

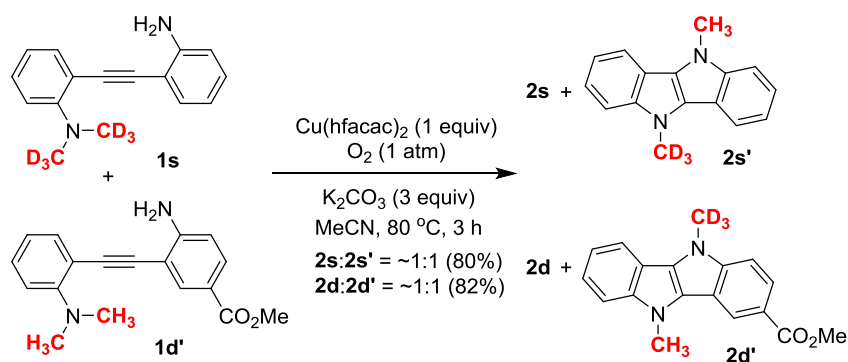
entry	metal salt (1 equiv)	base (3 equiv)	2a (%) ^b	1a (%) ^b
1	Cu(hfacac) ₂	K ₂ CO ₃	85 (80)	0
2	Cu(tfacac) ₂	K ₂ CO ₃	0	0
3	Cu(acac) ₂	K ₂ CO ₃	0	80
4	Cu(OAc) ₂	K ₂ CO ₃	6	trace
5	CuBr	K ₂ CO ₃	trace	0
6	CuBr ₂	K ₂ CO ₃	0	0
7	Cu(OTf) ₂	K ₂ CO ₃	0	20
8	Co(hfacac) ₂	K ₂ CO ₃	0	99
9	Ni(hfacac) ₂	K ₂ CO ₃	0	99
10	Fe ₂ (hfacac) ₃	K ₂ CO ₃	0	60
11	Mn(hfacac) ₂	K ₂ CO ₃	0	80
12	Cu(hfacac) ₂	Na ₂ CO ₃	7	0
13	Cu(hfacac) ₂	Cs ₂ CO ₃	22	77
14	Cu(hfacac) ₂	KOAc	10	0
15	Cu(hfacac) ₂	K ₃ PO ₄	45	15

^a Reaction conditions: **1a** (0.2 mmol), metal salt (1.0 equiv), base (6.0 equiv), O₂ balloon in MeCN (0.2 M) at 80 °C for 3 h. ^b ¹H NMR yield determined using CH₂Br₂ as an internal standard. Isolated is shown in parenthesis.

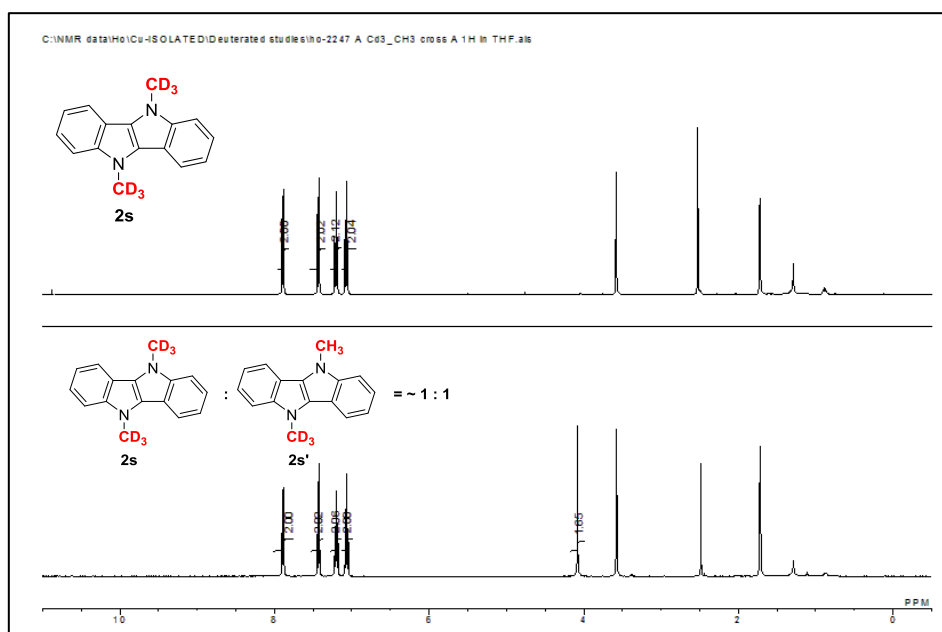
Figure S1. ORTEP drawing of the DHII compound **2a**. Hydrogen atoms are omitted for clarity. Thermal ellipsoids are shown at 50% probability.



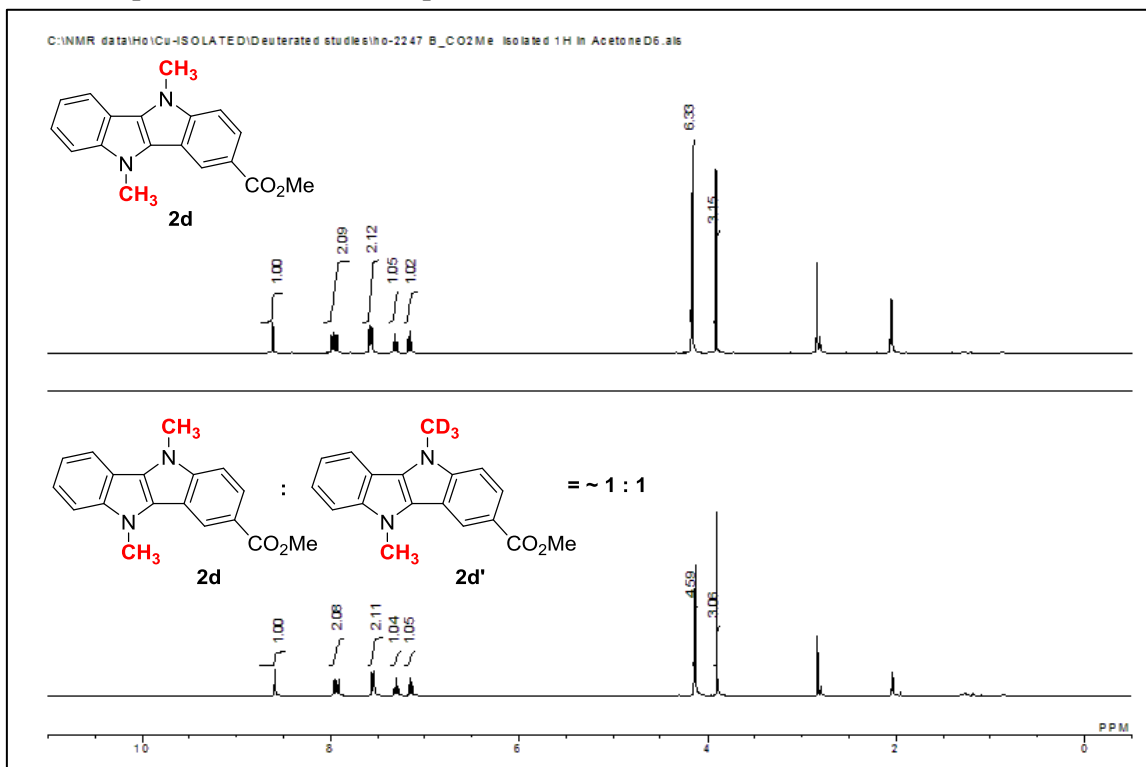
Scheme S1. Crossover experiments with the protonated **1d'** and the deuterated **1s**



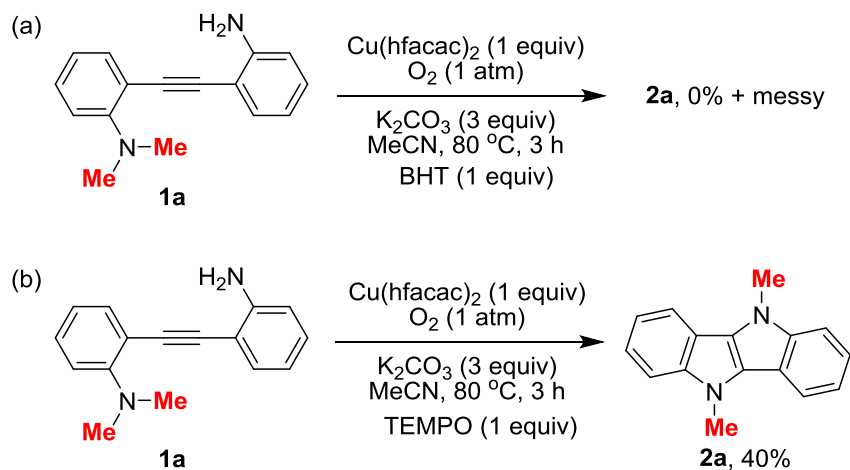
^1H NMR spectra of the crossover products: **2s and **2s'** mixture was measured in $\text{THF-}d_8$**



¹H NMR spectra of the crossover products: 2d and 2d' mixture was measured in acetone-*d*₆

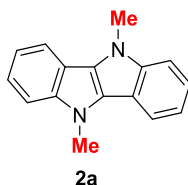


Scheme S2. Radical scavenging experiments in the presence of TEMPO or BHT.



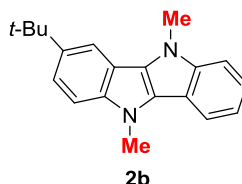
Analytical data for compounds.

5,10-Dimethyl-5,10-dihydroindolo[3,2-*b*]indole, (2a)



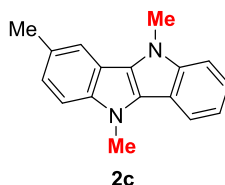
White solid (80%, 0.16 mmol, 37.5 mg); ^1H NMR (400 MHz, THF- d_8) δ 7.89 (d, J = 8.0 Hz, 2H), 7.44 (d, J = 8.0 Hz, 2H), 7.22 (t, J = 8.0 Hz, 2H), 7.06 (t, J = 8.0 Hz, 2H), 4.10 (s, 6H); ^{13}C NMR (100 MHz, THF- d_8) δ 141.42, 126.28, 121.33, 117.82, 117.19, 115.02, 109.28, 30.72; HRMS (APCI) calcd for $\text{C}_{16}\text{H}_{14}\text{N}_2$, $[\text{M}+\text{H}]^+$: 235.12297, found: 235.12290.

3-(*tert*-Butyl)-5,10-dimethyl-5,10-dihydroindolo[3,2-*b*]indole, (2b)



White solid (78%, 0.156 mmol, 45.3 mg); ^1H NMR (400 MHz, THF- d_8) δ 7.89 (d, J = 0.8 Hz, 1H), 7.87 (d, J = 8.0 Hz, 1H), 7.43 (d, J = 7.6 Hz, 1H), 7.38-7.31 (m, 2H), 7.18 (t, J = 8.0 Hz, 1H), 7.05 (d, J = 8.0 Hz, 1H), 4.10 (s, 3H), 4.05 (s, 3H), 1.42 (s, 9H); ^{13}C NMR (100 MHz, THF- d_8) δ 141.33, 140.47, 139.87, 126.50, 126.44, 121.09, 119.54, 117.71, 117.08, 115.11, 114.82, 113.09, 109.24, 108.92, 34.27, 31.05, 30.80, 30.76; HRMS (APCI) calcd for $\text{C}_{20}\text{H}_{22}\text{N}_2$, $[\text{M}+\text{H}]^+$: 291.18558, found: 291.18560.

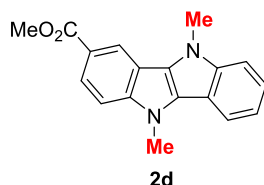
3,5,10-Trimethyl-5,10-dihydroindolo[3,2-*b*]indole, (2c)



White solid (from 1c: 81%, 0.162 mmol, 40.2 mg; from 1c': 45%, 0.09 mmol, 22.3 mg); ^1H NMR (400 MHz, CD_2Cl_2) δ 7.90 (d, J = 8.0 Hz, 1H), 7.71 (s, 1H), 7.44 (d, J = 8.4 Hz, 1H), 7.34 (d, J = 8.4 Hz, 1H), 7.29 (t, J = 8.0 Hz, 1H), 7.18-7.13 (m, 2H), 4.09 (s, 3H), 4.07 (s, 3H), 2.54 (s, 3H); ^{13}C NMR (100 MHz, CD_2Cl_2) δ 141.39, 140.00, 127.57, 126.74, 126.24, 123.41, 121.74, 118.20, 117.57, 117.45, 115.09, 115.06, 109.71, 109.48, 31.95, 31.89, 21.59; HRMS (APCI) calcd for

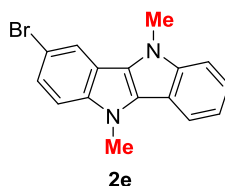
C₁₇H₁₆N₂, [M+H]⁺: 249.13862, found: 249.13865.

Methyl 5,10-dimethyl-5,10-dihydroindolo[3,2-*b*]indole-3-carboxylate, (2d)



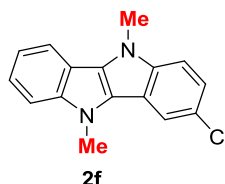
White solid (from 1d: 70%, 0.14 mmol, 40.9 mg; from 1d': 80%, 0.16 mmol, 46.7 mg); ¹H NMR (400 MHz, Acetone-*d*₆) δ 8.60 (d, *J* = 1.6 Hz, 1H), 7.98-7.91 (m, 2H), 7.56 (d, *J* = 8.8 Hz, 1H), 7.55 (d, *J* = 8.0 Hz, 1H), 7.33-7.28 (m, 1H), 7.15 (td, *J* = 8.4, 1.2 Hz, 1H), 4.15 (s, 3H), 4.14 (s, 3H), 3.90 (s, 3H); ¹³C NMR (100 MHz, Acetone-*d*₆) 168.10, 143.85, 142.26, 127.99, 127.13, 123.43, 123.05, 120.81, 120.75, 119.26, 118.47, 115.40, 115.03, 110.69, 110.06, 51.90, 31.97, 31.84; HRMS (APCI) calcd for C₁₈H₁₆N₂O₂, [M+H]⁺: 293.12845, found: 293.12846.

3-Bromo-5,10-dimethyl-5,10-dihydroindolo[3,2-*b*]indole, (2e)



White solid (from 1e: 75%, 0.15 mmol, 46.8 mg; from 1e': 87%, 0.174 mmol, 54.3 mg); ¹H NMR (400 MHz, Acetone-*d*₆/CD₂Cl₂) δ 8.01 (d, *J* = 2.0 Hz, 1H), 7.91 (d, *J* = 7.6 Hz, 1H), 7.47 (d, *J* = 8.4 Hz, 1H), 7.39 (d, *J* = 8.8 Hz, 1H), 7.34-7.27 (m, 2H), 7.15-7.11 (t, *J* = 8.0 Hz, 1H), 4.06 (s, 3H), 4.05 (s, 3H); ¹³C NMR (100 MHz, Acetone-*d*₆/CD₂Cl₂) δ 142.13, 140.20, 127.89, 125.61, 124.44, 122.89, 120.29, 118.82, 118.29, 116.50, 115.01, 111.77, 111.17, 110.28, 31.74, 31.61.; HRMS (APCI) calcd for C₁₆H₁₃BrN₂, [M+H]⁺: 313.03349, found: 313.03351.

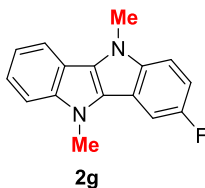
3-Chloro-5,10-dimethyl-5,10-dihydroindolo[3,2-*b*]indole, (2f)



White solid (80%, 0.16 mmol, 42.9 mg); ¹H NMR (400 MHz, CD₂Cl₂) δ 7.88 (d, *J* = 8.0 Hz, 1H), 7.83 (d, *J* = 2.0 Hz, 1H), 7.43 (d, *J* = 8.4 Hz, 1H), 7.35-7.30 (m, 2H), 7.23 (dd, *J* = 8.8, 2.0 Hz,

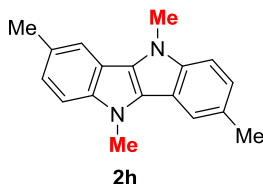
1H), 7.17 (t, $J = 7.6$ Hz, 1H), 4.03 (s, 3H), 4.00 (s, 3H); ^{13}C NMR (100 MHz, CD_2Cl_2) δ 141.66, 139.55, 127.71, 125.49, 123.60, 122.52, 121.59, 118.48, 117.86, 116.97, 115.42, 114.67, 110.71, 109.87, 31.98, 31.82.; HRMS (APCI) calcd for $\text{C}_{16}\text{H}_{13}\text{ClN}_2$, $[\text{M}+\text{H}]^+$: 269.08400, found: 269.08403.

3-Fluoro-5,10-dimethyl-5,10-dihydroindolo[3,2-b]indole, (2g)



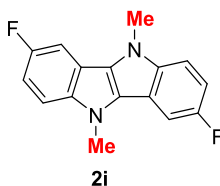
White solid (73%, 0.146 mmol, 36.8 mg); ^1H NMR (400 MHz, $\text{THF}-d_8$) δ 7.89 (d, $J = 7.6$ Hz, 1H), 7.60 (dd, $J = 9.6, 2.4$ Hz, 1H), 7.43 (d, $J = 8.4$ Hz, 1H), 7.38 (dd, $J = 8.8, 4.4$ Hz, 1H), 7.23 (t, $J = 7.6$, 1H), 7.07 (t, $J = 7.6$ Hz, 1H), 6.98 (td, $J = 9.2, 2.4$ Hz, 1H), 4.05 (s, 3H), 4.03 (s, 3H); ^{13}C NMR (100 MHz, $\text{THF}-d_8$) δ 157.00 (d, $J^I = 230.5$ Hz), 141.84, 137.98, 128.02, 125.90 (d, $J^6 = 4.2$ Hz), 121.96, 117.90, 117.48, 114.81, 114.38 (d, $J^I = 10.7$ Hz), 109.90 (d, $J^5 = 9.1$ Hz), 109.38, 108.94 (d, $J^2 = 25.5$ Hz), 102.35 (d, $J^3 = 24.7$ Hz), 30.83, 30.53; ^{19}F NMR (658.8 MHz, $\text{THF}-d_8$) δ -130.90; HRMS (MALDI) calcd for $\text{C}_{16}\text{H}_{13}\text{FN}_2$ $[\text{m/z}]$: 252.10573, found: 252.10574.

3,5,8,10-Tetramethyl-5,10-dihydroindolo[3,2-b]indole, (2h)



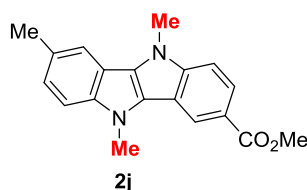
White solid (80%, 0.16 mmol, 41.9 mg); ^1H NMR (400 MHz, $\text{THF}-d_8$) δ 7.67 (s, 2H), 7.29 (d, $J = 8.4$ Hz, 2H), 7.02 (d, $J = 8.0$ Hz, 2H), 4.04 (s, 6H), 2.47 (s, 6H); ^{13}C NMR (100 MHz, $\text{THF}-d_8$) δ 140.06, 126.61, 126.31, 122.71, 117.00, 115.26, 108.95, 83.90, 30.74, 20.76; HRMS (APCI) calcd for $\text{C}_{18}\text{H}_{18}\text{N}_2$, $[\text{M}+\text{H}]^+$: 263.15428, 263.15430.

3,8-Difluoro-5,10-dimethyl-5,10-dihydroindolo[3,2-b]indole, (2i)



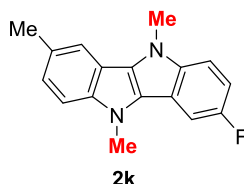
White solid (72%, 0.144 mmol, 38.9 mg); ^1H NMR (400 MHz, CDCl_3) δ 7.51 (dd, $J = 9.2, 2.4$ Hz, 2H), 7.31 (dd, $J = 8.8, 4.4$ Hz, 2H), 7.06 (td, $J = 9.2, 2.4$ Hz, 2H), 4.03 (s, 6H); ^{13}C NMR (100 MHz, CDCl_3) δ 156.74 (d, $J^I = 231.8$ Hz), 137.93, 127.43 (d, $J^J = 4.1$ Hz), 113.98 (d, $J^I = 10.7$ Hz), 105.10 (d, $J^J = 18.2$ Hz), 109.92 (d, $J^J = 1.7$ Hz), 102.77 (d, $J^J = 21.7$ Hz), 31.69; ^{19}F NMR (658.8 MHz, CDCl_3) δ -127.46; HRMS (APCI) calcd for $\text{C}_{16}\text{H}_{12}\text{F}_2\text{N}_2$ $[\text{M}+\text{H}]^+$: 271.10413, found: 271.10414.

Methyl 5,8,10-trimethyl-5,10-dihydroindolo[3,2-*b*]indole-3-carboxylate, (2j)



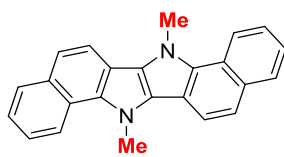
White solid (80%, 0.16 mmol, 49.0mg); ^1H NMR (400 MHz, $\text{THF-}d_8$) δ 8.60 (s, 1H), 7.91 (dd, $J = 8.8, 1.6$ Hz, 1H), 7.71 (d, $J = 0.8$ Hz, 1H), 7.46 (d, $J = 8.4$ Hz, 1H), 7.36 (d, $J = 8.4$ Hz, 1H), 7.09 (d, $J = 8.4$ Hz, 1H), 4.10 (s, 3H), 4.07 (s, 3H), 3.87 (s, 3H), 2.49 (s, 3H); ^{13}C NMR (100 MHz, $\text{THF-}d_8$) δ 167.01, 143.05, 140.12, 127.18, 126.87, 126.65, 123.46, 122.48, 119.99, 119.77, 117.13, 114.83, 114.39, 109.27, 108.70, 50.74, 30.87, 30.82, 20.74; HRMS (APCI) calcd for $\text{C}_{19}\text{H}_{18}\text{N}_2\text{O}_2$, $[\text{M}+\text{H}]^+$: 307.14410, 307.14413.

3-Fluoro-5,8,10-trimethyl-5,10-dihydroindolo[3,2-*b*]indole, (2k)



White solid (73%, 0.146 mmol, 38.9 mg); ^1H NMR (400 MHz, CD_2Cl_2) δ 7.55 (s, 1H), 7.38 (dd, $J = 9.6, 2.4$ Hz, 1H), 7.20-7.16 (m, 2H), 7.02 (dd, $J = 8.0, 1.2$ Hz, 1H), 6.90 (td, $J = 9.2, 2.4$ Hz, 1H), 3.89 (s, 3H), 3.84 (s, 3H), 2.41 (s, 3H); ^{13}C NMR (100 MHz, CD_2Cl_2) δ 156.97 (d, $J^I = 230.2$ Hz), 140.24, 137.94, 127.90, 127.63, 126.28 (d, $J^J = 4.2$ Hz), 124.00, 117.65, 114.86, 114.38 (d, $J^I = 10.8$ Hz), 110.18 (d, $J^J = 9.9$ Hz), 109.50, 109.28 (d, $J^J = 26.4$ Hz), 102.63 (d, $J^J = 24.7$ Hz), 31.96, 31.72, 21.56; ^{19}F NMR (658.8 MHz, CD_2Cl_2) δ -128.65; HRMS (APCI) calcd for $\text{C}_{17}\text{H}_{15}\text{FN}_2$, $[\text{M}+\text{H}]^+$: 267.12920, found: 267.12922.

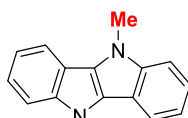
7,14-Dimethyl-7,14-dihydrobenzo[*g*]benzo[6,7]indolo[3,2-*b*]indole, (2l)



2l 50%

Yellow solid (50%, 0.1 mmol, 33.4 mg); ^1H NMR (400 MHz, $\text{CD}_2\text{Cl}_2/\text{CS}_2$) δ 8.68 (d, $J = 8.8$ Hz, 2H), 8.13 (d, $J = 8.8$ Hz, 2H), 8.00 (d, $J = 8.8$ Hz, 2H), 7.61 (d, $J = 9.2$ Hz, 2H), 7.60 (td, $J = 8.4$, 1.6 Hz, 2H), 7.49-7.45 (m, 2H), 4.71 (s, 6H); ^{13}C NMR (100 MHz, $\text{CD}_2\text{Cl}_2/\text{CS}_2$) δ 135.05, 131.51, 129.56, 127.45, 125.57, 124.18, 123.76, 121.55, 120.19, 117.71, 111.46, 37.55; HRMS (APCI) calcd for $\text{C}_{24}\text{H}_{18}\text{N}_2$, $[\text{M}]$: 335.15428, found: 335.15430.

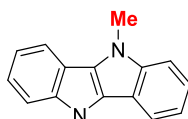
5-Ethyl-10-methyl-5,10-dihydroindolo[3,2-*b*]indole, (2m)



2m

White solid (75%, 0.15 mmol, 37.2 mg); ^1H NMR (400 MHz, CD_2Cl_2) δ 7.94 (d, $J = 7.6$ Hz, 1H), 7.88 (d, $J = 8.0$ Hz, 1H), 7.48 (t, $J = 8.0$, 2H), 7.35-7.29 (m, 2H), 7.22-7.16 (m, 2H), 4.55 (q, $J = 7.2$ Hz, 2H), 4.11 (s, 3H), 1.51 (t, $J = 7.2$ Hz, 3H); ^{13}C NMR (100 MHz, CD_2Cl_2) δ 141.55, 140.39, 126.92, 125.51, 121.97, 121.94, 118.48, 118.34, 117.84, 115.18, 114.90, 109.86, 40.18, 31.89, 15.40, 15.35; HRMS (APCI) calcd for $\text{C}_{17}\text{H}_{16}\text{N}_2$, $[\text{M}+\text{H}]^+$: 249.13862, found: 249.13869.

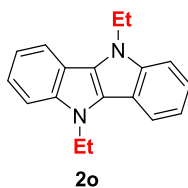
5-Benzyl-10-methyl-5,10-dihydroindolo[3,2-*b*]indole, (2n)



2n

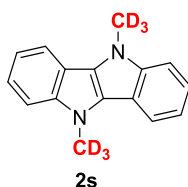
Yellow solid (25%, 0.05 mmol, 16.2 mg); ^1H NMR (400 MHz, $\text{Acetone-}d_6$) δ 8.01 (d, $J = 7.2$ Hz, 1H), 7.75 (d, $J = 7.2$ Hz, 1H), 7.61 (d, $J = 8.0$ Hz, 1H), 7.52 (d, $J = 8.4$ Hz, 1H), 7.25-7.12 (m, 7H), 7.14 (t, $J = 8.0$ Hz, 1H), 7.04 (t, $J = 7.2$ Hz), 5.82 (s, 2H), 4.17 (s, 3H); ^{13}C NMR (100 MHz, $\text{Acetone-}d_6$) δ 142.19, 141.88, 139.62, 129.41, 128.08, 127.51, 122.71, 122.52, 119.31, 118.97, 118.51, 118.48, 116.02, 115.56, 111.02, 110.51, 49.02, 31.78; HRMS (APCI) calcd for $\text{C}_{22}\text{H}_{18}\text{N}_2$, $[\text{m/z}]$: 311.15428, found: 311.15428.

5,10-Diethyl-5,10-dihydroindolo[3,2-*b*]indole, (2o)



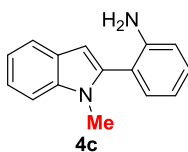
White solid (40%, 0.08 mmol, 20.9 mg); ^1H NMR (400 MHz, CDCl_3) δ 7.87 (d, J = 8.0 Hz, 2H), 7.48 (d, J = 8.4 Hz, 2H), 7.32 (t, J = 8.4 Hz, 2H), 7.20 (t, J = 7.6 Hz, 2H), 4.58 (q, J = 7.2 Hz, 4H), 1.55 (t, J = 7.2 Hz, 6H); ^{13}C NMR (100 MHz, CDCl_3) δ 139.94, 125.50, 121.47, 117.99, 117.56, 114.62, 109.41, 39.89, 15.33; HRMS (MALDI) calcd for $\text{C}_{18}\text{H}_{18}\text{N}_2$ [m/z]: 262.14645, found: 262.14646.

5,10-Bis(methyl- d_3)-5,10-dihydroindolo[3,2-*b*]indole, (2s)



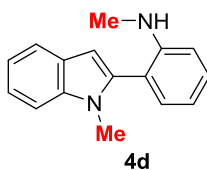
White solid (70%, 0.14 mmol, 33.6 mg); ^1H NMR (400 MHz, $\text{THF-}d_8$) δ 7.89 (d, J = 7.6 Hz, 2H), 7.43 (d, J = 8.8 Hz, 2H), 7.20 (t, J = 8.0 Hz, 2H), 7.06 (t, J = 8.0 Hz, 2H); ^{13}C NMR (100 MHz, $\text{THF-}d_8$) δ 141.40, 126.27, 121.31, 117.79, 117.19, 114.99, 109.28, 30.01 (m); HRMS (APCI) calcd for $\text{C}_{16}\text{H}_8\text{D}_6\text{N}_2$, [m/z]: 240.15281, found: 240.15284.

2-(1-Methyl-1*H*-indol-2-yl)aniline, (4c)



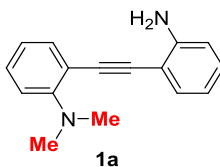
Yellow solid; ^1H NMR (400 MHz, CDCl_3) δ 7.66 (d, J = 7.6 Hz, 1H), 7.38 (d, J = 8.4 Hz, 1H), 7.29-7.23 (m, 2H), 7.20-7.14 (m, 2H), 6.86-6.80 (m, 2H), 6.55 (s, 1H), 3.84 (bs, 2H, $-\text{NH}_2$), 3.61 (s, 3H); ^{13}C NMR (100 MHz, CDCl_3) δ 145.21, 137.91, 137.72, 131.60, 129.79, 128.05, 121.53, 120.43, 119.71, 118.24, 118.06, 115.44, 109.57, 101.84, 30.46; HRMS (APCI) calcd for $\text{C}_{15}\text{H}_{14}\text{N}_2$, [$M+H$]: 223.12297, found: 223.12297.

N-Methyl-2-(1-methyl-1*H*-indol-2-yl)aniline



Pale yellow oil (70%, 0.14 mmol, 33.1 mg); ^1H NMR (400 MHz, CDCl_3) δ 7.66 (td, $J = 8.0, 0.8$ Hz, 1H), 7.39-7.34 (m, 2H), 7.29-7.25 (m, 1H), 7.17 (td, $J = 7.2, 1.6$ Hz, 2H), 6.79 (td, $J = 7.2, 0.8$ Hz, 1H), 6.73 (d, $J = 8.4$ Hz, 1H), 6.54 (s, 1H), 4.02 (bs, 1H), 3.60 (s, 3H), 2.80 (s, 3H); ^{13}C NMR (100 MHz, CDCl_3) δ 148.04, 137.94, 137.65, 131.31, 130.10, 128.05, 121.50, 120.40, 119.70, 117.51, 116.23, 109.65, 101.92, 30.45, 30.34.

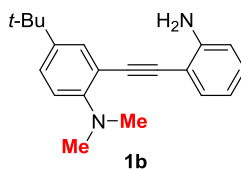
2-((2-Aminophenyl)ethynyl)-*N,N*-dimethylaniline (1a)



Pale yellow oil; ^1H NMR (400 MHz, CDCl_3) δ 7.50 (dd, $J = 8.0, 1.6$ Hz, 1H), 7.39 (dd, $J = 8.0, 2.0$ Hz, 1H), 7.28 (td, $J = 8.8, 2.0$ Hz, 1H), 7.14 (td, $J = 8.4, 1.6$ Hz, 1H), 6.99 (d, $J = 8.4$ Hz, 1H), 6.95 (td, $J = 8.0, 1.2$ Hz, 1H), 6.74-6.71 (m, 2H), 4.46 (bs, 2H), 2.97 (s, 6H); ^{13}C NMR (100 MHz, CDCl_3) δ 154.58, 147.67, 133.51, 131.50, 129.40, 129.01, 121.06, 117.66, 117.37, 116.15, 114.11, 108.45, 94.00, 91.24, 43.97.

HRMS (ESI positive) calcd for $\text{C}_{16}\text{H}_{16}\text{N}_2$, $[\text{M}+\text{Na}]^+$: 259.1188, found: 259.1188.

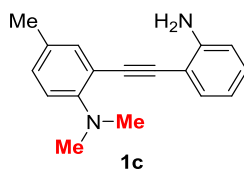
2-((2-Aminophenyl)ethynyl)-4-(*tert*-butyl)-*N,N*-dimethylaniline (1b)



Yellow oil; ^1H NMR (400 MHz, CDCl_3) δ 7.55 (d, $J = 2.4$ Hz, 1H), 7.43 (d, $J = 8.0$ Hz, 1H), 7.34 (dd, $J = 8.8, 2.4$ Hz, 1H), 7.16 (t, $J = 8.0$ Hz, 1H), 6.98 (d, $J = 8.8$ Hz, 1H), 6.77-6.74 (m, 2H), 4.53 (bs, 2H), 2.96 (s, 6H), 1.36 (s, 9H); ^{13}C NMR (100 MHz, CDCl_3) δ 152.29, 147.71, 143.81, 131.38, 130.16, 129.26, 126.08, 117.51, 117.05, 115.83, 114.02, 108.42, 94.42, 90.65, 44.05, 34.00, 31.31.

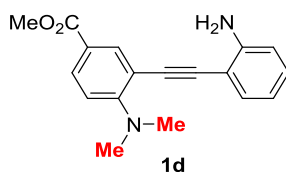
HRMS (ESI positive) calcd for $\text{C}_{20}\text{H}_{24}\text{N}_2$, $[\text{M}+\text{Na}]^+$: 315.1832, found: 315.1832.

2-((2-Aminophenyl)ethynyl)-*N,N*-4-trimethylaniline, (1c)



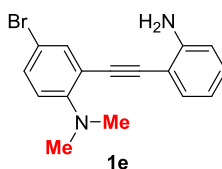
Yellow oil; ^1H NMR (400 MHz, CDCl_3) δ 7.40 (d, $J = 8.0$ Hz, 1H), 7.34 (s, 1H), 7.17-7.09 (m, 2H), 6.92 (d, $J = 8.0$ Hz, 1H), 6.75-6.72 (m, 2H), 4.50 (bs, 2H), 2.93 (s, 6H), 2.31 (s, 3H); ^{13}C NMR (100 MHz, CDCl_3) δ 152.55, 147.83, 133.72, 131.47, 130.67, 129.76, 129.38, 117.60, 117.44, 116.42, 114.08, 108.47, 94.06, 90.92, 44.13, 20.28; HRMS (ESI) calcd for $\text{C}_{17}\text{H}_{18}\text{N}_2$, $[\text{M}+\text{Na}]^+$: 273.1362, found: 273.1362.

Methyl 3-((2-aminophenyl)ethynyl)-4-(dimethylamino)benzoate, (1d)



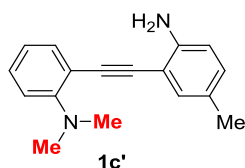
Yellow oil; ^1H NMR (400 MHz, CDCl_3) δ 8.13 (d, $J = 2.8$ Hz, 1H), 7.87 (dd, $J = 8.8, 2.0$ Hz, 1H), 7.35 (d, 8.0 Hz, 1H), 7.13 (td, $J = 8.0, 1.6$ Hz, 1H), 6.86 (d, $J = 8.8$, 1H), 6.74-6.70 (m, 2H), 4.34 (bs, 2H), 3.89 (s, 3H), 3.10 (s, 6H); ^{13}C NMR (100 MHz, CDCl_3) δ 166.51, 157.21, 147.63, 136.16, 131.66, 130.55, 129.63, 120.80, 117.83, 115.73, 114.28, 112.84, 108.18, 93.61, 91.37, 51.82, 42.98; HRMS (ESI) calcd for $\text{C}_{18}\text{H}_{18}\text{N}_2\text{O}_2$, $[\text{M}+\text{Na}]^+$: 317.1260, found: 317.1260.

2-((2-Aminophenyl)ethynyl)-4-bromo-N,N-dimethylaniline, (1e)



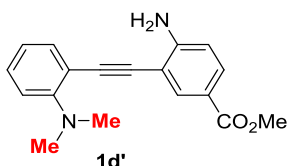
Yellow oil; ^1H NMR (400 MHz, CDCl_3) δ 7.57 (d, $J = 2.4$, 1H), 7.36-7.32 (m, 2H), 7.14 (td, $J = 8.0, 1.6$ Hz, 2H), 6.83 (d, $J = 8.0$ Hz, 1H), 6.73-6.70 (m, 2H), 4.40 (bs, 2H), 2.94 (s, 6H); ^{13}C NMR (100 MHz, CDCl_3) δ 153.58, 147.86, 135.72, 131.77, 131.71, 129.87, 118.94, 117.84, 117.82, 114.26, 112.94, 107.91, 92.60, 92.49, 43.73; HRMS (ESI) calcd for $\text{C}_{16}\text{H}_{15}\text{BrN}_2$, $[\text{M}+\text{Na}]^+$: 337.0311, found 337.0311.

2-((2-Amino-5-methylphenyl)ethynyl)-N,N-dimethylaniline, (1c')



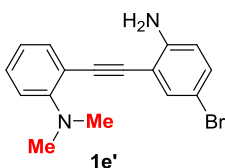
Yellow oil; ¹H NMR (400 MHz, CDCl₃) δ 7.48 (dd, *J* = 7.6, 1.2 Hz, 1H), 7.28 (m, 1H), 7.19 (s, 1H), 6.99-6.91 (m, 3H), 6.64 (d, *J* = 8.0 Hz, 1H), 4.24 (bs, 2H), 2.96 (s, 6H), 2.25 (s, 3H); ¹³C NMR (100 MHz, CDCl₃) δ 154.50, 145.33, 133.51, 131.56, 130.22, 128.91, 126.83, 120.96, 117.28, 116.13, 114.30, 108.44, 93.70, 91.44, 43.89, 20.32; HRMS (ESI) calcd for C₁₇H₁₈N₂, [M+H]⁺: 251.1543, found: 251.1543.

Methyl 4-amino-3-((2-(dimethylamino)phenyl)ethynyl)benzoate, (1d')



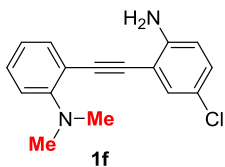
Pale yellow solid; ¹H NMR (400 MHz, CDCl₃) δ 8.06 (d, *J* = 2.0 Hz, 1H), 7.81 (dd, *J* = 8.4, 2.0 Hz, 1H), 7.48 (dd, *J* = 7.6, 1.6 Hz, 1H), 7.28 (td, *J* = 8.8, 1.6 Hz, 1H), 7.02 (d, *J* = 8.0 Hz, 1H), 6.97 (t, *J* = 7.6 Hz, 1H), 6.69 (d, *J* = 8.4 Hz, 1H), 4.94 (bs, 2H), 3.87 (s, 3H), 2.95 (s, 6H); ¹³C NMR (100 MHz, CDCl₃) δ 166.56, 151.48, 133.60, 133.49, 131.21, 129.33, 121.48, 119.07, 117.64, 115.98, 113.03, 107.58, 94.36, 90.19, 51.75, 44.13; HRMS (ESI) calcd for C₁₈H₁₈N₂O₂, [M+H]⁺: 295.1441, found: 295.1441.

2-((2-Amino-5-bromophenyl)ethynyl)-*N,N*-dimethylaniline, (1e')



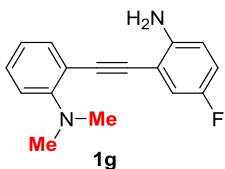
Pale yellow oil; ¹H NMR (400 MHz, CDCl₃) δ 7.49-7.46 (m, 2H), 7.31-7.27 (m, 1H), 7.20 (dd, *J* = 8.8, 2.4 Hz, 1H), 6.99 (d, *J* = 8.4 Hz, 1H), 6.95 (td, *J* = 7.6, 1.2 Hz, 1H), 6.59 (d, *J* = 8.8 Hz, 1H), 4.48 (br, 2H), 2.95 (s, 6H); ¹³C NMR (100 MHz, CDCl₃) δ 154.76, 146.67, 133.48, 133.36, 132.00, 129.35, 121.03, 117.37, 115.54, 115.48, 110.25, 108.60, 95.15, 89.73, 43.92; HRMS (ESI) calcd for C₁₆H₁₅BrN₂, [M+Na]⁺: 337.0311, found: 337.0311.

2-((2-Amino-5-chlorophenyl)ethynyl)-*N,N*-dimethylaniline, (1f)



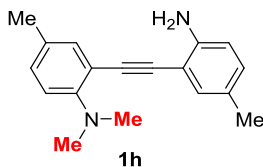
Yellow oil; ^1H NMR (400 MHz, CDCl_3) δ 7.41 (dd, $J = 8.0, 1.6$ Hz, 1H), 7.26 (d, $J = 2.4$ Hz, 1H), 7.22 (t, $J = 8.0$ Hz, 1H), 7.01 (dd, $J = 8.8, 2.4$ Hz, 1H), 6.93 (d, $J = 8.0$ Hz, 1H), 6.88 (t, $J = 7.6$ Hz, 1H), 6.58 (d, $J = 8.4$ Hz, 1H), 4.39 (bs, 2H), 2.89 (s, 6H); ^{13}C NMR (100 MHz, CDCl_3) δ 154.73, 146.29, 133.56, 130.62, 129.38, 129.28, 121.92, 121.14, 117.46, 115.63, 115.17, 109.78, 95.00, 89.94, 43.99; HRMS (ESI) calcd for $\text{C}_{16}\text{H}_{15}\text{ClN}_2$, $[\text{M}+\text{Na}]^+$: 293.0816, found: 293.0816.

2-((2-Amino-5-fluorophenyl)ethynyl)-N,N-dimethylaniline, (1g)



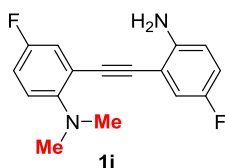
Pale yellow oil; ^1H NMR (400 MHz, CDCl_3) 7.48 (dd, $J = 8.0, 1.6$ Hz, 1H), 7.30-7.26 (m, 1H), 7.01 (dd, $J = 8.8, 3.2$ Hz, 1H), 6.99 (d, $J = 7.6$, 1H), 6.94 (td, $J = 8.0, 1.2$ Hz, 1H), 6.86 (td, $J = 8.8, 2.8$ Hz, 1H), 6.65 (dd, $J = 8.4, 4.0$ Hz, 1H), 4.31 (bs, 2H), 2.95 (s, 6H); ^{13}C NMR (100 MHz, CDCl_3) δ 155.16 (d, $J^1 = 234.7$ Hz), 154.88, 144.17 (d, $J^7 = 1.7$ Hz), 133.67, 129.43, 121.09, 117.45, 117.20 (d, $J^2 = 23.1$ Hz), 116.54 (d, $J^3 = 23.1$ Hz), 115.64, 115.06 (d, $J^5 = 8.2$ Hz), 109.2 (d, $J^4 = 9.0$ Hz), 94.76, 90.26 (d, $J^6 = 3.3$ Hz), 43.90; ^{19}F NMR (658.8 MHz, CDCl_3) δ -128.87; HRMS (ESI) calcd for $\text{C}_{16}\text{H}_{15}\text{FN}_2$, $[\text{M}+\text{Na}]^+$: 255.1292, found: 255.1292.

2-((2-Amino-5-methylphenyl)ethynyl)-N,N-dimethylaniline, (1h)



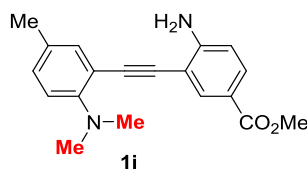
Yellow oil. ^1H NMR (400 MHz, CDCl_3) δ 7.31 (d, $J = 2.0$ Hz, 1H), 7.18, (s, 1H), 7.07 (dd, $J = 8.4, 2.0$ Hz, 1H), 6.95 (dd, $J = 8.4, 2.0$ Hz, 1H), 6.91 (d, $J = 8.0$ Hz, 1H), 6.65 (d, $J = 8.0$ Hz, 1H), 4.34 (bs, 2H), 2.92 (s, 6H), 2.29 (s, 3H), 2.25 (s, 3H); ^{13}C NMR (100 MHz, CDCl_3) δ 152.36, 145.40, 133.77, 131.56, 130.61, 130.19, 129.66, 126.83, 117.39, 116.40, 114.28, 108.52, 93.76, 91.16, 44.19, 20.39, 20.35; HRMS (ESI) calcd for $\text{C}_{18}\text{H}_{20}\text{N}_2$, $[\text{M}+\text{H}]^+$: 265.1699, found: 265.1699

2-((2-Amino-5-fluorophenyl)ethynyl)-4-fluoro-N,N-dimethylaniline, (1i)



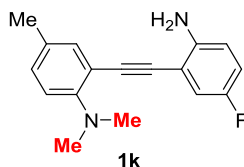
Yellow oil; ^1H NMR (400 MHz, CDCl_3) δ 7.17 (dd, $J = 8.4, 2.8$ Hz, 1H), 7.05 (dd, $J = 8.8, 3.2$ Hz, 1H), 7.01-6.92 (m, 2H), 6.87 (td, $J = 8.4, 2.8$ Hz, 1H), 6.65 (dd, $J = 8.8, 4.4$ Hz, 1H), 4.35 (bs, 2H), 2.88 (s, 6H); ^{13}C NMR (100 MHz, CDCl_3) δ 157.19 (d, $J^1 = 239.2$ Hz), 154.93 (d, $J^2 = 233.5$ Hz), 151.42 (d, $J^{11} = 2.5$ Hz), 144.39 (d, $J^{12} = 1.6$ Hz), 119.53 (d, $J^3 = 24.0$ Hz), 118.87 (d, $J^9 = 8.3$ Hz), 117.66 (d, $J^7 = 9.1$ Hz), 117.10 (d, $J^4 = 23.1$ Hz), 116.92 (d, $J^5 = 23.1$ Hz), 115.97 (d, $J^6 = 21.5$ Hz), 115.05 (d, $J^{10} = 8.2$ Hz), 108.41 (d, $J^8 = 9.1$ Hz), 93.387 (d, $J^{13} = 2.5$ Hz), 91.02 (d, $J^{14} = 2.4$ Hz), 44.35; ^{19}F NMR (658.8 MHz, CDCl_3) δ -128.77; HRMS (ESI) calcd for $\text{C}_{16}\text{H}_{14}\text{F}_2\text{N}_2$, $[\text{M}+\text{H}]^+$: 273.1198, found: 273.1198.

Methyl 4-amino-3-((2-(dimethylamino)-5-methylphenyl)ethynyl)benzoate, (1j)



Yellow solid; ^1H NMR (400 MHz, CDCl_3) δ 8.07 (d, $J = 1.6$ Hz, 1H), 7.80 (dd, $J = 8.4, 1.6$ Hz, 1H), 7.30 (s, 1H), 7.08 (dd, $J = 8.4, 2.0$ Hz, 1H), 6.91 (d, $J = 8.0$ Hz, 1H), 6.67 (d, $J = 8.8$ Hz, 1H), 5.05 (bs, 2H), 3.87 (s, 3H), 2.87 (s, 6H), 2.28 (s, 3H); ^{13}C NMR (100 MHz, CDCl_3) δ 166.61, 152.69, 151.70, 133.52, 133.42, 131.09, 130.91, 130.01, 118.78, 117.58, 116.16, 112.91, 107.53, 94.53, 89.70, 51.55, 44.17, 20.22; HRMS (ESI) calcd for $\text{C}_{19}\text{H}_{20}\text{N}_2\text{O}_2$, $[\text{M}+\text{Na}]^+$: 331.1417, found: 331.1417.

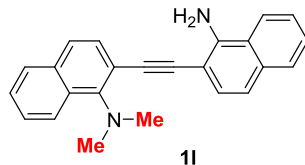
2-((2-Amino-5-fluorophenyl)ethynyl)-N,N-dimethylaniline, (1k)



Bright yellow oil; ^1H NMR (400 MHz, CDCl_3) δ 7.32 (s, 1H), 7.12-7.07 (m, 2H), 6.92 (d, $J = 8.4$, 1H), 6.86 (td, $J = 8.8, 2.8$ Hz, 1H), 6.65 (dd, $J = 8.8, 4.0$ Hz, 1H), 4.30 (bs, 2H), 2.92 (s, 6H), 2.31 (s, 3H); ^{13}C NMR (100 MHz, CDCl_3) δ 154.99 (d, $J^1 = 233.5$ Hz), 152.54, 144.16 (d, $J^6 = 1.6$ Hz), 133.74, 130.72, 130.08, 117.49, 116.73 (d, $J^2 = 24.0$ Hz), 116.41 (d, $J^3 = 23.1$ Hz), 115.83, 114.95 (d, $J^5 = 8.3$ Hz), 109.15 (d, $J^4 = 9.9$ Hz), 94.75, 89.96 (d, $J^7 = 3.3$ Hz), 44.18, 20.33; ^{19}F NMR (658.8 MHz, CDCl_3) δ -128.93; HRMS (ESI) calcd for $\text{C}_{17}\text{H}_{17}\text{FN}_2$, $[\text{M}+\text{H}]^+$: 269.1449, found:

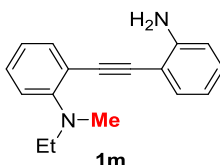
269.1449.

2-((1-Aminonaphthalen-2-yl)ethynyl)-*N,N*-dimethylnaphthalen-1-amine, (1l)



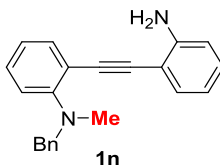
Yellow solid; ^1H NMR (400 MHz, CDCl_3) δ 8.33 (d, $J = 8.0$ Hz, 1H), 7.76 (t, $J = 8.0$, 3H), 7.56-7.41 (m, 7H), 7.24-7.19 (m, 1H), 4.95 (bs, 2H), 3.18 (s, 6H); ^{13}C NMR (100 MHz, CDCl_3) δ 151.37, 144.46, 134.30, 133.97, 131.84, 130.28, 128.56, 127.95, 126.54, 126.45, 126.08, 125.35, 124.62, 124.55, 122.49, 120.87, 118.09, 116.75, 102.61, 95.26, 92.49, 44.07; HRMS (ESI) calcd for $\text{C}_{24}\text{H}_{20}\text{N}_2$, $[\text{M}+\text{Na}]^+$: 359.1519, found: 359.1519.

2-((2-Aminophenyl)ethynyl)-*N*-ethyl-*N*-methylaniline, (1m)



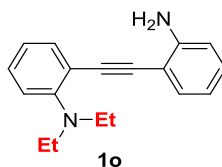
Pale yellow oil; ^1H NMR (400 MHz, CDCl_3) δ 7.52 (dd, $J = 7.6$, 2.0 Hz, 1H), 7.40 (dd, $J = 8.0$, 1.6 Hz, 1H), 7.29 (td, $J = 8.0$, 1.2 Hz, 1H), 7.15 (td, $J = 7.6$, 1.6 Hz, 1H), 7.02 (d, $J = 8.4$ Hz, 1H), 6.96 (td, $J = 8.0$, 0.8 Hz, 1H), 6.75-6.72 (m, 2H), 4.49 (bs, 2H), 3.37 (q, $J = 7.2$ Hz, 2H), 2.89 (s, 3H), 1.21 (t, $J = 7.2$ Hz, 3H); ^{13}C NMR (100 MHz, CDCl_3) δ 154.22, 147.80, 133.54, 131.45, 129.37, 128.90, 121.02, 118.49, 117.59, 116.66, 114.06, 108.42, 94.11, 90.74, 50.15, 39.87, 12.55; HRMS (ESI) calcd for $\text{C}_{17}\text{H}_{18}\text{N}_2$, $[\text{M}+\text{Na}]^+$: 273.1362, found: 273.1363.

2-((2-Aminophenyl)ethynyl)-*N*-benzyl-*N*-methylaniline, (1n)



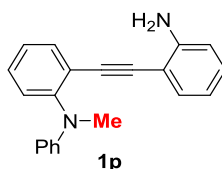
Yellow oil; ^1H NMR (400 MHz, CDCl_3) δ 7.53 (dd, $J = 8.0$, 2.0 Hz, 1H), 7.39-7.23 (m, 6H), 7.12-7.08 (m, 2H), 7.01-6.95 (m, 2H), 6.67-6.60 (m, 2H), 4.52 (s, 2H), 4.26 (bs, 2H), 2.81 (s, 3H); ^{13}C NMR (100 MHz, CDCl_3) δ 153.89, 147.66, 138.56, 133.90, 131.72, 129.39, 129.08, 128.34, 127.02, 121.18, 118.58, 117.64, 116.34, 114.04, 108.34, 93.90, 91.26, 59.90, 40.17; HRMS (ESI) calcd for $\text{C}_{22}\text{H}_{20}\text{N}_2$, $[\text{M}+\text{Na}]^+$: 335.1519, found: 335.1519.

2-((2-Aminophenyl)ethynyl)-*N,N*-diethylaniline, (1o)



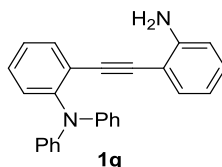
Pale yellow oil; ^1H NMR (400 MHz, CDCl_3) δ 7.48 (d, $J = 6.8$ Hz, 1H), 7.34 (dd, $J = 7.6, 1.6$ Hz, 1H), 7.24 (t, $J = 7.6$ Hz, 1H), 7.12 (t, $J = 7.6$ Hz, 1H), 7.02 (d, $J = 8.4$ Hz, 1H), 6.96 (t, $J = 7.6$ Hz, 1H), 6.73-6.68 (m, 2H), 4.58 (bs, 2H), 3.30 (q, $J = 6.8$ Hz, 4H), 1.07 (t, $J = 6.8$ Hz, 6H); ^{13}C NMR (100 MHz, CDCl_3) δ 152.41, 147.97, 133.11, 131.23, 129.33, 128.50, 121.70, 120.95, 118.90, 117.51, 113.95, 108.51, 94.50, 90.41, 46.61, 12.27; HRMS (ESI) calcd for $\text{C}_{18}\text{H}_{20}\text{N}_2$, $[\text{M}+\text{H}]^+$: 265.1699, found: 265.1700.

2-((2-Aminophenyl)ethynyl)-*N*-methyl-*N*-phenylaniline, (1p)



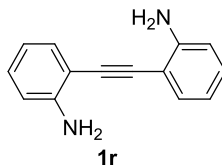
Yellow solid; ^1H NMR (400 MHz, CDCl_3) δ 7.63 (dd, $J = 8.0, 1.6$ Hz, 1H), 7.38 (t, $J = 8.0$ Hz, 1H), 7.28-7.20 (m, 5H), 7.07 (t, $J = 8.0$ Hz, 1H), 6.81 (td, $J = 7.6, 1.2$ Hz, 1H), 6.76 (dd, $J = 8.0, 1.2$ Hz, 2H), 6.65 (t, $J = 8.0$ Hz, 1H), 6.57 (d, $J = 8.0$ Hz, 1H), 3.79 (bs, 2H), 3.38 (s, 3H); ^{13}C NMR (100 MHz, CDCl_3) δ 149.23, 148.90, 147.95, 133.41, 131.84, 129.63, 129.00, 127.93, 125.74, 122.67, 117.67, 117.34, 113.97, 113.81, 107.51, 92.25, 90.85, 39.58.

2-((2-Aminophenyl)ethynyl)-*N,N*-diphenylaniline, (1q)



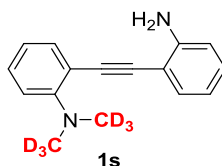
Pale yellow solid; ^1H NMR (400 MHz, CDCl_3) δ 7.52 (dd, $J = 8.0, 1.6$ Hz, 1H), 7.23 (td, $J = 7.6, 1.6$ Hz, 1H), 7.18-7.05 (m, 6H), 7.00-6.93 (m, 6H), 6.89 (t, $J = 7.6$ Hz, 2H), 6.55-6.48 (m, 2H), 3.68 (bs, 2H); ^{13}C NMR (100 MHz, CDCl_3) δ 147.64, 147.60, 147.30, 134.18, 132.25, 129.61, 129.54, 129.29, 129.11, 125.19, 122.40, 122.33, 122.00, 117.64, 114.18, 107.95, 92.42, 91.20.

2,2'-(Ethyne-1,2-diyl)dianiline, (1r)¹



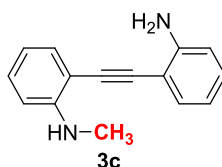
Pale yellow flake; ¹H NMR (400 MHz, CDCl₃) δ 7.37 (d, *J* = 8.0 Hz, 2H), 7.16 (t, *J* = 8.0 Hz, 2H), 6.75-6.72 (m, 4H), 4.14 (bs, 4H); ¹³C NMR (100 MHz, CDCl₃) δ 147.48, 131.93, 129.63, 117.93, 114.33, 108.00, 91.02.

2-((2-Aminophenyl)ethynyl)-*N,N*-bis(methyl-*d*₃)aniline (1s)



Pale yellow oil; ¹H NMR R (400 MHz, CDCl₃) δ 7.50 (dd, *J* = 7.2, 1.6 Hz, 1H), 7.39 (dd, *J* = 8.0, 1.6 Hz, 1H), 7.28 (td, *J* = 8.0, 1.6 Hz, 1H), 7.14 (td, *J* = 8.0, 1.6 Hz, 1H), 6.99 (d, *J* = 8.0 Hz, 1H), 6.95 (t, *J* = 8.0 Hz, 1H), 6.75-6.71 (m, 2H), 4.56 (bs, 2H); ¹³C NMR (100 MHz, CDCl₃) δ 154.70, 147.75, 133.58, 131.53, 129.43, 129.06, 120.95, 117.67, 117.27, 116.05, 114.13, 108.47, 94.05, 91.19, 42.90 (m).; HRMS (ESI) calcd for C₁₆H₁₀D₆N₂, [M+Na]⁺: 265.1582, found: 265.1582.

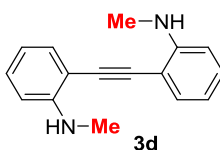
2-((2-Aminophenyl)ethynyl)-*N*-methylaniline, (3c)



Yellow oil; ¹H NMR (400 MHz, CDCl₃) δ 7.38-7.36 (m, 2H), 7.26 (t, *J* = 8.0 Hz, 1H), 7.15 (td, *J* = 8.0, 1.6 Hz, 1H), 6.77-6.62 (m, 4H), 4.73 (bs, 1H), 4.27 (bs, 2H), 2.92 (s, 3H); ¹³C NMR (100 MHz, CDCl₃) δ 149.67, 147.60, 131.99, 131.94, 130.06, 129.68, 117.94, 116.18, 114.34, 109.01, 108.03, 107.35, 91.20, 91.10, 30.27; HRMS (ESI) calcd for C₁₅H₁₄N₂ [M+Na]⁺: 245.1049, found: 245.1049.

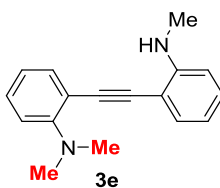
2,2'-(Ethyne-1,2-diyl)bis(*N*-methylaniline), (3d)

¹ Perea-Buceta, J. E.; Wirtanen, T.; Laukkanen, O.-V.; Makela, M. K.; Nieger, M.; Melchionna, M.; Huittinen, N.; Lopez-Sanchez, J. A.; Helaja, J. *Angew. Chem., Int. Ed.* **2013**, *52*, 11835.



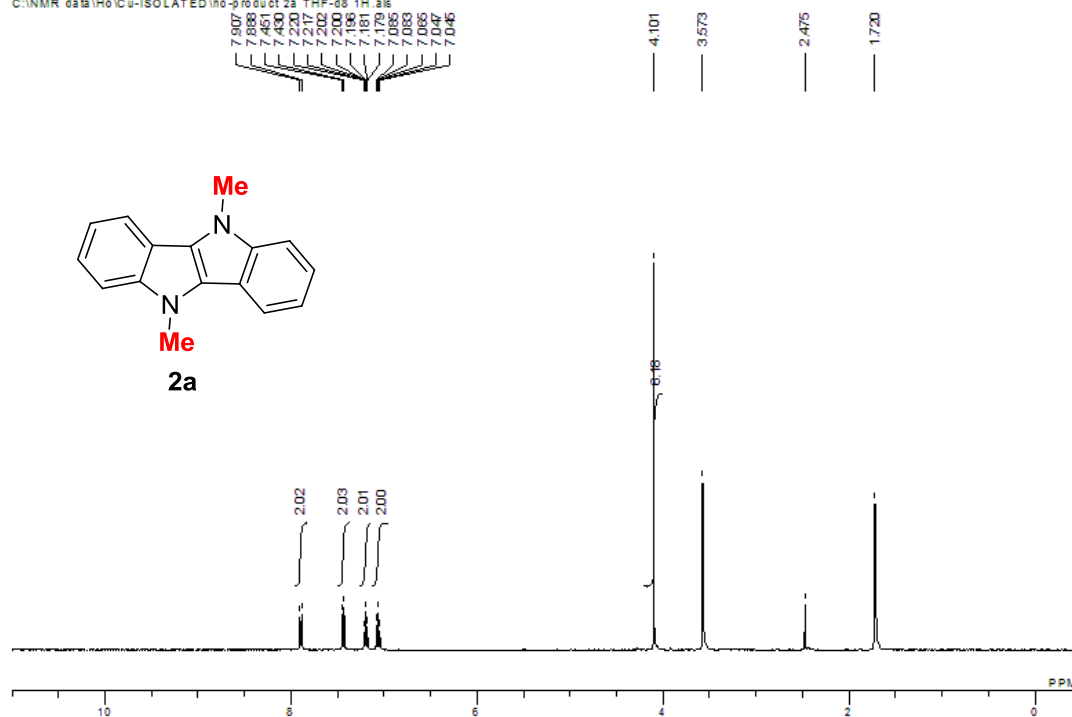
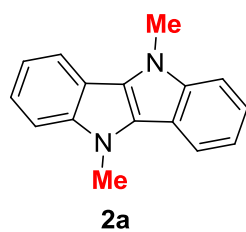
Pale yellow oil; ^1H NMR (400 MHz, CDCl_3) δ 7.37 (dd, $J = 7.2, 1.2$ Hz, 2H), 7.28-7.23 (m, 2H), 6.67 (t, $J = 7.6$ Hz, 2H), 6.63 (d, $J = 8.4$ Hz, 2H), 4.72 (br, 2H), 2.92 (s, 6H); ^{13}C NMR (100 MHz, CDCl_3) δ 149.67, 132.00, 130.08, 116.28, 109.11, 107.47, 91.29, 30.35. HRMS (APCI positive) calcd for $\text{C}_{16}\text{H}_{16}\text{N}_2$, $[\text{M}+\text{H}]^+$: 237.13862, found 237.13865.

***N,N*-Dimethyl-2-((2-(methylamino)phenyl)ethynyl)aniline, (3e)**

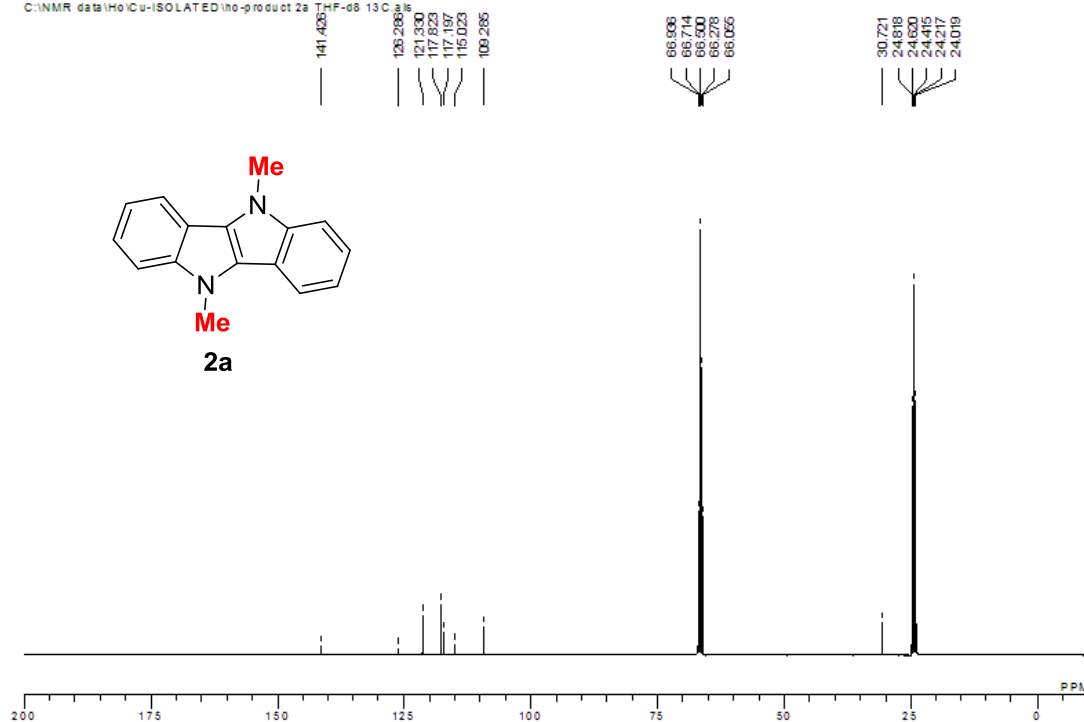
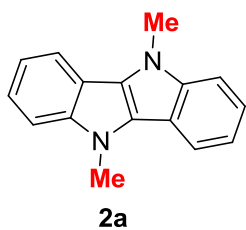


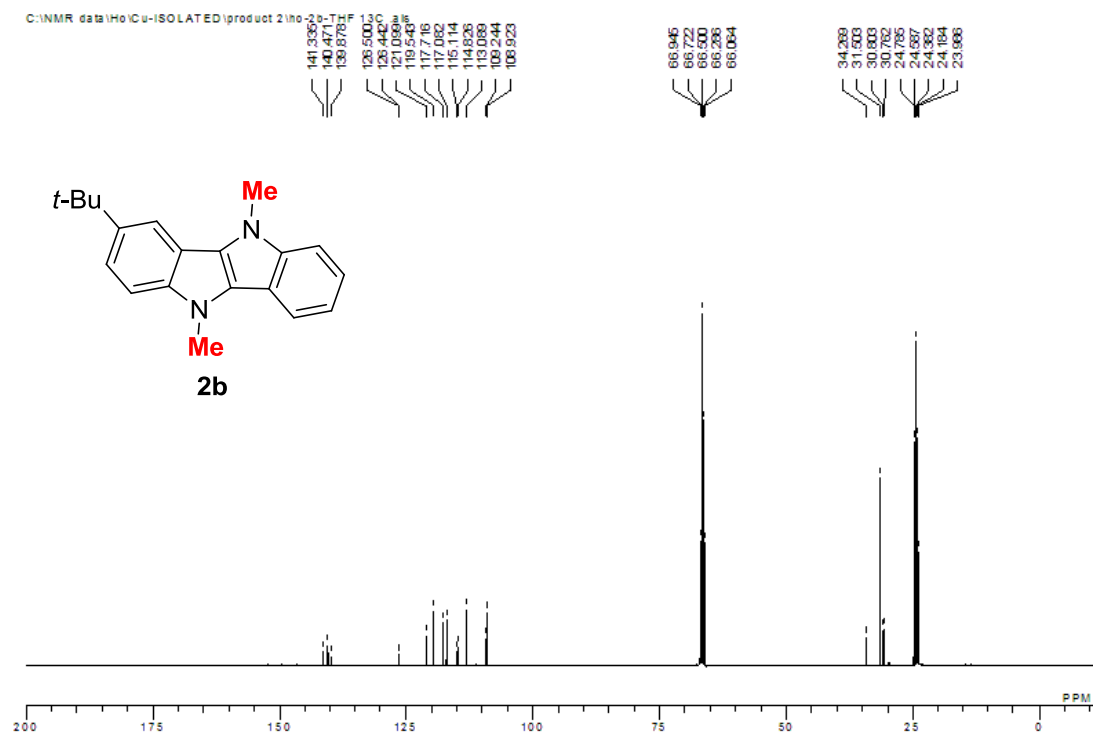
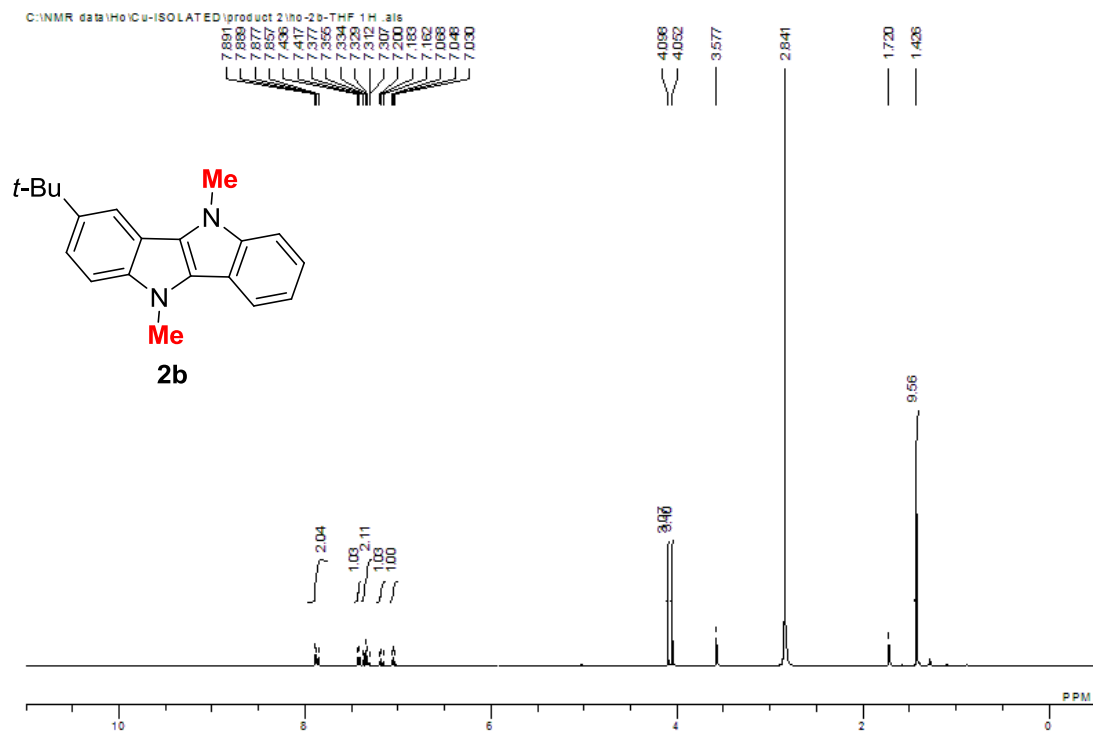
Yellow oil; ^1H NMR (400 MHz, CDCl_3) δ 7.48 (dd, $J = 7.6, 1.6$ Hz, 1H), 7.37 (dd, $J = 7.6, 1.6$ Hz, 1H), 7.28-7.21 (m, 2H), 7.00 (d, $J = 8.4$ Hz, 1H), 6.95 (td, $J = 7.6, 0.8$ Hz, 1H), 6.65 (td, $J = 7.6, 0.8$ Hz, 1H), 6.61 (d, $J = 8.0$ Hz, 1H), 5.19 (bs, 1H), 2.95 (s, 6H), 2.93 (s, 3H); ^{13}C NMR (100 MHz, CDCl_3) δ 154.66, 149.74, 133.20, 131.19, 129.74, 128.91, 121.25, 117.46, 116.50, 115.82, 108.66, 107.80, 94.29, 91.40, 44.08, 30.37.

C:\NMR data\Ho\Cu-ISOLATED\ho-product 2a THF-d8 1H.als

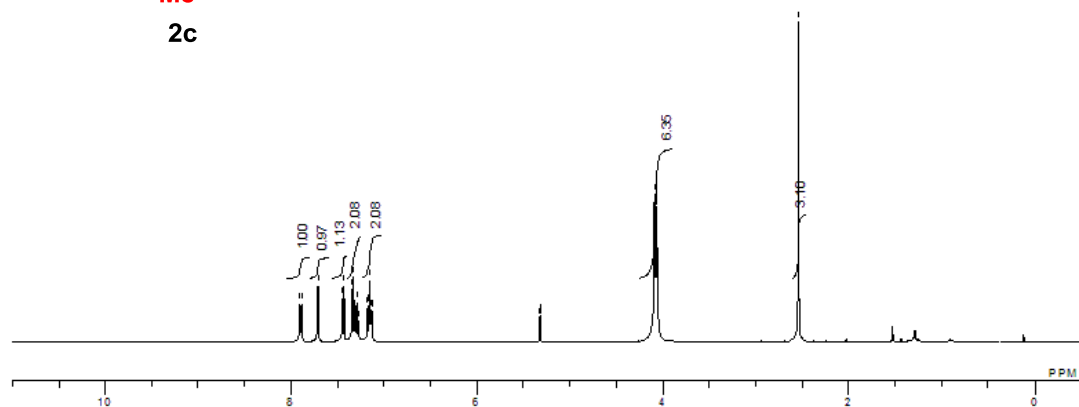
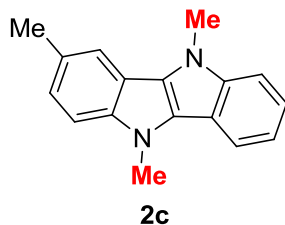


C:\NMR data\Ho\Cu-ISOLATED\ho-product 2a THF-d8 13C.als

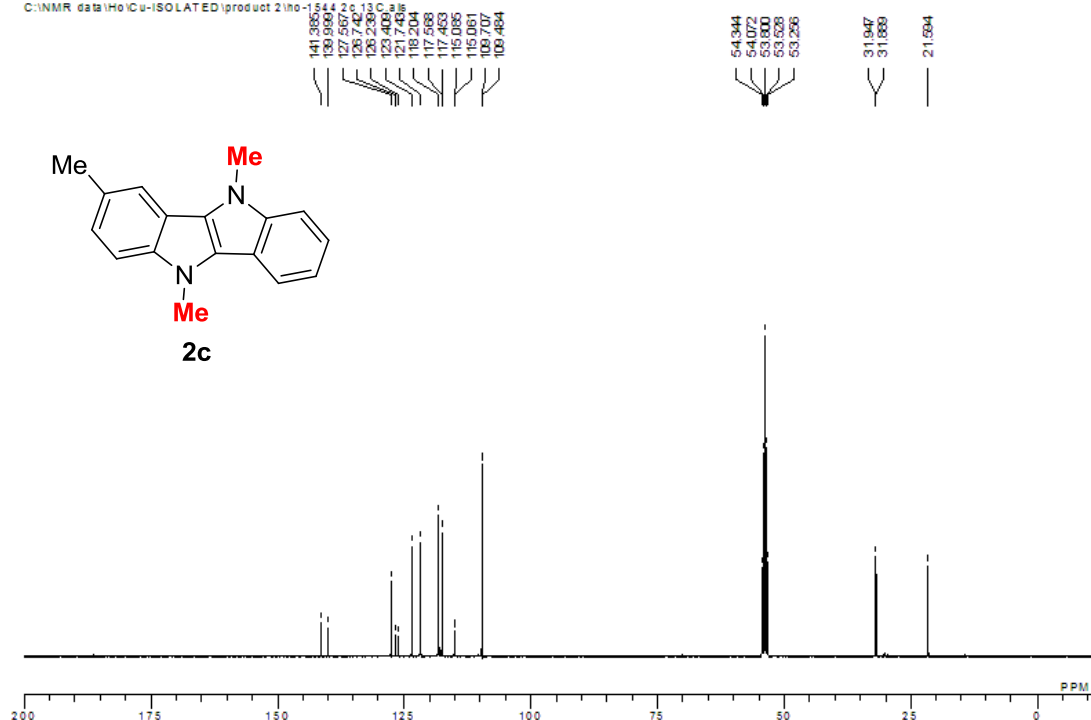
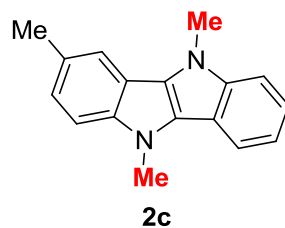


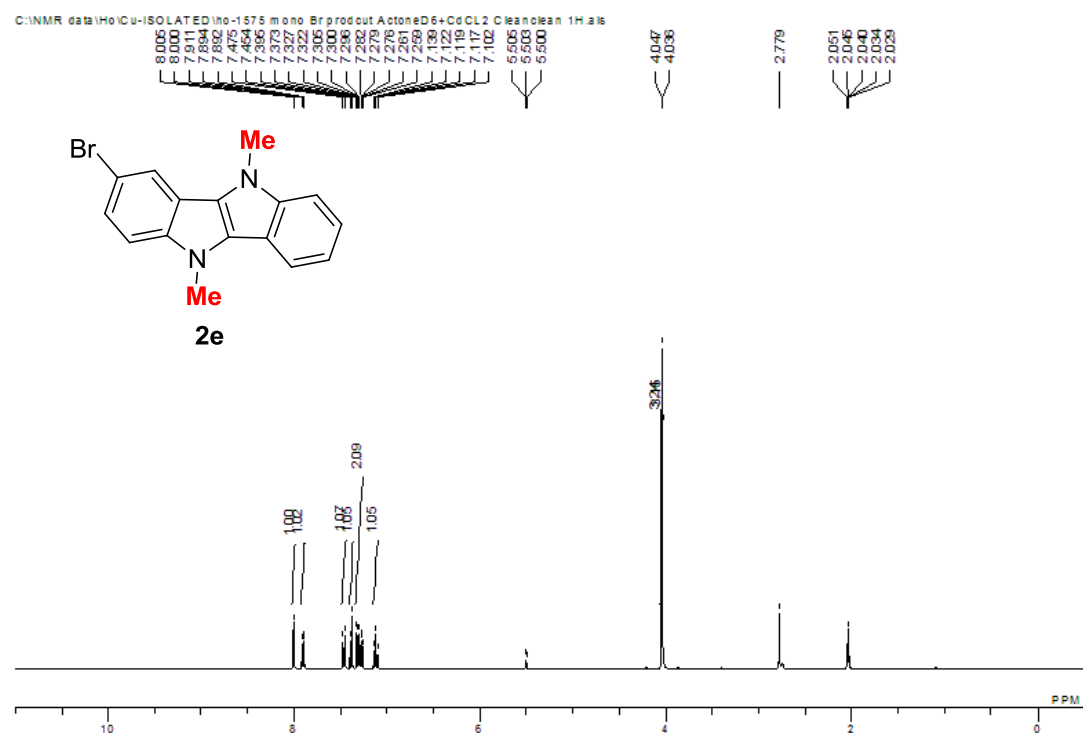
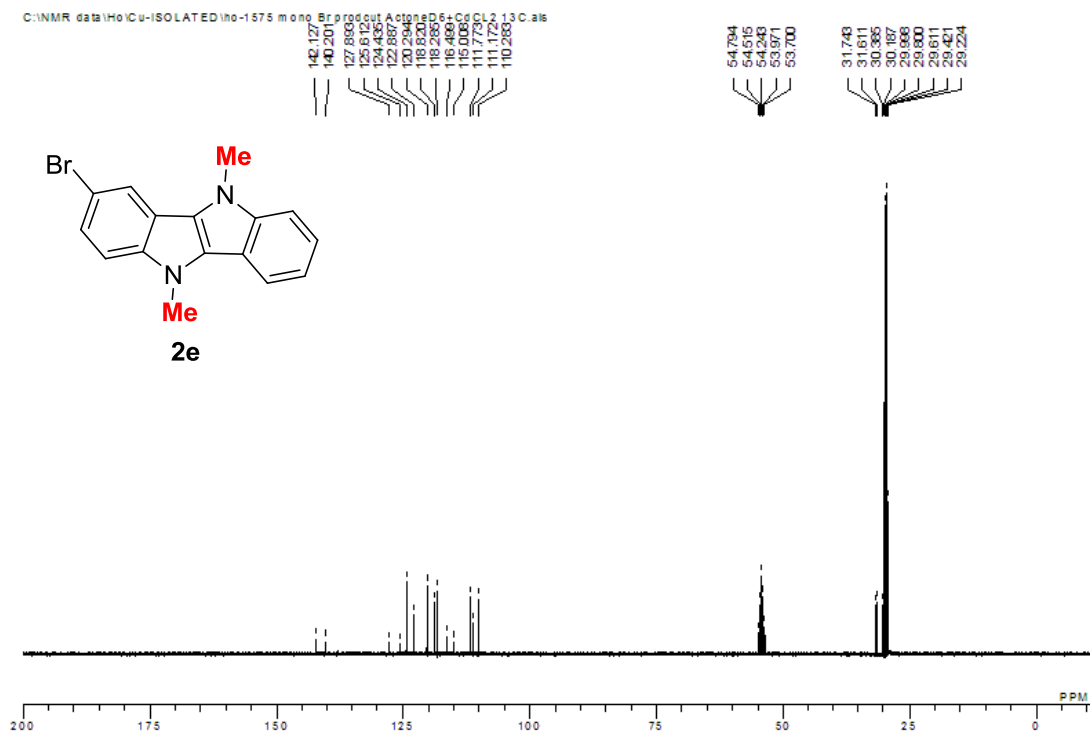


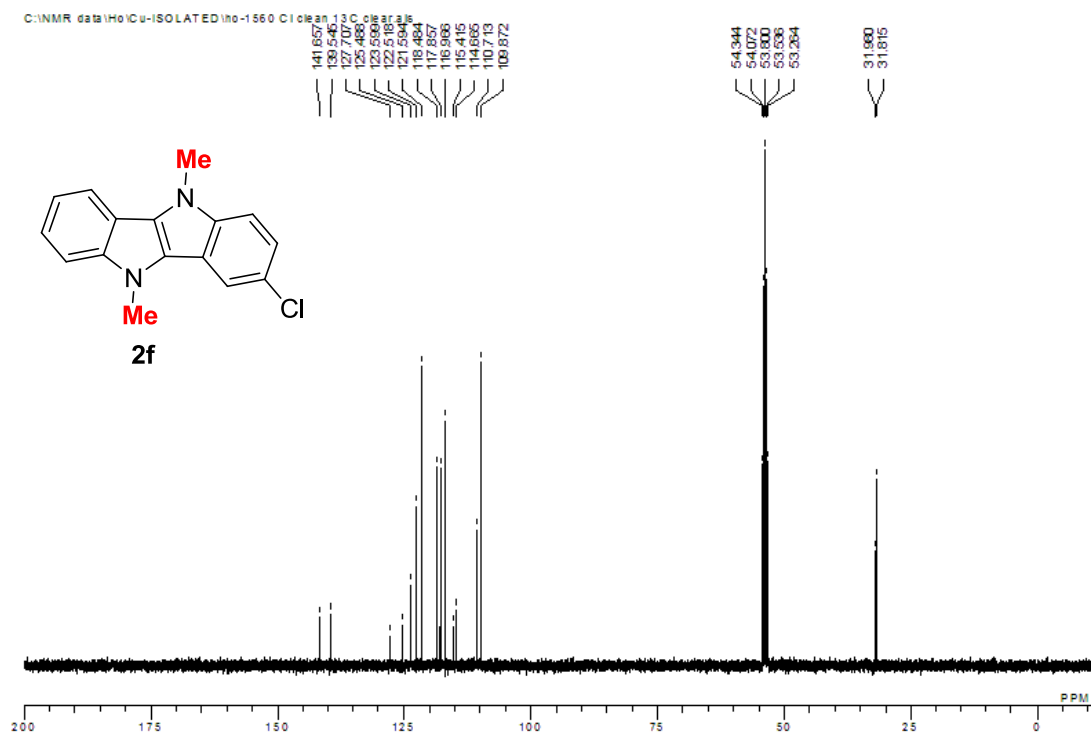
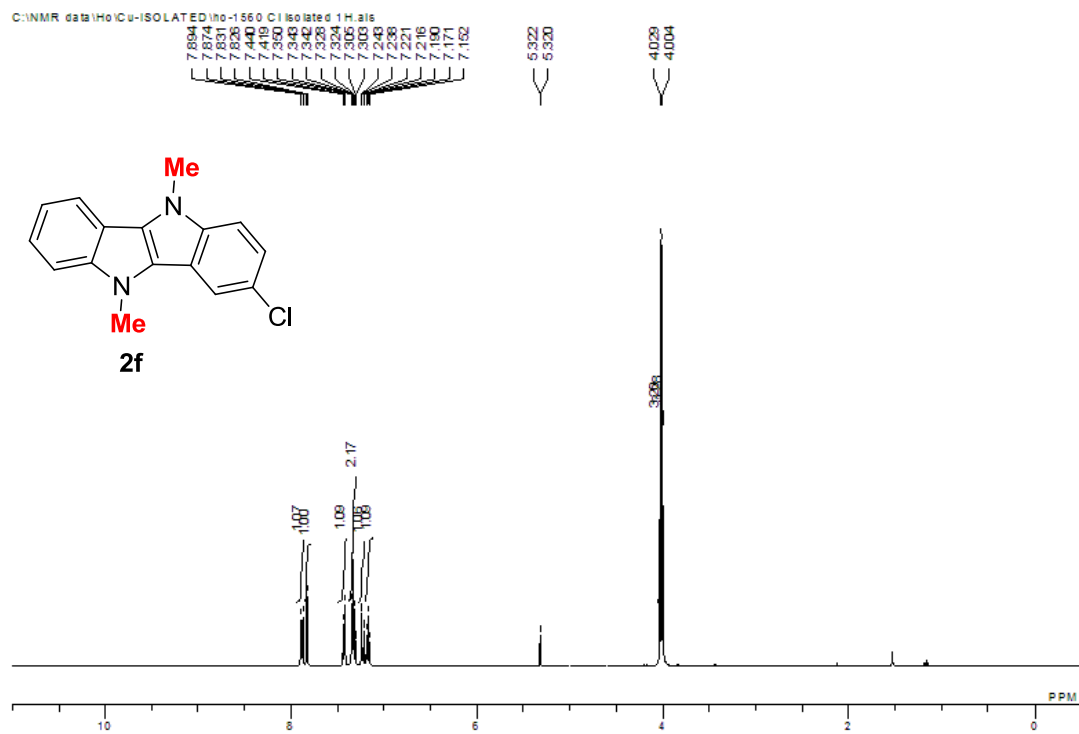
C:\NMR data\Ho\Cu-ISOLATED\product 2\ho-1544\iso 2c C6Cl2 1 H.a16

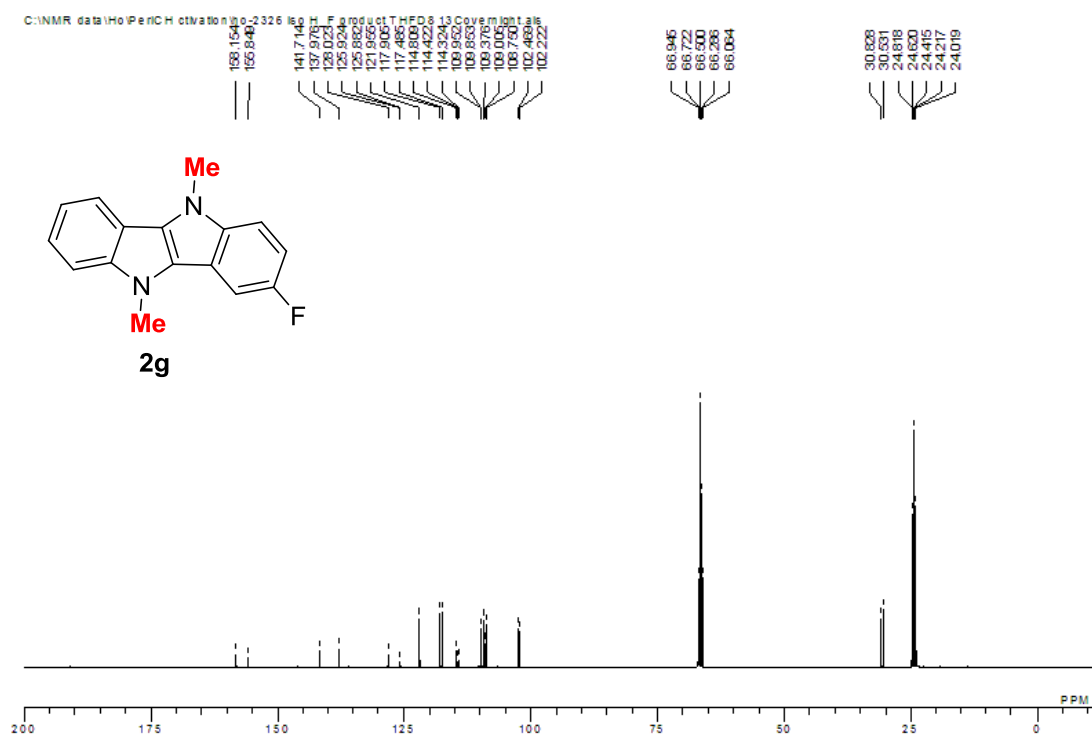
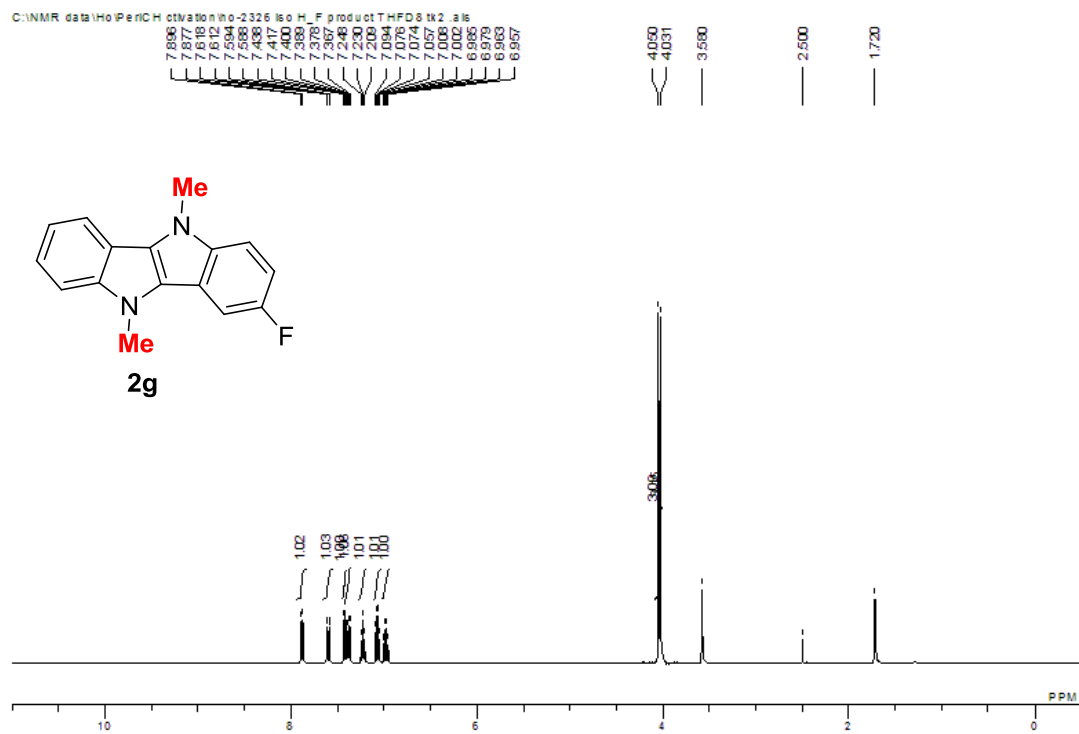


C:\NMR data\Ho\Cu-ISOLATED\product 2\ho-1544\iso 2c C6Cl2 1 H.a16

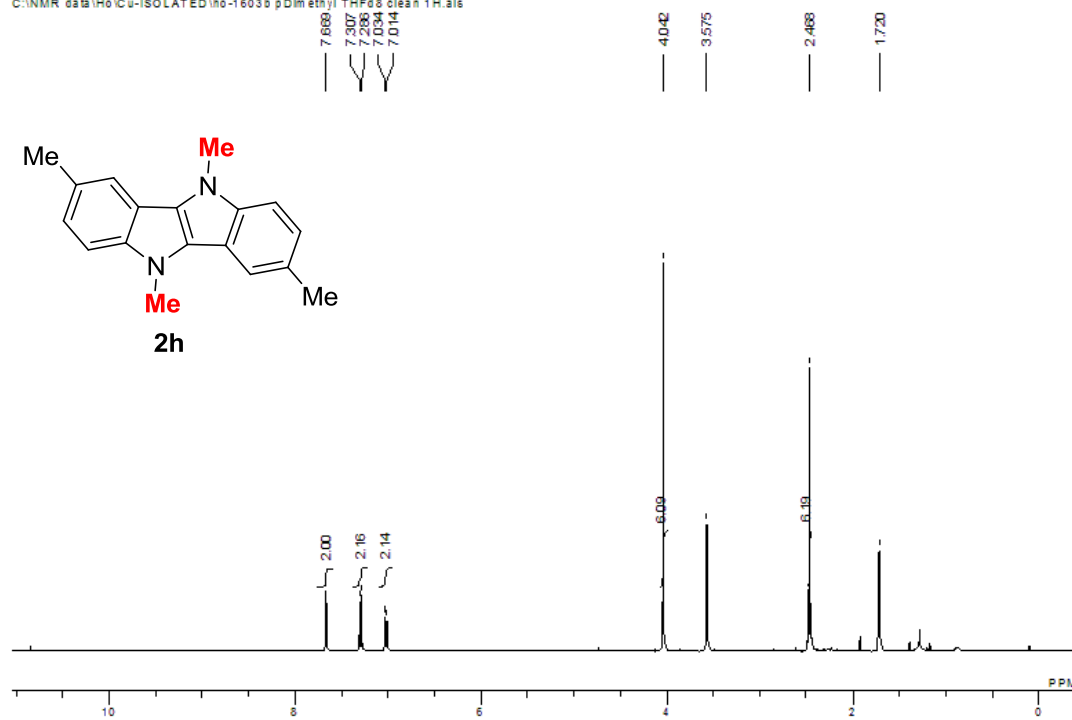




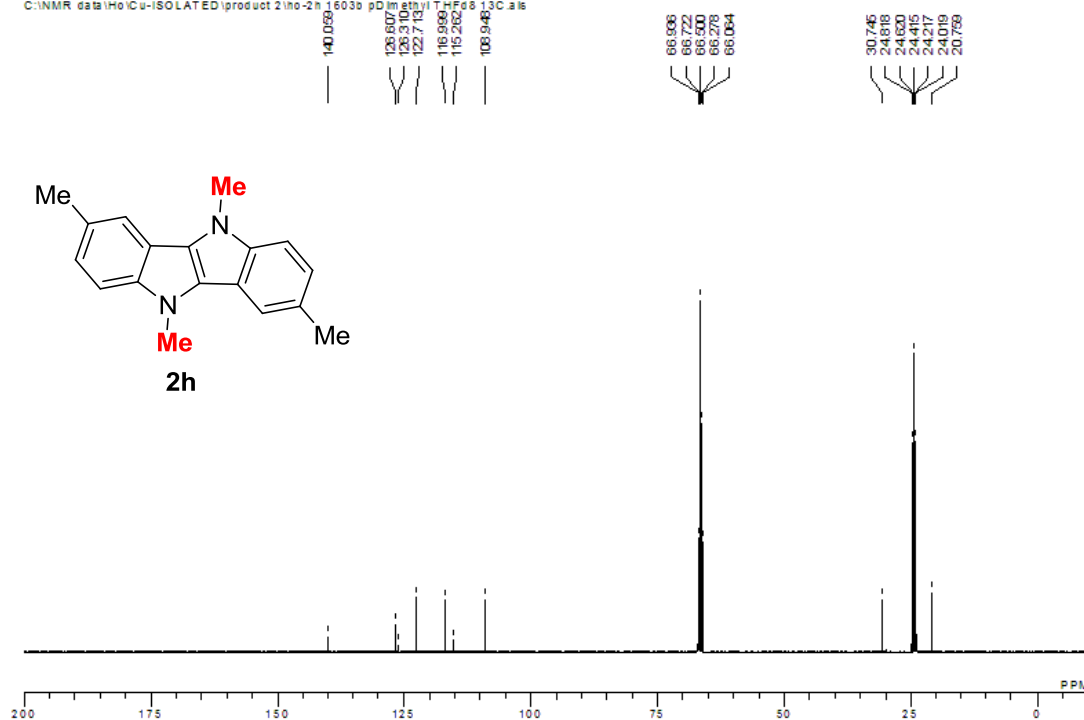




C:\NMR data\Ho\Cu-ISOLATED\ho-1603b pDImethyl THF d8 clean 1H.a16



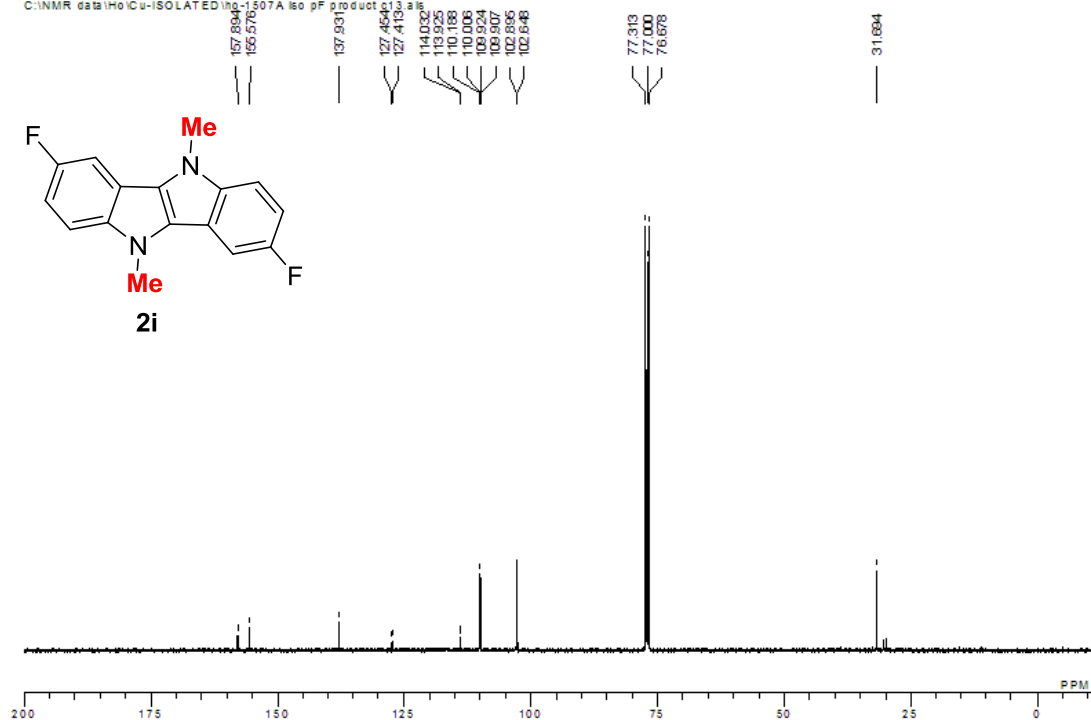
C:\NMR data\Ho\Cu-ISOLATED\product 2\ho-2h 1603b pDImethyl THF d8 13C.a16



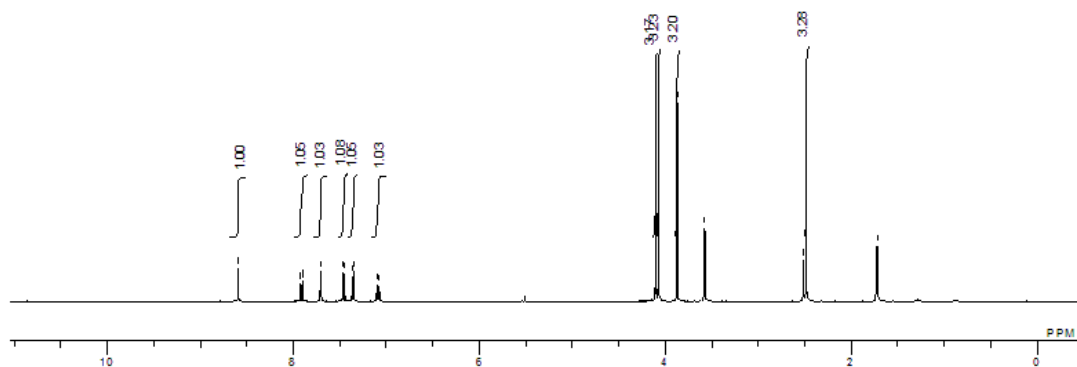
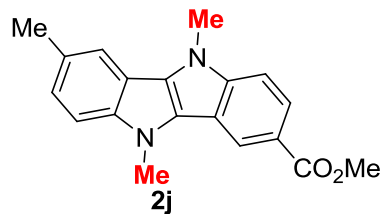
C:\NMR data\Ho\Cu-ISOLATED\product 2\ho-2i\1507a.pDI.F CdCL3 clean 1H.als.als



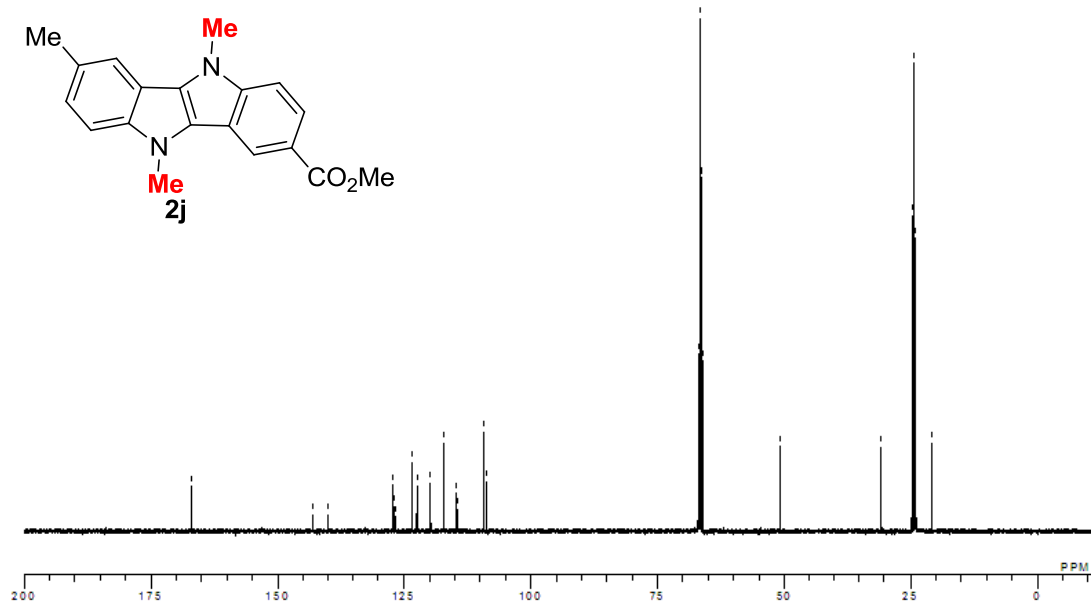
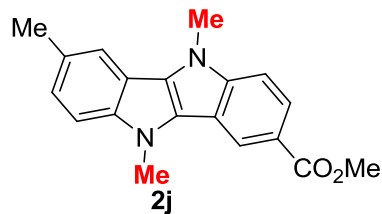
C:\NMR data\Ho\Cu-ISOLATED\ho-1507A Iso pF product\1.als

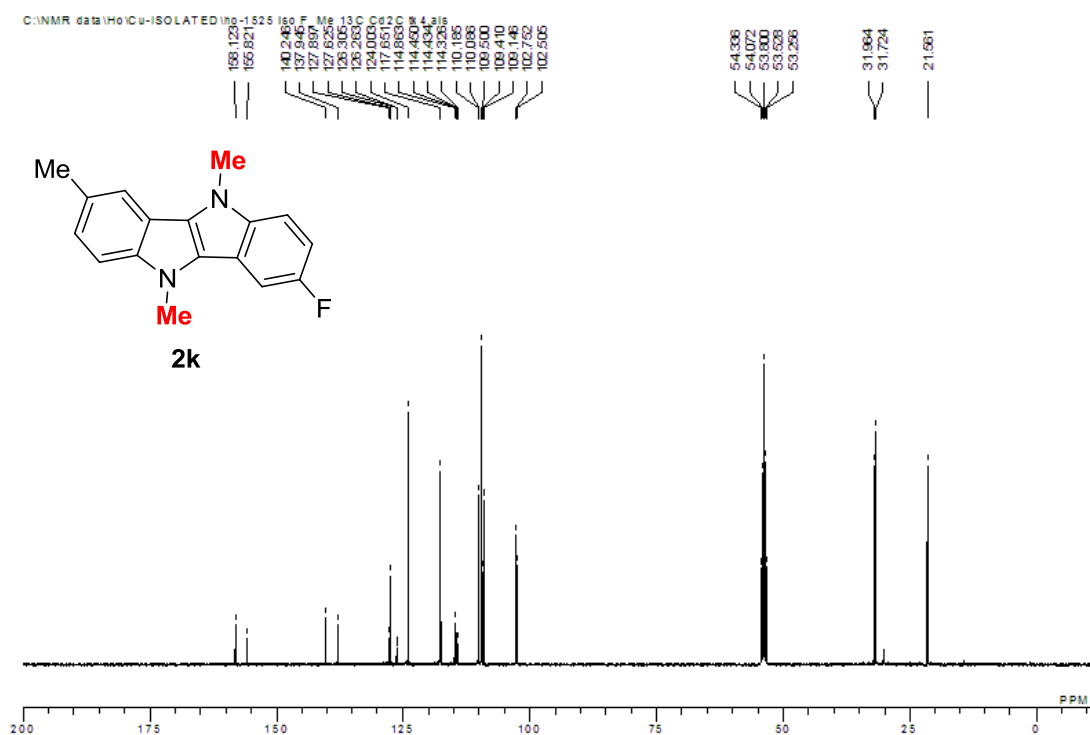
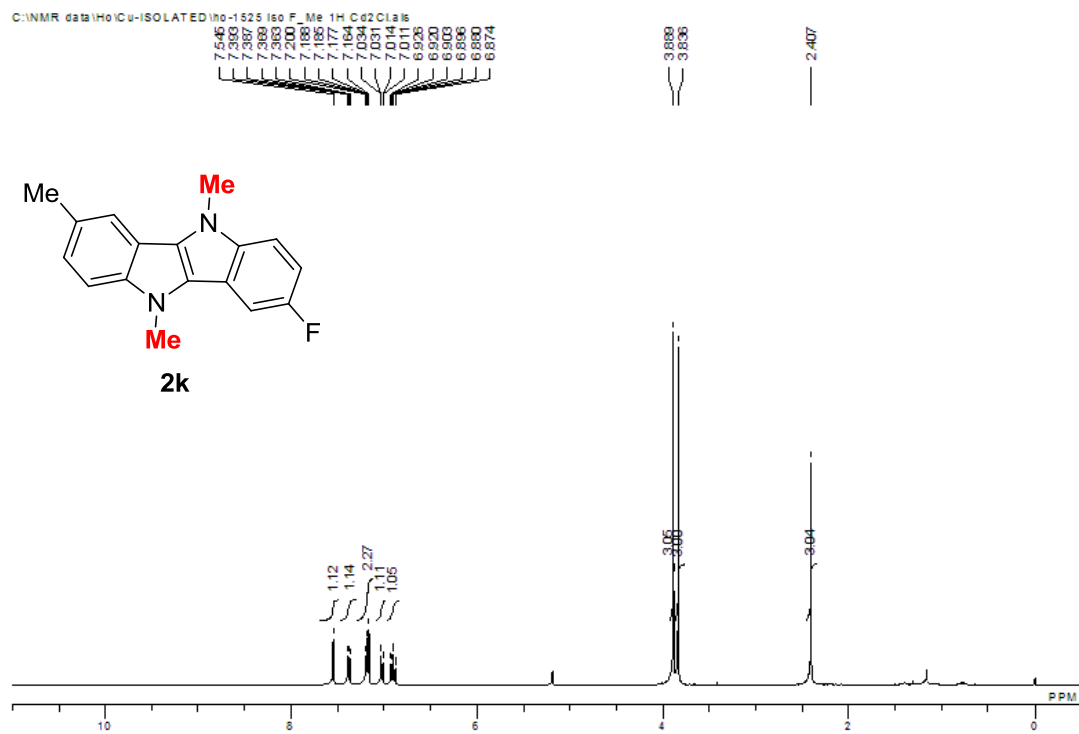


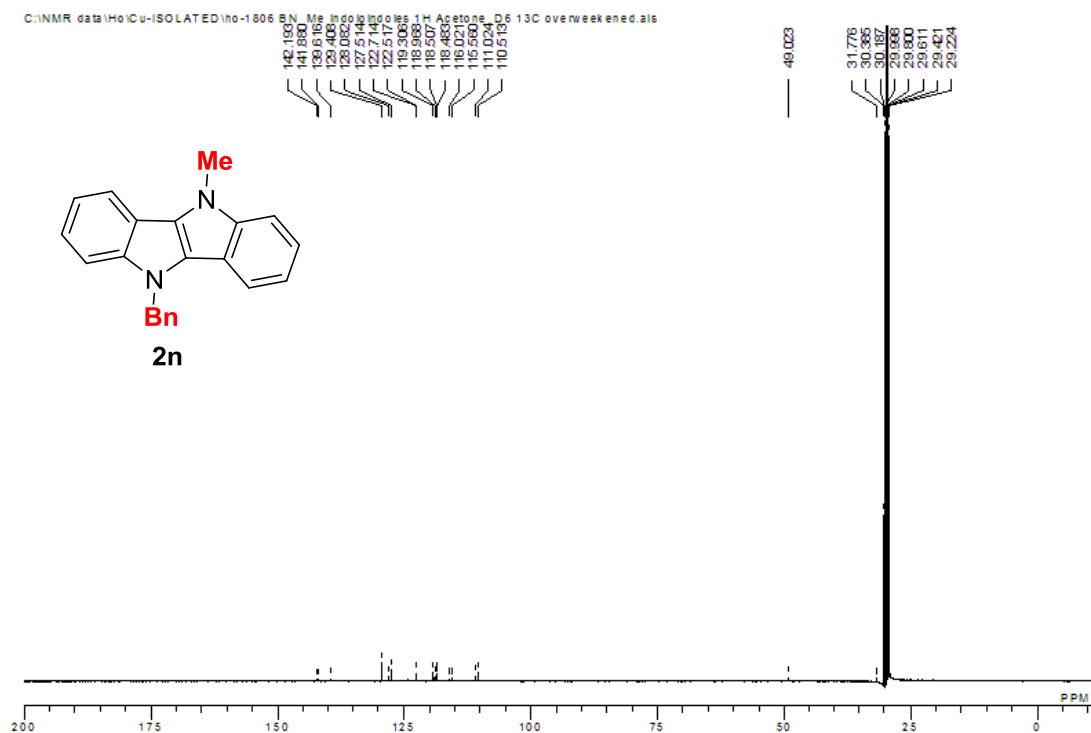
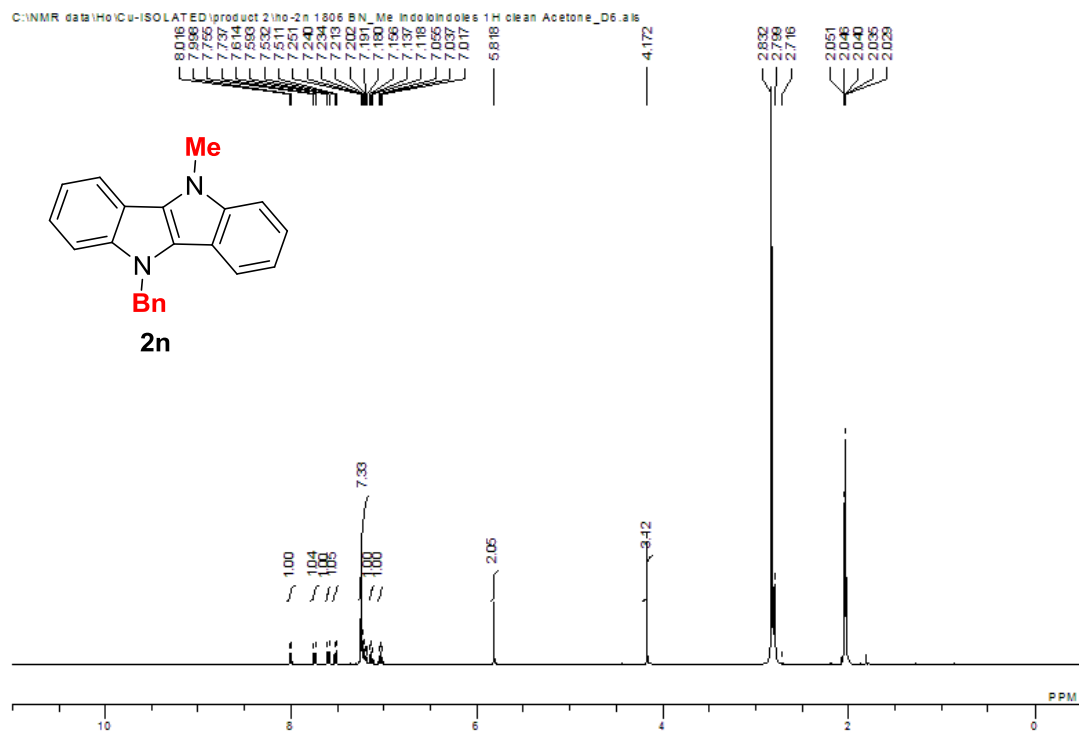
C:\NMR data\Ho\ICU-ISOLATED\ho-1583 Iso THF-D5 1H Me_CO2Me.ale



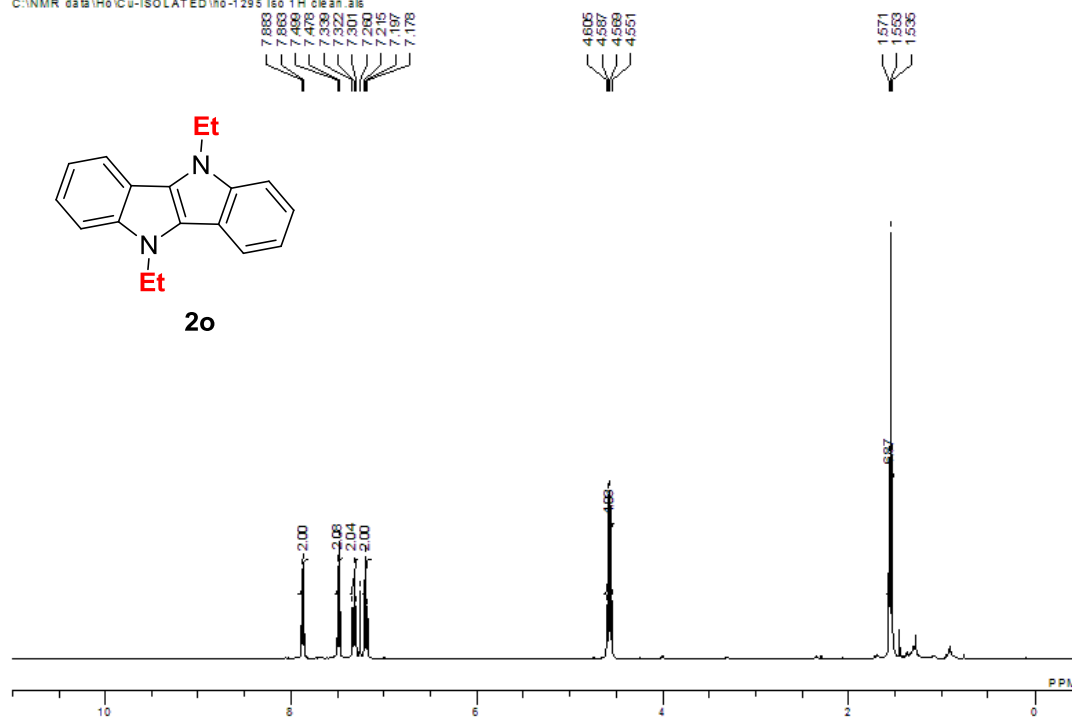
C:\NMR data\Ho\ICU-ISOLATED\ho-1583 Iso THF-D5 13C Me_CO2Me.ale



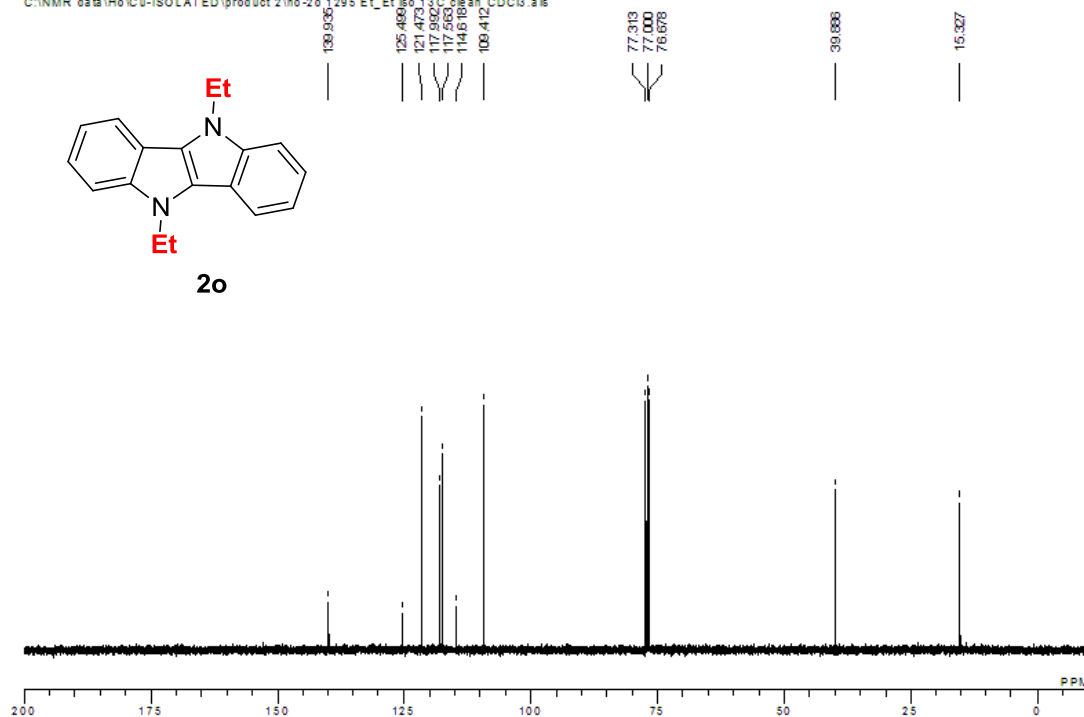




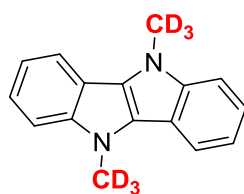
C:\NMR data\Ho\ICU-ISOLATED\ho-1295 iso 1H clean.a1s



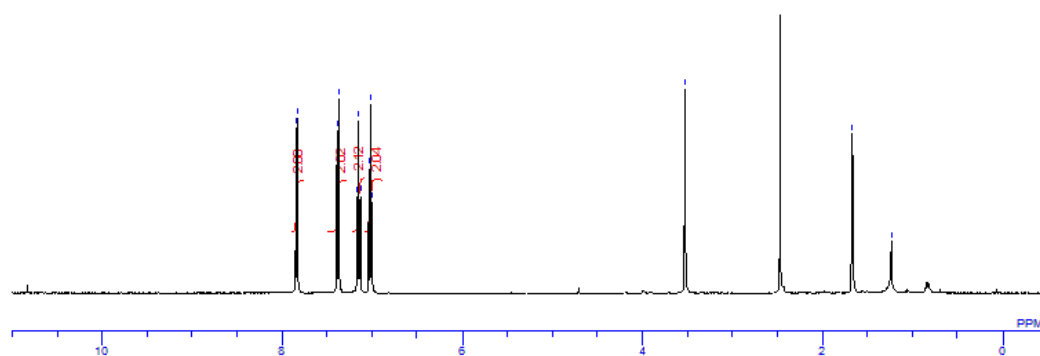
C:\NMR data\Ho\ICU-ISOLATED\product 2\ho-2o 1295 Et_Et iso 13C clean CDCl3.a1s



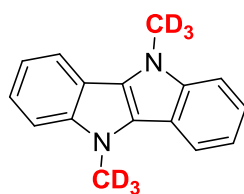
C:\NMR data\Ho\Cu-ISOLATED\ho-1650 CD3 product THF d8 ty. ais



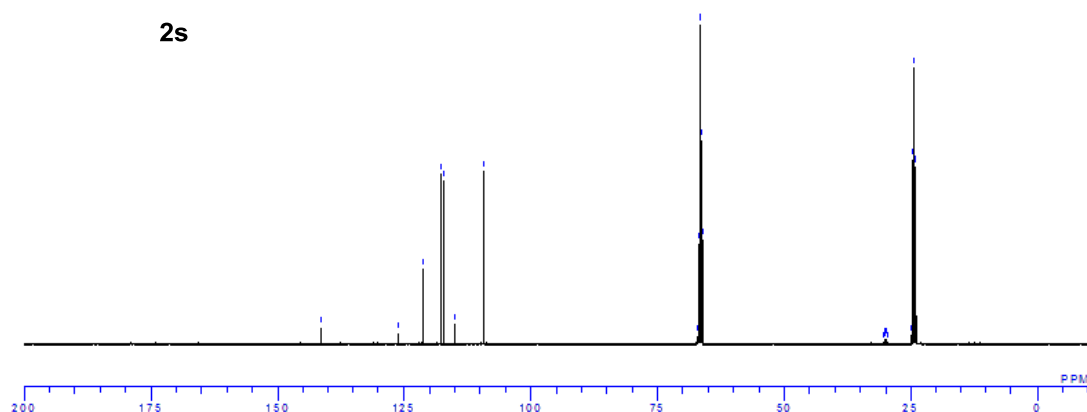
2s

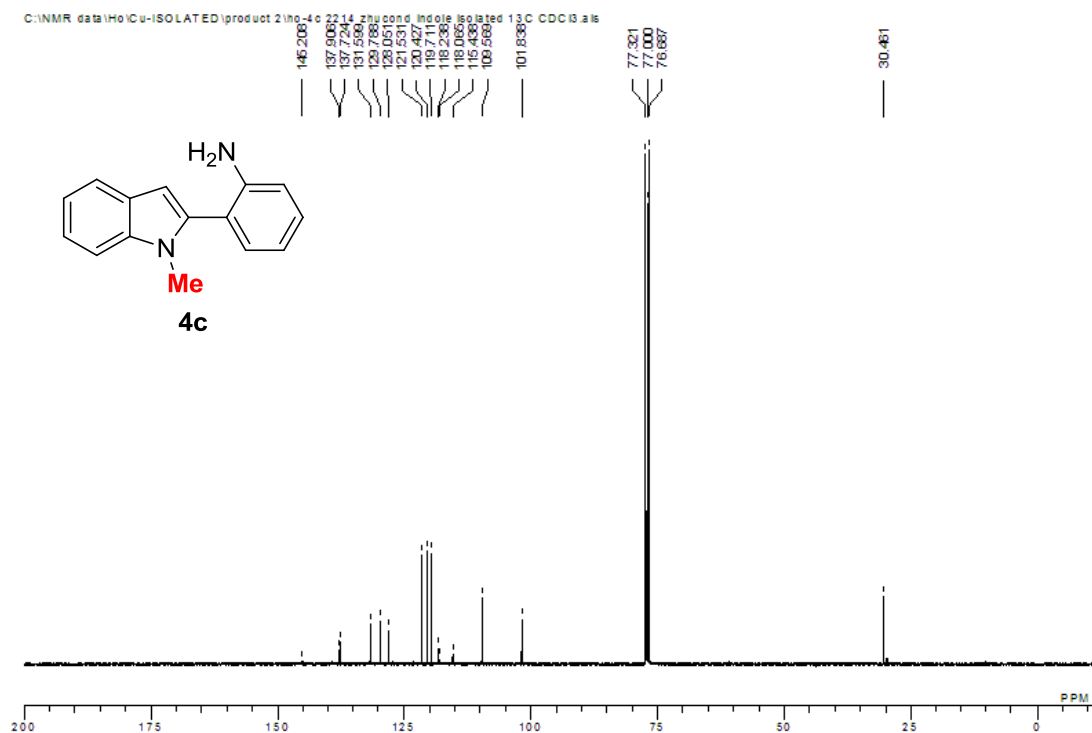
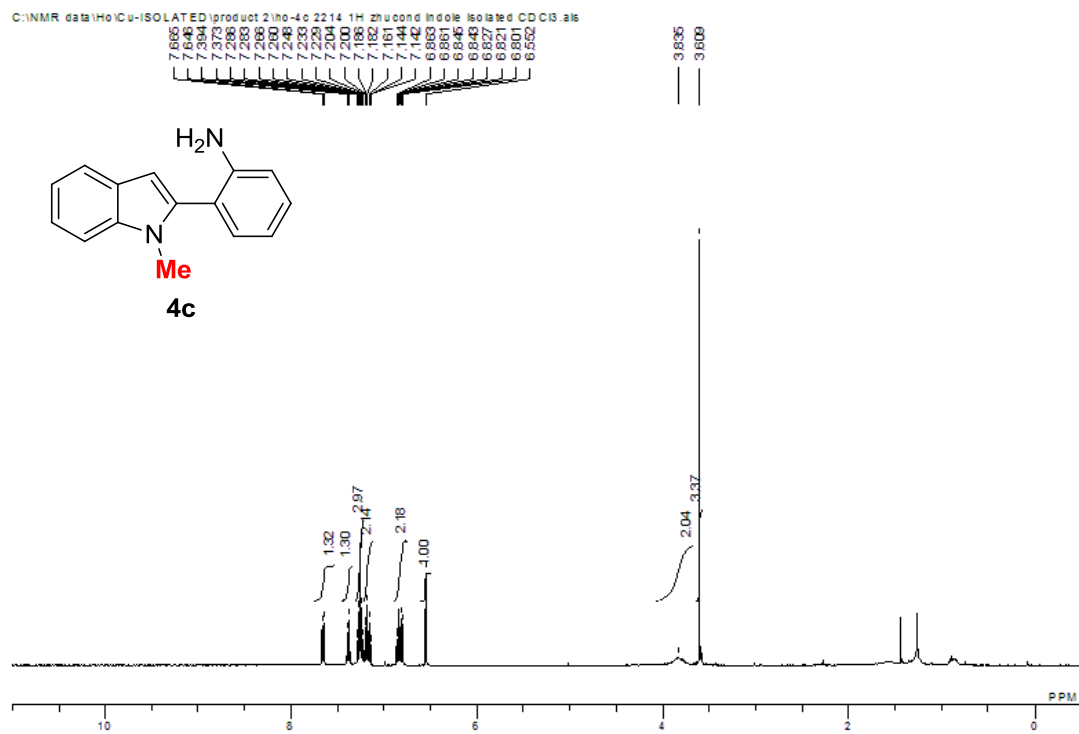


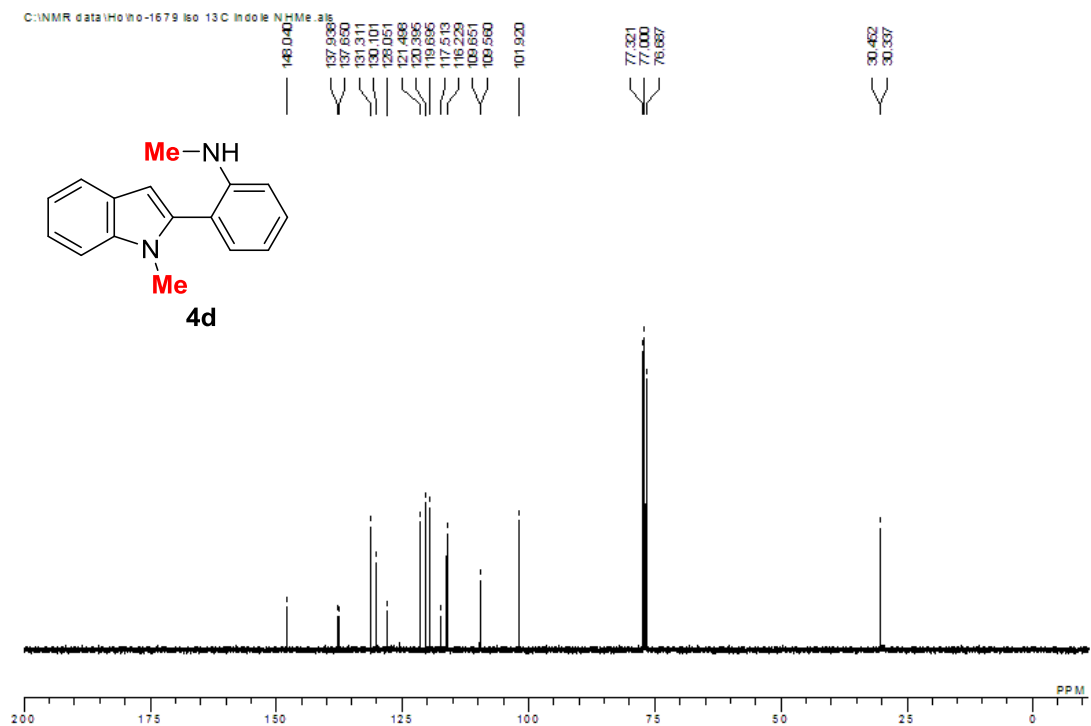
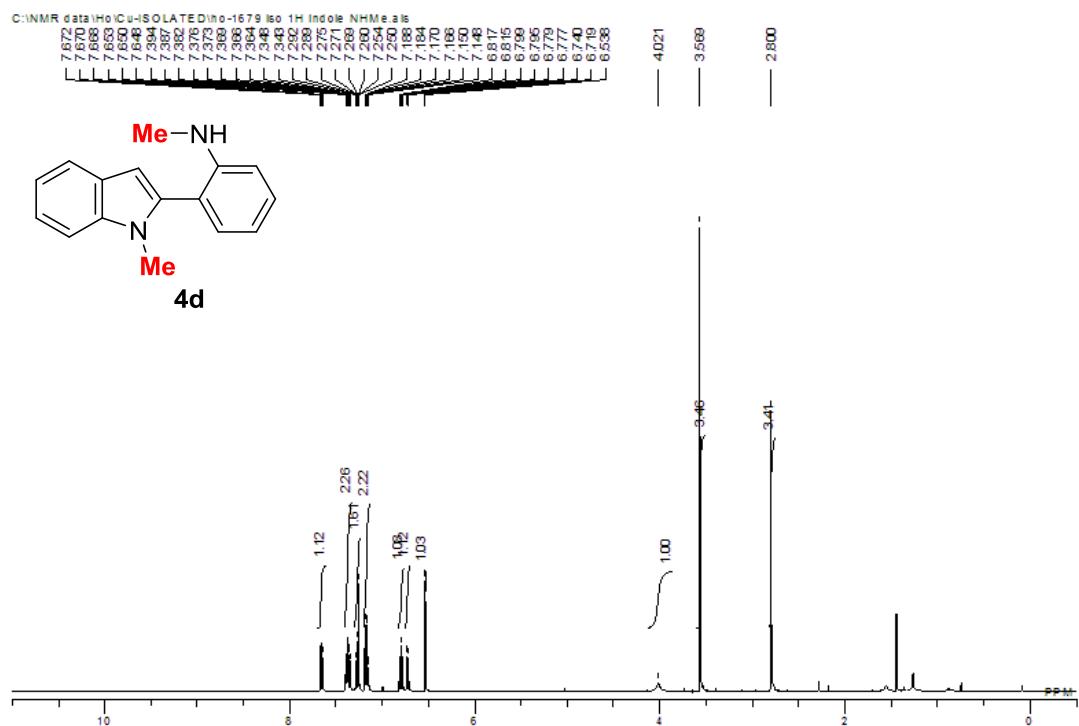
C:\NMR data\Ho\Cu-ISOLATED\product 2\ho-2s 1650 deuterated CD3 CD3 13 C THF d8. ais

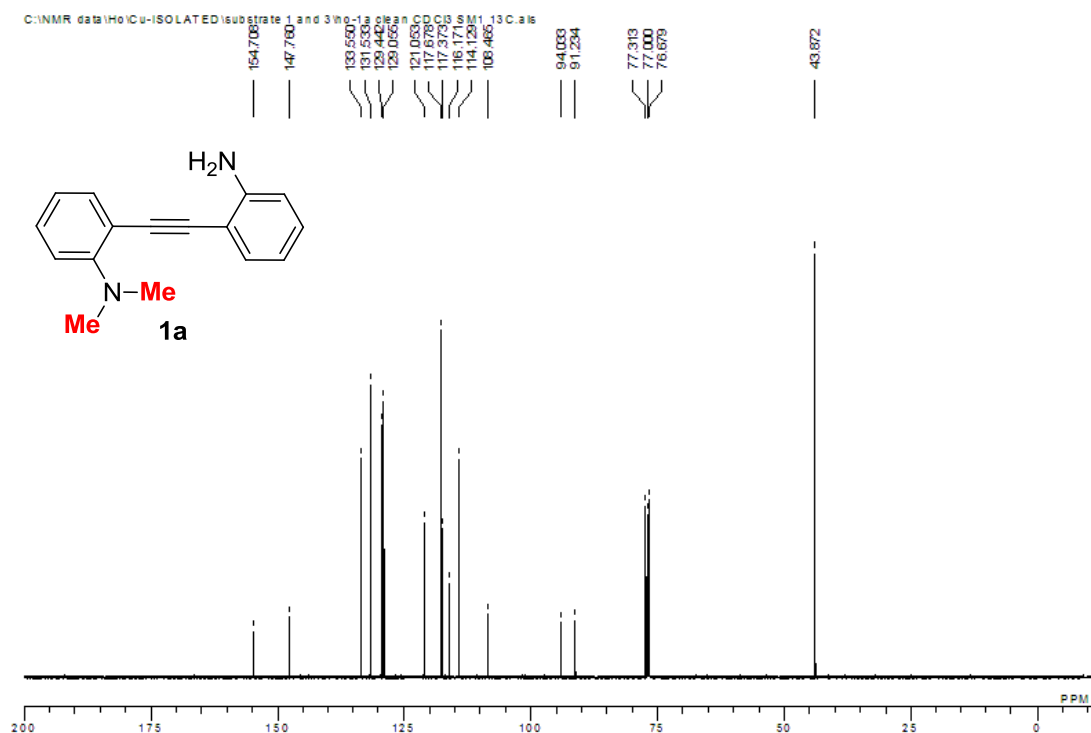
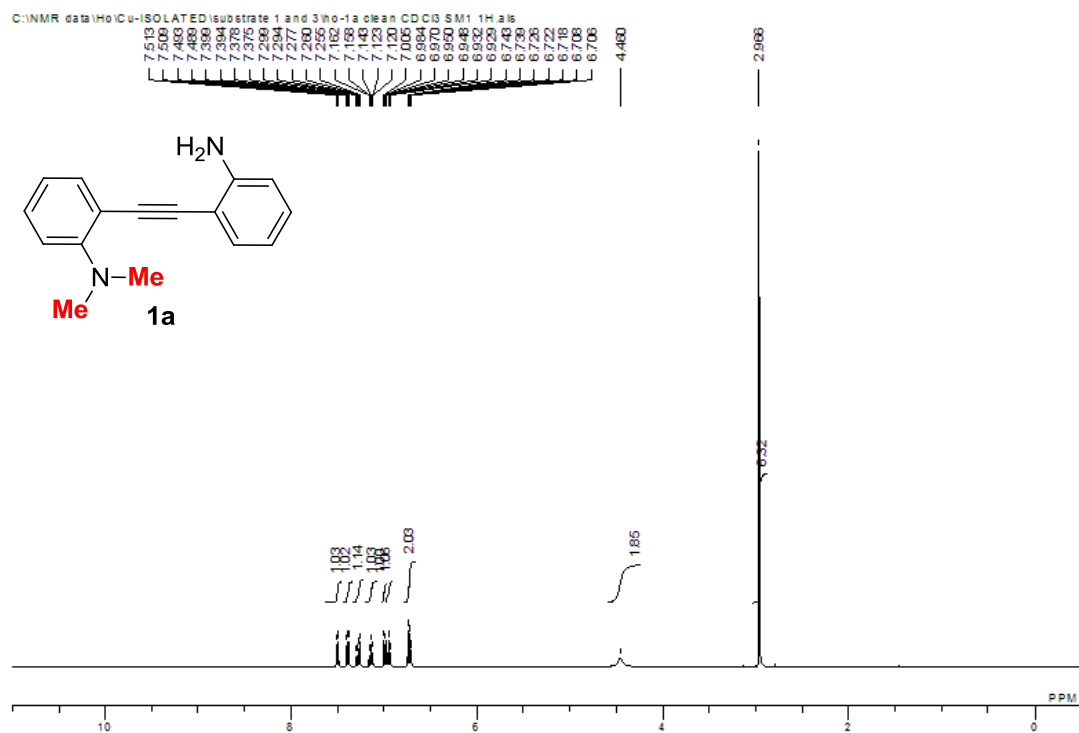


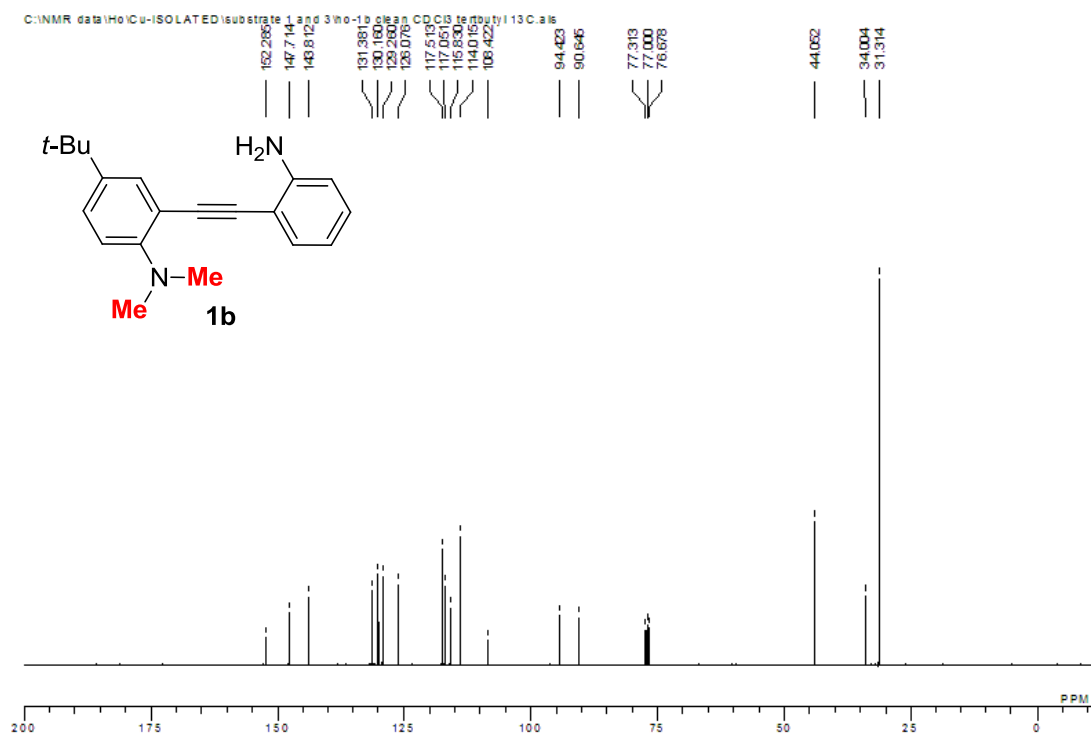
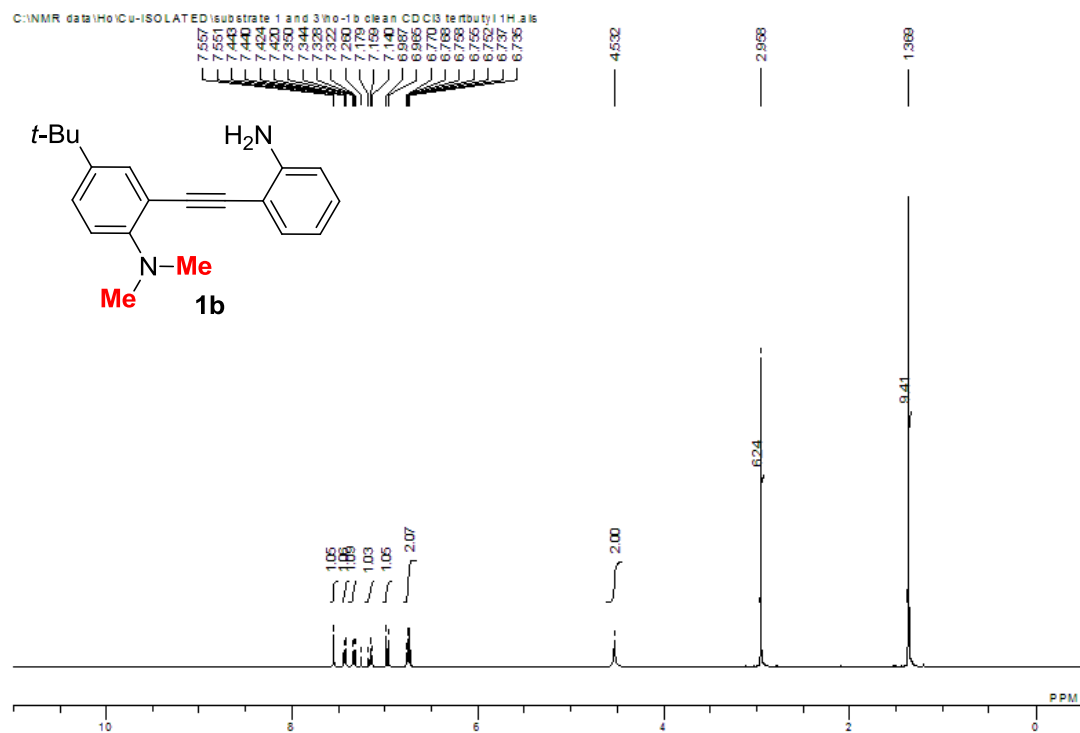
2s

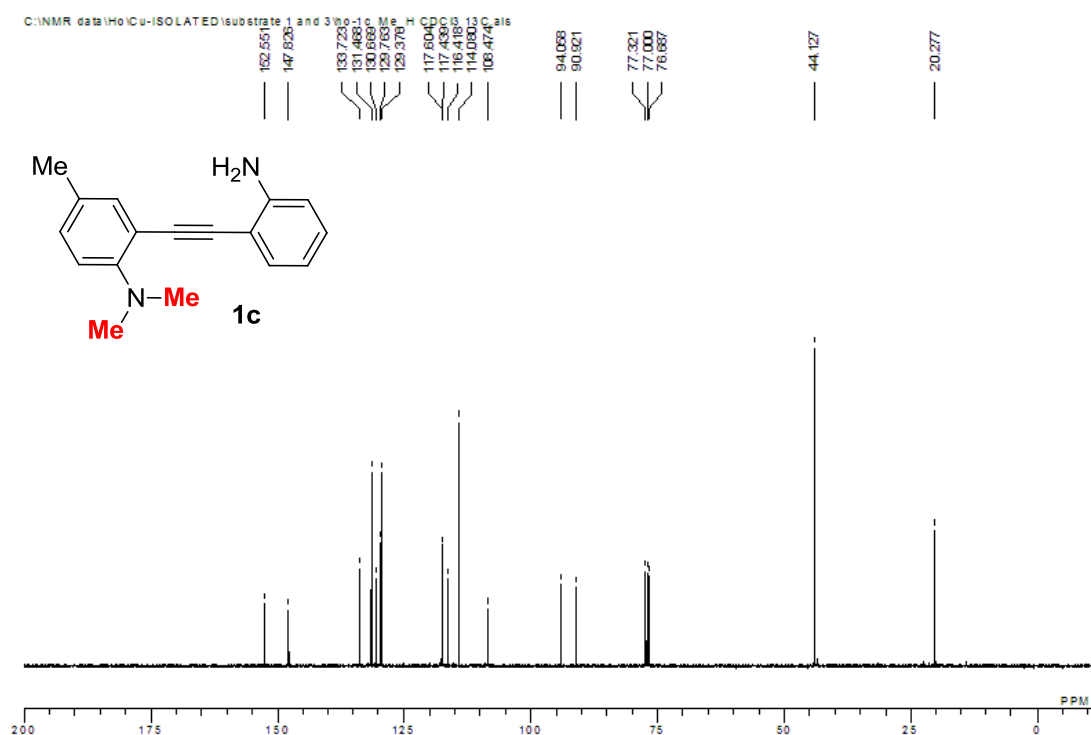
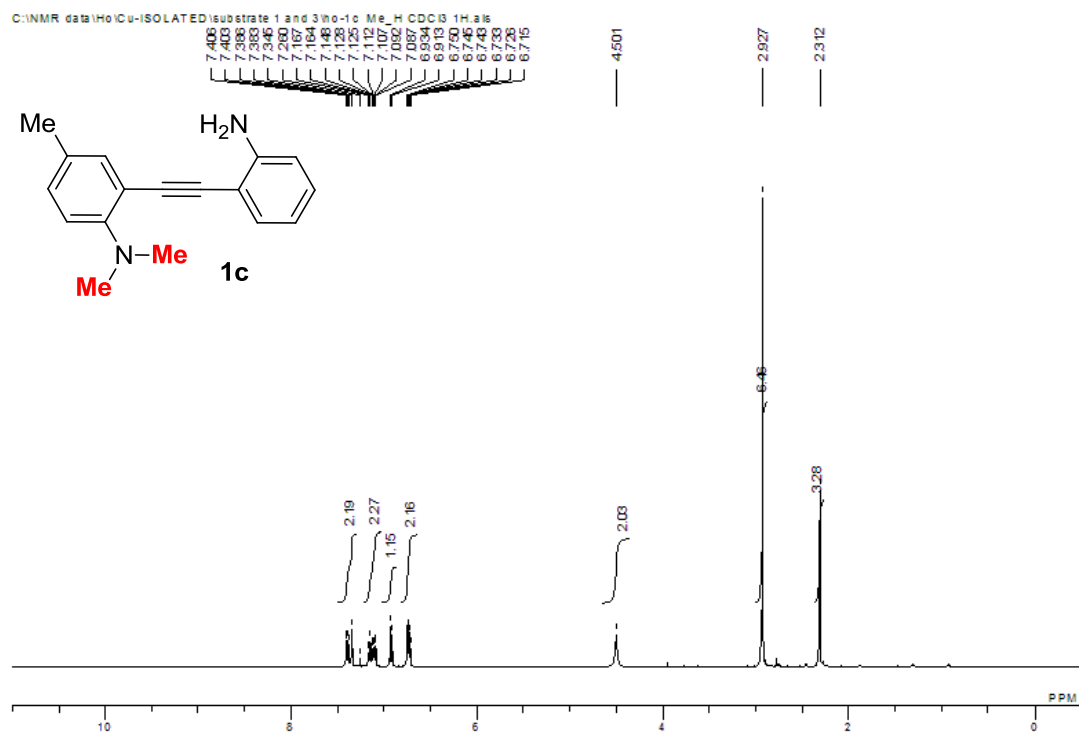


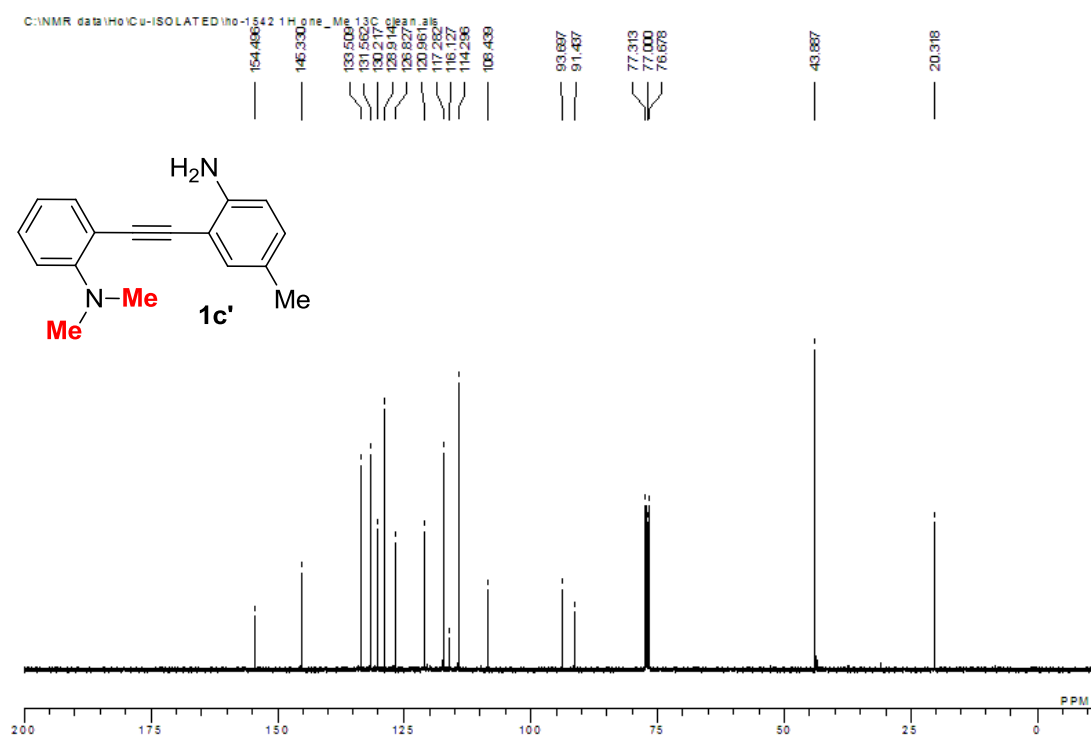
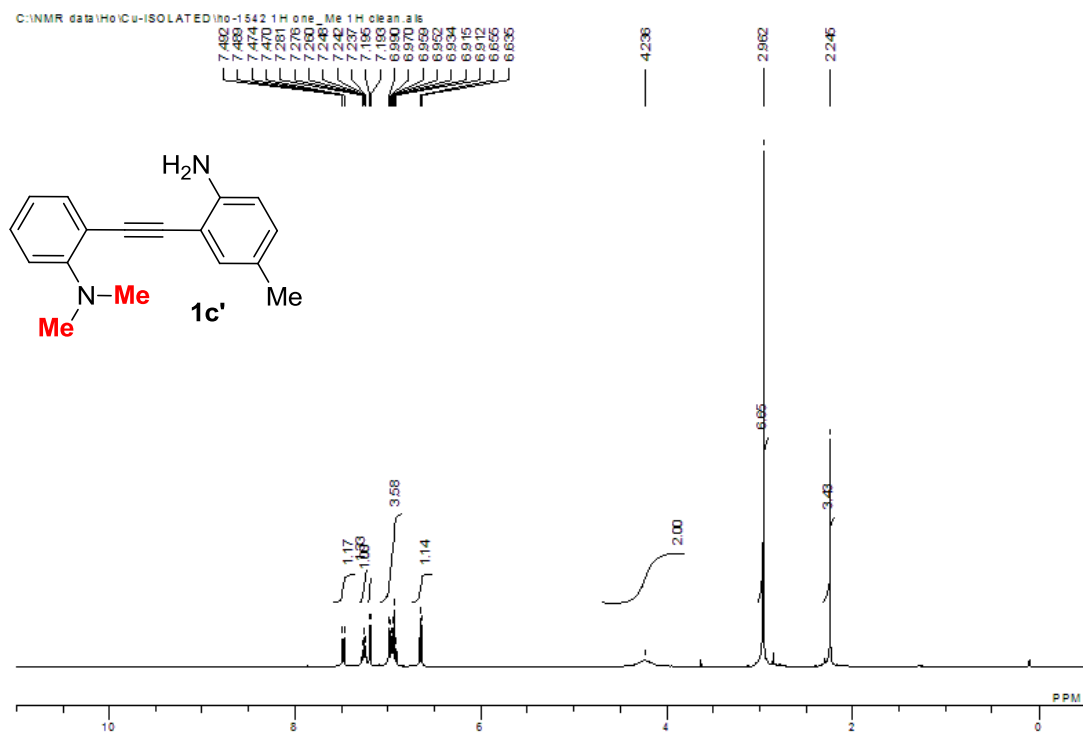


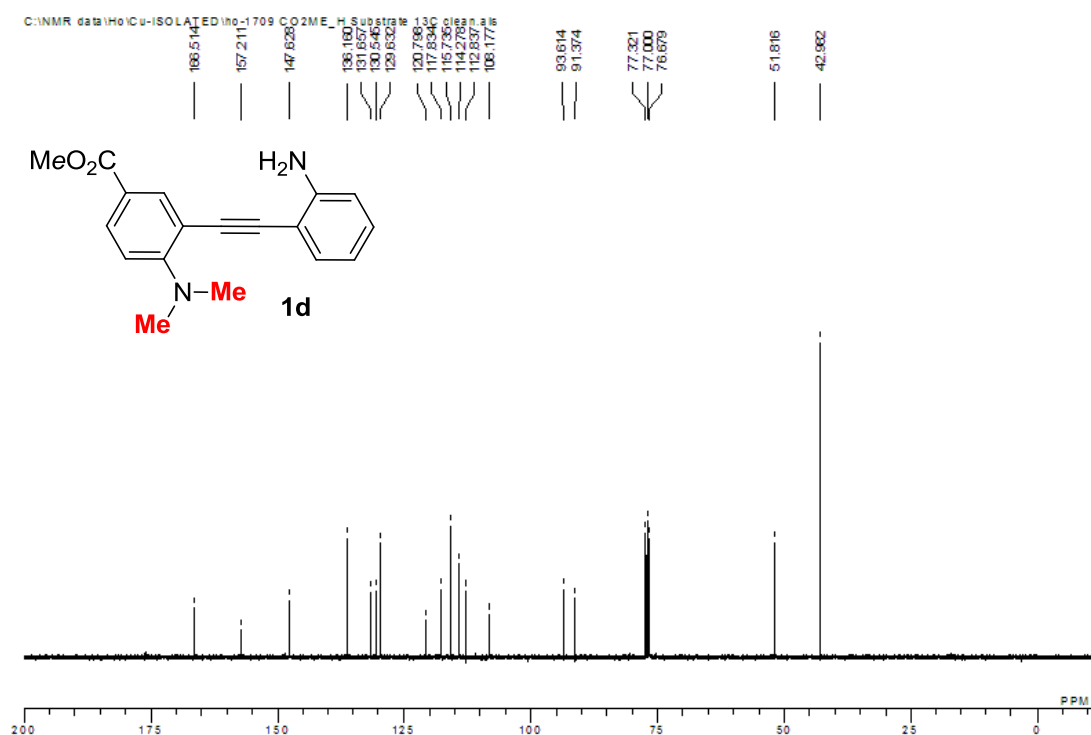
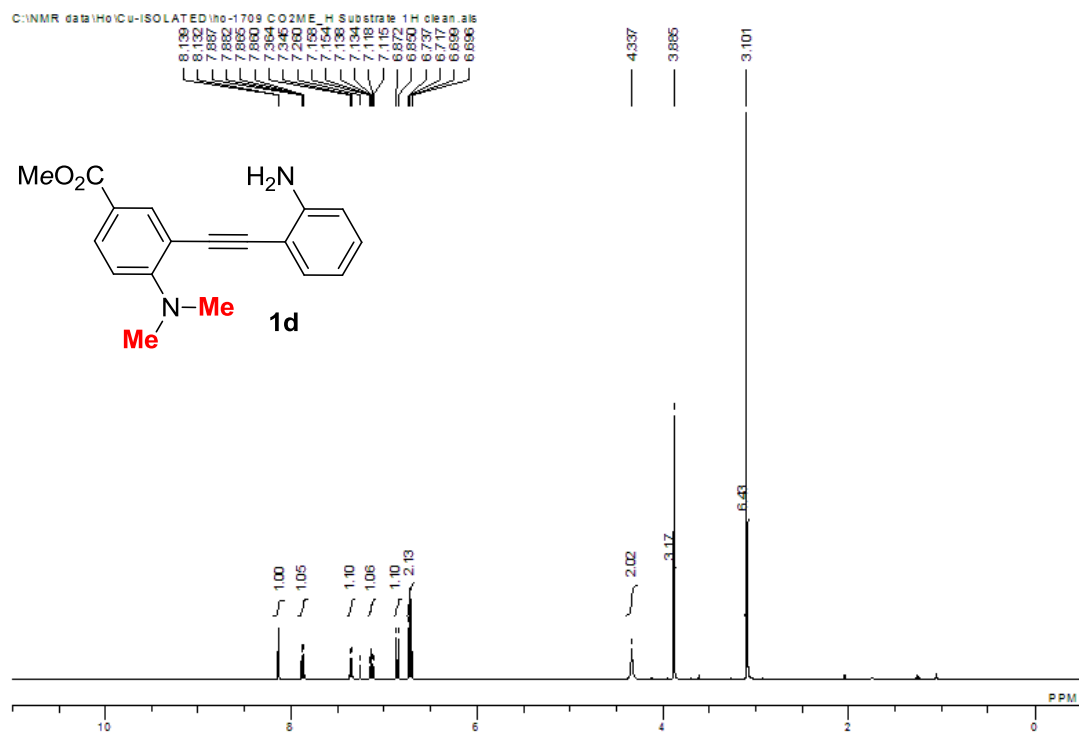


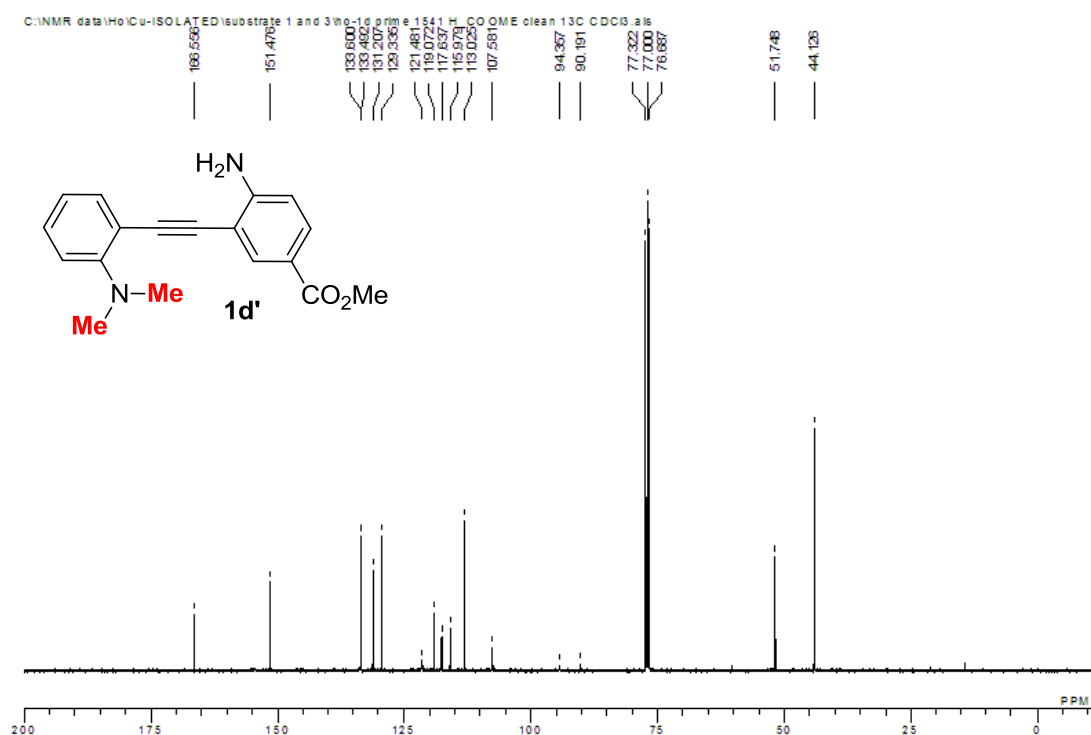
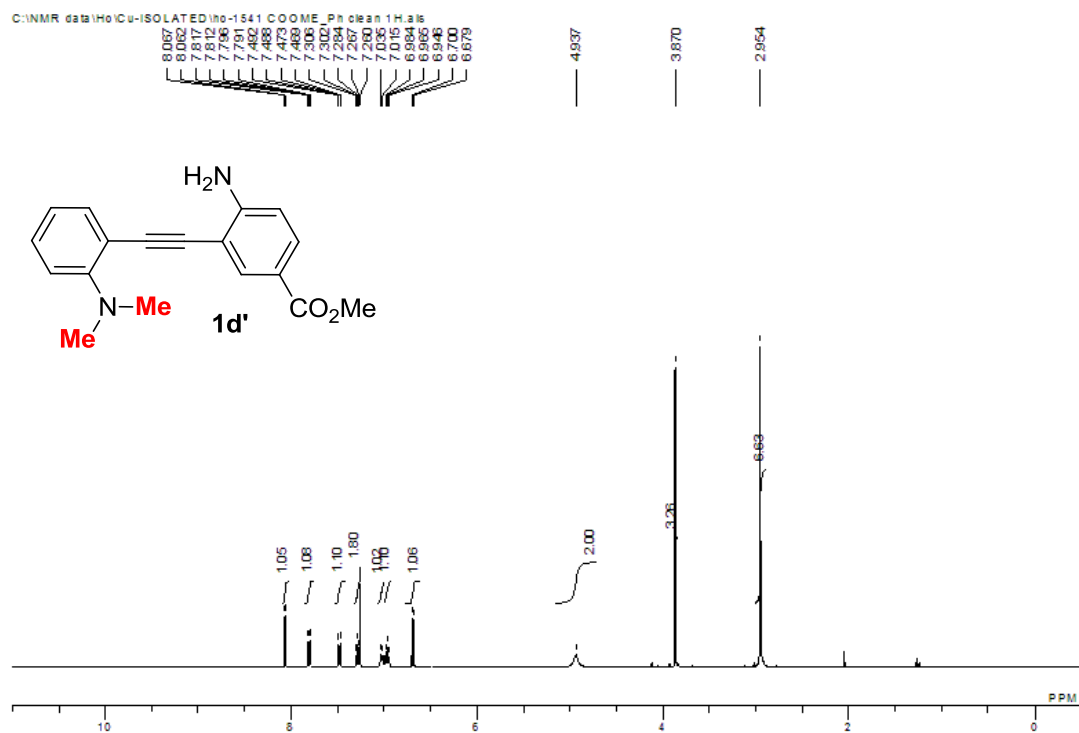


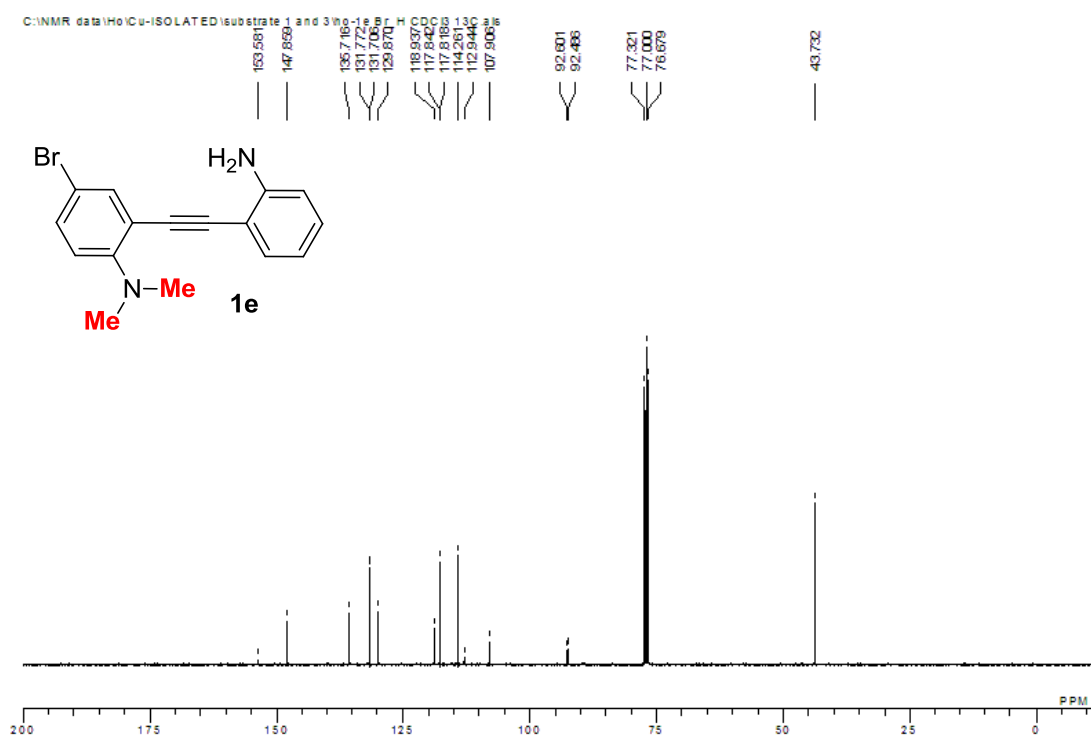
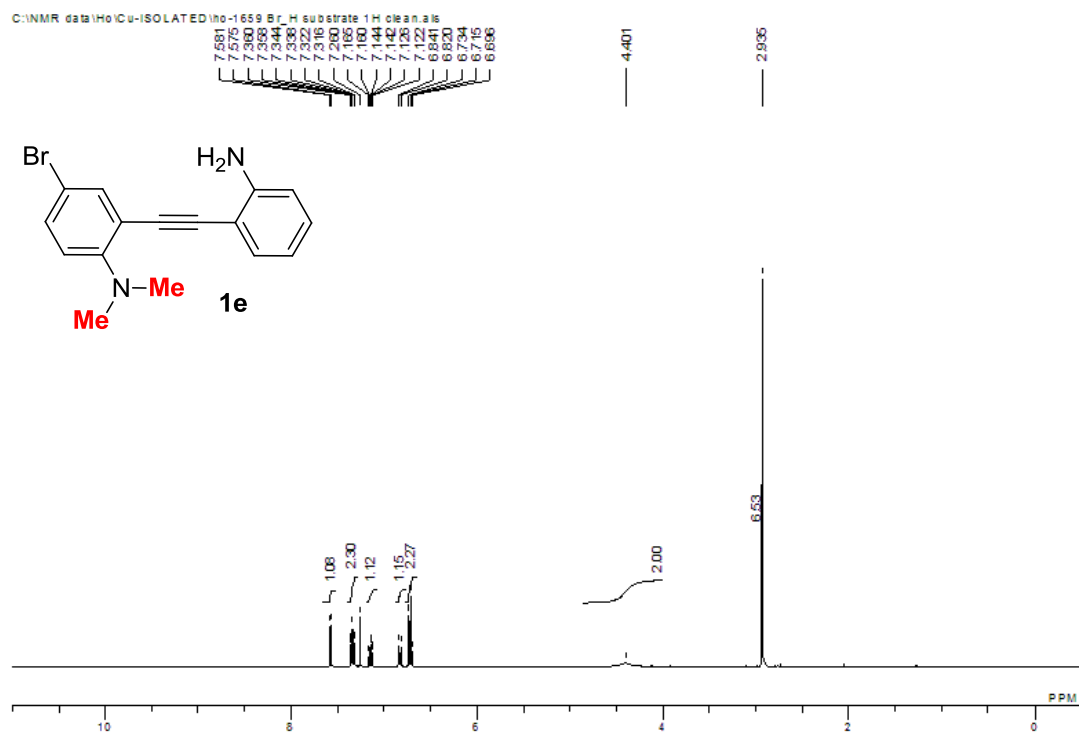


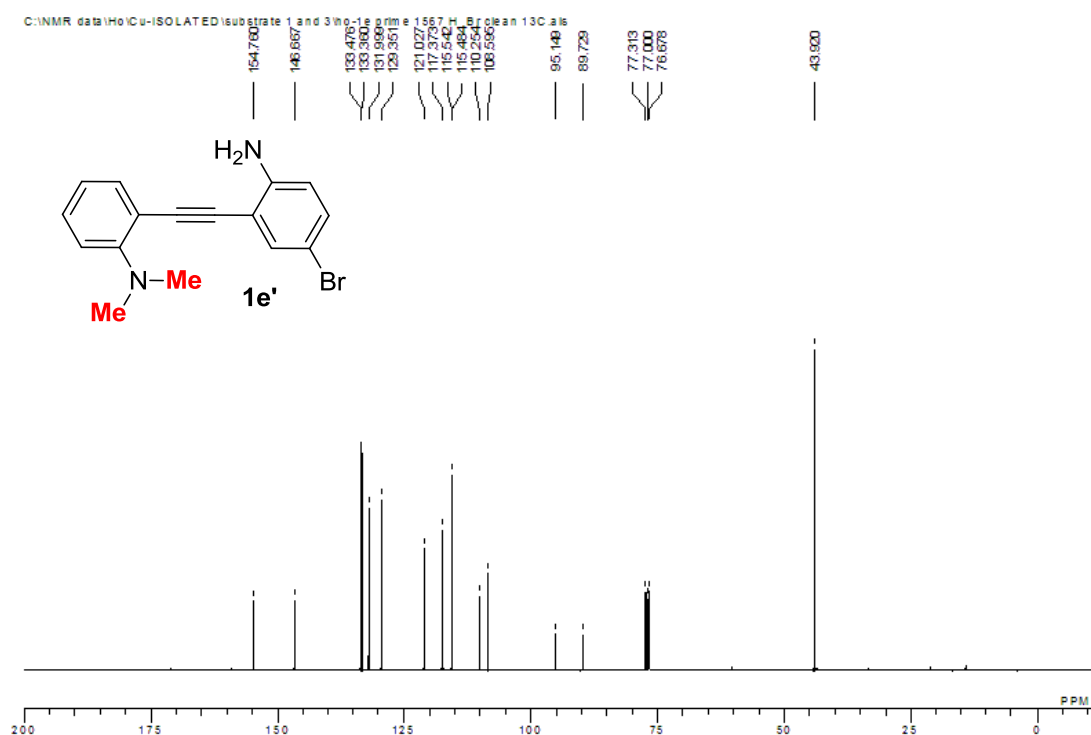
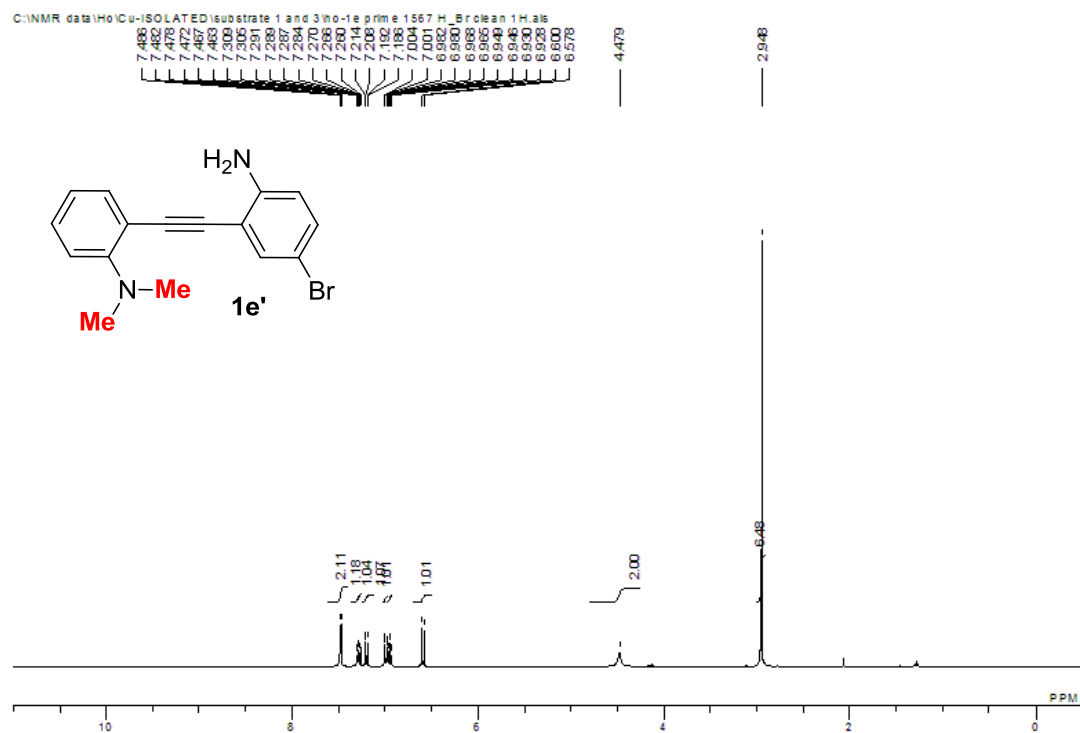


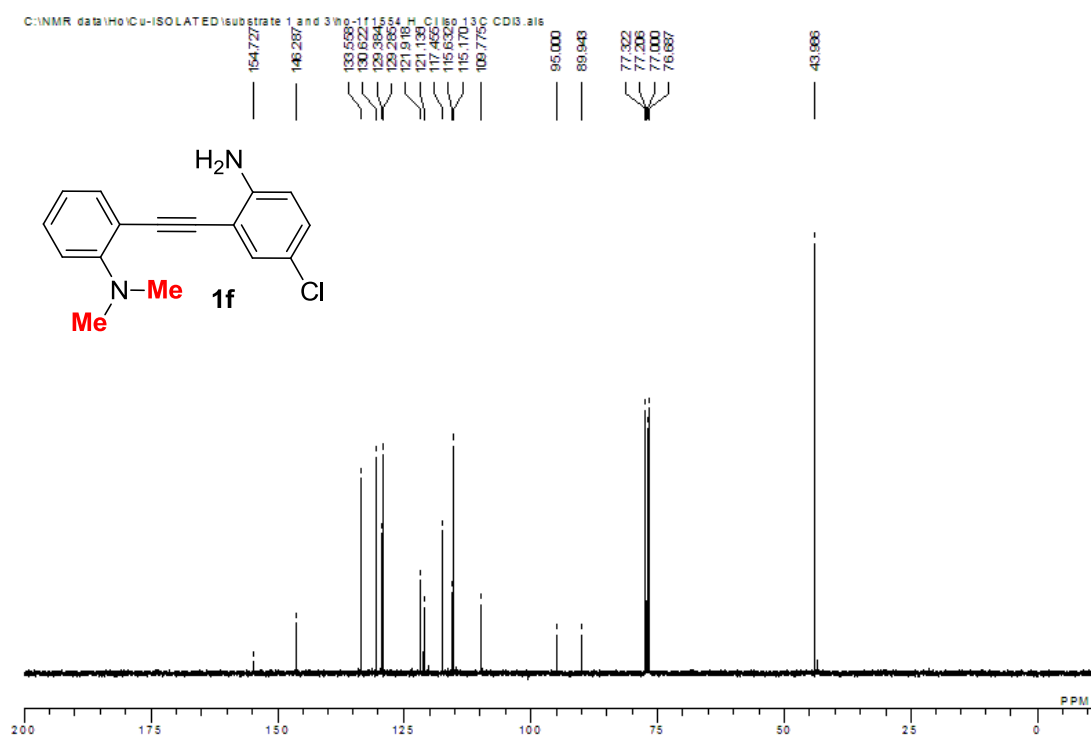
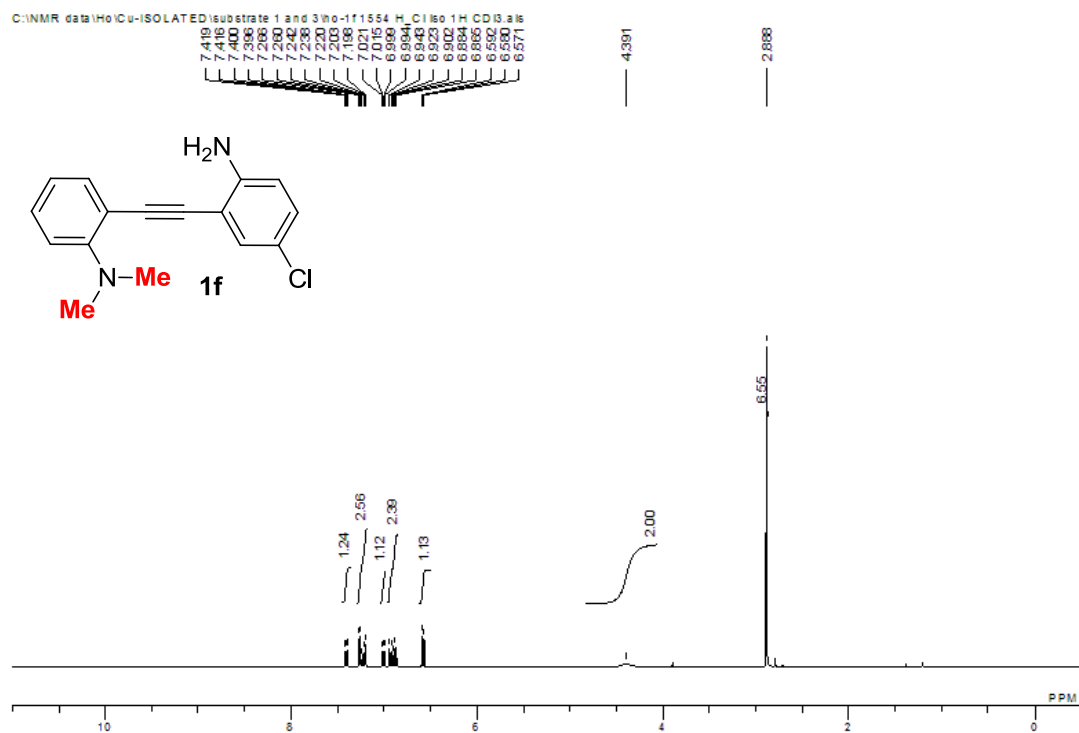


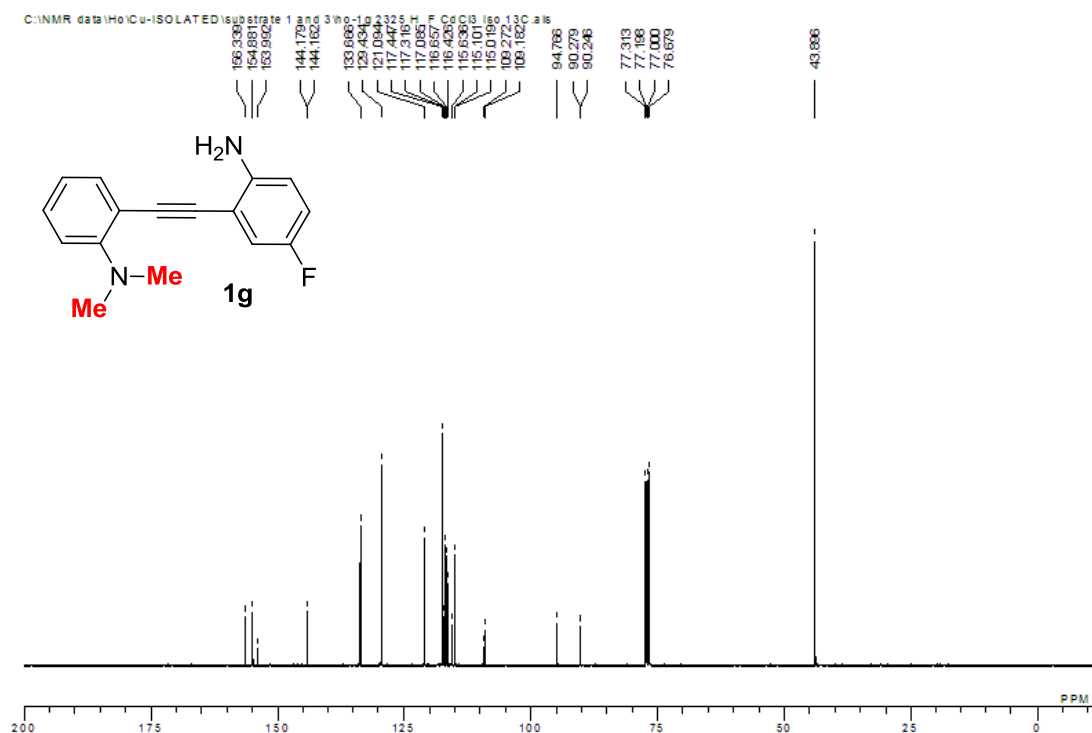
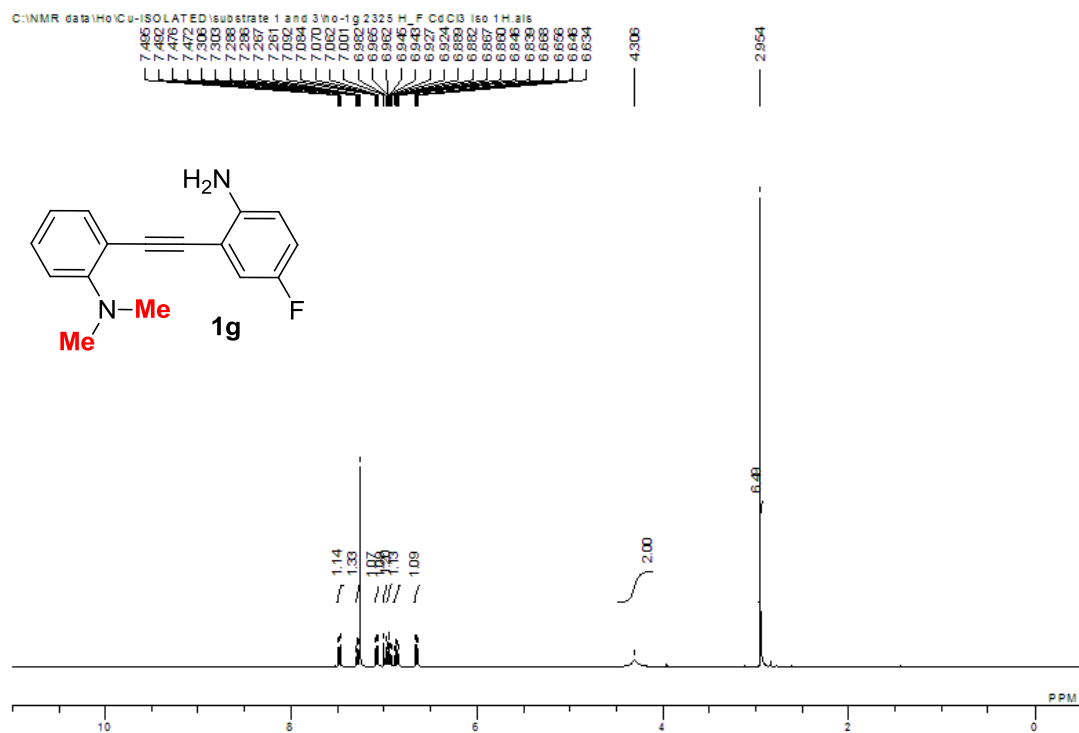


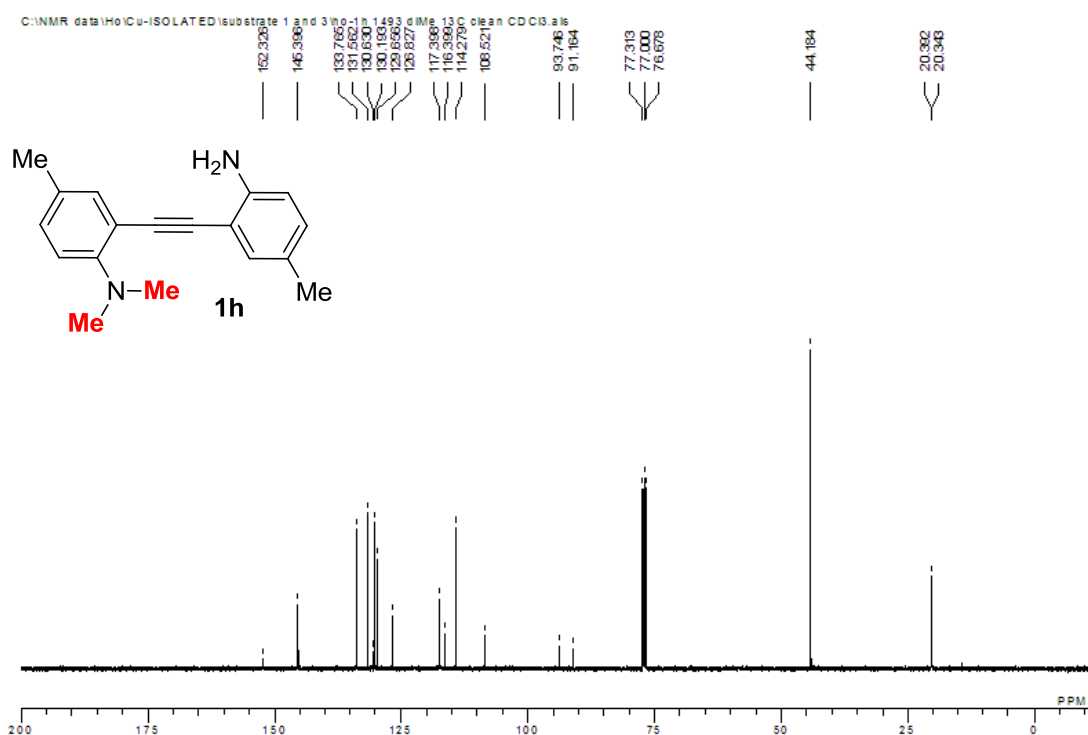
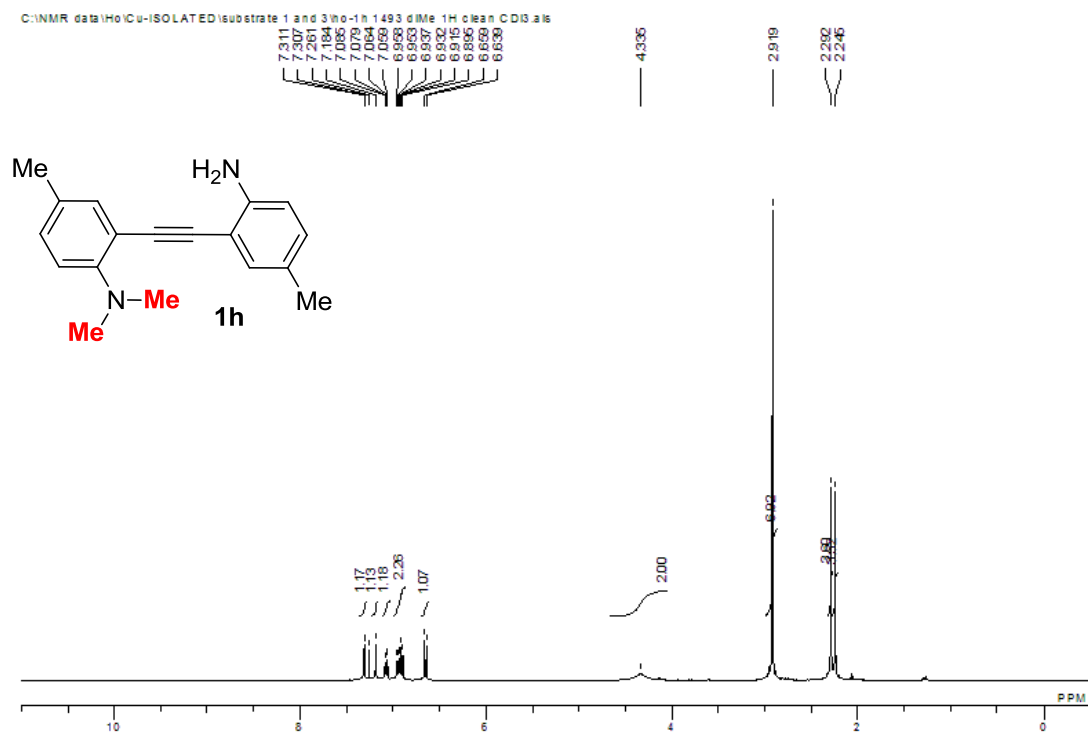


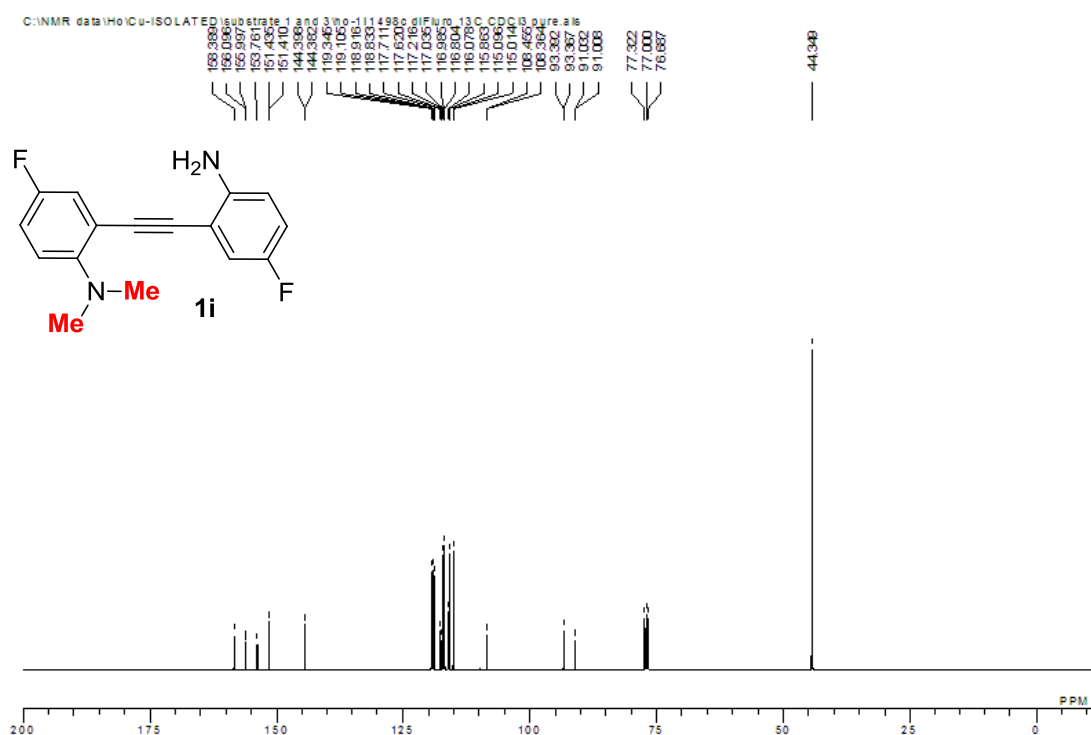
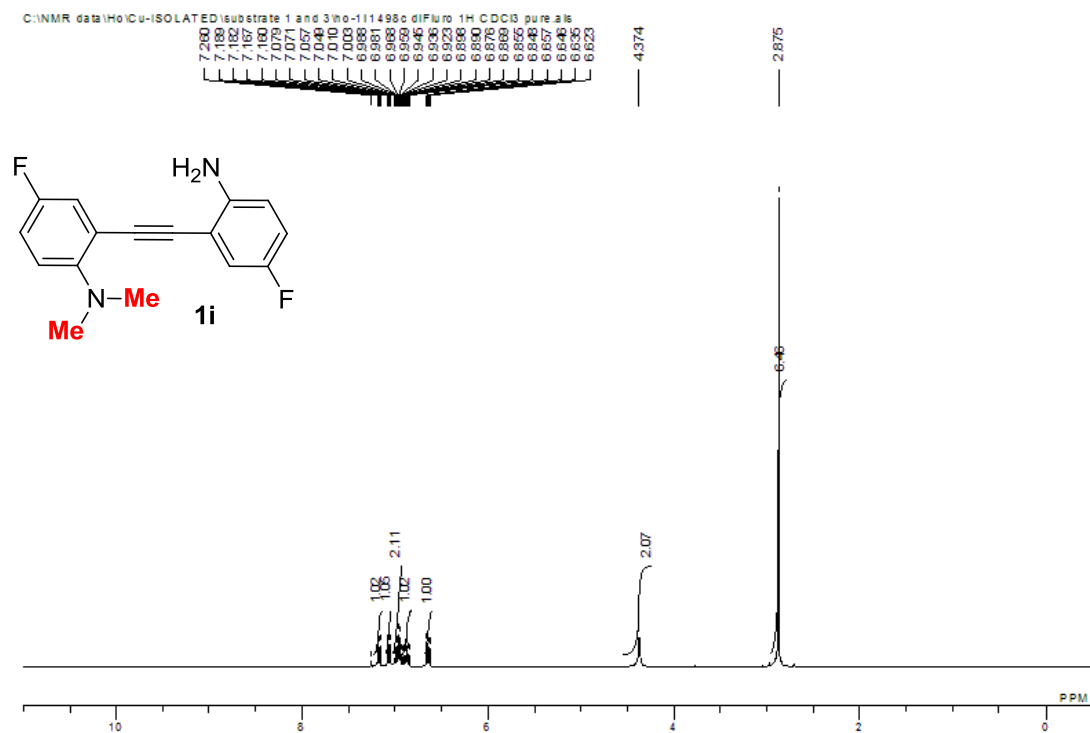


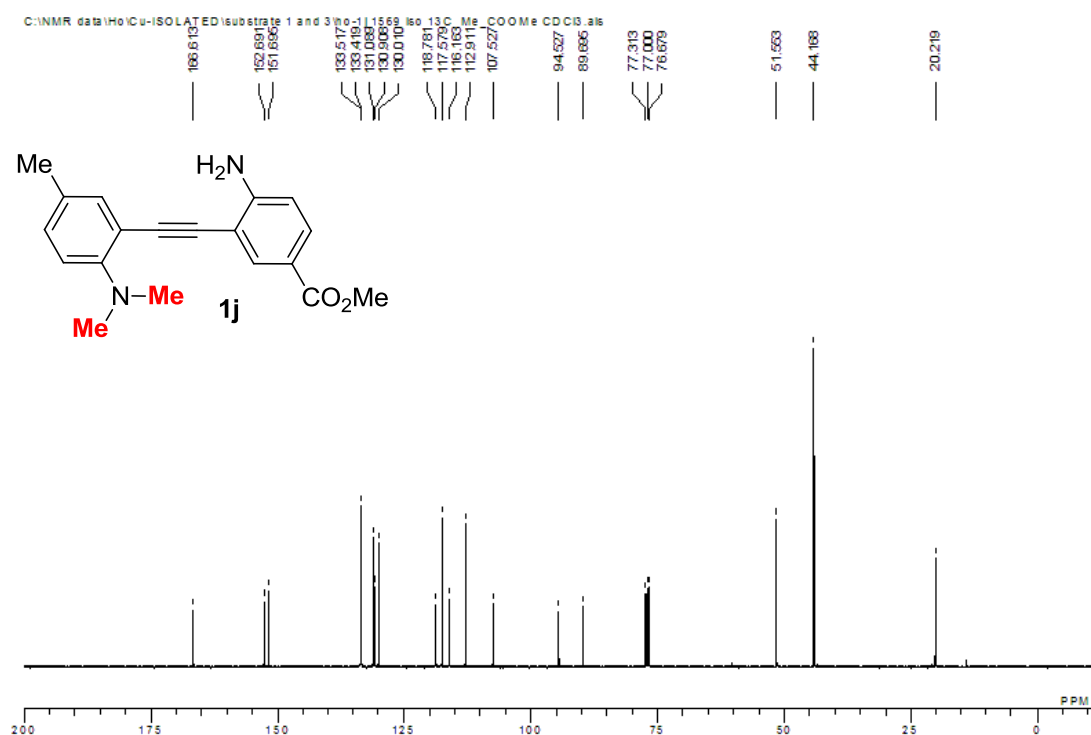
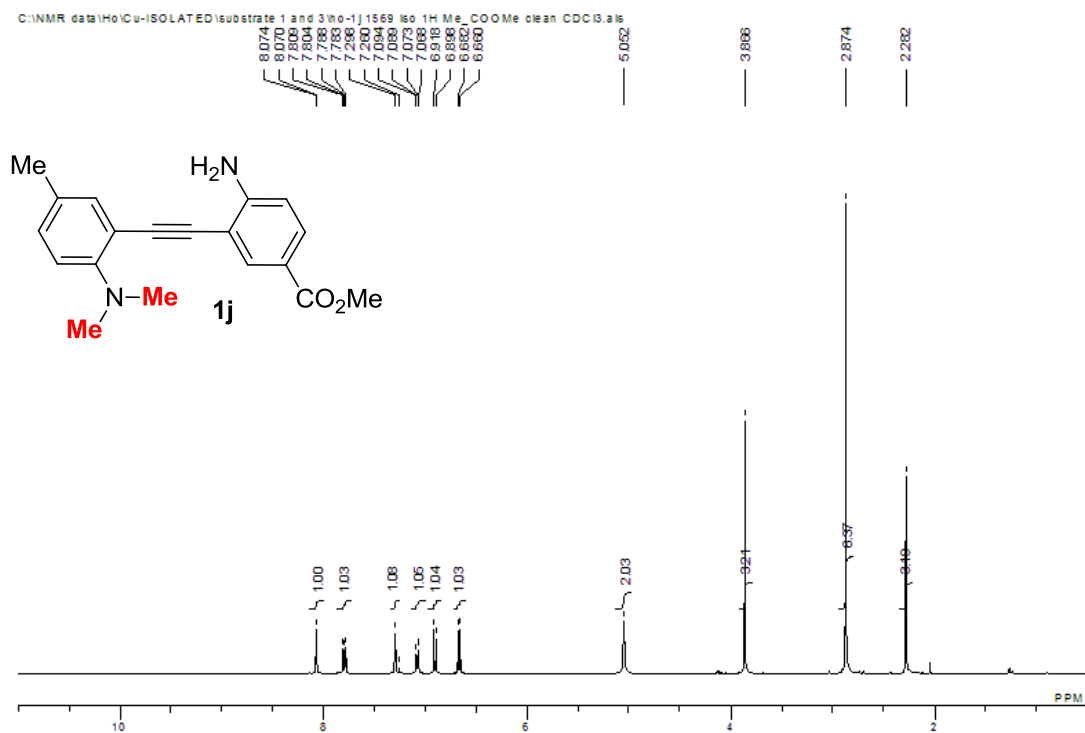


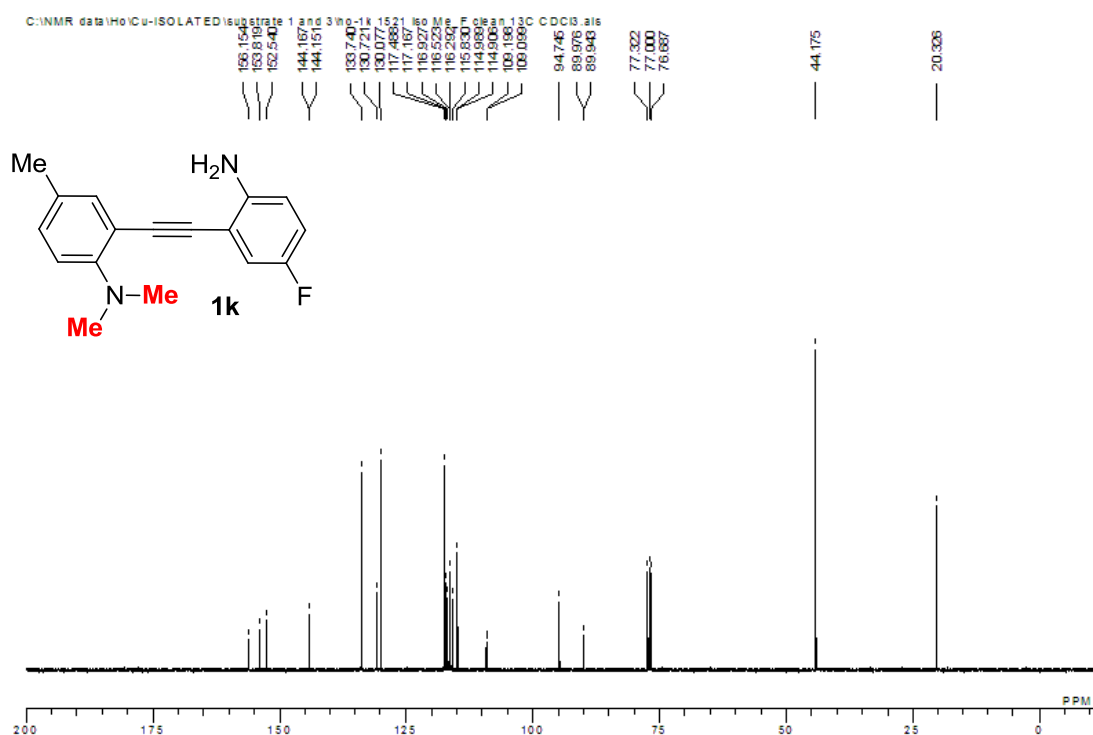
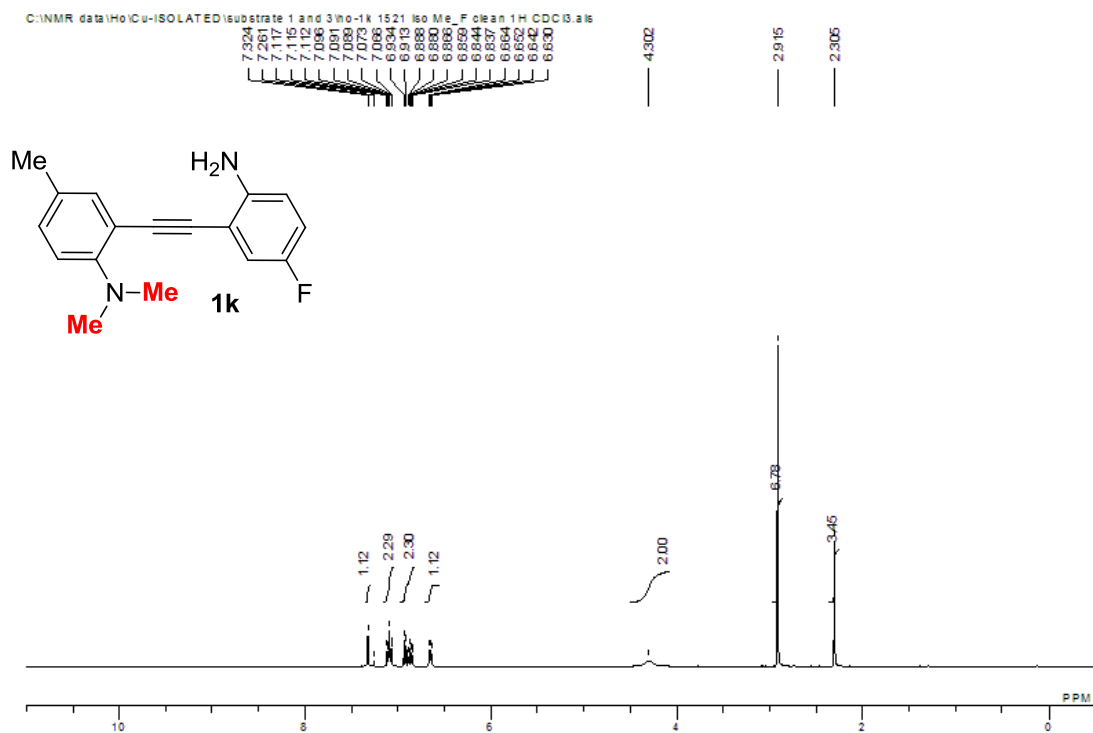




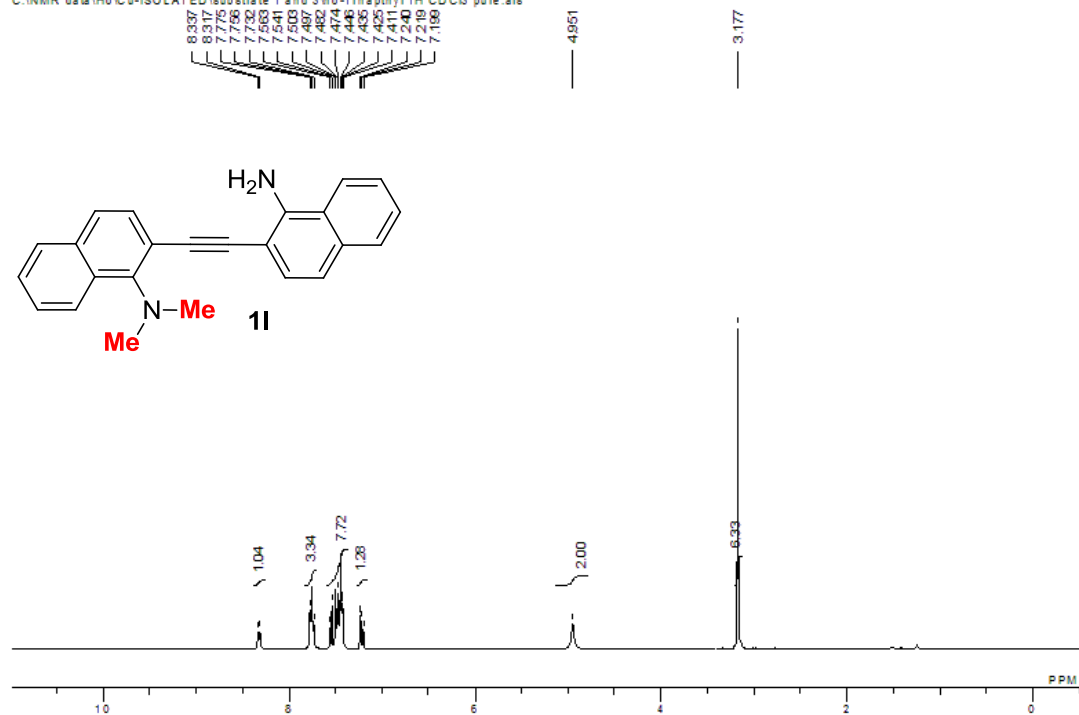




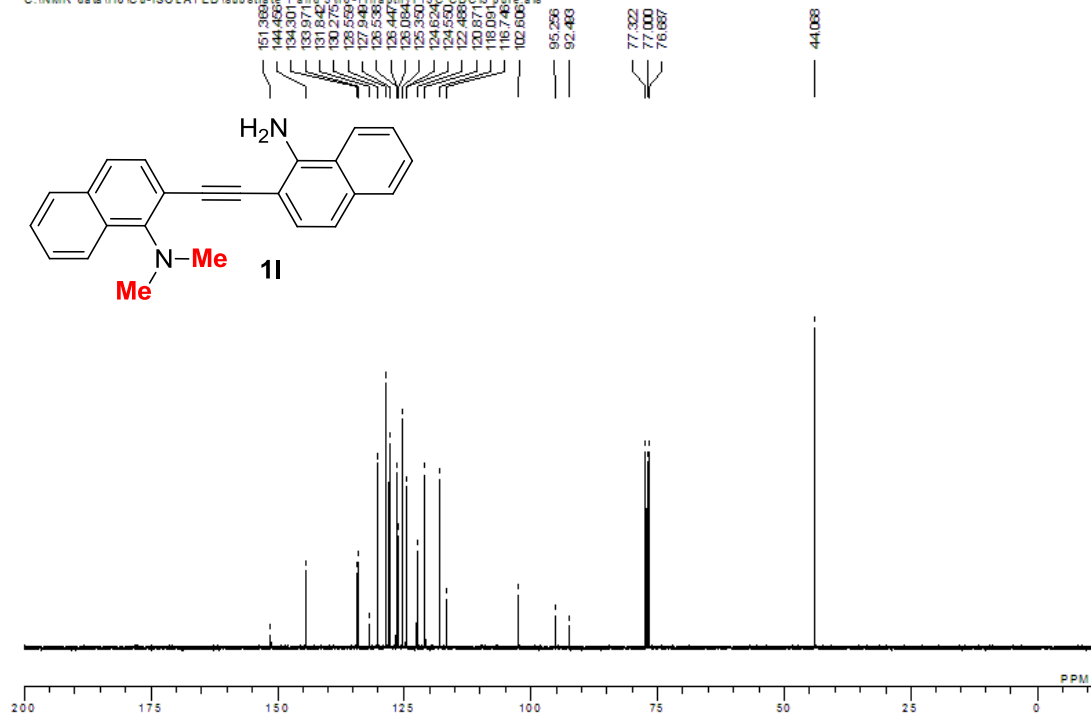


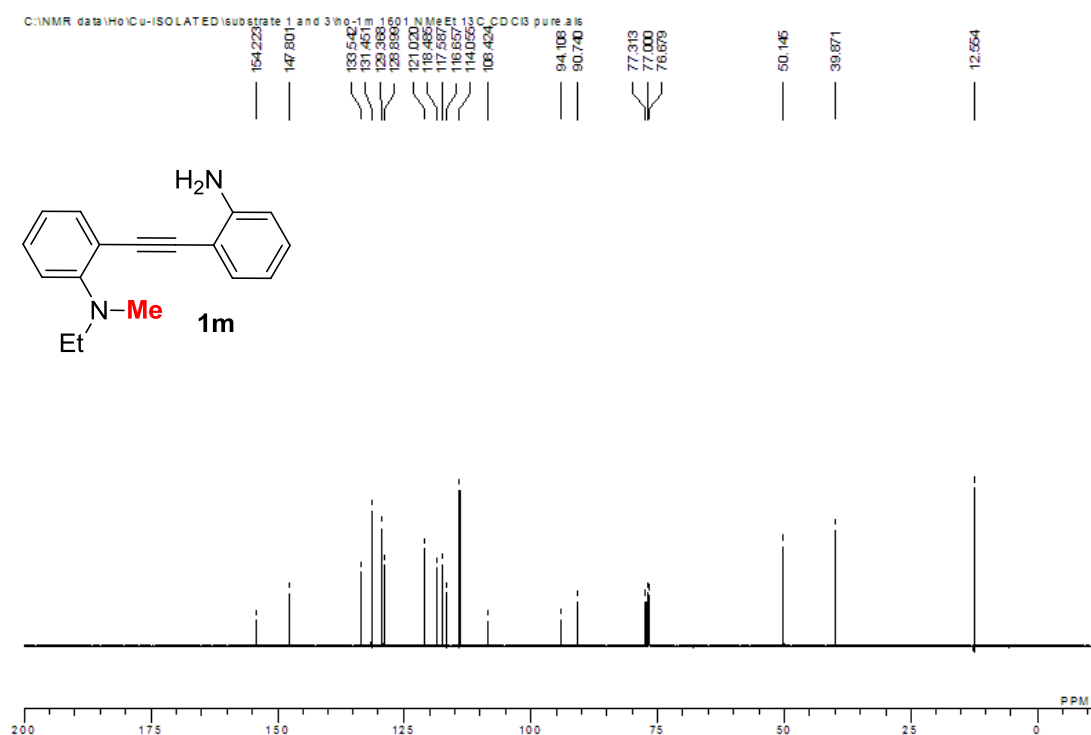
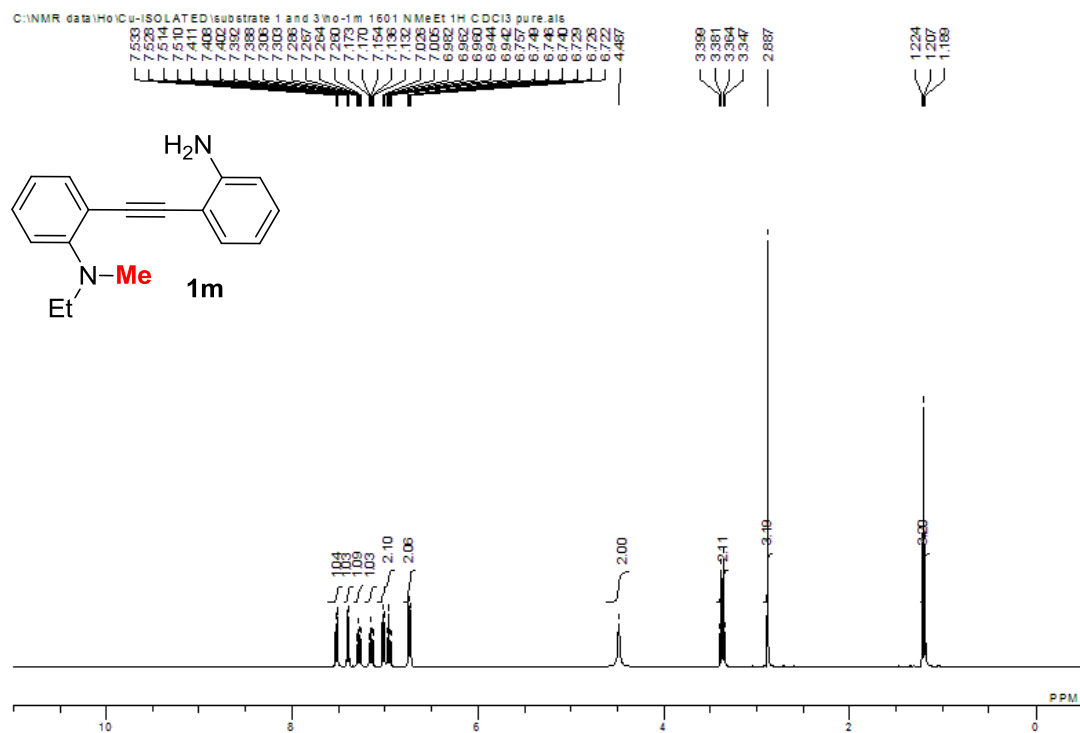


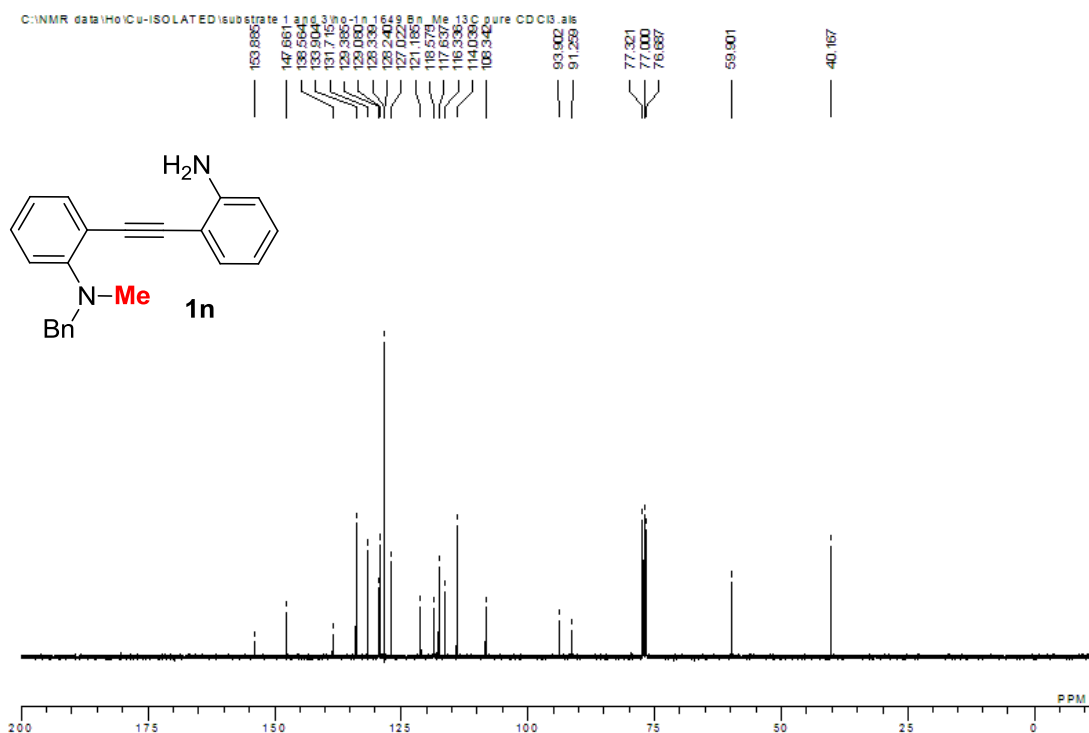
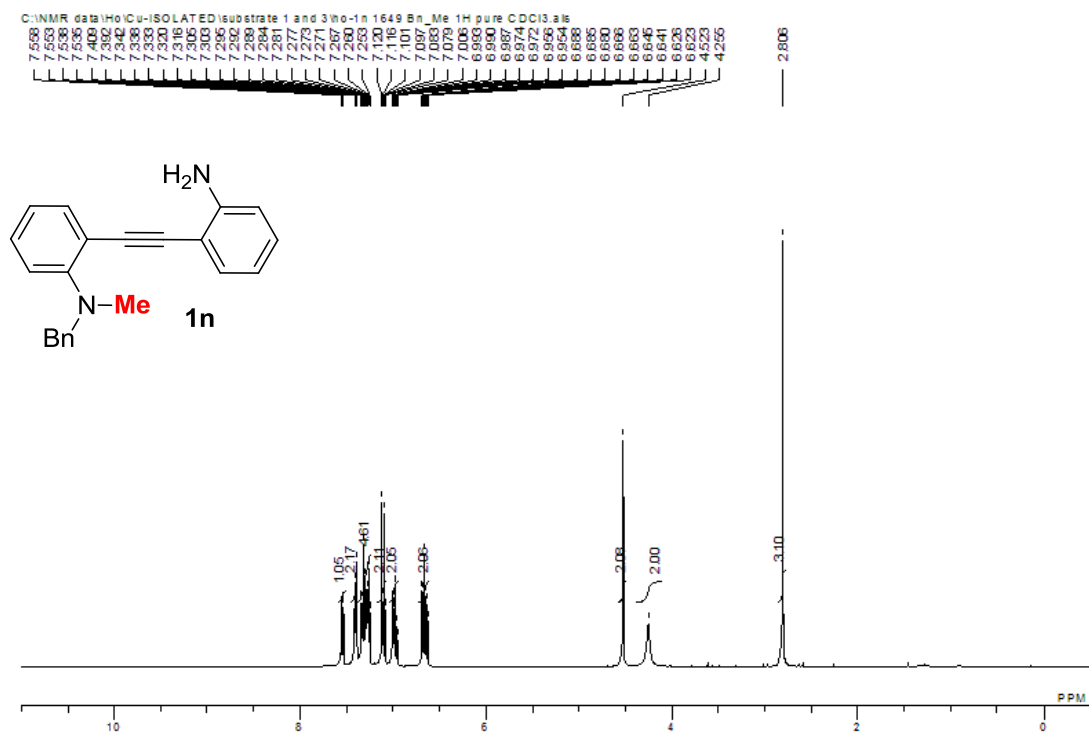
C:\NMR data\Ho\Cu-ISOLATED\substrate 1 and 3\ho-1\1naphthyl1\H CDCl3 pure.als

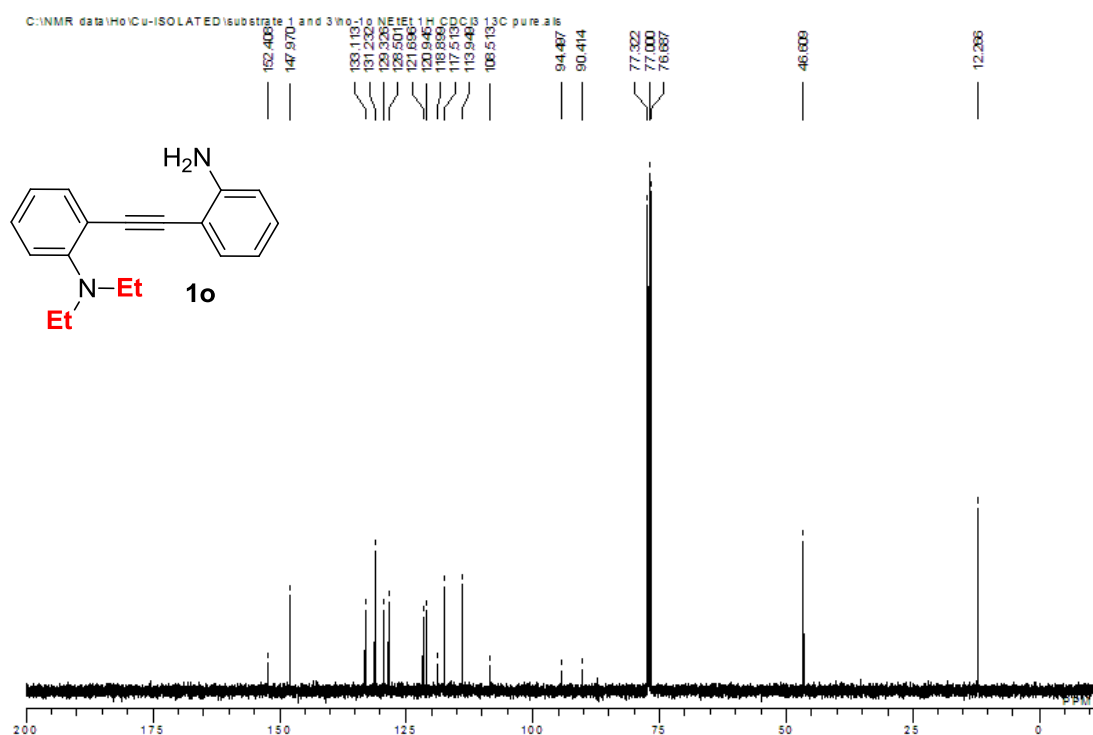
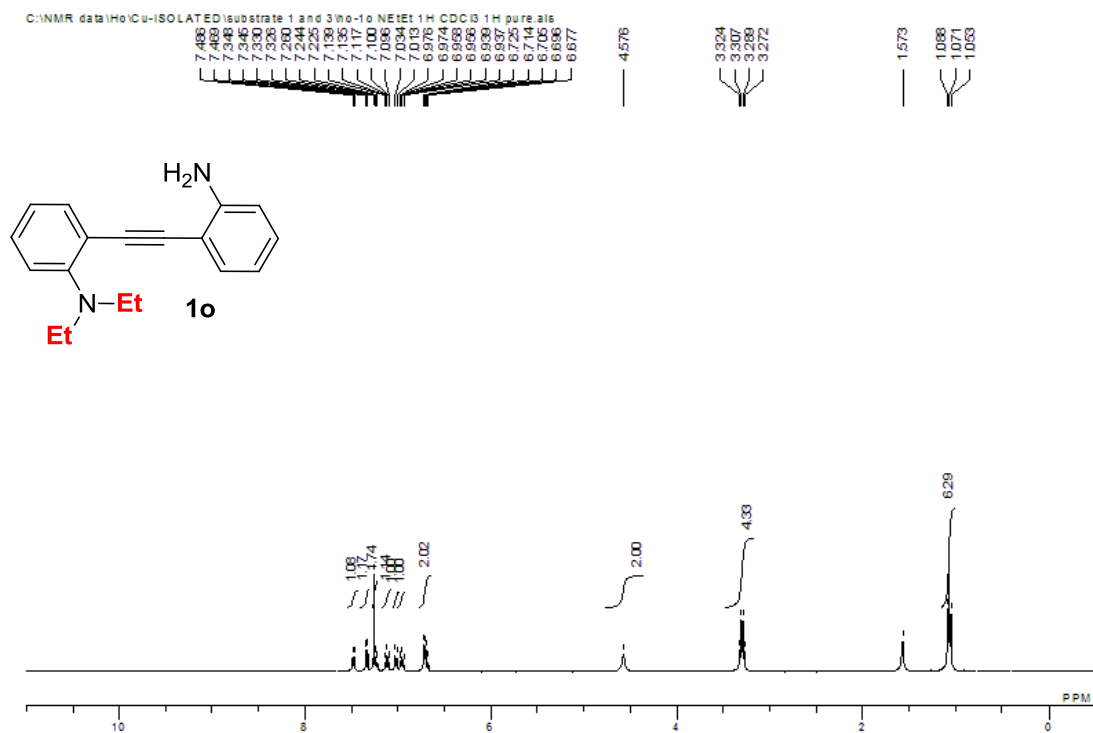


C:\NMR data\Ho\Cu-ISOLATED\substrate 1 and 3\ho-1\1naphthyl1\13C CDCl3 pure.als

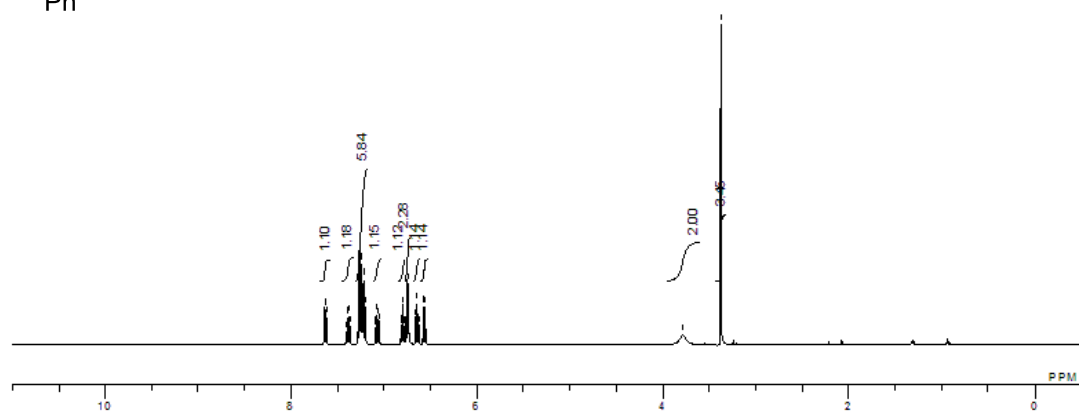
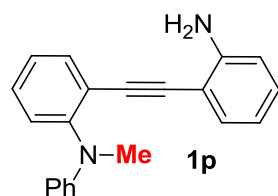




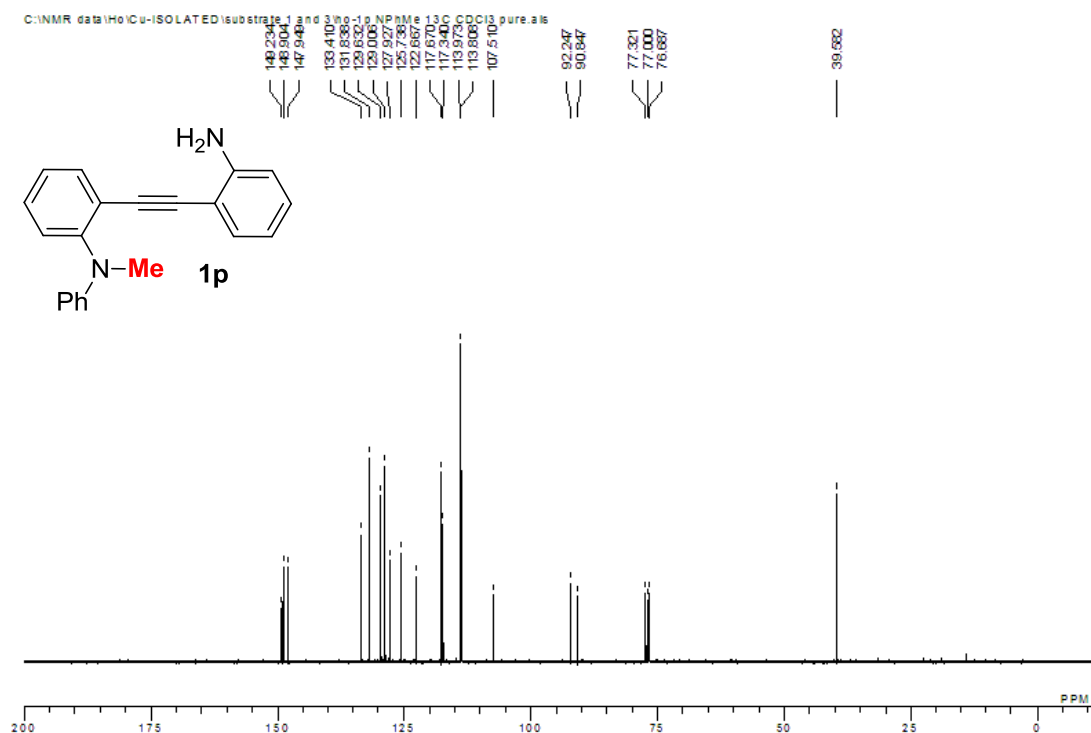
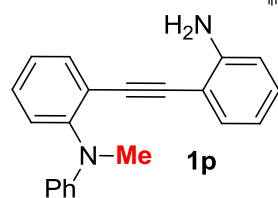


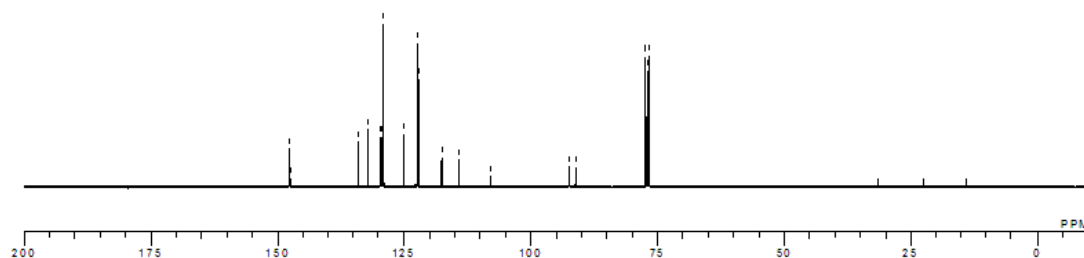
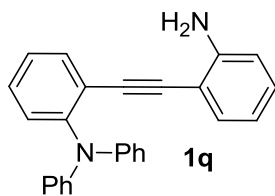
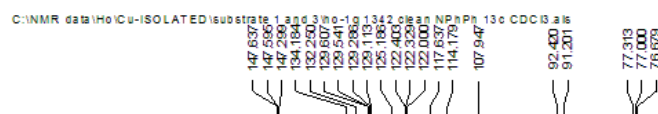
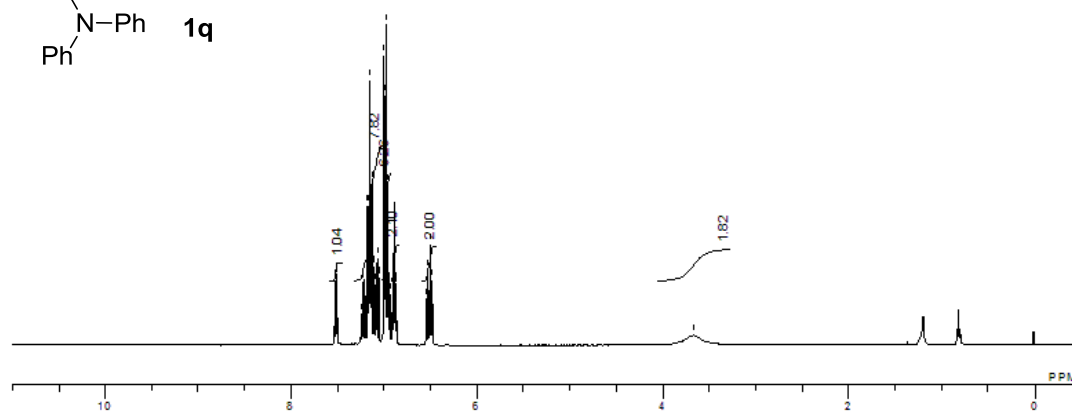
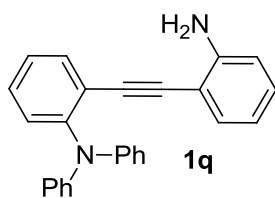
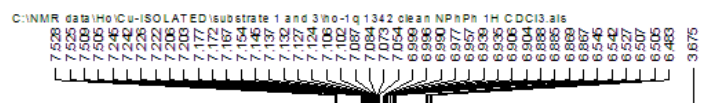


C-13 NMR data (H₂O)-ISOLATED substrate 1 and 3 (no-1p NPhMe 1H) ddle pure ails

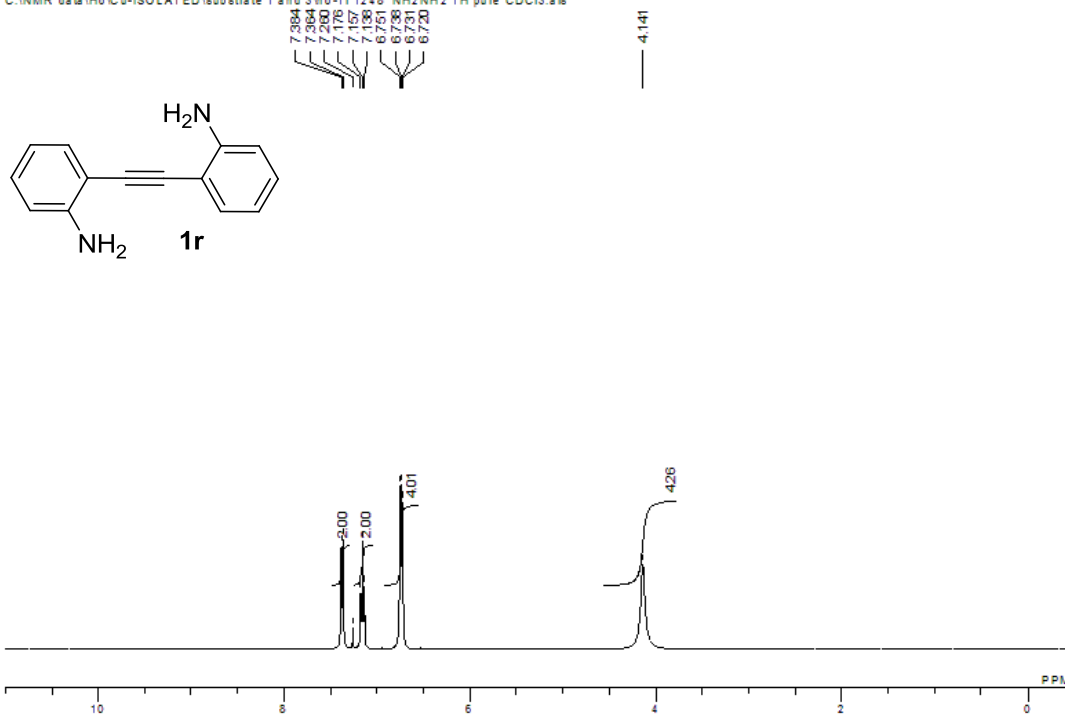


C-13 NMR data (H₂O)-ISOLATED substrate 1 and 3 (no-1p NPhMe 1H) ddle pure ails

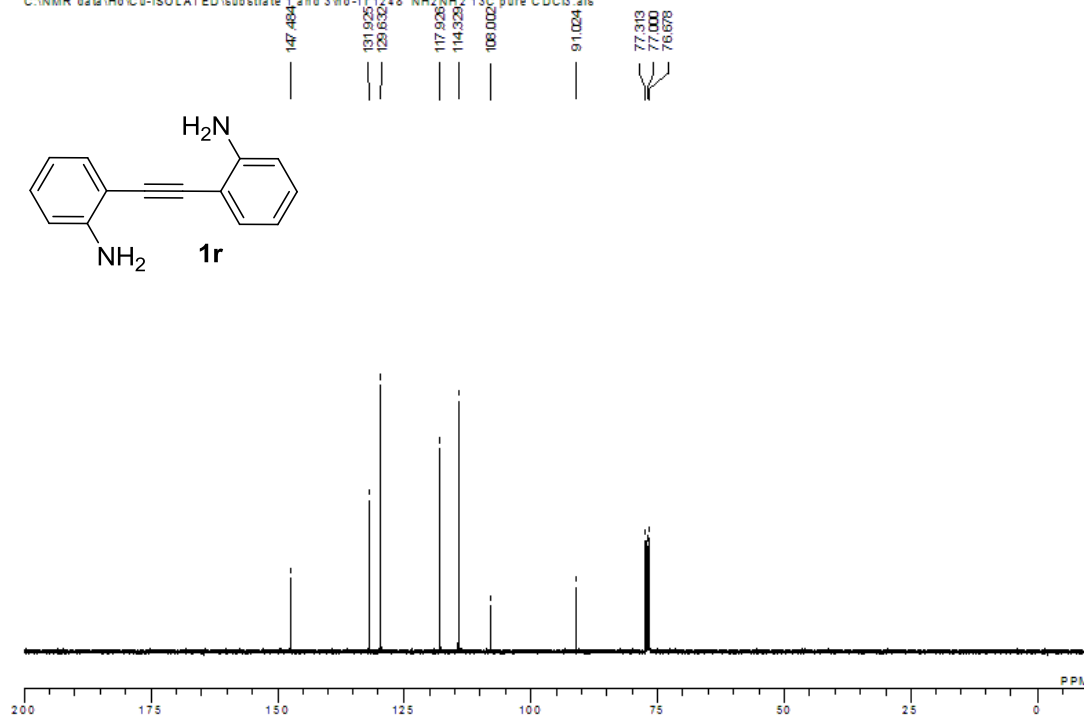


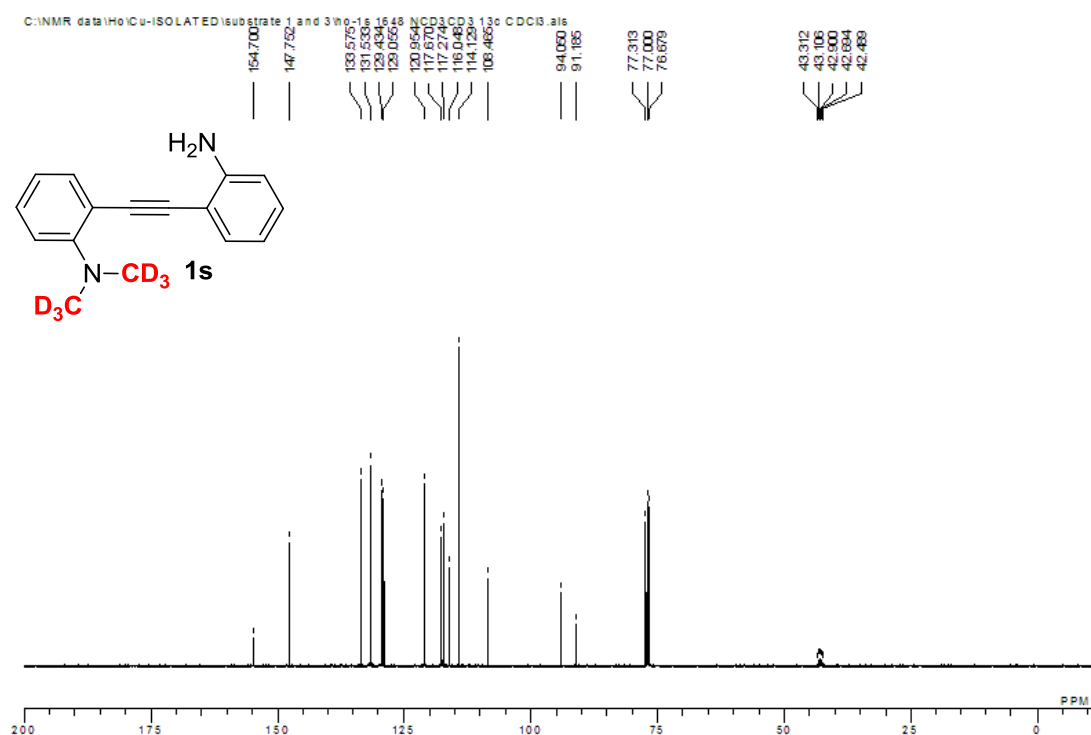
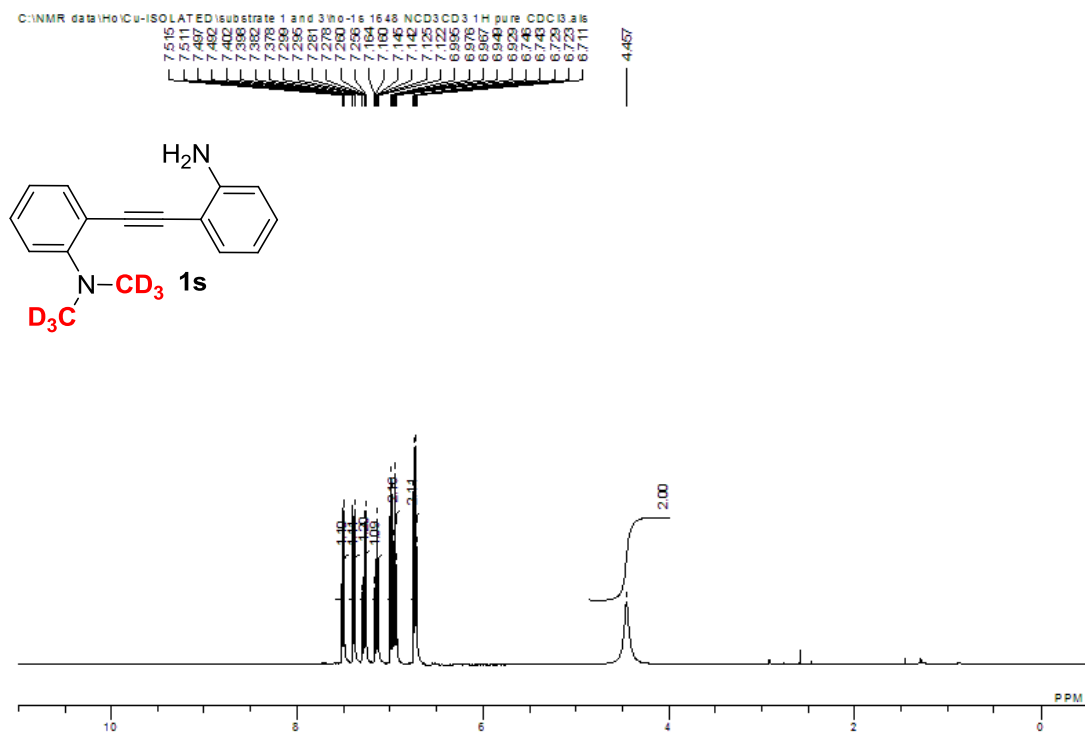


C:\NMR data\Ho\Cu-ISOLATED\substrate 1 and 3\ho-1r 1248 NH2NH2 1H pure CDCl3.a16

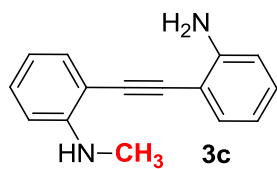
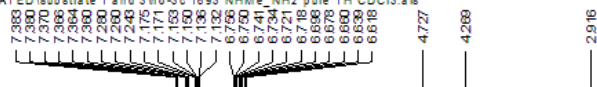


C:\NMR data\Ho\Cu-ISOLATED\substrate 1 and 3\ho-1r 1248 NH2NH2 13C pure CDCl3.a16

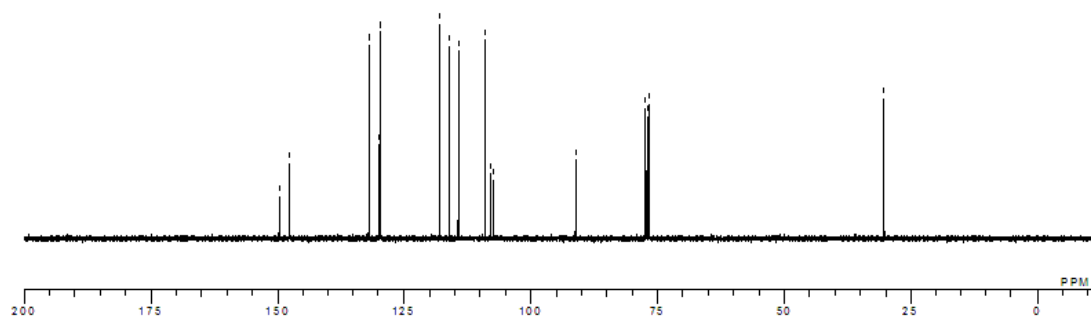
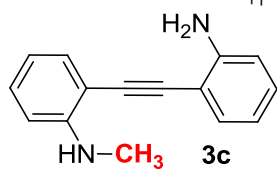
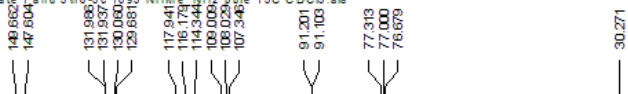




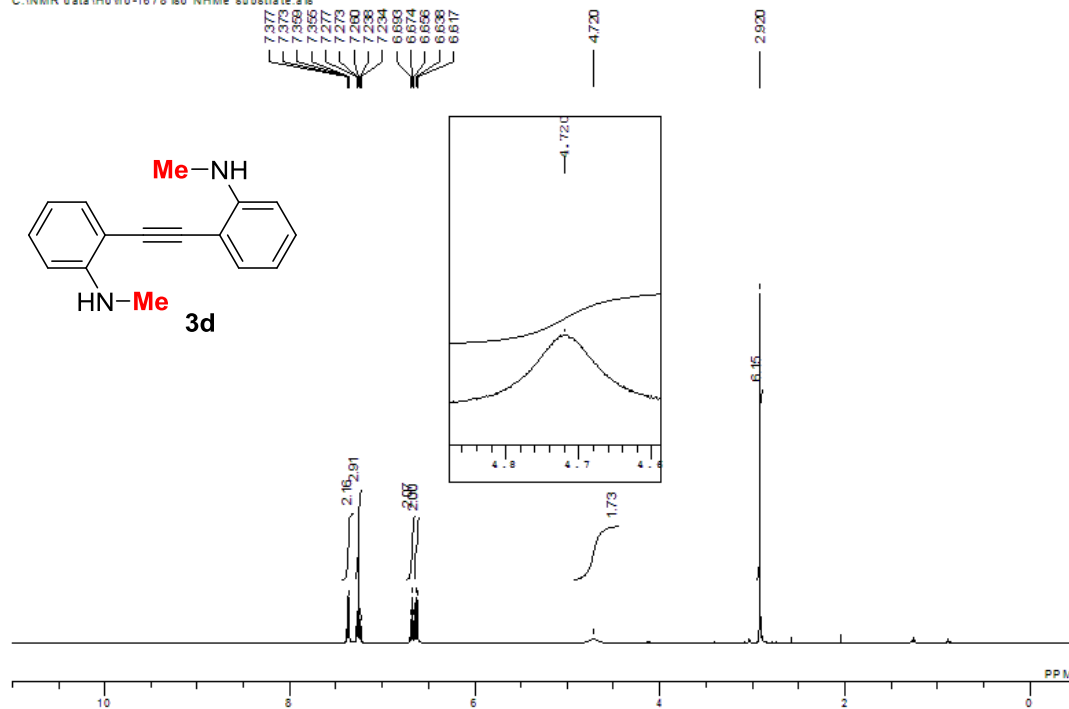
C:\NMR data\Ho\Cu-ISOLATED\substrate 1 and 3\ho-3c-1693 NHMe, NH2 pure 1H CDCl3.als



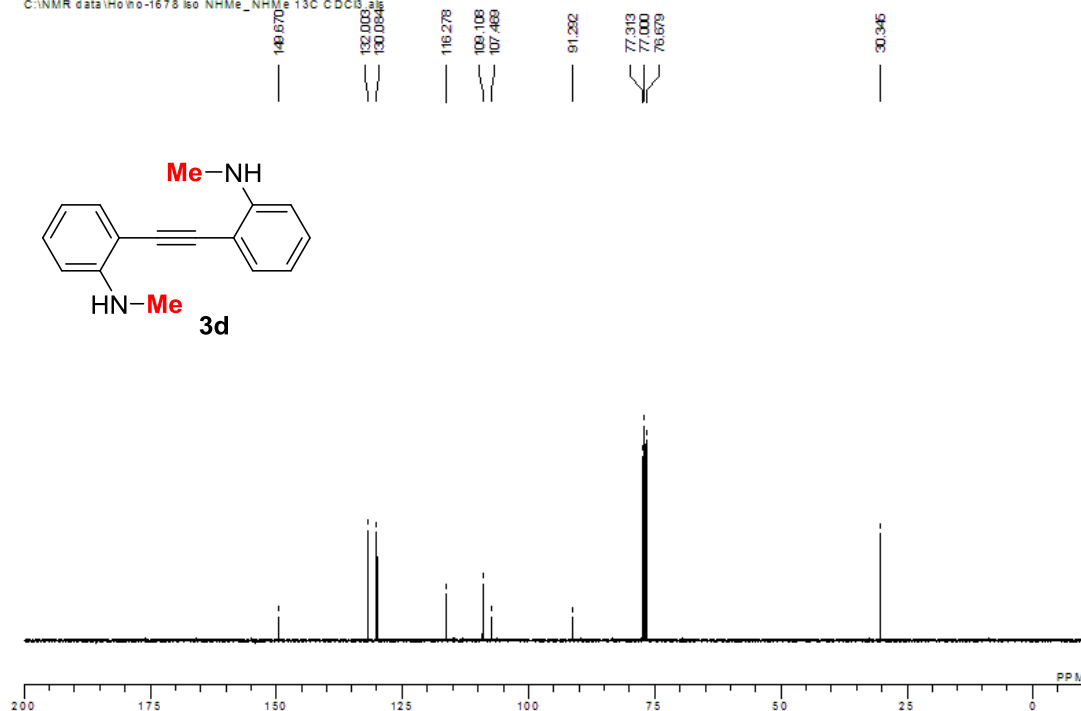
C:\NMR data\Ho\Cu-ISOLATED\substrate 1 and 3\ho-3c-1693 NHMe, NH2 pure 13C CDCl3.als

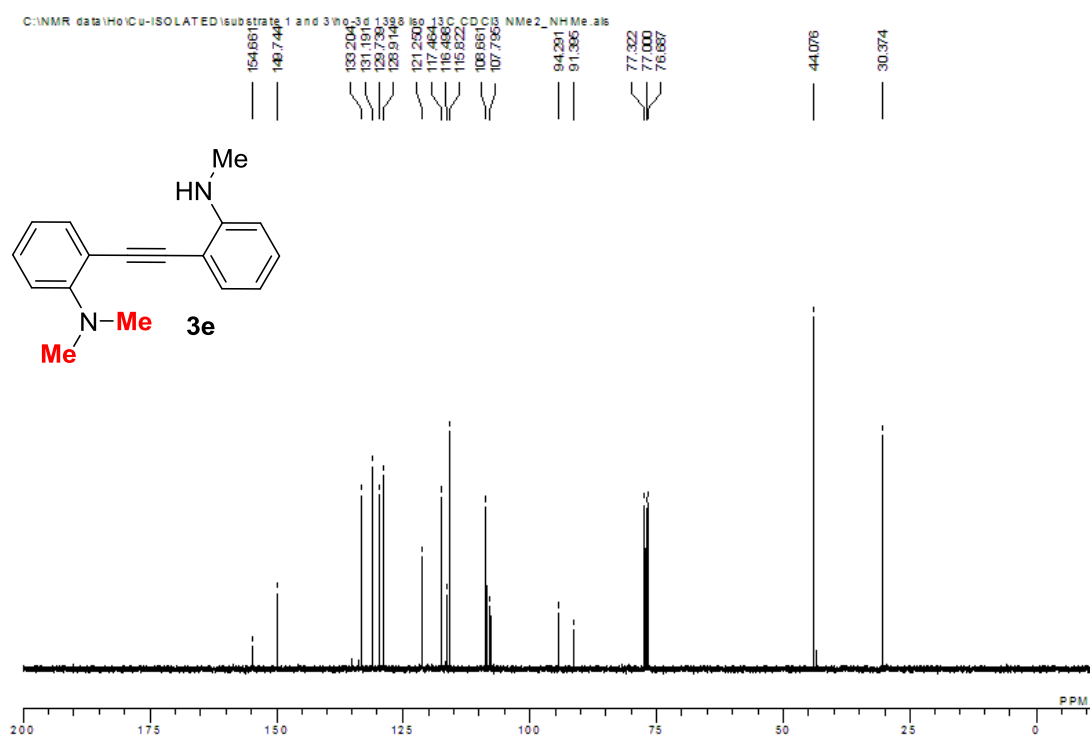
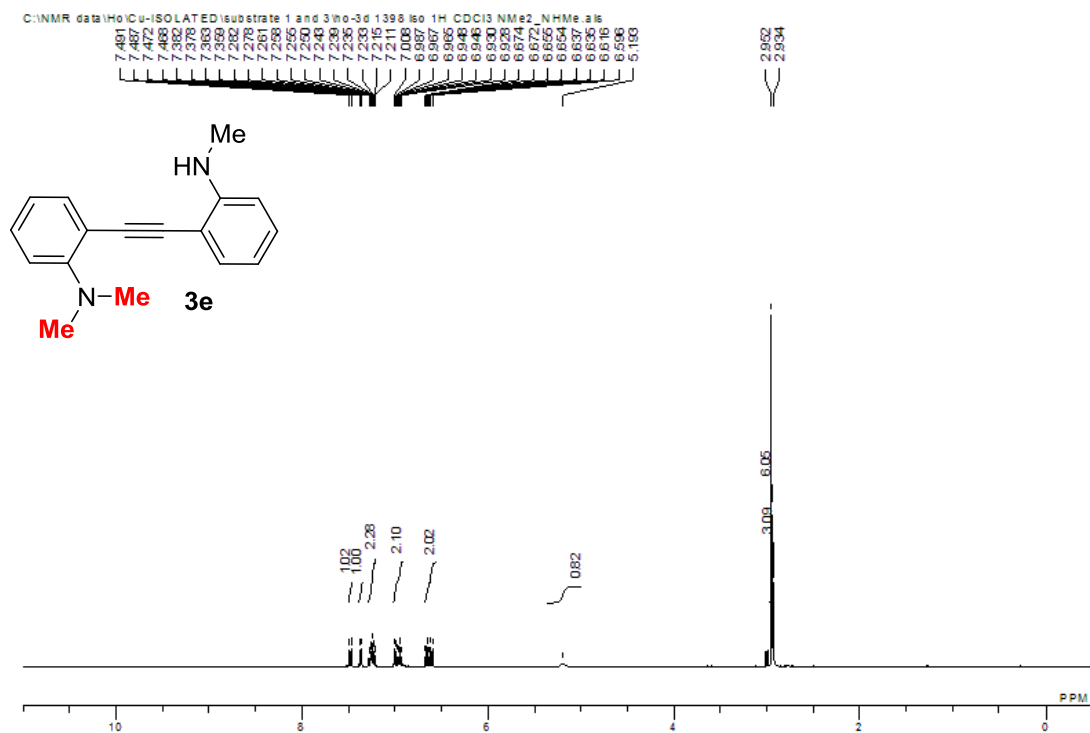


C:\NMR data\Ho\ho-1678 iso NHMe substrate 3d



C:\NMR data\Ho\ho-1678 iso NHMe_NHMe 13C CDCl3 3d





Chapter 3

Pd(II)-catalyzed Intramolecular Annulations of *ortho*-Alkynylaniline for Polyheterocyclics via C-N and *peri* C-H Bond Activation

1. Introduction

The excellent photophysical properties of cyclopentafused- polycyclic aromatics hydrocarbons (PAHs) or heteroaromatics (PHAs) have received much attention in materials science due to their high electron affinities and high stability for potential applications as organic semiconductors.¹ The presence of peripheral fused in PAH or PHA are often associated with lower bandgap organic target. In accordance, the rapid advancement of transition metal-catalyzed C-H bond functionalization has improved the synthetic toolbox for practical construction of target molecules in organic electronics.² For instance, the transition metals-catalyzed annulation *via* C-H activation have revolutionized the approach for efficient formation of C-C or C-heteroatoms without prefunctionlization. The π -coordination between C-C unsaturated and electrophilic metal-catalyst can assist C-H activation. This strategy has been successfully implemented in several cascade reaction with alkynes for C-H/C-heteroatoms bond activation to construct various complex π -extended PAHs or PHAs from readily accessible starting materials.^{2g, 3, 8a,b}

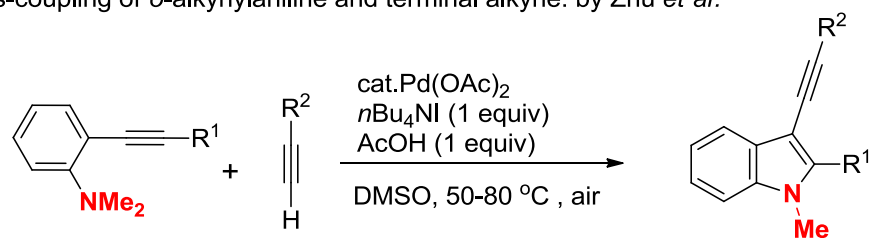
In the past, several groups have demonstrated the ability of Pd(II) to coordinate with C-C triple bond of *o*-alkynylaniline moiety to form σ -indolylpallada ammonium intermediate and subsequent dealkylation can lead to the successful annulation.⁴ This mechanistic approach has been successfully applied by Zhu et al. for the impressive Pd(II)-catalyzed intermolecular cross-coupling of *o*-alkynylaniline with terminal alkynes for efficient synthesis of 3-alkynylindoles scaffold (Scheme 1a).⁵ Liang et al. also demonstrated a Pd(II)-catatalyzed cascade cross-coupling of *o*-alkynylanilines with internal alkynes *via ortho*-C-H bond of bis-arylalkyne to afford the indole-containing heterocycles (Scheme 1b).⁶

Taking into consideration the aforementioned developments, an intramolecular cascade annulations of *o*-alkynylaniline was designed by introducing an indole-fused cyclopentadienyl-containing CP-PHAs. Previously, our group have demonstrated an efficient Rh(III)-catalyzed selective intermolecular alkenylation of nathylcarbamate by using internal alkynes *via* selective *peri* C-H and *ortho*-C-H for *N*-containing PHAs.⁷ As part of our recent research interest of developing new synthetic methodologies for π -extended PAH and PHAs,⁸ I herein report a novel methodology of Pd(II)-catalyzed intramolecular cascade annulation *via* C-N and *peri* C-H activation of *N,N*-dialkyl-2-(naphthalen-1-ylethynyl)aniline to construct 7-alkyl-7H-

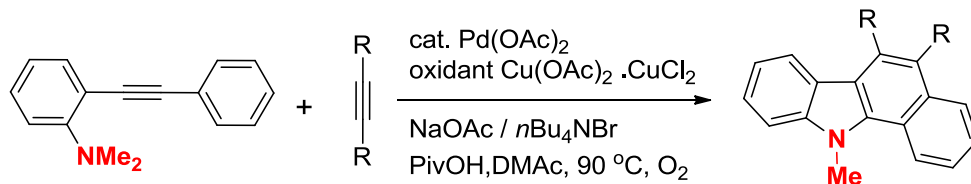
acenaphtho[1,2-*b*]indole (AAIs) scaffold (Scheme 1c). To date, reported methodologies to access the AAI scaffold are limited and relied on the use of classical functional group alteration which is restrictive and required multistep synthesis.⁹

Scheme 1. Pd-catalyzed Cascade Reaction for *N*-containing Heterocycles Synthesis

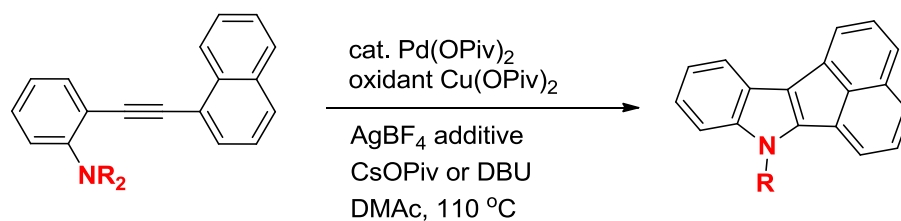
(a) Cross-coupling of *o*-alkynylaniline and terminal alkyne: by Zhu *et al.*



(b) Cross-coupling of *o*-alkynylaniline and internal alkyne: by Liang *et al.*



(c) Intramolecular annulation of *o*-alkynylaniline *via* C-N and *peri* C-H activation: **This work**



2. Results and Discussion

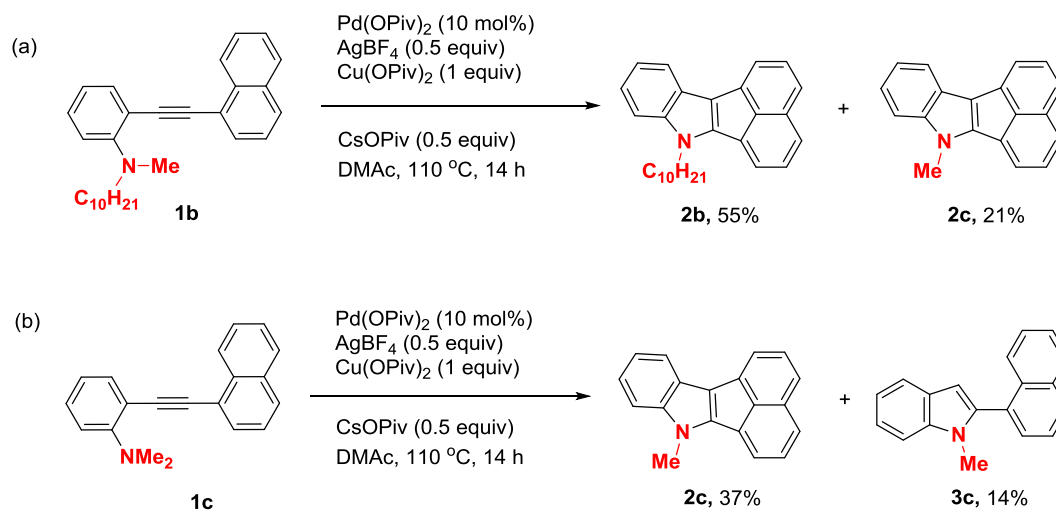
In the preliminary stage, using model substrate *N,N*-dihexyl-2-(naphthalen-1-ylethynyl)aniline (**1a**), several oxidative combination of Pd(II)-catalyzed cascade intramolecular condition were employed and the results are summarized in Table 1. In presence of Pd(OPiv)₂ catalyst, Cu(OPiv)₂ (oxidant), AgBF₄ (additives) gave a moderate yield of the desired product **2a** in 64% and noticeable amount of indole byproduct **3a** (Table 1, entry 1). Interestingly, the introduction CsOPiv as base reduced the formation of indole **3a** with a good yield of **2a** in 85%. The use of other bases, Cs₂CO₃ resulted in poor conversion and partial decomposition, while tributylamine yield 81% of **2a** accompanied by 12% of the indole byproduct **3a** (entry 3, 4). To my delights, by employing bulky organic base DBU improved the yield of **2a** up to 97% (entry 5). It is noted that without AgBF₄ hampered the turnover rate and only yielded 34% of **2a** (entry 6). Further screening of other commonly used oxidants used in Pd(II)-catalytic system, i.e. copper diacetate, copper dichloride, *o*-chloranil, or di-(pivaloyloxy)iodobenzene were less effective (entries 7-10). Blank tests confirmed that the excellent combination of Pd(OPiv)₂ catalyst and Cu(OPiv)₂ oxidant. (For details, see Supporting Information, Table S1-S4).

Table 1. Optimization^a

entry	base	oxidant	2a (%)	3a (%)	1a (%) ^a
1	-	Cu(OPiv) ₂	64	12	0
2	CsOPiv	Cu(OPiv) ₂	(85)	0	0
3	Cs ₂ CO ₃	Cu(OPiv) ₂	39	2	36
4	<i>n</i> Bu ₃ N	Cu(OPiv) ₂	81	12	0
5	DBU	Cu(OPiv) ₂	99 (97)	0	0
6 ^b	DBU	Cu(OPiv) ₂	34	0	50
7	DBU	Cu(OAc) ₂	21	0	66
8	DBU	CuCl ₂	16	12	10
9	DBU	<i>o</i> -Chloranil	8	2	43
10	DBU	PhI(OPiv) ₂	8	0	39

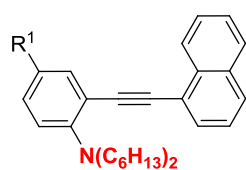
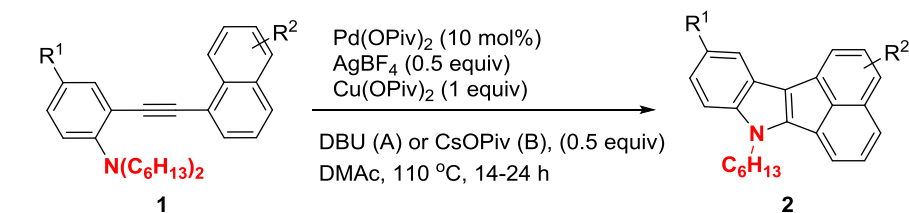
^a Reaction conditions: **1a** (0.1 mmol), Pd(OPiv)₂ (10 mol%), AgBF₄ (0.5 equiv), Cu-oxidant (1.0 equiv), base (1 equiv), DMAc (1.0 mL), stirred at 110 °C for 14 h under Ar atmosphere. ^b without AgBF₄.

Scheme 2. *N*-substituent effect of *o*-alkynylaniline.

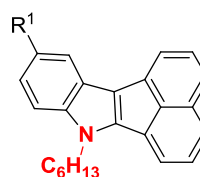


Under one of the optimal reaction conditions from entry 2 in Table 1, *N*-substituent effect of other *o*-alkynylanilines, namely **1b** and **1c** were examined as shown in Scheme 2. The *N*-decyl-*N*-methyl-2-(naphthalen-1-ylethynyl) (**1b**), afforded a mixture of the corresponding demethylated product **2b** in 55% and dedecylated product **2c** in 21%, without recovery of starting substrate. The *N,N*-dimethyl-2-(naphthalen-1-ylethynyl) (**1c**) only afforded the expected product **2c** in 37%, accompanied by formation of *N*-methyl-protected indole product **3c** in 14% without recovery of **1c**. It was apparent that the substrates with the longer *N,N*-dialkyl chain is far more superior in terms of stability and chemical yield for the construction of the AAI scaffold. Besides, the demethylation seemingly took place more readily than that of the longer *N*-alkyl substituent (Scheme 2a).

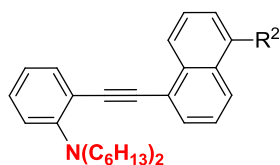
Scheme 3. Electronic Effect of Substituents^a



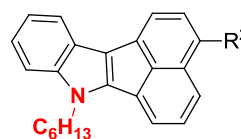
1d R¹ = Me
1e R¹ = F



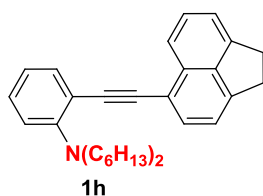
2d, R¹ = Me, A: 80% ; B: 80% (24 h)
2e, R¹ = F, A: 89%; B: 82%



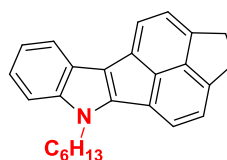
1f, R² = Me
1g, R² = F



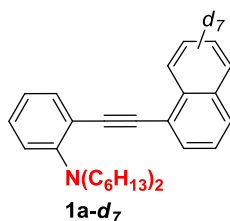
2f, R² = Me, A: 88% ; B: 84%
2g, R² = F, A: 72% (24 h); B: 85% (24 h)



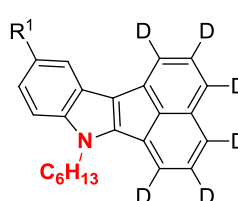
1h



2h, B: 43%^b



1a-d₇



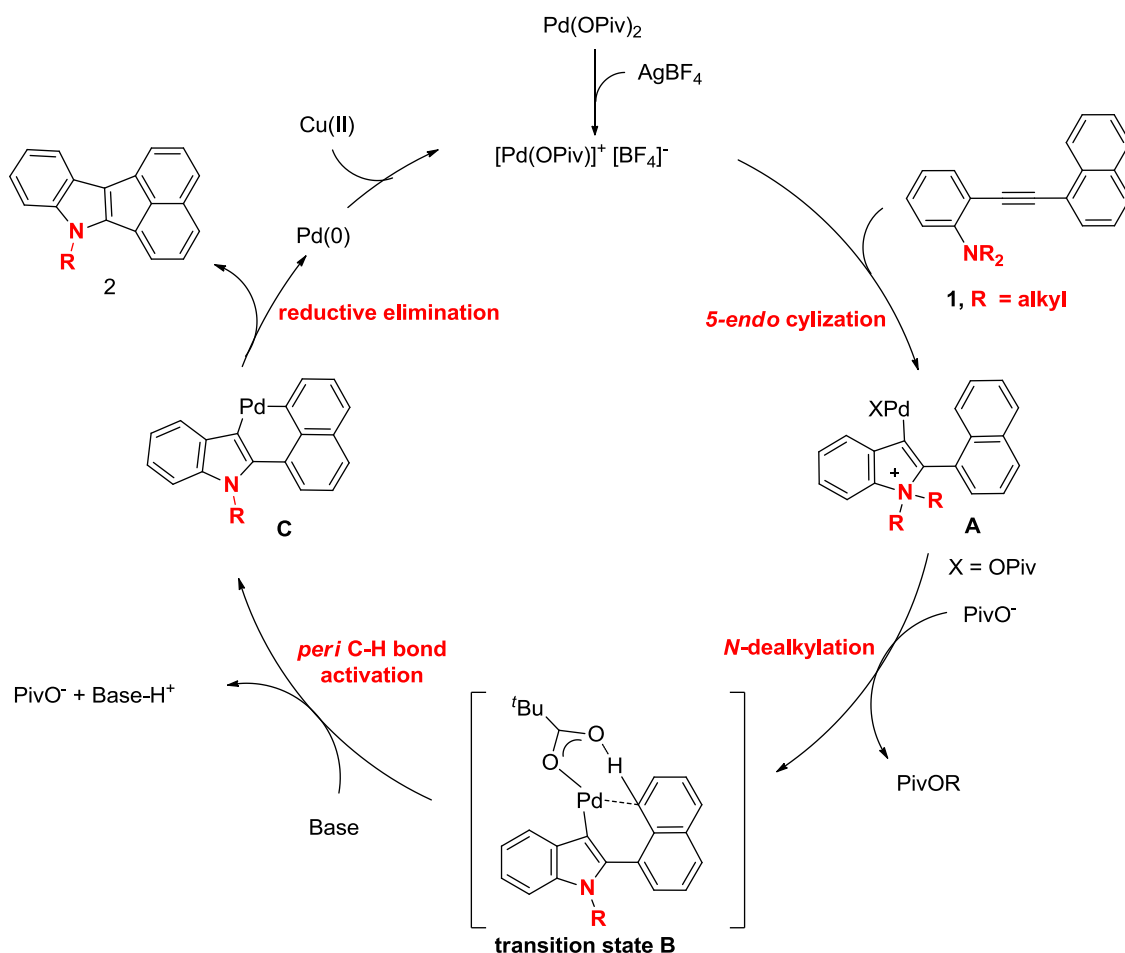
2a-d₆, B: 72% (> 99% D)

^a Reaction conditions: **1** (0.1 mmol), Pd(OPiv)₂ (10 mol%), AgBF₄ (0.5 equiv), Cu(OPiv)₂ (1.0 equiv), base (0.5 equiv): DBU (**A**) or CsOPiv (**B**), DMAc (0.1 M) at 110 °C for 14-24 h. The isolated yields are shown. ^b 150 °C, 12 h.

The electronic effect of substituents on the starting moieties has been studied under optimized conditions A (using DBU, 0.5 equiv) and B (using CsOPiv, 0.5 equiv) as shown in Scheme 3. Overall, we observed high compatibility of substrate scope with good yields and reproducibility (on an average yield of at least two runs), under both standard condition A and B. With electron-rich group at the *para* position of the *o*-alkynylaniline (R^1), substituent Me (**1d**) afforded high yield of **2d** in 80% in both optimized condition A and B. While the electron-deficient substituent **1e** ($R^1 = F$) rendered a higher yields of **2e** in 89% and 82% under A and B condition correspondingly. Meanwhile, substrate with electron-rich substituent *N,N*-dihexyl-2-((5-methylnaphthalen-1-yl)ethynyl)aniline (**1f**, $R^2 = Me$), resulted in comparable yields of **2f** in 88% under condition A and slightly lower yield of 82% under condition B. In contrast, electron-deficient substituent **1g** ($R^2 = F$) required a longer reaction time and afforded a slightly lower yield of **2g** in 72% and 85%, under condition A and B respectively. It is noted that of the indistinct correlation between substituent effects with the slight fluctuated chemical yields under different base system, both optimal conditions showed high compatibility and efficiency to furnish the corresponding AAs (**2a**, **2d-g**). Moreover, the 2-((1,2-dihydroacenaphthylen-5-yl)ethynyl)-*N,N*-dihexylaniline **1h**, yielded the structurally contorted **2h** in 43% under higher reaction temperature of 150 °C after 12 h. Under the standard condition B, the substrate having deuterated naphthalene **1a-d₇** yielded the corresponding product in 72% exclusively without the occurrence of D–H exchange (Scheme 3, **2a-d₆**).

To gain some insight of the mechanism, the kinetic isotope effect was examined by subjecting **1a** and the deuterated **1a-d₇** for one-pot reaction. After 7 h, **2a** was yielded in 68%. In contrast, **2a-d₆** was yielded in 20% (¹H-NMR yield). The K_H/K_D ratio was 3.40, indicating the cleavage of the *peri* C–H bond should be the rate determining step. (See Supporting Information (SI), Scheme S1). Although the addition of base and additives are not crucial to complete the Pd(0)-Pd(II) catalytic cycle, superior turnover numbers and reproducibility are associated in their presence. The exact role of base is not fully clear, however, we believe the bases can assist the deprotonation of *in situ* formation of pivalic acid and provide counter pivalate anion to stabilize the Pd(0) species before reoxidation, preventing or slowing the formation of palladium black.¹⁰ The beneficial impact of the catalytic additive AgBF₄ is less clear, based on reported works, we assume its presence may render a more electrophilic palladium (II) species early in the reaction.¹¹

Scheme 4. Plausible reaction mechanism



On the basis of reported works and experimental details derived from current reaction, a plausible reaction mechanism is proposed, as shown in Scheme 4. The electrophilic cationic Pd(II) coordinate with the C-C triple bond and induced 5-*endo* cyclization to give the σ -palladaindolium species **A**. The σ -indolylpallaindolium species undergoes dealkylation in presence of pivalate nucleophile (OPiv), and *via* transition state **B** directed the *peri* C-H bond activation under assistance of pivalate.¹² In the presence of base, deprotonation of resulting pivalic acid to generate of pivalate species. The resultant six-membered cyclopalladacycle **C** species undergoes reductive elimination to form the corresponding product **2a** and release Pd(0) . Regeneration of Pd(II) species under oxidative condition completes the catalytic cycle.

3. Conclusion

In conclusion, a highly efficient Pd(II)-catalytic system for intramolecular annulation of *o*-alkynylaniline via *peri* C-H and C-N bond activation has been developed to access 7-alkyl-7H-acenaphtho[1,2-*b*]indole (AAIs) scaffold. The combination of bases and additive under oxidative Pd(OPiv)₂ catalytic system is crucial for the successful intramolecular cascade annulation. Further investigation will focus on the expansion of the scope of the reaction towards larger π -extended CP-PHAHs and their high potential applications in organic electronic.

4. References and notes

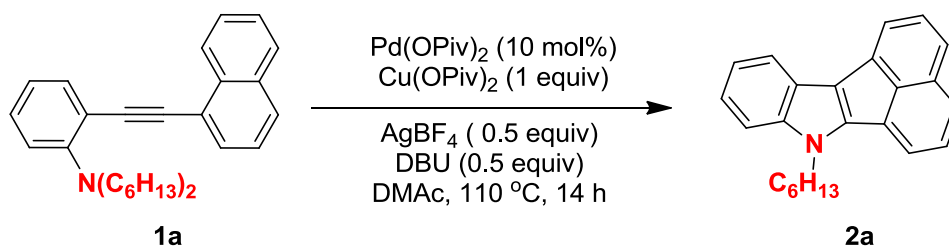
1. Stępień, M.; Gońka, E.; Żyła, M.; Sprutta, N. *Chem. Rev.* **2016**, Article ASAP. DOI: 10.1021/acs.chemrev.6b00076
2. For selected reviews on C-H activation, see: a) Liu, C.; Zhang, H.; Shi, W.; Lei, A.; *Chem. Rev.* **2011**, *111*, 1780–1824; b) Yeung, C. S.; Dong, V. M. *Chem. Rev.* **2011**, *111*, 1215–1292. c) Yamaguchi, J.; Yamaguchi, A. D.; Itami, K. *Angew. Chem. Int. Ed.* **2012**, *51*, 8960–9009; d) Lyons, T. W.; Sanford, M. S. *Chem. Rev.* **2010**, *110*, 1147–1169; e) Chen, X.; Engle, K. M.; Wang, D.-H.; Yu, J.-Q. *Angew. Chem. Int. Ed.* **2009**, *48*, 5094–5115. f) F. Gulías, M; Mascareñas, J. L. *Angew. Chem. Int. Ed.* **2016**, *55*, 27. g) Gandeepan, P.; Cheng, C-H. *Chem. Asian J.* **2015**, *10*, 824.
3. Shi, Z.; Ding, S.; Cui, Y.; Jiao, N. *Angew. Chem. Int. Ed.* **2009**, *48*, 7895.
4. Ouyang, K.; Hao, W.; Zhang, W.-X.; Xi, Z. *Chem. Rev.* **2015**, *115*, 12045.
5. Yao, B.; Wang, Q.; Zhu, J. *Angew. Chem. Int. Ed.* **2012**, *51*, 12311.
6. Xia, X. -F.; Wang, N.; Zhang, L. -L.; Song, X. -R.; Liu, X. -Y.; Liang, Y.-M. *J. Org. Chem.* **2012**, *77*, 9163.
7. Zhang, X.; Si, W.; Bao, M.; Asao, N.; Yamamoto, Y.; Jin, T. *Org. Lett.* **2014**, *16*, 4830
8. a) Zhao, J.; Oniwa, K.; Asao, N.; Yamamoto, Y.; Jin, T. *J. Am. Chem. Soc.* **2013**, *135*, 10222. b) Zhao, J.; Asao, N.; Yamamoto, Y.; Jin, T. *J. Am. Chem. Soc.* **2014**, *136*, 9540. c) Ho, H. E.; Oniwa, K.; Yamamoto, Y.; Jin, T. *Org. Lett.* **2016**, *18*, 2487. d) Jin, T.; Zhao, J.; Asao, N.; Yamamoto, Y. *Chem. Eur. J.* **2014**, *20*, 3554. e) Zhao, J.; Xu, Z.; Oniwa, K.; Asao, N.; Yamamoto, Y.; Jin, T. *Angew. Chem. Int. Ed.* **2016**, *55*, 259. f) Jiang, H.; Ferrara, G.; Zhang, X.; Oniwa, K.; Islam, A.; Han, L.; Sun, Y.-J.; Bao, M.; Asao, N.; Yamamoto, Y.; Jin, T.; *Chem. –Eur. J.* **2015**, *21*, 4065.
9. a) Donald, J. R.; Taylor, R. J. K. *Synlett*, **2009**, 1, 59. b) Wróbel, Z.; Mąkosza, M. *Tetrahedron*. **1997**, *53*, 5501.
10. Stuart, D. R.; Fagnou, K. *Science*. **2007**, *316*, 1172.
11. Lebrasseur, N.; Larrosa, I. *J. Am. Chem. Soc.* **2008**, *130*, 2926.
12. Lafrance M.; Fagnou, K. *J. Am. Chem. Soc.* **2006**, *128*, 16496.

5. Experimental section

General Information. ^1H NMR and ^{13}C NMR were recorded on JEOL JNM AL 400 (400 MHz), JEOL JNM AL 700 (700 MHz), and JNM ECA 700 (700MHz) spectrometers. ^1H NMR spectra are reported as follows: chemical shift in ppm (δ) relative to the chemical shift of CDCl_3 at 7.26 ppm, CD_2Cl_2 at 5.32 ppm, acetone- d_6 at 2.04 ppm, THF- d_8 at 3.58 ppm integration, multiplicities (s = singlet, d = doublet, t = triplet, q = quartet, m = multiplet, and br = broadened), and coupling constants (Hz). ^{13}C NMR spectra were recorded on JEOL JNM AL 400 (100.5 MHz) and JEOL JNM AL 400 (176.0 MHz) spectrometers with complete proton decoupling, and chemical shift reported in ppm (δ) relative to the central line for CDCl_3 at 77 ppm, CD_2Cl_2 at 53.8 ppm, Acetone- d_6 at 29.8 ppm, and THF- d_8 at 66.5 ppm. High-resolution mass spectra were obtained on a BRUKER APEXIII spectrometer and JEOL JMS-700 MStation operator. Column chromatography was carried out employing silica gel 60 N (spherical, neutral, 40~63 μm , Merck Chemicals) and basic silica gel NH-DM1020 (Fuji Silysia Chemical Ltd). Analytical thin-layer chromatography (TLC) was performed on 0.2 mm precoated plate Kieselgel 60 F254 (Merck).

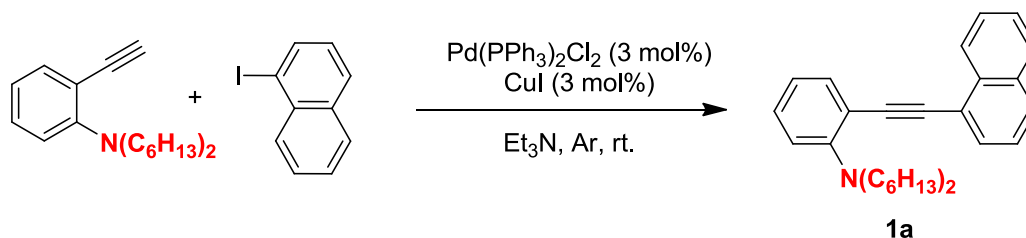
Materials. The commercially available chemicals were used as received. Structures of the products were identified by ^1H NMR, ^{13}C NMR, HRMS, and compared with reported works.

Representative procedure for Pd(II)-catalyzed synthesis of 7-hexyl-7H-acenaphtho[1,2-b]indole, **2a**



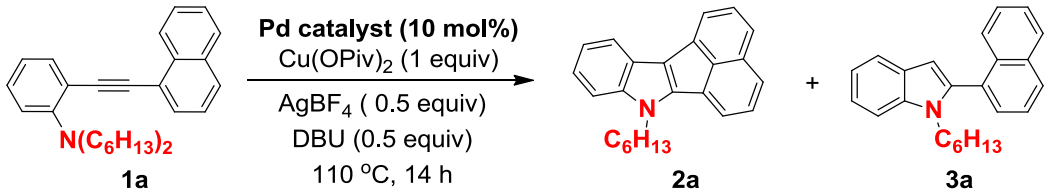
To a solution of starting material **1a** (41.1 mg, 0.1 mmol) in DMAc (1.0 mL) were added $\text{Pd}(\text{OPiv})_2$ (3.08 mg, 0.01 mmol), DBU (7.5 μL , 0.05 mmol), and AgBF_4 (9.74 mg, 0.05 mmol). The reaction mixture was stirred for 14 h at 110 °C under Ar atmosphere. The resulting mixture was filtered through a Florisil (Kanto Chemical, granularity: 150 nm-250 nm) using Et_2O or hexane/ EtOAc as eluent. After concentration, the residue was purified by short column chromatography using neutral silica gel (hexane:dichloromethane = 10:1) to give **2a** (31.6 mg, 0.097 mmol) in 97% yield as dark orange oil.

Representative procedure for synthesis of 2-((2-aminophenyl)ethynyl)-*N,N*-dimethylaniline, **1a**



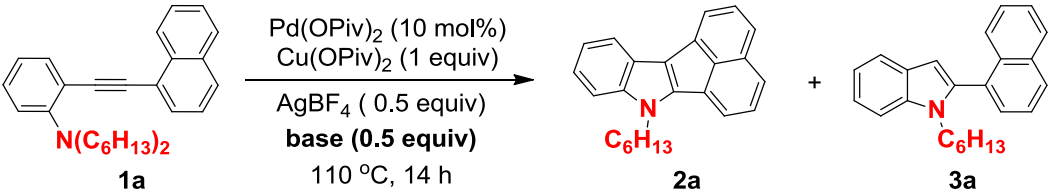
To a mixture of 2-ethynyl-*N,N*-dihexylaniline (2.85 g, 10.0 mmol), 1-iodonaphthalene (2.54 g, 10 mmol), $\text{PdCl}_2(\text{PPh}_3)_3$ (210 mg, 0.3 mmol), and CuI (57 mg, 0.3 mmol) was added triethylamine (0.3 M, 33 mL) in a 50 mL of Schlenk tube under Ar atmosphere. The reaction mixture was stirred for 12 h at room temperature. The resulting mixture was washed with Et_2O and filtered through a Celite pad. The filtrate was concentrated under reduced pressure to afford crude product, which was purified by silica gel chromatography (hexane:dichloromethane = 10:1) to give **1a** (3.70 g, 8.9 mmol) in 90% yield as pale yellow oil

Table S1. Screening of Pd catalyst ^a

				
entry	Pd-catalyst (10 mol%)	2a (%) ^b	1a (%) ^b	3a (%) ^b
1	-	0	98	0
2	Pd(OPiv) ₂	99(97)	0	0
3	Pd(OAc) ₂	74	14	0
4	PdCl ₂	69	20	2
5	Pd ₂ (dba) ₃	68	10	1

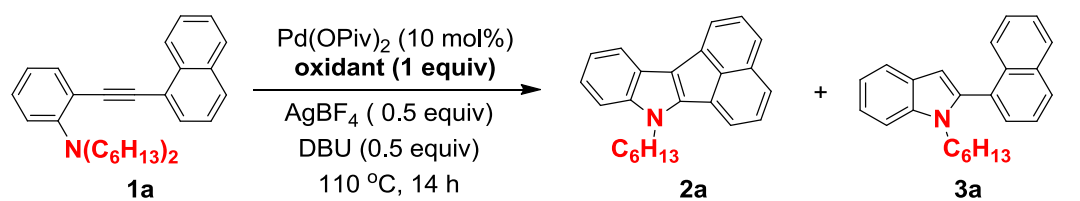
Conditions: ^a 1a (0.1 mmol), Pd catalyst (10 mol%), AgBF₄ (0.5 equiv), DBU (0.5 equiv), Cu(OPiv)₂ (1 equiv), DMAc (1.0 mL) stirred at 110 °C for 14 h under Ar. ^b NMR yields determined using CH₂Br₂ as internal standard. Isolated yields are shown in parentheses

Table S2. Screening of base ^a

				
entry	base (0.5 equiv)	2a (%) ^b	1a (%) ^b	3a (%) ^b
1	-	64	0	12
2	CsOPiv	(85)	0	0
3	Cs ₂ CO ₃	39	36	2
4	DABCO	28	24	26
5	DBU	99 (97)	0	0
6	<i>n</i> Bu ₃ N	81	0	12

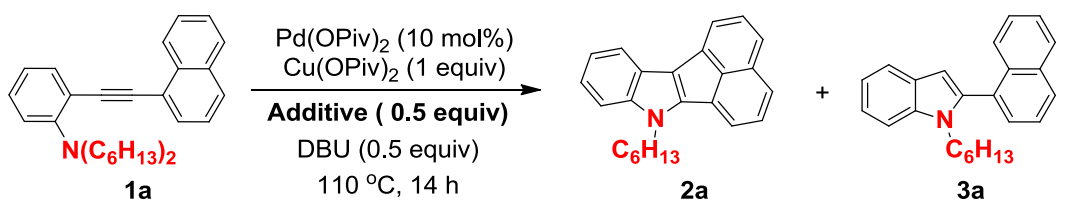
^a Conditions: 1a (0.1 mmol), Pd(OPiv)₂ (10 mol%), AgBF₄ (0.5 equiv), base (0.5 equiv), Cu(OPiv)₂ (1 equiv), DMAc (1.0 mL) stirred at 110 °C for 14 h under Ar. ^b NMR yields determined using CH₂Br₂ as internal standard. Isolated yields are shown in parentheses

Table S3. Screening of oxidant ^a

				
entry	Oxidant (1.0 equiv)	2a (%) ^b	1a (%) ^b	3a (%) ^b
1	-	15	80	0
2	Cu(OPiv) ₂	99(97)	0	0
3	Cu(OAc) ₂	21	61	0
4	CuCl ₂	61	10	12
5	K ₂ S ₂ O ₈	40	12	0
6	<i>o</i> -chloranil	8	43	2
7	PhI(OPiv) ₂	34	50	0
8 ^c	Cu(OPiv) ₂ / O ₂	49	18	4

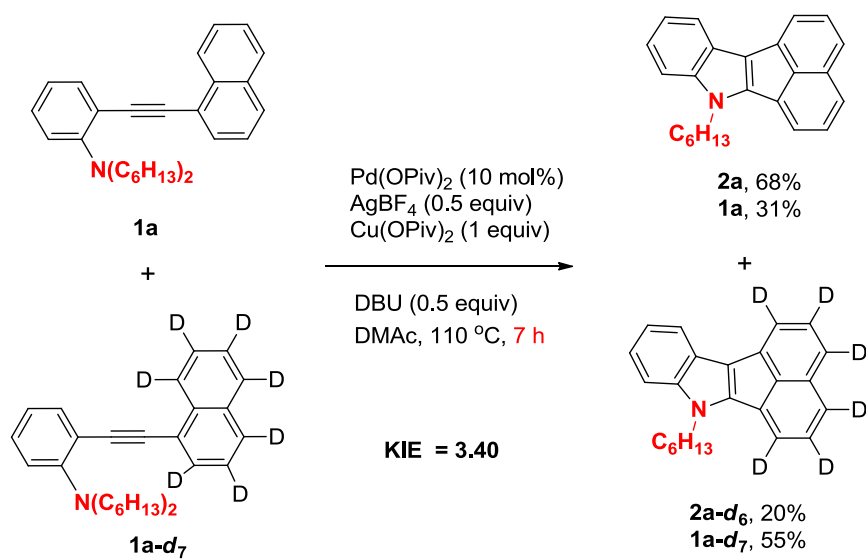
Conditions: ^a1a (0.1 mmol), Pd(OPiv)₂ (10 mol%), AgBF₄ (0.5 equiv), DBU (0.5 equiv), oxidant (1 equiv), DMAc (1.0 mL) stirred at 110 °C for 14 h under Ar. ^b NMR yields determined using CH₂Br₂ as internal standard. Isolated yields are shown in parentheses ^c Cu(OPiv) (0.4 equiv) and O₂ balloon.

Table S4. Screening of additives ^a

				
entry	Additive (0.5 equiv)	2a (%) ^b	1a (%) ^b	3a (%) ^b
1	-	34	50	0
2	AgBF ₄	99(97)	0	0
3	AgOTs	61	32	2
4	<i>n</i> Bu ₄ N.BF ₄	32	64	0
5	LiBF ₄	46	46	0

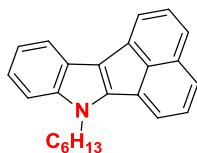
Conditions: ^a1a (0.1 mmol), Pd(OPiv)₂ (10 mol%), additive (0.5 equiv), DBU (0.5 equiv), Cu(OPiv)₂ (1 equiv), DMAc (1.0 mL) stirred at 110 °C for 14 h under Ar. ^b NMR yields determined using CH₂Br₂ as internal standard. Isolated yields are shown in parentheses

Scheme S1. Kinetic Isotope Effect.



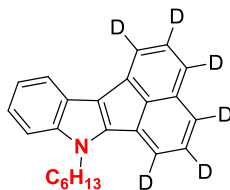
Analytical Data

7-hexyl-7H-acenaphtho[1,2-b]indole, 2a



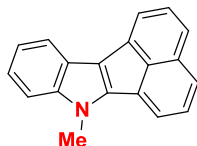
Dark orange oil (97%, 0.097 mmol, 31.54mg); ^1H NMR (400 MHz, CDCl_3) δ 7.87-7.83 (m, 1H), 7.74 (d, J = 8.0 Hz, 2H), 7.70 (d, J = 6.8 Hz, 1H), 7.59 (d, J = 8.0 Hz, 1H), 7.54-7.49 (m, 2H), 7.40-7.36 (m, 1H), 7.23-7.18 (m, 2H), 4.43 (t, J = 7.2 Hz, 2H), 2.03-1.95 (m, 2H), 1.49-1.24 (m, 4H), 0.86 (t, J = 7.2 Hz, 3H); ^{13}C NMR (100 MHz, CDCl_3) δ 144.74, 141.48, 134.01, 133.00, 129.73, 129.33, 128.19, 127.30, 126.96, 124.13, 122.94, 121.33, 120.55, 120.00, 119.82, 119.67, 119.36, 110.46, 45.52, 31.55, 29.94, 26.86, 22.51, 13.99; HRMS (MALDI) calcd for $\text{C}_{24}\text{H}_{23}\text{N}$, $[m/z]$: 325.18250, found: 325.18249.

[Deuterated] 7-hexyl-7H-acenaphtho[1,2-b]indole (2a-d₆)



Orange oil (72%, 0.072 mmol, 23.87mg); ^1H NMR (400 MHz, CDCl_3) δ 7.87-7.83 (m, 1H), 7.40-7.36 (m, 1H), 7.23-7.18 (m, 1H), 4.42 (t, J = 6.8 Hz, 2H), 2.03-1.95 (m, 2H), 1.49-1.42 (m, 2H), 1.37-1.24 (m, 4H), 0.86 (t, J = 6.8 Hz, 3H); ^{13}C NMR (100 MHz, CDCl_3) δ 144.74, 141.46, 133.88, 132.98, 129.60, 129.16, 122.94, 121.3, 120.64, 119.65, 119.32, 110.45, 45.50, 31.54, 29.93, 26.86, 22.50, 13.98; HRMS (MALDI) calcd for $\text{C}_{24}\text{H}_{17}\text{D}_6\text{N}$, $[m/z]$: 331.22016, found: 331.22015.

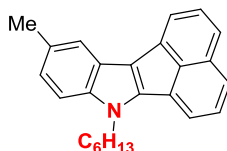
7-methyl-7H-acenaphtho[1,2-b]indole, 2c



Dark orange solid (34%, 0.034 mmol, 8.70mg); ^1H NMR (400 MHz, CDCl_3) δ 7.85-7.82 (m, 1H), 7.75-7.72 (m, 3H), 7.59 (d, J = 8.4 Hz, 1H), 7.51 (td, J = 8.4, 1.6 Hz, 2H), 7.38-7.34 (m, 1H), 7.19-7.24 (m, 2H), 4.04 (s, 3H); ^{13}C NMR (100 MHz, CDCl_3) δ 145.25, 142.06, 133.87, 132.89, 129.63, 129.30, 128.17, 127.37, 126.92, 124.13, 122.90, 121.42, 120.66, 119.89, 119.87, 119.60,

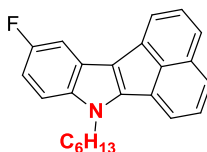
119.20, 110.19, 31.57; HRMS (APCI) calcd for C₁₉H₁₃N, [M+H]⁺: 256.11208, found: 256.11210.

7-hexyl-10-methyl-7H-acenaphtho[1,2-b]indole, 2d



Orange oil (88%, 0.088 mmol, 29.87mg); ¹H NMR (400 MHz, CDCl₃) δ 7.72 (d, *J* = 2.8 Hz, 1H), 7.70 (s, 1H), 7.68 (d, *J* = 6.8 Hz, 1H), 7.63 (s, 1H), 7.67 (d, *J* = 8.0 Hz, 1H), 7.52-7.48 (m, 2H), 7.26 (t, *J* = 2.8 Hz, 1H), 7.02 (d, *J* = 8.0 Hz, 1H), 4.39 (t, *J* = 7.2 Hz, 2H), 2.51 (s, 3H), 2.01-1.93 (m, 2H), 1.55-1.40 (m, 2H), 1.36-1.23 (m, 4H), 0.85 (t, *J* = 6.8 Hz, 3H); ¹³C NMR (100 MHz, CDCl₃) δ 144.79, 139.91, 134.15, 133.03, 129.91, 129.85, 129.31, 128.17, 127.14, 126.94, 123.94, 123.11, 122.90, 119.84, 119.63, 119.47, 118.83, 110.12, 45.54, 31.56, 29.94, 26.85, 22.50, 21.54, 14.00; HRMS (MALDI) calcd for C₂₅H₂₅N, [m/z]: 339.19815, found: 339.19815.

10-fluoro-7-hexyl-7H-acenaphtho[1,2-b]indole, 2e



Orange solid (89%, 0.089 mmol, 30.54mg); ¹H NMR (400 MHz, CDCl₃) δ 7.75 (d, *J* = 8.0 Hz, 1H), 7.69 (d, *J* = 5.2 Hz, 1H), 7.68 (d, *J* = 4.4 Hz, 1H), 7.60 (d, *J* = 8.4 Hz, 1H), 7.55-7.49 (m, 2H), 7.46 (dd, *J* = 9.6, 2.4 Hz, 1H), 6.93 (td, *J* = 9.2, 2.4 Hz, 1H), 4.39 (t, *J* = 6.8 Hz, 2H), 2.00-1.93 (m, 1H), 1.47-1.39 (m, 2H), 1.36-1.23 (m, 4H), 0.86 (t, *J* = 6.8 Hz, 3H); ¹³C NMR (100 MHz, CDCl₃) δ 158.53 (d, *J*¹ = 234.7 Hz), 146.16, 138.06, 133.25 (d, *J*² = 59.2 Hz), 129.39 (d, *J*⁷ = 5.0 Hz), 128.22, 127.60, 127.01, 124.22, 122.93 (d, *J*⁵ = 10.7 Hz), 120.17, 119.72, 119.05 (d, *J*⁸ = 4.1 Hz), 110.99 (d, *J*⁶ = 9.9 Hz), 109.40 (d, *J*³ = 26.4 Hz), 104.59 (d, *J*⁴ = 23.0 Hz), 56.69, 31.51, 29.90, 26.82, 22.49, 13.97; HRMS (MALDI) calcd for C₂₄H₂₂FN, [m/z]: 343.17308, found: 343.17305.

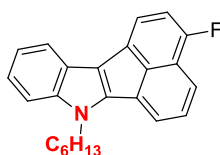
7-hexyl-3-methyl-7H-acenaphtho[1,2-b]indole, 2f



Dark orange oil (88%, 0.088 mmol, mg); ¹H NMR (400 MHz, CDCl₃) δ 7.83-7.81 (m, 1H), 7.71

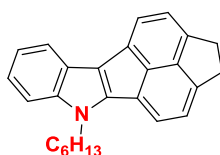
(dd, $J = 8.4, 6.8$ Hz, 2H), 7.55 (d, $J = 7.2$ Hz, 1H), 7.50 (dd, $J = 6.8$ Hz, 1H), (m, 1H), 7.27 (d, $J = 8.0$ Hz, 1H), 7.19-7.17 (m 1H), 4.40 (t, $J = 7.2$ Hz, 2H), 2.77 (s, 3H), 2.01-1.93 (m, 2H), 1.44-1.41 (m, 2H), 1.34-1.27 (m, 6H), 0.86 (t, $J = 7.6$ Hz, 3H). ^{13}C NMR (100 MHz, CDCl_3) δ 144.92, 141.33, 136.33, 134.48, 133.34, 129.46, 127.92, 127.84, 127.07, 123.04, 121.01, 120.99, 120.47, 120.16, 119.50, 119.46, 118.77, 110.38, 56.47, 31.56, 29.89, 26.85, 22.50, 18.24, 14.00; HRMS (MALDI) calcd for $\text{C}_{25}\text{H}_{25}\text{N}$, $[\text{m/z}]$: 339.19185, found: 339.19186.

3-fluoro-7-hexyl-7H-acenaphtho[1,2-b]indole, 2g



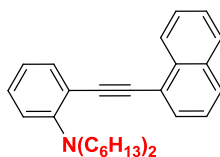
Dark orange solid (85%, 0.085 mmol, 29.17mg); ^1H NMR (400 MHz, CDCl_3) δ 7.83-7.79 (m, 1H), 7.75 (d, $J = 8.4$ Hz, 1H), 7.72 (d, $J = 8.4$ Hz, 1H), 7.55-7.51 (m, 2H), 7.38-7.34 (m, 1H), 7.22-7.18 (m, 2H), 7.09 (dd, $J = 11.2, 7.2$ Hz, 1H), 4.37 (t, $J = 7.2$ Hz, 2H), 2.00-1.92 (m, 2H), 1.55-1.36 (m, 2H), 1.34-1.23 (m, 4H), 0.86 (t, $J = 6.8$ Hz, 3H); ^{13}C NMR (100 MHz, CDCl_3) δ 160.00 (d, $J^1 = 256.8$ Hz), 142.29, 141.24, 134.82 (d, $J^3 = 6.6$ Hz), 133.80 (d, $J = 2.5$ Hz), 128.54, 125.99 (d, $J^4 = 4.1$ Hz), 123.01, 121.31, 120.72, 121.57, 120.36 (d, $J^5 = 3.3$ Hz), 120.28, 119.48, 119.08 (d, $J^6 = 3.3$ Hz), 117.62 (d, $J^7 = 1.6$ Hz), 110.76 (d, $J^2 = 22.2$ Hz), 110.52, 45.46, 31.52, 29.89, 26.85, 22.50, 13.98; HRMS (MALDI) calcd for $\text{C}_{24}\text{H}_{22}\text{FN}$, $[\text{m/z}]$: 343.17308, found: 343.17305.

5-hexyl-2,5-dihydro-1H-cyclopenta[5,6]acenaphtho[1,2-b]indole, 2h



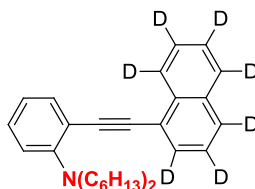
Yellow oil (43%, 0.043 mmol, 15.10mg); ^1H NMR (400 MHz, CDCl_3) δ 7.86 (br, 1H), 7.74 (d, $J = 6.8$ Hz, 1H), 7.72 (d, $J = 6.8$ Hz), 7.39-7.34 (m, 3H), 7.19 (br, 2H), 4.44 (t, $J = 6.8$ Hz, 2H), 3.46 (s, 4H), 2.03-1.95 (m, 2H), 1.55-1.35 (m, 2H), 1.33-1.21 (m, 4H), 0.83 (t, $J = 6.8$ Hz, 3H); ^{13}C NMR (100 MHz, CDCl_3) δ ; HRMS (MALDI) calcd for $\text{C}_{26}\text{H}_{25}\text{N}$, $[\text{m/z}]$: 351.19815, found: 351.19810.

N,N-diethyl-2-(naphthalen-1-ylethynyl)aniline, 1a



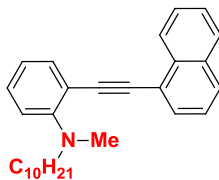
Bright yellow oil; ^1H NMR (400 MHz, CDCl_3) δ 8.55 (d, $J = 7.6$ Hz, 1H), 7.87 (d, $J = 8.0$ Hz, 1H), 7.82 (d, $J = 8.0$ Hz, 1H), 7.73 (d, $J = 7.2$ Hz, 1H), 7.61-7.51 (m, 3H), 7.45 (t, $J = 7.2$ Hz, 1H), 7.28-7.23 (m, 1H), 7.00 (d, $J = 8.0$ Hz, 1H), 6.92 (td, $J = 8.0, 1.2$ Hz, 1H), 3.35 (t, $J = 7.6$ Hz, 2H), 2.98 (s, 3H), 1.73-1.67 (m, 2H), 1.28-1.16 (m, 16H), 0.88 (t, $J = 7.2$ Hz, 3H) ^{13}C NMR (100 MHz, CDCl_3) δ 153.25, 134.32, 133.30, 133.24, 129.71, 128.86, 128.22, 128.16, 126.64, 126.48, 126.30, 125.27, 121.85, 120.42, 116.98, 94.22, 91.79, 52.63, 31.73, 27.27, 26.91, 22.62, 14.00; HRMS (MALDI) calcd for $\text{C}_{30}\text{H}_{37}\text{N}$, $[\text{m/z}]$: 410.28423, found: 410.28422.

[Deuterated] N,N-di(6-((2-((1-ethynyl-2-phenyl)ethynyl)naphthalen-1-yl)ethyl)aniline)aniline (1a-d₇)



Bright yellow oil; ^1H NMR (400 MHz, CDCl_3) δ 8.55 (d, $J = 7.6$ Hz, 1H), 7.87 (d, $J = 8.0$ Hz, 1H), 7.82 (d, $J = 8.0$ Hz, 1H), 7.73 (d, $J = 7.2$ Hz, 1H), 7.61-7.51 (m, 3H), 7.45 (t, $J = 7.2$ Hz, 1H), 7.28-7.23 (m, 1H), 7.00 (d, $J = 8.0$ Hz, 1H), 6.92 (td, $J = 8.0, 1.2$ Hz, 1H), 3.35 (t, $J = 7.6$ Hz, 2H), 2.98 (s, 3H), 1.73-1.67 (m, 2H), 1.28-1.16 (m, 16H), 0.88 (t, $J = 7.2$ Hz, 3H) ^{13}C NMR (100 MHz, CDCl_3) δ 153.24, 134.32, 128.84, 120.44, 120.04, 117.03, 94.18, 91.79, 52.64, 31.72, 27.27, 26.90, 22.62, 13.98; HRMS (MALDI) calcd for $\text{C}_{30}\text{H}_{30}\text{D}_7\text{N}$, $[\text{M}+\text{H}]^+$: 419.34381, found: 419.34383.

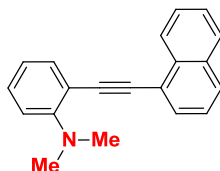
N-decyl-N-methyl-2-(naphthalen-1-ylethynyl)aniline, 1b



Bright yellow oil; ^1H NMR (400 MHz, CDCl_3) δ 8.54 (d, $J = 7.6$ Hz, 1H), 7.89 (d, $J = 7.2$ Hz, 1H), 7.85 (d, $J = 8.4$ Hz, 1H), 7.76 (d, $J = 6.8$ Hz, 1H), 7.64-7.53 (m, 3H), 7.47 (t, $J = 7.2$ Hz, 1H), 7.32-7.28 (m, 1H), 7.00 (d, $J = 8.4$ Hz, 1H), 6.95 (t, $J = 7.2$ Hz, 1H), 3.96 (t, $J = 7.6$ Hz, 2H), 2.98 (s, 3H), 1.73-1.67 (m, 2H), 1.28-1.16 (m, 16H), 0.88 (t, $J = 7.2$ Hz, 3H); ^{13}C NMR (100 MHz, CDCl_3) δ 154.61, 134.44, 133.27, 133.25, 129.79, 129.24, 128.33, 128.21, 126.57, 126.52, 126.32, 125.26, 121.70, 120.30, 217.96, 115.58, 93.97, 92.28, 56.02, 40.35, 31.85, 29.59, 29.56,

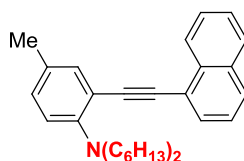
29.26, 27.73, 27.18, 22.65, 14.10 ; HRMS (MALDII) calcd for C₂₉H₃₅N, [M+H]⁺: 398.28423, found: 398.28425.

N,N-dimethyl-2-(naphthalen-1-ylethynyl)aniline, 1c



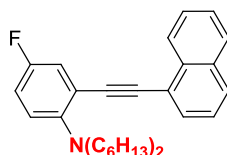
Bright yellow oil; ¹H NMR (400 MHz, CDCl₃) δ 8.52 (d, *J* = 8.0 Hz, 1H), 7.87 (d, *J* = 8.0 Hz, 1H), 7.83 (d, *J* = 8.0 Hz, 1H), 7.77 (dd, *J* = 7.8, 0.8 Hz, 1H), 7.64-7.52 (m, 3H), 7.47 (t, *J* = 7.2 Hz, 1H), 7.32-7.26 (m, 1H), 6.99 (d, *J* = 8.0, 1H), 6.95 (d, *J* = 8.0 Hz, 1H), 3.06 (s, 3H); ¹³C NMR (100 MHz, CDCl₃) δ 154.83, 134.37, 133.24, 133.21, 129.93, 129.37, 128.43, 128.24, 126.65, 126.40, 126.35, 125.29, 121.59, 120.63, 117.13, 115.50, 93.77, 92.85, 43.74.

N,N-diethyl-4-methyl-2-(naphthalen-1-ylethynyl)aniline, 1d



Bright yellow oil; ¹H NMR (400 MHz, CDCl₃) 8.57 (d, *J* = 8.4 Hz, 1H), 7.87 (d, *J* = 8.0 Hz, 1H), 7.82 (d, *J* = 8.0 Hz, 1H), 7.73 (d, *J* = 6.8 Hz, 1H), 7.59-7.51 (m, 2H), 7.46 (t, *J* = 7.2, 1H), 7.42 (d, *J* = 2.0 Hz, 1H), 7.08 (dd, *J* = 8.4, 2.4 Hz, 1H), 6.93 (d, *J* = 8.4 Hz, 1H), 3.28 (t, *J* = 7.6 Hz, 1H), 2.32 (s, 3H), 1.57-1.52 (m, 4H), 1.28-1.18 (m, 12H), 0.80 (t, *J* = 6.8 Hz, 1H); ¹³C NMR (100 MHz, CDCl₃) δ 151.01, 134.40, 133.32, 133.23, 130.23, 129.69, 129.67, 128.16, 128.13, 126.71, 126.45, 126.28, 125.26, 121.92, 120.55, 117.65, 94.24, 91.47, 52.99, 31.74, 27.21, 26.95, 22.62, 20.40, 14.00; HRMS (MALDI) calcd for C₃₁H₃₉N, [M+H]⁺: 426.31553, found: 426.31555.

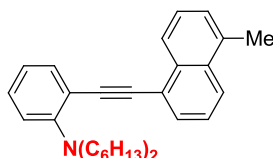
4-fluoro-N,N-diethyl-2-(naphthalen-1-ylethynyl)aniline, 1e



Bright yellow oil; ¹H NMR (400 MHz, CDCl₃) 8.59 (d, *J* = 8.0 Hz, 1H), 7.99 (d, *J* = 8.0 Hz, 1H), 7.87 (d, *J* = 8.0 Hz, 1H), 7.78 (dd, *J* = 7.2, 1.2 Hz, 1H), 7.63-7.56 (m, 2H), 7.49 (dd, *J* = 8.4, 7.2 Hz, 1H), 7.34 (dt, 9.2, 2.0 Hz, 1H), 7.02 (dd, *J* = 6.4, 1.6 Hz, 2H), 3.29 (t, *J* = 7.6 Hz, 4H), 1.60-1.52 (m, 4H), 1.35-1.22 (m, 12H), 0.84 (t, *J* = 6.8 Hz, 3H); ¹³C NMR (100 MHz, CDCl₃) δ 157.23

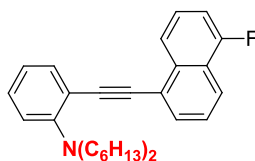
(d, $J^1 = 239.6$ Hz), 149.81 (d, $J^9 = 2.4$ Hz), 133.26 (d, $J^6 = 7.4$ Hz), 130.00, 128.64, 128.21, 126.58 (d, $J^5 = 8.2$ Hz), 126.39, 122.26 (d, $J^4 = 8.3$ Hz), 121.32, 119.88 (d, $J^7 = 3.3$ Hz), 119.74 (d, $J^3 = 10.7$ Hz), 115.70 (d, $J^2 = 22.2$ Hz), 92.76 (d, $J^8 = 3.3$ Hz), 92.56, 53.27, 31.72, 27.14, 26.90, 22.61, 13.99; HRMS (MALDI) calcd for $C_{30}H_{36}FN$, $[M+H]^+$: 430.29045, found: 430.29042.

N,N-dihexyl-2-((5-methylnaphthalen-1-yl)ethynyl)aniline, 1f



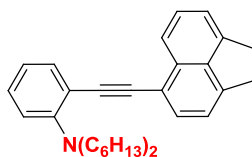
Bright yellow oil; 1H NMR (400 MHz, $CDCl_3$) δ 8.61-8.59 (m, 1H), 8.01-7.99 (m, 1H), 7.64 (d, $J = 7.2$ Hz, 1H), 7.61-7.53 (m, 3H), 7.29 (d, $J = 6.8$ Hz, 1H), 7.26-7.20 (m, 1H), 7.00 (d, $J = 7.6$ Hz, 1H), 6.91 (t, $J = 8.0$ Hz, 1H), 3.34 (t, $J = 8.0$ Hz, 4H), 2.70 (s, 3H), 1.60-1.52 (m, 4H), 1.30-1.19 (m, 12H), 0.80 (t, $J = 6.8$ Hz, 1H); ^{13}C NMR (100 MHz, $CDCl_3$) δ 153.16, 134.97, 134.23, 133.27, 132.40, 129.48, 128.68, 127.25, 126.15, 126.12, 124.30, 120.44, 120.11, 120.03, 117.24, 93.60, 32.13, 52.59, 31.73, 27.25, 26.91, 22.62, 19.61, 14.00. HRMS (MALDI) calcd for $C_{31}H_{39}N$, $[M+H]^+$: 426.31553, found: 426.31548.

2-((5-fluoronaphthalen-1-yl)ethynyl)-N,N-dihexylaniline, 1g



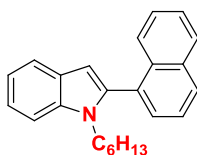
Bright yellow oil; 1H NMR (400 MHz, $CDCl_3$) δ 8.54 (d, $J = 6.8$ Hz, 1H), 8.13 (dd, $J = 7.2, 2.4$ Hz, 1H), 7.68-7.57 (m, 4H), 7.26 (td, $J = 8.4, 2.0$ Hz, 1H), 7.14 (dd, $J = 8.4$ Hz, 1H), 7.00 (d, $J = 8.4$ Hz, 1H), 6.93 (t, $J = 7.2$ Hz, 1H), 3.33 (t, $J = 8.0$ Hz, 2H), 1.59-1.52 (m, 4H), 1.28-1.17 (m, 12H), 0.80 (t, $J = 7.2$ Hz, 6H). ^{13}C NMR (100 MHz, $CDCl_3$) δ 158.55 (d, $J^1 = 253.6$ Hz), 153.25, 134.71 (d, $J^5 = 4.9$ Hz), 134.24, 129.62 (d, $J^2 = 8.3$ Hz), 128.90, 127.44, 126.69 (d, $J^4 = 5.8$ Hz), 126.67, 123.58 (d, $J^3 = 7.3$ Hz), 118.01 (d, $J^6 = 4.1$ Hz), 116.95, 93.7 (d, $J^7 = 2.4$ Hz), 91.00, 52.68, 31.72, 27.27, 26.91, 22.62, 13.99. HRMS (MALDI) calcd for $C_{30}H_{36}FN$, $[M+H]^+$: 430.29045 found: 430.29044.

2-((1,2-dihydroacenaphthylen-5-yl)ethynyl)-N,N-dihexylaniline, 1h

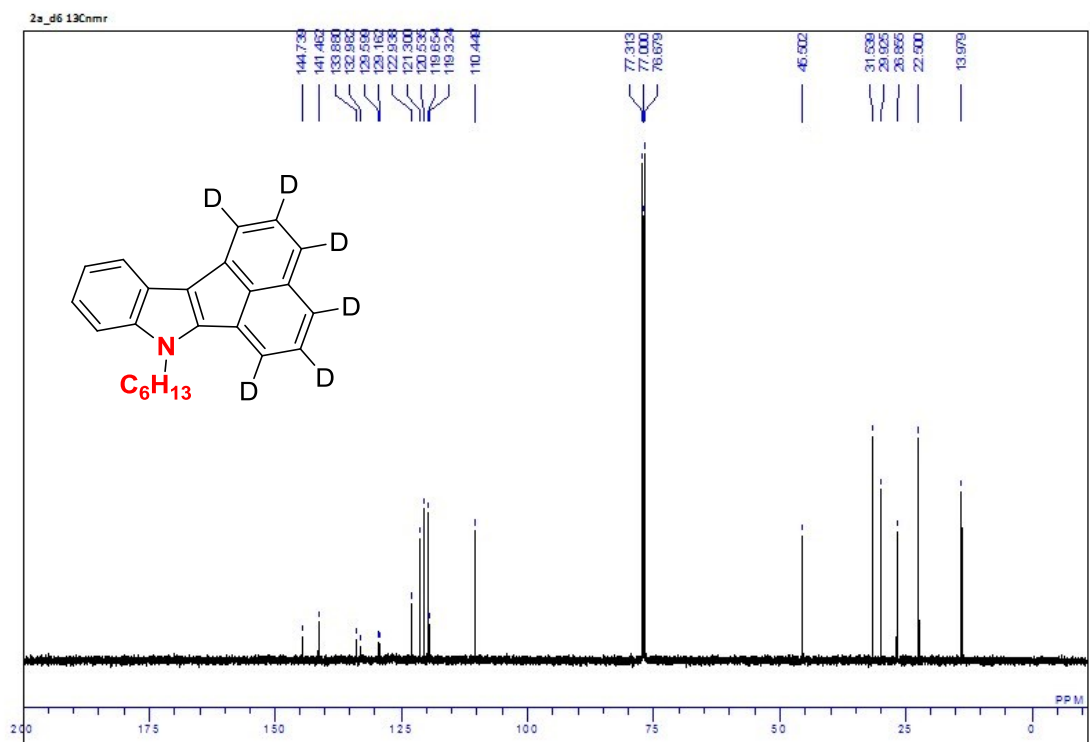
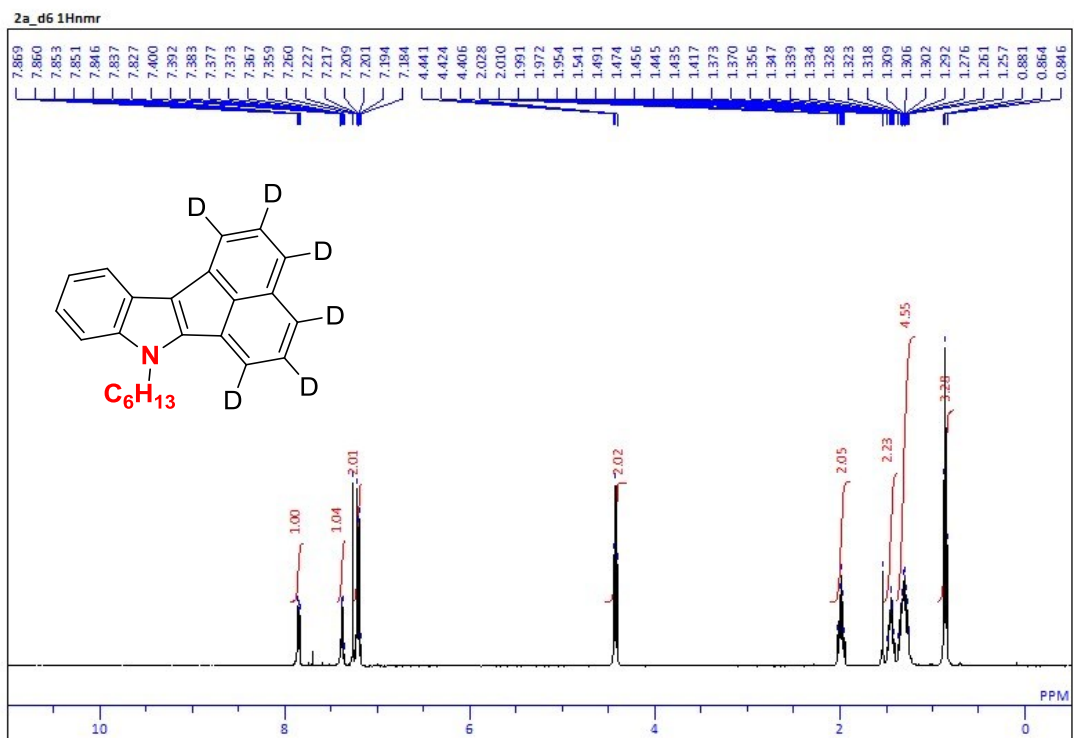


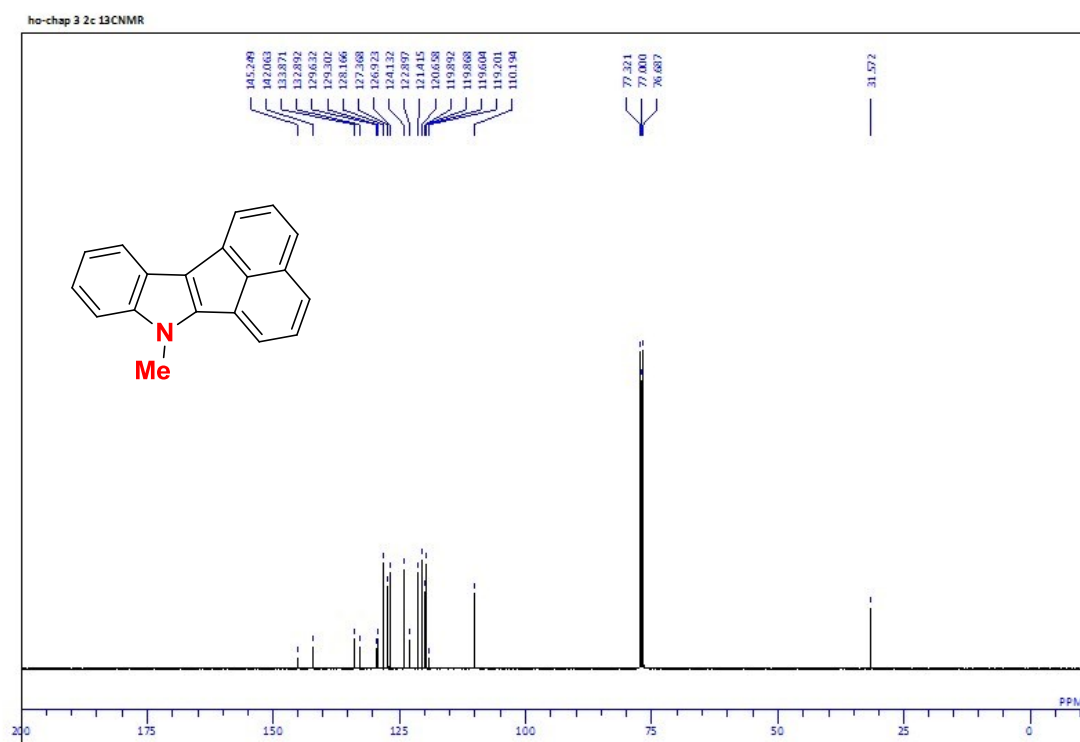
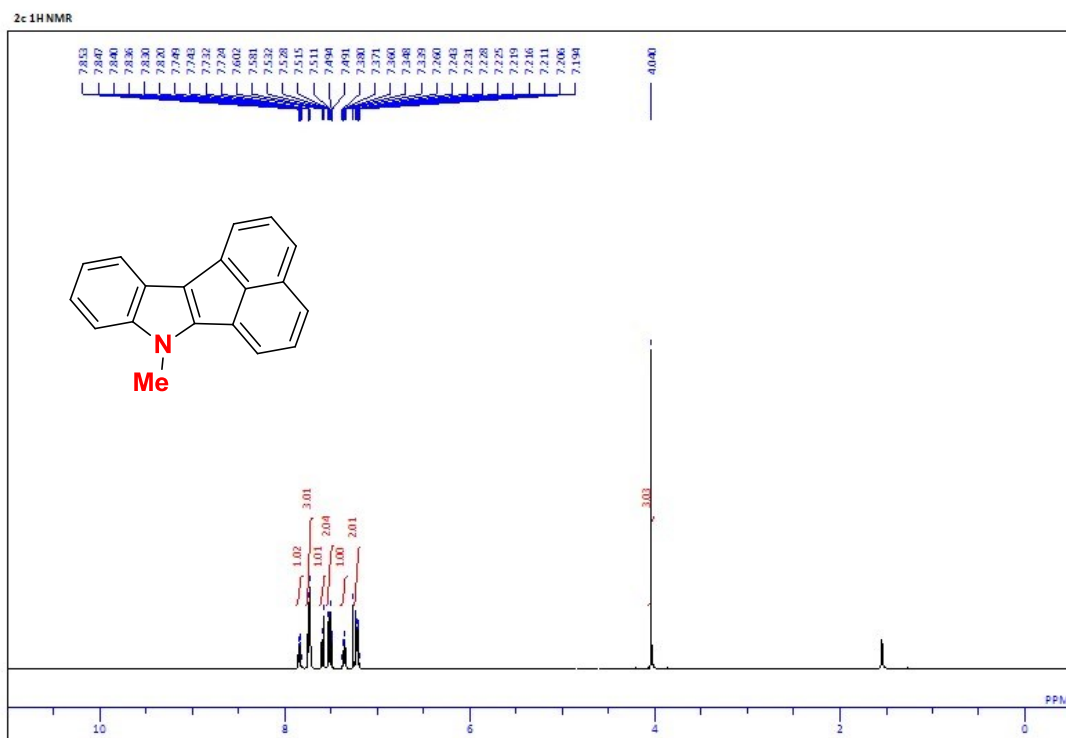
Yellow oil; ^1H NMR (400 MHz, CDCl_3) δ 8.08 (d, $J=8.4$ Hz, 1H), 7.67 (d, $J=7.6$ Hz, 1H), 7.58 (d, $J=8.0$, 1.2 Hz, 1H), 7.53 (t, $J=6.8$ Hz, 1H), 7.33 (d, $J=6.4$ Hz, 1H), 7.27-7.22 (m, 2H), 6.68 (d, $J=8.4$ Hz, 1H), 6.91 (t, $J=7.6$ Hz, 1H), 3.42 (s, 4H), 3.35 (t, $J=8.0$ Hz, 4H), 1.60-1.52 (m, 4H), 1.36-1.18(m, 12H), 0.80 (t, $J=6.8$ Hz, 1H); ^{13}C NMR (100 MHz, CDCl_3) δ 153.09, 146.66, 146.14, 138.99, 134.34, 131.80, 131.48, 128.56, 128.33, 121.52, 120.33, 119.93, 119.79, 118.97, 117.21, 116.92, 92.86, 91.93, 52.55, 31.74, 30.48, 30.44, 27.28, 26.93, 22.64, 14.01; HRMS (MALDI) calcd for $\text{C}_{32}\text{H}_{39}\text{N}$, $[\text{M}+\text{H}]^+$: 438.31553, found: 438.31555.

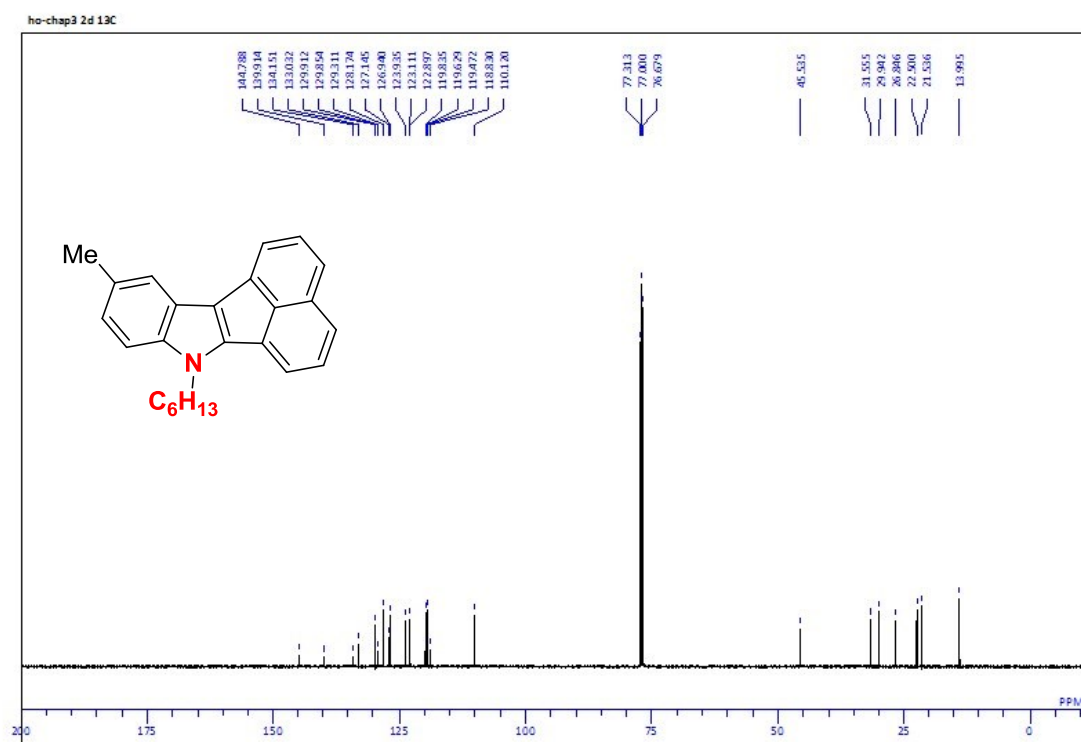
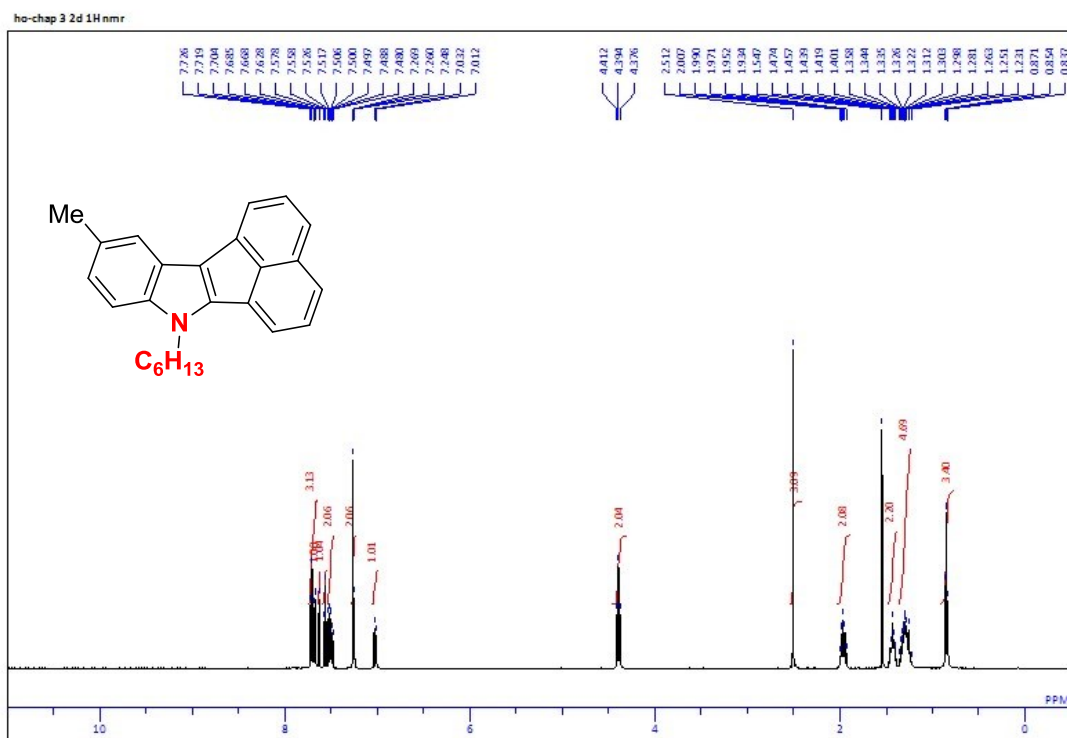
1-hexyl-2-(naphthalen-1-yl)-1H-indole, 3a

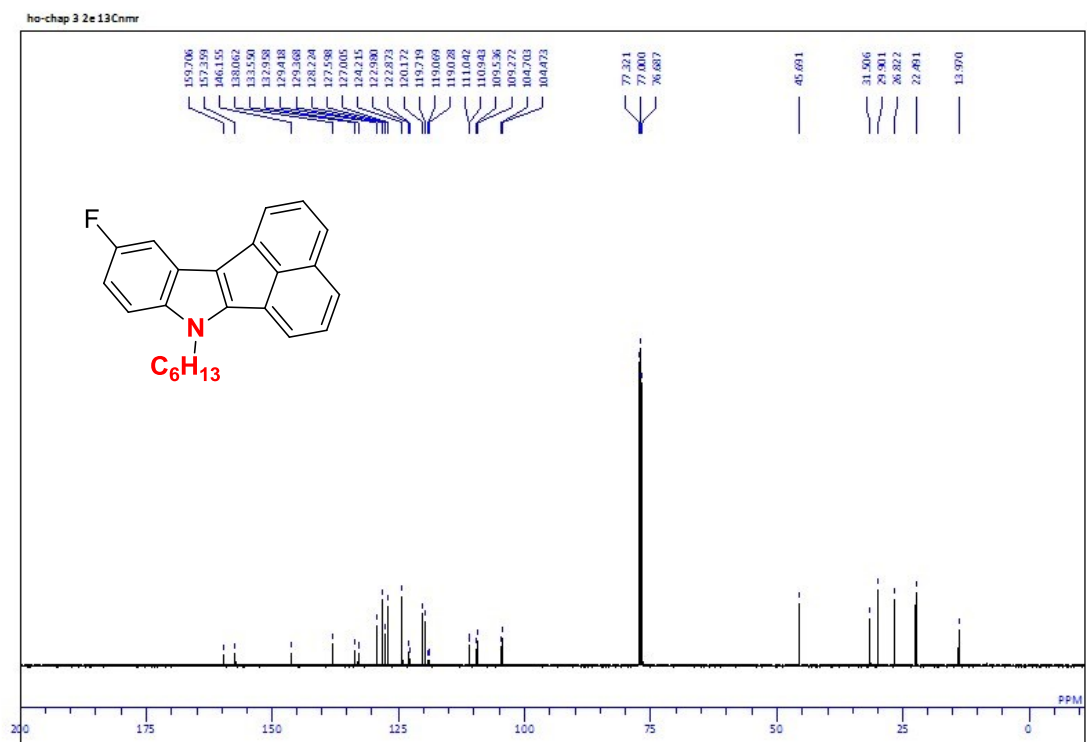
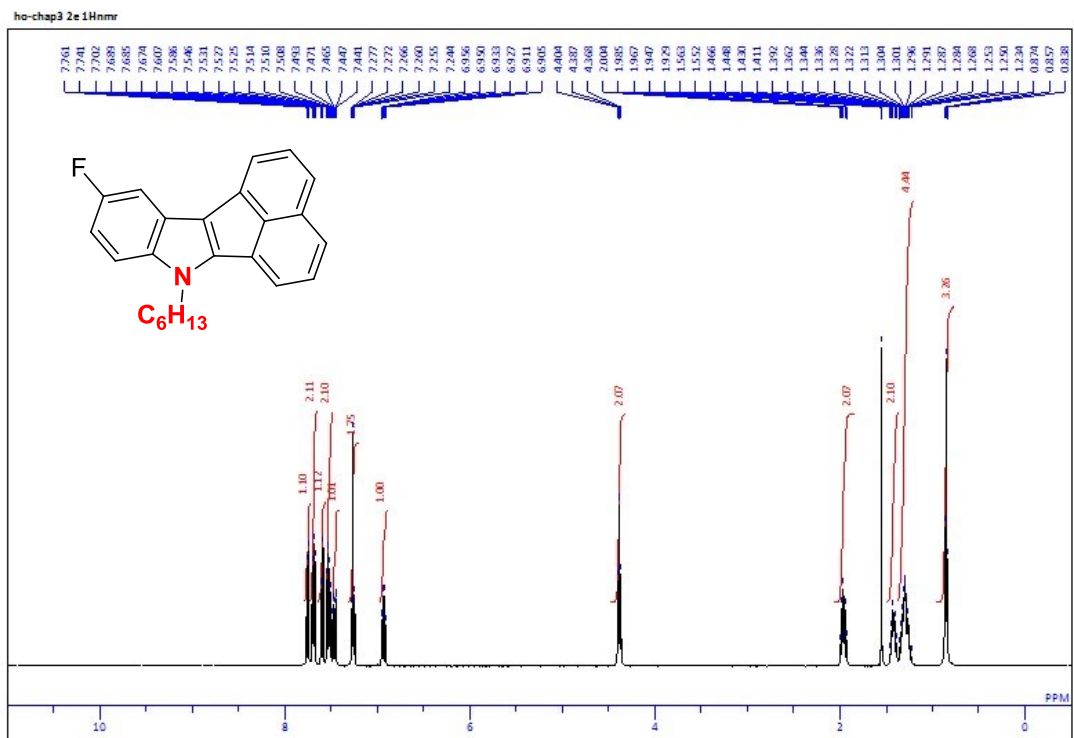


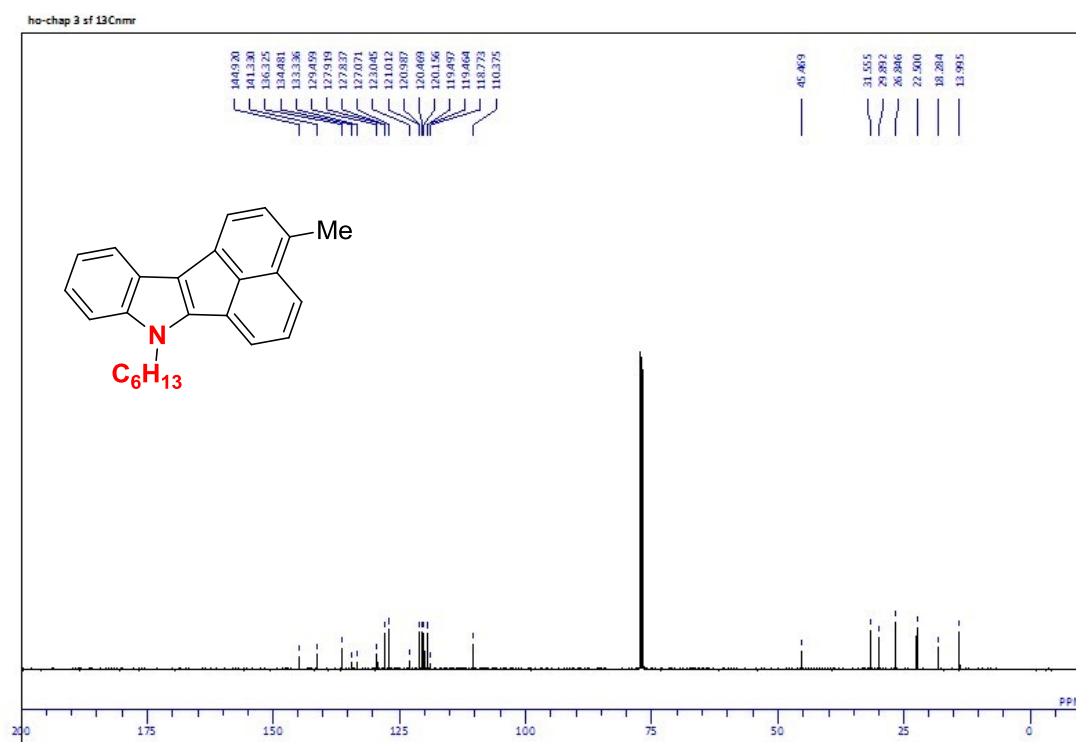
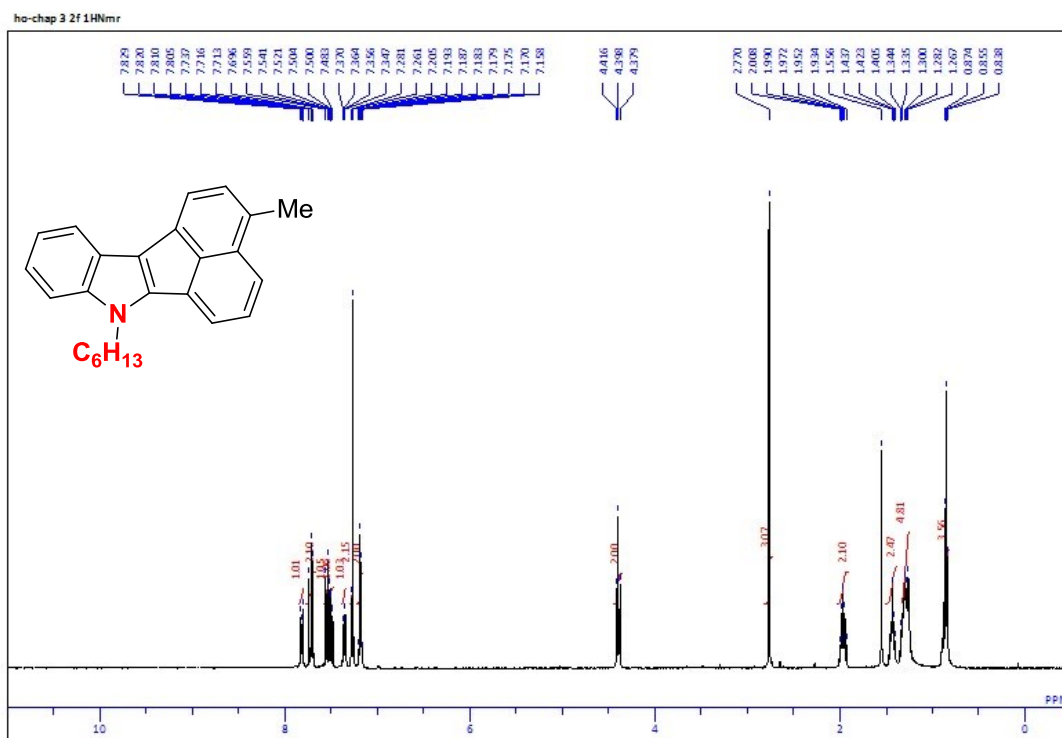
Yellow oil; ^1H NMR (400 MHz, CDCl_3) 7.98-7.92 (m, 1H), 7.71 (d, $J=7.8$ Hz, 2H), 7.59-7.50 (m, 3H), 7.45-7.41(m, 2H), 7.31-7.26 (m, 1H), 7.21-7.17(m, 1H), 6.61 (s, 1H), 4.08-4.01 (m, 1H), 3.82-3.76 (m, 1H), 1.07-0.98 (m, 6H), 0.71(t, $J=7.6$ Hz, 3H); ^{13}C NMR (100 MHz, CDCl_3) δ 138.84, 136.72, 133.48, 133.00, 130.83, 128.92, 128.87, 128.27, 128.50, 126.50, 126.11, 126.06, 125.08, 121.33, 120.55, 119.59, 109.94, 103.34, 44.02, 31.07, 29.84, 26.28, 22.27, 13.83; HRMS (MALDI) calcd for $\text{C}_{24}\text{H}_{25}\text{N}$, $[\text{m}/\text{z}]$: 327.19815, found: 327.19814.

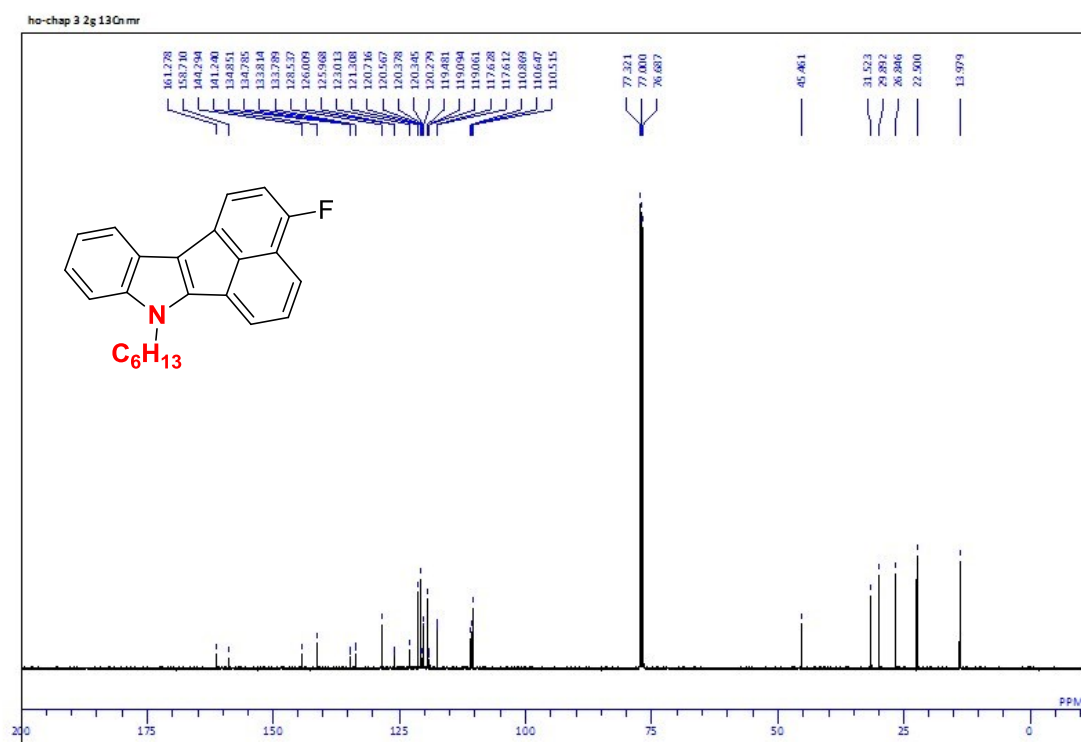
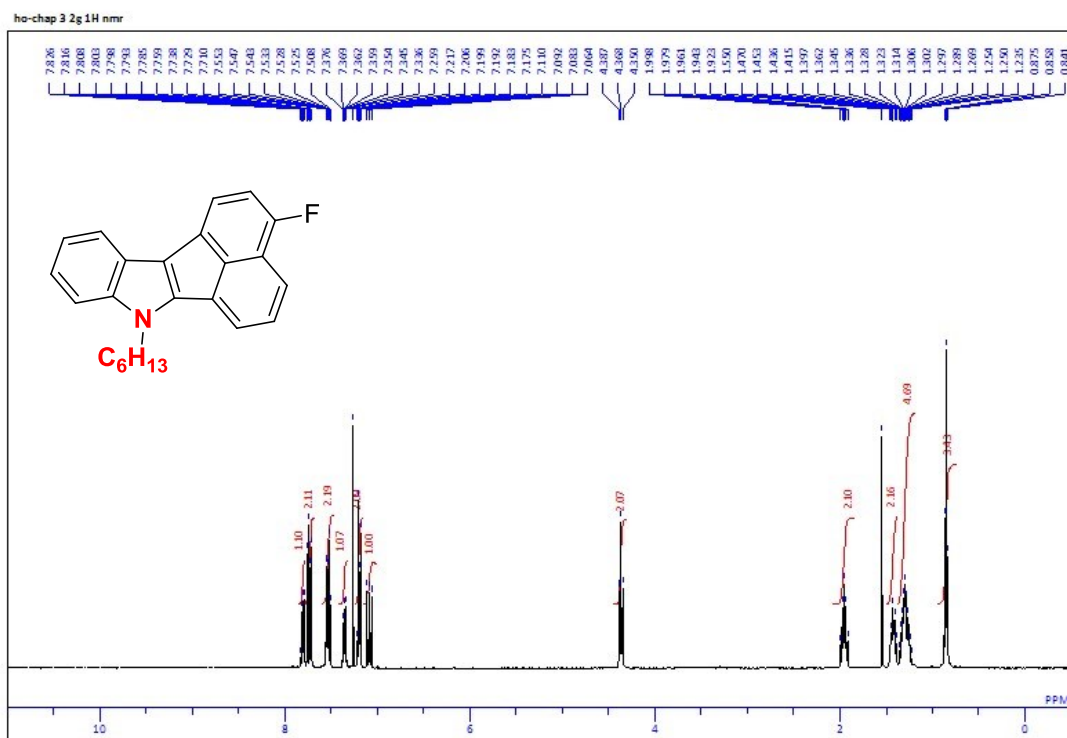


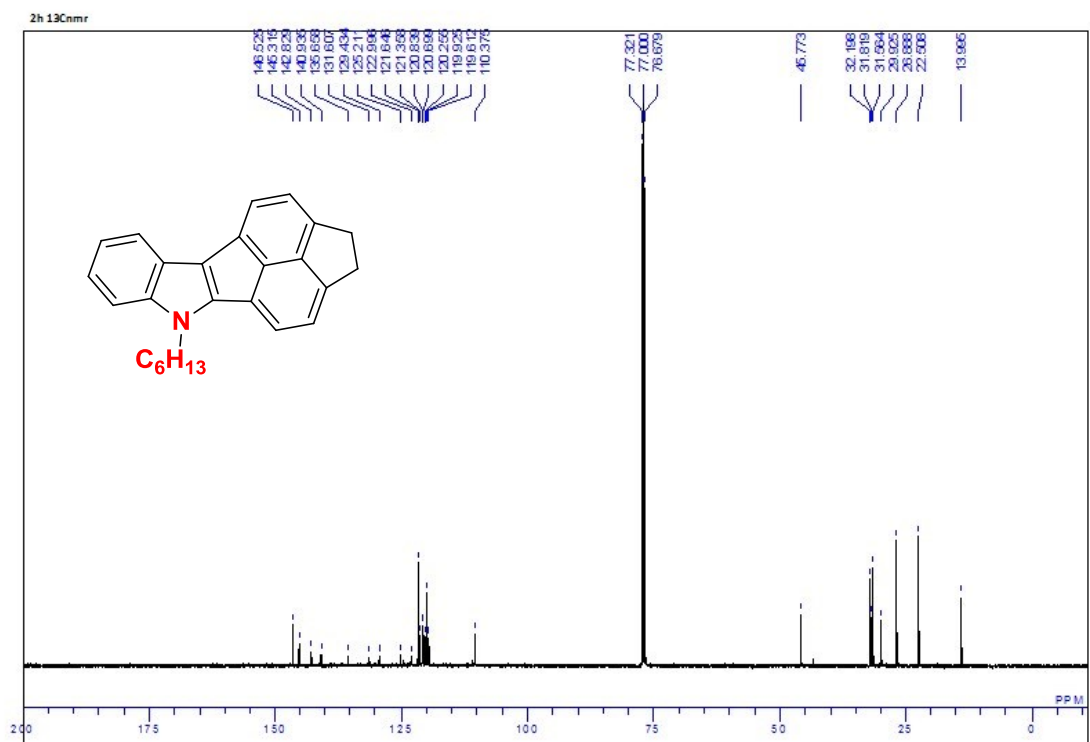
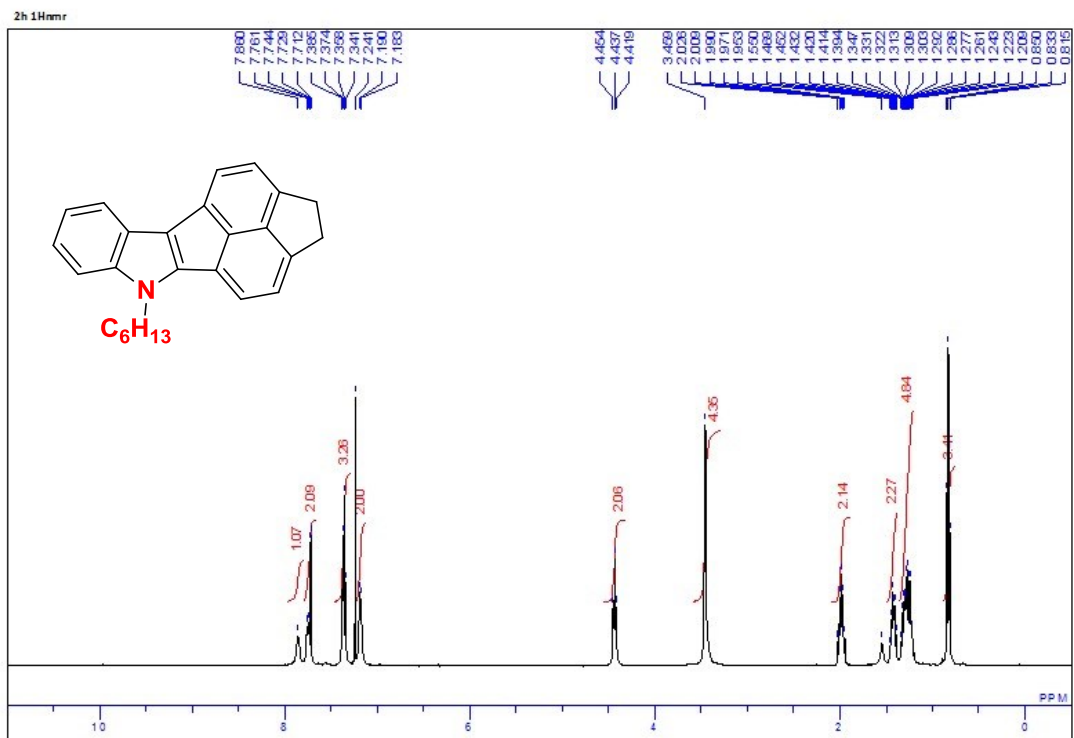


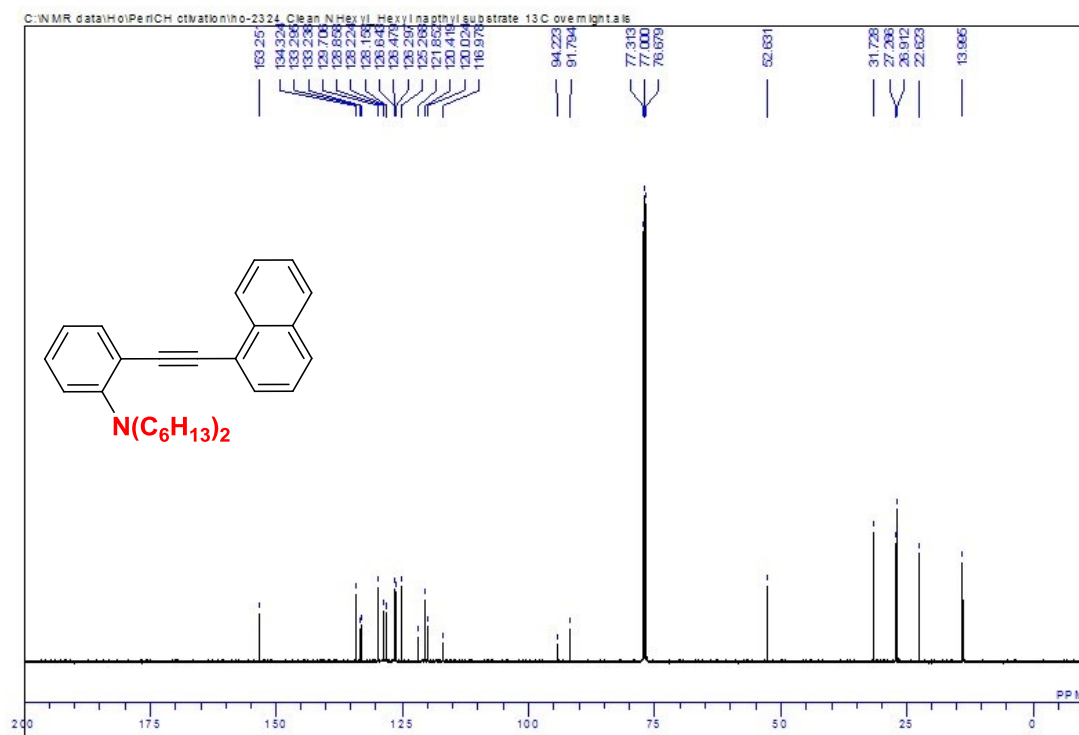
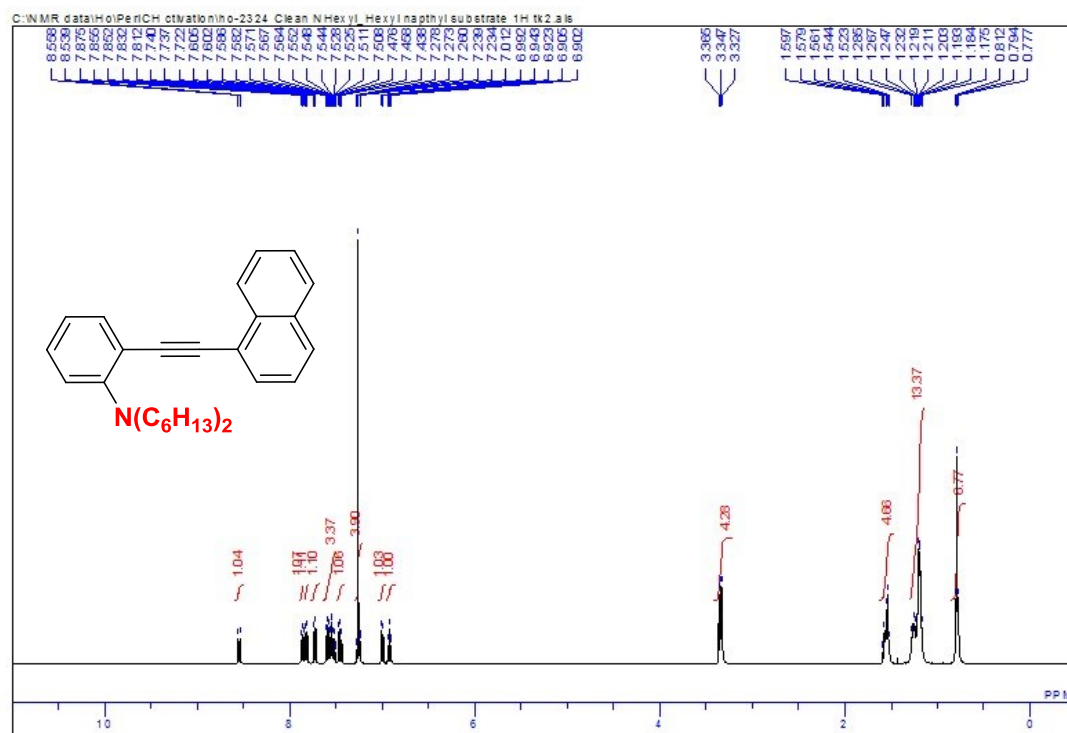


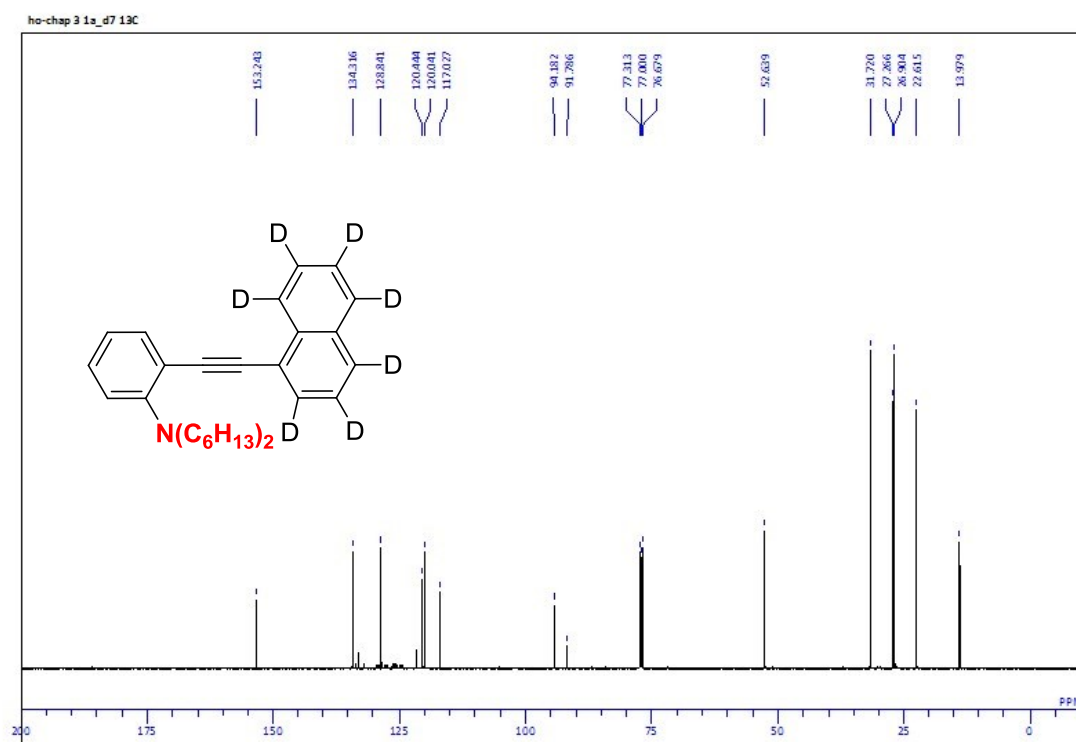
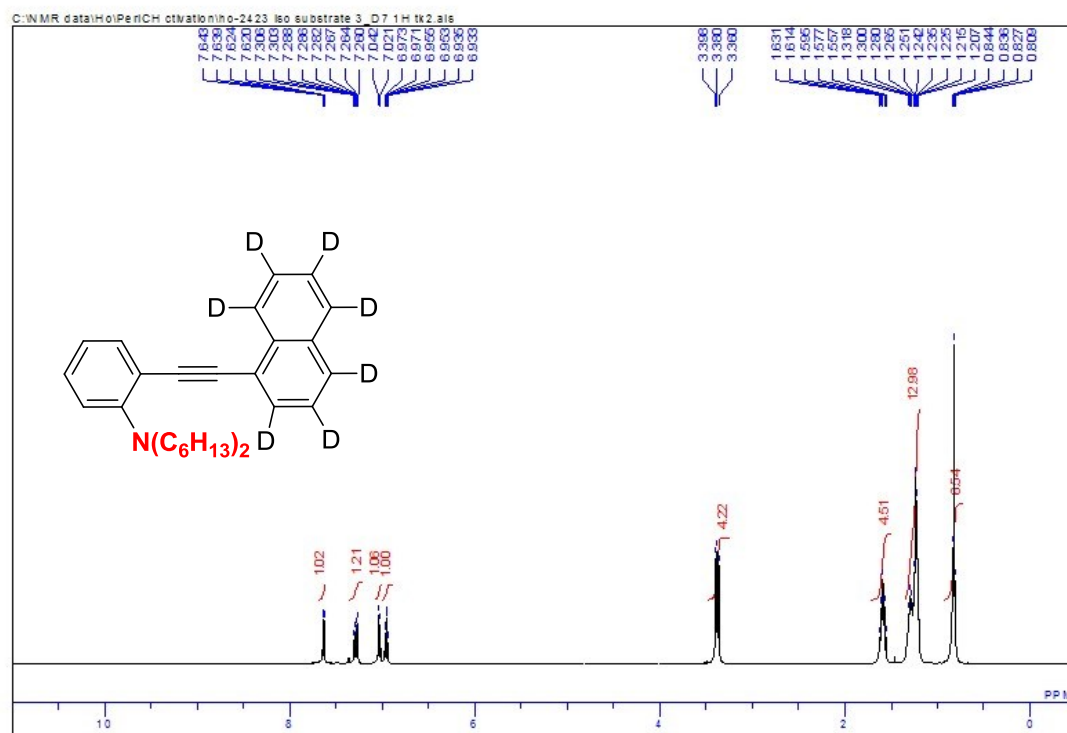


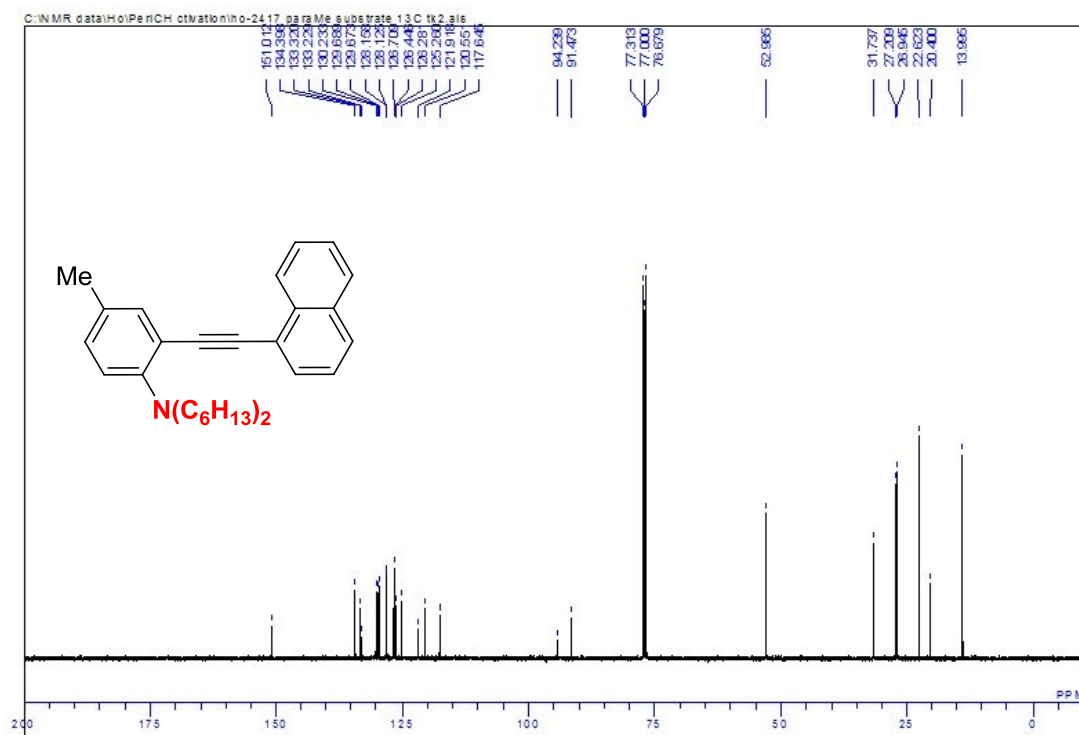
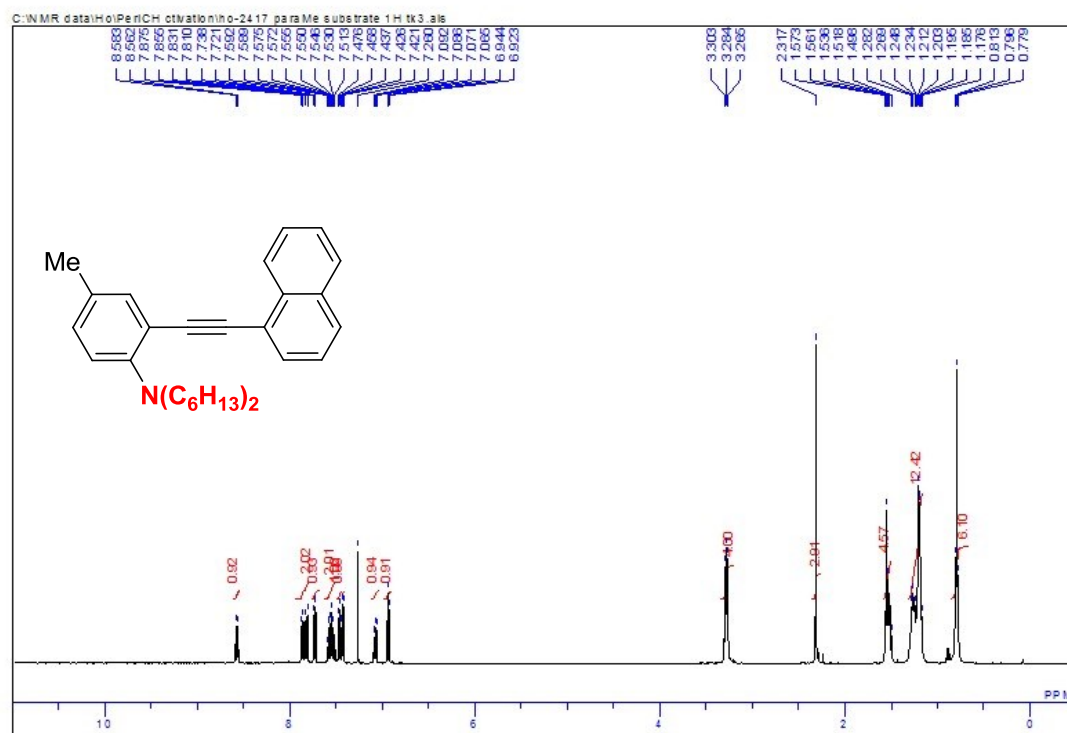


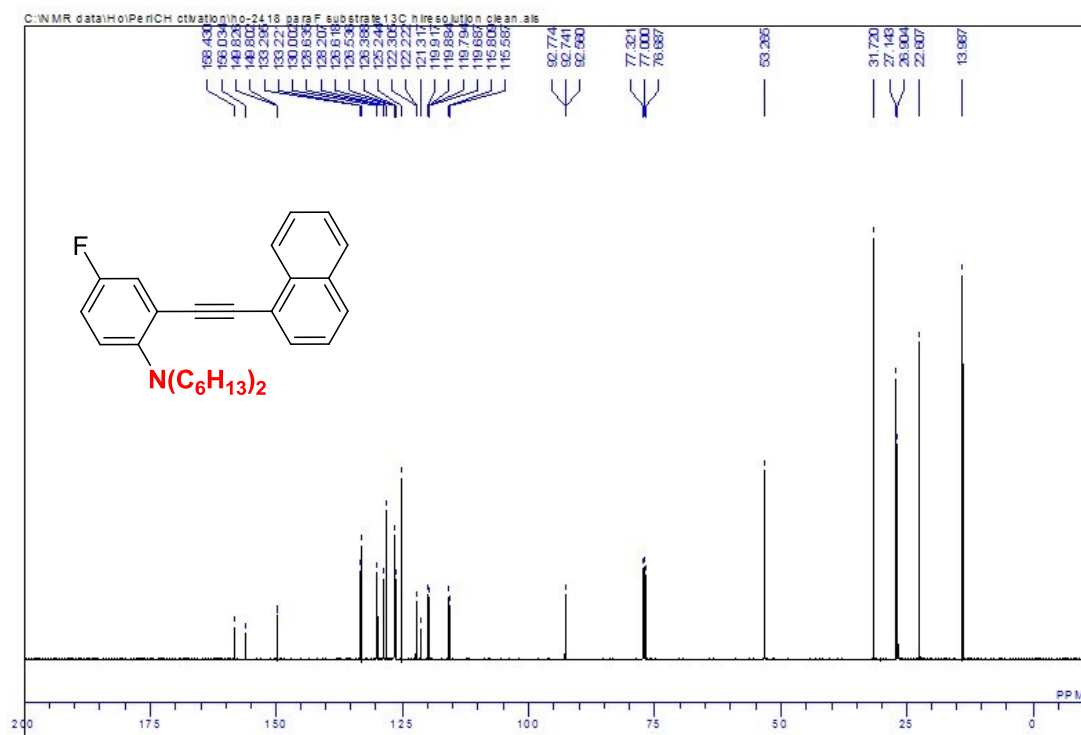
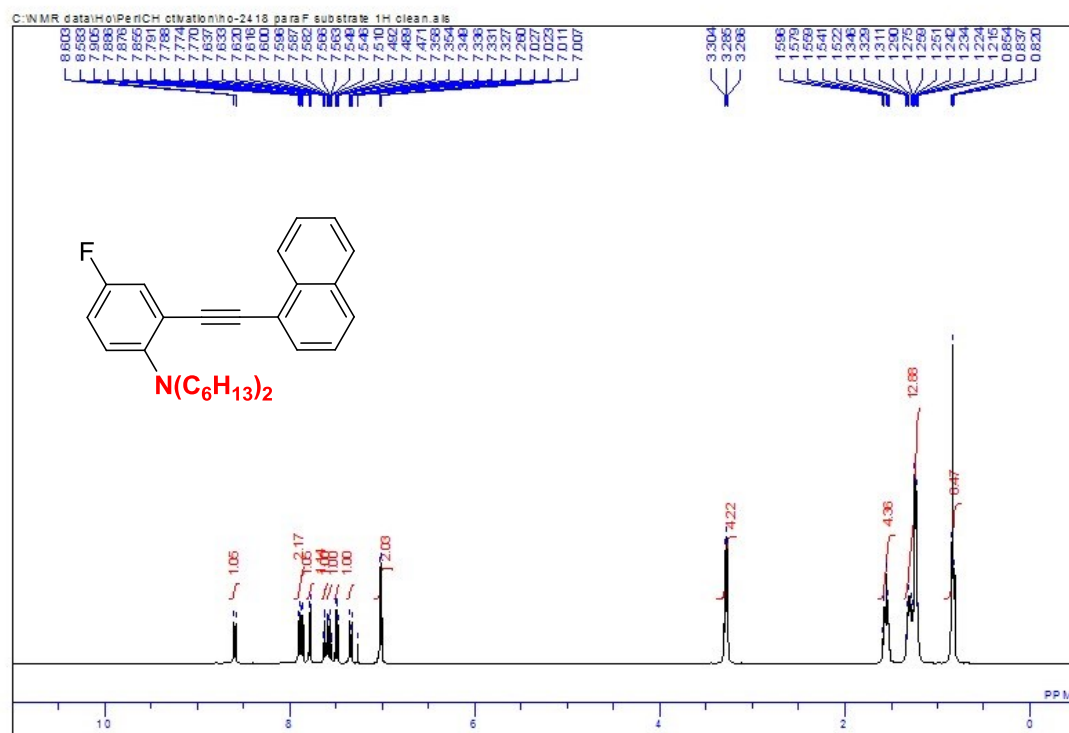


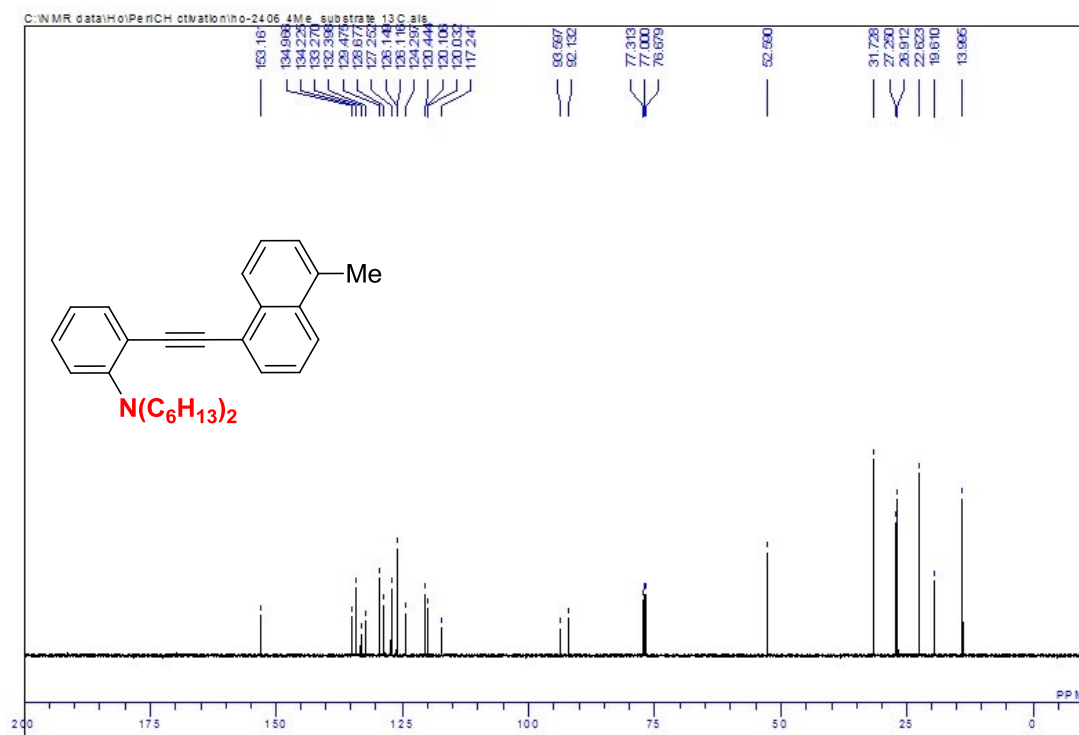
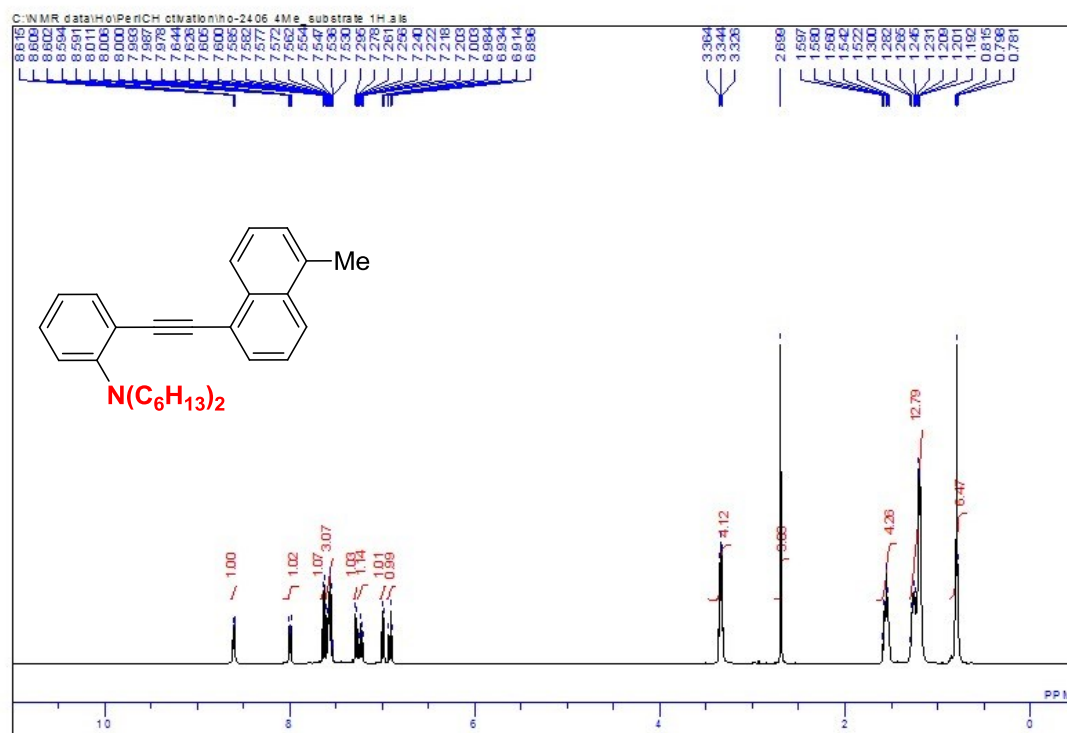


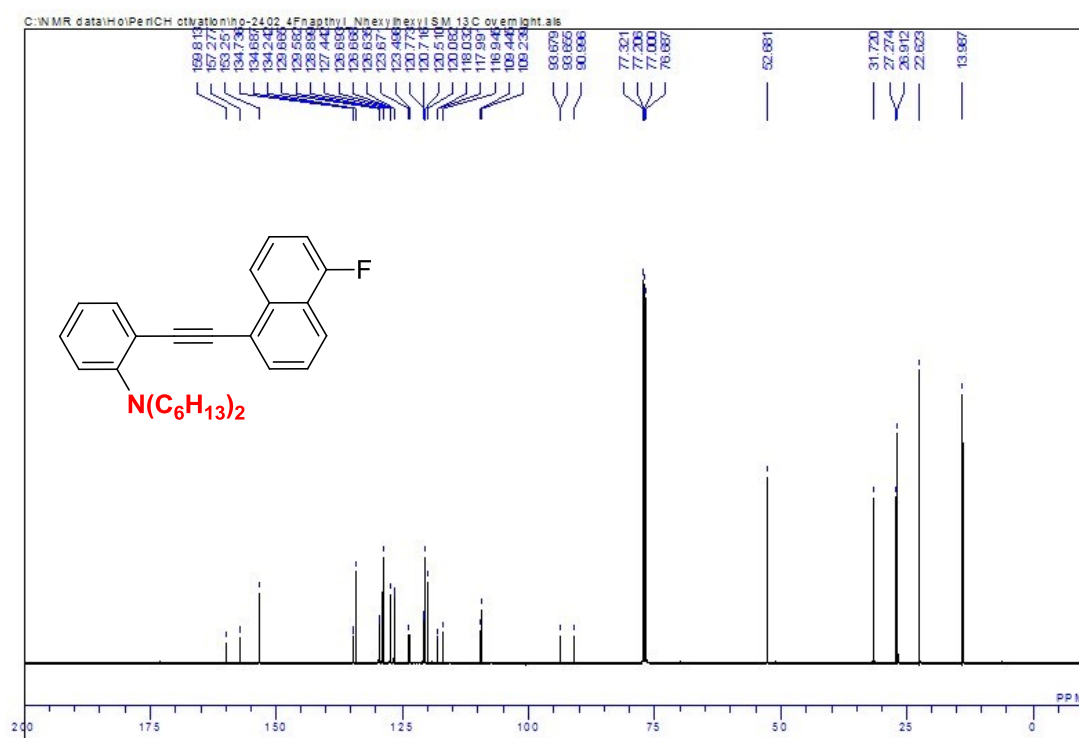
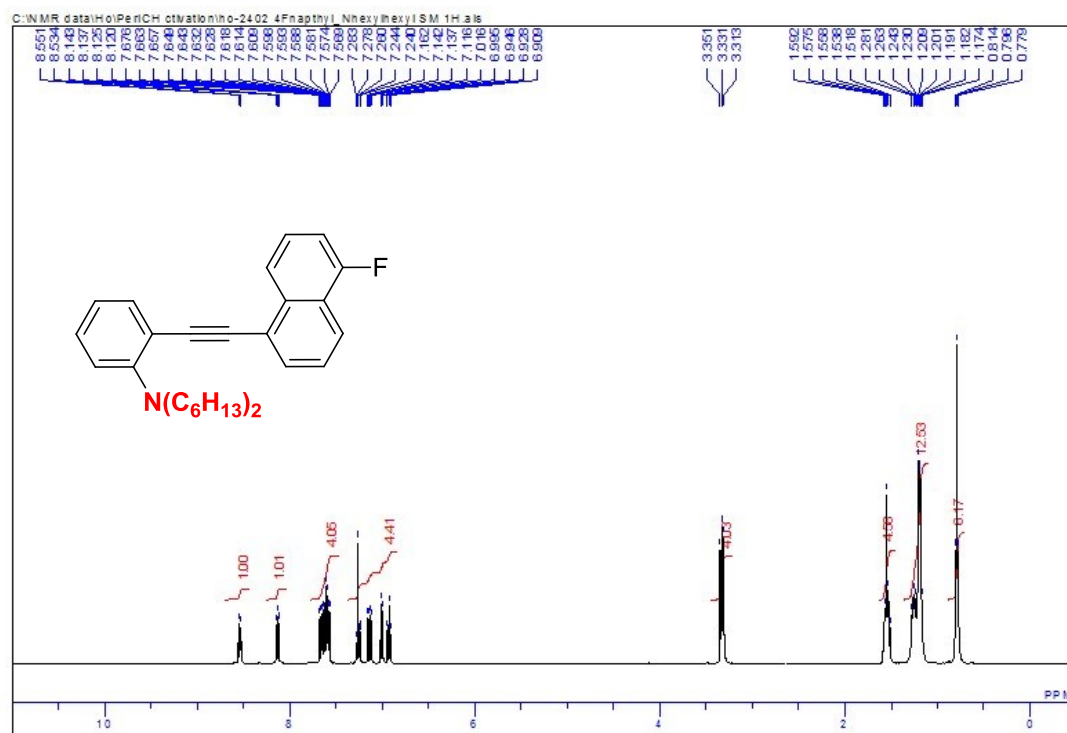


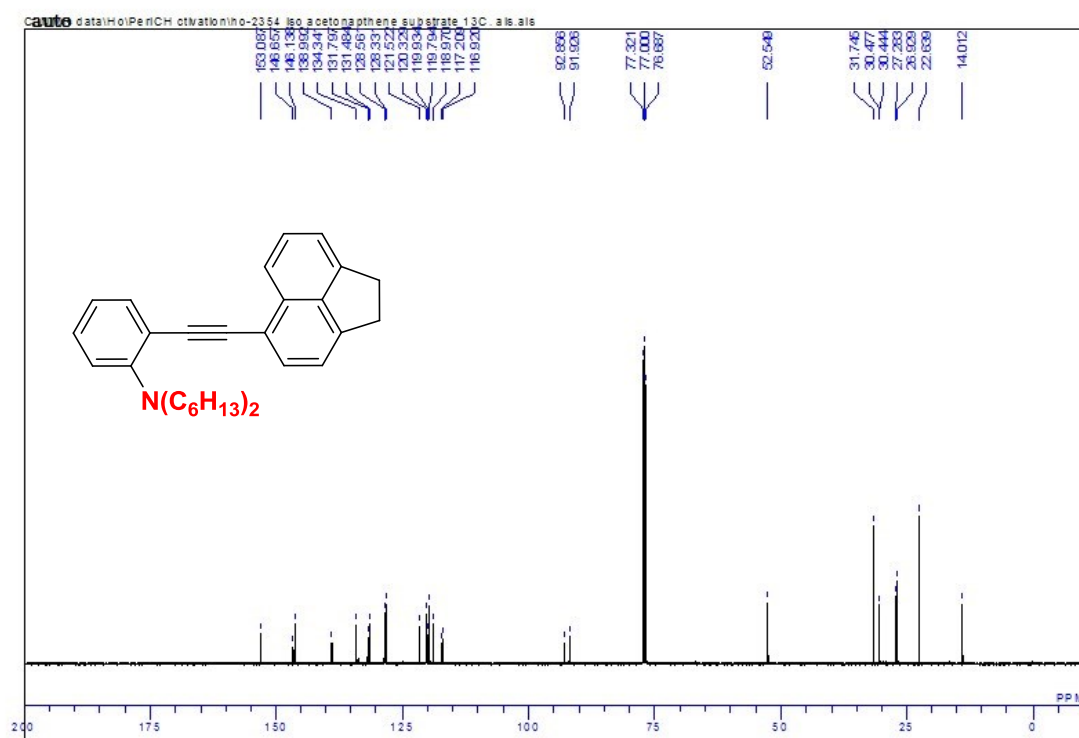
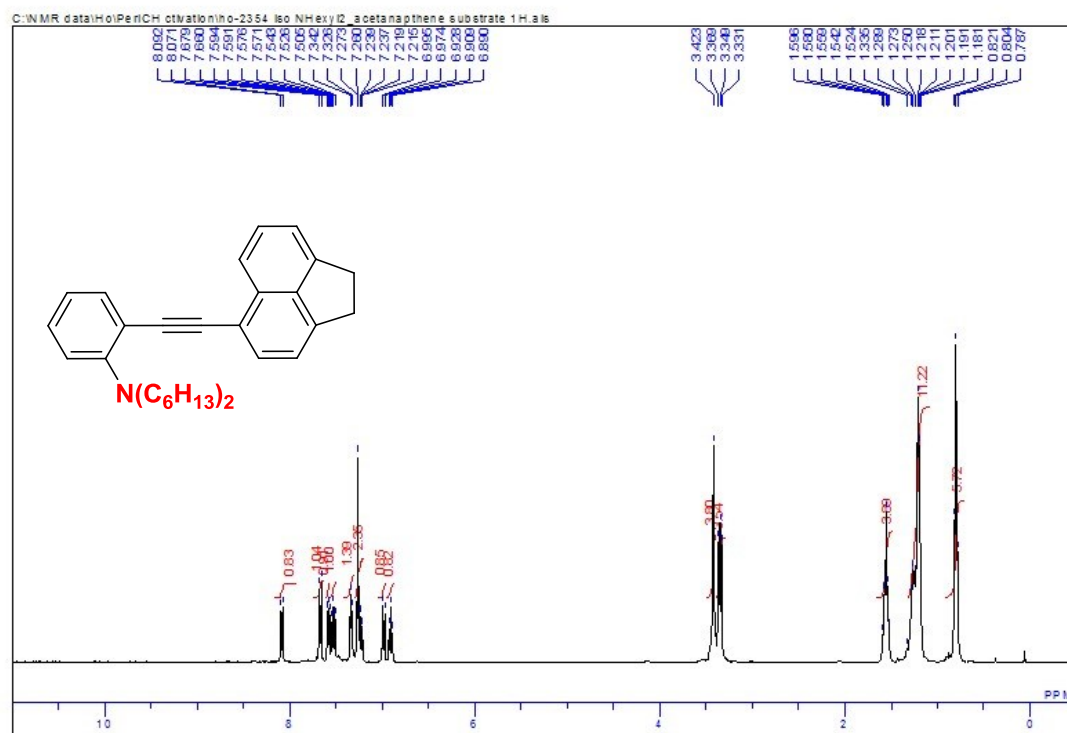


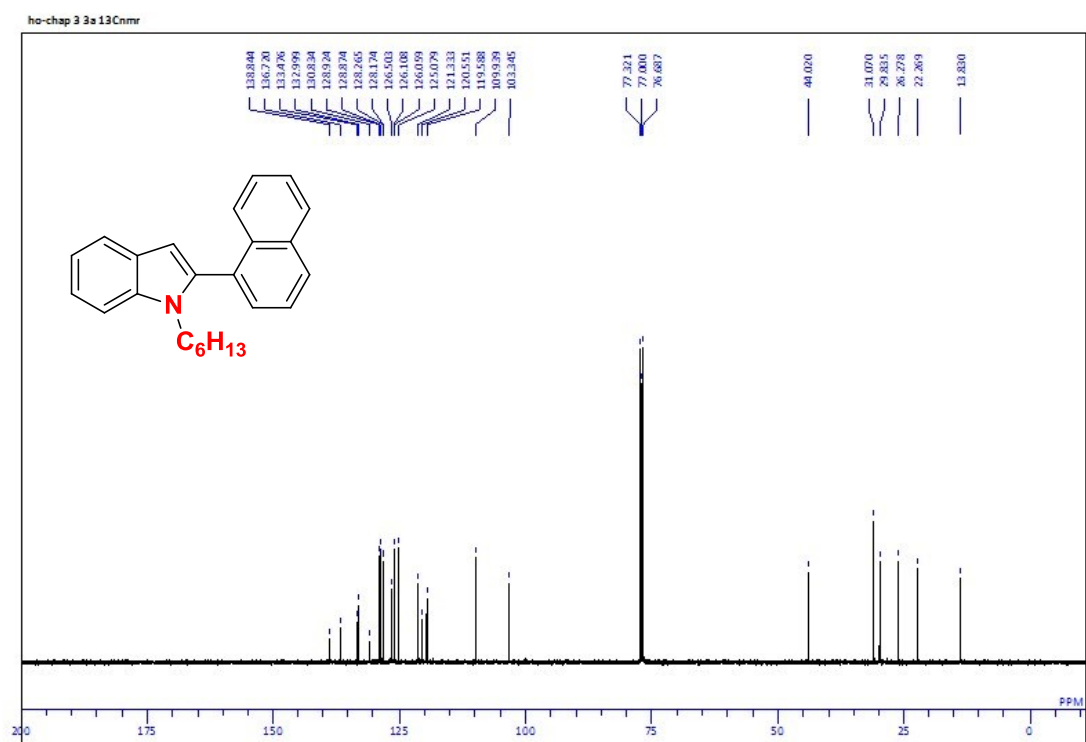
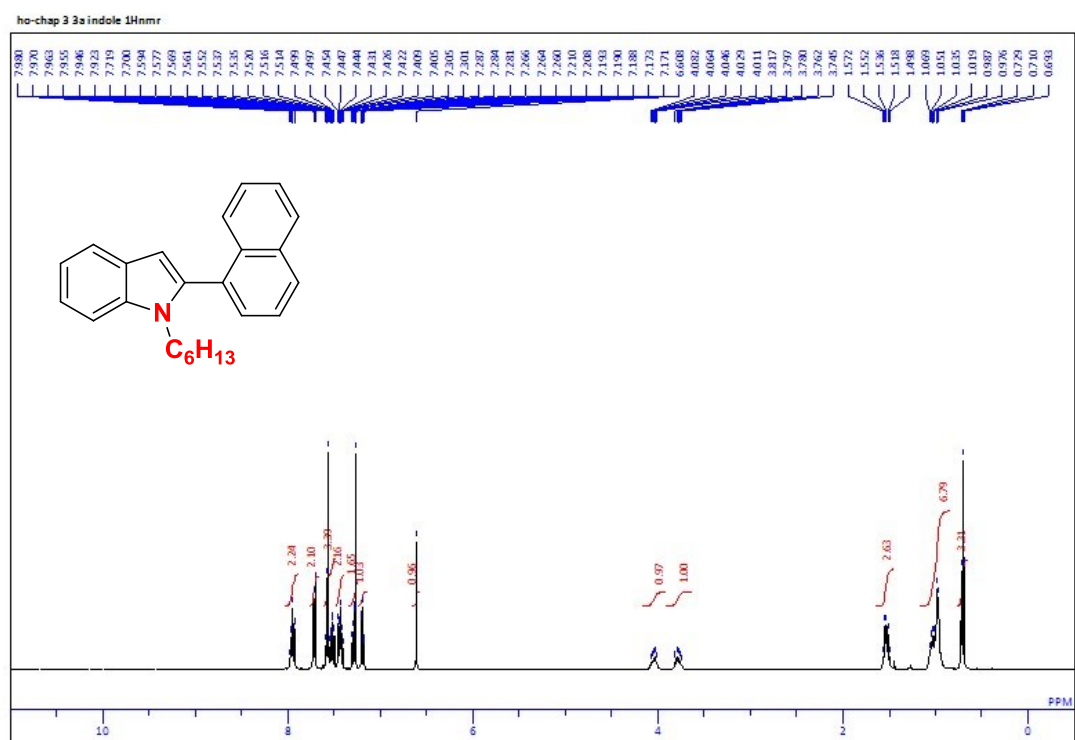










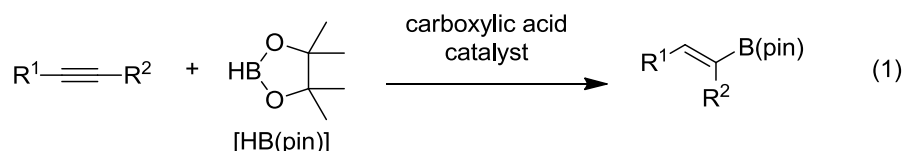


Chapter 4

Carboxylic Acid-Catalyzed Highly Efficient and Selective Hydroboration of Alkynes with Pinacolborane

1. Introduction

It is well-known that the C-B bond of organoboranes is cleaved through C-B bond protonolysis with carboxylic acids.¹ It has been for a long time that carboxylic acids are reagents for C-B bond cleavage. Quite surprisingly, I discovered that carboxylic acids can catalyze the hydroboration of alkynes with pinacolborane [HB(pin)], giving the alkenylboranes in good to high yields with exclusive regio- and stereoselectivities (eq 1).



The direct hydroboration of alkynes is one of the most powerful and straightforward methods to form the alkenylboronates, which are important synthetic intermediates in various useful transformations,^{2,3} such as Pd-catalyzed Suzuki-Miyaura cross-coupling to construct complex molecules for useful organic semiconductors and pharmaceuticals. During the last five decades, diverse alkyne–hydroboration reactions, including uncatalyzed,⁴ metal-catalyzed,^{2b,5} and base-catalyzed,⁶ have been developed using various hydroborating reagents. Among them, the hydroboration of alkynes with HB(pin) or bis(pinacolato)diboron [B₂(pin)₂] by using transition-metal-catalysts has been extensively studied in an effort to improve the efficiency and selectivity of the resulting alkenyl pinacolboronate esters, which are highly dependent on the catalyst species, ligands, base additives, and alkyne structures.⁵ The alkenyl pinacolboronate esters have been found to exhibit excellent thermal stability air- and water-insensitivity, which can be purified by aqueous workup and silica chromatography.^{2b}

The selective synthesis of 1,1-diborylalkenes is particularly attractive because they enable the construction of useful π -conjugated molecules through the Pd-catalyzed multiple carbon-carbon formation.⁷ In spite of their important synthetic utility, the direct hydroboration of alkynylboronates with organoborane to the corresponding 1,1-diborylalkenes has never been explored.⁸ This class of compounds has been prepared by Hiyama and co-workers using 1-halo-1-lithioalkenes and B₂(Pin)₂.⁹ The research groups of Marder and Iwasawa reported independently

the catalytic dehydrogenative borylation of alkenes with $B_2(Pin)_2$ using rhodium and Pd-pincer complexes.¹⁰ In this paper, we began our investigation by using alkynylboronates and HB(pin) to realize a new and direct hydroboration for synthesis of 1,1-diborylalkenes without using metal catalysts.

2. Results and discussion

Initially, a variety of organocatalysts have been screened in the hydroboration of 2-phenyl-1-ethynylboronic acid pinacol ester (**1a**) with HB(pin) (5 equiv) as a boron source in octane at 100 °C for 12 h. In the absence of catalysts, the reaction was sluggish without producing the desired 1,1-diborylalkene product **2a** (Table 1, entry 1). Surprisingly, the reaction proceeded smoothly in the presence of a catalytic amount of acetic acid to afford **2a** in high yield with an exclusive regioselectivity (entry 2). This unusual result led us to further examine various carboxylic acids and their analogues. Formic acid exhibits almost the same catalytic activity as acetic acid, while the sterically hindered pivalic acid and 2,2,2-triphenylacetic acid and rather strong acid such as trifluoroacetic acid decreased the yield of **2a** (entries 3-6). The use of triflic acid, one of the strongest Brønsted acids, resulted in decomposition of **1a** without yielding **2a** (entry 7). We were pleased to find that benzoic acid catalyzed the hydroboration reaction efficiently to give **2a** in almost quantitative yield (entry 8).

In order to figure out the relationship between chemical yield and acidity of carboxylic acid catalysts,¹¹ various benzoic acids bearing different functional groups have been studied. The use of benzoic acids having electron-withdrawing groups of nitro or acyl on the benzene ring resulted in substantially diminished yield of **2a** (entries 9 and 10). On the contrary, benzoic acids with an electron-donating group at the *para*-position of the benzene ring showed a remarkably high catalytic activity. For example, the use of 4-methyl-, 4-methoxy-, and 4-dimethylamino-substituted benzoic acids as catalysts, respectively, resulted in a quantitative yield of the corresponding product **2a** being obtained (entries 11-13). Among them, 4-(dimethylamino)benzoic acid having a strong electron-donating group exhibited the highest catalytic activity, furnishing **2a** within 8 h (entry 13). These results showed a clear trend that the chemical yield roughly depends on the acidity of carboxylic acids; weaker aromatic carboxylic acids give higher chemical yields (entries 8-13). It is worth noting that the totally different catalytic activity between 2-(dimethylamino)benzoic acid (0%) and (1,1'-biphenyl)-2-carboxylic acid (80%) indicates that the chelation of 2-dimethylamino group to boron may form a stable, inactive four-coordinate boron species bound to N and O atoms of benzoic acid (entries 14 and 15). It was noted that we did not observe any reduced compounds of carboxylic acids under the reaction conditions.

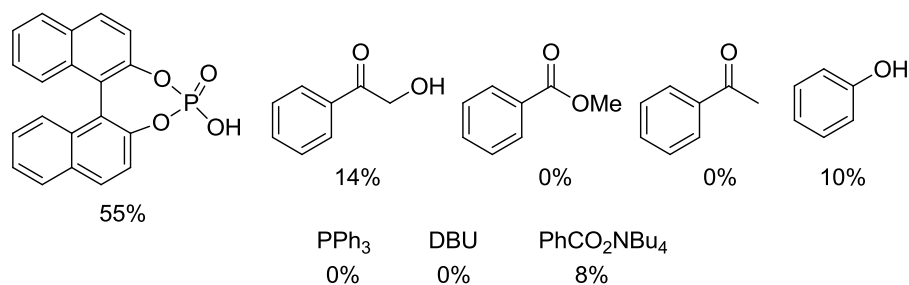
Table 1. Screening of Various Organocatalysts for Hydroboration of 2-Phenyl-1-ethynylboronic Acid Pinacol Ester (**1a**) with HB(pin)^a

$\text{Ph}-\text{C}\equiv\text{C}-\text{B}(\text{pin}) + \text{HB}(\text{pin}) \xrightarrow[\text{octane, 100 } ^\circ\text{C, 12 h}]{\text{Brønsted acid (5 mol \%)}} \text{Ph}-\text{CH}=\text{C}(\text{B}(\text{pin}))_2$

1a **2a**

entry	catalyst (pK _a) ^b	yield (%) ^c
1	none	0
2	AcOH (4.76)	94
3	HCO ₂ H (3.75)	85
4	PivOH (5.03)	79
5	(Ph) ₃ CCO ₂ H	79
6	CF ₃ CO ₂ H (0.52)	83
7	TfOH	0
8	PhCO ₂ H (4.20)	99 (94)
9	R = 4-NO ₂ (3.44)	72
10	R = 4-Ac	85
11	R = 4-Me (4.34)	99
12	R = 4-OMe (4.47)	99
13	R = 4-NMe ₂ (5.03)	99 (94) ^d
14	R = 2-NMe ₂ (8.42)	0
15	R = 2-C ₆ H ₅ (3.46)	80

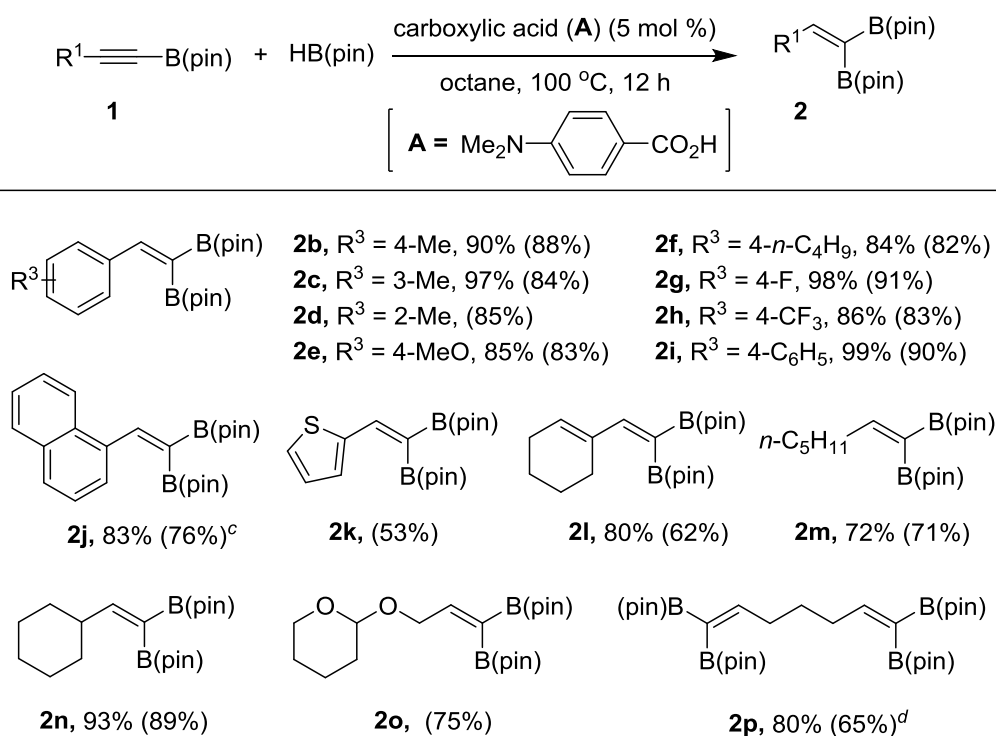
other organocatalysts:



^a Reaction conditions: **1a** (0.4 mmol), HB(pin) (2 mmol), catalyst (5 mol %), octane (1 M), 100 °C for 12 h under an argon atmosphere. ^b Thermodynamic pK_a values according to ref 11. ^c The ¹H NMR yield of **2a** determined using CH₂Br₂ as an internal standard. Isolated yields are shown in parentheses. ^d The reaction was carried out for 8 h.

Organic phosphoric acid also can be used as a Brønsted acid catalyst; the yield of **2a** (55%) is lower than that of carboxylic acids (Table 1). Other organocatalysts without a carboxylic acid group, such as 2-hydroxy-1-phenylethanone, methyl benzoate, acetophenone, phenol, and triphenylphosphine, were found to be ineffective in catalyzing the present hydroboration (Table 1). The results indicate that the carboxylic group is essentially crucial for catalytic hydroboration of alkynes with HB(pin). Additionally, the solvent examination revealed that the use of nonpolar solvents is preferred for obtaining high yields of **2a** and the polar solvents, such as dichloroethane, tetrahydrofuran, acetonitrile, ethyl acetate, and 1,4-dioxane afforded **2a** in low yields of 20-40% (Table S2, Supporting Information). Other hydroborating reagents, 9-BBN and HB(cat), are incompatible with the present reaction conditions, which resulted in a complex mixture of products. Finally, it should be noted that the use of lesser amounts of HB(pin) (3 equiv) resulted in a decreased yield of **2a** (75%) due to the consumption of HB(pin) by water under the present conditions leading to the formation of HOB(pin) and [(pin)B]₂O. Overall, the use of 4-(dimethylamino)benzoic acid as a catalyst in octane was chosen as the optimal conditions for regio- and stereoselective hydroboration of alkynes with HB(pin).

Scheme 1. Carboxylic Acid-Catalyzed Hydroboration of Various Alkynylboronates (1) with HB(pin)^{a,b}

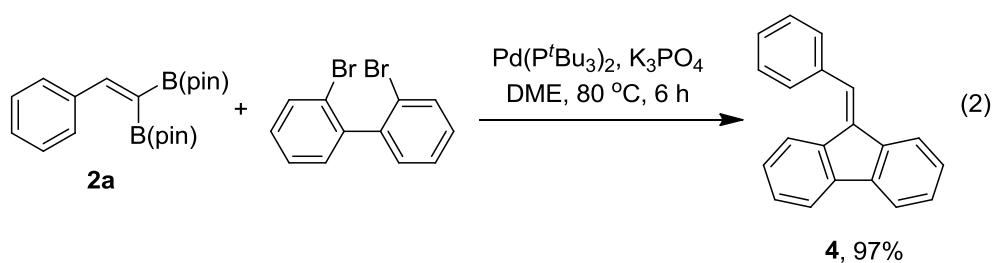


^a Reaction conditions: **1** (0.4 mmol), HB(pin) (2 mmol), 4-(dimethylamino)benzoic acid (5 mol %), octane (1 M, 0.4 mL), Ar atmosphere, 100 °C, 12 h. ^b ¹H NMR yield determined using CH₂Br₂ as an internal standard. Isolated yields are shown in parentheses. ^c The reaction temperature for **2j** is 120 °C and reaction time is 8 h. ^d The reaction for forming **2p** carried out at 120 °C for 12 h using 10 equiv of HB(pin).

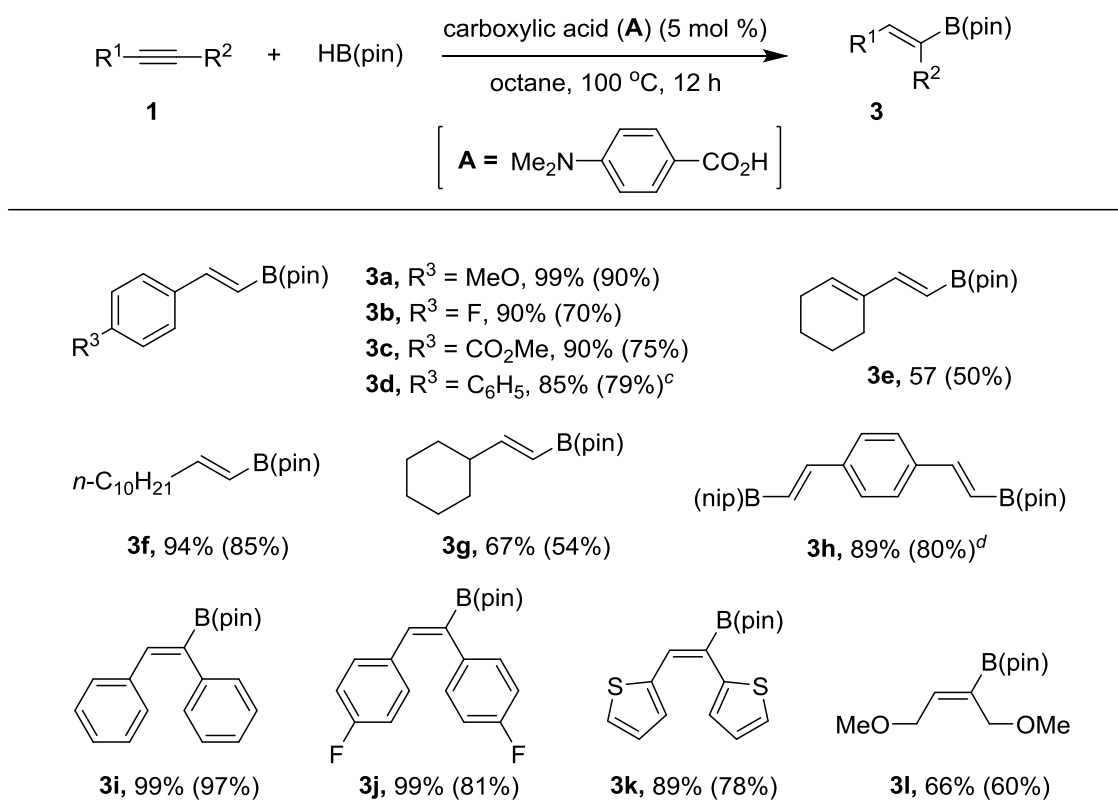
To explore the generality and scope of this method, various alkynylboronates were examined under the optimized conditions. All products were isolated using Kugelrohr distillation to remove low boiling-point compounds, followed by a short silica gel column chromatography. It should be mentioned that the hydroboration of every alkyne employed in the present work almost did not proceed in the absence of catalysts. As shown in Scheme 1, a wide range of functional group tolerance and an exclusive regioselectivity were observed. The reactions of 2-(tolyl)ethynylboronates having an electron-donating methyl group at the phenyl ring proceeded efficiently to afford the corresponding 1,1-diborylalkenes **2b-d** in high yields regardless of the position of methyl substituent. The reactions of arylalkynes bearing electron-donating and electron-withdrawing groups at the phenyl ring did not exhibit a large difference to the reaction outcome. For example, arylalkynylboronates having methoxyl, *n*-butyl, fluorine, and trifluoromethyl groups at R¹ produced the desired products **2e-h** in good to high yields.

Alkynylboronates having biphenyl and naphthyl groups at the alkynyl terminus also worked uneventfully to afford **2i** and **2j** in high yields. 2-Thienyl alkynylboronate suffered from decomposition of the starting material together with a small amount of the semihydrogenated alkenylboronate, which lowered the yield of **2k** to 53%. The cyclohexenyl-substituted conjugated enynylboronate was also compatible with the acid-catalyzed conditions, in which the trisubstituted alkene moiety remained intact (**2l**). Likewise, the aliphatic alkynylboronates substituted with *n*-pentyl and cyclohexyl groups, and tetrahydropyran-protected propargyl alcohol were also good substrates to give the corresponding products **2m-o** in good to high isolated yields. The double hydroboration also took place when 1,6-diynylboronate was used as a substrate to give the corresponding tetraboryl diene **2p** in a 65% isolated yield. Other alkynylboronate such as 5,5-dimethyl-2-(phenylethynyl)-1,3,2-dioxaborinane failed to give the corresponding diboryl alkene, resulting in decomposition of the starting material due to its low stability under the standard conditions (Scheme S1, Supporting Information).

The resulting 1,1-diborylalkenes are synthetically useful substrates for further functionalization by Suzuki-Miyaura coupling. Thus, following the method developed by Shimizu and Hiyama et al.,⁷ 1,1-diborylalkene **2a** was treated with 2,2'-dibromo-1,1'-biphenyl in the presence of Pd catalyst, which gave the corresponding product 9-benzylidene-9*H*-fluorene **4** in 97% yield through the double cross-coupling annulation (eq. 2).



Scheme 2. Carboxylic Acid-Catalyzed Common Alkynes with HB(pin)^{a,b}



^a Reaction conditions: **1** (0.4 mmol), $HB(pin)$ (3 equiv), octane (0.4 mL), 4-(dimethylamino)benzoic acid (5 mol %), 100 °C, 12 h, Ar atmosphere. ^b ¹H NMR yield was determined using CH_2Br_2 as an internal standard. Isolated yields are shown in parentheses. ^c The reaction time for **3d** is 6 h. ^d $HB(pin)$ (5 equiv) was used for the formation of **3h**.

This method was further extended to the hydroboration of common alkynes (Scheme 2). To my delight, both terminal and internal alkynes were well tolerated to give monoboryl alkenes in good to high yields. Remarkably, this hydroboration proceeded through a perfect *anti*-Markovnikov and exclusive *syn*-addition of $HB(pin)$ to alkynes. The reaction with terminal arylalkynes having electron-donating and electron-withdrawing groups, such as methoxy, fluorine, and ester groups at the phenyl ring produced the desired *E*-isomers **3a-c** exclusively, in which the methoxy-substituted electron-rich alkyne exhibited a better reactivity, giving **3a** in a 90% isolated yield. Biphenyl terminal alkyne is also a rather reactive substrate, giving a high yield of alkenylboronate **3d** within 6 h. The reaction of the conjugated 1-ethynylcyclohex-1-ene exhibited an exclusive chemoselectivity to the C-C triple bond, affording the corresponding diene **3e** in moderate yield. The hydroboration with aliphatic terminal alkynes also proceeded smoothly, converting dodec-1-yne and ethynylcyclohexane to the corresponding alkenylboronates **3f** and **3g** in good to high

yields. Terminal diyne such as 1,4-diethynylbenzene underwent double hydroboration to give the corresponding diboronate **3h** in a 80% isolated yield. The hydroboration of symmetric internal alkynes also took place uneventfully. 1,2-Diphenylethyne, 1,2-bis(4-fluorophenyl)ethyne, 1,2-di(thiophen-2-yl)ethyne, and 1,4-dimethoxybut-2-yne were selectively hydroborated under the standard conditions to give the corresponding *Z*-isomers **3i-l** in good to excellent yields.

In an early paper, Brown and co-workers reported that the reaction of propionic acid with sodium borohydride could produce hydrogen gas and $[\text{EtCO}_2\text{BH}_3]^- \text{Na}^+$ which is an effective hydroborating reagent.¹² Ganem et al. proposed that the catecholboronate ester should be a key intermediate for the reaction of carboxylic acids with amines to form amides in the presence of catecholborane, which has been demonstrated by the infrared absorption.¹³ Most recently, Antilla and co-workers reported that organic phosphoric acid reacted with HB(cat) to generate hydrogen gas and phosphoryl catechol boronate, and the latter species was an effective hydroborating reagent for reduction of ketones.¹⁴ Although it is not yet clear at the present time how carboxylic acids catalyze the hydroboration reaction of pinacolborane toward alkynes, the present finding provides a synthetically useful procedure of hydroboration..

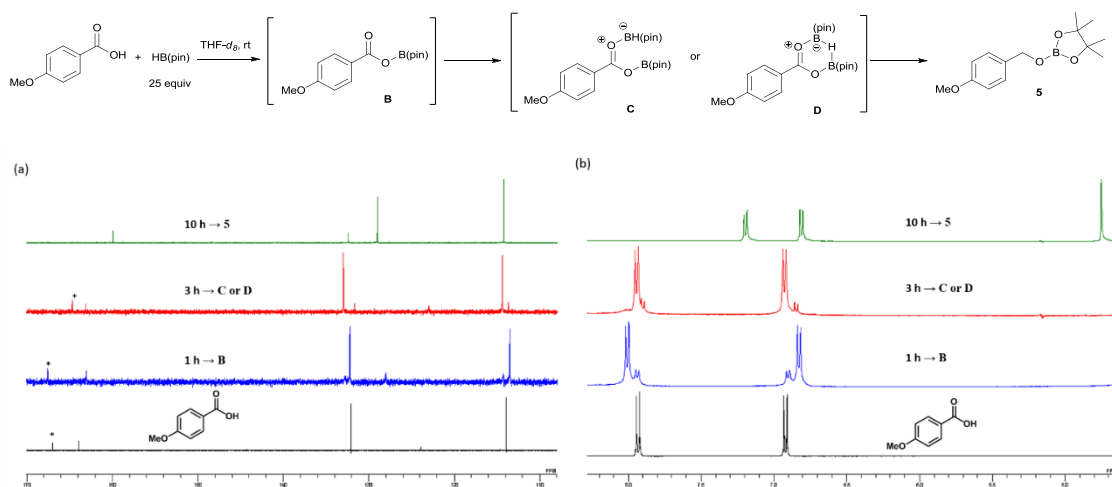


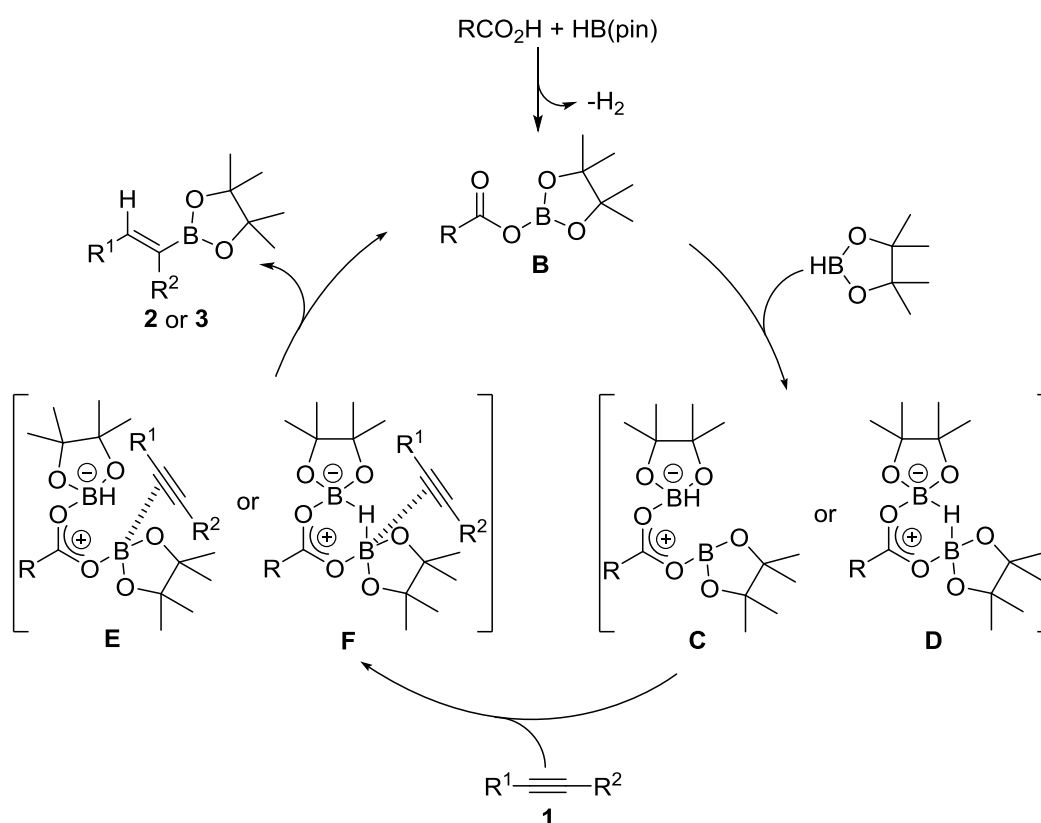
Fig. 1 Time-dependent NMR studies of the reaction between anisic acid and HB(pin) at rt, in THF-d₈. (a) ¹³C NMR spectra and (b) ¹H NMR spectra.

In terms of the reported literatures, NMR experiments were carried out in order to examine the new catalyst species in the present hydroboration process. A THF-d₈ solution of anisic acid was placed in a NMR tube under Ar in the glove-box, and was treated with excess amounts of HB(pin) (25 equiv) at rt. It was noted that the use of a 1:5 mixture of anisic acid and HB(pin) gave a very poor conversion. The gas evolution was observed at the beginning of the reaction, which we

assumed to be hydrogen gas. After 30 min, the ^{13}C NMR spectrum showed that the C=O (166.97 ppm) signal of anisic acid almost disappeared and a new C=O signal was observed at 167.55 ppm (Fig. 1a). Correspondingly, the slightly shifted aromatic C-H signals were appeared in the ^1H NMR spectrum compared to the anisic acid (Fig. 1b). The ^{11}B NMR spectrum (^1H -coupled) showed a new broad singlet at 24.62 ppm compared with the chemical shifts of HB(pin), [(pin)B] $_2$ O, and HOB(pin) (Fig. S1, ESI). These distinct observations supported the formation of a new boronate ester species which we considered to be 4-methoxyphenyl-CO $_2$ B(pin) (**B**) derived through the reaction between anisic acid and HB(pin). Interestingly, after 3 h at rt, a new chemical shift change of the C=O signal was observed at 164.69 ppm in the ^{13}C NMR spectrum along with the apparent changes of aromatic C-H signals in the ^1H NMR spectrum (Fig. 1). In the ^{11}B NMR spectrum, the new peak at 24.62 ppm increased in intensity compared to the boron species **B** (Fig. S1, Supporting Information). These NMR evidences suggested the formation of a second boronate ester species upon prolonged reaction time, which we tentatively assigned to the diboryl ester species **C** or **D** formed from the reaction between the intermediate **B** and HB(pin). It should be mentioned that after overnight, the new intermediate **C** or **D** was further reduced to give the product 4-methoxybenzyl-OB(pin) (**5**) cleanly which did not show any catalytic activity in the reaction of alkyne with HB(pin) under the standard conditions. We also carried out the NMR studies for the reaction of anisic acid, HB(pin), and 4-ethynylanisole. The formation of the intermediate **C** (or **D**) was confirmed after 1 h in the reaction of anisic acid with HB(pin) in THF- d_8 and octane- d_{18} (1:1). Subsequently, 4-ethynylanisole was added to the reaction mixture. The ^{13}C NMR showed a new terminal alkynyl carbon signal with a chemical shift of 76.79 ppm which is obviously shifted in comparison with the chemical shifts of 4-ethynylanisole (76.46 ppm), a mixture of anisic acid and 4-ethynylanisole (76.54 ppm), and a mixture of HB(pin) and 4-ethynylanisole (76.59 ppm) (Fig. S2, Supporting Information). This evidence suggested an interaction between alkyne and the intermediate **C** (or **D**). Finally, it should be noted that the intermediates **B** and **C** (or **D**) are air sensitive and unstable in the absence of solvents and we failed to isolate these intermediates.

Although different possible mechanisms should be considered, on the basis of the experimental observations, the proposed mechanism illustrated in Scheme 3 seems reasonable. Initially, the carboxylic acid catalyst would react with HB(pin) to form RCO $_2$ B(pin) (**B**) along with the evolution of H $_2$. In terms of the NMR results, we assume that the carbonyl group in the intermediate **B** may further react with HB(pin) to generate an electron-deficient oxocarbenium ion **C** which may also exist as the three-center two-electron bonded species **D**. The enhanced electrophilicity of boron in species **C** or **D** may accelerate the interaction between alkyne and boron to form the boron-alkyne π -complex **E** or **F**.¹⁵ The π -complex **E** (or **F**) may direct the

selective *syn*-addition of HB(pin) to alkynes, resulting in the corresponding hydroboration products **2** and **3** with a high stereoselectivity together with the regeneration of the intermediate **B**. It is noted that the analogues of the reduction product **5** did not observed in the presence of alkynes, that we ascribed to the readily formation of the π -complex **E** (or **F**) in preference to the reduction.



Scheme 3. Proposed reaction mechanism.

3. Conclusion

In conclusion, for the first time that the carboxylic acids catalyze the hydroboration of alkynes with HB(pin) has been demonstrated. The hydroboration takes place with various terminal and internal alkynes having a wide range of functional groups without using any metal catalysts and additives, affording the synthetically important alkenyl diboronates and monoboronates in good to high yields with exclusive regio- and stereoselectivities. This method not only provides an efficient and general approach for formation of alkenylboronates, it also may open a new avenue for hydroboration of versatile unsaturated C-C multiple bonds using organocatalysts.

4. References and notes

1. a) Brown, H. C.; Murray, K. *J. Am. Chem. Soc.* **1959**, *81*, 4108. b) Brown, H. C.; Zweifel, G. *J. Am. Chem. Soc.* **1961**, *83*, 3834. c) Zweifel, G.; Arzoumanian, H. *J. Am. Chem. Soc.* **1967**, *89*, 5086. d) Brown, H. C.; Gupta, S. K. *J. Am. Chem. Soc.* **1972**, *94*, 4370.
2. a) Brown, H. C. *Pure Appl. Chem.* **1976**, *47*, 49. b) Beletskaya, I.; Pelter, A. *Tetrahedron* **1997**, *53*, 4957.
3. a) Pelter, A.; Smith, K.; Brown, H. C. *Borane Reagents*; Academic Press: London, **1988**. (b) Matteson, D. S. *Stereodirected Synthesis with Organoboranes*; Springer: Berlin, **1995**. (c) Hall, D. G., Ed. *Boronic Acids. Preparation, Applications in Organic Synthesis and Medicine*; Wiley-VCH: Weinheim, **2005**. (d) Miyaura, N.; Suzuki, A. *Chem. Rev.* **1995**, *95*, 2457. e) Hayashi, T.; Yamasaki, K. *Chem. Rev.* **2003**, *103*, 2829. f) Crudden, C. M.; Glasspoole, B. W.; Lata, C. J. *Chem. Commun.* **2009**, 6704.
4. a) Brown, H. C.; Gupta, S. K. *J. Am. Chem. Soc.* **1972**, *94*, 4370. b) Lane, C. F.; Kabalka, G. W. *Tetrahedron* **1976**, *32*, 981. (c) Tucker, C. E.; Davidson, J.; Knochel, P. *J. Org. Chem.* **1992**, *57*, 3482.
5. For selected transition-metal-catalyzed hydroboration of alkynes with pinacolborane, see: a) Ohmura, T.; Yamamoto, Y.; Miyaura, N. *J. Am. Chem. Soc.* **2000**, *122*, 4990. b) Pereira, S.; Srebnik, M. *Organometallics* **1995**, *14*, 3127. c) Pereira, S.; Srebnik, M. *Tetrahedron Lett.* **1996**, *37*, 3283. d) Lee, T.; Baik, C.; Jung, I.; Song, K. H.; Kim, S.; Kim, D.; Kang, S. O.; Ko, J. *Organometallics* **2004**, *23*, 4569. e) Xue, C.; Kung, S.-H.; Wu, J.-Z.; Luo, F.-T. *Tetrahedron* **2008**, *64*, 248. f) Gunanathan, C.; Hölscher, M.; Pan, F.; Leitner, W. *J. Am. Chem. Soc.* **2012**, *134*, 14349. g) Sundararaju, B.; Fürstner, A. *Angew. Chem., Int. Ed.* **2013**, *52*, 14050. h) Semba, K.; Fujihara, T.; Terao, J.; Tsuji, Y. *Chem.—Eur. J.* **2012**, *18*, 4179. i) Haberberger, M.; Enthaler, S. *Chem.—Asian J.* **2013**, *8*, 50. j) Kim, H. R.; Yun, J. *Chem. Commun.* **2011**, 47, 2943.
6. Wen, K.; Chen, J.; Gao, F.; Bhadury, P. S.; Fan, E.; Sun, Z. *Org. Biomol. Chem.* **2013**, *11*, 6350.
7. a) Shimizu, M.; Nakamaki, C.; Shimono, K.; Schelper, M.; Kurahashi, T.; Hiyama, T. *J. Am. Chem. Soc.* **2005**, *127*, 12506. b) Shimizu, M.; Nagao, I.; Kiyomoto, S.-i.; Hiyama, T. *Aust. J. Chem.* **2012**, *65*, 1277.
8. Takaya, J.; Iwasawa, N. *ACS Catal.* **2012**, *2*, 1993.
9. Hata, T.; Kitagawa, H.; Masai, H.; Kurahashi, T.; Shimizu, M.; Hiyama, T. *Angew. Chem., Int. Ed.* **2001**, *40*, 790.
10. a) Coapes, R. B.; Souza, F. E. S.; Thomas, R. L.; Hall, J. J.; Marder, T. B. *Chem. Commun.* **2003**, 614. b) Takaya, J.; Kirai, N.; Iwasawa, N. *J. Am. Chem. Soc.* **2011**, *133*, 12980.

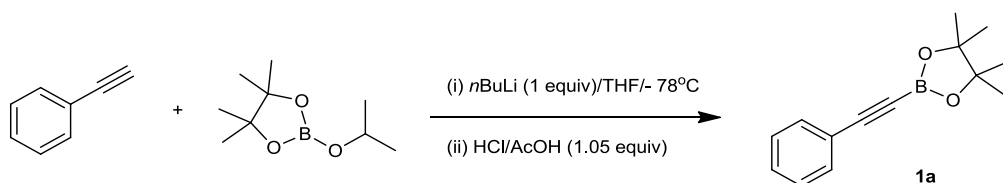
11. For pK_a values, see: a) Brown, H. C.; McDaniel, D. H.; Häfliger, O. *Determination of Organic Structures by Physical Methods*; Braude, E. A., Nachod, F. C., Eds.; Academic Press: New York, 1955; pp 567—662. b) Dippy, J. F. J.; Hughes, S. R. C.; Rozanski, A. *J. Chem. Soc.* **1959**, 2492.
12. Brown, H. C.; Subba Rao, B. C. *J. Am. Chem. Soc.* **1960**, 82, 681.
13. Collum, D. B.; Chen, S. C.; Ganem, B. *J. Org. Chem.* **1978**, 43, 4393.
14. Zhang, Z.; Jain, P.; Antilla, J. C. *Angew. Chem., Int. Ed.* **2011**, 50, 10961.
15. Jones, P. R. *J. Org. Chem.*, 1972, **37**, 1886.

5. Experimental Section

General Information. GC-MS analysis was performed on an Agilent 6890N GC interfaced to an Agilent 5973 mass-selective detector (30 m x 0.25 mm capillary column, HP-5MS). ^1H NMR and ^{13}C NMR spectra were recorded on JEOL JNM AL 400 (400 MHz) spectrometer. ^1H NMR spectra are reported as follows: chemical shift in ppm (δ) relative to the chemical shift of CDCl_3 at 7.26 ppm, integration, multiplicities (s = singlet, d = doublet, t = triplet, q = quartet, dt = doublet of triplets, m = multiplet, and br = broadened), and coupling constants (Hz). ^{13}C NMR spectra were recorded on JEOL JNM AL 400 (100.5 MHz) spectrometers with complete proton decoupling, and chemical shift reported in ppm (δ) relative to the central line of triplet for CDCl_3 at 77 ppm. ^{11}B NMR spectra were recorded on JEOL JNM AL 700 (225MHz) spectrometers. High-resolution mass spectra were obtained on a Bruker Daltonics Solarix 9.4T spectrometer and JEOL JMS-T100GCV. Column chromatography was carried out employing silica gel 60 N (spherical, neutral, 40~63 μm , Merck Chemicals). Analytical thin-layer chromatography (TLC) was performed on 0.2 mm precoated plate Kieselgel 60 F254 (Merck). Kugelrohr distillation was performed under vacuum by using Sibata Glass Tube Oven (GTO-250RS).

Materials. Pinacolborane (4,4,5,5-tetramethyl-1,3,2-dioxaborolane) (Aldrich), carboxylic acids (Tokyo Chemical Industry), alkynes were purchased and used as received. The structures of new compounds are determined by using ^1H , ^{13}C , ^{11}B NMR, and HRMS. The corresponding products, **2a**, **2e**, **3i**, and **3k** of the internal alkynes were determined unambiguously by the reported authentic compounds and the references are shown. Alkynes **1** were prepared following the reported literature from the terminal alkynes precursors.² Internal alkynes **3i** and **3l** were prepared by Sonogashira coupling reaction.

General procedure for synthesis of 1-alkynyldioxaborolanes, **1**

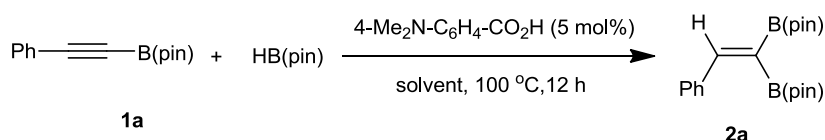


Synthesis of 4,4,5,5-tetramethyl-2-(phenylethynyl)-1,3,2-dioxaborolane (1a**).** To a solution of phenylacetylene (0.62 mL, 6 mmol) in THF (0.4 M, 15 mL) in a 50 mL of Schlenk tube -78 °C under an Ar atmosphere was added $n\text{-BuLi}$ (3.75 mL, 1.6 M hexane solution, 6 mmol). The reaction mixture was stirred for 1 h at -78 °C. A THF solution (0.4 M, 13 mL) of 4,4,5,5-

² Brown, H. C.; Bhat, N. G.; Srebnik, M.; *Tetrahedron Lett.* **1998**, 29, 2631.

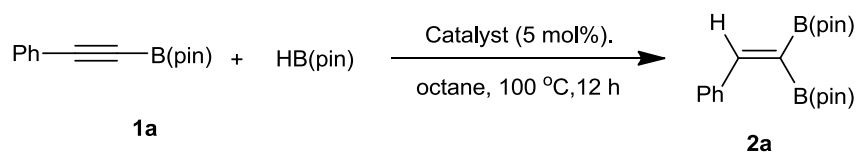
tetramethyl-2-(1-methylethoxy)-1,3,2-dioxaborolane [(*i*-PrO)B(pin), 5 mmol] was added to the lithiated reaction mixture at -78 °C. After being stirred for 2 h at -78 °C, the reaction mixture was quenched with 1.0 M HCl/Et₂O solution (5.25 mL, 5.25 mmol), and the mixture was warmed to room temperature with additional 1 h stirring. Filtration and evaporation afforded pale yellow oil. Bulb to bulb distillation gave **1a** in 98% yield (1.12 g) as a white solid.

Representative procedure for carboxylic acid-catalyzed hydroboration of alkynes

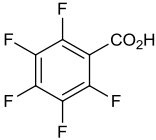
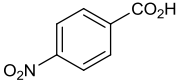
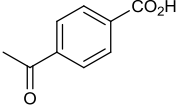
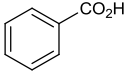
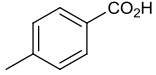
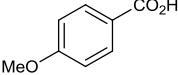
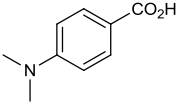
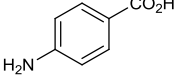
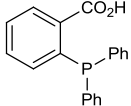
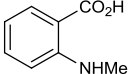
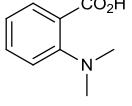
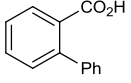


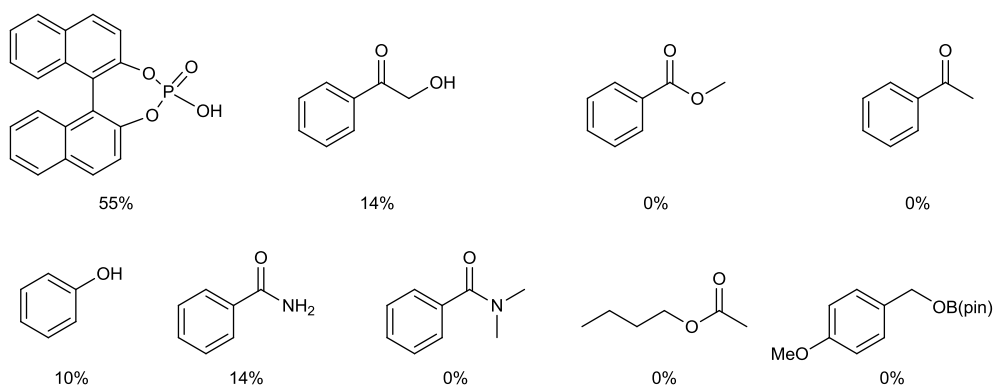
To an octane solution (0.4 mL, 1 M) were added 4,4,5,5-tetramethyl-2-(phenylethynyl)-1,3,2-dioxaborolane (**1a**, 91.2 mg, 0.4 mmol), and 4-(dimethylamino)benzoic acid (3.3 mg, 5 mol%), and pinacol borane (0.29 mL, 2.0 mmol) under an Ar atmosphere. The reaction was stirred at 100 °C for 12 h. After cooling to room temperature, the reaction mixture was concentrated under vacuum. The low-boiling point impurities were removed by Kugelrohr distillation and the residue was further purified by passing through a short silica column chromatography using hexane/ethyl acetate (10/1) as eluents to afford **2a** in 94% (134 mg) as pale yellow oil.

Table S1. Optimization of various organocatalysts^a



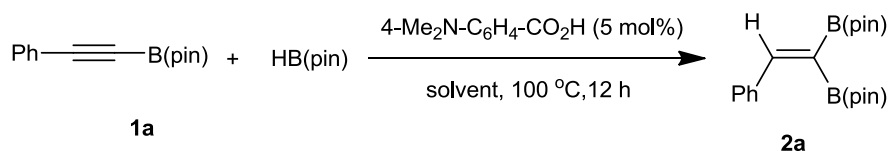
entry	catalyst (5 mol%)	yield of 2a (%) ^b
1	HCOOH	85
2	AcOH	94
3	CF ₃ COOH	83
4	Pivalic acid	79
5	Adamantane carboxylic acid	72
6	(Ph) ₃ CCO ₂ H	79
7	PhCO ₂ H	99 (94)
8	TfOH	0
9	H ₃ PO ₄	50
10	PPh ₃	0
11	NaOtBu	0
12	-	0

 48%	 72%	 85%	 99%
 99%	 99%	 99 (94), ^c 72 ^d	 82%
 33%	 0%	 0%	 80%



^a Reaction condition: **1a** (0.4 mmol), HB(pin) (2 mmol), octane (1 M), 100 °C, 12 h. ^b Yield determined by using CH₂Br₂ as internal standard. Isolated yield is shown in parenthesis. ^c 8 h. ^d 3 mol% of catalyst loading.

Table S2. Screening of solvent.^a



entry	solvent	yield of 2a (%) ^b
1	octane	99 (94)
2	decane	85
3	cyclooctane	80
4	toluene	37
5	1,4-dioxane	38
6	DCE	33
7	ethyl acetate	40
8	acetonitrile	20
9	THF	40

^a Reaction condition: **1a** (0.4 mmol), HBPin (5 equiv), 4-(dimethylamino)benzoic acid (5 mol %), solvent (1 M), 100 °C, 12 h. ^b Yield determined by using CH₂Br₂ as internal standard. Isolated yield is shown in parenthesis.

Scheme S1. Reaction of 5,5-dimethyl-2-(phenylethynyl)-1,3,2-dioxaborinane with HB(pin) under the standard conditions.

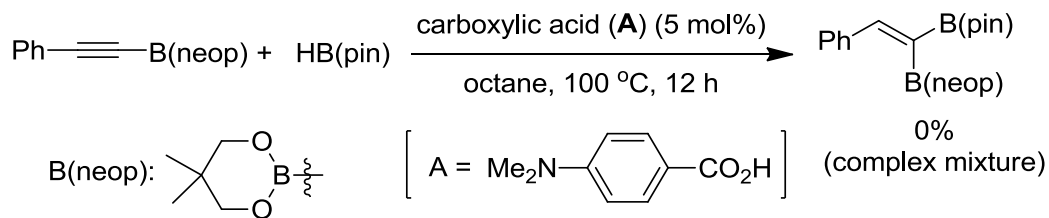


Figure S1. Time-dependent ^{11}B NMR study of the reaction between anisic acid and HB(pin) at rt in THF- d_8 (a) and comparison with related boron compounds (b).

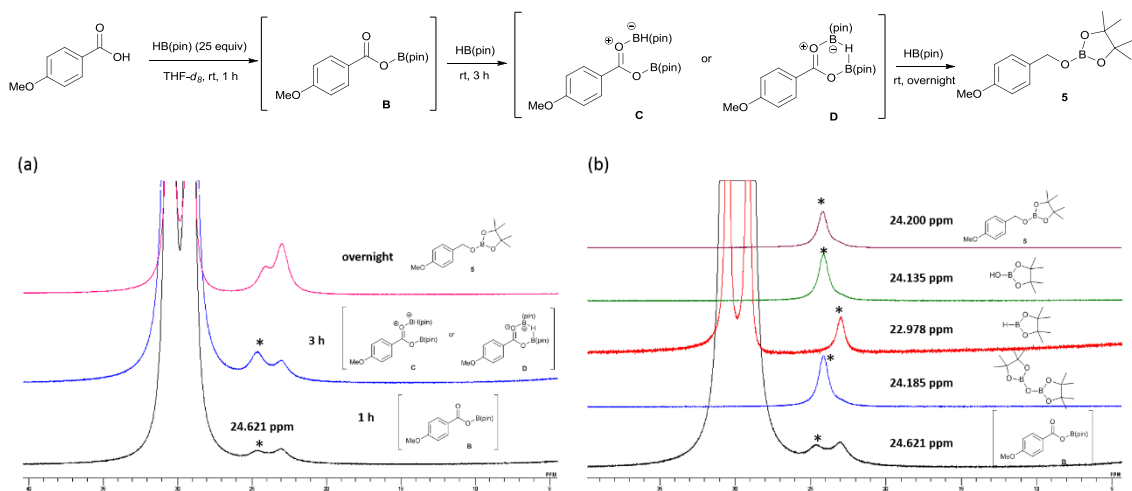
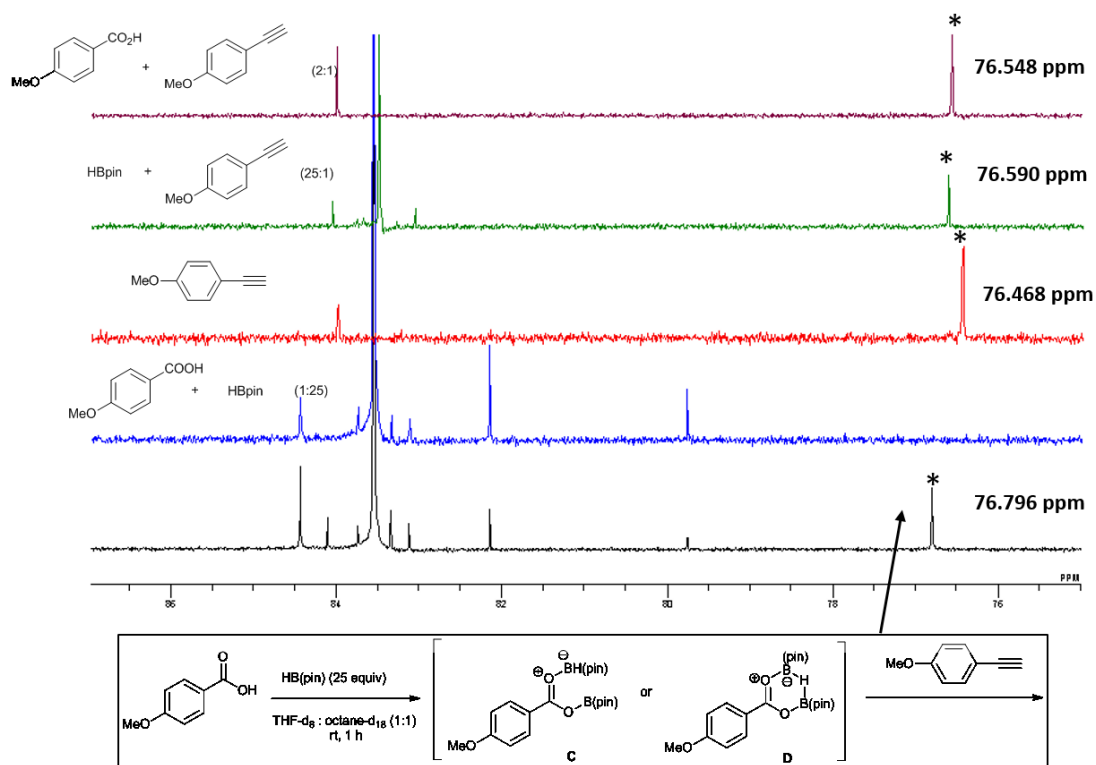
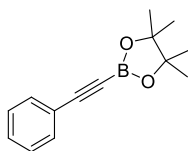


Figure S2. Controlled ^{13}C NMR study for the reaction of anisic acid, HB(pin), and 4-ethynylanisole at rt in octane- d_{18} and THF- d_8 (1:1): the chemical shift changes of terminal alkynyl carbon of 4-ethynylanisole.



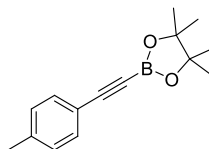
Analytical data of alkynes 1.

4,4,5,5-Tetramethyl-2-(phenylethynyl)-1,3,2-dioxaborolane (1a)³



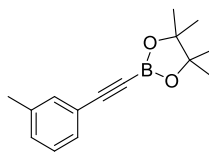
White solid; ¹H NMR (400 MHz, CDCl₃) δ 7.54-7.51 (m, 2H), 7.38-7.28 (m, 3H), 1.32 (s, 12H); ¹³C NMR (100 MHz, CDCl₃) δ 132.4, 129.3, 128.1, 121.7, 84.4, 24.7. The carbon signals of triple bond were not observed due to low intensity.

4,4,5,5-Tetramethyl-2-(*p*-tolylethynyl)-1,3,2-dioxaborolane (1b)



White solid. ¹H NMR (400 MHz, CDCl₃) δ 7.42 (d, *J* = 8.0 Hz, 2H), 7.11 (d, *J* = 8.0 Hz, 2H), 2.35 (s, 3H), 1.32 (s, 12H); ¹³C NMR (100 MHz, CDCl₃) δ 139.6, 132.4, 128.9, 118.7, 84.3, 24.7, 21.6 (The carbon signals of triple bond were not observed due to low intensity); HRMS (ESI): calcd for C₁₅H₁₉BO₂ [M+Na]: 265.1370; found 265.1369.

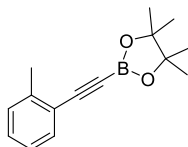
4,4,5,5-Tetramethyl-2-(*m*-tolylethynyl)-1,3,2-dioxaborolane (1c)



Pale yellow oil. ¹H NMR (400 MHz, CDCl₃) δ 7.34-7.31 (m, 2H), 7.20-7.15 (m, 2H), 2.30 (s, 3H), 1.31 (s, 12H); ¹³C NMR (100 MHz, CDCl₃) δ 137.8, 132.9, 130.1, 129.5, 128.0, 121.5, 101.9, 84.3, 24.7 (The carbon signal attached to B was not observed due to low intensity); HRMS (APCI): calcd for C₁₅H₁₉BO₂ [M+H]: 243.1550; found, 243.1550.

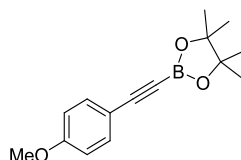
4,4,5,5-Tetramethyl-2-(*o*-tolylethynyl)-1,3,2-dioxaborolane (1d)

³ Takaya, J.; Kirai, N.; Iwasawa, N. *J. Am. Chem. Soc.* **2011**, *133*, 12980.



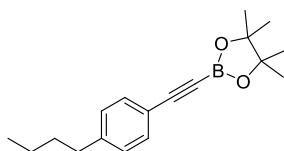
Colorless oil. ^1H NMR (400 MHz, CDCl_3) δ 7.50 (d, $J = 7.6$ Hz, 1H), 7.27-7.23 (m, 1H), 7.19-7.10 (m, 2H), 2.48 (s, 3H), 1.33 (s, 12H). ^{13}C NMR (100 MHz, CDCl_3) δ 141.1, 132.9, 129.3, 129.2, 125.3, 121.6, 100.5, 84.2, 24.7, 20.7 (The carbon signal attached to B was not observed due to low intensity); HRMS (APCI): calcd for $\text{C}_{15}\text{H}_{19}\text{BO}_2$ $[\text{M}+\text{H}]$: 243.1550; found, 243.1550.

2-((4-Methoxyphenyl)ethynyl)-4,4,5,5-tetramethyl-1,3,2-dioxaborolane (1e)⁴



Yellow oil. ^1H NMR (400 MHz, CDCl_3) δ 7.46 (d, $J = 9.0$ Hz, 2H), 6.82 (d, $J = 9.0$ Hz, 2H), 3.80 (s, 3H), 1.31 (s, 12H); ^{13}C NMR (100 MHz, CDCl_3) δ 160.3, 134.1, 113.8(8), 113.8(1), 102.1, 84.2, 55.2, 24.7 (The carbon signal attached to B was not observed due to low intensity); HRMS (APCI): calcd for $\text{C}_{15}\text{H}_{19}\text{BO}_3$ $[\text{M}+\text{H}]$: 259.1500; found, 259.1499.

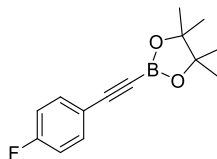
2-((4-Butylphenyl)ethynyl)-4,4,5,5-tetramethyl-1,3,2-dioxaborolane (1f)



Pale yellow oil. ^1H NMR (400 MHz, CDCl_3) δ 7.43 (d, $J = 8.4$ Hz, 2H), 7.11 (d, $J = 8.4$ Hz, 2H), 2.59 (t, $J = 7.6$ Hz, 2H), 1.61-1.53 (m, 2H), 1.38-1.27 (m, 14H), 0.91 (t, $J = 7.2$ Hz, 3H); ^{13}C NMR (100 MHz, CDCl_3) δ 144.5, 132.4, 131.9, 128.3, 118.8, 102.1, 84.3, 35.6, 33.2, 24.7, 24.6, 22.3, 13.9 (The carbon signal attached to B was not observed due to low intensity); HRMS (APCI): calcd for $\text{C}_{18}\text{H}_{25}\text{BO}_2$ $[\text{M}+\text{H}]$: 285.2020, found: 285.2020.

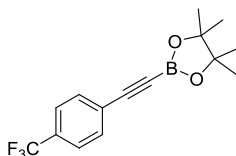
2-((4-Fluorophenyl)ethynyl)-4,4,5,5-tetramethyl-1,3,2-dioxaborolane (1g)

⁴ Coapes, R. B.; Souza, F. E. S.; Thomas, R. L.; Hall, J. J.; Marder, T. B. *Chem. Commun.* **2003**, 614.



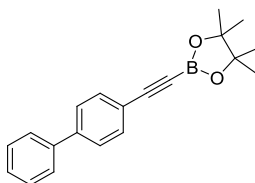
White solid. ^1H NMR (400 MHz, CDCl_3) δ 7.48-7.44 (m, 2H), 6.99-6.94 (m, 2H), 1.27 (s, 12H); ^{13}C NMR (100 MHz, CDCl_3) δ 162.8 (d, $J^1 = 249.1$ Hz), 134.3 (d, $J^3 = 9.1$ Hz), 117.8 (d, $J^4 = 3.3$), 115.5 (d, $J^2 = 22.3$), 100.4, 84.3, 24.6 (The carbon signal attached to B was not observed due to low intensity); HRMS (APCI): calcd for $\text{C}_{14}\text{H}_{16}\text{BFO}_2$ $[\text{M}+\text{H}]$: 247.1300, found: 247.1299.

4,4,5,5-Tetramethyl-2-((4-(trifluoromethyl)phenyl)ethynyl)-1,3,2-dioxaborolane (1h)⁵



White solid. ^1H NMR (400 MHz, CDCl_3) δ 7.62 (d, $J = 8.4$ Hz, 2H), 7.57 (d, $J = 8.4$ Hz, 2H), 1.33 (s, 12H); ^{13}C NMR (100 MHz, CDCl_3) δ 132.6, 130.9 (q, $J^2 = 32.2$ Hz), 125.7, 125.1 (q, $J^3 = 4.1$ Hz), 123.7 (q, $J^1 = 270.6$ Hz), 99.7, 84.6, 24.7 (The carbon signal attached to B was not observed due to low intensity); HRMS (APCI): calcd for $\text{C}_{15}\text{H}_{16}\text{BFO}_3$ $[\text{M}+\text{H}]$: 297.1268, found: 297.1267.

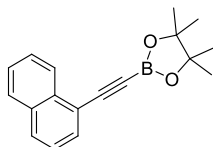
2-(Biphenyl-4-ylethynyl)-4,4,5,5-tetramethyl-1,3,2-dioxaborolane (1i)



Brown solid. ^1H NMR (400 MHz, CDCl_3) δ 7.61-7.53 (m, 6H), 7.46-7.42 (m, 2H), 7.38-7.34 (m, 1H), 1.34 (s, 12H); ^{13}C NMR (100 MHz, CDCl_3) δ 142.0, 140.0, 132.9, 132.4, 128.7, 127.7, 126.9(8), 126.9(0), 120.5, 101.68, 84.4, 24.7 (The carbon signal attached to B was not observed due to low intensity); HRMS (APCI): calcd for $\text{C}_{20}\text{H}_{21}\text{BO}_2$ $[\text{M}+\text{H}]$: 305.1707, found: 305.1707.

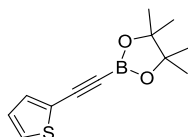
4,4,5,5-Tetramethyl-2-(naphthalen-1-ylethynyl)-1,3,2-dioxaborolane (1j)

⁵ Nishihara, Y.; Miyasaka, M.; Okamoto, M.; Takahashi, H.; Inoue, E.; Tanemura, K.; Takagi, K. *J. Am. Chem. Soc.* **2007**, *129*, 12634.



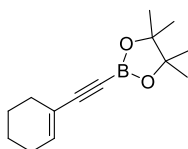
Yellow solid. ^1H NMR (400 MHz, CDCl_3) δ 8.42 (d, $J = 8.0$ Hz, 1H), 7.85 (t, $J = 9.2$ Hz, 2H), 7.79 (dd, $J = 7.2, 1.2$ Hz, 1H), 7.59-7.49 (m, 2H), 7.41 (dd, $J = 8.0, 7.2$ Hz, 1H), 1.37 (s, 12H); ^{13}C NMR (100 MHz, CDCl_3) δ 133.4, 132.8, 132.0, 129.8, 128.1, 126.9, 126.4, 126.2, 124.9, 119.4, 99.6, 84.4, 24.7 (The carbon signal attached to B was not observed due to low intensity); HRMS (APCI): calcd for $\text{C}_{18}\text{H}_{19}\text{BO}_2$ $[\text{M}+\text{H}]$: 279.1550, found: 279.1550.

4,4,5,5-Tetramethyl-2-(thiophen-2-ylethynyl)-1,3,2-dioxaborolane (1k)



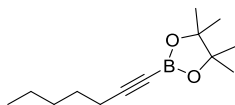
Brown solid. ^1H NMR (400 MHz, CDCl_3) δ 7.34 (d, $J = 3.6$ Hz, 1H), 7.30 (d, $J = 5.2$ Hz, 1H), 6.97 (dd, $J = 5.2, 3.6$ Hz, 1H), 1.32 (s, 12H); ^{13}C NMR (100 MHz, CDCl_3) δ 134.4, 128.8, 126.9, 121.7, 84.5, 24.7 (The carbon signals of triple bond were not observed due to low intensity); HRMS (APCI): calcd for $\text{C}_{12}\text{H}_{15}\text{BO}_2\text{S}$ $[\text{M}+\text{H}]$: 235.0958, found: 235.0957.

2-(Cyclohexenylethynyl)-4,4,5,5-tetramethyl-1,3,2-dioxaborolane (1l)



Yellow oil. ^1H NMR (400 MHz, CDCl_3) δ 6.29-6.27 (m, 1H), 2.13-2.05 (m, 4H), 1.61-1.53 (m, 4H), 1.26 (s, 12H); ^{13}C NMR (100 MHz, CDCl_3) δ 138.8, 119.9, 104.0, 84.0, 28.5, 25.7, 24.6, 22.0, 21.3 (The carbon signal attached to B was not observed due to low intensity); HRMS (APCI): calcd for $\text{C}_{14}\text{H}_{21}\text{BO}_2$ $[\text{M}+\text{H}]$: 233.1707, found: 233.1706.

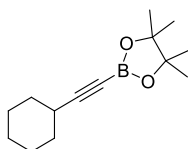
2-(Hept-1-ynyl)-4,4,5,5-tetramethyl-1,3,2-dioxaborolane (1m)



Colorless oil. ^1H NMR (400 MHz, CDCl_3) δ 2.24 (t, $J = 7.2$ Hz, 2H), 1.58-1.49 (m, 2H), 1.38-

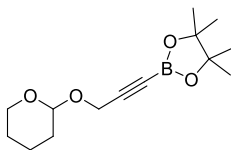
1.28 (m, 4H), 1.26 (s, 12H), 0.88 (t, $J=7.2$ Hz, 3H); ^{13}C NMR (100 MHz, CDCl_3) δ 105.2, 83.9, 31.0, 27.8, 24.7, 22.2, 19.5, 13.9 (The carbon signal attached to B was not observed due to low intensity); HRMS (APCI): calcd for $\text{C}_{13}\text{H}_{23}\text{BO}_2$ [M+H]: 223.1863, found: 223.1863.

2-(Cyclohexylethynyl)-4,4,5,5-tetramethyl-1,3,2-dioxaborolane (1n)



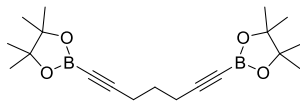
White solid. ^1H NMR (400 MHz, CDCl_3) δ 2.44-2.39 (m, 1H), 1.83-1.79 (m, 2H), 1.74-1.67 (m, 2H), 1.56-1.39 (m, 3H), 1.28-1.26 (m, 14H); ^{13}C NMR (100 MHz, CDCl_3) δ 83.9, 32.0, 29.7, 25.7, 24.8, 24.7 (The carbon signals of triple bond were not observed due to low intensity); HRMS (APCI): calcd for $\text{C}_{14}\text{H}_{21}\text{BO}_2$ [M+H]: 235.1863, found: 235.1863.

4,4,5,5-Tetramethyl-2-(3-(tetrahydro-2H-pyran-2-yloxy)prop-1-ynyl)-1,3,2-dioxaborolane (1o)



Pale yellow oil. ^1H NMR (400 MHz, CDCl_3) δ 4.81 (t, $J = 3.2$ Hz, 1H), 4.28 (d, $J = 3.2$ Hz, 2H), 3.83-3.77 (m 1H), 3.54-3.48 (m, 1H), 1.84-1.70 (m, 2H), 1.69-1.48 (m, 2H), 1.26 (s, 12H); ^{13}C NMR (100 MHz, CDCl_3) δ 98.9, 96.5, 84.3, 61.8, 54.1, 30.1, 25.3, 24.6, 18.9 (The carbon signal attached to B was not observed due to low intensity); HRMS (APCI): calcd for $\text{C}_{14}\text{H}_{23}\text{BO}_4$ [M+Na]: 289.1581, found: 289.1581.

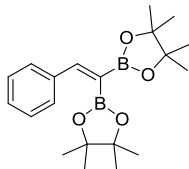
1,7-Bis(4,4,5,5-tetramethyl-1,3,2-dioxaborolan-2-yl)hepta-1,6-diyne (1p)



White solid. ^1H NMR (400 MHz, CDCl_3) δ 2.39 (t, $J = 6.8$ Hz, 4H), 1.76 (m, 2H), 1.26 (s, 12H). ^{13}C NMR (100 MHz, CDCl_3) δ 103.4, 84.0, 26.6, 24.7, 18.7 (The carbon signal attached to B was not observed due to low intensity); HRMS (APCI): calcd for $\text{C}_{22}\text{H}_{28}\text{B}_2\text{O}_4$ [M+H]: 345.2403, found: 345.2402.

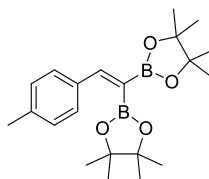
Analytical data of products 2 and 3

2,2'-(2-Phenylethene-1,1-diyl)bis(4,4,5,5-tetramethyl-1,3,2-dioxaborolane) (2a)⁶



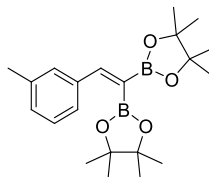
Colorless oil (134 mg, 94%). ¹H NMR (400 MHz, CDCl₃) δ 7.70 (s, 1H), 7.48-7.46 (m, 2H), 7.30-7.23 (m, 3H), 1.30 (s, 12H), 1.26 (s, 12H); ¹³C NMR (100 MHz, CDCl₃) δ 155.0, 139.4, 128.3, 128.0, 127.9, 83.5, 83.1, 24.9, 24.6 (The carbon signal attached to B was not observed due to low intensity); ¹¹B NMR (CDCl₃, 225 MHz, rt) δ 32.17, 30.62; HRMS (ESI): calcd for C₂₀H₃₀B₂O₄ [M+Na]: 379.2222, found: 379.2221.

2,2'-(2-*p*-Tolylethene-1,1-diyl)bis(4,4,5,5-tetramethyl-1,3,2-dioxaborolane) (2b)



Colorless oil (130.3 mg, 88%). ¹H NMR (400 MHz, CDCl₃) δ 7.67 (s, 1H), 7.38 (d, *J* = 8.0 Hz, 2H), 7.09 (d, *J* = 8.0 Hz, 2H), 2.33 (s, 3H), 1.32 (s, 12H), 1.27 (s, 12H). ¹³C NMR (100 MHz, CDCl₃) δ 155.0, 138.3, 136.7, 128.7, 128.1, 83.5, 83.0, 24.9, 24.7, 21.3 (The carbon signal attached to B was not observed due to low intensity); ¹¹B NMR (CDCl₃, 225 MHz, rt) δ 32.35, 30.79; HRMS (ESI) calcd for C₂₁H₃₂B₂O₄ [M+Na]: 393.2378, found: 393.2378.

2,2'-(2-*m*-Tolylethene-1,1-diyl)bis(4,4,5,5-tetramethyl-1,3,2-dioxaborolane) (2c)

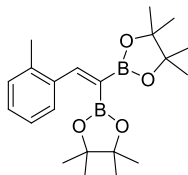


Colorless oil (124.4 mg, 84%). ¹H NMR (400 MHz, CDCl₃) δ 7.69 (s, 1H), 7.33 (s, 1H), 7.27 (d, *J* = 7.6 Hz, 1H), 7.18 (t, *J* = 7.6 Hz, 1H), 7.07 (d, *J* = 7.6 Hz, 1H), 2.32 (s, 3H), 1.32 (s, 12H), 1.28 (s, 12H); ¹³C NMR (100 MHz, CDCl₃) δ 155.1, 139.4, 137.4, 129.1, 128.3, 127.9, 125.4, 83.4, 83.0, 24.8, 24.6, 21.3 (The carbon signal attached to B was not observed due to low intensity).

⁶ Takaya, J.; Kirai, N.; Iwasawa, N. *J. Am. Chem. Soc.* **2011**, *133*, 12980.

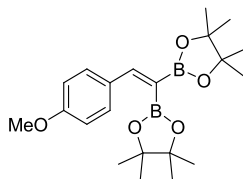
intensity); ^{11}B NMR (CDCl_3 , 225 MHz, rt) δ 32.67, 30.64; HRMS (ESI): calcd for $\text{C}_{21}\text{H}_{32}\text{B}_2\text{O}_4$ $[\text{M}+\text{Na}]$: 393.2378, found: 393.2378.

2,2'-(2-*o*-Tolylethene-1,1-diyl)bis(4,4,5,5-tetramethyl-1,3,2-dioxaborolane) (2d)



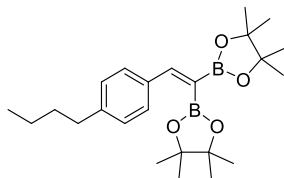
Colorless oil (125.9 mg, 85%). ^1H NMR (400 MHz, CDCl_3) δ 7.89 (s, 1H), 7.45 (d, $J = 7.2$ Hz, 1H), 7.18-7.08 (m 3H), 2.35 (s, 3H), 1.28 (s, 12H), 1.24 (s, 12H); ^{13}C NMR (100 MHz, CDCl_3) δ 153.9, 139.0, 136.1, 129.6, 128.1, 127.5, 125.3, 83.3, 83.0, 24.8, 24.5, 19.7 (The carbon signal attached to B was not observed due to low intensity); ^{11}B NMR 32.09, 30.53; (CDCl_3 , 225 MHz, rt) δ HRMS (ESI): calcd for $\text{C}_{21}\text{H}_{32}\text{B}_2\text{O}_4$ $[\text{M}+\text{Na}]$: 393. 2378, found: 393.2378.

2,2'-(2-(4-Methoxyphenyl)ethene-1,1-diyl)bis(4,4,5,5-tetramethyl-1,3,2-dioxaborolane) (2e)⁷



Pale yellow oil (128.2 mg, 83%). ^1H NMR (400 MHz, CDCl_3) δ 7.65 (s, 1H), 7.44 (d, $J = 8.4$ Hz, 2H), 6.81 (d, $J = 8.4$ Hz, 2H), 3.79 (s, 3H), 1.32 (s, 12H), 1.27 (s, 12H); ^{13}C NMR (100 MHz, CDCl_3) δ 159.8, 154.6, 132.3, 129.6, 113.4, 83.4, 82.9, 55.2, 24.8, 24.7 (The carbon signal attached to B was not observed due to low intensity); ^{11}B NMR (CDCl_3 , 225 MHz, rt) δ 32.48, 30.89; HRMS (ESI): calcd for $\text{C}_{21}\text{H}_{32}\text{B}_2\text{O}_5$ $[\text{M}+\text{Na}]$: 409.2328, found: 409.2327.

2,2'-(2-(4-Butylphenyl)ethene-1,1-diyl)bis(4,4,5,5-tetramethyl-1,3,2-dioxaborolane) (2f)

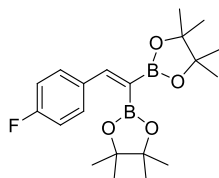


Pale yellow oil (135.2 mg, 82%). ^1H NMR (400 MHz, CDCl_3) δ 7.68 (s, 1H), 7.40 (d, $J = 8.0$ Hz, 2H), 7.10 (d, $J = 8.0$ Hz, 2H), 2.58 (t, $J = 7.6$ Hz, 2H), 1.62-1.54 (m, 2H), 1.33-1.31 (s, 14H),

⁷ Coapes, R. B.; Souza, F. E. S.; Thomas, R. L.; Hall, J. J.; Marder, T. B. *Chem. Commun.* **2003**, 614.

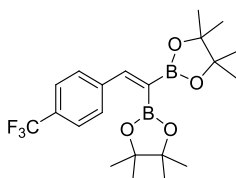
1.27 (s, 12H), 0.91 (t, $J = 7.6$ Hz, 3H); ^{13}C NMR (100 MHz, CDCl_3) δ 155.0, 143.3, 136.8, 128.0, 127.8, 83.4, 83.0, 35.4, 33.4, 24.8, 24.6, 22.3, 13.9 (The carbon signal attached to B was not observed due to low intensity); ^{11}B NMR (CDCl_3 , 225 MHz, rt) δ 32.59, 31.11; HRMS (ESI): calcd for $\text{C}_{24}\text{H}_{38}\text{B}_2\text{O}_4$ [$\text{M}+\text{Na}$]: 435.2848, found: 435.2847.

2,2'-(2-(4-Fluorophenyl)ethene-1,1-diyl)bis(4,4,5,5-tetramethyl-1,3,2-dioxaborolane) (2g)



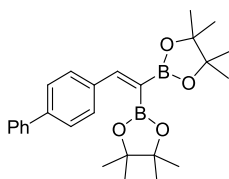
Pale yellow oil (136.2 mg, 91%). ^1H NMR (400 MHz, CDCl_3) δ 7.65 (s, 1H), 7.49-7.44 (m, 2H), 6.99-6.95 (m, 2H), 1.30 (s, 12H), 1.27 (s, 12H); ^{13}C NMR (100 MHz, CDCl_3) δ 162.6 (d, $J^1 = 246.7$ Hz), 153.6, 135.7 (d, $J^d = 3.3$ Hz), 129.7 (d, $J^3 = 8.3$ Hz), 114.9 (d, $J^2 = 21.5$ Hz), 83.6, 83.2, 24.8, 24.6 (The carbon signal attached to B was not observed due to low intensity); ^{11}B NMR (CDCl_3 , 225 MHz, rt) δ 30.84; HRMS (ESI): calcd for $\text{C}_{20}\text{H}_{29}\text{B}_2\text{FO}_4$ [$\text{M}+\text{Na}$]: 397.2128, found: 397.2128.

2,2'-(2-(4-(Trifluoromethyl)phenyl)ethene-1,1-diyl)bis(4,4,5,5-tetramethyl-1,3,2-dioxaborolane) (2h)



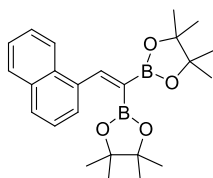
Pale yellow oil (140.8 mg, 83%). ^1H NMR (400 MHz, CDCl_3) δ 7.70 (s, 1H), 7.59-7.53 (m, 4H), 1.31 (s, 12H), 1.28 (s, 12H); ^{13}C NMR (100 MHz, CDCl_3) δ 152.9, 142.8, 129.9 (q, $J^2 = 32.2$ Hz), 128.5, 125.0 (q, $J^3 = 4.0$ Hz), 124.0 (q, $J^1 = 276$ Hz), 83.8, 83.4, 24.9, 24.6 (The carbon signal attached to B was not observed due to low intensity); ^{11}B NMR (CDCl_3 , 225 MHz, rt) δ 31.54; HRMS (ESI): calcd for $\text{C}_{20}\text{H}_{29}\text{B}_2\text{FO}_4$ [$\text{M}+\text{Na}$]: 447.2096, found: 447.2096.

2,2'-(2-(Biphenyl-4-yl)ethene-1,1-diyl)bis(4,4,5,5-tetramethyl-1,3,2-dioxaborolane) (2i)



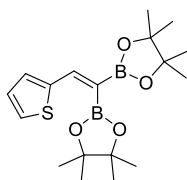
Yellow oil (155.6 mg, 90%). ^1H NMR (400 MHz, CDCl_3) δ 7.76 (s, 1H), 7.62-7.54 (m, 6H), 7.43

(t, $J = 7.2$ Hz, 2H), 7.36-7.32 (m, 1H), 1.35 (s, 12H), 1.30 (s, 12H); ^{13}C NMR (100 MHz, CDCl_3) δ 154.4, 141.0, 138.4, 132.4, 128.6, 128.5, 127.2, 126.9, 126.7, 83.6, 83.1, 24.9, 24.7. The carbon signal attached to B was not observed due to low intensity; ^{11}B NMR (CDCl_3 , 225 MHz, rt) δ 30.71; HRMS (ESI): calcd for $\text{C}_{26}\text{H}_{34}\text{B}_2\text{O}_4$ $[\text{M}+\text{Na}]$: 307.1863, found: 307.1863. **2,2'-(2-(Naphthalen-1-yl)ethene-1,1-diyl)bis(4,4,5,5-tetramethyl-1,3,2-dioxaborolane) (2j)**



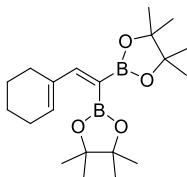
White solid. (123.5 mg, 76%). ^1H NMR (400 MHz, CDCl_3) δ 8.40 (s, 1H), 8.12 (d, $J = 7.2$ Hz, 1H), 7.83-7.76 (m, 2H), 7.62 (d, $J = 7.2$ Hz, 1H), 7.50-7.40 (m, 2H), 7.37 (t, $J = 7.6$ Hz, 1H), 1.32 (s, 12H), 1.17 (s, 12H); ^{13}C NMR (100 MHz, CDCl_3) δ 153.4, 137.7, 133.2, 131.2, 128.5, 128.0, 125.8, 125.7, 125.4, 125.0, 124.8, 83.4, 83.2, 25.0, 24.5 (The carbon signal attached to B was not observed due to low intensity); ^{11}B NMR (CDCl_3 , 225 MHz, rt) δ 32.09; HRMS (ESI): calcd for $\text{C}_{24}\text{H}_{32}\text{B}_2\text{O}_4$ $[\text{M}+\text{Na}]$: 429.2378, found: 429.2378.

2,2'-(2-(Thiophen-2-yl)ethene-1,1-diyl)bis(4,4,5,5-tetramethyl-1,3,2-dioxaborolane) (2k)



Pale yellow oil (76.8 mg, 53%). ^1H NMR (400 MHz, CDCl_3) δ 7.71 (s, 1H), 7.27-7.26 (m, 1H), 7.19-7.18 (m, 1H), 6.96 (dd, $J = 5.2, 3.6$ Hz, 1H), 1.37 (s, 12H), 1.26 (s, 12H); ^{13}C NMR (100 MHz, CDCl_3) δ 145.8, 144.2, 129.2, 127.1, 127.0, 83.6, 83.1, 24.8, 24.5. The carbon signal attached to B was not observed due to low intensity; ^{11}B NMR (CDCl_3 , 225 MHz, rt) δ 31.22; HRMS (ESI): calcd for $\text{C}_{18}\text{H}_{28}\text{B}_2\text{O}_4\text{S}$ $[\text{M}+\text{Na}]$: 385.1786, found: 385.1786.

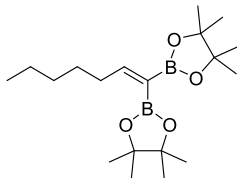
2,2'-(2-Cyclohexenylethene-1,1-diyl)bis(4,4,5,5-tetramethyl-1,3,2-dioxaborolane) (2l)



Colorless oil (89.3 mg, 62%). ^1H NMR (400 MHz, CDCl_3) δ 7.17 (s, 1H), 6.00-5.98 (m, 1H), 2.20-2.12 (m, 4H), 1.66-1.53 (m, 4H), 1.30 (s, 12H), 1.22 (s, 12H); ^{13}C NMR (100 MHz, CDCl_3)

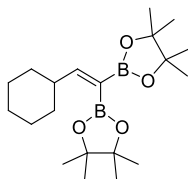
δ 157.8, 138.6, 134.9, 83.3, 82.7, 26.2, 25.8, 24.8, 24.7, 22.3, 22.0 (The carbon signal attached to B was not observed due to low intensity); ^{11}B NMR (CDCl_3 , 225 MHz, rt) δ 32.49; HRMS (ESI): calcd for $\text{C}_{20}\text{H}_{34}\text{B}_2\text{O}_4$ $[\text{M}+\text{Na}]$: 383.2535, found: 383.2535.

2,2'-(Hept-1-ene-1,1-diyl)bis(4,4,5,5-tetramethyl-1,3,2-dioxaborolane) (2m)



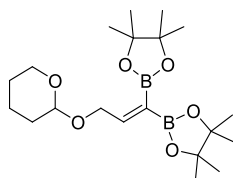
Yellow oil. (99.5 mg, 71%). ^1H NMR (400 MHz, CDCl_3) δ 6.92 (t, $J = 7.2$ Hz, 1H), 2.24 (dt, $J = 7.2, 7.2$ Hz, 2H), 1.44-1.36 (m, 2H), 1.28-1.22 (m, 28H), 0.86 (t, $J = 7.2$ Hz, 3H); ^{13}C NMR (100 MHz, CDCl_3) δ 162.4, 83.0, 82.7, 35.4, 31.5, 28.7, 24.8, 24.7, 22.5, 14.0 (The carbon signal attached to B was not observed due to low intensity); ^{11}B NMR 34.08, 31.47; (CDCl_3 , 225 MHz, rt) δ HRMS (ESI): calcd for $\text{C}_{19}\text{H}_{36}\text{B}_2\text{O}_4$ $[\text{M}+\text{Na}]$: 373.2691, found: 373.2691.

2,2'-(2-Cyclohexylethene-1,1-diyl)bis(4,4,5,5-tetramethyl-1,3,2-dioxaborolane) (2n)



Colorless oil (128.9 mg, 89%). ^1H NMR (400 MHz, CDCl_3) δ 6.74 (d, $J = 8.8$ Hz, 1H), 2.30-2.21 (m, 1H), 1.73-1.70 (m, 4H), 1.29 (s, 12H), 1.22-1.08 (m, 16H). ^{13}C NMR (100 MHz, CDCl_3) δ 166.8, 83.0, 82.7, 44.1, 32.6, 25.9, 25.8, 24.8, 24.6 (The carbon signal attached to B was not observed due to low intensity); ^{11}B NMR (CDCl_3 , 225 MHz, rt) δ 31.56; HRMS (ESI): calcd for $\text{C}_{20}\text{H}_{36}\text{B}_2\text{O}_4$ $[\text{M}+\text{Na}]$: 385.2691, found: 385.2691.

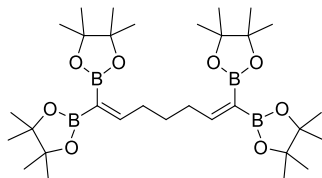
2,2'-(3-(Tetrahydro-2H-pyran-2-yloxy)prop-1-ene-1,1-diyl)bis(4,4,5,5-tetramethyl-1,3,2-dioxaborolane) (2o)



Colorless oil (118.3 mg, 75%). ^1H NMR (400 MHz, CDCl_3) δ 7.00 (dd, $J = 6.0, 5.2$ Hz, 1H), 4.63 (t, $J = 3.6$ Hz, 1H), 4.38 (dd, $J = 14.0, 5.2$ Hz, 1H), 4.21, (dd, $J = 14.0, 6.0$ Hz, 1H), 3.87-3.82 (m 1H), 3.51-3.45 (m, 1H), 1.88-1.77 (m, 1H), 1.74-1.65 (m, 1H), 1.63-1.48 (m, 4H), 1.28 (s,

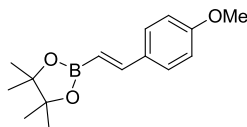
12H), 1.24 (s, 12H); ^{13}C NMR (100 MHz, CDCl_3) δ 157.5, 97.7, 83.2, 83.0, 68.2, 61.9, 30.5, 25.5, 24.8, 24.7, 19.3; ^{11}B NMR (CDCl_3 , 225 MHz, rt) δ 30.87; HRMS (ESI): calcd for $\text{C}_{20}\text{H}_{36}\text{B}_2\text{O}_6$ $[\text{M}+\text{Na}]$: 417.2590, found: 417.2589.

1,1,7,7-Tetrakis(4,4,5,5-tetramethyl-1,3,2-dioxaborolan-2-yl)hepta-1,6-diene (2p)



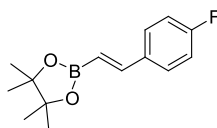
Colorless oil (156.1 mg, 65%). ^1H NMR (400 MHz, CDCl_3) δ 6.90 (t, $J = 7.2$ Hz, 2H), 2.28-2.23 (m, 4H), 1.56-1.49 (m, 2H), 1.25 (s, 24H), 1.20 (s, 24H); ^{13}C NMR (100 MHz, CDCl_3) δ 161.9, 82.9, 82.6, 35.0, 31.5, 28.5, 24.8, 24.7; ^{11}B NMR (CDCl_3 , 225 MHz, rt) δ 31.16; HRMS (ESI): calcd for $\text{C}_{31}\text{H}_{56}\text{B}_4\text{O}_8$ $[\text{M}+\text{Na}]$: 623.4239, found: 623.4239.

(E)-2-(4-Methoxystyryl)-4,4,5,5-tetramethyl-1,3,2-dioxaborolane (3a)⁸



White solid (93.6 mg, 85%). ^1H NMR (400 MHz, CDCl_3) δ 7.43 (d, $J = 8.8$ Hz, 1H), 7.35 (d, $J = 18.4$ Hz, 1H), 6.85 (d, $J = 8.4$ Hz, 1H), 6.01 (d, $J = 18.4$ Hz, 1H), 3.79 (s, 3H), 1.30 (s, 12H); ^{13}C NMR (100 MHz, CDCl_3) δ 160.1, 148.9, 130.2, 128.3, 113.8, 83.1, 55.2, 24.8. The carbon signal attached to B was not observed due to low intensity.

(E)-2-(4-Fluorostyryl)-4,4,5,5-tetramethyl-1,3,2-dioxaborolane (3b)⁹

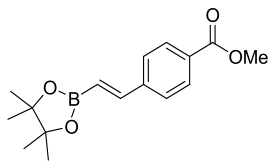


Colorless oil (69.5 mg, 70%). ^1H NMR (400 MHz, CDCl_3) δ 7.47-7.42 (m, 2H), 7.35 (d, $J = 18.4$ Hz, 1H), 7.04-6.98 (m, 2H), 6.07 (d, $J = 18.4$ Hz, 1H), 1.30 (s, 12H); ^{13}C NMR (100 MHz, CDCl_3) δ 162.9 (d, $J = 247.0$ Hz), 148.2, 133.5 (d, $J = 2.5$ Hz), 128.5 (d, $J = 8.2$ Hz), 115.4 (d, $J = 21.4$ Hz), 83.1, 24.8. The carbon signal attached to B was not observed due to low intensity.

⁸ Stewart, S. K.; Whiting, A. *J. Organomet. Chem.* **1994**, 482, 293.

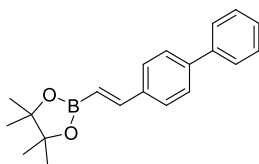
⁹ Wen, K.; Chen, J.; Gao, F.; Bhadury, P. S.; Fan, E.; Sun, Z. *Org. Biomol. Chem.* **2013**, 11, 6350.

(E)-Methyl 4-(2-(4,4,5,5-tetramethyl-1,3,2-dioxaborolan-2-yl)vinyl)benzoate (3c)¹⁰



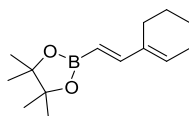
White solid (86.4 mg, 75%). ¹H NMR (400 MHz, CDCl₃) δ 8.01-7.98 (m, 2H), 7.52 (d, *J* = 8.4 Hz, 2H), 7.40 (d, *J* = 18.4 Hz, 1H), 6.27 (s, *J* = 18.4, 1H), 3.90 (s, 3H), 1.31 (s, 12H); ¹³C NMR (100 MHz, CDCl₃) δ 166.2, 147.9, 141.5, 130.0, 129.8, 126.8, 83.5, 52.1, 24.8. The carbon signal attached to B was not observed due to low intensity; HRMS (APCI): calcd for C₁₆H₂₁BO₄ [M+H]: 289.1605, found: 289.1605.

(E)-2-(2-(Biphenyl-4-yl)vinyl)-4,4,5,5-tetramethyl-1,3,2-dioxaborolane (3d)



Yellow solid (96.8 mg, 79%). ¹H NMR (400 MHz, CDCl₃) δ 7.61-7.56 (m, 6H), 7.46-7.41 (m, 3H), 7.36-7.34 (m, 1H), 6.21 (d, *J* = 18.4 Hz, 1H), 1.33 (s, 12H); ¹³C NMR (100 MHz, CDCl₃) δ 148.8, 141.5, 140.4, 136.4, 128.7, 127.4, 127.3, 127.1, 126.9, 83.6, 24.8. The carbon signal attached to B was not observed due to low intensity; HRMS (APCI): calcd for C₂₀H₂₃BO₂ [M+H]: 307.1863, found: 307.1863.

(E)-2-(2-Cyclohexenylvinyl)-4,4,5,5-tetramethyl-1,3,2-dioxaborolane (3e)¹¹

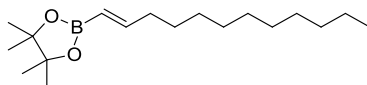


Colorless oil (46.8 mg, 50%). ¹H NMR (400 MHz, CDCl₃) δ 7.01 (d, *J* = 18.4 Hz, 1H), 5.97-5.95 (m, 1H), 5.42 (d, *J* = 18.4 Hz, 1H), 2.14 (br, 4H), 1.69-1.55 (m, 4H), 1.27 (s, 12H); ¹³C NMR (100 MHz, CDCl₃) δ 153.1, 137.0, 134.1, 82.9, 26.2, 24.8, 23.7, 22.4, 22.3. The carbon signal attached to B was not observed due to low intensity.

¹⁰ Haberberger, M. and Enthaler, S. *Chem. Asian J.* **2013**, 8, 50

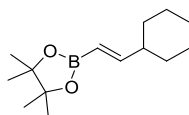
¹¹ Shade, R. E.; Hyde, A. M.; Olsen, J.-C.; Merlic, C. *J. Am. Chem. Soc.* **2010**, 132, 1202.

(E)-2-(Dodec-1-en-1-yl)-4,4,5,5-tetramethyl-1,3,2-dioxaborolane (3f)¹²



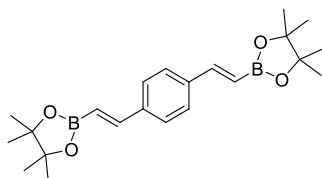
Colorless oil (100 mg, 85%). ¹H NMR (400 MHz, CDCl₃) δ 6.65 (dt, *J* = 18.0, 6.4 Hz, 1H), 5.41 (d, *J* = 18.0, 1.6 Hz, 1H), 2.16-2.11 (m, 2H), 1.42-1.26 (m, 28H), 0.87 (t, *J* = 6.8 Hz 3H); ¹³C NMR (100 MHz, CDCl₃) δ 154.7, 82.9, 35.8, 31.9, 29.6(6), 29.6(2), 29.5, 29.3, 29.2(7), 29.2(6), 24.8, 22.7, 14.1. The carbon signal attached to B was not observed due to low intensity.

(E)-2-(2-Cyclohexylvinyl)-4,4,5,5-tetramethyl-1,3,2-dioxaborolane (3g)¹³



Colorless oil (51.0 mg, 54%). ¹H NMR (400 MHz, CDCl₃) δ 6.55 (dd, *J* = 18.4, 6.0 Hz, 1H), 5.37 (d, *J* = 18.4 Hz, 1H), 2.06-1.99 (m, 1H), 1.75-1.62 (m, 6H), 1.27 (s, 12H), 1.19-1.05 (m, 4H); ¹³C NMR (100 MHz, CDCl₃) δ 159.7, 82.9, 43.2, 31.9, 26.1, 25.9, 24.8. The carbon signal attached to B was not observed due to low intensity. HRMS (ESI): calcd for [M+H]⁺: 237.1913, found: 237.1913.

1,4-Bis((E)-2-(4,4,5,5-tetramethyl-1,3,2-dioxaborolan-2-yl)vinyl)benzene (3h)¹⁴



White solid (122.3 mg, 80%). ¹H NMR (400 MHz, CDCl₃) δ 7.45 (s, 4H), 7.36 (d, *J* = 18.4 Hz, 2H), 6.16 (d, *J* = 18.4 Hz, 2H), 1.31 (s, 24H); ¹³C NMR (100 MHz, CDCl₃) δ 148.7, 137.8, 127.2, 119.6, 83.8, 24.8. The carbon signal attached to B was not observed due to low intensity.

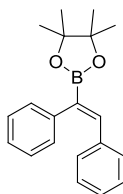
(Z)-2-(1,2-Diphenylvinyl)-4,4,5,5-tetramethyl-1,3,2-dioxaborolane (3i)¹⁵

¹² Quigley, B. L.; Grubbs, R. H. *Chem. Sci.* **2014**, *5*, 501.

¹³ Haberberger, M. and Enthaler, S. *Chem. Asian J.* **2013**, *8*, 50

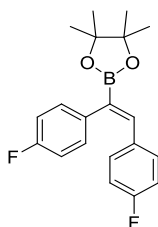
¹⁴ Lee, T.; Baik, C.; Jung, I.; Song, K. H.; Kim, S.; Kim, D.; Kang, S. O.; Ko, J. *Organometallics*. **2004**, *23*, 4569.

¹⁵ Grirrane, A.; Corma, A.; Garcia, H. *Chem. Eur. J.* **2011**, *17*, 2467.



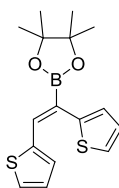
Pale yellow solid (118.8 mg, 97%). ^1H NMR (400 MHz, CDCl_3) δ 7.36 (s, 1H), 7.28-7.03 (m, 10H), 1.31 (s, 12H); ^{13}C NMR (100 MHz, CDCl_3) δ 143.0, 140.2, 136.8, 129.8, 128.7, 128.1, 127.7, 127.4, 126.1, 83.7, 24.8. The carbon signal attached to B was not observed due to low intensity.

(Z)-2-(1,2-Bis(4-fluorophenyl)vinyl)-4,4,5,5-tetramethyl-1,3,2-dioxaborolane (3j)



White solid (110.9 mg, 81%). ^1H NMR (400 MHz, CDCl_3) δ 7.33 (s, 1H), 7.13-6.95 (m, 6H), 6.83 (t, $J = 8.4$ Hz, 2H), 1.32 (s, 12H); ^{13}C NMR (100 MHz, CDCl_3) δ 161.8 (d, $J = 246.7$ Hz), 161.5 (d, $J = 243.4$ Hz), 142.1, 135.7 (d, $J = 3.3$ Hz), 132.7 (d, $J = 3.3$ Hz), 131.4 (d, $J = 8.3$ Hz), 130.2 (d, $J = 8.2$ Hz), 115.2 (d, $J = 20.7$ Hz), 114.8 (d, $J = 20.7$ Hz), 83.8, 24.8; HRMS (APCI): calcd for $\text{C}_{20}\text{H}_{21}\text{BF}_2\text{O}_2$ $[\text{M}+\text{H}]$: 343.1675, found: 343.1675.

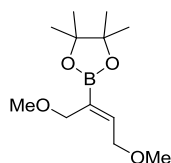
(Z)-2-(1,2-Di(thiophen-2-yl)vinyl)-4,4,5,5-tetramethyl-1,3,2-dioxaborolane (3k)¹⁶



Yellow oil (99.2 mg, 78%). ^1H NMR (400 MHz, CDCl_3) δ 7.63 (s, 1H), 7.38 (dd, $J = 5.2, 1.2$ Hz, 1H), 7.21-7.19 (m, 1H), 7.12-7.11 (m, 1H), 7.08 (dd, $J = 5.2, 3.2$ Hz, 1H), 6.93-6.90 (m, 2H), 1.31 (s, 12H); ^{13}C NMR (100 MHz, CDCl_3) δ 140.7, 139.8, 139.1, 131.4, 128.7, 127.3, 126.0, 125.7, 83.8, 24.7; HRMS (APCI): calcd for $\text{C}_{14}\text{H}_{16}\text{BO}_2\text{S}_2$ $[\text{M}+\text{H}]$: 319.0992, found: 319.0991.

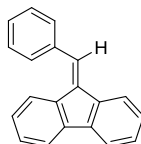
(Z)-2-(1,4-Dimethoxybut-2-en-2-yl)-4,4,5,5-tetramethyl-1,3,2-dioxaborolane (3l)

¹⁶ Sundararaju, B. and Fürstner, A. *Angew. Chem. Int. Ed.* **2013**, 52, 14050



Colorless oil (58.1 mg, 60%). ^1H NMR (400 MHz, CDCl_3) δ 6.58 (t, $J = 5.6$ Hz, 1H), 4.14 (d, $J = 5.6$ Hz, 2H), 4.02 (s, 2H), 3.34 (s, 3H), 3.28 (s, 3H), 1.24 (s, 12H); ^{13}C NMR (100 MHz, CDCl_3) δ 146.5, 83.4, 69.6, 68.9, 58.3, 57.8, 24.7. The carbon signal attached to B was not observed due to low intensity; HRMS (ESI): calcd for $\text{C}_{12}\text{H}_{23}\text{BO}_4$ $[\text{M}+\text{Na}]$: 265.1581, found: 265.1580.

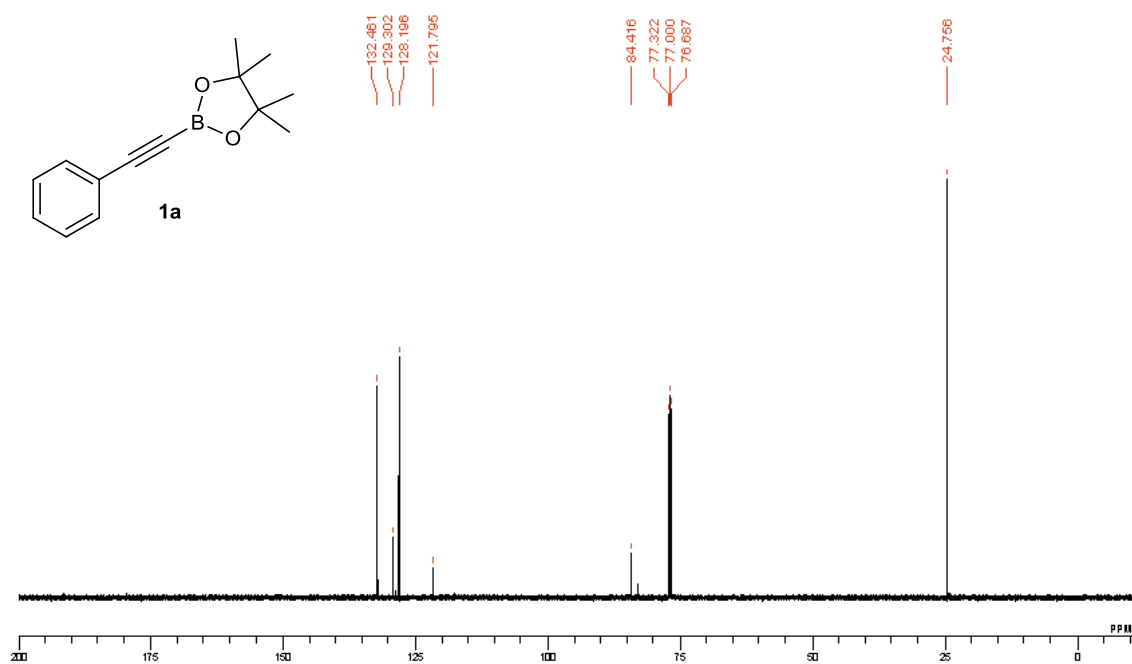
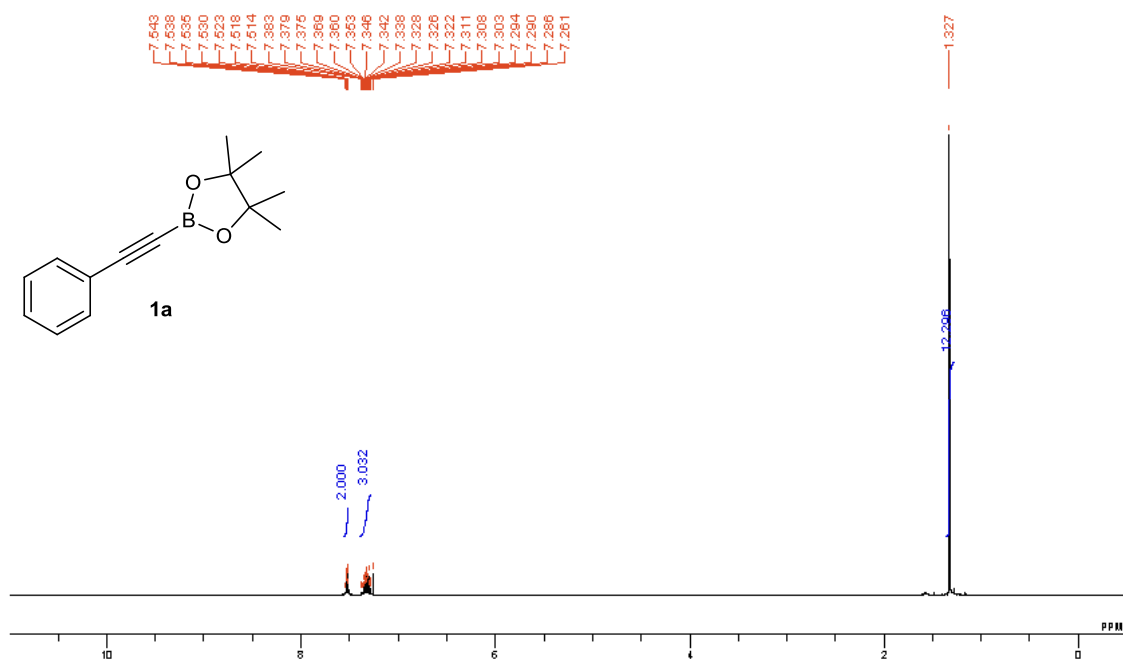
9-Benzylidene-9*H*-fluorene (**4**)¹⁷

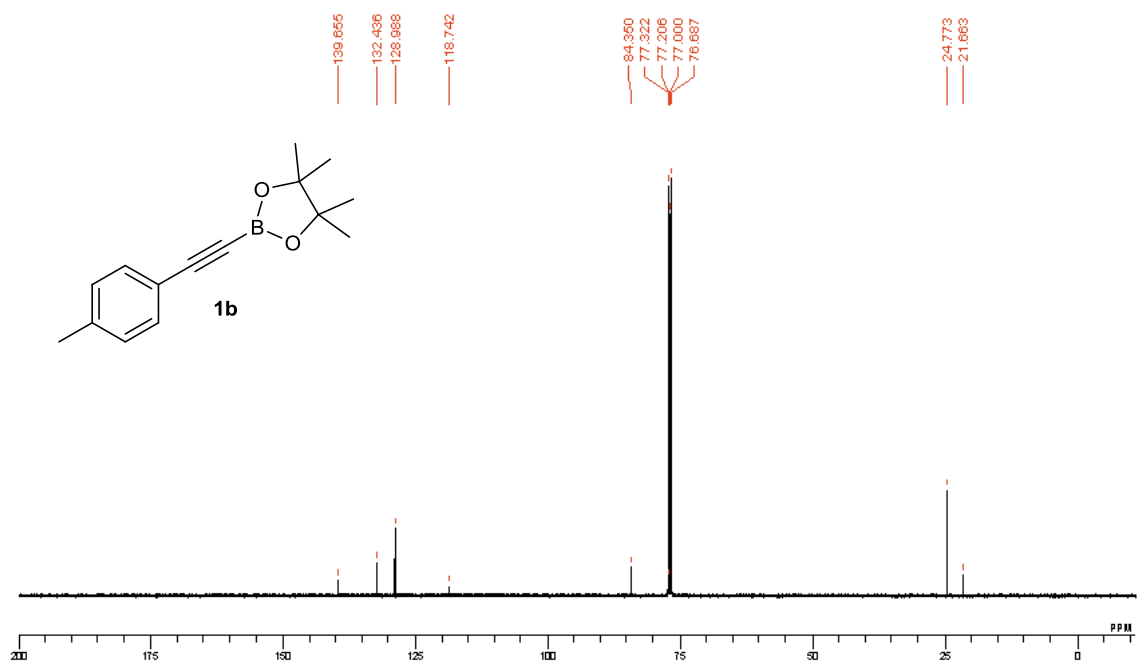
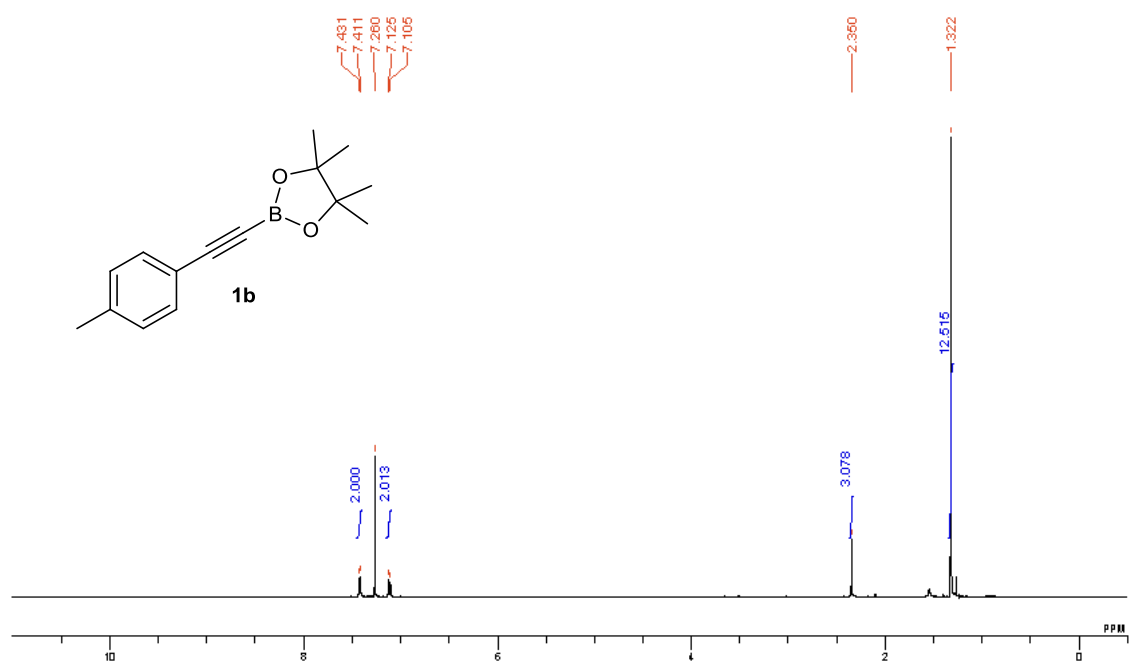


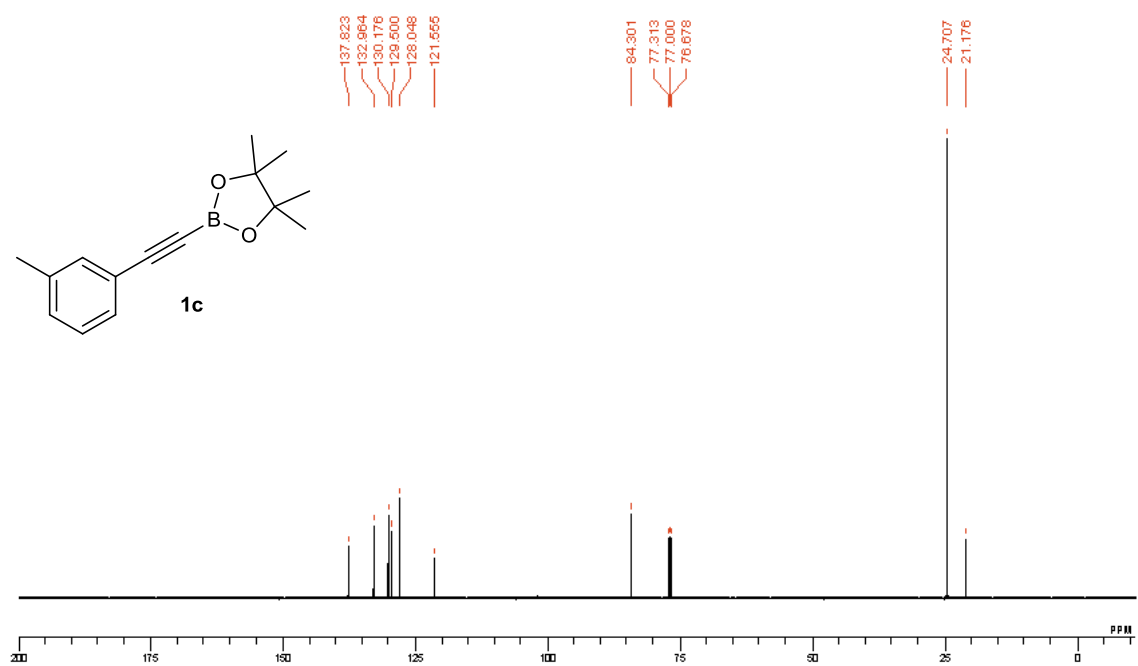
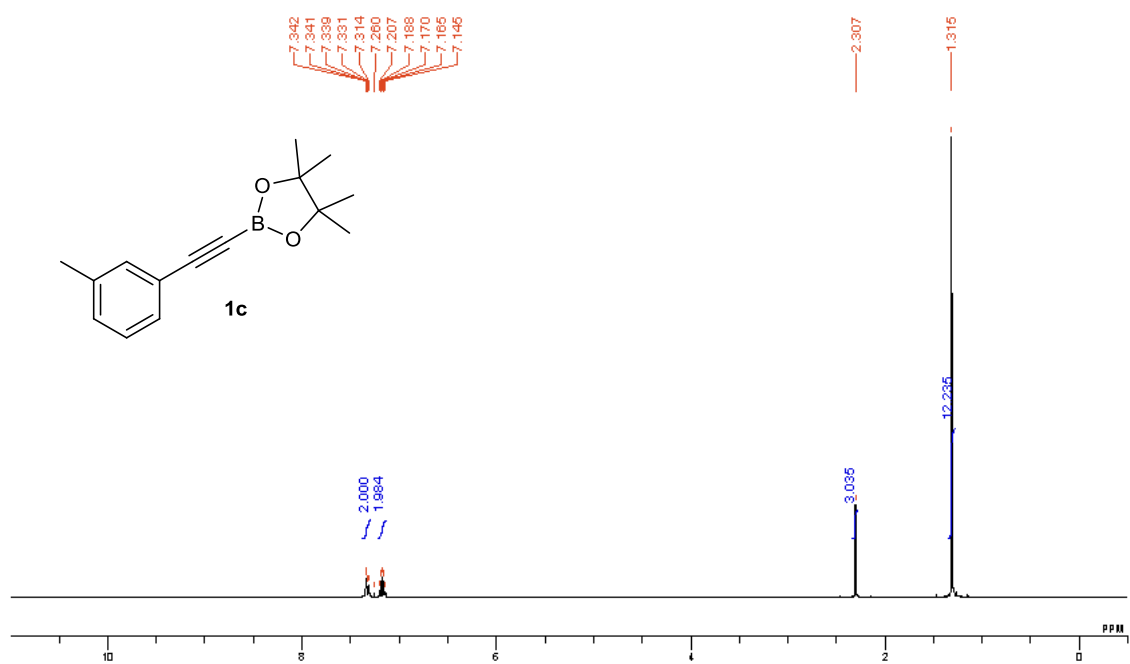
White solid (74 mg, 97%). ^1H NMR (400 MHz, CDCl_3) δ 7.80 (d, $J = 7.6$ Hz, 1H), 7.73-7.70 (m, 3H), 7.60-7.54 (m, 3H), 7.48-7.44 (m, 2H), 7.48-7.45 (m, 2H), 7.41-7.29 (m, 4H), 7.07-7.03 (m, 1H); ^{13}C NMR (100 MHz, CDCl_3) δ 141.1, 139.3, 139.0, 136.8, 136.4, 136.3, 129.1, 128.4, 128.1, 127.9, 127.1, 126.9, 126.5, 124.3, 120.1, 119.6, 119.5.

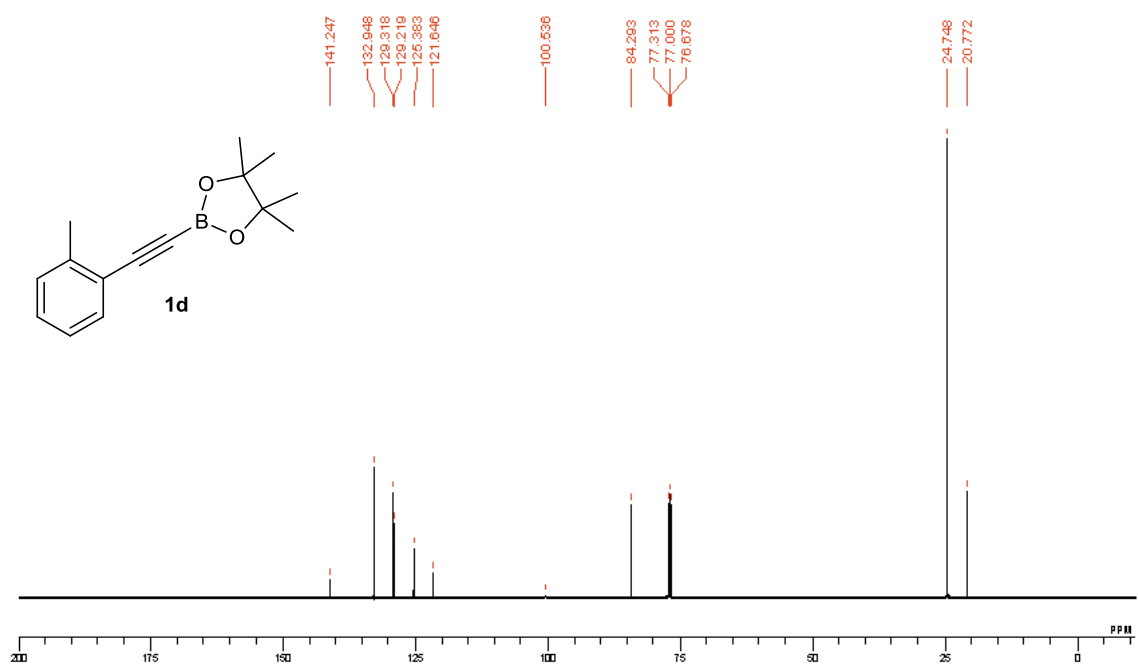
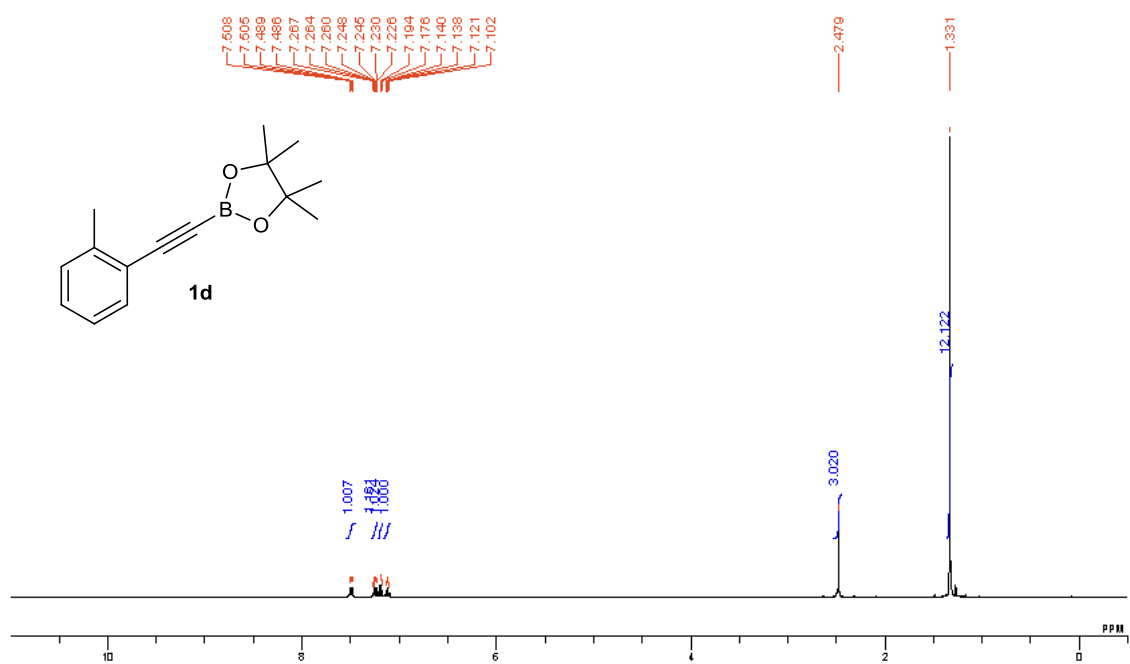
¹⁷ Chernyak, N.; Gevorgyan, V. *J. Am. Chem. Soc.* **2008**, *130*, 5636.

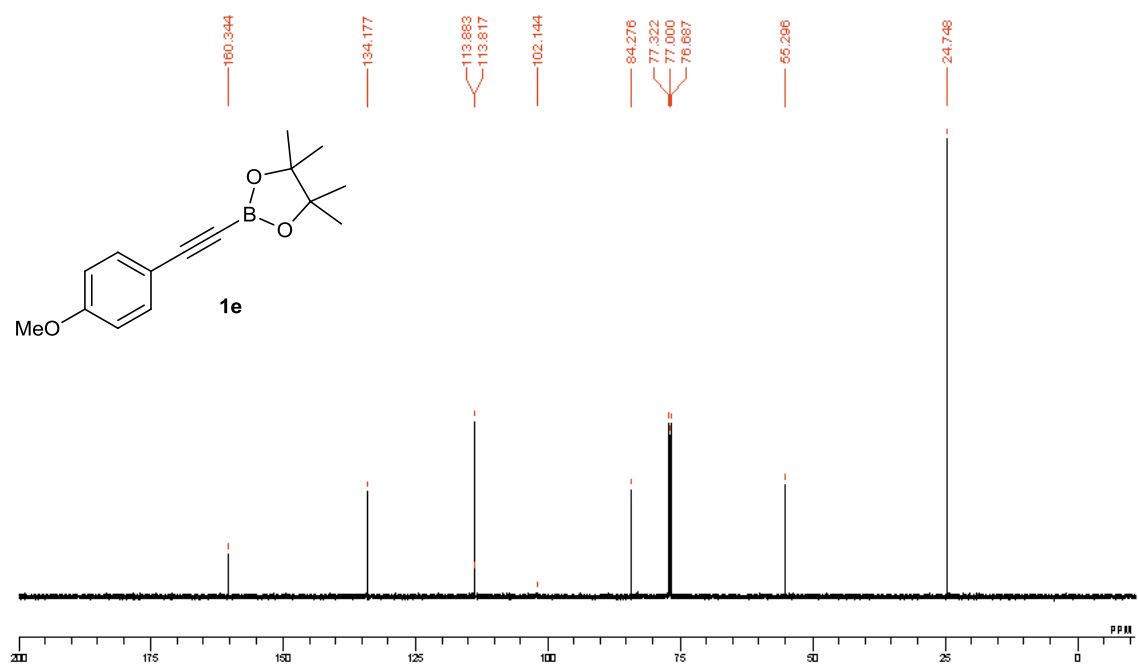
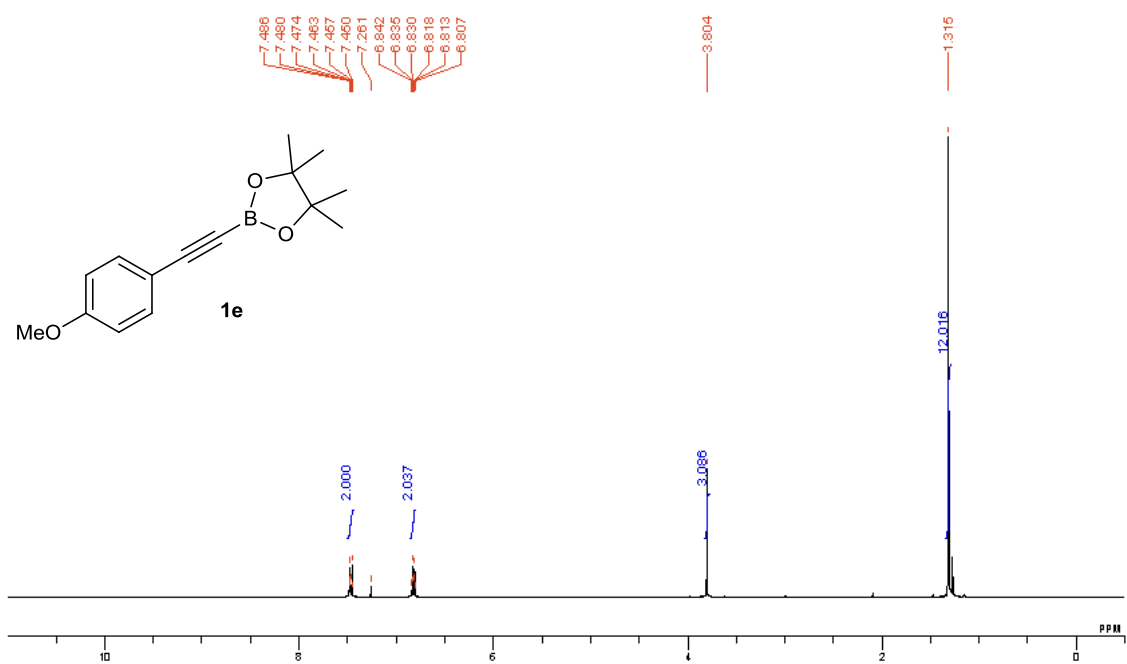
NMR Spectra

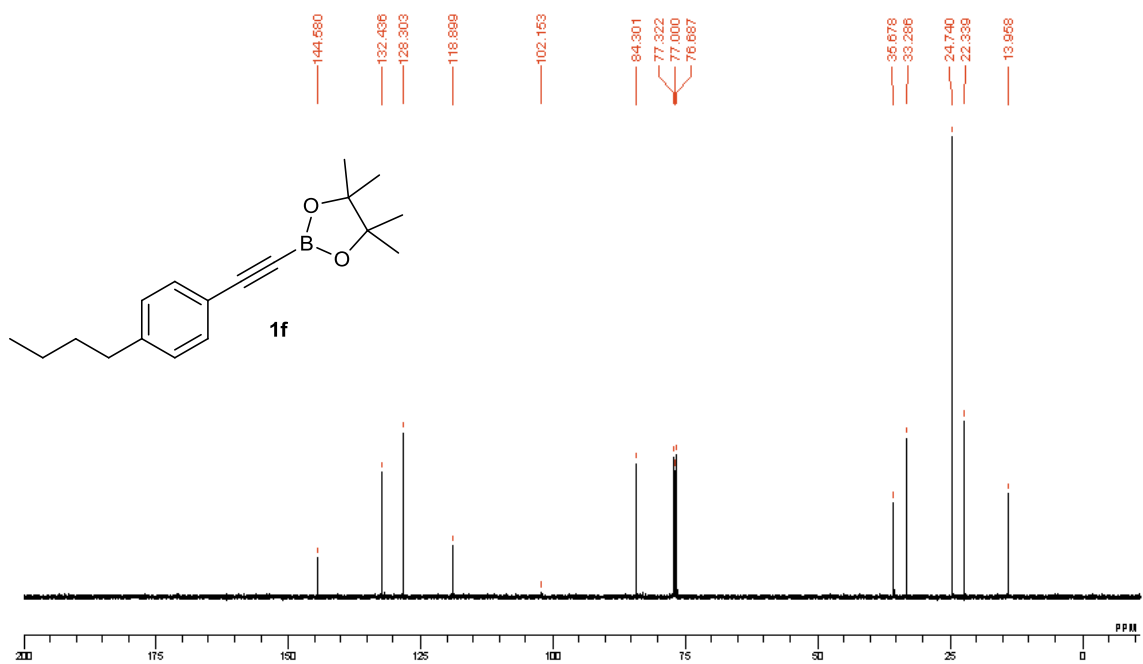
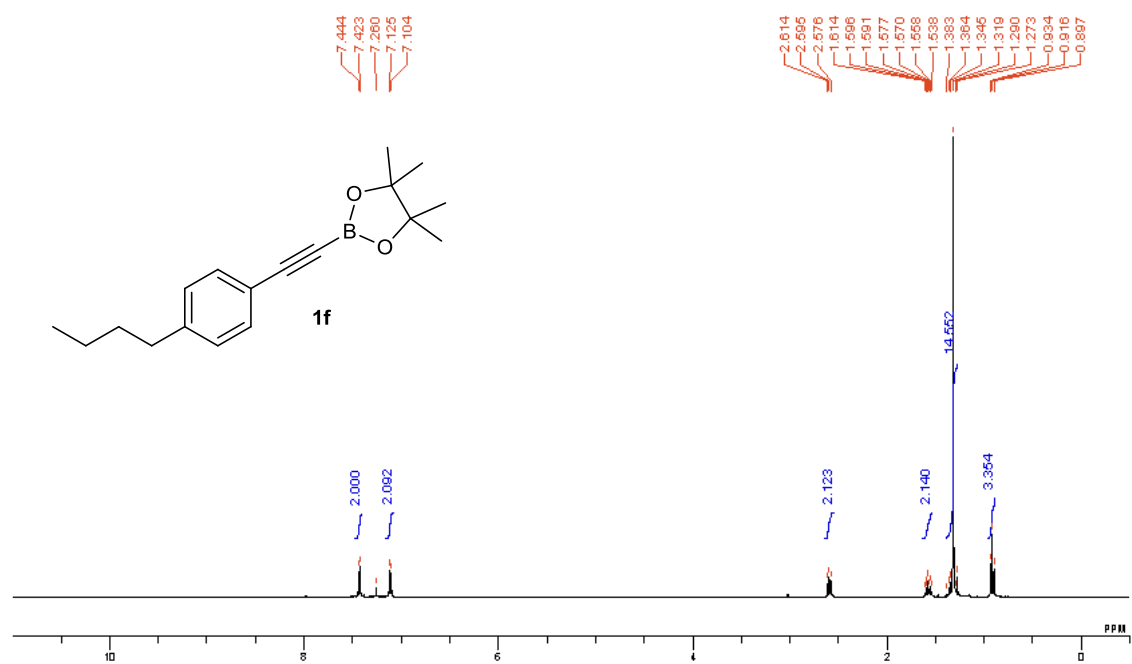


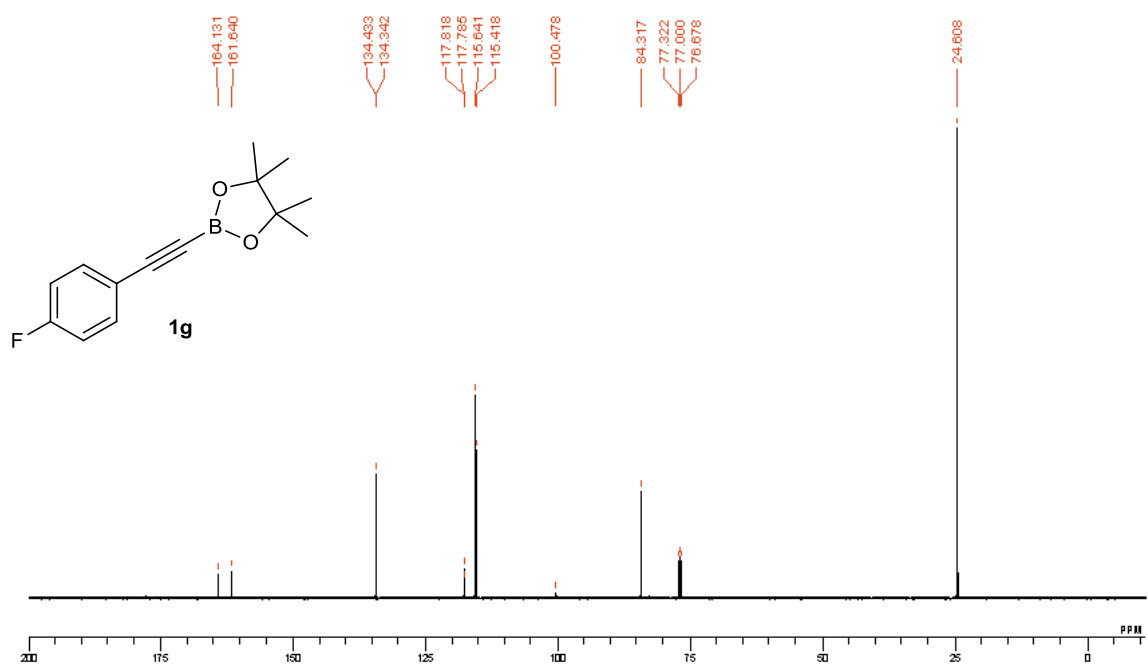
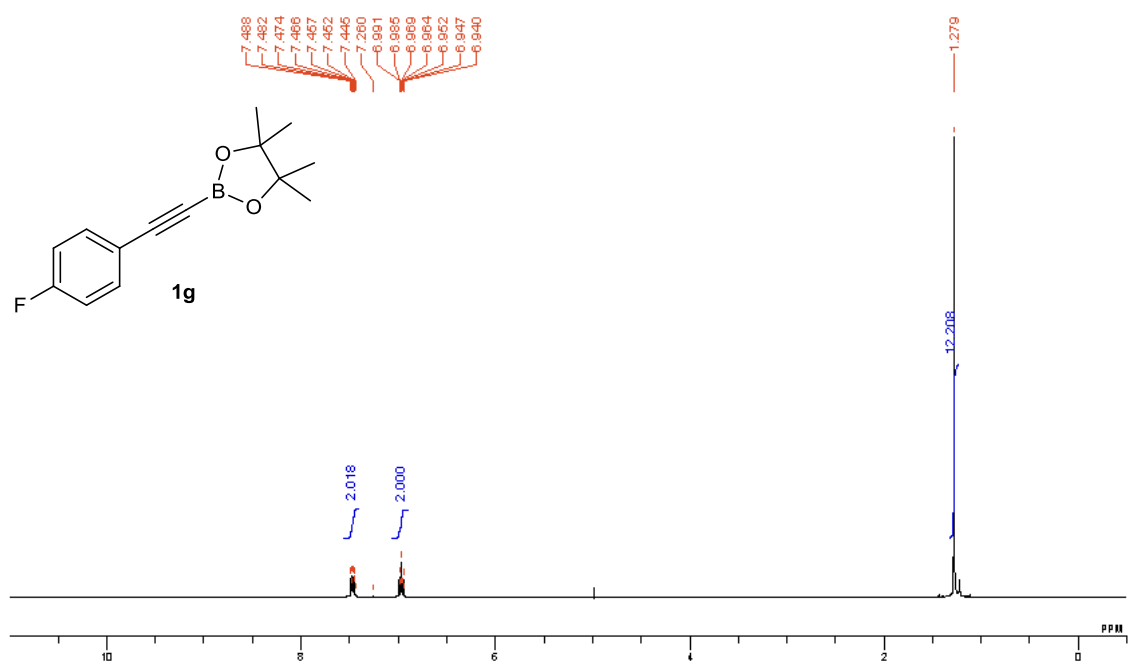


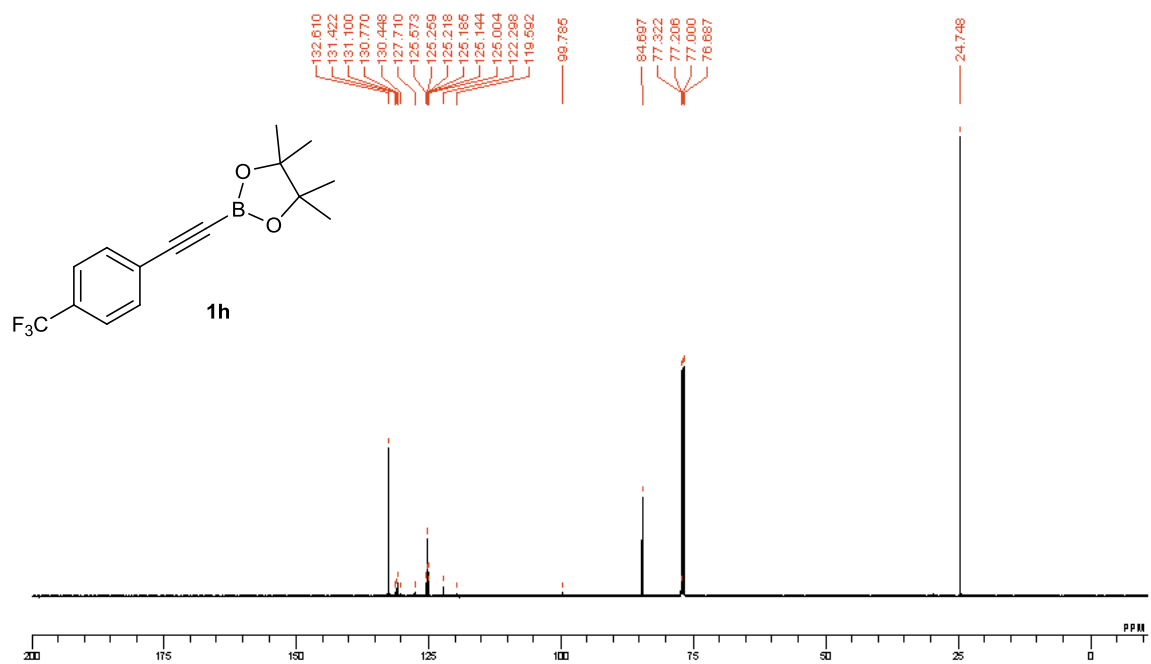
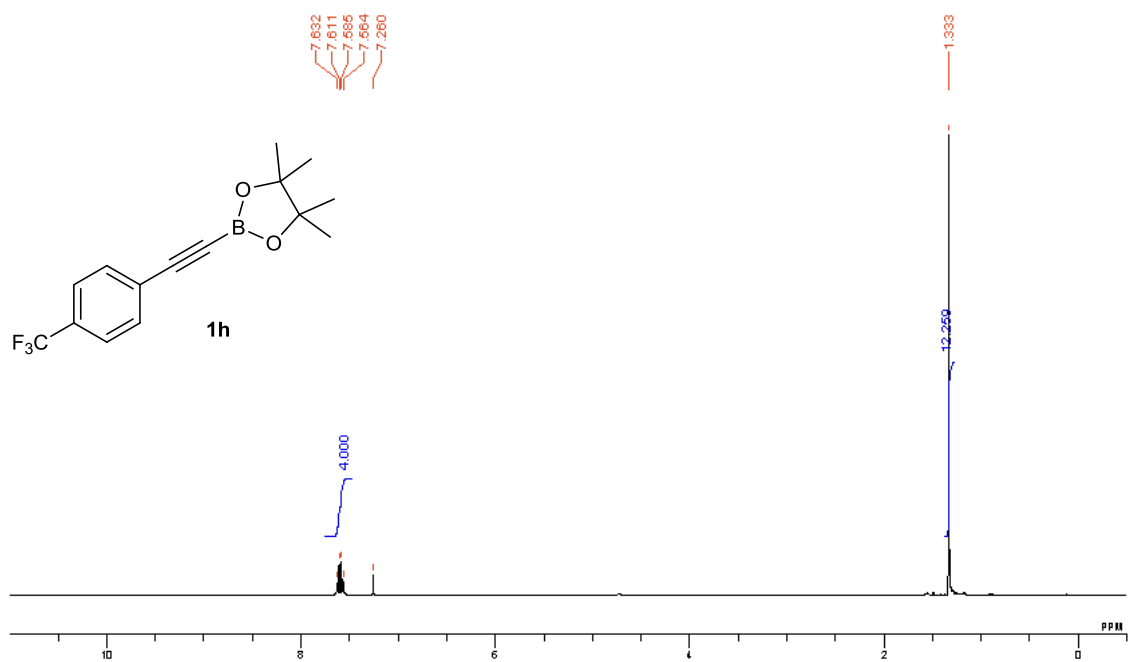


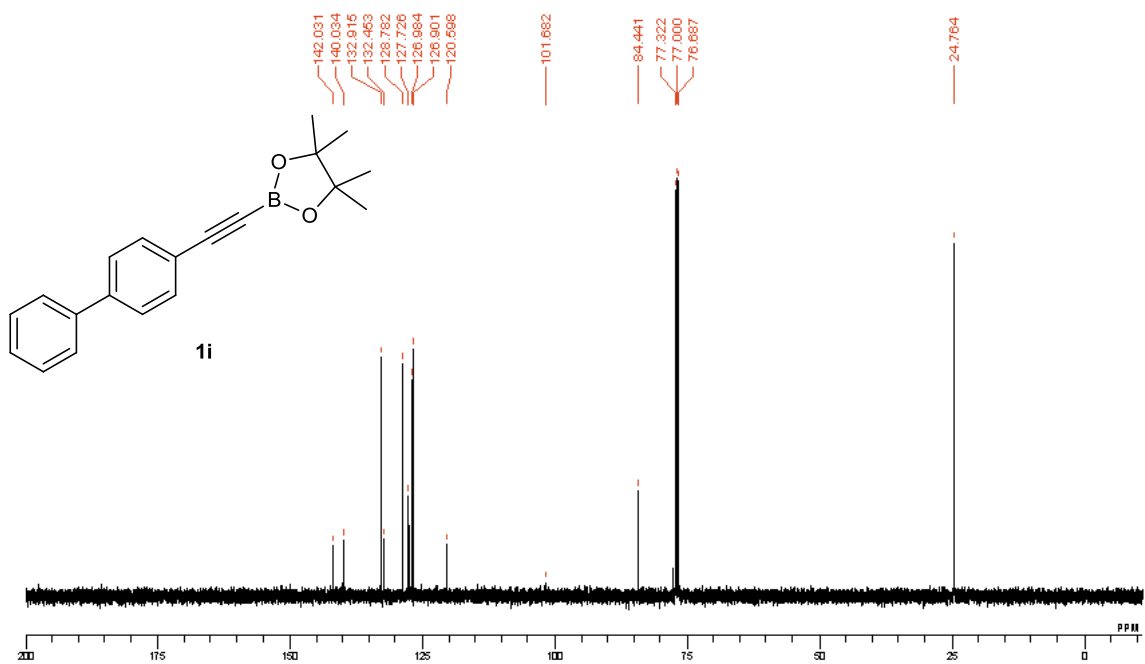
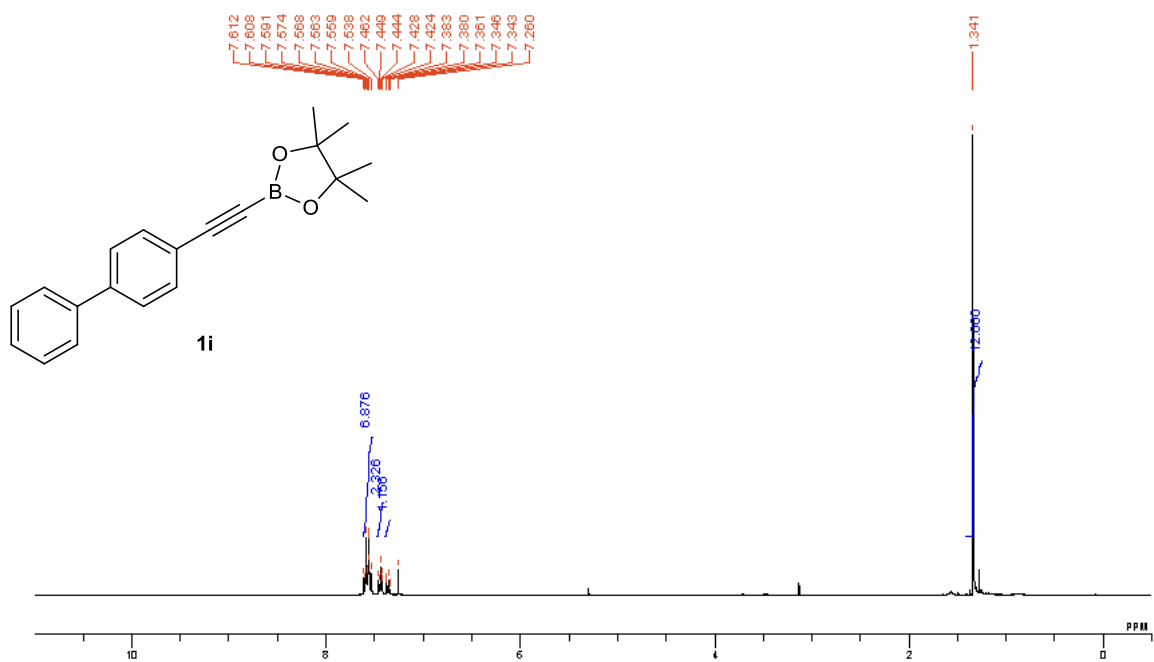


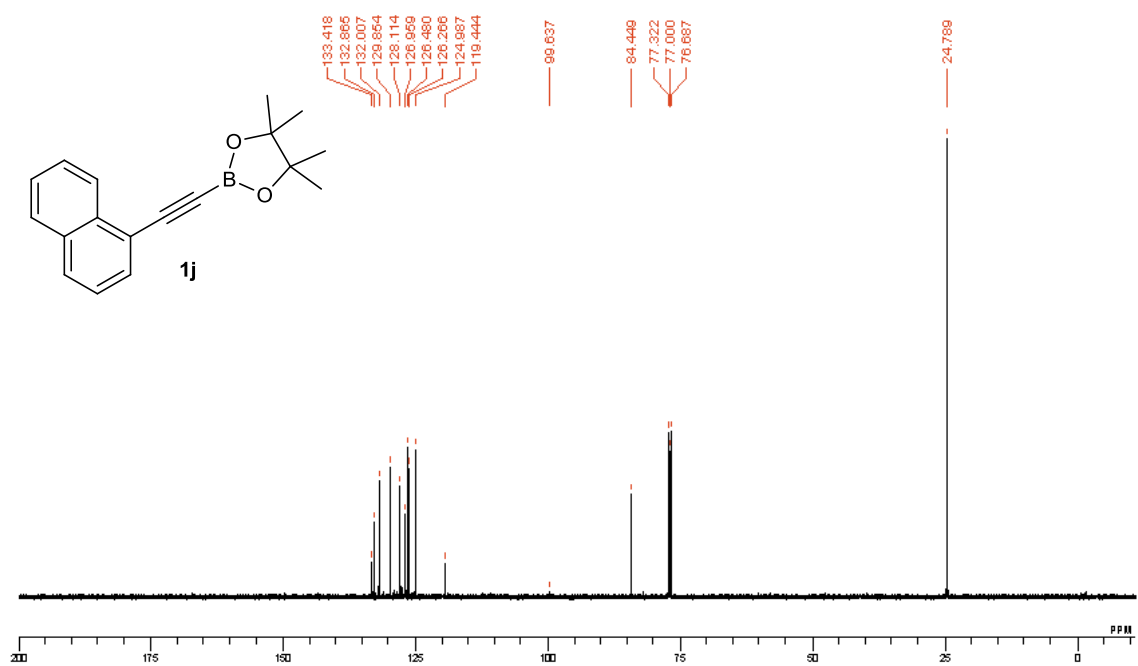
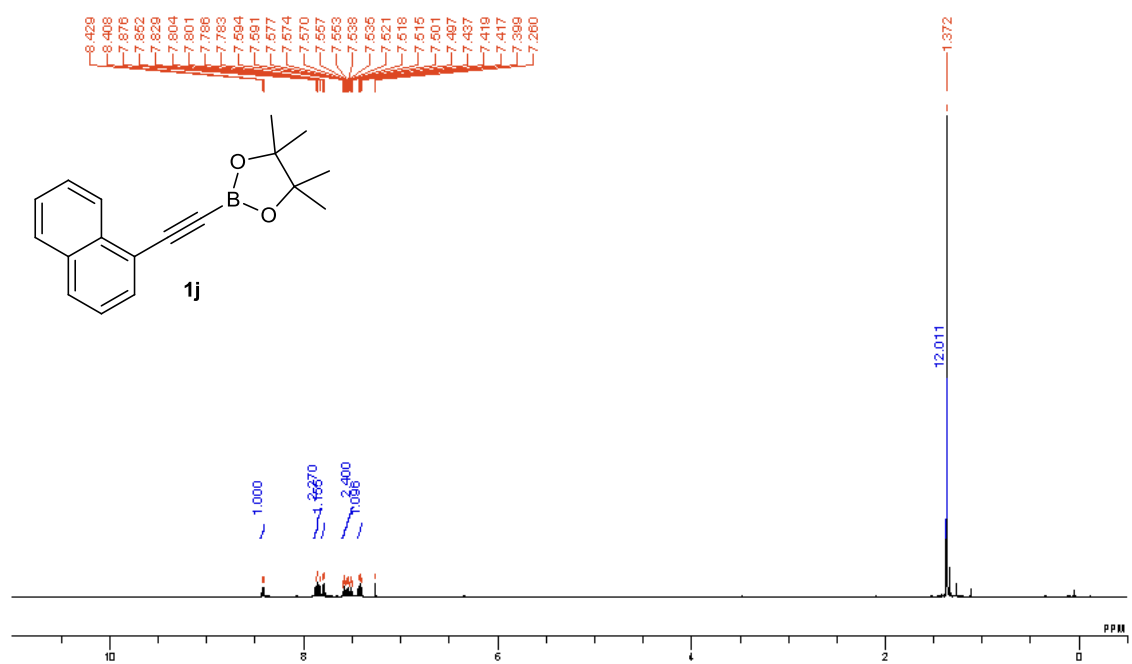


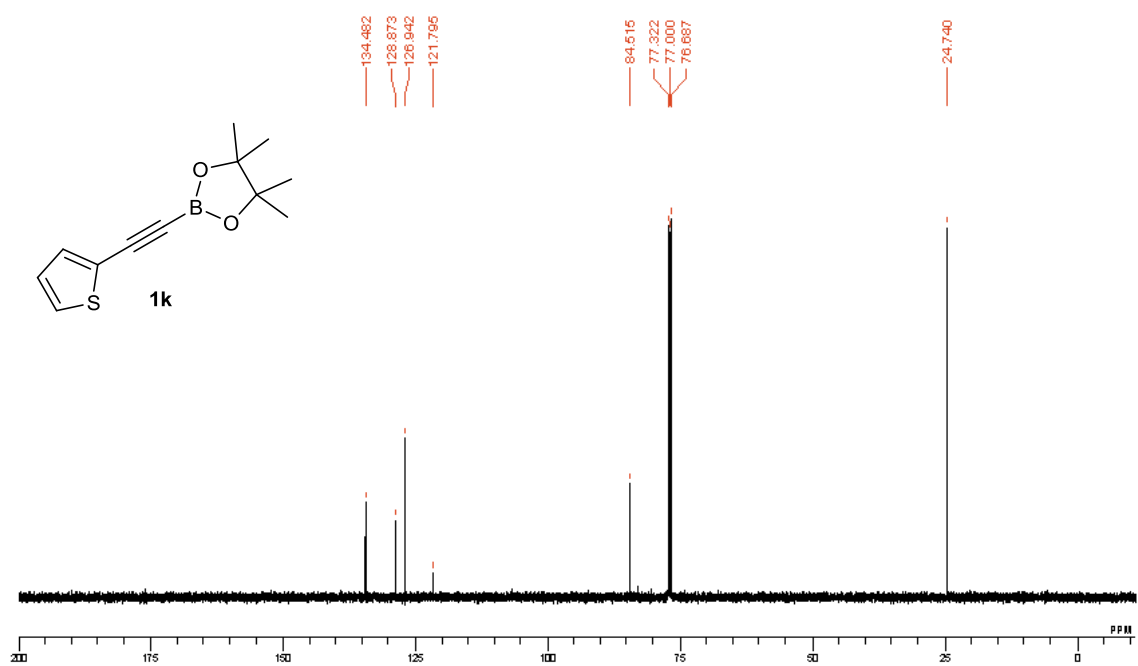
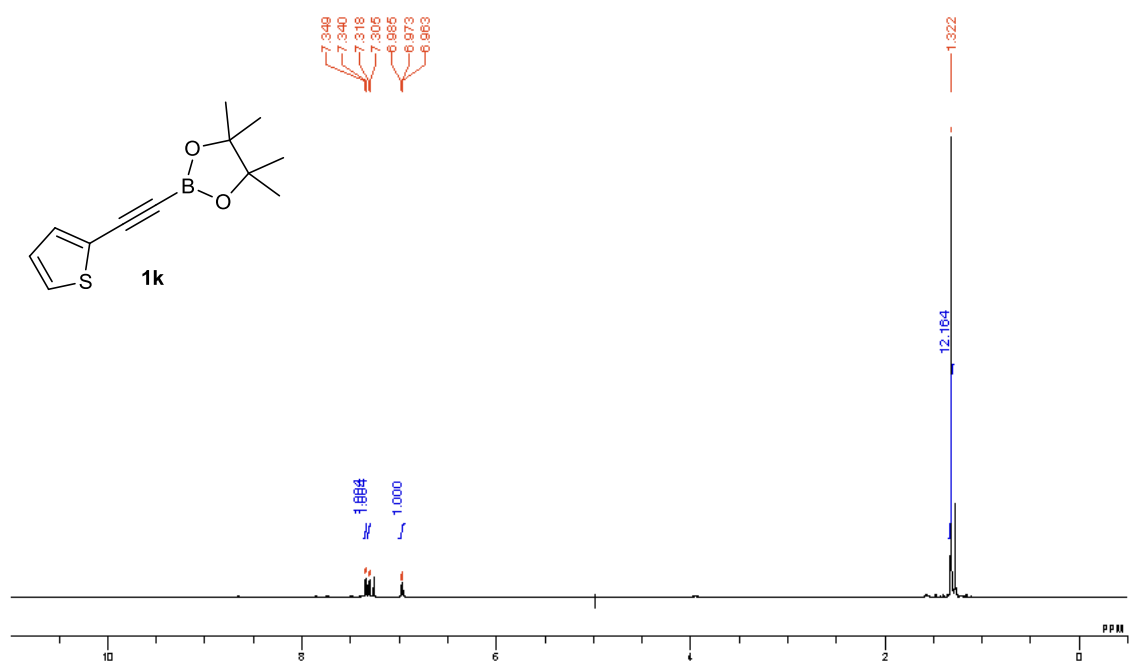


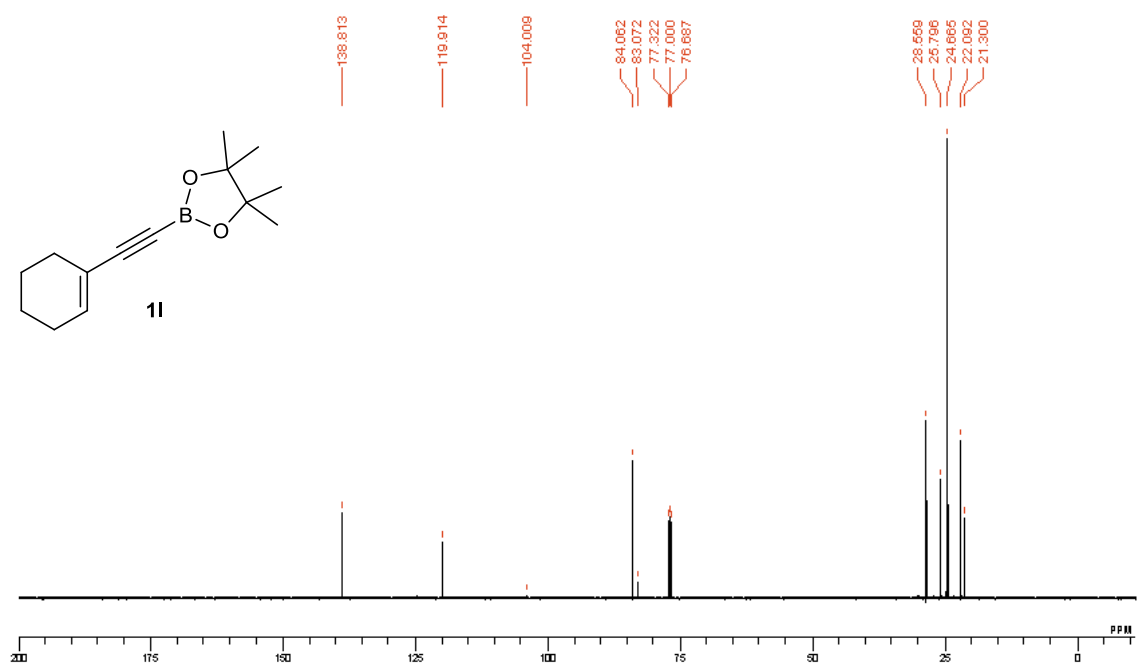
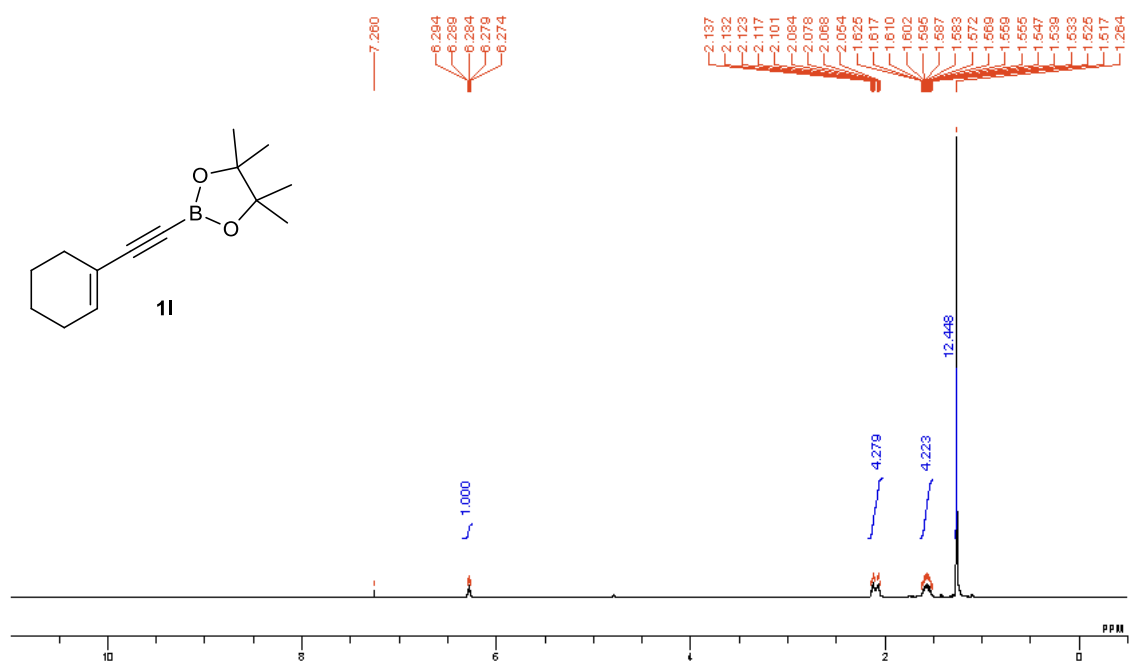


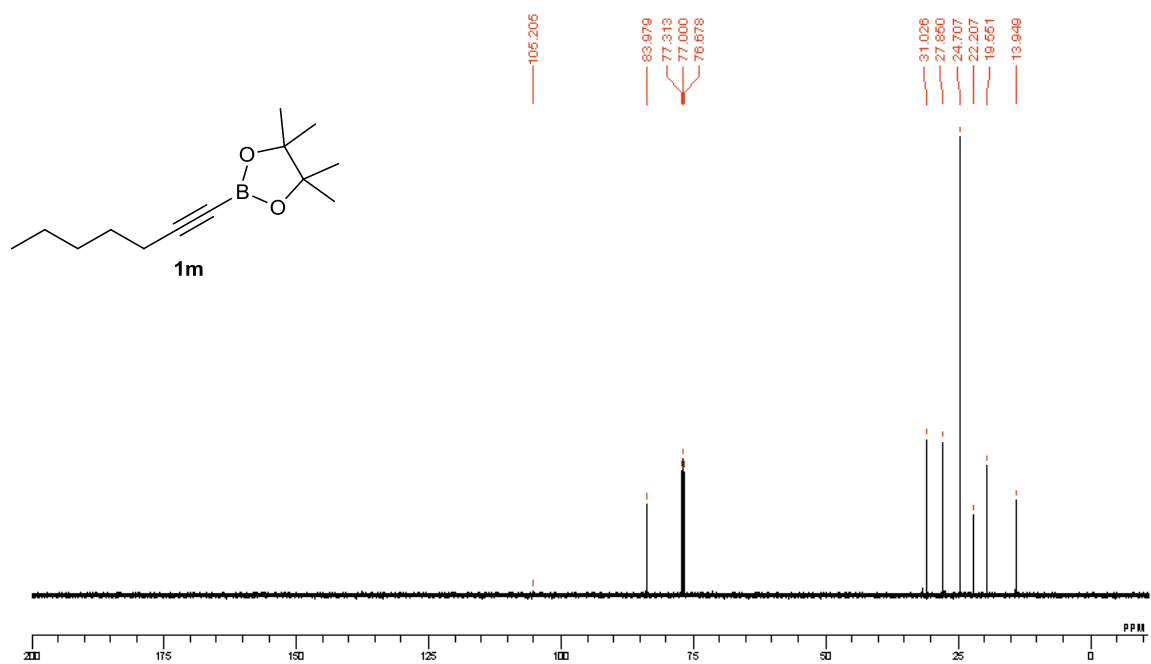
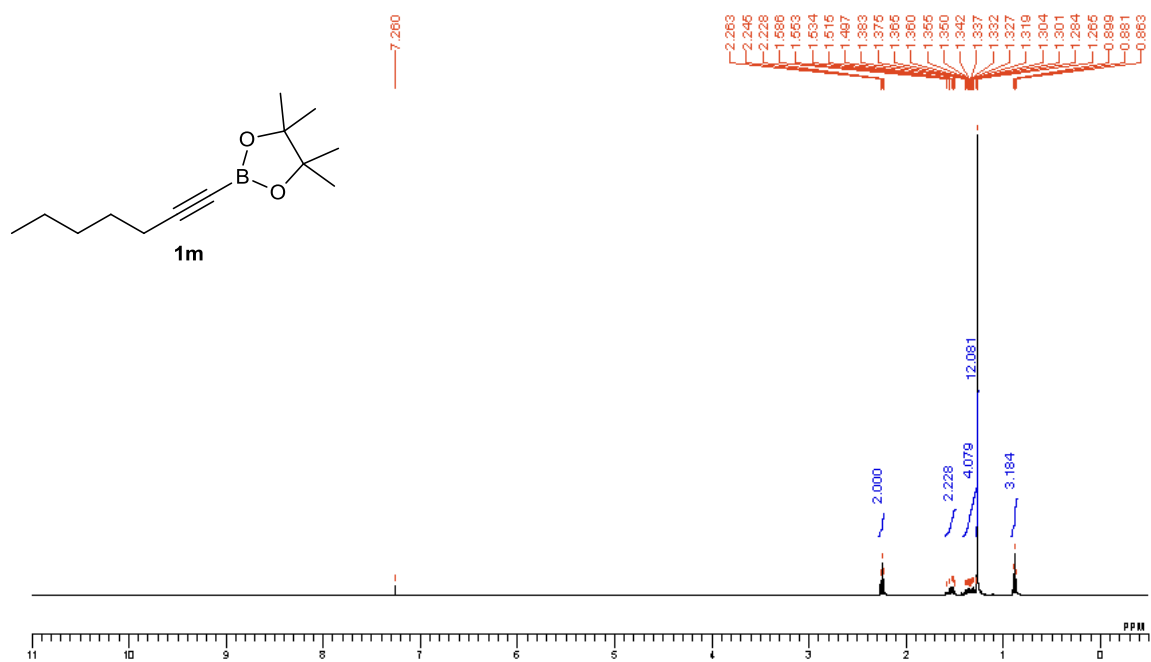


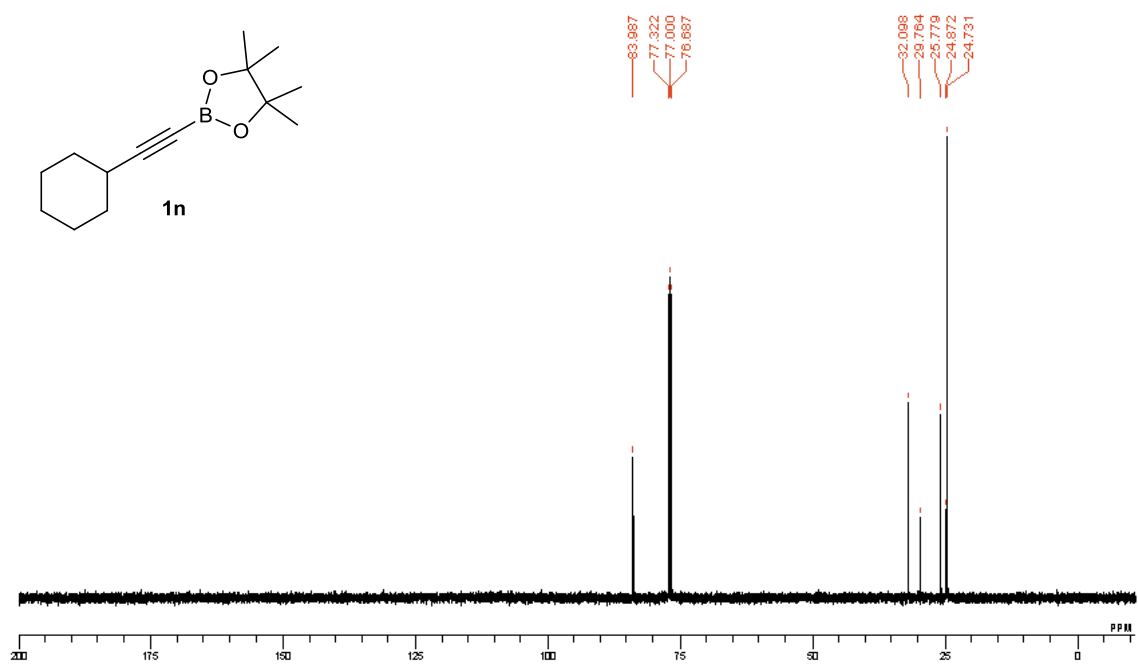
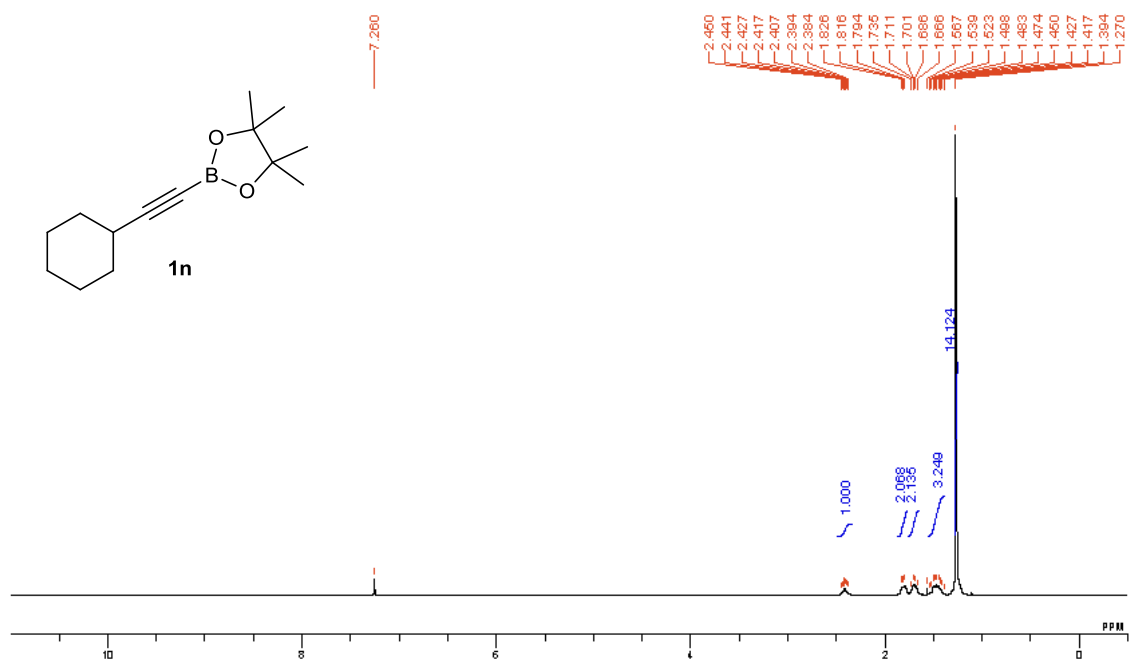


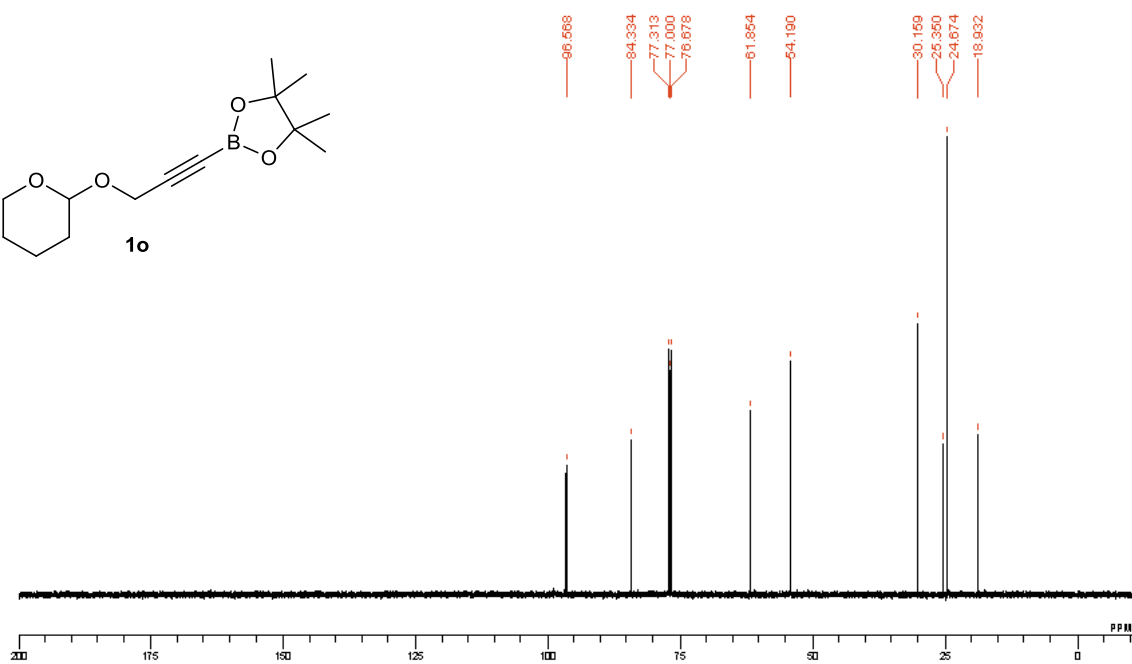
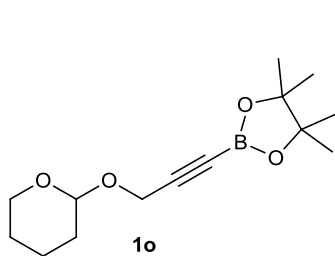
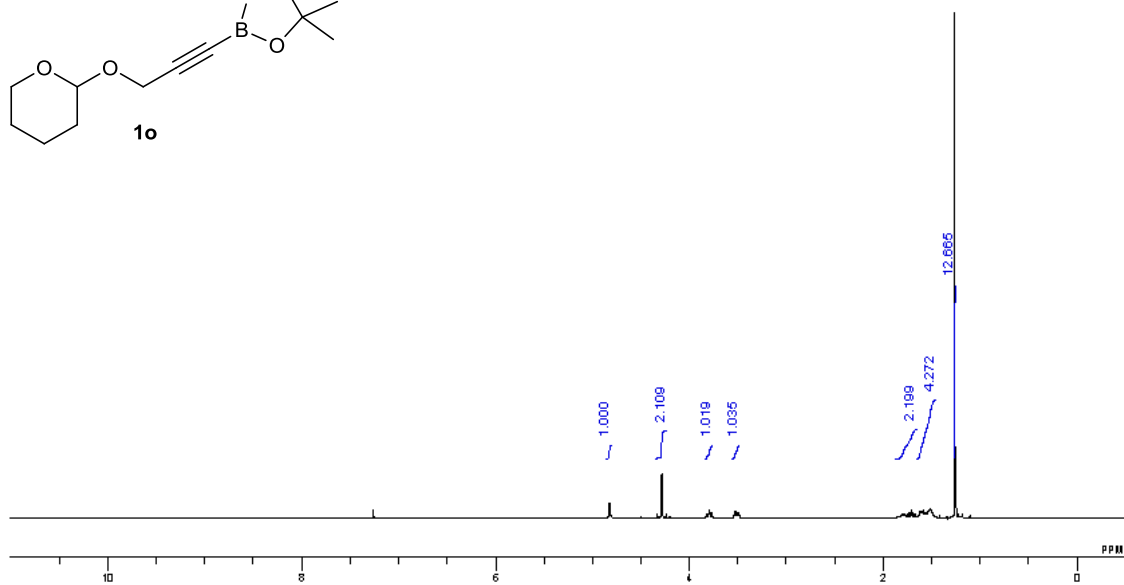
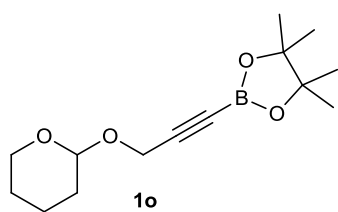


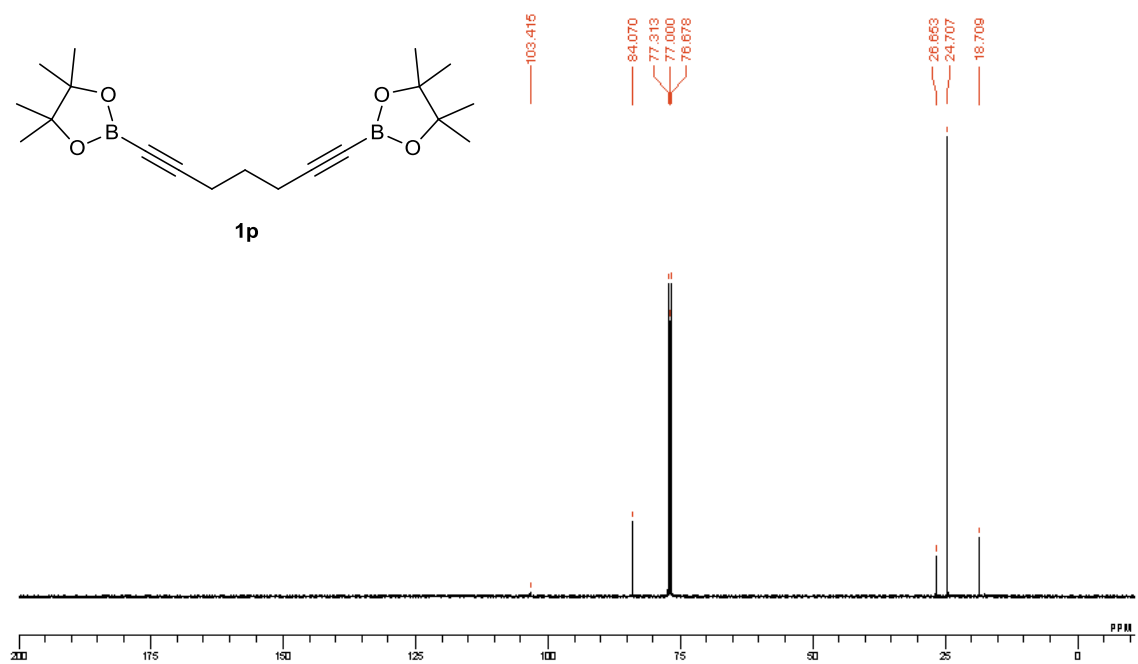
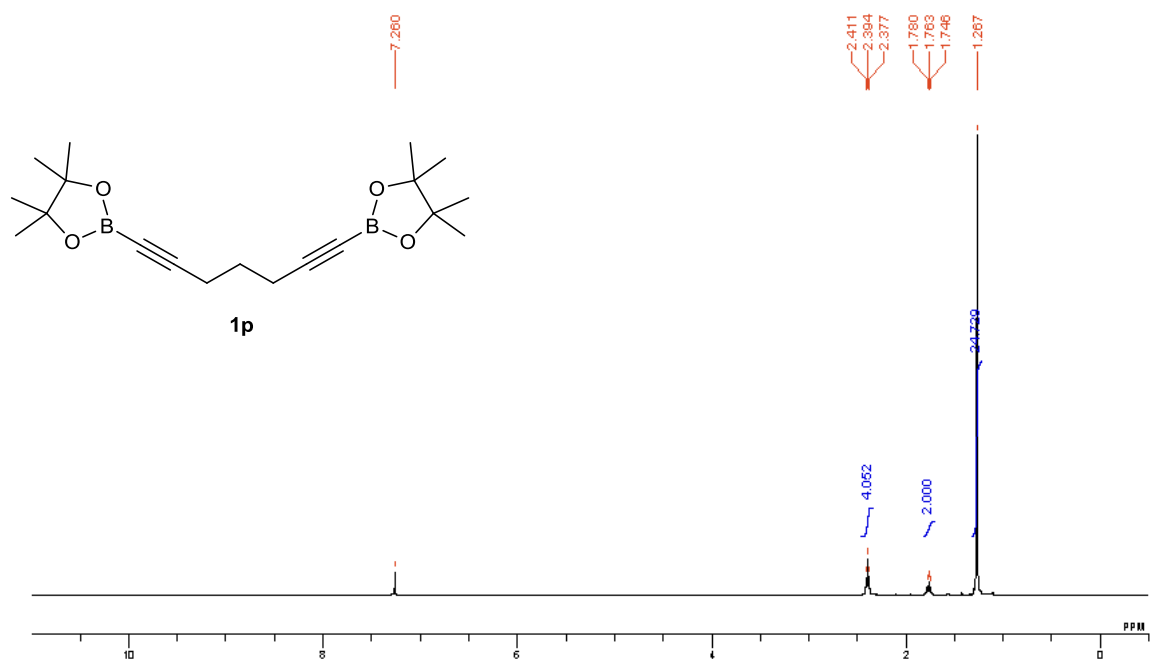


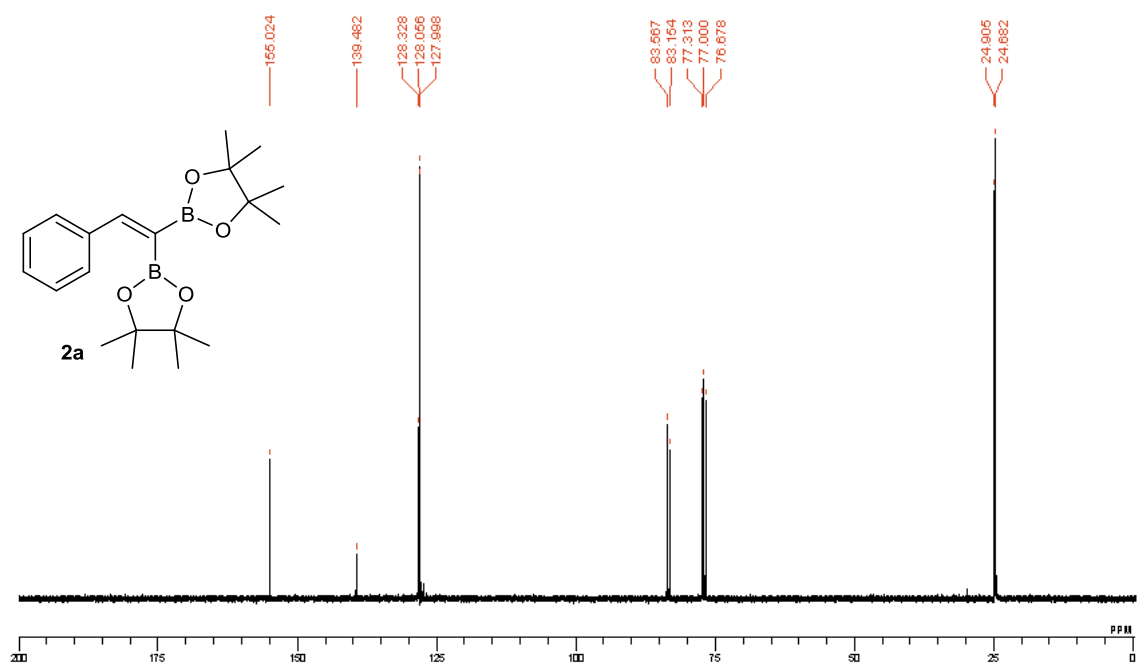
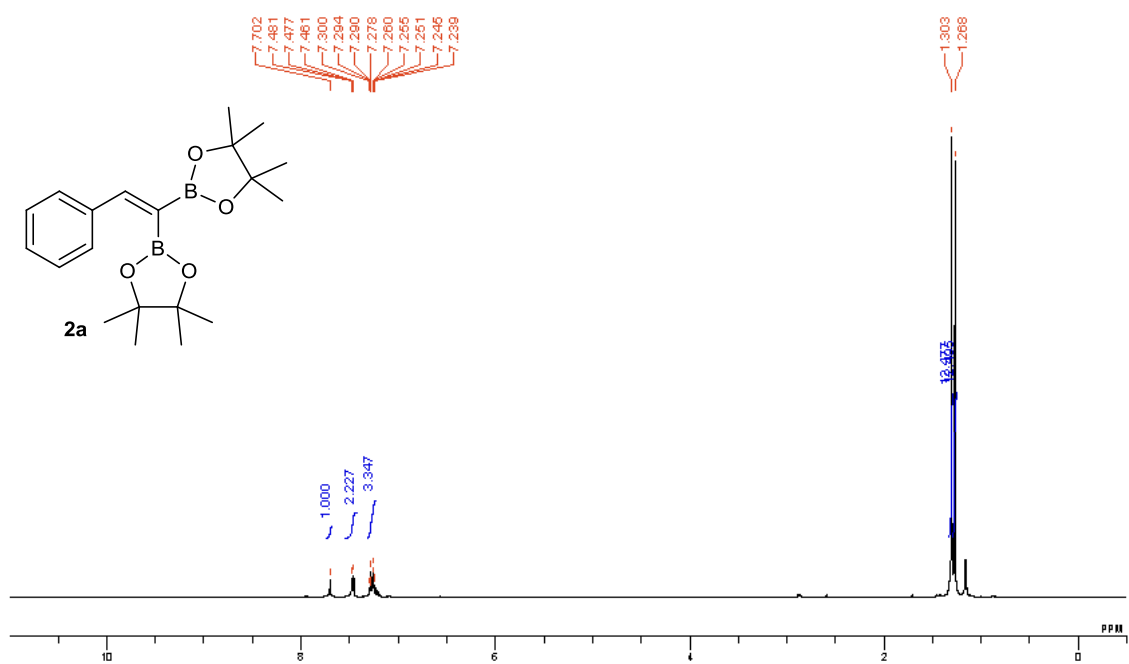


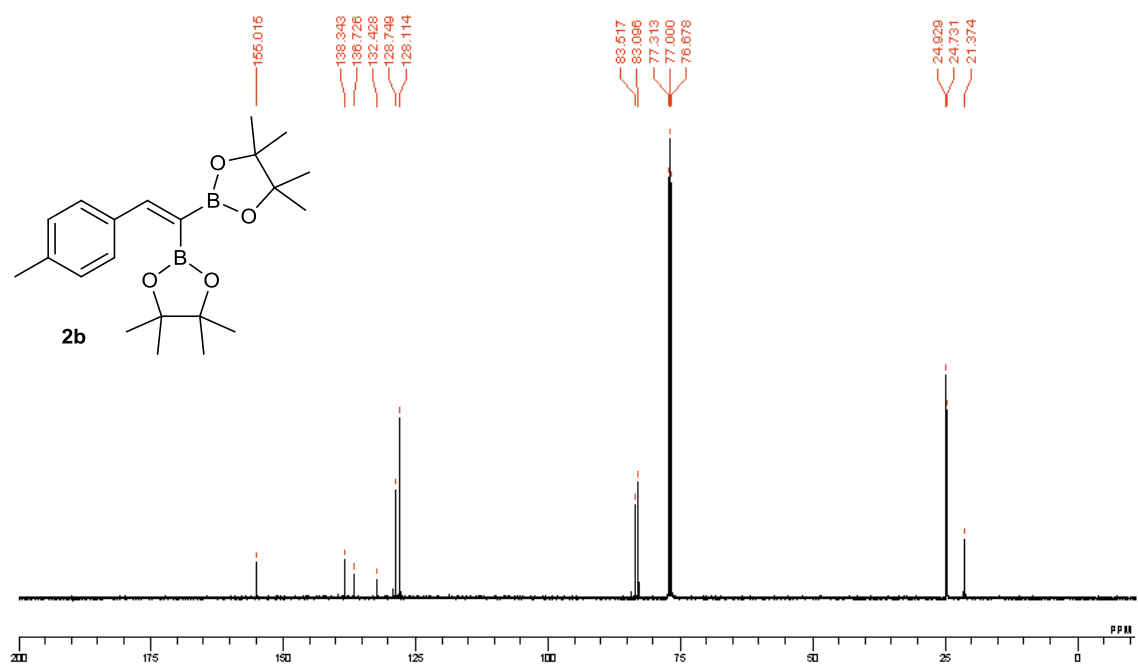
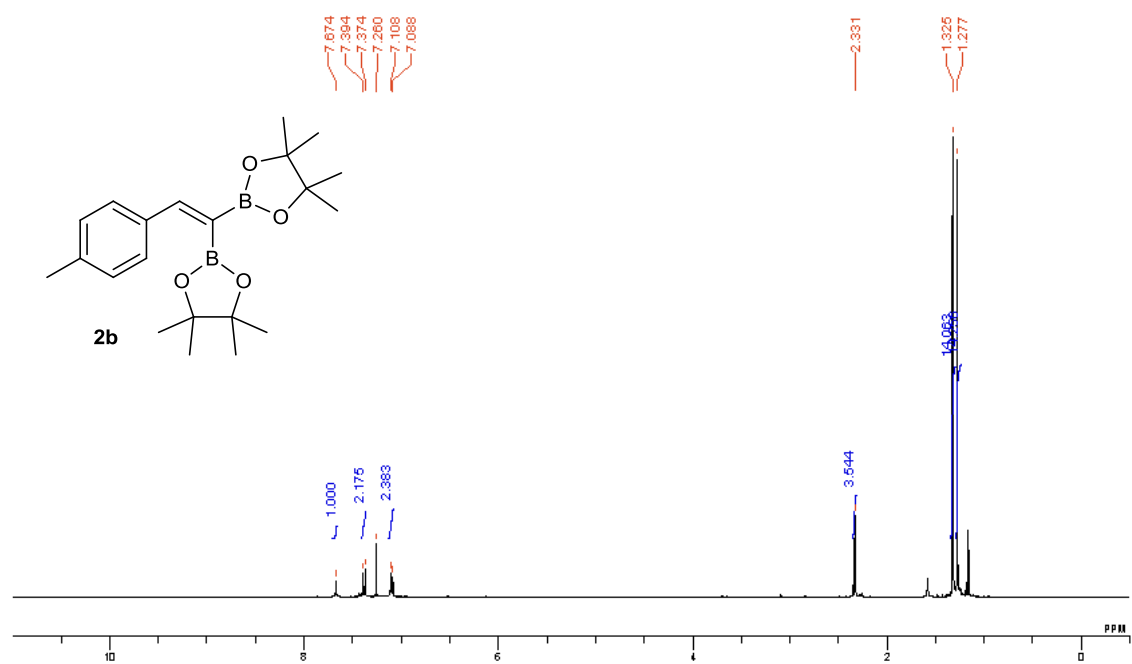


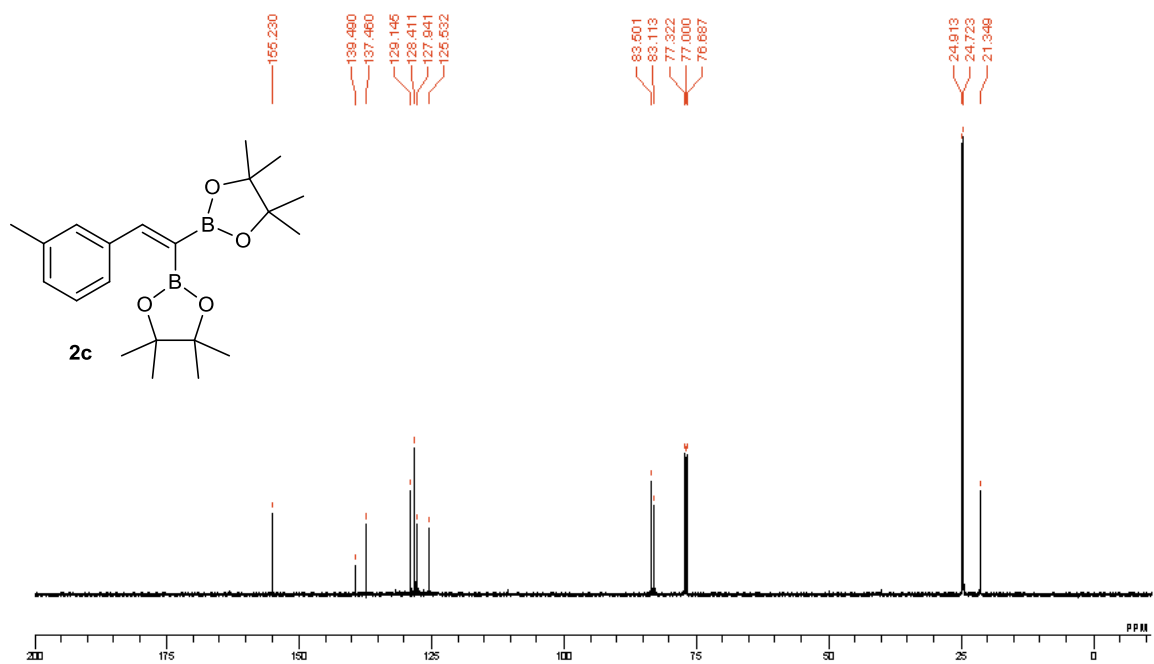
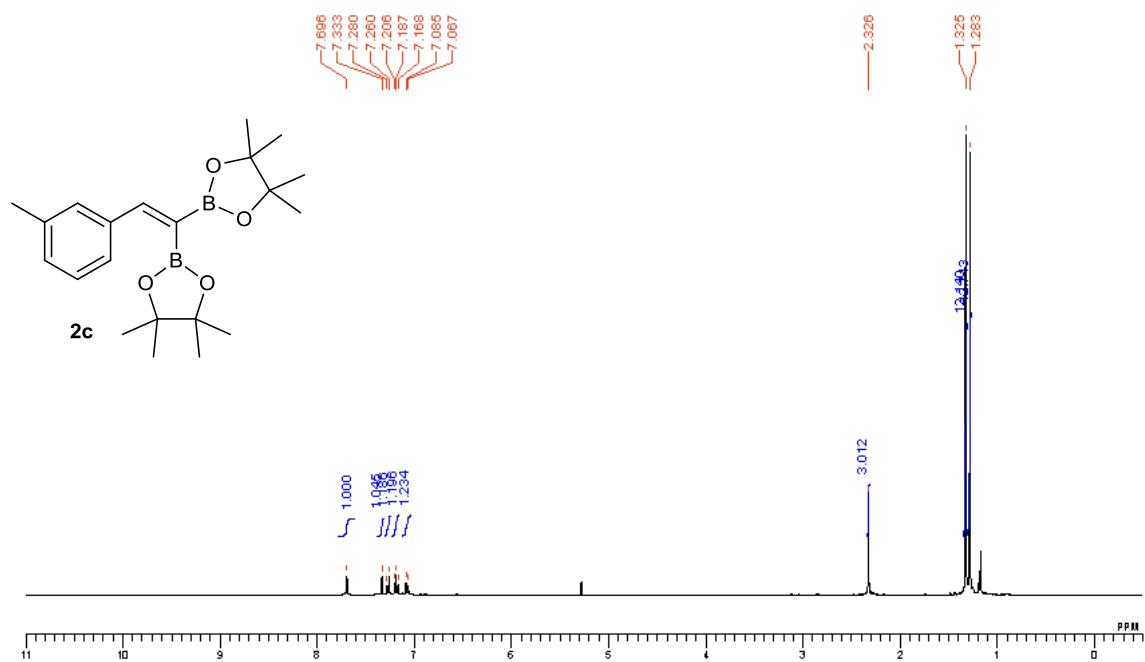


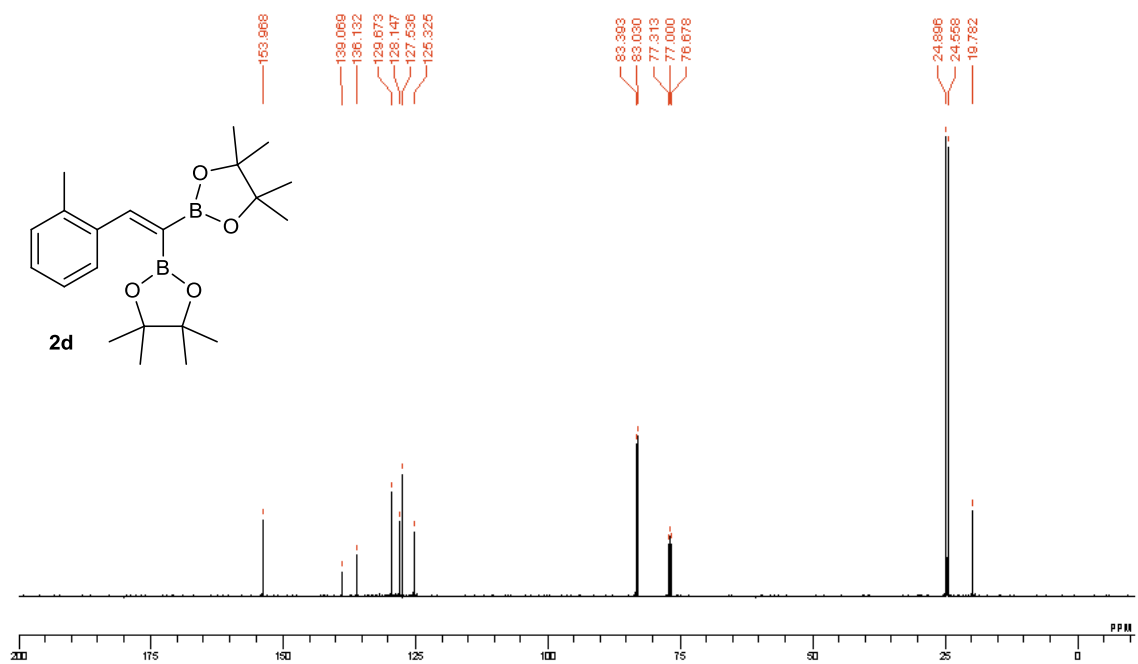
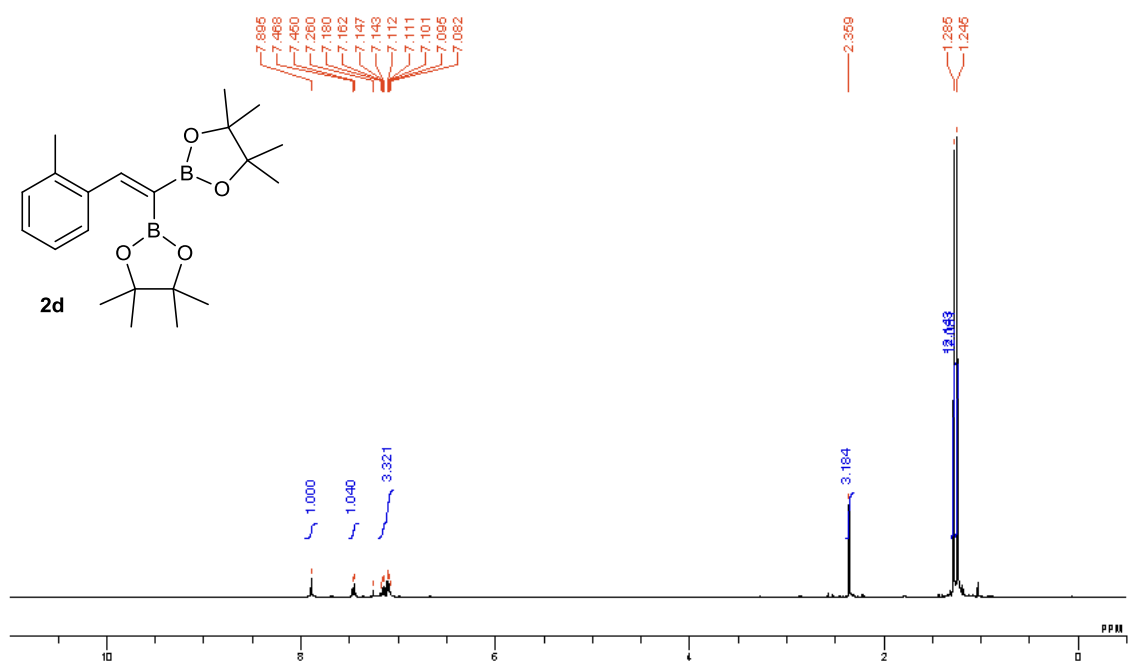


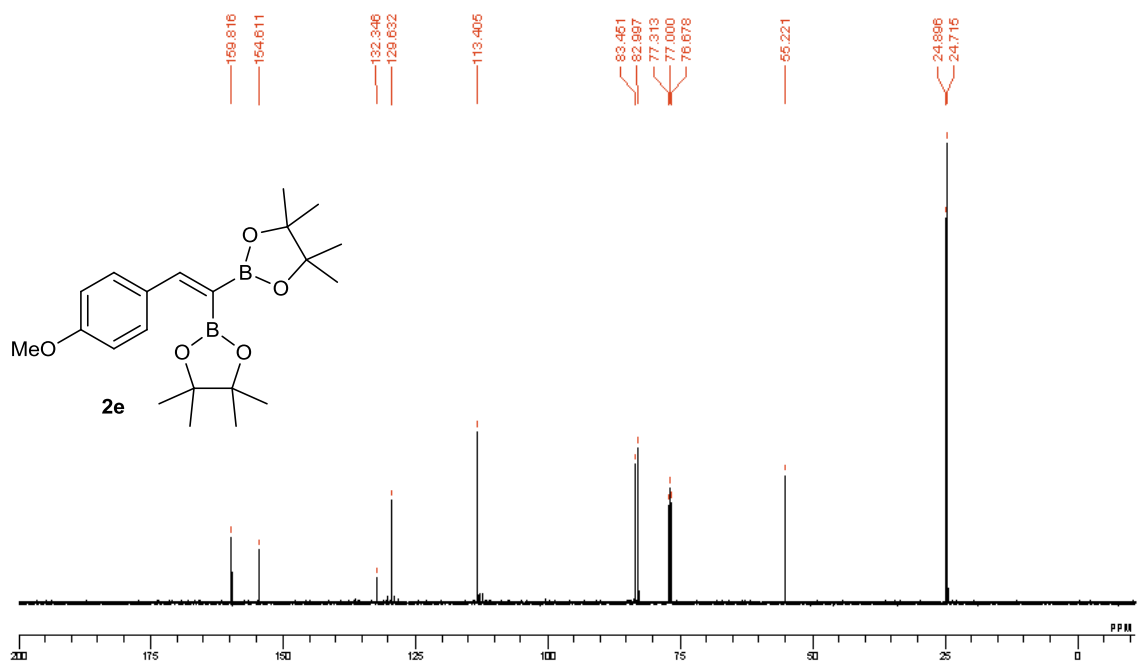
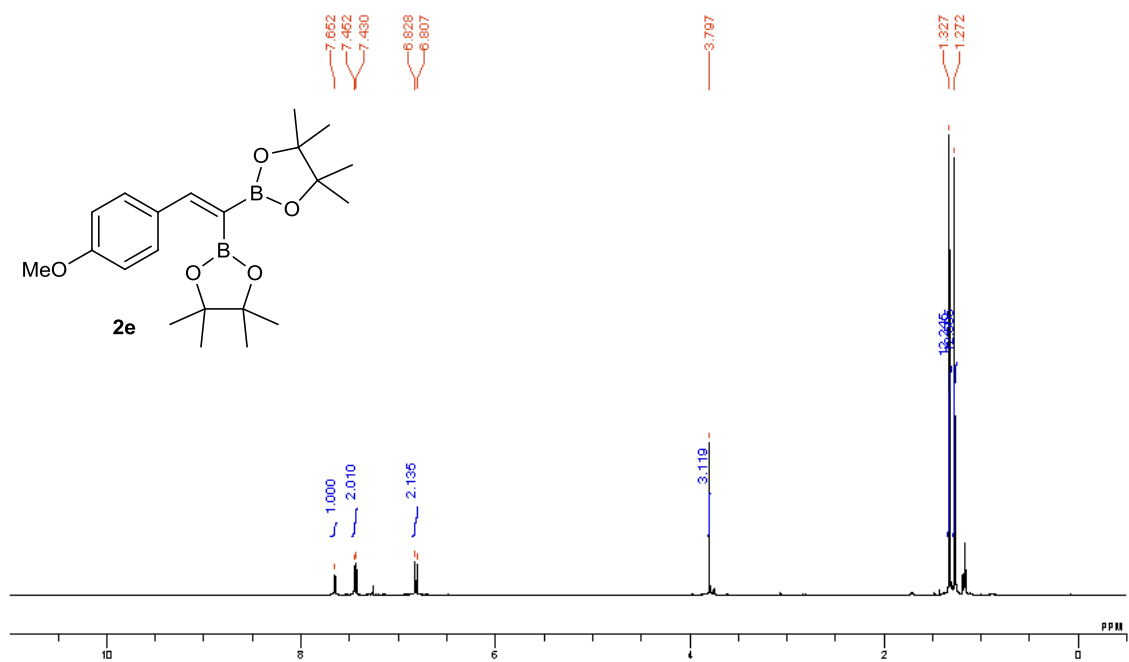


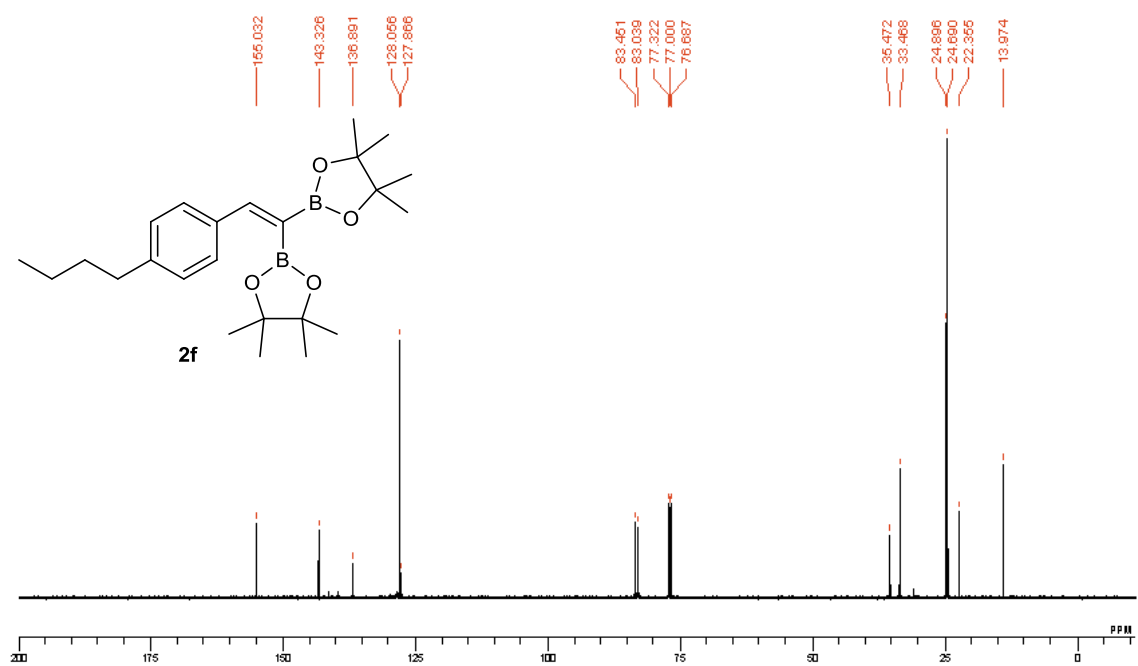
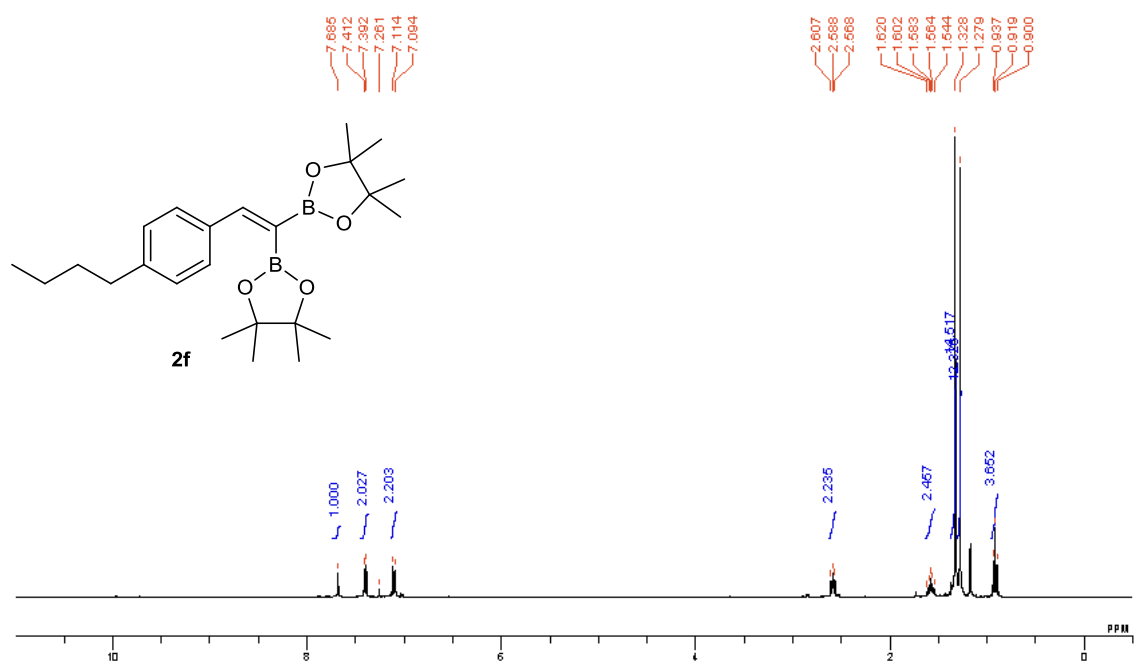


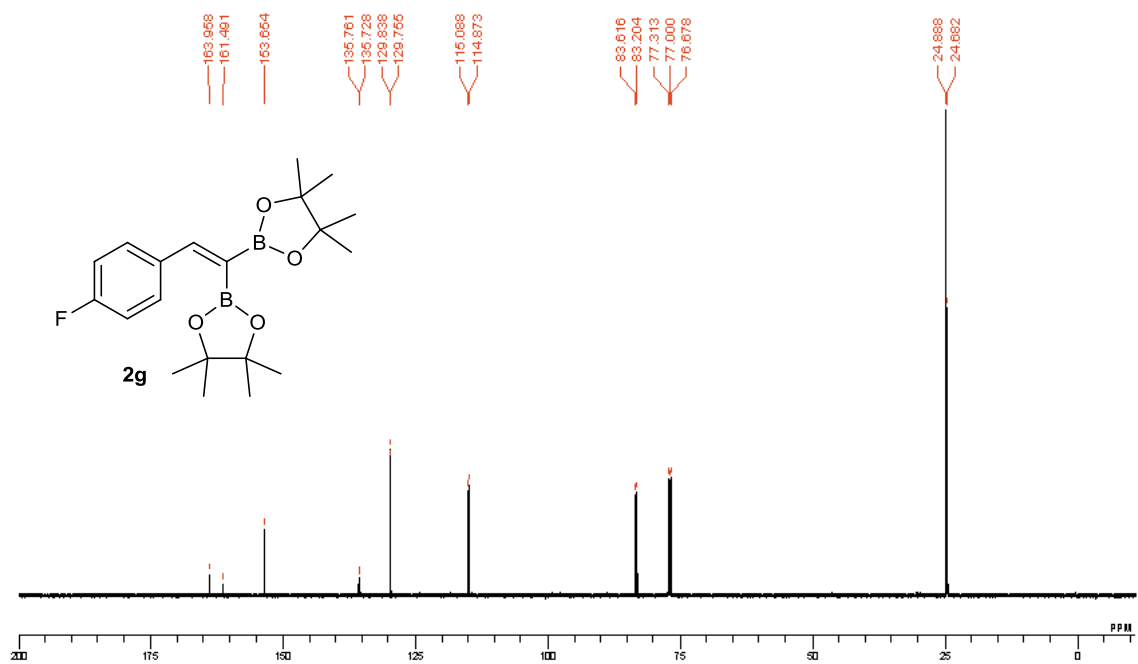
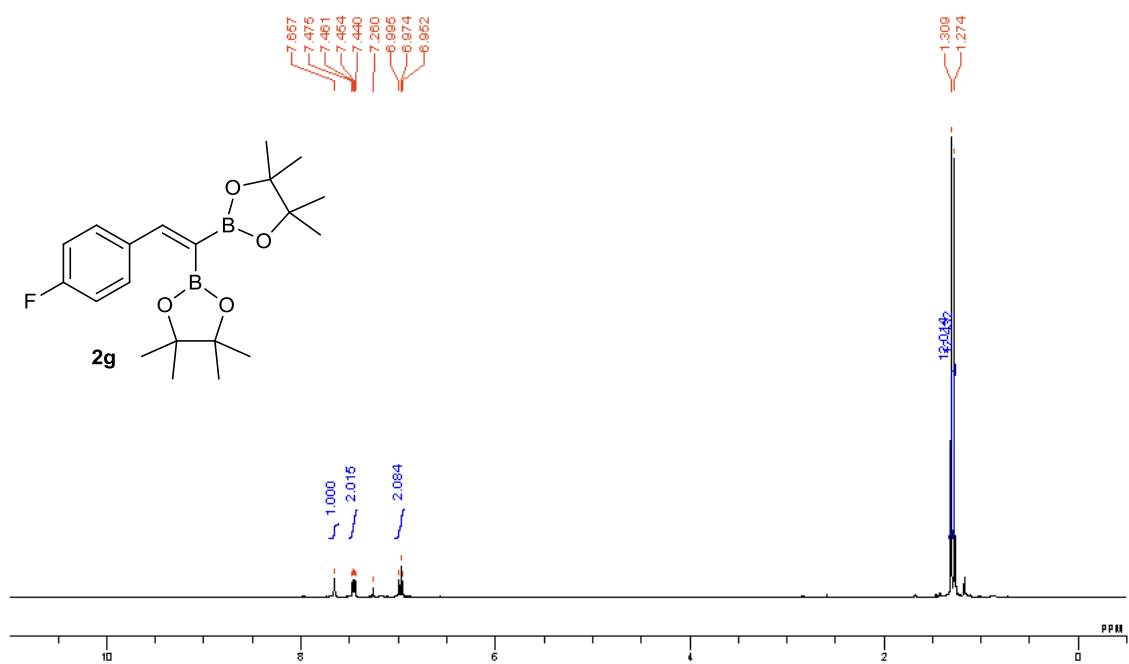


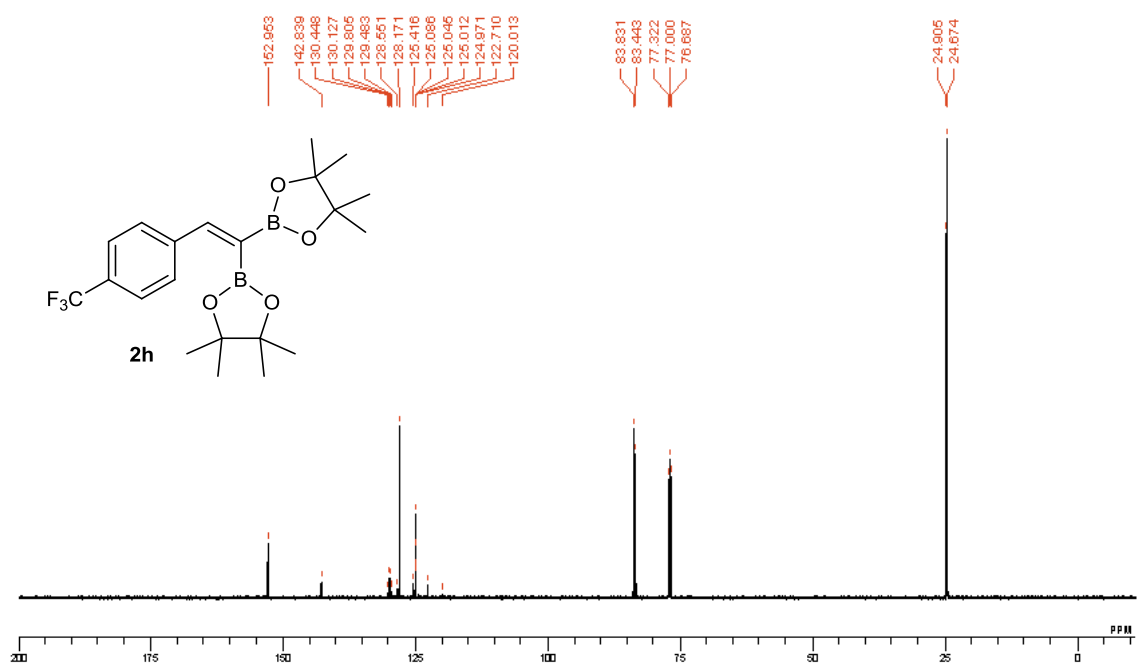
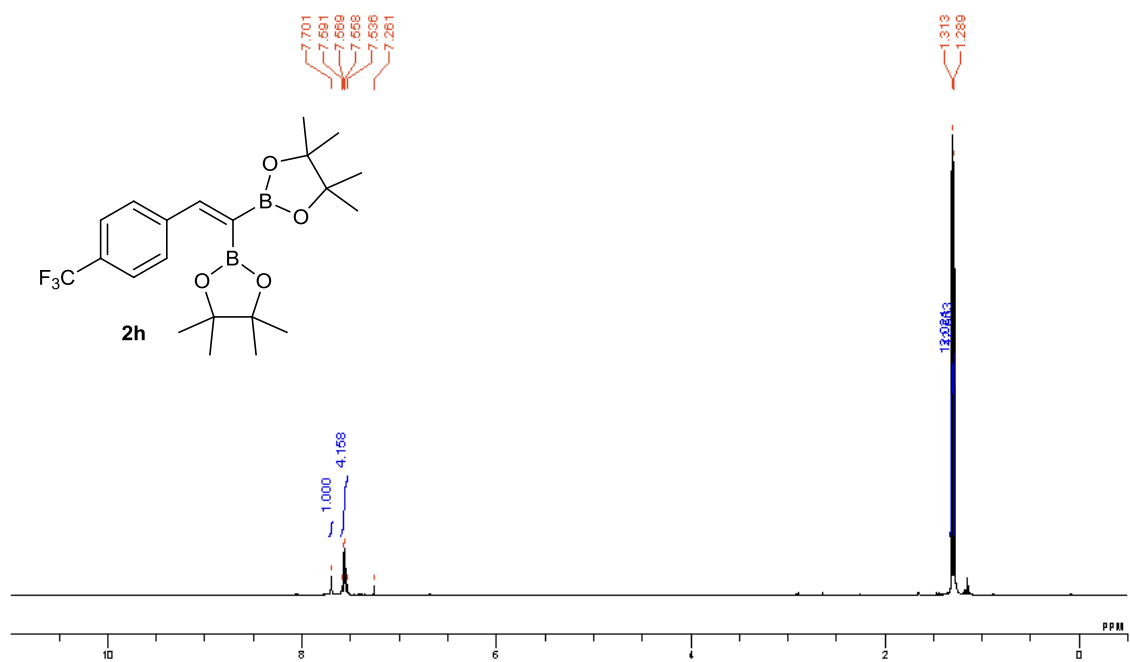


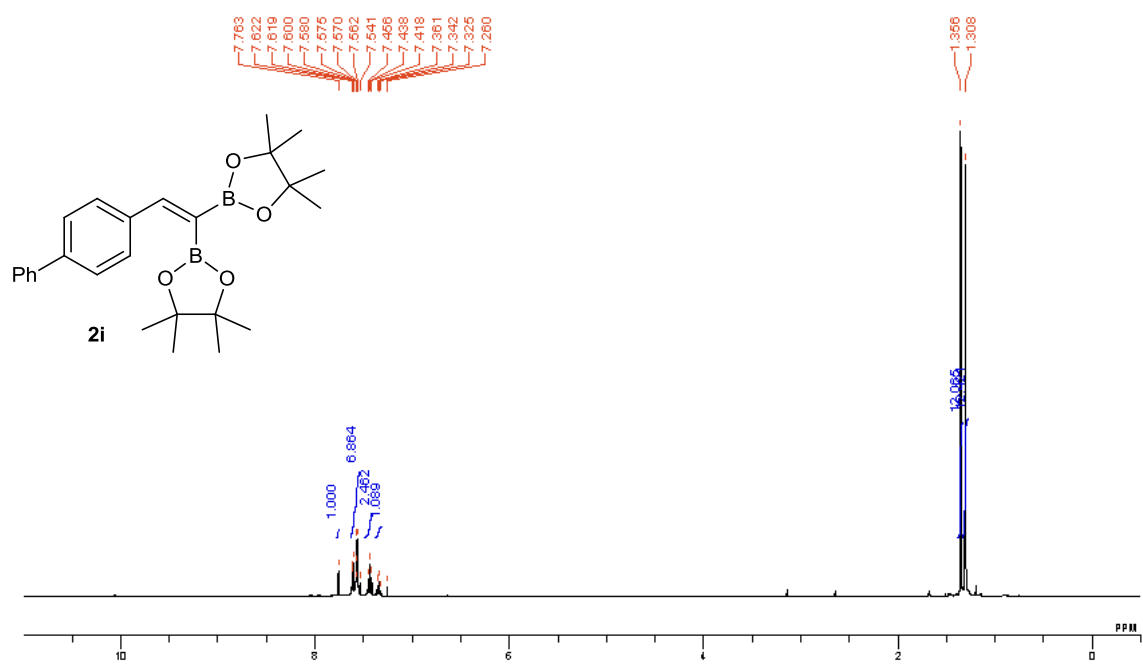


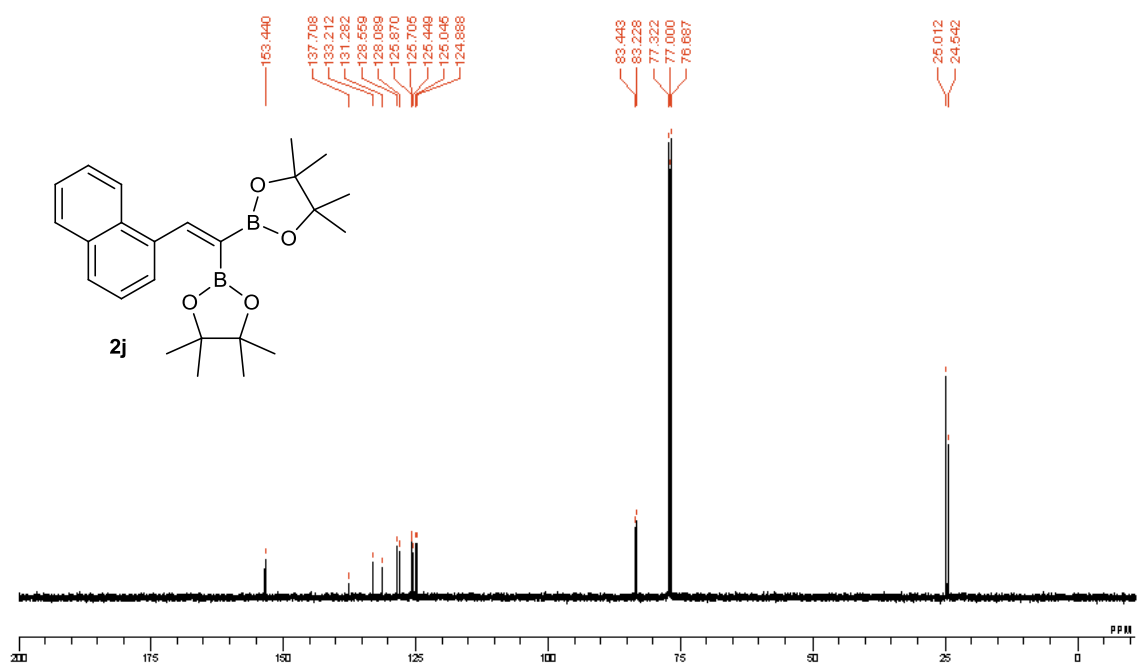
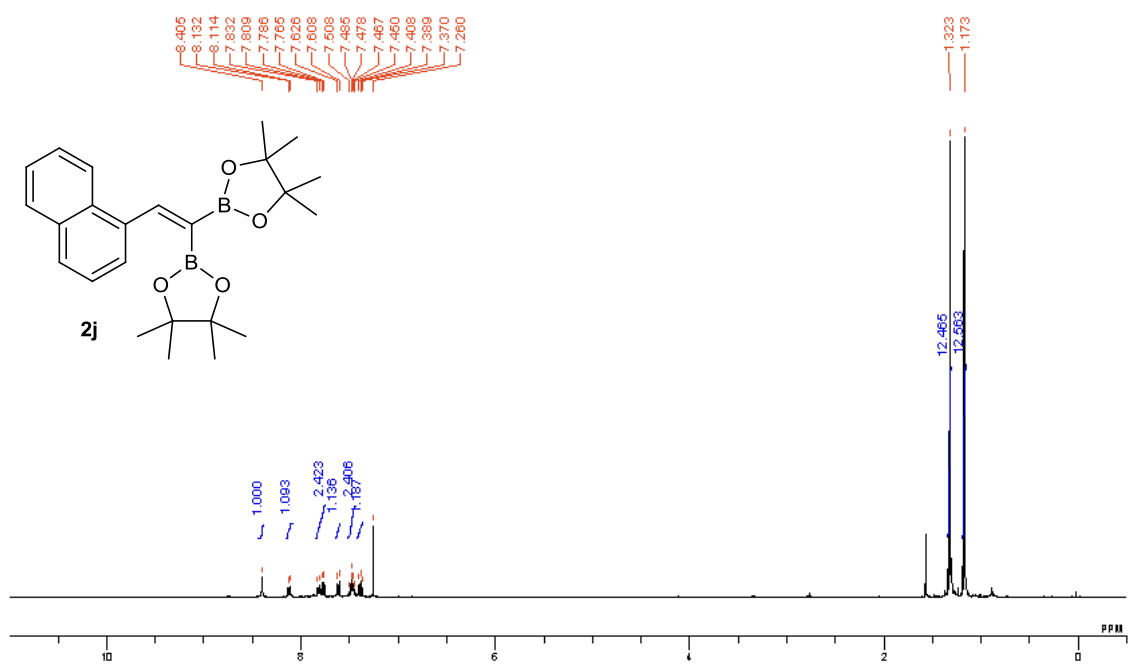


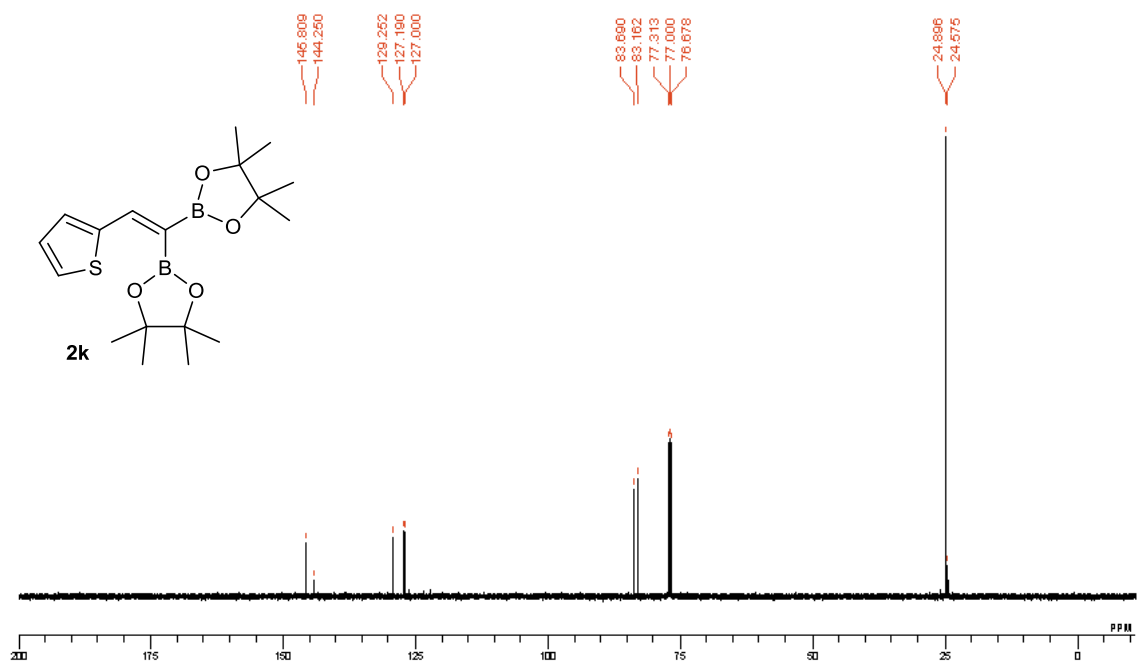
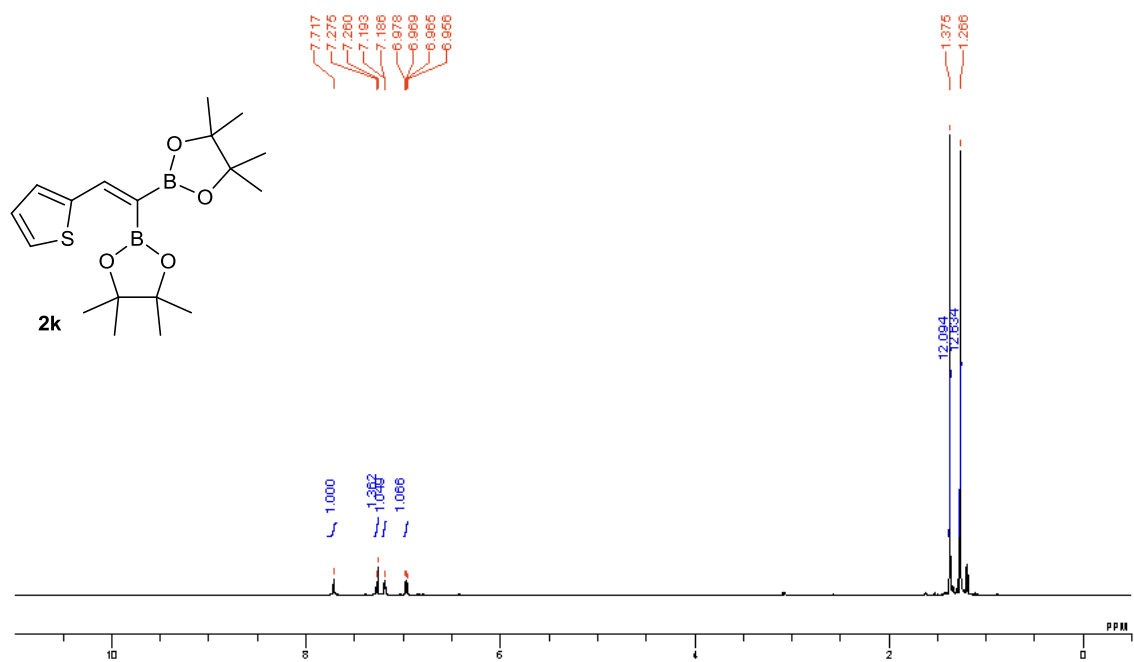


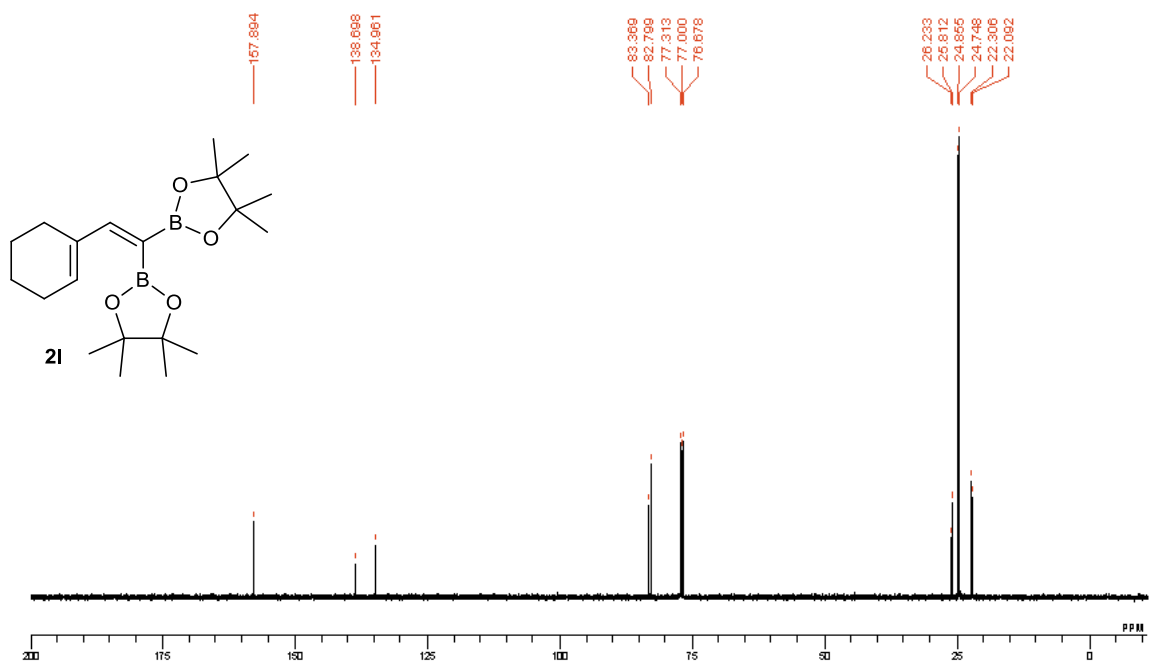
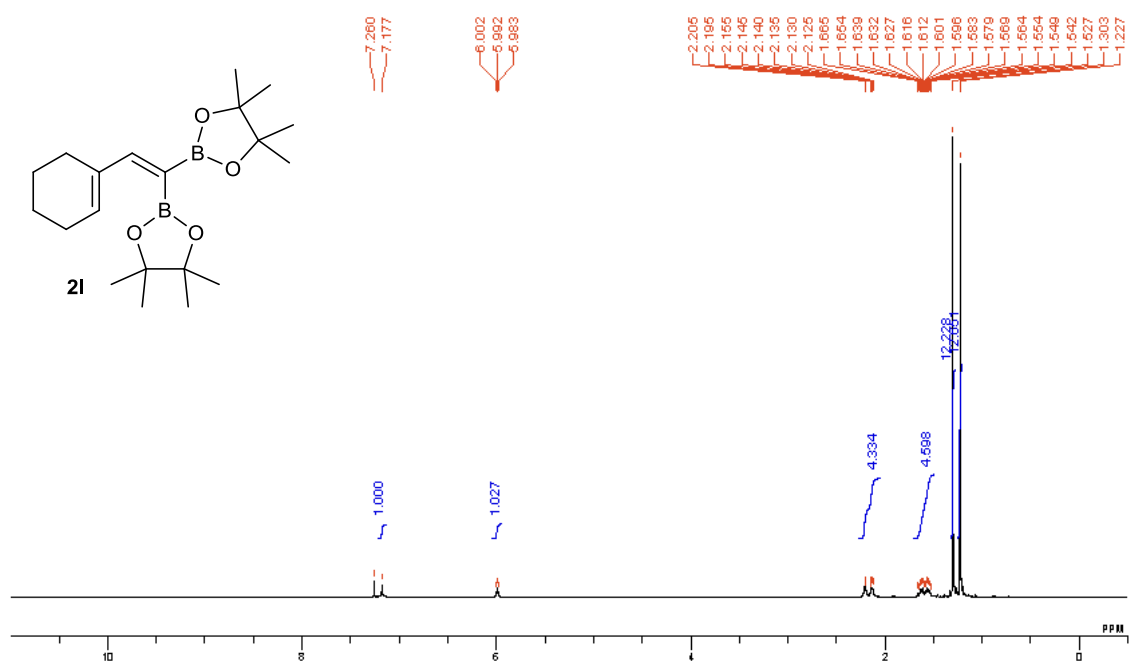


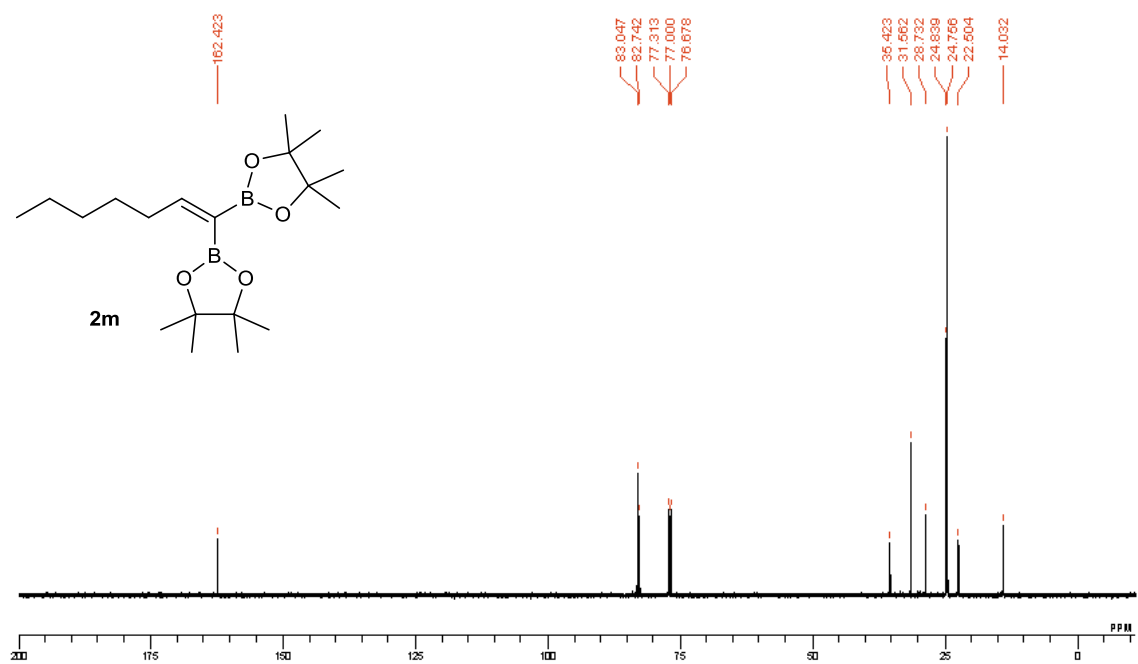
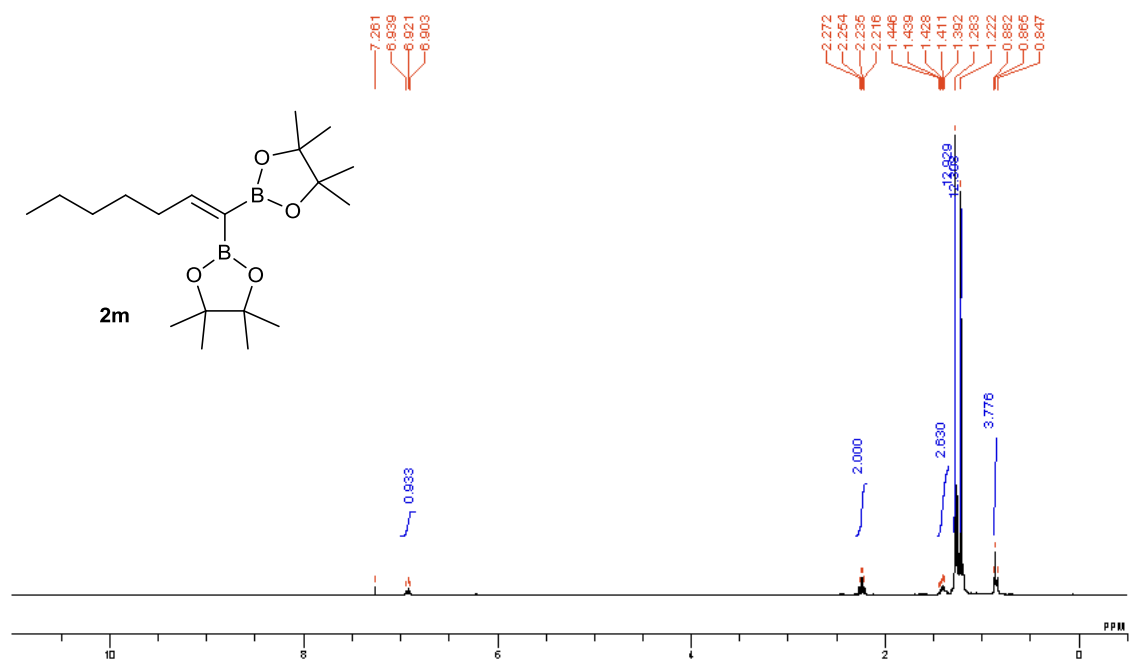


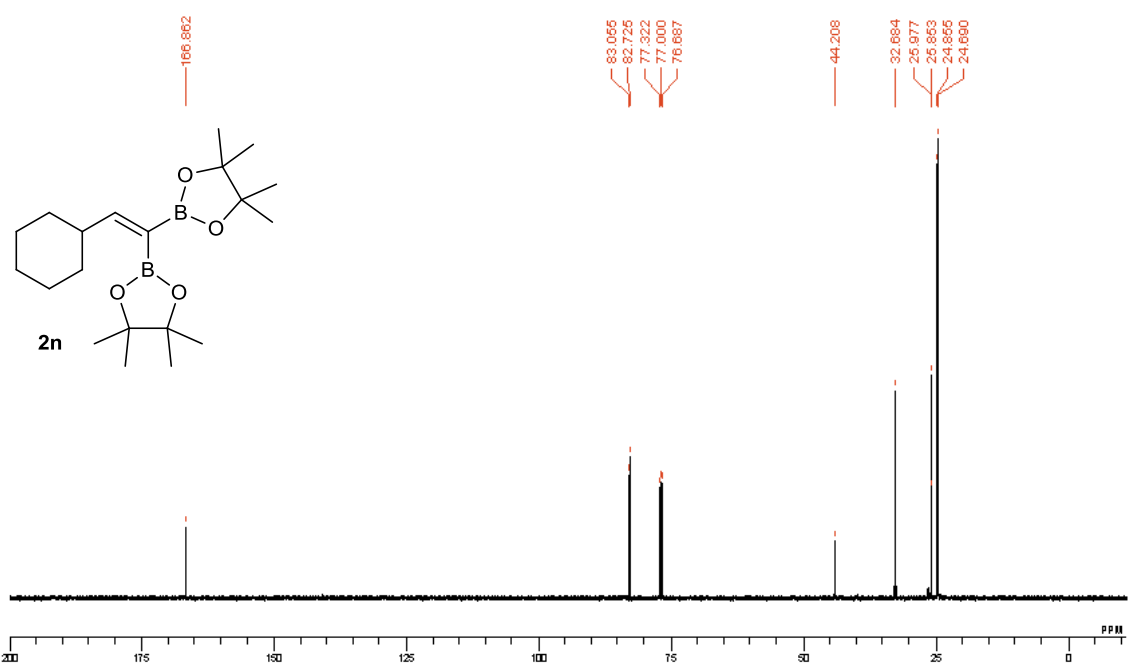


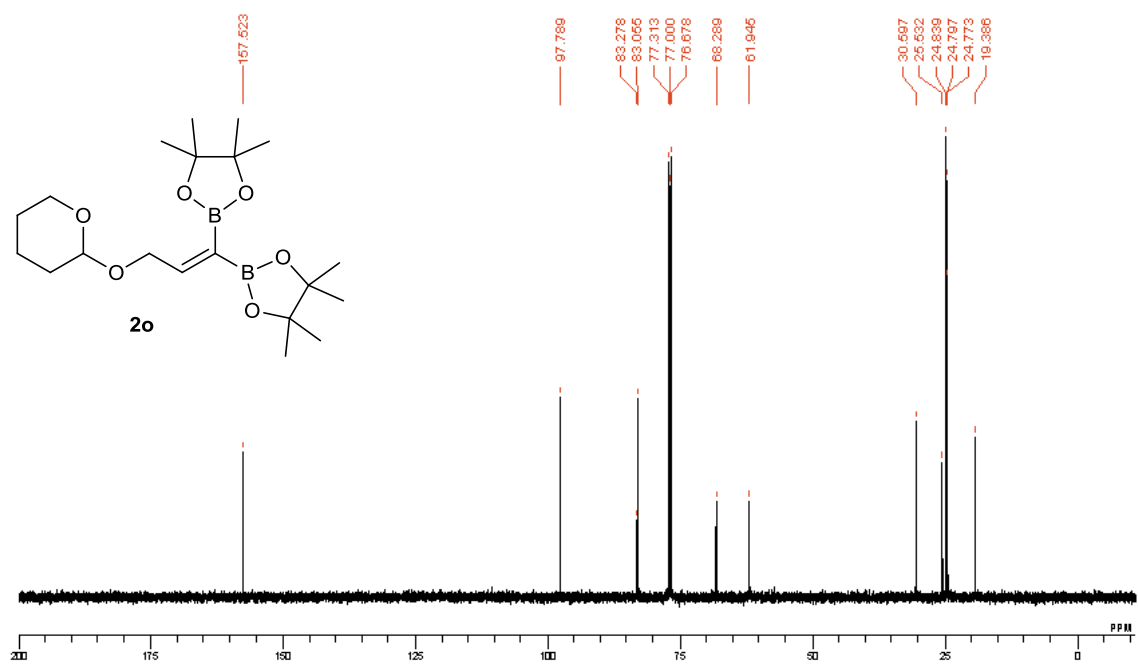
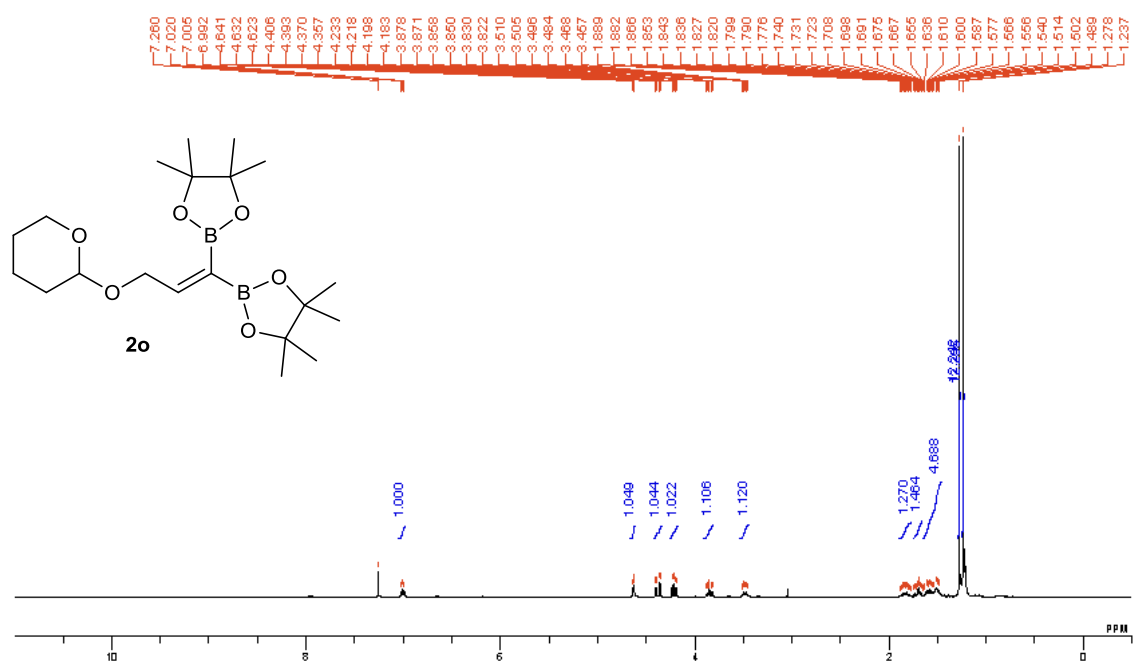


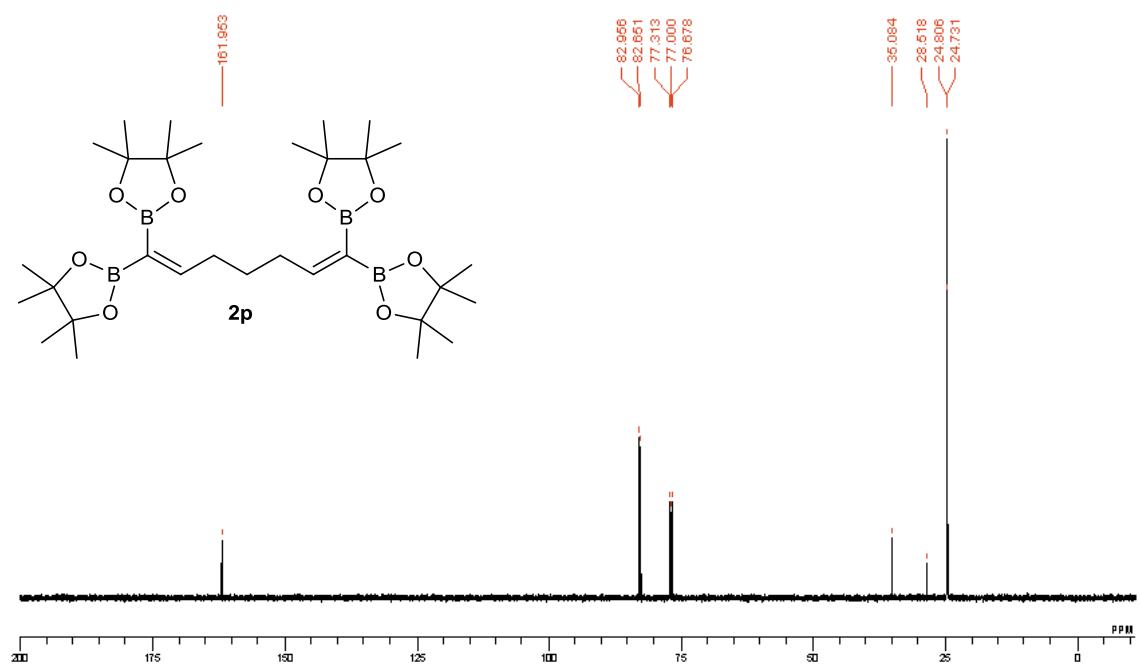
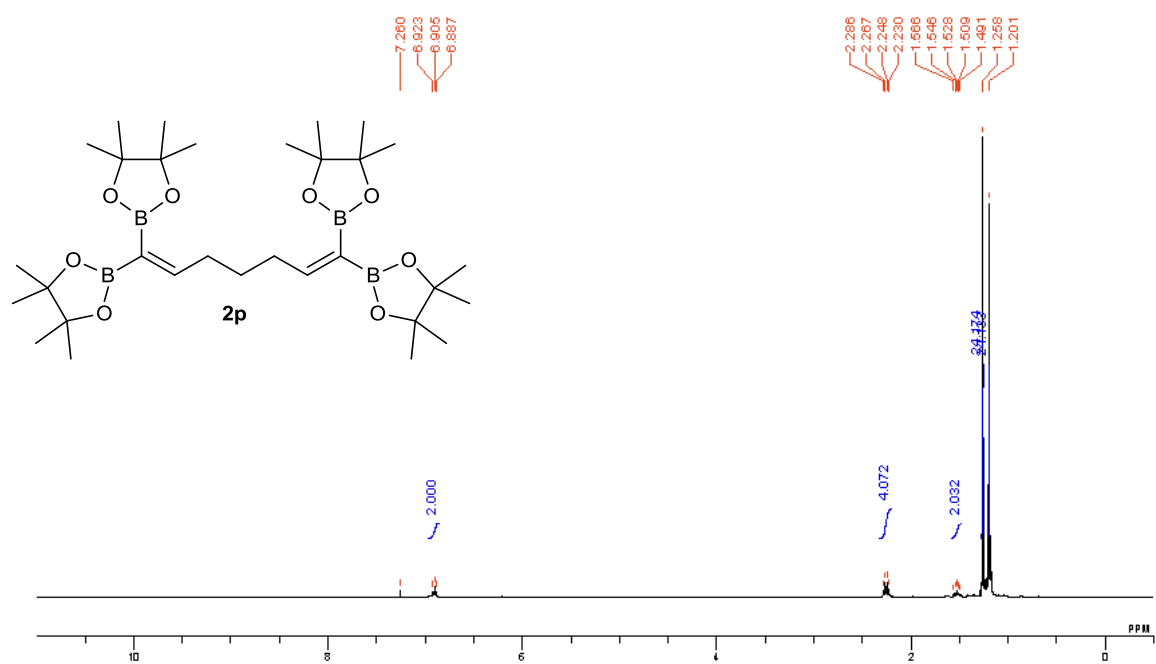


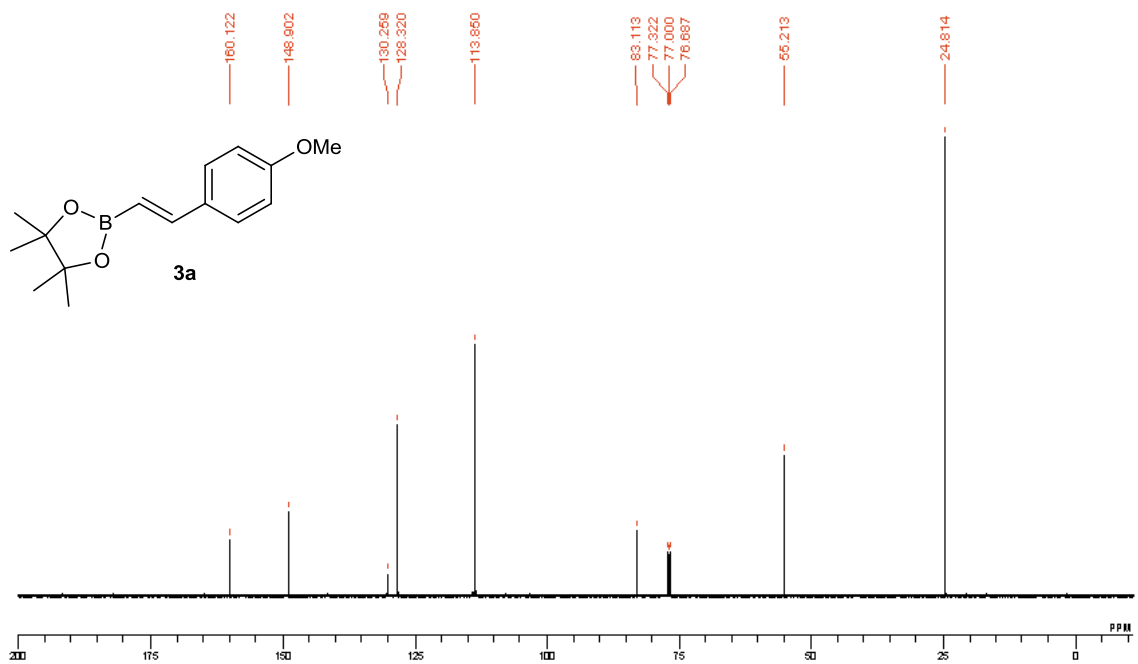
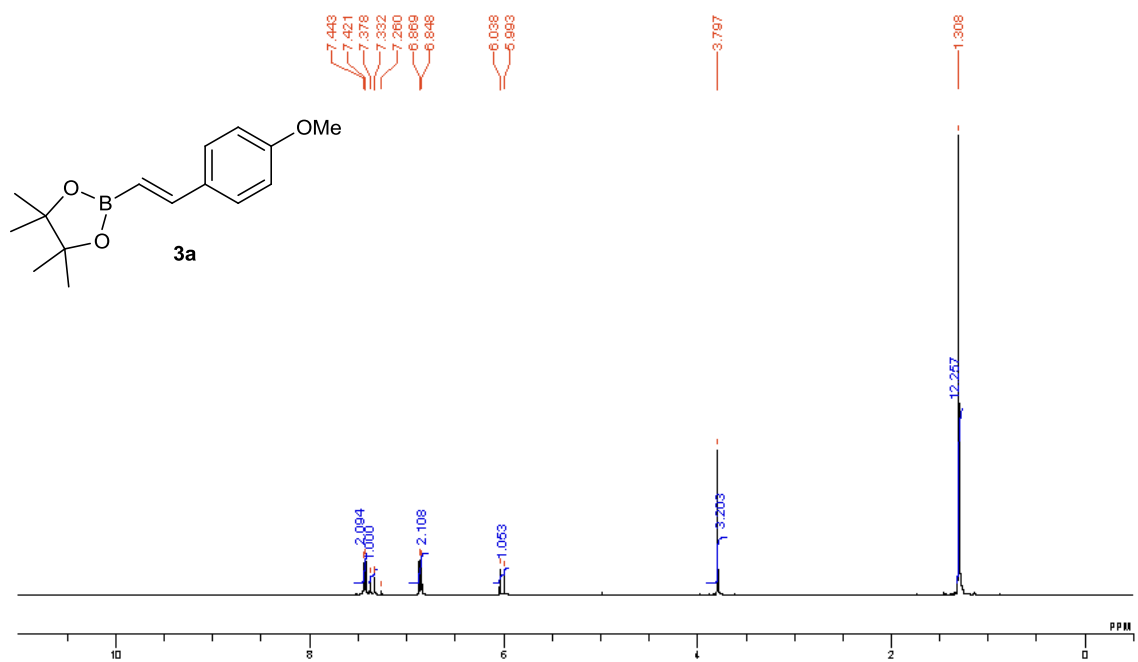


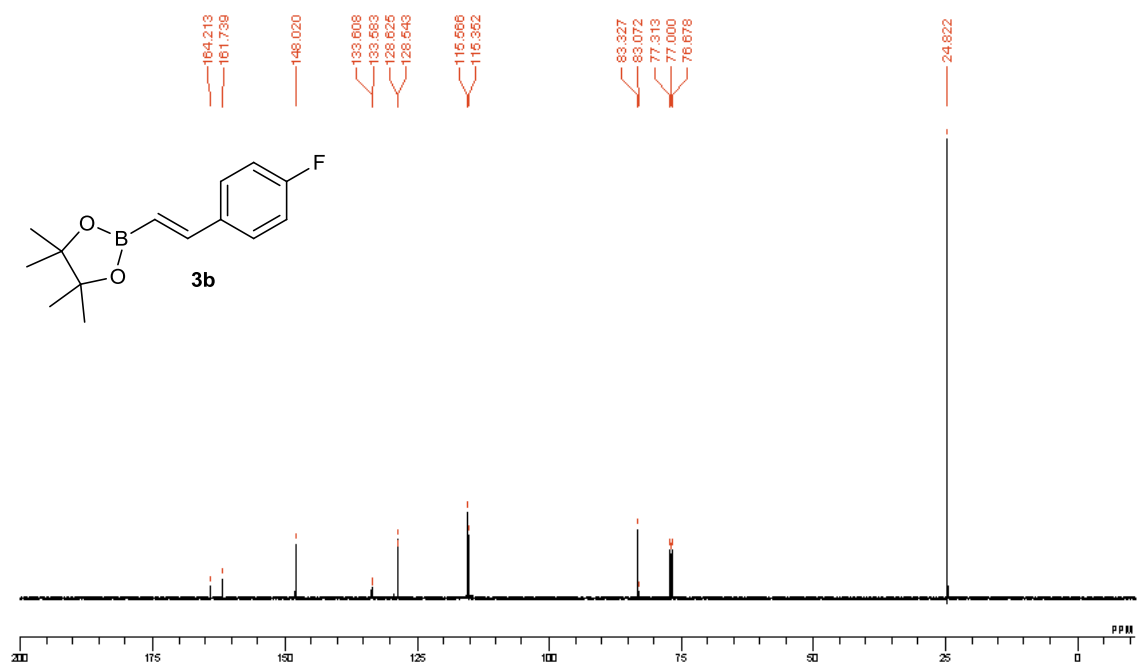
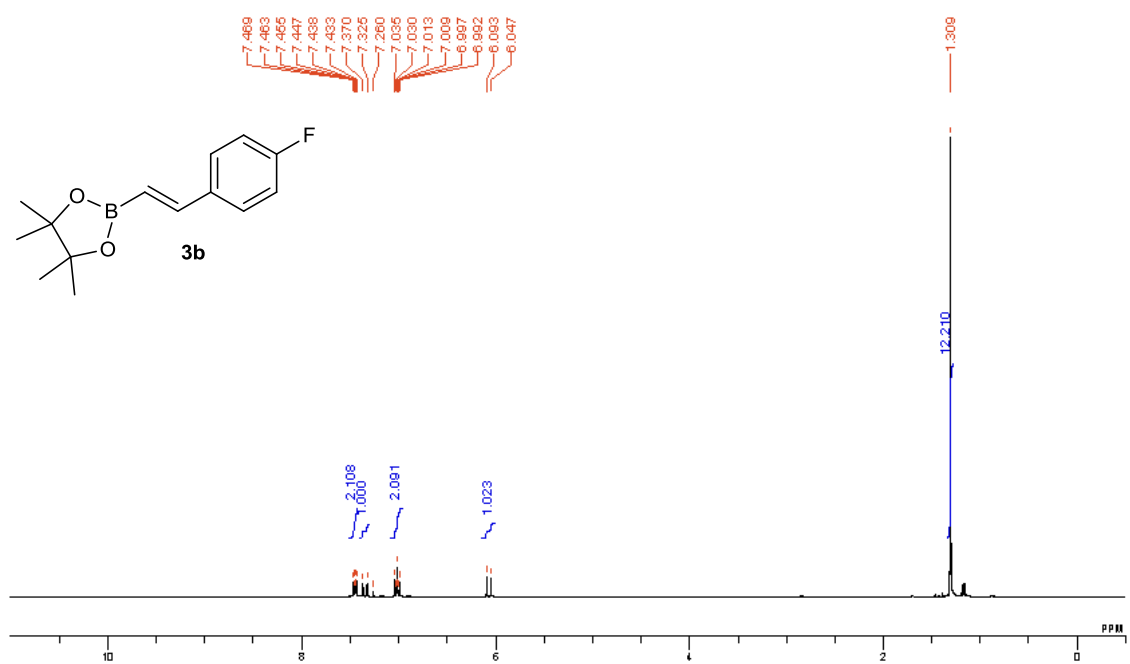


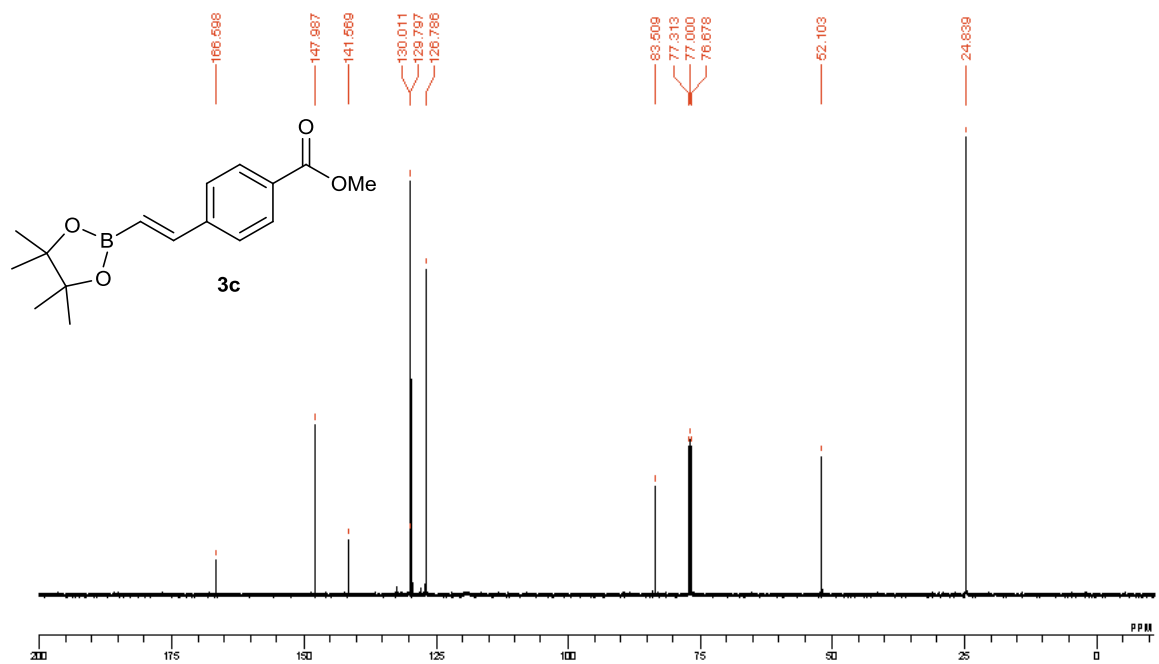
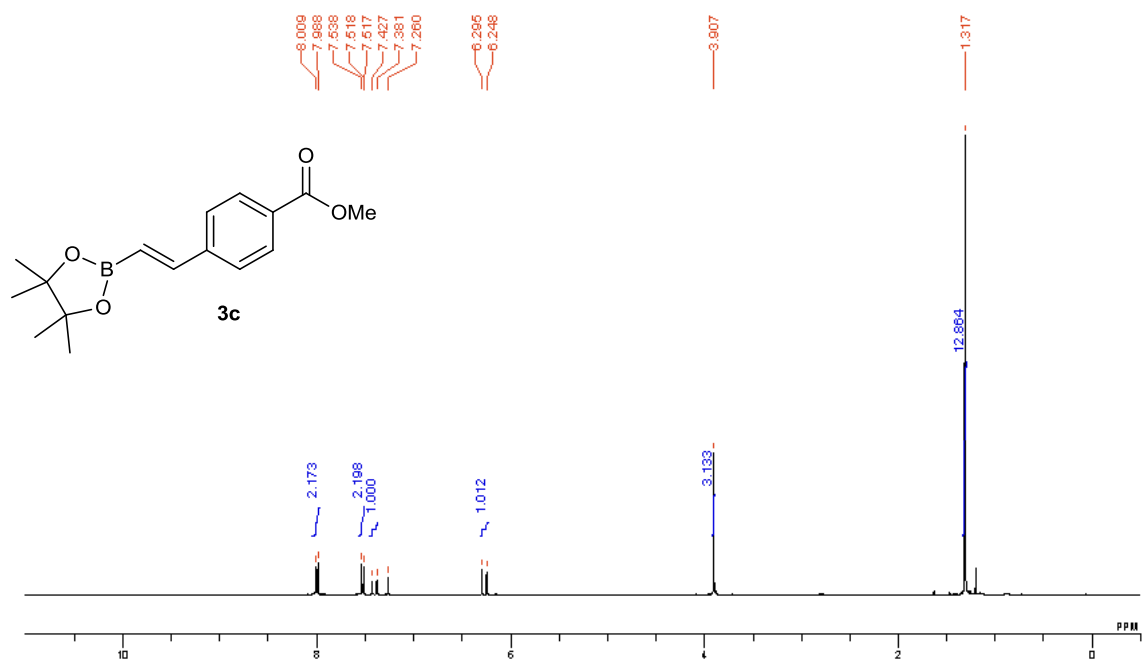


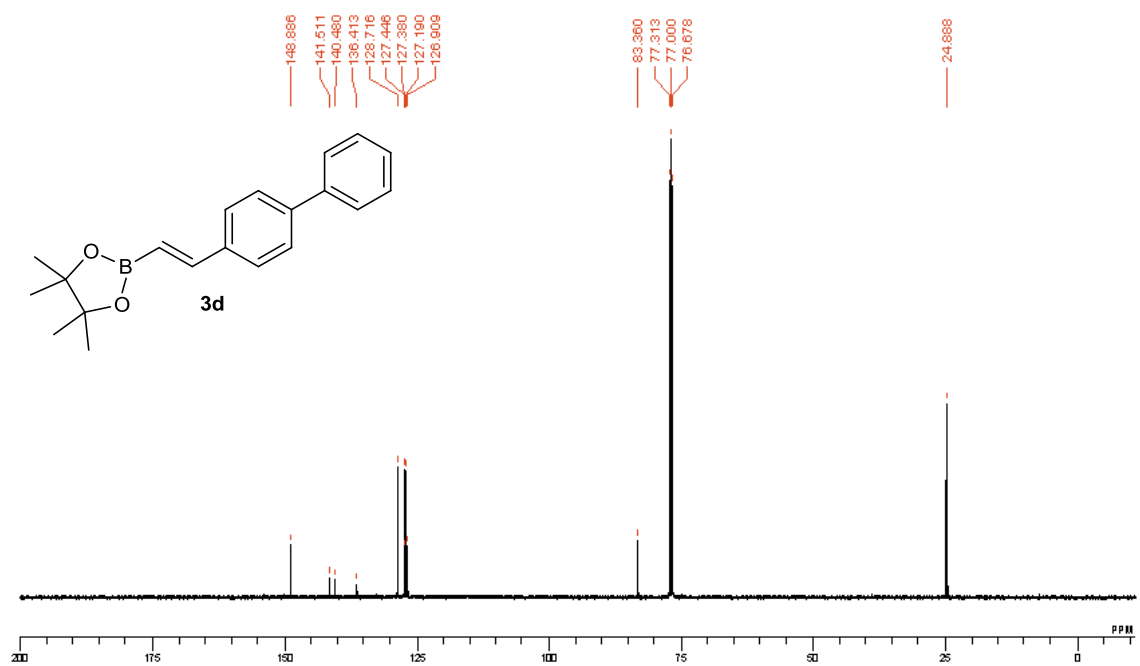
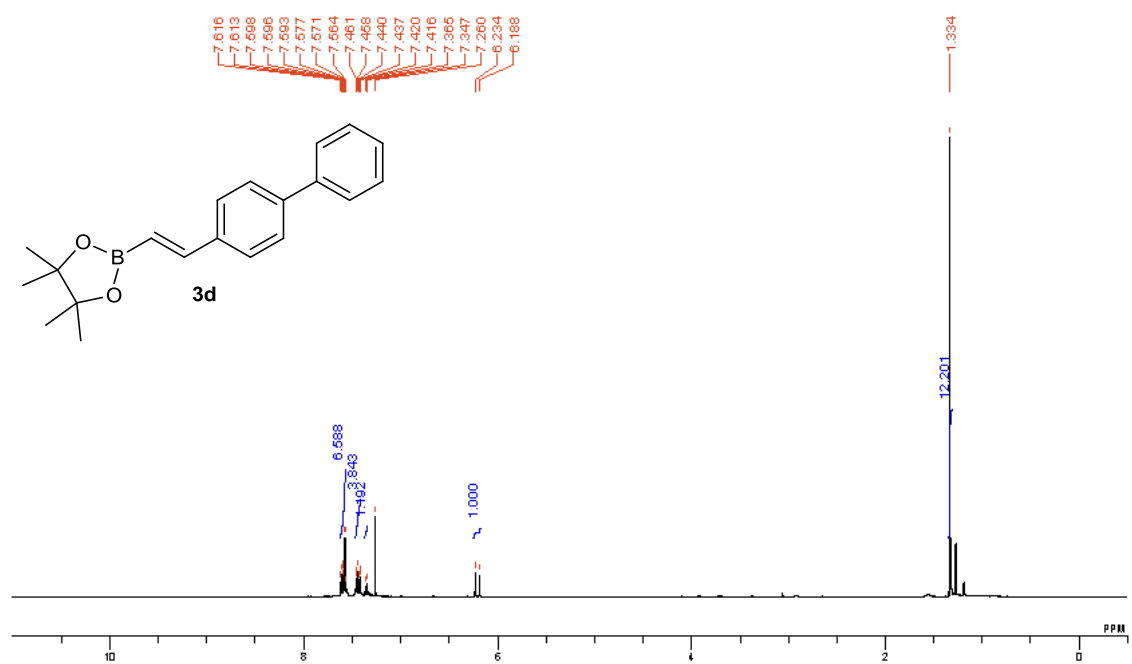


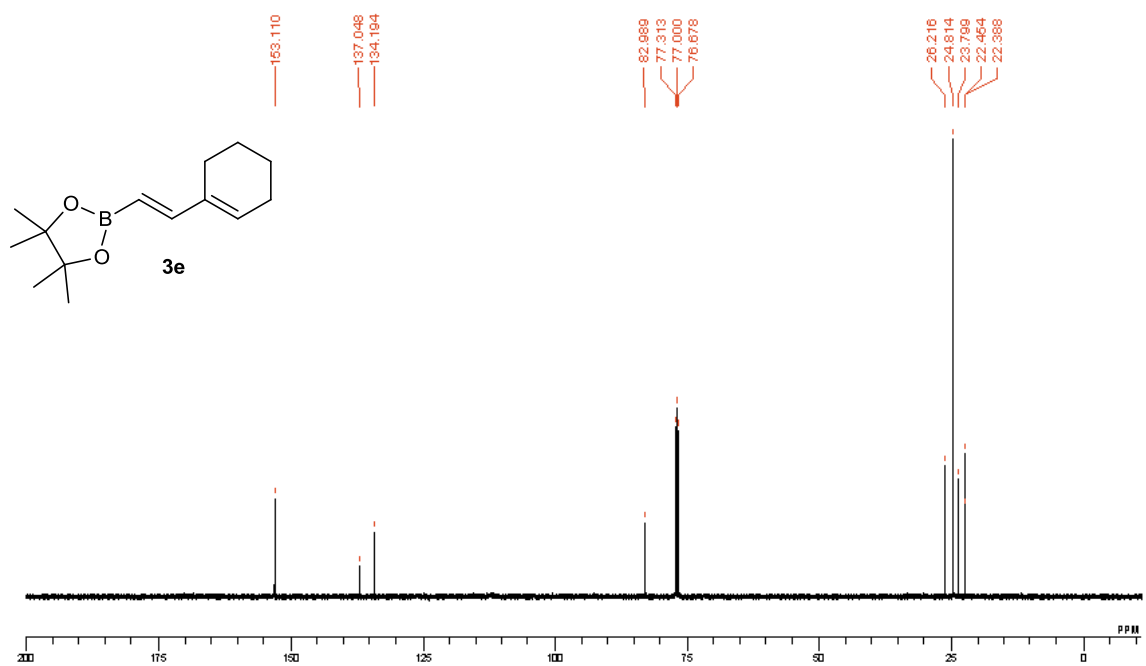
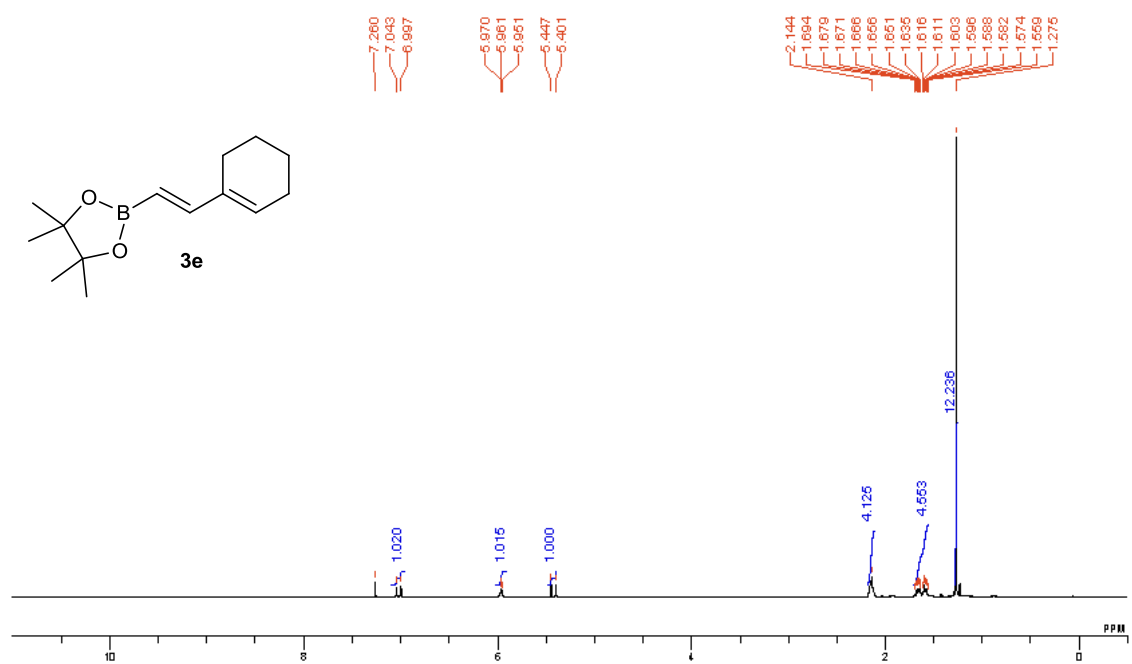


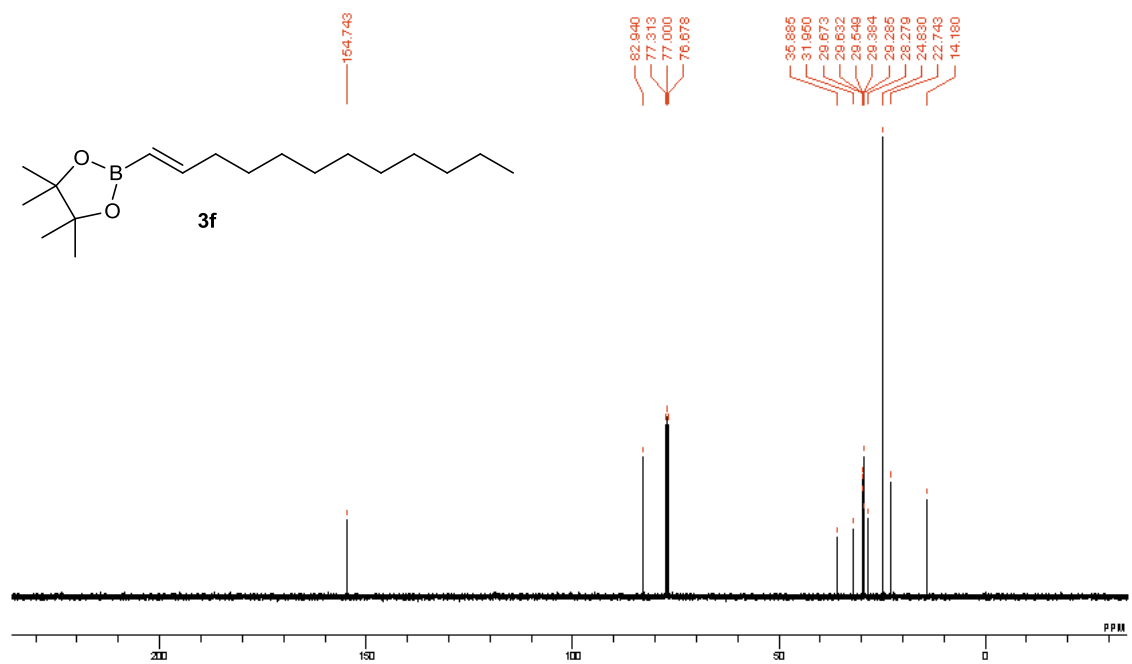
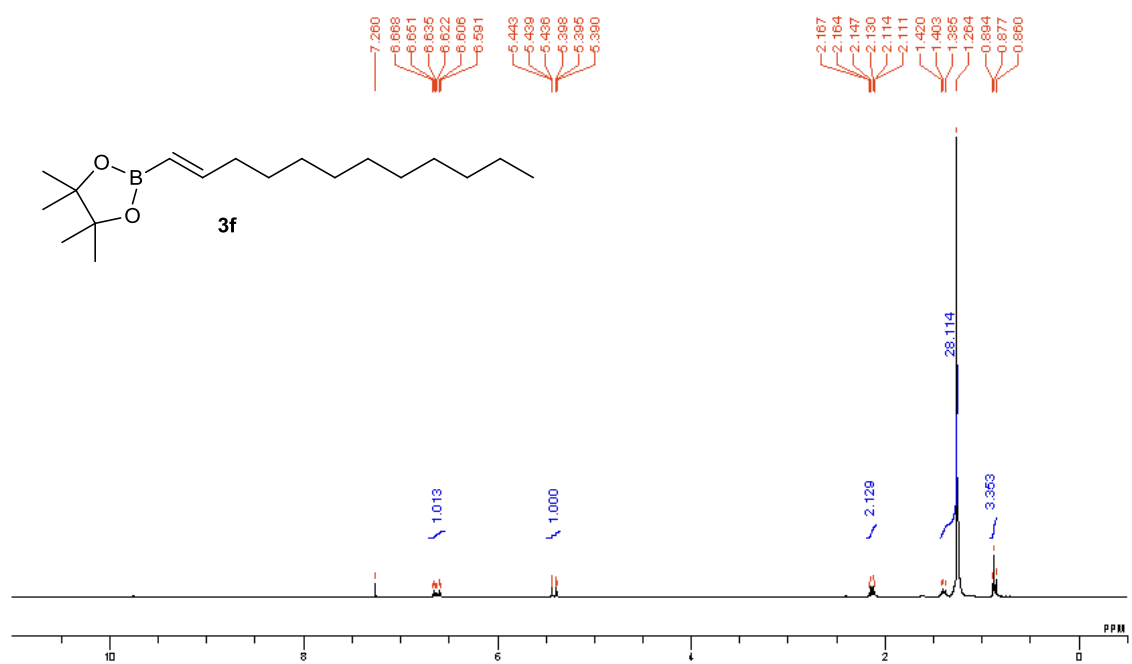


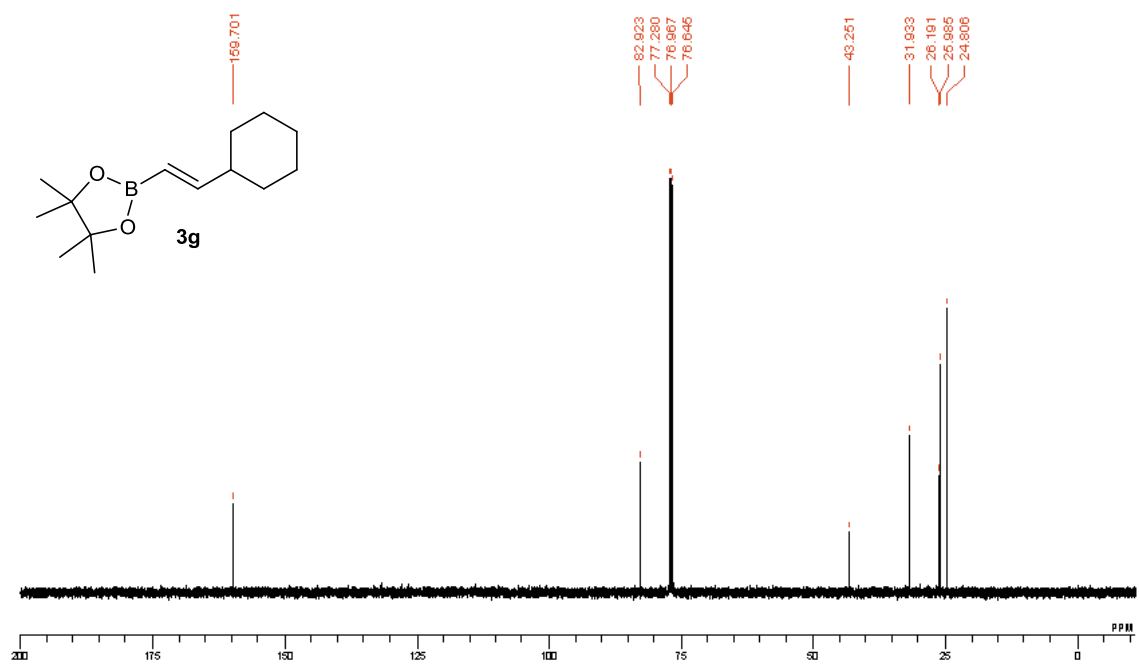
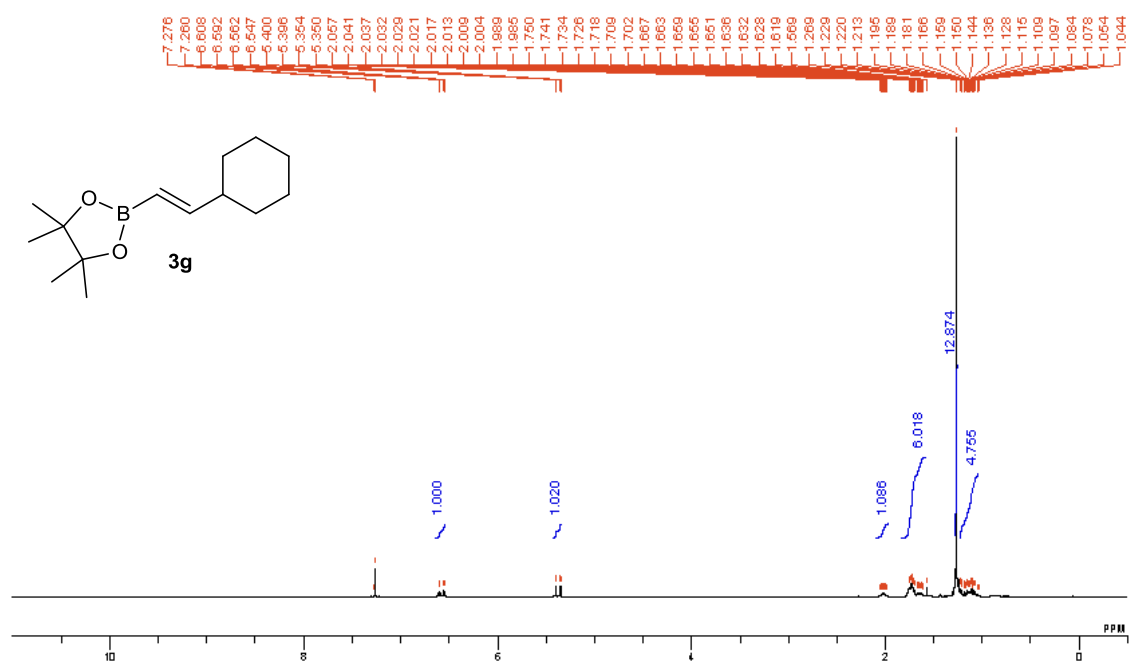


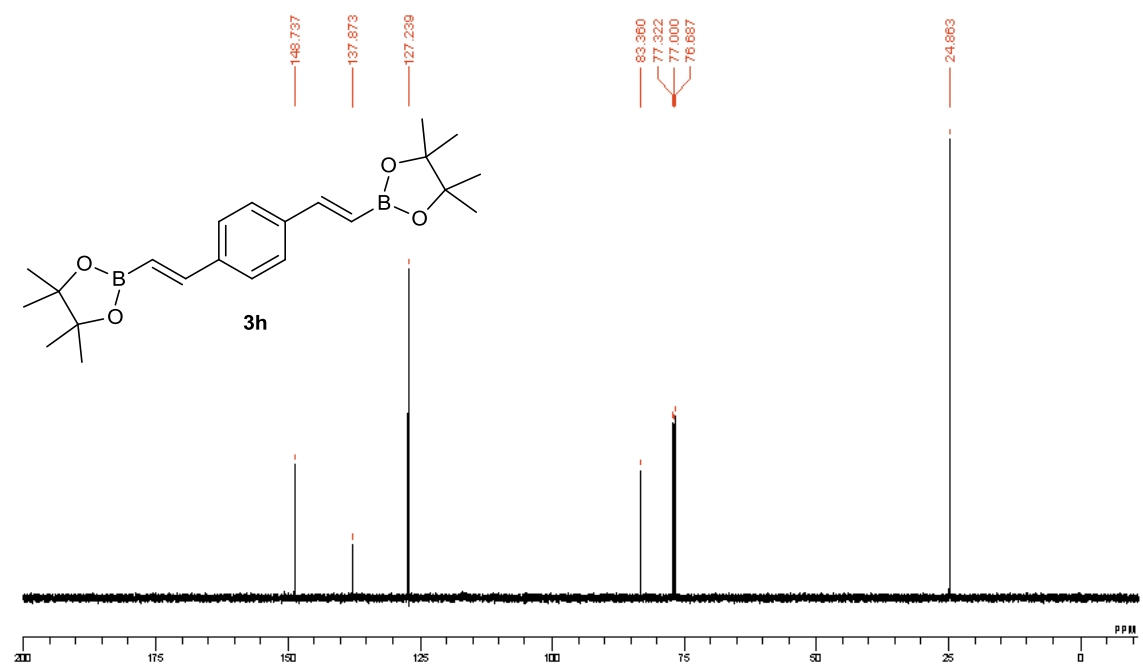
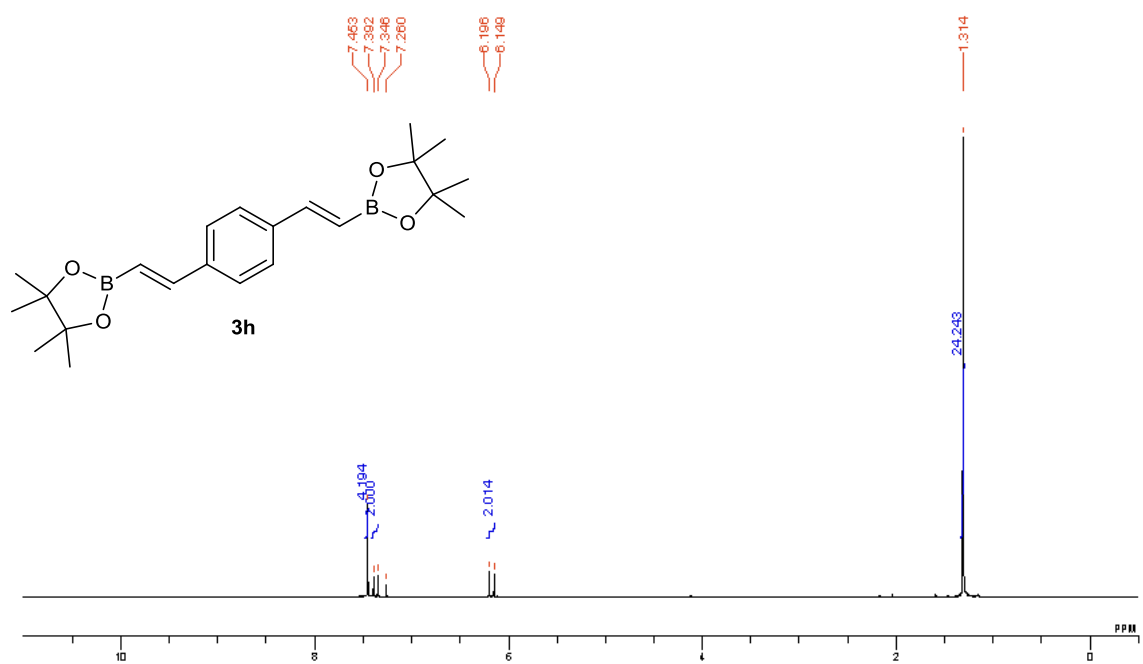


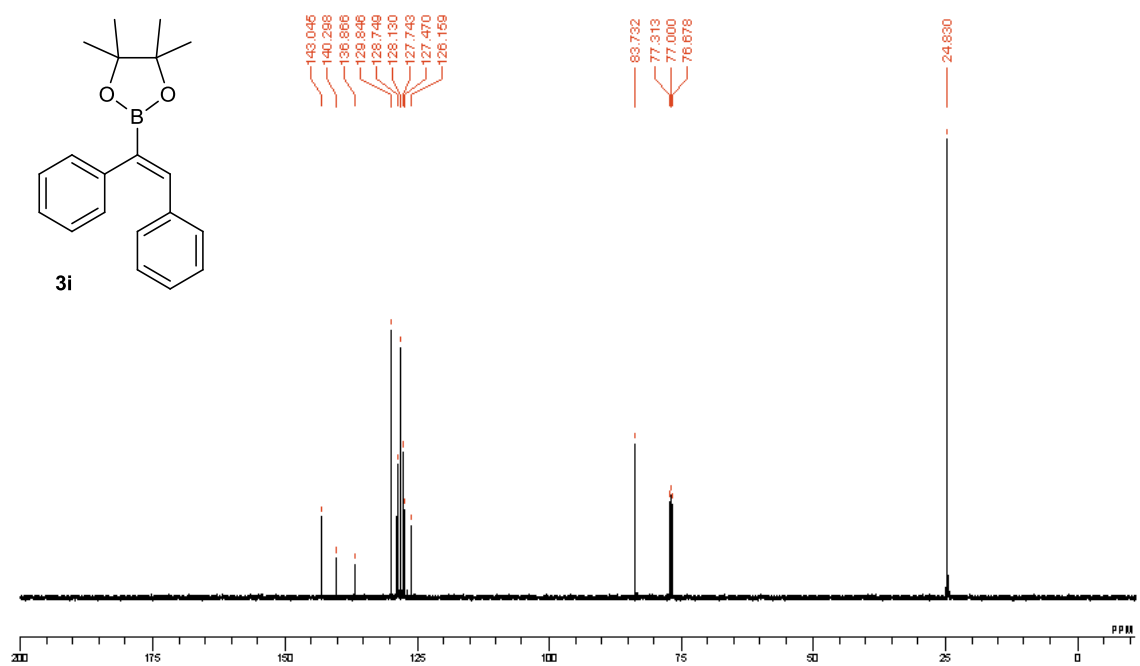
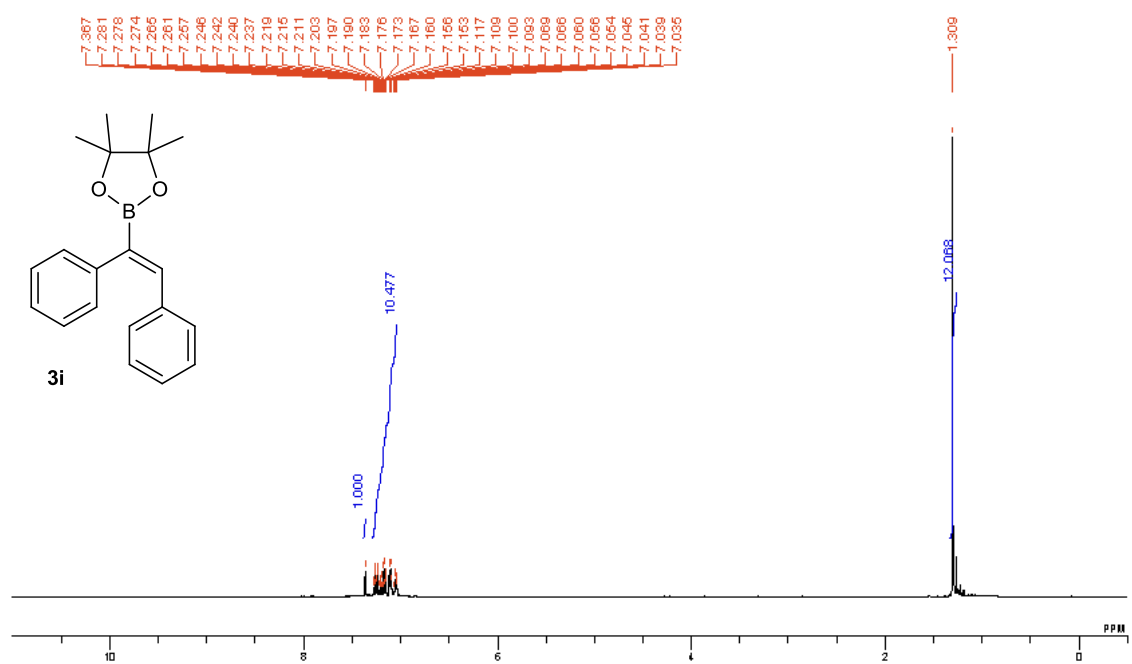


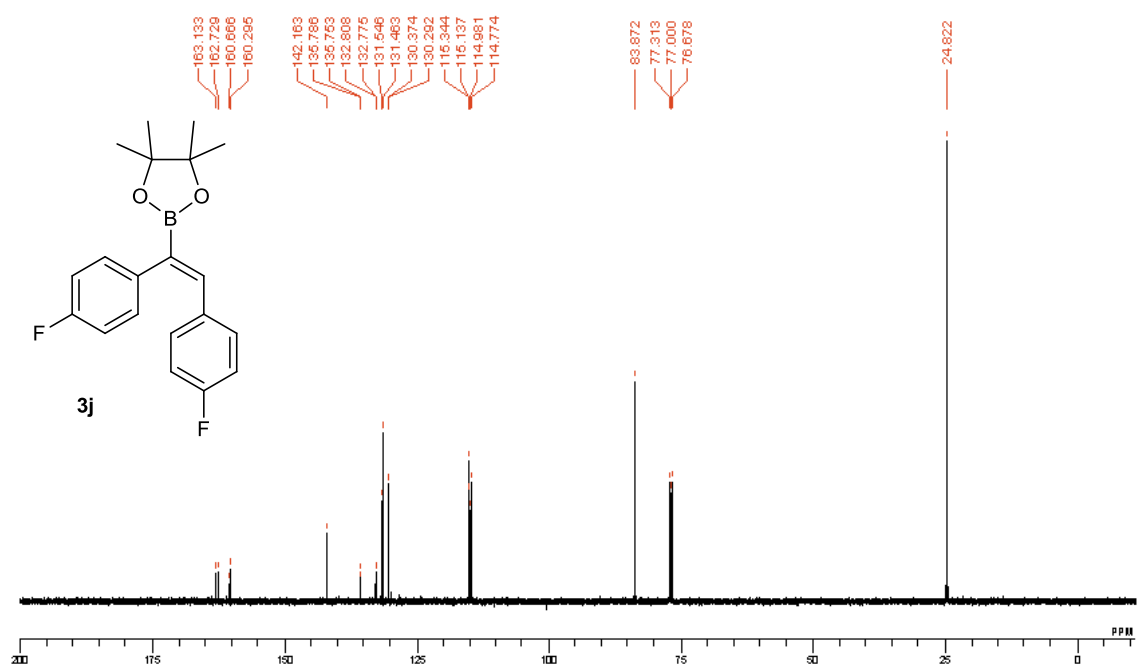
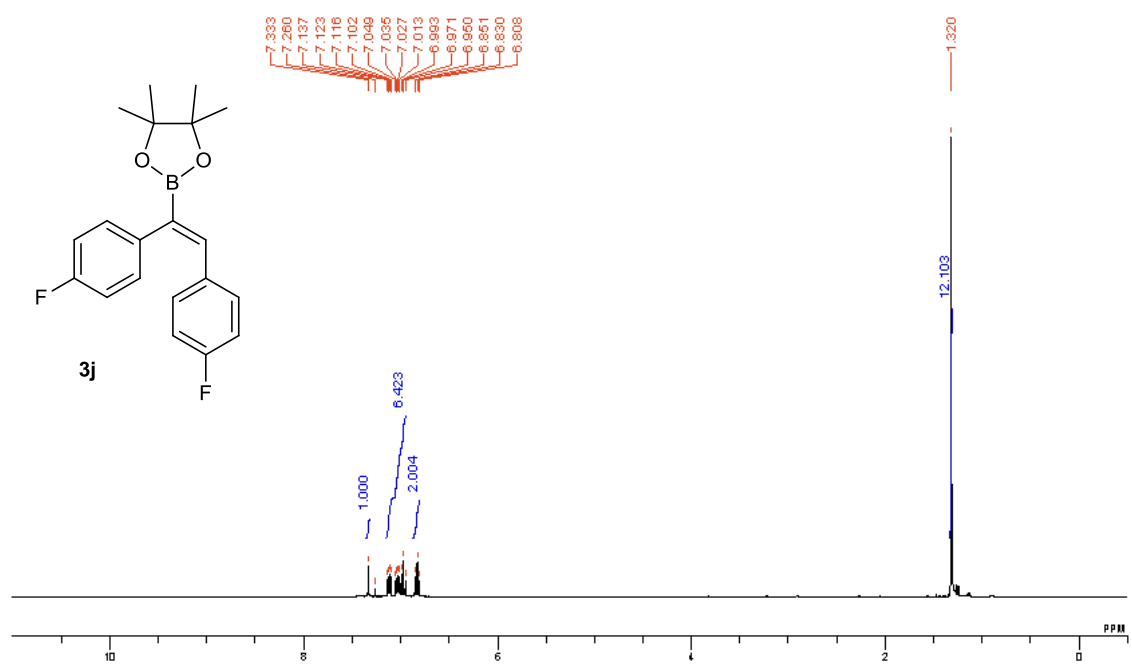


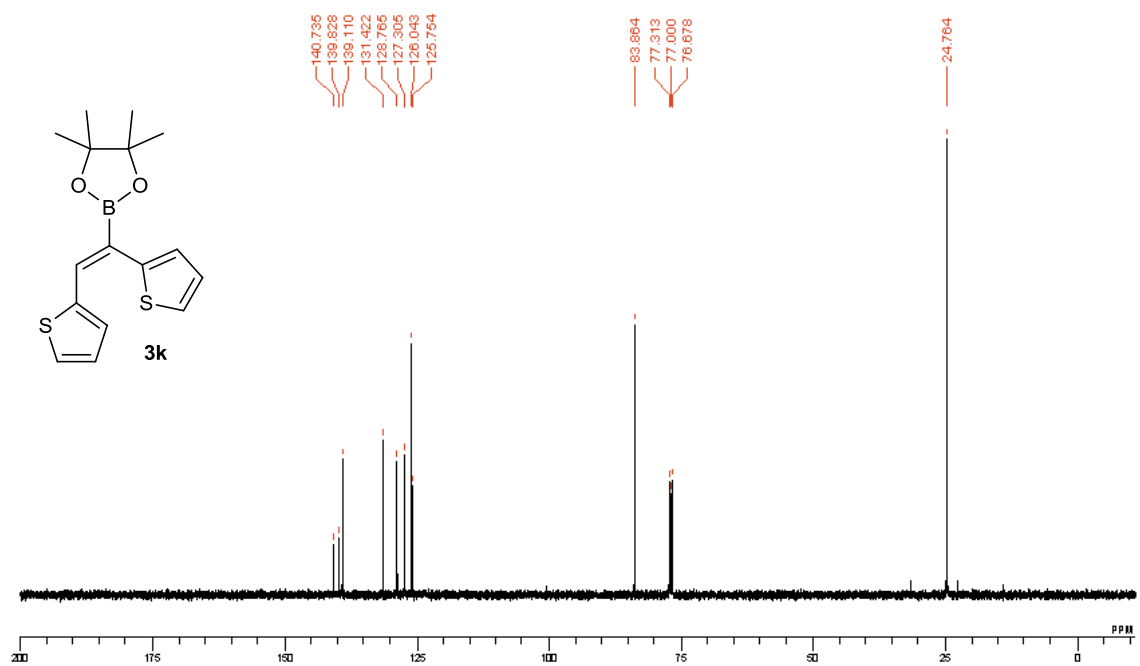
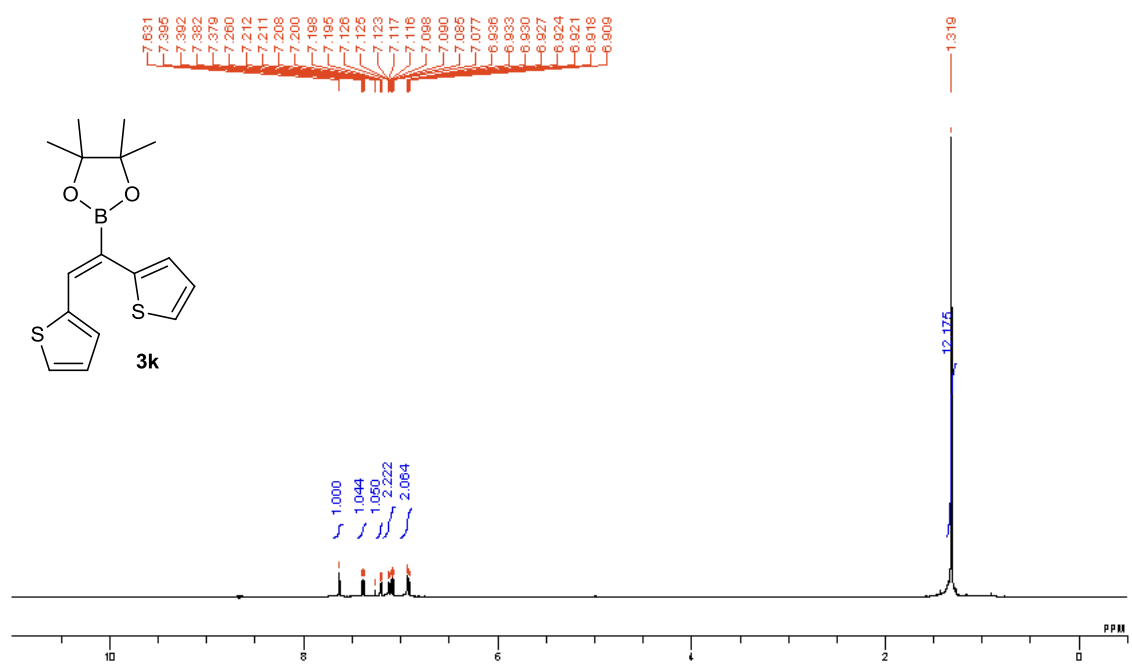


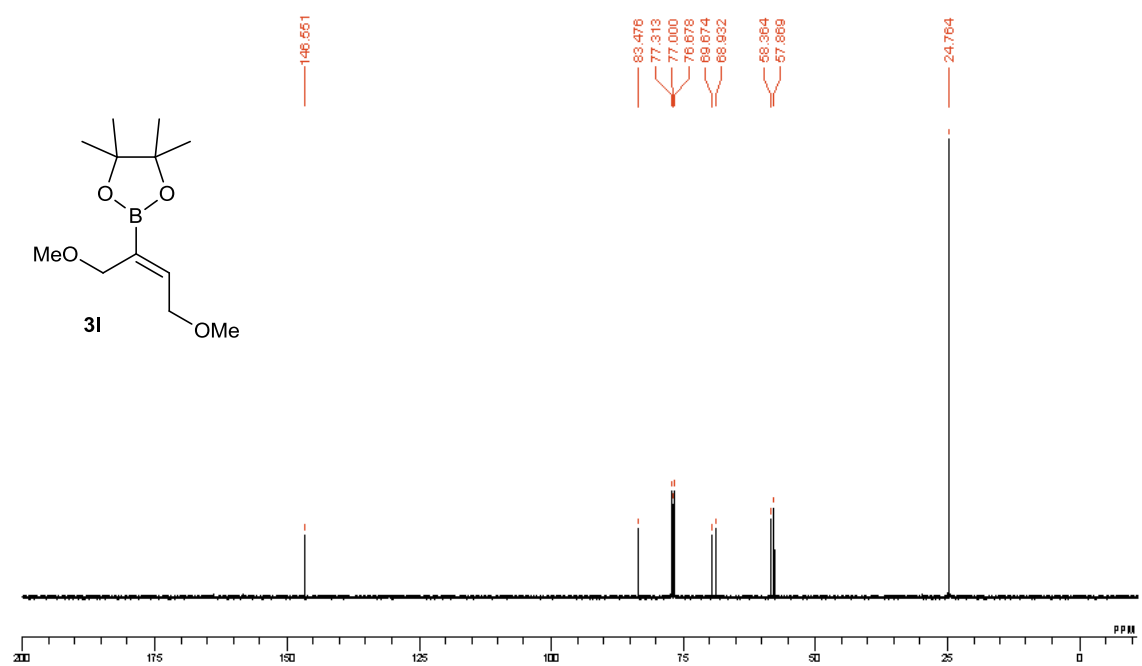
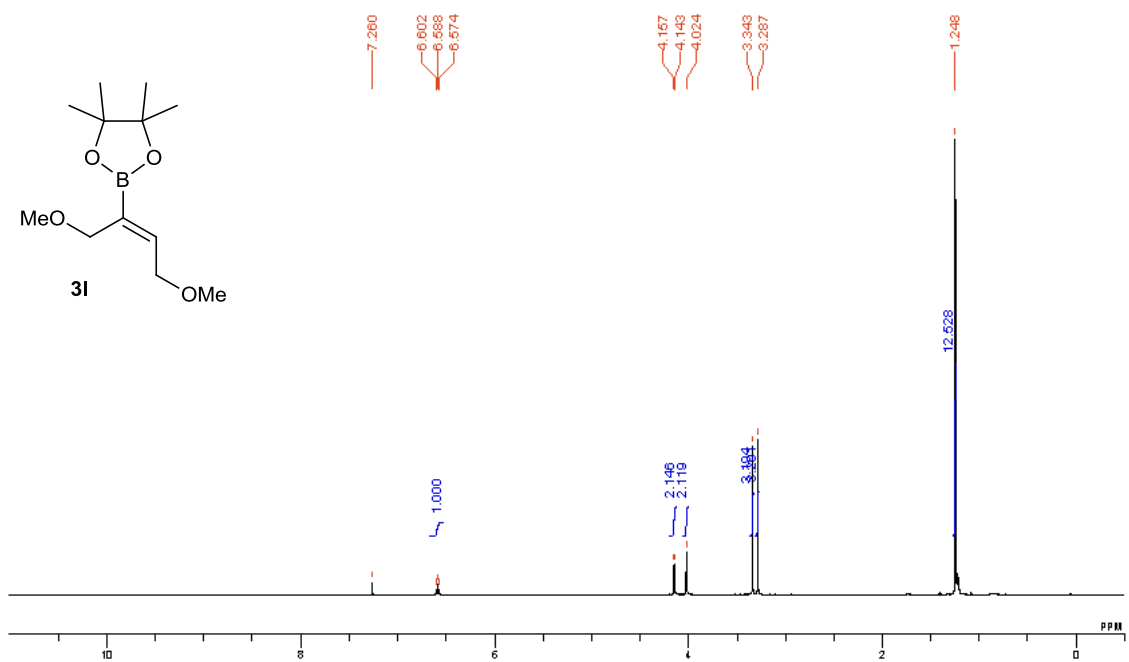


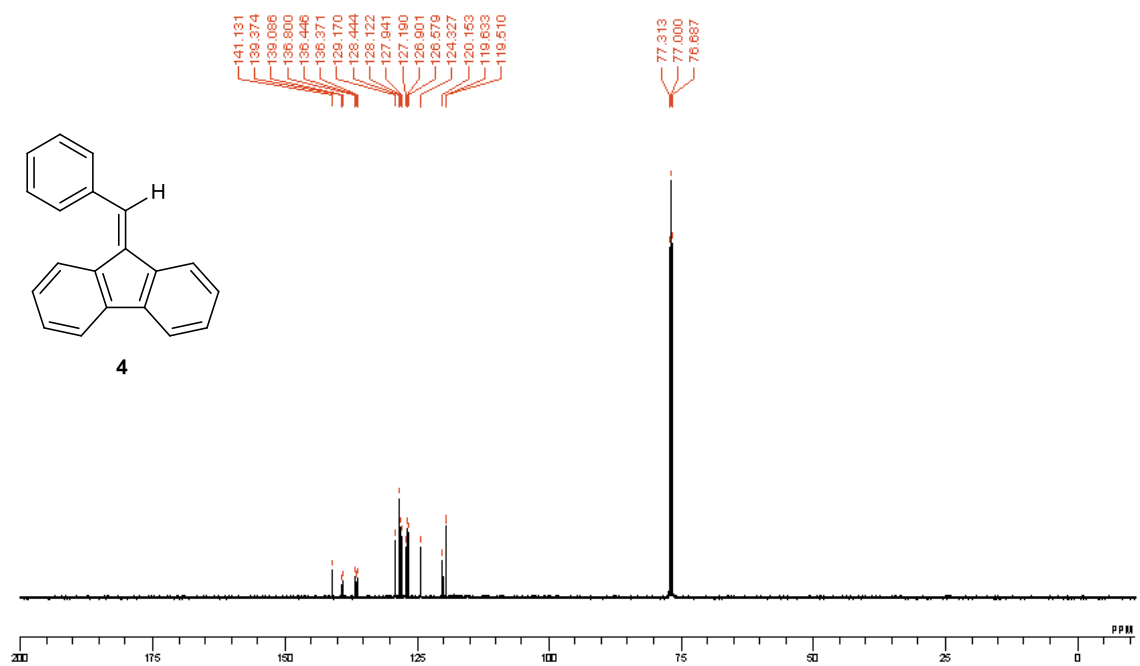
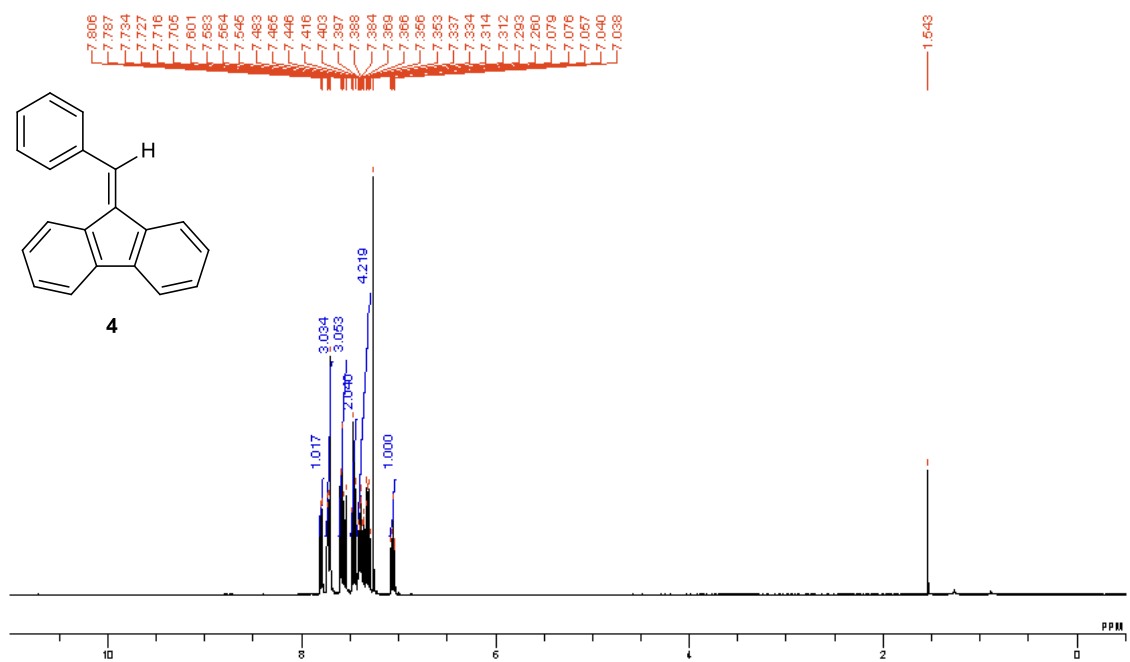












Acknowledgement

This dissertation would not have been possible without the invaluable academic, educational, psychological, humanitarian support and belief from many personalities. Here is a small tribute to all those who supported and believed in me throughout my studies in Tohoku University.

To Professor Yamamoto Yoshinori,

I am very grateful for the opportunity to learn chemistry in your established and world-class laboratory. I am especially grateful for your mentorship and admire your philosophy in science which has been imparted generously to me in each and every group meetings. Thank you for the inspiration in chemistry and gave me the much needed encouragements during difficult periods.

To Professor Jin Tienan,

I am deeply indebted to you for your guidance in chemistry research. This fruitful research is the outcome of your philosophy, “details determine success.” Thank you for giving me supports, advices, encouragements, and your precious time whenever I needed them. You patiently and laboriously guided me since my first day in Tohoku University. Your love for chemistry and perseverance are some of the many other good qualities I will always look up to.

To Professor Asao Naoki,

Thank you for the support, insightful comments, and valuable suggestions in my research works.

I am blessed to have worked and collaborated with some of the best colleagues, brainiest lab mates, wittiest jokesters, and good friends in this laboratory. Thanks for the valuable discussions, companionships, friendships, assistances, information, and all the fun we had together.

I want to express my gratitude to the secretaries who assisted me in many aspects during my stay in Tohoku University. They are: Sunaga Rika, Furuya Saya, and Onodera Sakoto. I would also like to thank the Ministry of Education, Culture, Sports, Science and Technology (MEXT) of Japan for the scholarship and financial support during my stay in Japan from 2011-2016.

Lastly and most importantly, I want to thank my family for loving me since my arrival on Earth. My special thanks to my wife who supported and encouraged me every day since we first met. Lastly, I want to thank my parents. They gave me life, raised me, supported me, and love me. To them I dedicate this dissertation.

Ho Hon Eong, July 2016